UNIVERSITÀ DEGLI STUDI DI MILANO

University of Glasgow

The omega-6: omega-3 fatty acid ratio in swine nutrition: long-term effects on performance, milk fatty acid profiles, oxidative status, and proteomes

Thi Xuan Nguyen
BSc, MSc

Submitted in fulfilment of the requirements for the degree of
Doctor of Philosophy

Supervisors:

Università degli Studi di Milano	**Prof. Giovanni Savoini**
	Prof. Alessandro Agazzi
University of Glasgow	**Dr. Richard Burchmore**
	Prof. David Eckersall
Acuvet Biotech	**Dr. Matilde Pineiro**

September 2022

UNIVERSITÀ DEGLI STUDI DI MILANO

University of Glasgow

The omega-6: omega-3 fatty acid ratio in swine nutrition: long-term effects on performance, milk fatty acid profiles, oxidative status, and proteomes

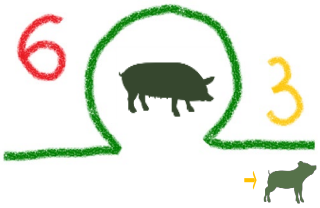

Thi Xuan Nguyen
BSc, MSc

Submitted in fulfilment of the requirements for the degree of
Doctor of Philosophy

Dipartimento di Medicina Veterinaria e Scienze Animali
Università degli Studi di Milano

Institute of Biodiversity, Animal Health and Comparative Medicine
College of Medical, Veterinary and Life Sciences
University of Glasgow

September 2022

Abstract

The ω3 polyunsaturated fatty acids (PUFAs) are characterized as micronutrients and are usually deficient in animal diets. Frequently excessive animal consumption of ω6 PUFAs from corn and other grains compared to ω3 PUFAs (or high dietary ω6:ω3 ratio) leads to various performance and health problems in animals and can also affect human health – the primary consumers of animal products. In recent years, lowering the ratio between ω6 and ω3 PUFAs in animal diets has gained increasing attention as a nutritional intervention to enhance performance and health.

This thesis aimed to improve growth performance and immune system in weaned pigs through early nutritional programs (maternal low ratio of ω6:ω3 (LR) diet during gestation and lactation) combined with later-life nutritional interventions (post-weaned seaweed (SW) diet). Effects of LR in sow diet and SW supplementation in piglet diet on performance, colostrum and milk fatty acids (FA) profiles, and oxidative status, were studied *in vivo* (Chapter 2). The performance and zootechnical data showed the effects of maternal LR diet during gestation and lactation alone or in combination with the SW supplementation in post-weaned piglets on piglet growth and antioxidant status. Also, the influence of SW supplementation alone on piglet growth was revealed. To discover the fundamental molecular processes that activate biological systems such as reproduction and oxidative status, influenced by gestational and lactational LR diet, sow plasma proteomic pattern changes and related biological pathways associated with LR diet were characterized (Chapter 3). Moreover, the alterations in the serum and ileal proteomes and related pathways induced by the interplay between maternal LR diet and offspring SW diet were studied (Chapters 4 and 5). In the final chapter, the findings of the thesis were summarized, and implications of the results for future feeding regime practices were addressed (Chapter 6).

Zootechnical performance: Maternal LR diet during gestation and lactation combined with the SW supplementation in post-weaned piglets did not enhance piglets' growth or antioxidant status. Nevertheless, the maternal LR diet alone increased total ω3 PUFAs (mainly α-linolenic acid - ALA) in the colostrum and milk, improving the weaning survival rate and suckling piglets' weight gain. Additionally, SW supplementation enhanced piglets' growth from sows fed control ratio of ω6:ω3 (CR) diet.

Sow plasma proteomics: LR diet altered the plasma levels of several acute phase proteins (APPs) such as HP, SERPINA1, and APCS that might be involved in protective mechanisms against accelerated stresses and, in particular, oxidative stress at later stages of gestation and lactation. Furthermore, significant shifts were found over the late gestation-late lactation period affecting the plasma lipoproteins and the APPs. The end of pregnancy is associated with an acute phase reaction (APR) demonstrated by the increased abundance of positive APPs (i.e., HP and ITIH4 (pig-MAP)) and a decrease in negative APPs, i.e., APOA1, while by the end of lactation, this APR has dissipated and APOA1, APOA2, and APOC3 were all increased.

Piglet serum proteomics: Maternal LR diet enhanced piglet host protective response via regulating the expression of C3, SAA, SERPINA3, SERPINC1, and TF and their association with anti-inflammatory activities and innate immunity. Post-weaned piglets' SW diet enriched C5a and KNG1, stimulating coagulation cascade regulation and the connection between innate and adaptive immunity to enhance the host defence during inflammation conditions. The potential regulator proteins associated with the early development of piglet post-weaning were also underlined, including serum lipoproteins (APOA1, APOB, APOE); pro-coagulation proteins (F2, HRG, ORM1); coagulation regulator (PLG); and APPs (HP, ITIH4, TF, SAA, SERPINA1). These proteins participate in platelet metabolism, haemostasis, and cross-talk between coagulation pathways and inflammation, particularly in the innate immune system.

Piglet ileum proteomics: Maternal LR diet positively regulated RPSA regarding protein synthesis process but may induce uncontrolled proliferation and overexpression of cell cycle regulators in the offspring via affecting CCT2. SW supplementation reduced the inflammation severity in post-weaning piglets by regulating ATP5A1 and ATP5B, promoting ileal epithelial growth in piglets fed seaweed from the mother provided a control ratio of ω6:ω3 (CRSW piglets) (HBA, HBB, RPL10A, and RPL24). However, it decreased the fat absorptive capacity in piglets fed seaweed from the mother received a low ratio of ω6:ω3 (LRSW piglets) (FABP6).

Overall, the results suggest maternal and offspring nutritional interventions play a vital role in sow reproduction and piglet development. Moreover, potential protein regulators of pig performance and health over sensitive periods were revealed. These can be used as the basis of future studies to understand how nutrition programs can be enhanced to improve the quality and safety of animal products for human consumption.

Table of Contents

List of Tables

List of Figures

Acknowledgement

First and foremost, I would like to express my sincerest gratitude to my supervisor team, Prof. Giovanni Savoini and Prof. Alessandro Agazzi (University of Milan), Dr Richard J. Burchmore and Prof. David Eckersall (University of Glasgow), and Dr Matilde Pineiro (Acuvet Biotech) for their insightful supervision, guidance, support, and encouragement throughout this PhD project. Their invaluable supervision and support at each milestone, especially during the covid lockdown, helped in getting my thesis to the form that I am now submitting.

I would like to sincerely thank Prof. Alessandro Agazzi for his willingness, time, and availability in research and assistance in my administrative and bureaucratic procedures in Italy. My heartfelt thanks to Prof. David Eckersall for his excellent support, great advice and opportunity, and encouragement, especially through a trial-and-error procedure during the lab work and writing process.

I acknowledge the funding from the EU 2020-ITN project – MANNA (No 765423) under Marie Skłodowska-Curie's early-stage researcher fellowships program. My gratitude goes to the MANNA consortium for offering me a position in the ESR1 project to pursue my doctoral studies and to attend numerous conferences. The 3-year PhD program was a unique learning experience and fantastic opportunity that will always value for the rest of my career. Particularly, I owe a huge debt of gratitude to Prof. Fabrizio Ceciliani, the Principal Investigator of the MANNA project at University of Milan, for his invaluable support from the beginning and throughout my PhD journey and the chance to learn several techniques in his lab.

I would like to thank numerous others for their technical support and encouragement. I could not have gotten to this stage without each of you. I thank Marcello Comi, Valentino Bontempo, Invernizzi Guido, Sara Panseri, Vera Perricone, Fabio Omodei Zorini, Jacob Ranghetti, and Francesca Maffetti (University of Milan) for help with the in-vivo trials, Barbara Heitkoenig and Thomas Blees (University of Bonn) for technical assistance with the oxidative status experiments, Suzanne McGill and Stefan Weidt, and Dr Mark McLaughlin (University of Glasgow) for their technical supports on proteomic experiments and validations, Andrea Gelemanović (Mediterranean Institute for Life Sciences) for her preliminary advice and guidance on statistical and bioinformatic analysis on

proteomic data. I also thank Michaela Scigelova (Thermo Fisher Scientific, Charlotte, North Carolina, USA) for assistance with Proteome Discoverer software and Ting Huang (Khoury College of Computer Sciences, Northeastern University, Boston, MA, USA) for assistance with the MSstatsTMT R package.

My thanks go to Prof. Helga Sauerwein (University of Bonn) for giving me the opportunity to visit her research group and learn basic techniques on measuring parameters of oxidative stress and encourage me to write and publish my first paper on Animals journal.

To all my friends from MANNA: Tamil, Gaby, Arash, Yron, Punit, Ruben, Morena, Francesca, Jorge, and Rafaela, thank you for all your support during this 3-year journey. To Carlotta and Valentina, thank you for your time and assistance with Milan's administrative and bureaucratic procedures. To Ngoc, Trang, Lan Anh, and Tu Anh, thank you for always being beside me whenever I need you with your warm heart and love. I will never forget the time laugh and cry we had together in the San Mamete family.

Finally, my warmest gratitude and love go to my husband Quang Hanh and my daughter Quynh Thu for their infinite love, everlasting assistance, and encouragement over the last years. I am also extremely thankful to my parents, Van Thang and Thi Sau, for being my backbone. I could never have completed this journey without your unconditional love and support.

Thank you all,

Xuan

Author's Declaration

I declare that, except otherwise cited or acknowledged, this thesis is entirely the result of my own work and has not been submitted for any other degree at the University of Milan, University of Glasgow, or any other institution.

Signature:

Printed name: Thi Xuan Nguyen

September 2022

Abbreviations

Abbreviation	*Meaning*	*Abbreviation*	*Meaning*
A. nodosum	*Ascophyllum nodosum*	DNA	Deoxyribonucleic acid
× *g*	times gravity	IGF	Insulin growth factor
°C	Degrees Celsius	IL	Interleukins
µg	Microgram	IS	Internal standard
µl	Microliter	iTRAQ	Isobaric tag for relative and absolute quantitation
µm	Micrometer	kg	kilogram
µM	Micromolar	KGF	Keratinocyte growth factor
AA	Arachidonic acid	L	Lactation
ACN	Acetonitrile	LA	Linoleic acid
ADFI	Average daily feed intake	LC	Liquid chromatography
ADG	Average daily gain	LDL	Low-density lipoprotein
ALA	α-linolenic acid	L-End	End of lactation
AOPP	Advanced oxidation products of proteins	LR	Low ratio of ω6:ω3
APP	Acute phase protein	LSM	Least square means
APR	Acute phase responses	LTs	Leukotrienes
ATP	Adenosine triphosphate	m/z	Mass to charge ratio
BCA	Bicinchoninic acid method	MCP1	monocyte chemoattractant protein-1
BCS	Body condition scores	MF	Molecular Function
BP	Biological Process	MIF	Migration inhibitory factor
BV	Blood vessels	min	Minute
BW	Body weight	mL	Milliliter
CC	Cellular Component	mM	Millimolar
CLA	Conjugated linoleic acid	mm	Millimeter
CR	Control ratio of ω6:ω3	MMPs	Matrix metalloproteinases
CT	Piglet basal diet without seaweed supplementation	MS	Mass spectrometry
CVs	Coefficients of variation	MS/MS	Tandem mass spectrometry
CXCL2	Chemokine	MUFA	Mono-unsaturated fatty acid
d	Day	NF-kB	Nuclear factor-kappaB
DAPs	Differentially abundant proteins	NO	Nitric oxide
DE	Dimensional gel electrophoresis	OA	Oleic acid
DGLA	Dihomo-γ-linolenic acid	PA	Palmitoleic acid
DHA	Docosahexaenoic acid	PCA	Principal Component Analysis
DIGE	Difference gel electrophoresis	PD	Piglet diet
DM	Dry matter	PDGF	Platelet-derived growth factor

DPA	Docosapentaenoic acid	PGs	Prostaglandins
d-ROMs	Derivatives of reactive oxygen metabolites	PIs	Prostacyclins
DTT	Dithiothreitol	PPI	Protein-protein interaction
ECL	Enhanced chemiluminescence	PSM	Peptide spectrum match
EDTA	Ethylenediaminetetra acetic acid	PTMs	Post-translational modifications
EFAs	Essential fatty acids	PUFA	Polyunsaturated fatty acids
EGF	Epithelial growth factor	PW	Post-weaning
ELISA	Enzyme-linked immunosorbent assay	ROS	Reactive oxygen species
EPA	Eicosapentaenoic acids	s	second
ESI	Electrospray ionisation	SD	Sow diet
ETA	Eicosatrienoic acid	SDA	Stearidonic acid
FA	Fatty acids	SDS	Sodium dodecyl sulfate
FAMEs	Fatty acid methyl esters	SDS-PAGE	Sodium-dodecyl Sulphate Polyacrylamide Gel Electrophoresis
FASP	Filter-aided sample preparation	SE	Standard error
FC	Fold-change	SEM	Standard error of the means
FDR	False discovery rate	SFAs	Saturated fatty acids
FGF	Fibroblast growth factor	SILAC	Stable isotope labeling with amino acids in cell culture
FRAP	Ferric reducing ability of plasma	SW	Seaweed
G	Gestation	TBARS	Thiobarbituric acid reactive substances
g	gram	TEAB	Triethylammonium bicarbonate
G:F	Gain-to-feed ratio	TFA	Trifluoroacetic acid
GEE	Generalized estimating equations	TG	Triglycerides
GLA	Gamma linolenic acid	TGF-beta	Transforming growth factor beta
GLM	General Linear Model	TIMPs	Tissue inhibitors of metalloproteinases
GO	Gene Ontology	TLR	Toll-like receptor
GSH-Px	Glutathione peroxidase activity	TMT	Tandem Mass Tag
h	Hour	TNF	Tumour necrosis factor
HCl	Hydrochloric acid	TXs	Thromboxanes
HDL	High-density lipoprotein	VEGF	Vascular endothelial growth factor
IAA	Iodoacetamide	VLDL	Very low-density proteins
IFN	Interferon	ω6:ω3	Omega 6: omega 3 ratio

Chapter 1 Introduction

The increasing demand for high-quality and safe animal products drives the production system towards sustainable development. Nutritional management focusing on lipids is widely used in animal diets as energy sources and essential FAs. Potential benefits of supplemental lipids as functional substances are obvious when animals experience management and environmental challenges [1]. This introduction considers the functional effects of essential FAs on sows' and progeny performance and changes to the proteome, the entire set of proteins present in a biological sample.

1.1 THE ROLE OF LIPIDS IN ANIMAL NUTRITION

Lipids are water-insoluble but organic-solvent-soluble molecules (except phospholipids, which are water-soluble). The chemical structure of lipids is characterized by hydrocarbon chains, of which fatty acids (FAs) and steroids are the main types [2]. Fatty acids are carboxylic acids [R-(CH2)nCOO-] with an even number of carbon atoms up to 28 [3]. Steroids are cholesterol-derived and complex lipophilic molecules [4]. In general, lipids in animals, such as swine, contain oil-liquid at room temperature and originated from vegetable sources, and fat which is solid at room temperature and originated from the animal.

1.1.1 Lipid digestion and absorption in swine

Nutrient digestion and absorption determine growth and health in swine [5]. Lipid supplementation significantly affects the sow's reproductive and milk performance, piglets' intestinal health and development [6]. Dietary lipids are firstly digested in the mouth with salivation, mastication, and liberation of lingual lipase [7]. When the digesta is transferred to the stomach, lingual lipase hydrolyzes medium- and long-chain triglycerides to free FAs [8]. At the stomach, gastric lipase continues hydrolyzing triacyl-glycerides to short-chain FAs [8]. However, the primary lipid digestion location is the small intestine, where more than 70% of triacyl-glycerides are hydrolyzed [7].

In the small intestine, lipids are digested by bile salts (formed from cholesterol in the liver and stored in the gallbladder) [9] and pancreatic lipase. Bile salts are essential for micelle formation, and pancreatic lipase hydrolyzes the triacylglycerol to generate two free FAs and a monoacylglycerol [10]. Micellar

formation starts from bile salts and phospholipids, which are released from the gallbladder [7]. Micelles have a greater affinity for polyunsaturated FAs (PUFAs) and saturated monoacylglycerols [11]. A mixed micelle increases lipids' free FAs content and absorption rate [12]. A general schematic of lipid digestion and absorption is illustrated in Figure 1-1.

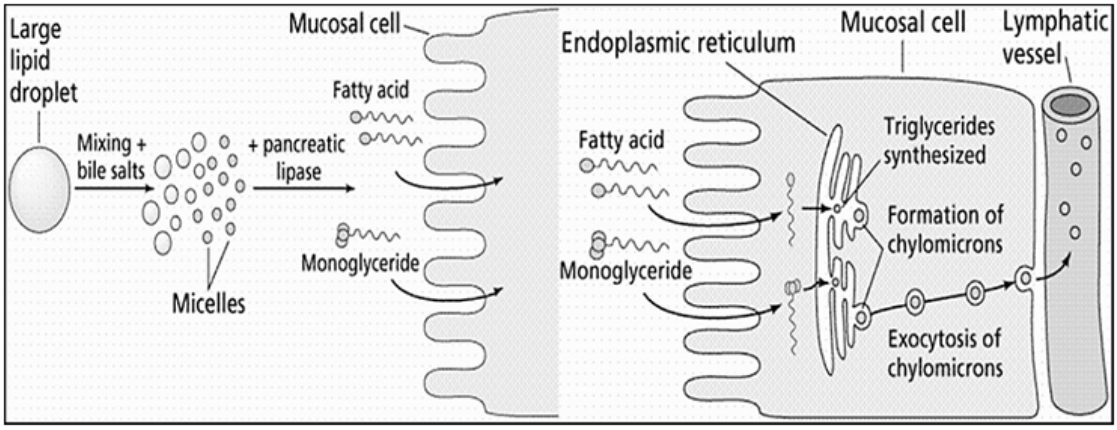

Figure 1-1 General schematic of lipid digestion and absorption [2].

1.1.2 The ω6 and ω3 fatty acids in nutrition

Fatty acids (FAs) are straight-chain carboxylic acids (with the general formula R-COOH) based on hydrogen and carbon atoms [13]. The FAs are categorized according to the number of double bonds, and whether they are saturated (no double bonds) or unsaturated (with double bonds). Fatty acids containing one double bond in the acyl chain are called monounsaturated fatty acids (MUFAs), and two or more double bond fatty acids are called PUFAs [14]. Double bonds make unsaturated FAs more chemically reactive than saturated FAs: the more double bonds that unsaturated FAs have, the more reactive they will be [15].

Based on the parent fatty acid from which PUFAs are synthesized, PUFAs comprise four groups: the ω3 family derived from α-linolenic acid (ALA, 18:3 ω3); the ω6 family derived from *cis*-linoleic acid (LA, 18:2 ω6); the ω9 family derived from oleic acid (OA, 18:1 ω9); the ω7 family derived from palmitoleic acid (PA, 16:1 ω7) [16]. Among these PUFAs, the ω3 and ω6 families are the most significant due to their role in human and other mammals' health and nutrition [15]. The ω9 and ω7 families are "non-essential FAs" because mammals can synthesize them from simple precursors [17].

ALA and LA cannot be synthesized in mammalian cells due to the lack of the Δ12 and 15-desaturase enzymes to put an unsaturated site at the ω6 or ω3 location of the fatty acid chain [18]. Consequently, they are naturally essential FAs (EFAs) and necessary components of human and animal diets [15,16]. Moreover, dietary LA and ALA are required to generate C20 and C22 ω6 and ω3 PUFAs in the membrane lipids, which are crucial for the brain's function, circulating cells including red blood cells and leukocytes and skin [15]. The PUFAs containing 20C-atoms such as dihomo-γ-linolenic acid (DGLA, C20:3 ω6), arachidonic acid (AA, C20:4 ω6), and eicosapentaenoic acids (EPA, C20:5 ω3) are converted to eicosanoid hormone-like compounds comprising prostaglandins (PGs), thromboxanes (TXs), prostacyclins (PIs), and leukotrienes (LTs) [19]. The C22 PUFAs such as docosapentaenoic acid (DPA, C22:5 ω3) and docosahexaenoic acid (DHA, 22:6 ω3) are the precursor of docosanoids such as protectins, resolvins, and maresins [20,21]. Eicosanoids and docosanoids regulate many physiological activities involving blood pressure, clotting, and lipid profiles; platelet aggregation, immune response, and inflammation response to injury and infection [15,22]. Structures of several common fatty acids found in plant and animal based-diets are illustrated in Figure 1-2.

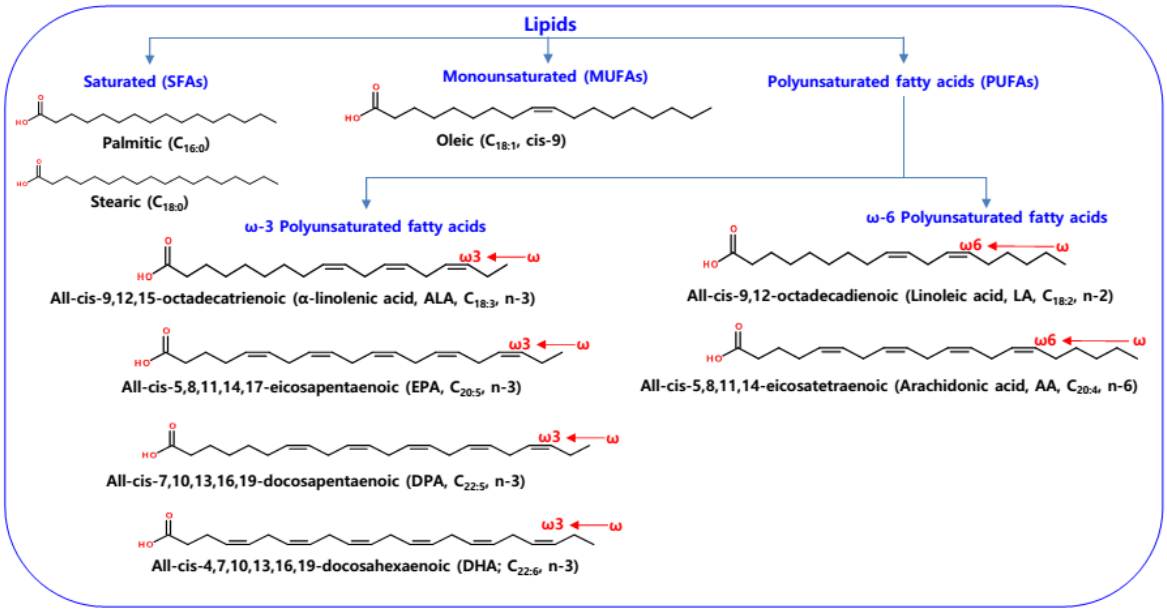

Figure 1-2 Structures of common fatty acids found in plant and animal-based diets [23].

1.1.2.1 ω6 PUFAs

The parent FA of the ω6 PUFAs is LA. LA has 18 carbon atoms and 2 unsaturated sites in which the first one is the sixth carbon from the methyl end of the FA structure. LA is broadly distributed and abundant in dietary fat and several regular vegetable oils including canola (~75%) [24], sunflower (~66%) [25], corn, perilla [26], cotton seeds (~61%) [27], and soybean (46-54%) [28]. Accordingly, human and animal consumptions of LA are far greater than that of ω3 PUFAs.

1.1.2.2 ω3 PUFAs

The parent FA of the ω3 PUFAs is ALA. ALA has 18 carbon atoms and 3 unsaturated sites in which the first one is the third carbon from the methyl end of the fatty acid chain. ALA mainly occurs in vegetable oils such as perilla (~60%), linseed (also known as flaxseed, ~55%), camelina (~38%) [29,30], canola (6-10%), soybean (5-8%) [15], genetically modified soybean (7.4-11.8%) [31], and seaweed (0.4-3.9% in brown species, 4.4% in green species and 0.2-4.3% in red species) [32]. ALA is firstly converted to stearidonic acid (SDA, 18:4 ω3) before being further transformed to EPA, DPA, and DHA. SDA is present in animal and vegetable oils, including fish (up to 4%); seeds such as blackcurrant, redcurrant, alpine currant, *Echium* [33]; and soybean. EPA (20:5 ω3), DPA (22:5 ω3) and DHA (22:6 ω3) are the available ω3 PUFAs in fish sources involving lean fish (e.g., cod), fatty fish (e.g., salmon, mackerel, sardines, and tuna) and their lipids [15].

1.1.3 Synthesis and metabolism of ω6 and ω3 PUFAs

The ω3 and ω6 FAs occur in feed sources in triglyceride form [34]. After digestion in the small intestine, these EFAs can undergo three metabolic fates, including 1) ß-oxidation to produce ATP-energy, 2) esterification into cellular lipids containing triglycerides, cholesterol esters, and phospholipids, and 3) desaturation and elongation reactions to transform into other longer unsaturated chains (Figure 1-3) [35].

A high proportion of dietary derived PUFA are ß-oxidized, including 60-85% of ALA [36], 50% of ω6 PUFA, and ~65% of DHA; thus, PUFA biosynthesis is relatively poor [37]. Therefore, dietary PUFAs are highly utilised by tissues (e.g., heart and muscle) for energy. Moreover, dietary PUFAs are recycled by tissues (e.g., brain

and liver) to provide carbon for forming saturated fatty acids, amino acids, and sterols within 5-10 minutes [37].

According to the third metabolism, the acyl chain of EFAs will be desaturated and elongated by microsomal desaturase and elongase enzymes [14,38]. In the ω6 series, linoleic acid (LA; C18:2 ω6) will be altered through γ-linolenic (C18:3 ω6) and dihomo-γ-linolenic (C20:3 ω6) to arachidonic (C20:4 ω6) and other FAs (Figure 1-4.). In the ω3 series, α-linolenic acid (ALA; C18:3 ω3) will be altered through stearidonic (C18:4 ω3), eicosatetraenoic (C20:4 ω3) and eicosapentaenoic (EPA; C20:5 ω3) to docosahexaenoic (DHA; C22:6 ω3) and other FAs (Figure 1-4) [14]. EPA is a precursor of PGs and TXs and DHA is a precursor of docosanoids [15].

The ω3 and ω6 FAs compete for identical enzymes, including fatty acyl-CoA synthetases, Δ-6 and Δ-5 desaturases, and respective elongases (ELOV) via a comparable set of reactions to biosynthesize to their long-chain PUFAs (LC-PUFAs) [1,14,39]. These enzymes have a higher affinity to ω3 FAs than that to ω6 FAs [1]. However, immoderate consumption of LA can influence these enzymes, particularly Δ-6 desaturase (FADS2), therefore decreasing the conversion of ALA to EPA and DHA [39]. Higher availability of ω3 FAs (or lower the ω6:ω3 FAs ratio) will lessen the biosynthesis of ω6 FAs to LC-PUFAs [1].

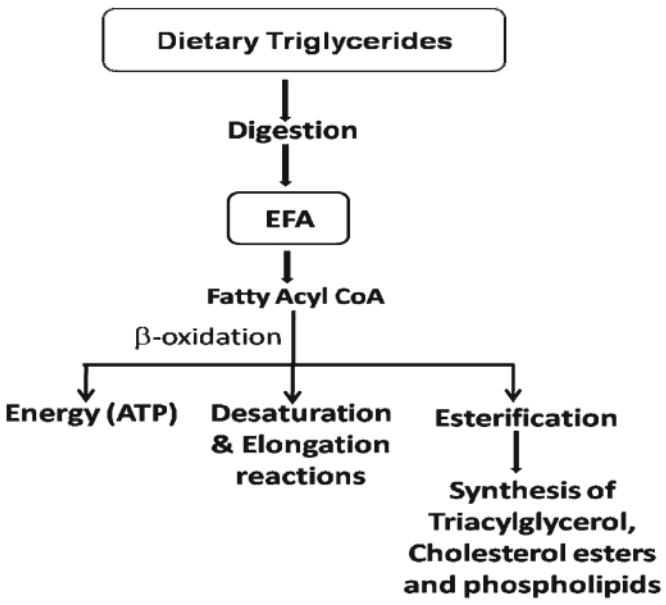

Figure 1-3 Metabolic fate of essential fatty acids (EFA) [35].

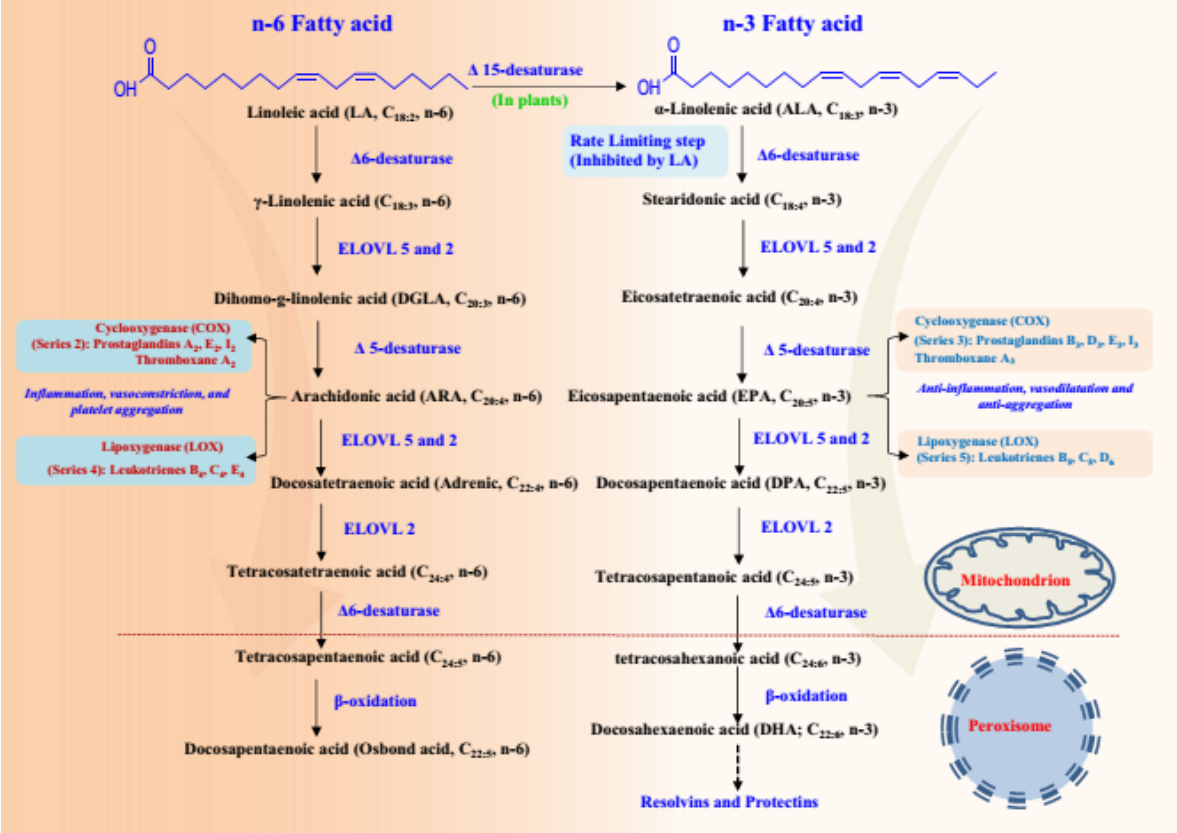

Figure 1-4 Biosynthetic pathway of very long chain ω3 and ωa6 polyunsaturated fatty acids (PUFAs) [23] (ELOVL: elongation of very long fatty acids).

1.1.4 Importance of ω6 and ω3 PUFAs balance

The wide distribution and abundance of ω6 PUFAs over ω3 PUFAs results in a dietary imbalance of ω6:ω3 PUFAs ratio [40]. This ratio varies from 15:1 [41] to 20:1 [42] in the typical Western diet. Moreover, ω3 cannot be converted to ω6 PUFAs in the animal body due to the absence of ω3 desaturase enzyme, and these two PUFAs are different in metabolic and physiological roles [41]. The ω6 PUFAs are pro-inflammatory molecules, whereas ω3 PUFAs have anti-inflammatory properties and thus help maintain homeostasis and health [43]. Therefore, the balance of ω6:ω3 PUFAs ratio is important for good health and normal development [44]. High dietary ω6:ω3 PUFAs ratios can increase inflammation by promoting the production of pro-inflammatory cytokines, e.g., tumour necrosis factor-alpha (TNF-α), interleukin-1 (IL-1), and interleukin-6 (IL-6) [41,45], and are associated with many health problems such as cardiovascular disease, diabetes, cancer, obesity, autoimmune diseases, rheumatoid arthritis, asthma and depression [41,46]. Consequently, ω6:ω3 PUFA ratios should be reduced to near 4:1 – 1:1 [40] for optimal performance, immunity, and health benefits [41,44].

1.1.5 The balance of ω6 and ω3 PUFAs during lactation in sows

An overview of the balance of ω6 and ω3 PUFAs (or EFAs) during lactation is presented in Figure 1-5 [1]. A negative balance (intake minus milk output) of LA and ALA is pronounced throughout lactation due to over EFAs secretion in milk compared to the daily consumption, resulting in tissue mobilization. The balance of EFAs throughout lactation is the difference between the inflow (intake minus FAs not absorbed) and the outflow of EFAs [1]. EFAs can be absorbed through body tissues such as adipose tissue, cell membranes, synthesized to other LC-PUFAs or bioactive compounds, and energy oxidation. However, the mammary gland takes the substantial EFAs and is secreted into milk [47]. Therefore, assessment of EFAs balance during lactation is essential to provide more accurate estimates of the requirements for EFAs and support the reproductive performance of sows. The recommended minimum LA of 100 g/d should be provided to the sows to maintain the EFAs balance during lactation, but no requirement for ALA is suggested [1].

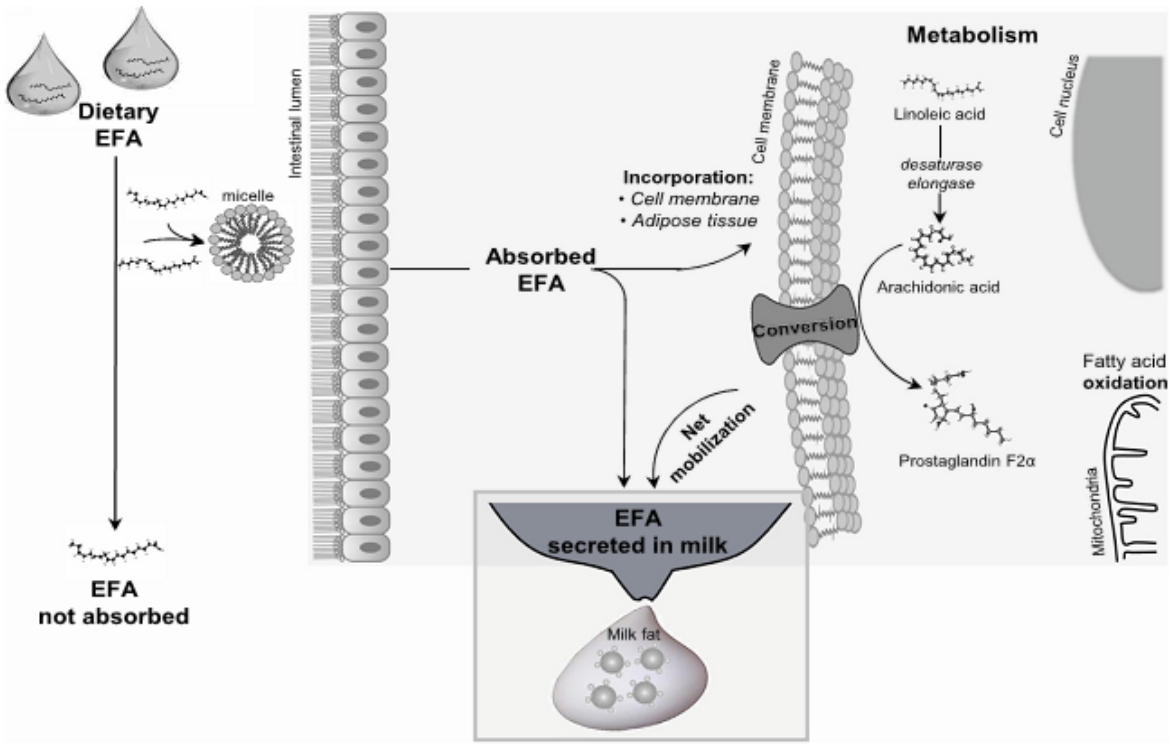

Figure 1-5 Simplified overview of the source, partitioning, and net balance of essential fatty acids (EFAs) during lactation of sows. After absorbed into the body, fatty acids can be deposited into tissues (e.g., adipose tissue, cell membranes), elongated to long chain PUFA, biosynthesized to active metabolites, or oxidized for energy. The substantial amount of absorbed EFA is anticipated to be extracted by the mammary gland and secreted in milk [1].

1.1.6 The role of ω6 and ω3 PUFAs in the sow and litter performance

Swine use dietary lipids as energy and EFAs sources. Many studies have been performed to assess the effect of dietary lipids on the lactating sow and progeny over the last 30 years; however, the results are still conflicting [1]. Therefore, we need more research to clarify the benefit of including lipids, especially EFAs, in swine diets on their performance [1].

EFAs are significant components of all cell membranes, influencing membrane-fluidity and membrane-bound enzymes and receptors [16]. LC-PUFAs, particularly DHA and AA, play an essential role in fetal growth and development [39,44]. The embryo and infant can convert LA to AA and ALA to DHA [48], but their synthesis rate is inadequate [18]. Therefore, the LC-PUFA source of the embryo entirely depends on maternal circulation through the placenta [18] and the infant depends on uptake of LC-PUFAs from its mother's milk or diet.

Moreover, the ω6 PUFAs positively regulate all wound healing phases (Figure 1-6) [49]. Studies on healthy humans, mice, and zebrafish showed that LA could promote wound healing by maintaining hydration and elasticity during the inflammatory phase of tissue repair [49]. Conjugated LA (CLA) expressed antioxidant and anti-inflammatory effects on the later inflammatory phase of tissue repair in healthy mice and dogs. GLA (gamma-linolenic acid) positively influences inflammation control in healthy humans. AA and its metabolites stimulate cell migration and angiogenesis, improving wound healing in pigs [49]. However, the mechanisms associated with these processes need to be clarified [49]. The effects of LA, CLA, GLA, and AA on wound healing phases are presented in Figure 1-6 and Figure 1-7.

1.1.7 ω6, ω3 PUFAs and cytokine regulation during pregnancy

Pregnancy contains three phases distinguished by many pro- and anti-inflammatory compounds [50]. In the first phase of gestation, pro-inflammatory compounds, e.g., cytokines, are increasingly synthesized for fetus recognition, successful implantation, and synchronized maternal – embryonic dialogue [50]. During this phase, fetus implantation involves the actions of some cytokines, e.g., interleukins (IL), leukemia inhibitory factor (LIF), interferon (IFN)-γ, tumour

necrosis factor (TNF)-α, and migration inhibitory factor (MIF) [51]. In the second phase of gestation, a high concentration of anti-inflammatory compounds is needed for uterine quiescence and embryo development. The last stage of gestation observed an increasing concentration of IL-1β and IL-8 [52].

Metabolism of ω6 PUFAs produces pro-inflammatory compounds, and ω3 PUFAs metabolism creates anti-inflammatory compounds, although they share the same synthesizing enzymes [51]. The ω3 PUFAs against inflammation by preventing the formation of nuclear factor-kappaB (NF-kB), which perform transcription for pro-inflammatory cytokines, e.g., TNF-α (tumour necrosis factor), and IL (interleukin) [53]. Moreover, the gene expression of IL-6 and IL-1β can be lowered by ω3 PUFAs [54]. Cell culture studies showed that the anti-inflammatory effect of ω3 PUFAs refers to macrophage, endothelial cells regulation [55], and monocyte immune modulation [56].

During pregnancy, ω3 PUFAs prolong gestation length by interfering with pro-inflammatory cytokine expression and activities in the uterus and reducing the production of prostaglandins [51]. Consequently, the weight of infants at birth increases. Nevertheless, the influence of ω3 PUFAs at each phase of pregnancy on its establishment and outcome is still unknown [51].

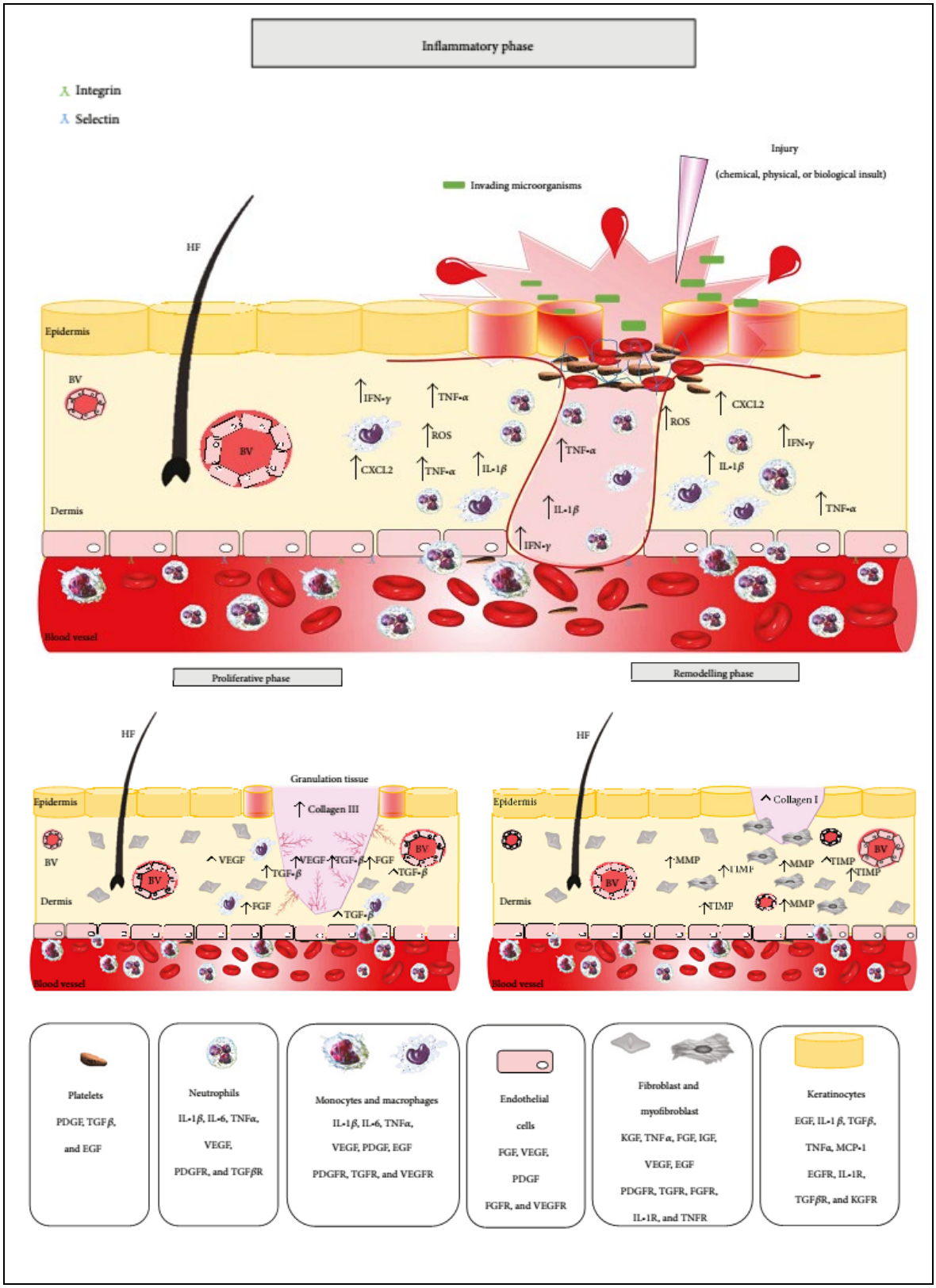

Figure 1-6 Wound healing process [49], including three stages: the inflammatory, proliferative, and remodelling. Early phases of wound healing involve coagulation and activation of inflammatory cells. The proliferative phase includes proliferation offibroblasts and angiogenesis. The remodelling stage involves restoration of the barrier and contraction of the wound by myofibroblasts. The procedure is coordinated by immune cells and growth factors and cytokines and chemokines as followings: HF = hair follicle; BV = blood vessels; TNF = tumour necrosis factor; IL-1beta = interleucina 1beta; IL-6 = interleucina 6; ROS = reactive oxygen species; CXCL2 = chemokine (C-X-C motif) ligand 2; IFN-gamma = interferon-gamma; VEGF = vascular endothelial growth factor; TGF-beta = transforming growth factor beta; FGF = fibroblast growth factor; KGF = keratinocyte growth factor; MCP1 = monocyte chemoattractant protein-1; IGF = insulin growth factor; TIMPs = tissue inhibitors of metalloproteinases; MMPs = matrix metalloproteinases; PDGF = platelet-derived growth factor; EGF = epithelial growth factor.

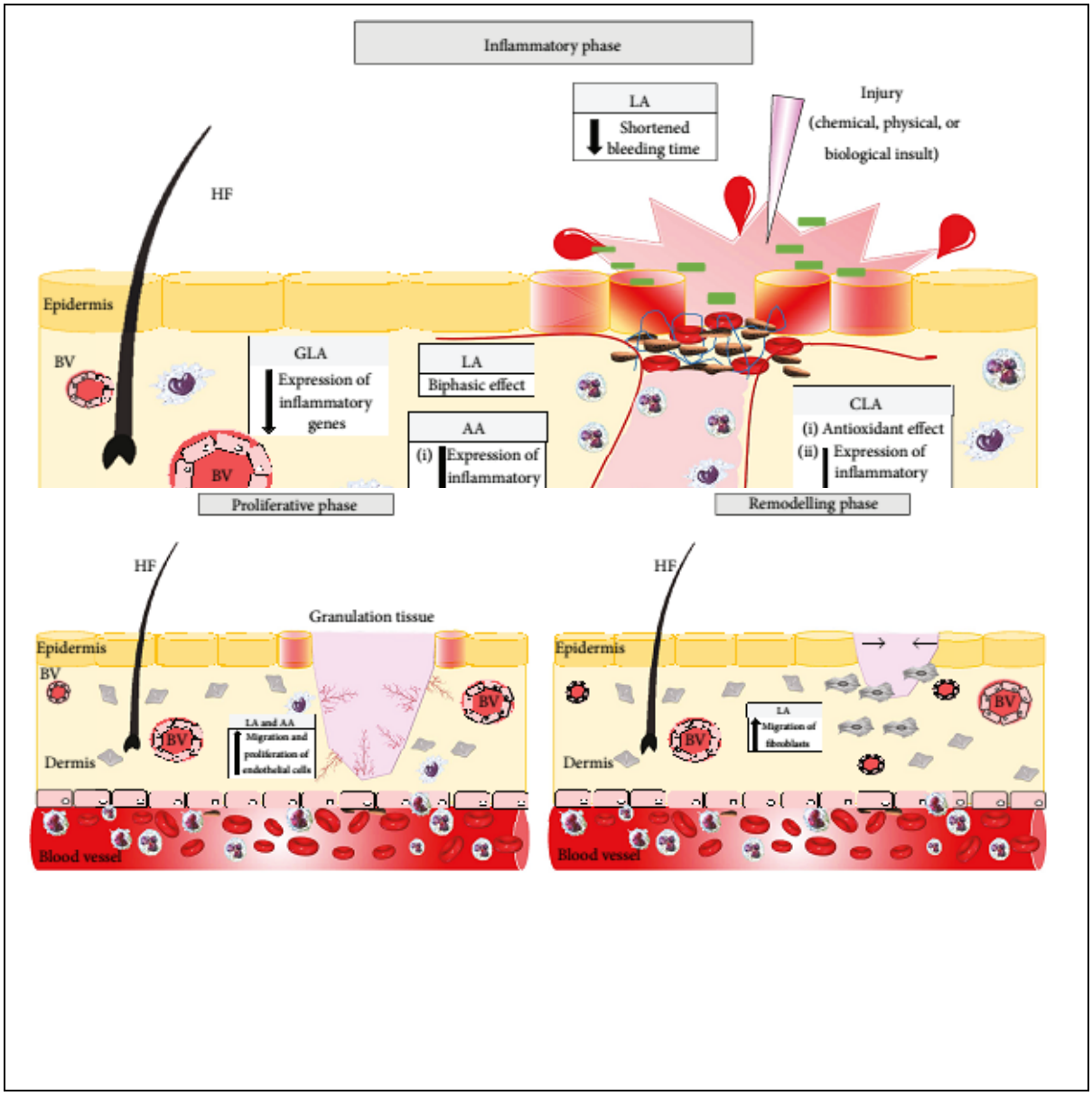

Figure 1-7 Effects of linoleic acid (LA), conjugated linoleic acid (CLA), gamma linolenic acid (GLA), and arachidonic acid on wound healing phases [49].

1.2 PROTEOMICS-BASED APPROACH IN SWINE STUDIES

Proteomics is the study of the proteome – entire protein complement present in a biological sample under a specific set of environmental and physiological conditions; these conditions change result in altered protein expressions [57]. Proteomics technologies provide valuable insights into the dynamic and complex processes influencing animal biology [58]. Besides discovering protein's expression and cellular functions, proteomics can identify their interactions, cellular localization, post-translational modifications (PTMs), and turnover [59]. PTMs such as acetylation, methylation, glycosylation, and phosphorylation regulate protein

activity, stability, localization, and function, and are involved in critical intracellular signalling pathways [60].

1.2.1 Background on proteomics technologies and workflows

The development of proteomics technologies is associated with updated methods for peptide/protein separation, isotope labelling for quantification, and bioinformatic data analysis with mass spectrometry is the core tool [61]. There are three main proteomics approaches, with details presented in Figure 1-8 and explained below.

Firstly, the bottom-up proteomics strategy analyses short peptides released from complete proteolytic digestion of protein [62]. The bottom-up analysis is called shotgun proteomics when a protein mixture is measured indirectly through proteolytic peptides [61]. In a shotgun proteomics study, the peptide mixture is fractionated into multiple samples according to their charge, size, polarity, or hydrophobicity, separated using liquid chromatography (LC), and subjected to MS/MS (tandem mass spectrometry) analysis [63]. The tandem mass spectra from peptide fragmentation are compared to the theoretical best match from a protein database to identify peptides [61]. Then, peptide sequences are mapped to proteins, noticing that peptides can be unique to a single protein or shared by >1 protein [61,64]. Relative differences in protein can be quantified (based on the relative changes in abundance across samples) or measured absolutely (absolute concentration of a protein in a sample) [63,64]. However, absolute quantification is only suitable for measurement of selected proteins of interest because it requires expensive spiked-in standards [65].

Similar to bottom-up analysis in the proteolysis step, the middle-down strategy generates longer proteolytic peptides; hence, more unique peptides are generated and better sequence coverage is achieved [62]. Consequently, this approach enhances the number of detected PTMs and proteoforms (intact protein forms) [62]. Middle-down proteomics reflects the actual protein level in the biological samples better than the bottom-up method because it reduces shared peptides and the effect of protein degradation and the completeness of proteolytic digestion [61].

Thirdly, the 'top-down' approach measures intact proteins [64], representing advantages for PTMs and protein isoform determination [61]. Nevertheless, the top-down approach is more challenging than bottom-up proteomics in protein fractionation, protein ionization, and fragmentation in the gas phase [61,66]. Higher and more diverse charge states of intact proteins reduce the signal-to-noise ratio, increase error-prone to proteoform identifications, and mislocalize PTMs [66].

In proteomic analysis, different protein separation techniques are applied. Gel-based techniques include 2-DE (dimensional gel electrophoresis), DIGE (difference gel electrophoresis), and 1-DE [62]. The most common gel-free technique is Liquid Chromatography (LC) [62,67]. 2-DE separates proteins according to their isoelectric point and molecular weight and generates a complex proteome map with numerous protein 'spots' [68]. DIGE is an advanced 2-DE technique where proteins are fluorescent-labeled with Cy-dyes, and an internal standard (the pooled represents all samples) is used between multiplexes; thus, saving gels and reducing experimental variation [69]. The main disadvantage of the 2-DE technique is the masking by high-abundance proteins of low-abundance proteins and poor separation of acidic, basic, and hydrophobic ones [70]. LC is the high-performance separation technique for proteolytic peptides or intact proteins, based on the mobile phase (solvents) and stationary phase [62].

In current shotgun proteomic workflows, isotope labeling methods are selected to improve quantitative accuracy and avoid false-positive protein changes resulting from co-eluting high-abundant peptides, such as SILAC (stable isotope labeling with amino acids in cell culture), iTRAQ (isobaric tag for relative and absolute quantitation), and TMT (tandem mass tag) [69]. In iTRAQ and TMT, the peptides are labeled after digestion and are maintained in their equal mass to charge (m/z) ratios after labeling (in the MS1 spectrum) [63]. Upon fragmentation (MS/MS), the isobaric tags break and release different reporter ions with unique mass depending on their condition and provide relative protein abundance between samples [71].

After the digestion, samples are subjected to mass spectrometry (MS) analysis for protein/peptide sequences identification [72]. Mass spectrometers contain ion sources, the mass analyser, and an ion detection system [70]. MS analysis involves three main phases: 1) protein ionization and generation of gas-phase ions, 2) ion

separation based on their *m*/*z* ratios, and 3) ion detection [73]. Next, the identified peptide sequences are re(mapped) to their originated proteins of origin [74]. MS/MS combines two different MS analyses in which each tryptic peptide is fragmented after a liquid phase separation [70]. Overall, MS technologies provide an accurate, high throughput, and robust proteome characterization in biological samples [75].

The final step is protein identification and validation, where MS/MS spectra are assigned to predicted fragment ion masses derived from a protein sequence database, using searching algorithms [70]. SEQUEST is a search engine that correlates observed MS/MS spectral data of peptides with known amino acid sequences in a database [76]. Another common search algorithm is Mascot which generates a probability-based score by assessing the chances that a particular fragment is associated with the observed spectrum, integrating mass spectra with protein sequence information, the molecular weight of tryptic peptides, and MS/MS data [77]. Peptide sequences are identified individually before inferring a set of peptide sequences to a protein based on their uniqueness [78].

Proteomics findings are usually validated using additional assays to support data in expression or differential abundance of proteins between two treatments at measurably different levels [79]. This confirmation step significantly improves data quality but should be considered carefully because it requires more resources, time, and potential failure of experiments [79]. The most common validation approaches are western blots and enzyme-linked immunosorbent assay (ELISA).

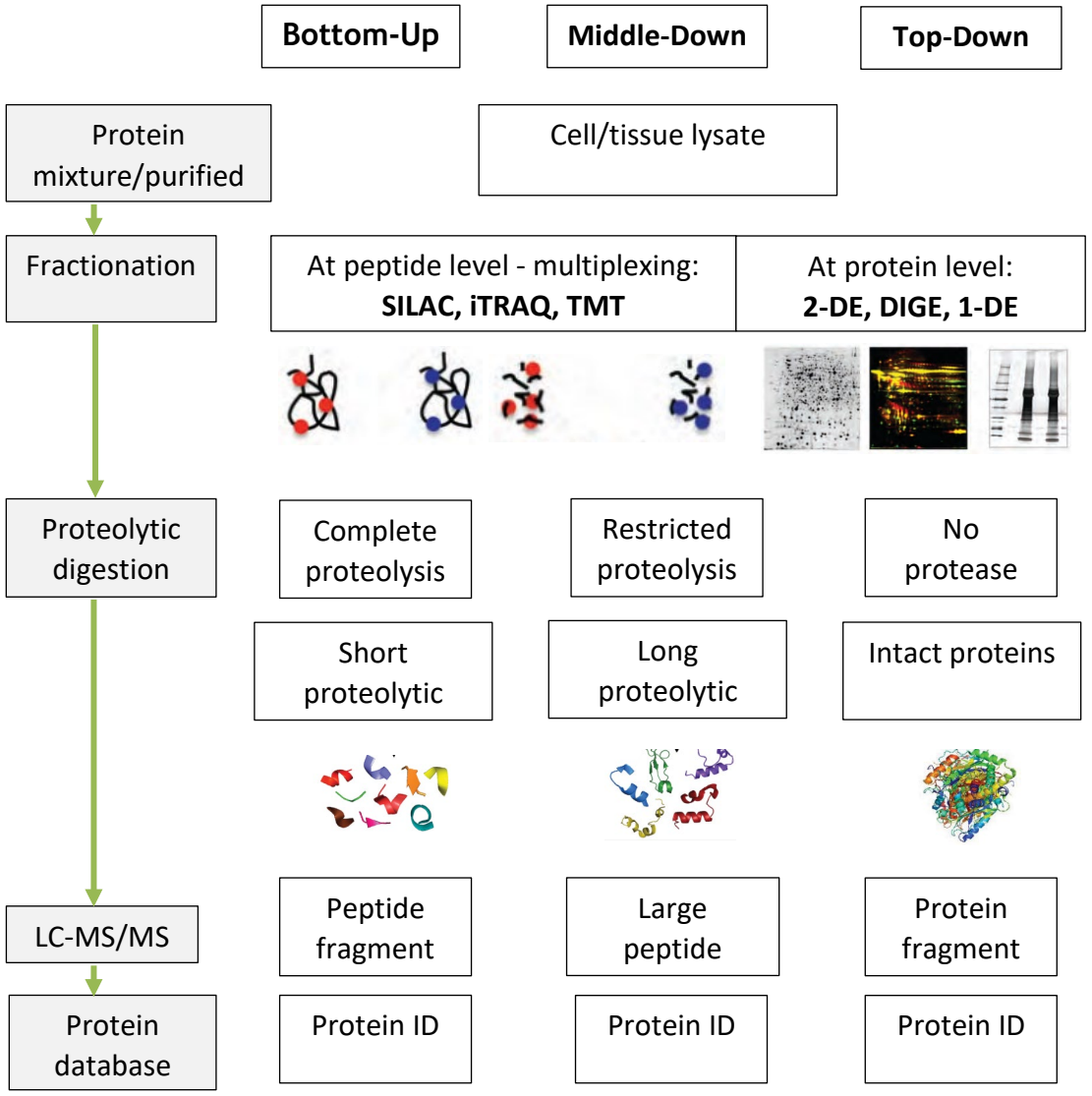

Figure 1-8 Proteomics approaches: bottom-up, middle-down, and top-down. The bottom-up strategy measures short proteolytic peptides produced from complete digestion (typically by trypsin). The middle-down method analyses longer peptides released from restricted digestion or more selective proteases. The top-down approach analyses the intact proteins. In three approaches, protein extracts were fractionated at the protein level (before proteolytic digestion) or at the peptide level (after proteolytic digestion). Labeling was performed in culture by incorporation of heavy or light amino acids (SILAC – stable isotope labeling with amino acids in cell culture) or at the peptide level (iTRAQ – isobaric tag for relative and absolute quantitation or TMT-tandem mass tag). In DIGE (difference gel electrophoresis), protein extracts are labeled with different fluorescent dyes before they are separated by 2-DE (dimensional gel electrophoresis). LC-MS/MS: Liquid chromatography – Tandem mass spectrometry. (Modified from [61,62,69]).

1.2.2 Proteomics studies in sows and piglets

Proteomic studies in swine have been developed rapidly and widely in recent years, covering various topics [80–82].

Several studies have focused on proteome changes in the sow, especially in the pregnancy stage. Specifically, protein alteration in the uterine endometrium during pregnancy (days 12, 40, 70, and 93) was compared to the non-pregnancy condition [83,84]. Quantitative proteomic analysis using two-dimensional differential gel electrophoresis (2D-DIGE) revealed the upregulation of a pregnancy-dependent protein profile, i.e., serpins, cofilin, annexin A2 related to uterine preparation pathways for embryo implantation (day 12), i.e., calcium signalling, angiogenesis, leukocyte migration, and cell movement [83], cell adhesion and cytoskeletal organization [85]. At later stages of pregnancy, development-, cytoskeleton- and chaperon-related proteins, i.e., transferrin, galectin-1, heat shock protein (HSP) 27 and HSP 90b, were changed in abundance, and participated in the regulation of endometrium function and development and maintaining pregnancy [84].

The 2D-DIGE procedure disclosed aldolase, fatty acid-binding proteins, and lipogenic enzyme regulation in subcutaneous adipose tissue of fetuses carried by sows of either pure and crossbred Large White or Meishan during late gestation (days 90 and 110) [86]. The label-free LC/MS shotgun proteomics approach discovered altered mammary tissue proteins associated with the fatty acid synthesis of sows supplemented with valine from day 75 of gestation until farrowing [87]. TMT-based quantitative proteomic analysis revealed the influence of different housing systems on the colostrum composition of pregnant sows via affecting their immune system and fat metabolism processes [88]. However, inadequate attention was given to the lactation stage in the sow.

Pregnant and lactating sows' nutrition and metabolism significantly affect piglets' survival, growth, and health by reprogramming sows and their offspring's proteome. An iTRAQ coupled with 2D LC-MS/MS analysis revealed that maternal obesity (with high backfat thickness, ≥ 23 mm) substantially reduced placental efficiency and increased sow's plasma and placental levels of proinflammatory cytokines and triglyceride, resulting in decreased placental total antioxidant

capacity [89]. Excessive backfat in sows is related to placental abnormal carbohydrate and lipid metabolism, mitochondrial dysfunction, and elevated oxidative stress and inflammation [89].

A 2D-DIGE based study demonstrated that a maternal low protein diet upregulated newborn offspring's subcutaneous adipose tissue proteins associated with glucose and FA metabolisms, lipid transport, and apoptosis regulation while maternal high protein diet upregulated proteins in new-born offspring (i.e., transaldolase, annexin II, and apolipoprotein A4) related to amino acid metabolism and protein turnover [90]. Piglets from the same trial were fed high protein diet from day 2 to 28 before weaning, expressed adipose tissue protein alterations associated with signal transduction (annexin 2), redox status (peroxiredoxin 6, glutathione S-transferase omega 1, cyclophilin-A), carbohydrate metabolism (ribose-5-phosphate dehydrogenase, lactate dehydrogenase), amino acid metabolism (glutamate dehydrogenase 1) and cell cytoskeleton dynamics (dynactin and cofilin-1) [91].

Shotgun proteomics analysis on days 4 and 7 postnatal milk in gestating and lactating sows supplemented with oat and yeast culture (as prebiotic + probiotic sources) benefitted piglets via upregulating milk-related immune and antimicrobial proteins such as lactoferrin and chitinase [92]. In addition, the TMT approach uncovered the testicular proteome changes of male offspring born from mother-fed fibre during pregnancy [93]. The testicular proteome is related to starch and sucrose metabolism pathways, FA, glutathione, and the renin-angiotensin system [93].

1.3 PREVIOUS STUDIES SHOWING Ω6:Ω3 RATIOS EFFECTS ON THE SOW'S AND PIGLET'S PERFORMANCE AND PROTEOME

Several studies have been performed to investigate the effect of different ω6:ω3 ratios on sow and piglet performances, lipid metabolism, immune response, gene expression, and transcriptome.

Different ratios of ω6:ω3 PUFAs can affect sow performance and their suckling piglets [94,95]. Changing the dietary ratio of ω6:ω3 PUFAs in lactating sows from

13:1 to 9:1 and 3:1 has influenced the sow's (plasma, colostrum, milk) and her litter's performance, fatty acid composition; immune and inflammatory response comprising immunoglobulin and cytokines, respectively [94]. In addition, reducing ω6:ω3 PUFAs ratio in gestation-lactation sow diets from 20:1 to 10:1 can improve reproductive performance by decreasing sow body weight loss after farrowing to weaning [95].

Several studies have been published on the effect of altering dietary PUFAs on lipid metabolism and inflammatory and immune response [96–100]. The ω6:ω3 PUFAs ratios of 1:1 and 5:1 influenced lipid metabolism and inflammation, providing more energy and nutrients for high performance and homeostatic pathways [99]. Furthermore, feeding PUFAs diets (2% fish oil) to the gestating and lactating sows activated their antioxidant defense procedure against oxidative stress, and this mechanism was transferred to their piglets [101].

Increased dietary intake of ω3 PUFAs resulted in reducing the ratio of ω6:ω3 PUFAs in the liver, regulating gene expression and influencing a group of genes that relate to energy metabolism, signalling pathways, inflammation, and immune response [102]. Altering ω6:ω3 PUFAs ratio affected the transcriptomic profile of the pig liver and their health status [102]. Lowering ω6:ω3 ratio by adding 0.5% ω3 PUFAs in male pig diet alleviates the immunosuppression and oxidative stress by decreasing the expression of tumour necrosis factor (TNF)-α, nuclear factor (NF)-κB, interferon (IFN)-γ, and interleukin (IL)-8, alleviating the activities of liver injury markers, and modulated serum oxidative stress markers [103]. Moreover, increasing dietary fat content (30 g/kg higher than control diet) by high PUFAs (ω6:ω3 ratio is 5.2) for gestating sows does not influence their reproduction or gene expression in their blood or the liver and blood of their progeny [104].

In general, although several results have been published, the actual requirements of ω6 and ω3 PUFAs in sow diets and the ideal ratio of these two PUFAs are still debated. Additionally, no proteome studies have linked the effects of different ω6:ω3 ratios with sow and their offspring developments.

1.4 BROWN SEAWEED AND PIGLET DEVELOPMENT

1.4.1 Introduction of brown seaweed

Weaning piglets are susceptible to numerous stressors, including separating from the sow, mixing with other piglets, dietary and environmental changes [105]. These changes modify gut microflora, and piglets are easily infected with enteric pathogens [106], thus, reducing feed consumption and daily gain [107]. In recent years, controlling these problems by using alternatives to in-feed antibiotics such as macroalgae (also known as seaweeds) [108] or probiotic feed additives such as microalgae [109,110] has been commonly performed.

Several studies stated that seaweeds and their products could be substituted for antibiotics to improve animal performance and reduce pathogenic bacteria [111]. Seaweeds are the source of bioactive constituents that produce many secondary substances with a broad spectrum of biological activities [112]. Furthermore, they are rich sources of minerals, e.g., Ca, P, Na, K, and vitamins, e.g., A, B_1, B_{12}, C, D, E, riboflavin, niacin, pantothenic acid, and folic acid [113]. Seaweeds are categorized into green, brown, and red algae based on their pigment [112].

Brown seaweeds are an excellent source of iodine and soluble fiber and, thus, are a source of prebiotics that can be used to maintain the equilibrium of intestinal flora [112]. Moreover, brown species contain many polysaccharides such as laminarin, fucoidan, and alginic acid [114]. Laminarin is a group of water-soluble and low molecular weight ß-glucans, a substrate for bifidobacteria and *Lactobacilli* spp. [115]; thereby enhancing growth performance, feed intake, and feed conversion ratio in nursery pigs [116]. Moreover, ß-glucans have antibacterial activity and can trigger cytokine release, e.g., tumour necrosis factor (TNF)-α from macrophages [117]. The second polysaccharide family in brown seaweeds, fucoidans, has profound biological activities [118], including antitumour [119], antiviral [120], and antibacterial features [121]. Besides that, polysaccharides have beneficial effects on inflammation and immune systems by protecting cells from viral infection [112]. Brown algae also contain a high level of phlorotannin, a phenolic compound with strong antioxidant, anti-inflammatory, antiviral, antimicrobial, anti-tumour, and anti-cancer activities [122].

In recent years, many studies focused on the brown seaweed *Laminaria sp.*; however, very little data are published on the effect of brown seaweed *Ascophyllum nodosum (A. nodosum)* [123]. *A. nodosum* is a common species of the Fucaceae family that occurs in the North Atlantic Ocean [123,124]. Like other brown seaweed species, *A. nodosum* is an excellent source of bioactive compounds. These algae species can contain up to 70% of total polysaccharides on a dry matter basis that could act as prebiotics to enhance gastro-intestinal microflora health status and other health-promoting bioactivities [32].

1.4.2 Previous studies showing brown seaweeds effects on piglet performance, health, and proteome

Several studies have been performed to examine the effect of diet containing *A. nodosum* products on animal performance and health status.

Dietary addition of extract of *A. nodosum* on weaned piglets shows several beneficial influences on growth performance (e.g., average daily gain (ADG), final weight, average daily feed intake (ADFI)) but no effect on immune response to challenge with *Salmonella typhimurium* [125]. Dietary inclusion of 500 and 1000 ppm *A. nodosum* extract for ten-day-old chicks remarkably decreased caecal *Campylobacter jejuni* (a zoonotic microorganism) level but also decreased growth parameters [126]. Therefore, further studies are required to investigate the exact composition and timing of administration of the extract to support the growth and health status of the chicks [126]. An e*x-vivo* study in the porcine colonic tissue challenged with lipopolysaccharide showed the immunomodulatory and anti-inflammatory bioactivities of *A. nodosum* extract [127]. Nevertheless, these effects need further investigation in the mammalian intestine [127].

Feeding dried intact *A. nodosum* (10 and 20 g/kg) for weaned piglets can improve their gastro-intestinal health and positively affect piglet performance [128]. However, the dietary inclusion of 2.5, 5.0, or 10.0 g/kg dried intact *A. nodosum* did not improve performances nor some gut health parameters and plasma oxidative status of weaned piglets [123]. This result can be explained by the additional level of *A. nodosum* being too low for a prebiotic influence or a masking influence of some available bioactive constituents.

To our knowledge, despite the high content in bioactive compounds, little and inconsistent information is published about the effect of *A. nodosum* seaweed supplementation on the health status of weaning piglets. Moreover, no previous research had combined the mother diet's effect to emphasize better the potential impact of *A. nosodum* on piglets' overall health status and proteome profile.

1.5 CONCLUSIONS, AIM, AND OUTLINE OF THIS THESIS

Polyunsaturated fatty acids (PUFAs) are beneficial bioactive compounds for animal health. The ratio of ω6:ω3 PUFAs can affect many biological processes and metabolic homeostasis [102], such as modulating immune-cell function [129]. The ω6 PUFAs are the precursors of multiple pro-inflammatory molecules, including prostaglandins, leukotrienes, and related compounds. The ω3 PUFAs are anti-inflammatory and immunomodulatory compounds [129] thus, they are beneficial for reproduction, including fetal growth and development [101].

Although several studies investigated the effect of dietary ω6:ω3 PUFAs on sow performance and their piglets, the actual requirements and optimal ratio of ω6:ω3 PUFA ratio in the diet of gestating and lactating sows is still debated, and previous studies did not exploit -omics techniques. Additionally, there are few publications on the effects of seaweed administration on postweaning piglets, and none of them examined prior dietary treatments on sows during gestation and lactation.

The research described in this thesis is project 01 "ω6/ω3 Fatty acid (FA) ratio effect on piglet microbiome and immunity", a collaborative project between Università degli Studi di Milano (Department of Health, Animal Science and Food Safety "Carlo Cantoni" (VESPA)) and University of Glasgow (College of Veterinary, Medical and Life sciences, School of Veterinary Medicine). This project is supported by the European Unions' Horizon 2020 research and innovation program H2020-MSCA-ITN-2017-EJD under the Marie Skłodowska-Curie Innovative Training Networks (European Joint Doctorate in Molecular Animal Nutrition, MANNA), grant agreement No 765423.

The project's overall aim was to improve growth performance and immunity of piglets that received seaweed (SW) supplementation and were born from mothers

fed low dietary ratio (LR) of ω6:ω3 PUFAs, by modulating their proteome profile. In this thesis, the focus was on an advanced understanding of the underlying mechanisms for the role of maternal dietary LR on sow's and piglet's performances and oxidative status, concerning proteomics alterations in sow plasma, piglet serum, and piglet ileum. The choice of omega 6:3 ratio (13:1 as the control and 4:1 as the low ratio) was based on previous literature. Brown seaweed was considered in EU feed legislation as feed materials not requiring any registration as feed additives (Regulation UE 2017/1017).

First, the effects of LR in sow diet and SW supplement in piglet diet on performance, colostrum and milk FA profiles, and oxidative status, were revealed (Chapter 2). These zootechnical studies assessed the combined effect of LR in sow diets and SW supplementation in piglet diets on piglets' growth and oxidative status. Furthermore, the influence of maternal LR diet on reproduction, milk FA profile, oxidative status, and plasma leptin concentration was discovered. The molecular mechanism of the interaction between dietary treatments in sows and piglets remains to be addressed. The effects of nutritional interventions on molecular outcomes in sows and their progeny were studied.

An extensive proteomics study in the plasma of sows (Chapter 3) was conducted to examine the protein expression alteration following the long-term decrease in dietary ω6:ω3 ratio during gestation and lactation periods. To better understand the interplay between maternal and offspring nutritional interventions, and identify whether maternal LR diet and progeny SW diet can boost progeny immunity and performance, altered serum and ileal proteomes in post-weaned piglets were studied in detail (Chapter 4 and 5). Lastly, the findings of this thesis were summarized and discussed in Chapter 6.

Chapter 2 Performance, Milk Fatty Acid Profiles, and Oxidative Status

Animals 2020, 10, 2049. https://doi.org/10.3390/ani10112049.

Thi Xuan Nguyen[1,2]
Alessandro Agazzi[1]
Marcello Comi[3]
Valentino Bontempo[1]
Invernizzi Guido[1]
Sara Panseri[1]
Helga Sauerwein[4]
Peter David Eckersall[2]
Richard Burchmore[2]
Giovanni Savoini[1]

[1] Department of Health, Animal Science and Food Safety 'Carlo Cantoni' (VESPA), Università degli Studi di Milano, Via dell' Università 6, 26900 Lodi, Italy

[2] College of Medical, Veterinary and Life Sciences, School of Veterinary Medicine, University of Glasgow, Garscube Estate, Switchback Road, Bearsden G61 1QH, UK

[3] Department of Human Science and Quality of Life Promotion, Università Telematica San Raffaele Roma, Via di Val Cannuta 247, 00166 Rome, Italy

[4] Institute of Animal Science, Physiology and Hygiene Unit, University of Bonn, 53115 Bonn, Germany

Thi Xuan Nguyen contribution: methodology, software, validation, formal analysis, investigation, data curation, writing—original draft preparation, visualization, writing—review and editing, corresponding author.

Other contributions: Conceptualization, A.A., V.B. and G.S.; methodology, A.A., G.S., S.P., H.S., G.I.; software, A.A.; validation, A.A.; formal analysis, A.A.; investigation, A.A., M.C., and G.I.; resources, A.A., M.C., V.B., G.S., S.P., and H.S.; data curation, A.A., and M.C.; writing—review and editing, G.S., A.A., H.S., D.E., R.B.; supervision, G.S., A.A., R.B., D.E.; project administration, G.S. and A.A.; funding acquisition, G.S.; all authors approved the final version to be submitted.

2.1 SUMMARY

Feeding maternal animals divergent ratios of omega-6 (ω6) and omega-3 (ω3) fatty acids can change not only their health, physiological condition, and performance but also do the same for their offspring. In swine production, various ω6:ω3 ratios have been tested, but the search for an optimal proportion in the sow diet is still in progress. For piglets, weaning oxidative stress has been alleviated by supplementing with abundant sources of bioactive compounds. In this case, brown seaweed, a rich source of natural antimicrobials and antioxidants, can be a good candidate, but studies on its supplementation in piglet diet is limited. This study explores the hypothesis that feeding a low ω6:ω3 ratio diet to sows during gestation and lactation, together with the supplementation of *Ascophyllum nodosum* for piglets during the post-weaning period, could benefit piglets' performance and oxidative status more than the respective single treatment provided to the mother or the piglet. Results showed that the low dietary ω6:ω3 ratio (4:1) and seaweed supplement did not affect the post-weaning piglets' growth rate and oxidative status. However, a low ω6:ω3 ratio diet alone improved weaning survival rate, suckling piglets' weight gain, and total ω3 fatty acids in colostrum and milk.

2.2 GRAPHICAL ABSTRACT

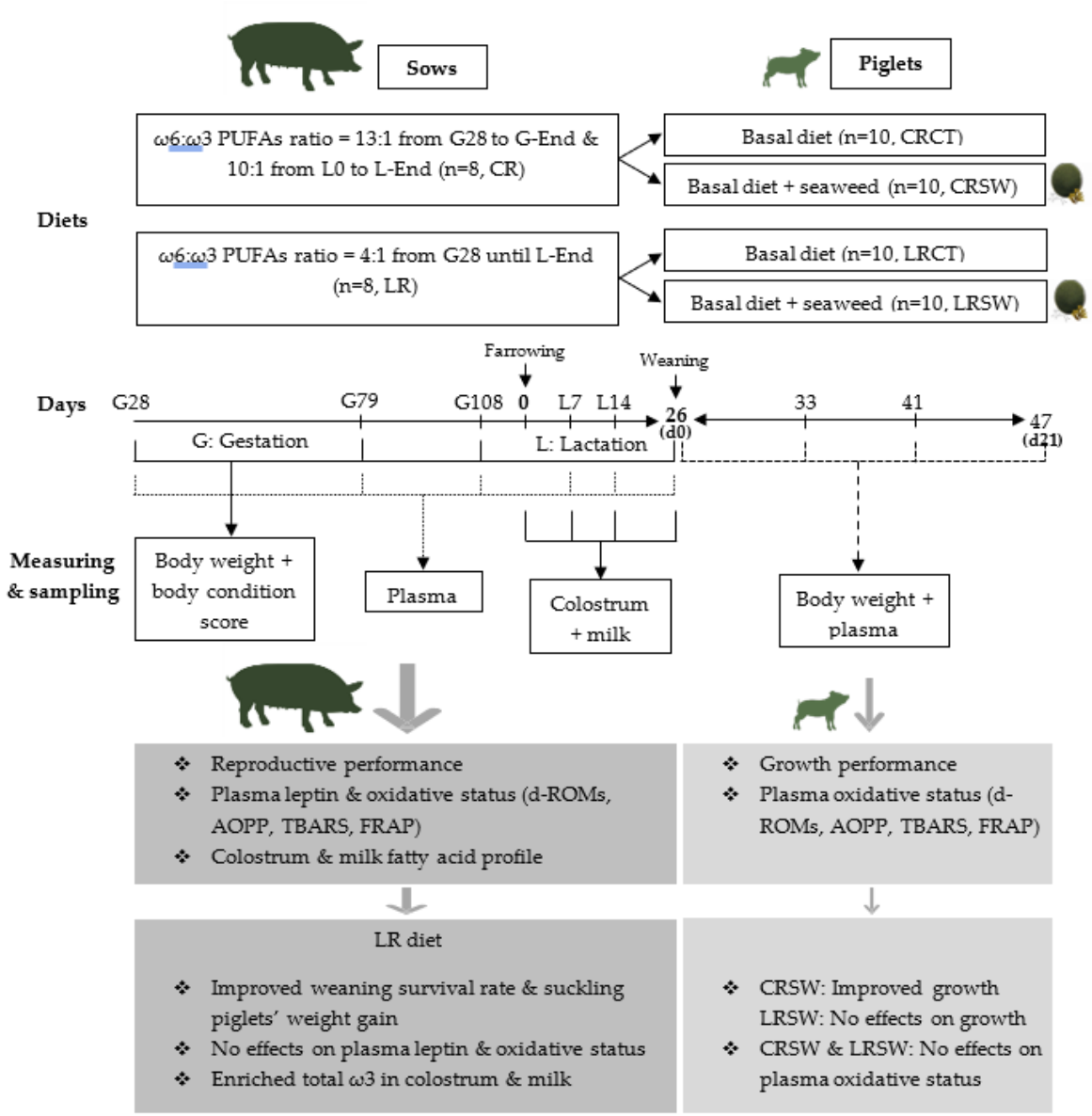

2.3 ABSTRACT

The ratio of omega-6 (ω6) to omega-3 (ω3) polyunsaturated fatty acids (PUFAs) in the diet contributes to animal health and performance modulations because they have mostly opposite physiological functions. Increasing ω3 PUFAs content in the maternal diet can stimulate antioxidative capacity in sow and piglets; however, the optimal ratio of ω6 and ω3 PUFAs in the sow diet is still under discussion. Rich sources of bioactive constituents such as brown seaweed are an excellent supplementation to promote animal health and antioxidant status. However, the knowledge of the effects of brown seaweed, specifically in post-weaning piglets, is still limited. Moreover, the combined effect of a low ω6:ω3 PUFAs ratio in sow diet and seaweed supplementation in post-weaning piglets' diet has never been studied.

This research aims to assess the combined effect of a low ω6:ω3 ratio in sow diets and seaweed supplementation in piglet diets on their growth and oxidative status. We also assessed the impact of a low ω6:ω3 ratio in the maternal diet on reproduction, milk fatty acid (FA) profile, and plasma leptin concentration. Two sow diets (n = 8 each) contained either a control ratio (CR, 13:1 during gestation, starting from day 28 (G28) and 10:1 during lactation) or a low ratio (LR, 4:1 from G28 until the end of lactation (L-End)) of ω6:ω3 FA by adding soybean oil or linseed oil, respectively. Reproductive performance was evaluated. Colostrum and milk at lactation day 7 (L7) and L-End were collected to analyse FA profile. Plasma was collected at G28, G79, G108, L7, L14, and L-End for determination of leptin and oxidative status. At weaning, 20 male piglets were selected per sow group to form 4 diet treatments (n = 10 each), which were supplemented with or without 4g/kg seaweed. Recording of growth performance and collection of blood were performed at days 0, 7, 15, and 21 of post-weaning for oxidative status.

LR diet increased ($p < 0.05$) the survival rate of piglets at weaning, and individual and litter weight gains. Colostrum and milk at L7 and L-End had lower ($p < 0.05$) ω6:ω3 ratio in LR sows. Interaction between dietary treatments on sows and piglets was revealed for all examined growth parameters at most time points ($p < 0.05$). LR diet did not affect plasma leptin levels and oxidative status. These findings suggest that the seaweed supplement during post-weaning could not improve growth rate and oxidative status of piglets born from mothers receiving

a low dietary ω6:ω3 ratio (4:1) during gestation and lactation. However, this low ratio was beneficial for weaning survival rate, sucking piglets' weight gain, and ω3 enrichment in colostrum and milk.

Keywords: sow; ω6:ω3 polyunsaturated fatty acids; seaweed; piglet

2.4 INTRODUCTION

In pig production, there is a growing interest in lowering the ratio of omega-6 (ω6) : omega-3 (ω3) polyunsaturated fatty acids (PUFAs) below 10:1 in maternal diets by using divergent sources of ω3 PUFAs (e.g., fish oil, linseed oil) to promote the health and performance of sows and piglets [1–5]. The enrichment of ω3 PUFAs in the diet has been shown to stimulate the antioxidative capacity in sow plasma and glutathione peroxidase activity (GSH-Px, an enzyme protecting cells against oxidative damage) in piglet liver, and decreased lipid peroxidation in piglet plasma [6]. A previous study found that increasing ω3 PUFAs in the maternal diet enhanced anti-inflammatory properties and reduced the pro-inflammatory effects of ω6 PUFAs, thus maintaining homeostasis [7]. A recent meta-analysis supports this notion in human studies [8], which showed that increasing the portion of ω3 PUFAs in the diet enhances the antioxidant defense mechanisms. However, there continues to be a debate about the optimal ratio of ω6 and ω3 PUFAs in the sow diet and how these effects can be transmitted from mother to offspring via milk, especially effects on piglets' performance and oxidative status.

For piglets, weaning is the most stressful event in life: the transition from a milk-based to a solid diet and changes in the environment and social relationships can reduce feed intake and conversion efficiency, disrupting gut mucosal barriers, and leading to reduced growth and health [9]. Moreover, piglets undergo oxidative stress and inflammation after weaning that can further contribute to poor performance [10]. These adverse outcomes can be alleviated by supplementing with abundant sources of bioactive compounds [10–13]. Brown seaweed *Ascophyllum nodosum (A. nodosum)* is a rich source of natural antioxidants [14] and antimicrobials [15], which can inhibit or impede oxidative damage by neutralizing free radicals in the cell [16]. Therefore, supplementing *A. nodosum* in the post-weaning diet can promote piglet health and performance. To our knowledge, only a few studies have investigated the effect of intact *A. nodosum* meal on the oxidative status of post-weaning piglets [17,18]. Moreover, none of them examined the possible combined or additive effect of low ω6: ω3 PUFAs ratio in sow diet and *A. nodosum* supplementation in post-weaning piglets' diet.

Herein, we hypothesized that feeding a low ω6:ω3 ratio diet to sows during gestation and lactation, together with the supplementation of *A. nodosum* for

piglets during the post-weaning period could benefit piglets' performance and oxidative status more than the respective single treatment provided to the mother or the piglet. With this purpose, we also considered the effects of maternal dietary low ω6:ω3 ratio on their reproductive performance, milk fatty acids (FA) profile, regulation of plasma leptin concentrations (which indicates sows' body fat content), and oxidative status.

2.5 MATERIALS AND METHODS

2.5.1 Animals and Housing

The sow experiment was conducted on a commercial swine farm (Arioli and Sangalli Agricultural Company S.S., Genzone, Italy). Sows (Landrace x Large White) were artificially inseminated with pooled semen (Topdelta boar, Large White) and kept in groups (8 sows per group) from one week after artificial insemination until one week before farrowing. Sixteen multiparous sows had similar body weight (202.57 ± 7.16 kg, mean ± SEM) and body condition score (2.36 ± 0.12, mean ± SEM) at the beginning of the trial. On day 108, gestating sows were moved to individual farrowing crates and stayed there until weaning. Within 24 h of birth, ear notching and tagging, iron injection, needle teeth clipping, and tail docking were performed.

The piglet trial was performed at the Animal Production Research and Teaching Centre, University of Milan (Lodi, Italy). Piglets were weaned at day 26 (± 1.76) of age (6.46 ± 0.15 kg of body weight, mean ± SE), and 20 male piglets per dietary treatment were selected from the sows (40 piglets in total). They were housed for 21 days in individual pens (0.47 m2/pen) equipped with a bite nipple drinker and self-feeder. The experimental protocols were approved by the Ethical Committee of the University of Milan (OPBA 67/2018) and the Italian Ministry of Health (authorization n. 168/2019 PR).

2.5.2 Experimental Diets

Sows were randomly allocated to one of two diet treatments that contained either a control ratio (CR, 13:1 during gestation, starting from day 28 (G28) and 10:1 during lactation) or a low ratio (LR, 4:1, from G28 until the end of lactation) of ω6:ω3 PUFAs. CR ratio was a usual ratio in European swine farms, and LR ratio

was selected according to the literature. The ω6 and ω3 fatty acids for this study were derived from soybean oil and linseed oil (Mazzoleni s.pa., Bergamo, Italy). The ω6 and ω3 PUFAs content (per total fatty acids) of soybean oil was 54.3% and 8.5%, (ω6:ω3 = 6.26), of linseed oil was 16.2% and 52.9% (ω6:ω3 = 0.31). Experimental diets were calculated to be isonitrogenous and isoenergetic and to meet the estimated nutrient requirements for sows during gestation and lactation [19], according to the total amount of the basal diet (Table 2-1) provided to adjust the final ratios of ω6:ω3 PUFAs in the diets to 13:1 during gestation and 10:1 during lactation, and 4:1 from G28 until the end of lactation (Table 2-2).

Table 2-1 Composition of Basal Sow Diets.

Item	Gestation	Lactation
Ingredients (g/kg as fed basis)		
Corn	284.60	249.10
Barley	224.20	216.70
Wheat bran	208.00	115.80
Distillers 'grains	125.00	40.00
Biscuit	50.20	52.10
Rice	35.00	35.00
Commercial concentrate *	25.00	250.00
Soybean oil	12.90	14.00
Fish meal	-	14.50
Mineral-vitamin premix **	20.00	11.70
HCl-Lysine	11.20	15.00
Composition (% DM)		
Crude protein	15.85	19.92
Crude fat	4.55	4.93
Crude fiber	5.69	5.66
Ash	5.68	4.46
Ca	1.70	1.21
P	0.56	0.57
Ca/P	3.04	2.12
Lysine	1.04	1.34
Methionine	0.18	0.22
Met +Cis	0.37	0.50
Digestible energy (DE, kcal/kg)	3069	2973
Metabolizable energy (ME, kcal/kg)	3123	3032

* Providing (as fed basis): 32.36% crude protein, 6.80% crude fat, 6.77% crude fiber, 0.80% Na, 2.43% lysine, 0.56% methionine. ** Providing (per kg of complete diet): vitamin A, 10 000 IU; vitamin D3, 2000 IU; vitamin E, 48 IU; vitamin K3, 1.5 mg; riboflavin, 6 mg; niacin, 40 mg; biotin, 0.2 mg; d-pantothenic, 17 mg; folic acid, 2 mg; choline, 166 mg; vitamin B6, 2 mg; and vitamin B12, 28 mg. Fe (as FeSO4), 90 mg; Cu (as CuSO4), 15 mg; Zn (as ZnSO4), 50 mg; Mn (as MnO2), 54 mg; I (as KI), 0.99 mg; and Se (as Na2SeO3), 0.25 mg.

Table 2-2 Fatty Acid (g/100g total fatty acids) of sow diets.

Item	Gestation CR	Gestation LR	Lactation CR	Lactation LR
10:0	0.26	0.22	-	-
12:0	0.35	0.30	1.80	1.56
14:0	0.25	0.21	-	-
16:0	20.23	18.08	17.58	16.06
16:1 ω7	0.50	0.42	-	-
18:0	3.06	3.30	4.36	4.40
18:1 ω9 cis	19.88	19.80	24.51	23.84
18:1 ω7	1.05	1.03	-	0.12
18:2 ω6 cis 9,12	49.79	44.73	46.92	42.90
18:3 ω3	3.72	11.12	4.83	11.12
20:0	0.28	0.24	-	-
20:1 ω9	0.41	0.35	-	-
22:0	0.23	0.20	-	-
ω6	49.79	44.73	46.92	42.90
ω3	3.72	11.12	4.83	11.12
ω6:ω3	13.40	4.02	9.71	3.88

Control ratio (CR): sow diet with ω6:ω3 ratio = 13:1 during gestation, starting from day 28 (G28) and 10:1 during lactation; low ratio (LR): sow diet with ω6:ω3 ratio = 4:1 from G28 until the end of lactation.

Experimental diets (fed as a liquid feed by mixing 25% solid feed with 75% water) were supplied from day (d) 28 of gestation until the end of lactation. Soybean oil and linseed oil were added to the barley meal at a rate of 10% to create a mixture before the daily feeding of the sows. The gestation diet was provided at 2.4 kg/d with 15g/d of soybean or linseed oil from d 28 to d 79 and 2.9 kg/d with 18g/d of soybean or linseed oil from d 80 to the end of gestation. Sows were fed per pen (8 sows/pen). The lactation diet was fed at 1 kg/d on the farrowing day (d 0) and then gradually increased to a maximum of 7.5 kg/d at weaning. During lactation, soybean oil and linseed oil were added daily to the individually basal diet administered according to the lactation feeding plan. Feed was provided twice a day and sows had unlimited access to freshwater. Feed was offered (increased daily) based on the sows' feed consumed during the previous day.

For piglets, the meal-based commercial diet (Table 2-3) was supplemented with or without 4g/kg seaweed powder (*A. nodosum*; Prodotti Arca S.r.l, Monza, Italy), providing 6.5% crude protein, 3.0% crude fat, 22.5% ash, and 52.5% polysaccharides on an as fed basis. Four groups (n = 10 each) were formed: CRCT (maternal ω6:ω3 = 13:1 during gestation and 10:1 during lactation, without seaweed (SW) supplementation); CRSW (ω6:ω3 = 13:1 during gestation and 10:1

during lactation, with SW); LRCT (ω6:ω3 = 4:1 during gestation and lactation, without SW); and LRSW (ω6:ω3 = 4:1 during gestation and lactation, with SW).

Table 2-3 Ingredients and Chemical Composition of the Basal Diet (CT) of post-weaning piglets. Seaweed powder (SW) was added to the basal diet at 4g/kg feed rate.

Item	Post-weaning basal diet
Ingredients (g/kg as fed basis)	
Barley	220.0
Wheat	161.7
Soy protein concentrate (Soicomil R)	98.0
Wheat, flaked	80.0
Corn	80.0
Corn, flaked	60.0
Soybean, meal	59.0
Biscuits	50.0
Whey	50.0
Dextrose, mono	40.0
Barley, flaked	40.0
Soybean oil	20.0
Dicalcium phosphate	10.0
Cocoa oil	10.0
L-Lysine	6.0
DL-Methionine	3.6
L-Threonine	3.5
Sodium chloride	2.7
Vitamin + trace elements	2.5
L-Valine (96.5%)	2.2
L-Tryptophan	0.8
Composition (%, DM)	
Dry matter (DM)	89.60
Crude protein	20.10
Crude fat	5.68
Fiber	3.29
Neutral detergent fiber (NDF)	12.91
Acid detergent fiber (ADF)	4.67
Acid detergent lignin (ADL)	0.97
Lysine (Lys), total	1.57
Cystine	0.32
Methionine (Met), total	0.66
Threonine, total	1.09
Tryptophan, total	0.32
Valine	1.08
Phenylalanine	0.85
Tyrosine	0.55
Isoleucine	0.74
Leucine	0.32
Net energy (NE, Mcal/kg)	2.90

2.5.3 Recording and Sampling

The sows' body weights and body condition scores (BCS) were assessed at the beginning of the trial (G28), middle of gestation (G79), at transferring time to the farrowing crates (G108), and at the end of lactation (L-End). The BCS was estimated using the five points scale (1 = emaciated, 2 = thin, 3 = ideal, 4 = fat, and 5 = obese; [20]). Two sows from the CR group had to be removed from the study because they had early parturition.

Piglets born, born alive, and born dead (stillborn, mummified, crushed, and abnormal) were counted within 24 h postpartum to calculate the survival rate at birth. The number of live piglets was recorded at d 7, d 14, and at weaning to calculate the weaning survival rate. Piglets were weighed at 24 h postpartum, d 7, d 14, and at weaning to calculate average daily weight gain.

Colostrum and milk samples (8–40 mL per sample) were collected after an overnight fast (12 h), by manual milking of all functional mammary glands of each sow within 24 h postpartum and on d 7, d 14, and at weaning. Samples were aliquoted and stored in pools per sow at −80 °C until analysis.

Blood samples were collected at G28, G79, G108, L7, L14, and L-End using ethylenediaminetetraacetic acid (EDTA) tubes and centrifuged (15 min.; 3000× *g*; room temperature). The EDTA plasma was aspirated and transferred to storage tubes before being stored at −80 °C until analysis.

For post-weaning piglets, feed supply and residuals per head were recorded every morning, from d 0 (weaning day) until d 21 to calculate average daily feed intake and feed conversion ratio. On d 0, 7, 15, and 21, piglets were weighed, and blood samples were collected from the jugular vein. The EDTA plasma obtained was stored at −80 °C until analysis.

2.5.4 Colostrum and Milk Fatty Acid Analysis

Fat in colostrum and milk was extracted [21] and then derivatized [22]. The resulting fatty acid methyl esters (FAMEs) were measured in a gas chromatographer equipped with a flame ionization detector (TraceTM GC Ultra, Thermo Fisher Scientific S.p.A., Rodano, Milan, Italy). The internal standard was

nonadecanoic acid (C19:0; 10 mg/mL of hexane), and the carrier gas was helium (He). FAMEs were separated by a fused silica capillary column (Rt-2560, 100 m × 0.25 mm × 0.25 µm) and followed the given program: 50 °C for 6 min; increased by 10 °C min−1 until 170 °C, constant for 30 min; increased by 4 °C min−1 to 220 °C, constant for 20 min. Individual FAME was verified by comparing peak retention times with standard mixtures (Supelco 37 FAME Mix, Bellefonte, Pennsylvania, USA) and pure standard methyl esters from Sigma-Aldrich (Saint Louis, Missouri, USA).

2.5.5 Leptin and Indicators of Oxidative Status in Plasma

Leptin was measured by an in-house developed ELISA validated for use on porcine samples [130]; the intra- and inter-assay CVs were 7.27 and 8.70%, respectively.

Oxidative damage was measured on levels of hydroperoxides (by-products of free radicals) using the d-ROMs (derivatives of reactive oxygen metabolites) test [131] with modifications [132]. Oxidative damage of proteins was assessed by the AOPP (advanced oxidation products of proteins) assay [133]. The AOPP concentrations are expressed both as molar concentrations and per mg of total protein. Total protein concentrations were measured with the Bradford assay [134]. Oxidative damage of lipids was estimated using the TBARS (thiobarbituric acid reactive substances) assay [135]. The total antioxidative capacity was assessed via the FRAP (ferric reducing ability of plasma) assay [136]. The intra- and inter-assay variations of all four assays were below 8%.

2.5.6 Statistical Analysis

Data relative to the length of gestation and lactation, body weight (BW) and BW gain/loss, reproductive performance, fatty acids (FAs) profile, leptin, and oxidative stress indicators of sows were analysed using the Generalized Linear Model (GLM) procedure in SAS Studio 3.8, on SAS version 9.04.01M6P11072018 (SAS Institute Inc., Cary, North Carolina, USA). The statistical model considered the ω6:ω3 ratio, day, and their interactions as fixed effects, and individual sows as the repeated effect.

Data on post-weaning piglet performance and oxidative stress indicators were analysed with a repeated-measures model using a MIXED procedure. The statistical

model considered ω6:ω3 ratio, seaweed supplement, day, and their interactions as fixed effects, individual piglets as a repeated effect, and weaning time as a random effect. GENMOD procedure (using generalized estimating equations (GEE) method) was performed to fit the generalized linear models on data that were not normally distributed. This included gain-to-feed ratio of piglets; some FAs (∑SFA, TLA, ∑ω3 and ALA in colostrum; DGLA, EPA, and DHA in milk at d 7 of lactation; GLA, DGLA, ETA, EPA, DHA, and ω6:ω3 ratio in milk at the end of lactation); some oxidative stress indicators in sows (leptin at L7, advanced oxidation products of proteins (AOPP) at G79 and G108, thiobarbituric acid reactive substances (TBARS) at L-End, Ferric reducing ability of plasma (FRAP) at G108 and L7, derivatives of reactive oxygen metabolites (d-ROM) at G28, L7, and L-End) and piglets (AOPP and FRAP at d 7, 15 and 21; TBARS at weaning and d 15; d-ROM from weaning to d 21).

Data are presented as LSM (least square means) ± SEM in tables and LSM ± SE in figures. Figures were plotted using GraphPad Prism version 8.4.2 (GraphPad software, La Jolla, CA, USA). Significance was set at $p \leq 0.05$.

2.6 RESULTS

2.6.1 Sow reproductive performance

Low dietary ω6:ω3 ratio (LR) had no effect on sow body weight, weight gain and loss during gestation and lactation (data not shown). LR diet caused an increase in perinatal mortality. The LR diet did not affect total number of piglets born (LSM ± SE: LR 13.75 ± 0.83 piglets; CR 16.33 ± 0.96 piglets; $p > 0.05$) but decreased the number of born alive by 3.45 piglets compared to CR diet (LR 11.38 ± 0.46 piglets; CR 14.83 ± 0.54 piglets; $p < 0.001$). Total piglets weaned per sow of LR group (10.38 ± 0.57 piglets) and of CR group (11.17 ± 0.65 piglets) were similar ($p > 0.05$). Consequently, the LR diet increased the survival rate of piglets at weaning (LR 90.95 ± 3.66 %; CR 75.95 ± 4.23 %; $p < 0.05$).

The LR diet increased individual and litter weight gains compared with the CR diet ($p < 0.05$, Figure 2-1). The LR diet did not affect piglet weight at weaning (LR 7.05 ± 0.44 kg; CR 5.84 ± 0.50 kg; $p > 0.05$) and piglet weight gain from d 7 to weaning (LR 4.49 ± 0.42 kg; CR 3.32 ± 0.49 kg; $p > 0.05$).

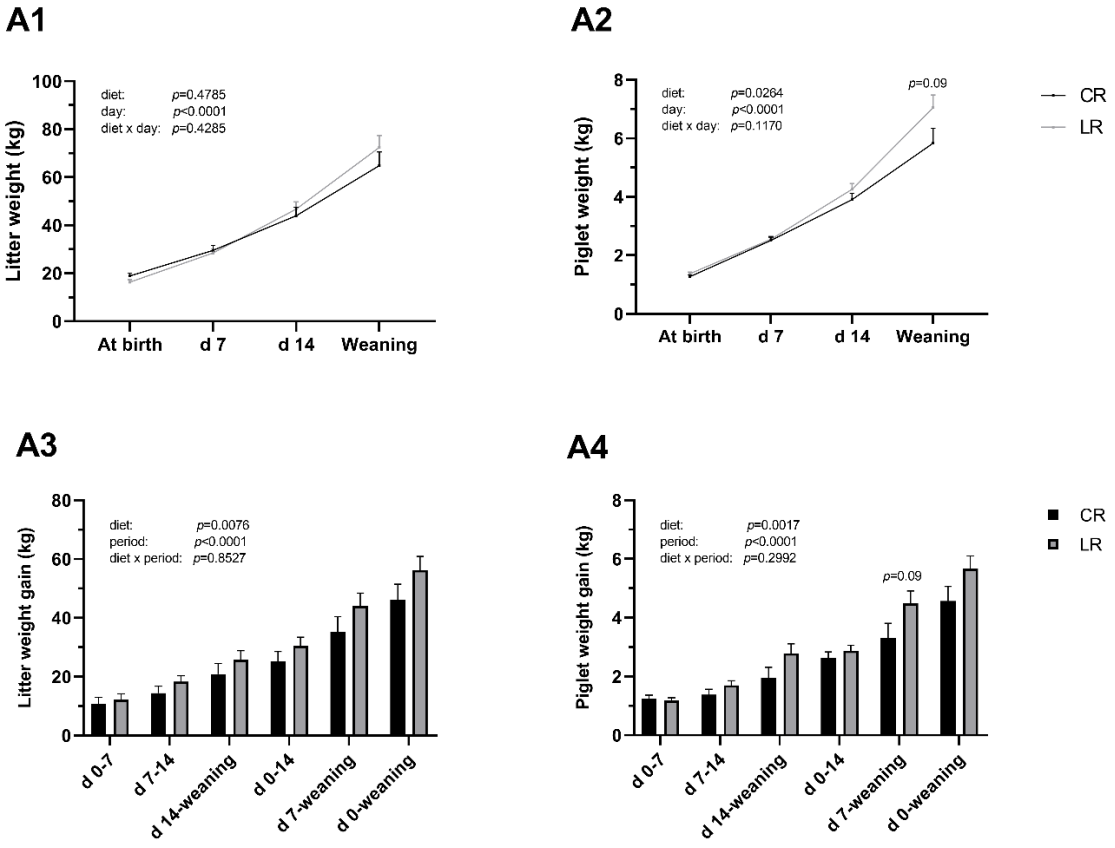

Figure 2-1 Low dietary ω6:ω3 ratio in sow improves body weight gain of neonatal piglets. Sows were fed diets with ω6:ω3 ratio = 13:1 during gestation, starting from day 28 (G28) and 10:1 during lactation (CR) or ω6:ω3 ratio = 4:1 from G28 until the end of lactation (LR). A1: Litter weight development during neonatal period. A2: Piglet weight development. A3: Litter weight gain per subperiod. A4: Piglet weight gain per subperiod. Data are LSM ± SE, n = 6 for CR group and n = 8 for LR group.

2.6.2 Growth Performance of Post-Weaning Piglets

Low maternal dietary ω6:ω3 ratio and seaweed supplementation in the post-weaning piglets' diet had no influence ($p > 0.05$) on piglet growth (Table 2-4, full details are presented in Table 2-5). However, interactions between dietary treatments on sow and piglet were revealed ($p < 0.05$) for BW, average daily gain (ADG), average daily feed intake (ADFI), and gain-to-feed ratio (G:F), mostly related to CRSW vs CRCT groups. At d 21, BW was higher ($p < 0.05$) in the CRSW than the CRCT group. ADG was improved ($p < 0.05$) during post-weaning. Higher ADFI ($p < 0.05$) was observed during post-weaning for CRSW and LRCT groups compared to LRSW group. G:F ratio was ameliorated ($p < 0.05$) during the first two weeks of post-weaning in CRSW vs. CRCT piglets.

Table 2-4 Growth performance of post-weaning piglets fed seaweed (SW) (brief).

Sow diets (SD)	CR		LR		SEM[1]	*p*-Value		
Piglet diets (PD) *	CT	SW	CT	SW		SD	PD	SD × PD
No. of piglets **	10	10	10	10				
BW[a] (kg)								
d 0	6.19	6.19	6.66	6.36	0.55	ns[4]	ns	ns
d 7	6.86	7.21	7.58	6.89	0.59	ns	ns	ns
d 15	9.56	10.72	10.62	9.32	0.98	ns	ns	0.018
d 21	12.41[b]	14.14[a]	13.64	12.13	1.17	ns	ns	0.010
ADG[2] (g/d)								
d 0 to 7	51.86	101.30	157.50	100.20	62.74	ns	ns	ns
d 0 to 15	202.76	279.59	275.82	211.51	55.73	ns	ns	0.017
d 0 to 21	276.15[b]	358.55[a]	345.63	289.71	52.20	ns	ns	0.013
ADFI[2] (g/d)								
d 0 to 7	154.46	194.17	222.59	196.79	44.58	ns	ns	ns
d 0 to 15	345.07	394.71	373.65	313.38	56.11	ns	ns	ns
d 0 to 21	458.59	527.04[a]	474.17[a]	387.27[b]	55.81	ns	ns	0.009
G: F[3]								
d 0 to 7	0.59	0.48	0.70	0.57	0.27	ns	ns	ns
d 0 to 15	0.55[b]	0.75[a]	0.71	0.67	0.16	ns	ns	0.033
d 0 to 21	0.62	0.73	0.70	0.70	0.08	ns	ns	0.050

CR: sow diet with ω6:ω3 ratio = 13:1 during gestation, starting from day 28 (G28) and 10:1 during lactation; LR: sow diet with ω6:ω3 ratio = 4:1 from G28 until the end of lactation. CT: post-weaning piglets' diet supplemented without intact seaweed powder. SD: sow diets, PD: piglet diets. BW: body weight, ADG: average daily gain, ADFI: average daily feed intake, G:F: gain-to-feed ratio. * The trial was performed from weaning to day 21 of post-weaning with 4 g seaweed supplementation per kg of feed. Feed residual and daily feed intake of each piglet were recorded every morning, from day 0 (weaning) to day 21 post-weaning to calculate average daily feed intake and feed conversion ratio. Individual body weight of piglets was measured on day 0, 7, 15 and 21 of post-weaning. ** Piglets were kept in individual pens (0.47 m2) with ad libitum feed and water. 1 SEM: Standard error of the means. Means are presented as least square means. a have normal distribution so mixed procedure was performed. 3 do not have normal distribution so GENMOD procedure (using generalized estimating equations (GEE) method) was performed to fit the generalized linear models. 4 ns: not significant.

2.6.3 Fatty acids Composition of Colostrum and Milk

Low ω6:ω3 ratio in the maternal diet significantly influenced the fatty acids (FA) profile of both colostrum and milk (Figure 2-2). In the colostrum, low ω6:ω3 ratio reduced concentrations of γ-linolenic acid (GLA, C18:3 ω6) by two-fold ($p < 0.05$). Low ω6:ω3 ratio also decreased the concentration of docosahexaenoic acid (DHA, C22:6 ω3) by two-fold and the overall ω6:ω3 ratio by one-third ($p < 0.05$). In the milk collected on day 7, low ω6:ω3 ratio increased concentrations of total ω3 FAs and α-linolenic acid (ALA, C18:3 ω3) by 1.6-fold ($p < 0.01$) and consequently decreased the overall ω6:ω3 ratio by one-third ($p = 0.0001$). In the milk collected at the end of lactation, low ω6:ω3 ratio increased concentrations of total ω3 FAs and α-linolenic acid (ALA, C18:3 ω3) by three-fold ($p < 0.0001$), increased concentration of eicosatrienoic acid (ETA, C20:3 ω3) by two-fold ($p < 0.05$), and

also increased level of eicosapentaenoic acid (EPA; C20:5 ω3) ($p < 0.01$). Overall, ω6:ω3 ratio was two-thirds declined in the low ratio treatment ($p < 0.0001$). Interactions between sow diet and sampling point were significant in total ω3, α-linolenic acid (ALA, C18:3 ω3) and the overall ω6:ω3 ratio.

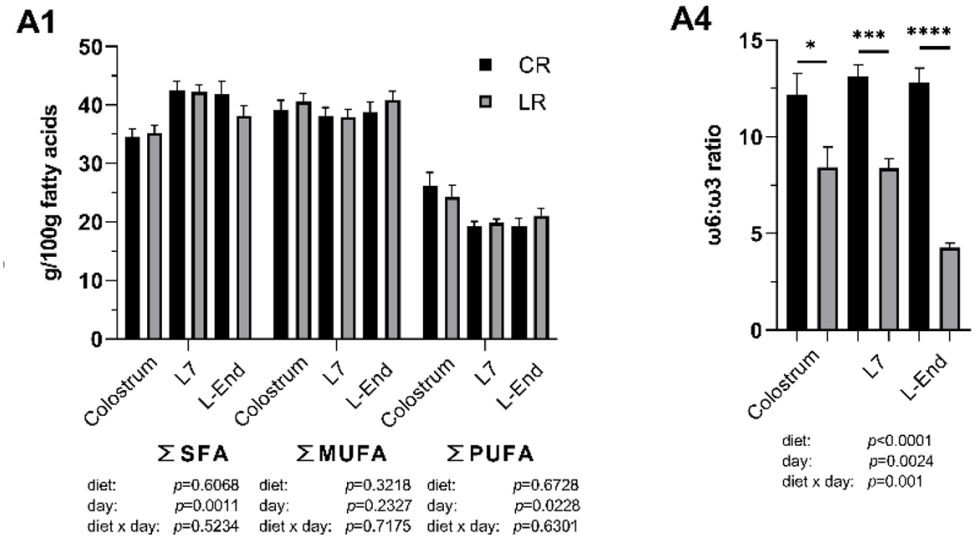

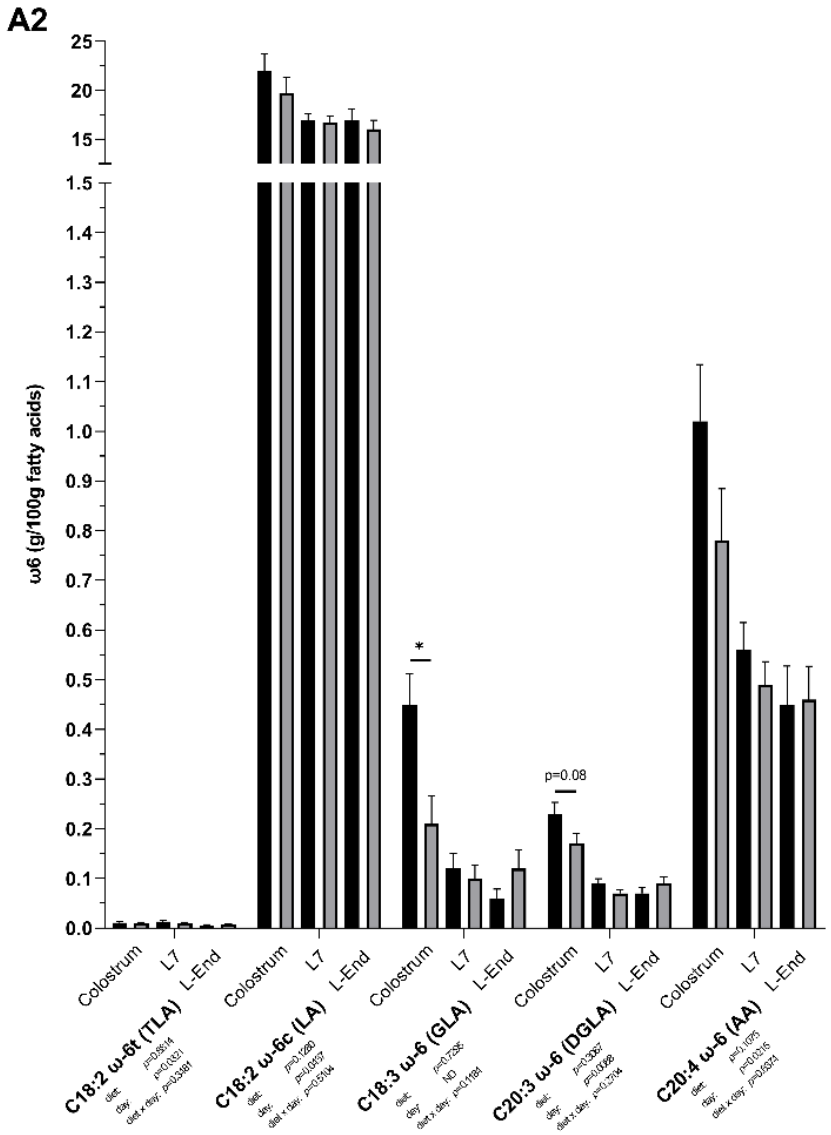
A2
ω6 (g/100g fatty acids)
25
20
15
1.5
1.4
1.3
1.2
1.1
1.0
0.9
0.8
0.7
0.6
0.5
0.4
0.3
0.2
0.1
0.0
*
p=0.08
Colostrum
L7
L-End
C18:2 ω-6t (TLA)
C18:2 ω-6c (LA)
C18:3 ω-6 (GLA)
C20:3 ω-6 (DGLA)
C20:4 ω-6 (AA)

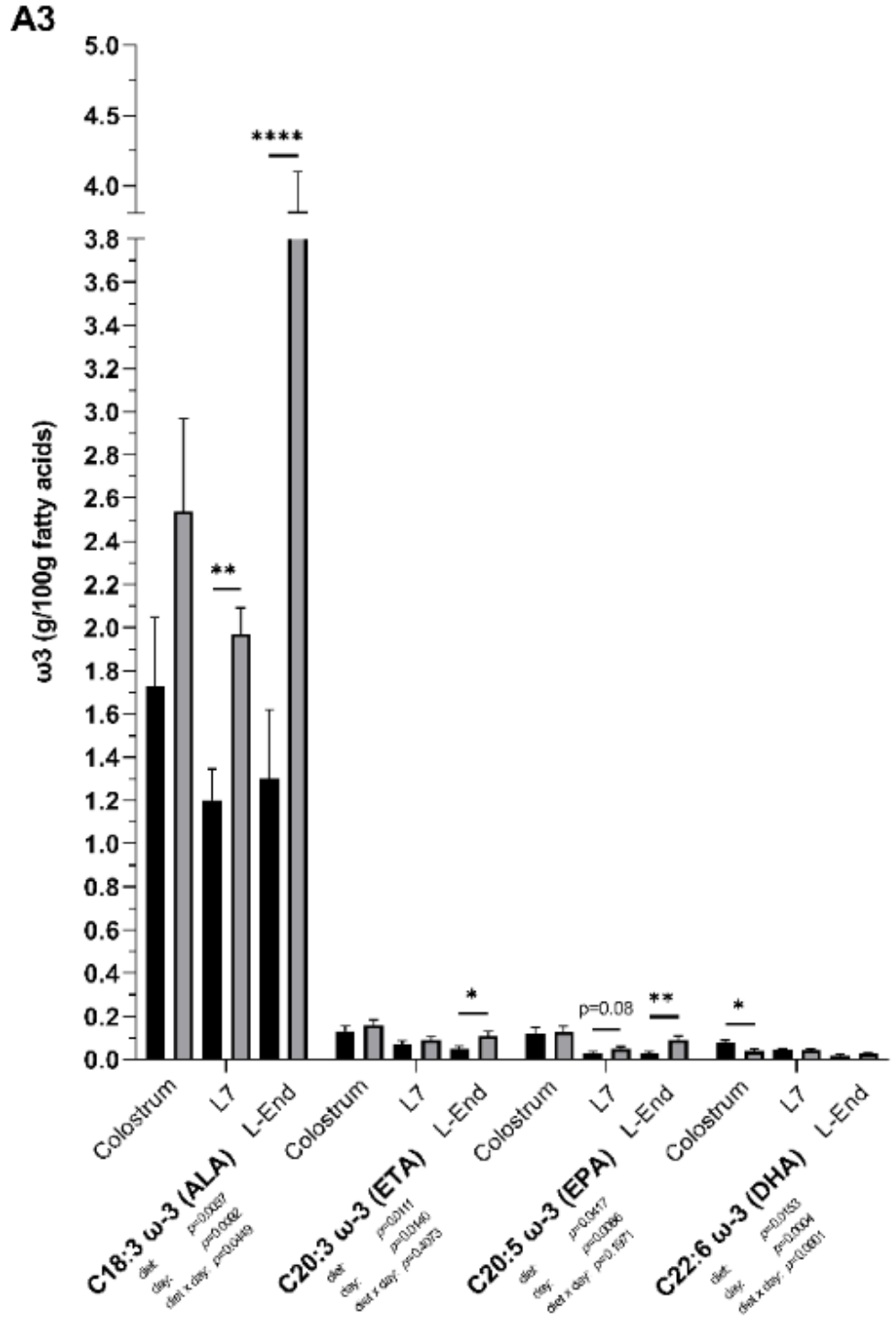

Figure 2-2 Fatty acid (FA) profile (g/100g FAs) of colostrum and milk. Milk collected on day 7 (L7) and the end of lactation (L-End) from sows fed diets included ω6:ω3 ratio = 13:1 during gestation, starting from day 28 (G28) and 10:1 during lactation (CR) or ω6:ω3 ratio = 4:1 from G28 until L-End (LR). A1: SFA, MUFA and PUFA concentrations. A2: Individual concentrations of ω6 PUFAs. A3: Individual concentrations of ω3 PUFAs. A4: ω6:ω3 ratio. SFA = Saturated FAs, MUFA = Monounsaturated FAs, PUFA = Polyunsaturated FAs, TLA = Linoleaidic acid, LA = Linoleic acid, GLA = γ-linolenic acid, DGLA = dihomo-γ-linolenic acid, AA = Arachidonic acid, ALA = α-linolenic acid, ETA = Eicosatrienoic acid, EPA = Eicosapentaenoic acid, DHA = Docosahexaenoic acid. Data are LSM ± SE; n = 5, 5 and 6 for CR group and 6, 7, 8 for LR group for colostrum, milk collected at L7 and L-End. * p < 0.05, ** p < 0.01, *** p < 0.001, **** p < 0.0001.

2.6.4 Leptin Concentrations and Oxidative Status in Sow Plasma

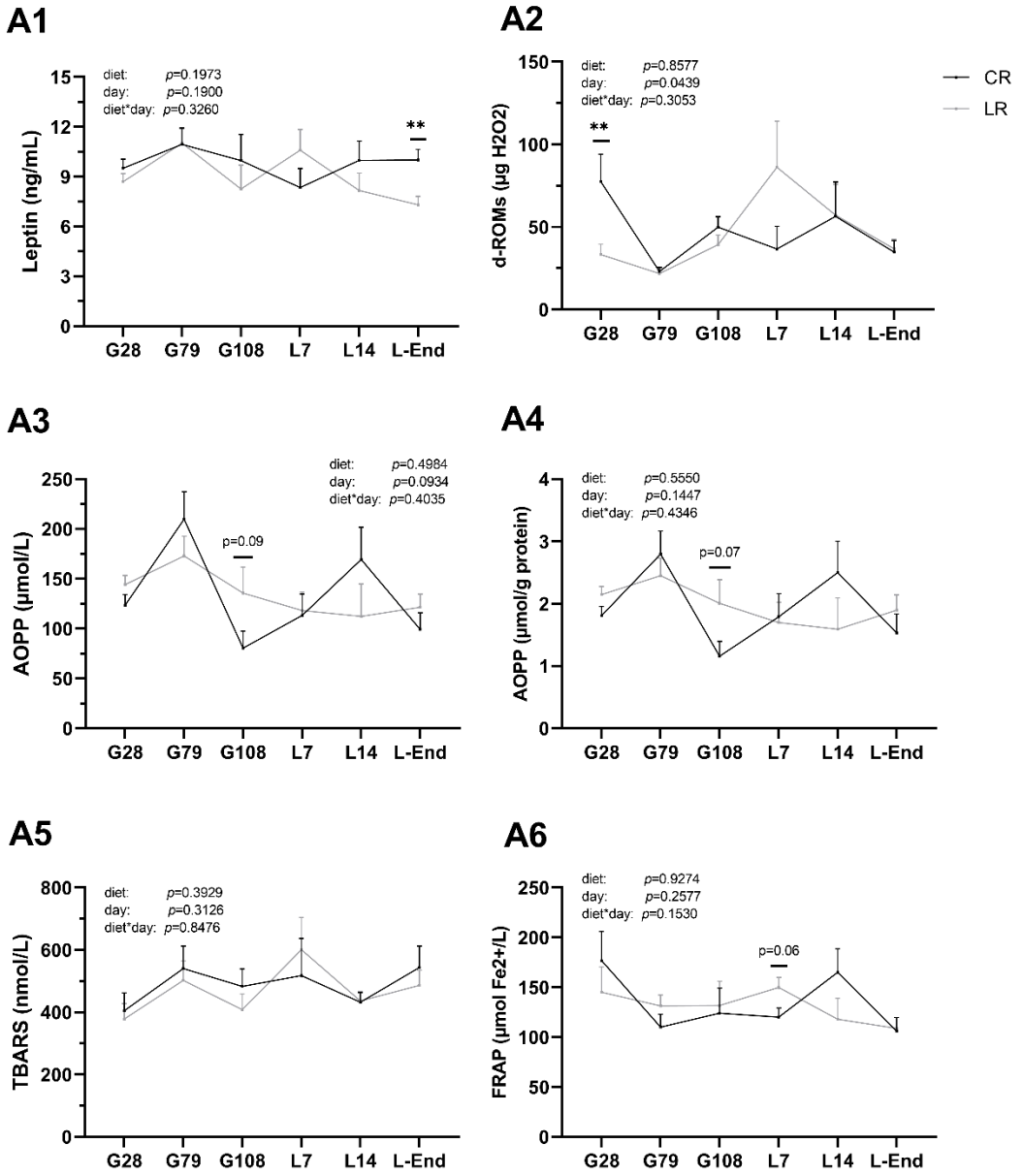

Figure 2-3 Concentrations of leptin and oxidative stress indicators of sow plasma during gestation and lactation periods. A1: Leptin; A2: The derivatives of reactive oxygen metabolites (d-ROMs); A3, A4: Advanced oxidation products of proteins (AOPP); A5: Thiobarbituric acid reactive substances (TBARS); A6: Ferric reducing ability of plasma (FRAP). CR: sow diet with ω6:ω3 ratio = 13:1 during gestation, starting from day 28 (G28) and 10:1 during lactation; LR: sow diet with ω6:ω3 ratio = 4:1 from G28 until L-End. G: days of gestation, L: days of lactation. Data are LSM ± SE; n = 6-8 sows per group. ** p < 0.01.

Low dietary ω6:ω3 ratio (LR) had some effects on the concentrations of leptin and oxidative stress indicators in sow plasma (Figure 2-3). LR diet decreased concentrations of plasma leptin at L-End and d-ROMs at G28 ($p < 0.01$) but had no effect on TBARS, AOPP, and FRAP levels at any time point. Regarding the impact of time on oxidative levels, concentrations of d-ROMs decreased in the middle of gestation and at the end of lactation but increased at the end of gestation and

middle of lactation ($p < 0.05$). No interaction between diet and time point was found for all measured indicators in sow plasma.

2.6.5 Oxidative Status in Plasma of Post-Weaning Piglets

Low maternal dietary ω6:ω3 ratio (LR) and seaweed supplementation (SW) in the post-weaning piglets' diet did not affect levels of d-ROMs in CRSW and LRCT piglets at weaning ($p > 0.05$, Figure 2-4). LR diet increased concentrations of d-ROMs at d 21 ($p < 0.05$): d-ROMs in LRSW piglets was 1.5-fold greater than LRCT and CRCT piglets and was 2-fold higher than CRSW piglets ($p = 0.01$).

SW diet lowered concentration of FRAP at d 7 ($p < 0.05$) but LR diet did not affect levels of FRAP during post-weaning ($p > 0.05$). There were no effects of either sow diet, piglet diet, or their interaction on plasma concentrations of AOPP and TBARS at any time point.

The effects of time on all examined oxidative parameters were significant ($p < 0.01$). Interaction between sow diet and time point, between sow diet, piglet diet and time point were revealed for d-ROMs levels through the post-weaning period ($p < 0.05$).

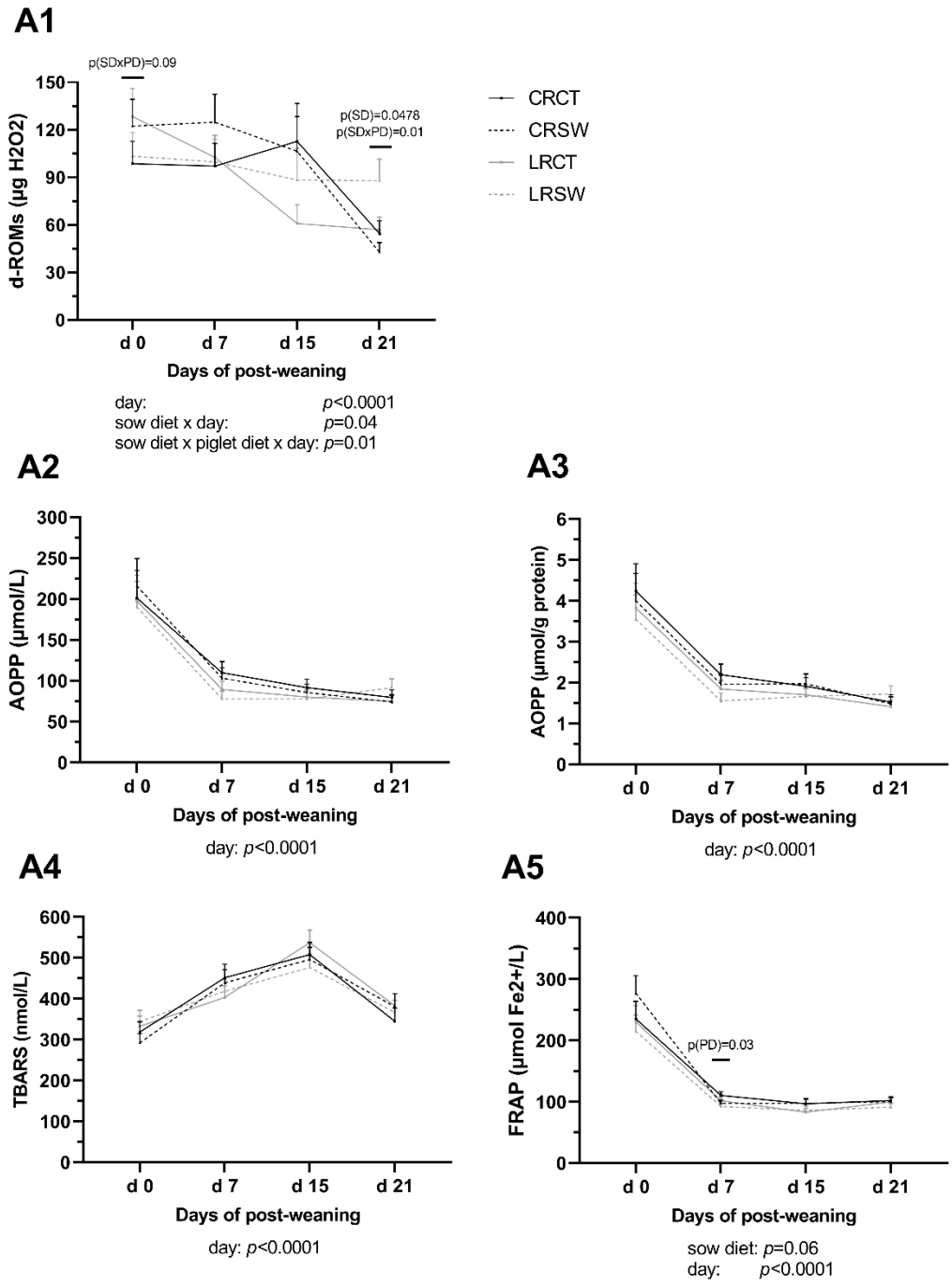

Figure 2-4 Concentrations of oxidative stress indicators of piglet plasma during the post-weaning period. A1: The derivatives of reactive oxygen metabolites (d-ROMs); A2: Advanced oxidation products of proteins (AOPP, µmol/L); A3: AOPP (µmol/g protein); A4: Thiobarbituric acid reactive substances (TBARS); A5: Ferric reducing ability of plasma (FRAP). CRCT: piglets fed no seaweed (SW, *Ascophyllum nodosum*), which were nursed by sows fed dietary ω6:ω3 ratio = 13:1 during gestation, starting from day 28 (G28) and 10:1 during lactation. CRSW: piglets fed SW, which were nursed by sows fed dietary ω6:ω3 ratio = 13:1 during gestation and 10:1 during lactation. LRCT: piglets fed no SW, which were nursed by sows fed dietary ω6:ω3 ratio = 4:1 from G28 until the end of lactation. LRSW: piglets fed SW, which were nursed by sows fed dietary ω6:ω3 ratio = 4:1 from G28 until the end of lactation. Data are LSM ± SE; n = 10 piglets/group. SD, PD, and SD × PD: effect of sow diet, piglet diet and their interaction between 4 groups at the same sample point.

2.7 DISCUSSION

In this study, we examined whether a low ω6:ω3 ratio (LR) in the sow diet and the supplementation of *A. nodosum* for piglets during the post-weaning period can benefit piglet performance and oxidative status more than the respective single treatment provided to the mother or the piglet. We also considered the effects of low ω6:ω3 ratio in the sows' diet on reproduction, milk FA profile, plasma leptin concentrations, and oxidative status. We found that the LR diet enhanced total ω3 FA in colostrum and milk, weaning survival rate, and suckling piglets' weight gain. The interaction between CR and SW diets enhanced piglets' growth. But LR and SW diets did not affect growth and oxidative status in sows and post-weaning piglets.

We observed that LR diet increased weaning survival rate and sucking piglets' weight gain compared with the control diet. The enhancement of total ω3 PUFAs in the sows' colostrum and milk in LR diet could lead to a positive modulation of the intestinal microflora, thus promoting the intestinal health in suckling piglets by inhibiting Toll-like receptor 4 (TLR4) and signalling to reduce inflammation [137]. Our results support previous research findings that link low ω6:ω3 ratio in the maternal diet with piglet growth improvement. Specifically, a trend in improving piglets' growth rate in the first week of life was reported when a ω6:ω3 ratio of 5:1 was provided to sows compared to an 11:1 ratio [104]. Similarly, lowering dietary ω6:ω3 ratio from 20:1 and 15:1 to 10:1 increased piglet body weight and litter ADG at weaning [95]. Moreover, a 3:1 diet tended to increase litter size on the second and third weeks of life while a 9:1 diet tended to increase litter ADG in the first 14 days of age compared with a 13:1 diet [94]. In our study, LR sows had fewer piglets born alive than CR sows, but their performance was similar to previous research when sows were fed low ω6:ω3 ratios (from 1:1 to 5:1) [138]. The reduction in the number of piglets born alive on the LR diet is difficult to explain: it could be due to low dietary ω6:ω3 ratio and some unaccounted factors might be involved in the obtained results. The total number of piglets born and the number of born alive are affected by genetic factors of both sows and piglets [139]. However, these traits' heritabilities are low (ranging from 0.16 to 0.19 and 0.04 to 0.29, respectively) [140,141]. Therefore, they are strongly affected by the environment. The low heritability of these parameters could explain for their variability between the sows and between CR and LR

groups, although we kept these two groups in the same environmental conditions during the feeding trial.

To our knowledge, this is the first study that accounts for a possible combined positive effect of ω3 enriched maternal diet and seaweed supplementation in the post-weaning piglets' diet on their growth and oxidative status. Results showed that seaweed (*A. nodosum*) supplementation in post-weaning piglets increased BW, ADG, ADFI, and G:F when born from control sow compared with non-seaweed supplemented piglets. *A. nodosum* is considered to be a source of ω3 PUFAs with a high concentration of EPA (C20:5 ω3) and low ω6:ω3 ratio of 2.75 [142]. Thus, this can add more ω3 PUFAs and lower ω6:ω3 ratios in piglets, which were born from control sows and received the seaweed diet. However, this positive result of additional ω3 PUFAs from *A. nodosum* was not seen in piglets born from sows fed ω3 enriched diet. Thus, the combined effect of LR and SW diets is difficult to explain. The literature reports that offering too low a ratio of ω6:ω3 (0.38) to pigs (from growing to finishing) did not affect their growth performance, although it improved total ω3 PUFAs (including ALA, EPA, and DHA) and reduced ω6:ω3 ratio in pork [143].

Lowering the ratio of ω6:ω3 PUFAs by adding linseed oil to the maternal diet can decrease ω6:ω3 ratio in colostrum and milk by enriching ALA concentration [94], thus, increasing concentrations of ALA in piglet liver, brain, and muscle tissues [144], plasma, carcass [145], and intestinal mucosa [146]. Our results are consistent with the findings of Yao et al. [94] when offering high ALA combined with the low LA diet.

However, high ALA intake was found not to affect the DHA level in piglet liver [101] or even decreased DHA concentration in human red blood cells, although it increased EPA level [147]. In line with recent research, the low concentration of DHA in our study was due to the inefficient conversion of ALA to EPA (i.e., 0.2 ~ 5%) and DHA (i.e., 0.05–0.5%) [148,149], which may be explained by several reasons: First, the high rate (59%) of ALA was β-oxidized for the whole body utilization [150]. Second, the lack of elongase-2 expression to elongate C22:5 ω3 to C24:5 ω3 [37], which supports the EPA generation. Third, the competition between LA and ALA for enzyme Δ-6 desaturase, which has a higher affinity for ALA; thus, high LA intake prevents the conversion from ALA to EPA [148,151].

Collectively, our results demonstrate that a linseed oil enriched ω3 diet is a substantial source for endogenous ALA rather than for endogenous DHA concentrations.

Leptin is an important adipocyte-secreted hormone regulating appetite, body weight, reproduction, energy homeostasis, and acts as a pro-inflammatory cytokine [152]. The ω3 enriched diet can regulate leptin *in vivo* [153]. It tended to decrease leptin in adipose tissue [154], and lower plasma leptin level [155]. In this study, the reducing effect of ω3 enriched diet on plasma leptin in sows at the end of lactation might go with increased ß-oxidation of FAs in the liver and skeletal muscle (to a smaller extent) [156].

Pregnancy, delivery process, and lactation are all associated with elevated levels of oxidative stress due to intensive metabolism and lipid peroxidation [157]. We found that a low ratio of ω6:ω3 PUFAs in the maternal diet tended to increase AOPP concentrations at the end of gestation, decreased the number of piglets born and piglets born alive, which could be explained by the involvement of AOPP levels in embryonic mortality [158]. However, the increased level of AOPPs in LR sows did not seem to cause intracellular ROS (H202) production because d-ROMs levels were the same between LR and CR sows at the end of gestation. In this study, ω3 enriched diet did not influence lipid peroxidation of sow plasma. It might be that the malondialdehyde measured in the TBARS test was absorbed quickly in the liver before being eliminated in urine without influencing TBARS levels in blood circulation [159]. Here, we observed that FRAP values of LR sows were similar at the end of gestation and tended to increase at the beginning of lactation, compared with CR sows. The hypothesis may explain that when protein oxidation increased, the sow's antioxidant system was stimulated and led to FRAP concentrations increasing when sows were offered more ω3 PUFAs.

Weaning is a stressful event for piglets, challenging for health and growth due to various stressors [160]. The post-weaning period is associated with increased oxidative products in plasma: the highest ROM found in the first-week post-weaning was linked to reduced growth rates [161]; NO and H2O2 were highest at weaning and decreasing after weaning [162]. Similar results were observed in our study.

We could not see any effects of the low ratio of ω6:ω3 PUFAs in the maternal diet and seaweed supplementation in the piglets' diet on the piglets' oxidative status. However, the higher ADG and G:F ratio of the LRCT and CRSW piglets indicated benefits of ω3 enriched diet and seaweed supplementation on stimulating antioxidants to reduce excessive ROS production, therefore, improving piglets' growth performance. Growth performance reflects overall influences over a period, whereas plasma measurements are a single test at a time point [163]. Moreover, this improvement can be explained by the bioactivity of ω3 PUFAs in the maternal diet and seaweed-derived elements (i.e., ascophyllan, laminarin, fucoidans, and phlorotannins) in the post-weaning piglet diet [164]. Maternal diets enriched in ω3 PUFAs with optimal ω6:ω3 ratio might regulate progeny immune response and improve anti-inflammatory activity against pathogens [165], especially the inflammatory response causing by post-weaning stress [166]. Post-weaning diets supplemented with *A. nodosum* can promote piglet intestinal health through its immunomodulatory, anti-inflammatory, antioxidant, and antimicrobial properties [127,167,168], thereby improving piglets' growth rates.

Overall, our study showed that the ω3 enriched diet during gestation and lactation did not affect the oxidative stress of sows and their post-weaning piglets. Similar results were reported when feeding a dietary ω6:ω3 ratio of 4:1 or 6:1 to sows [101] or feeding a dietary ω6:ω3 ratio of 5:1 to piglets (10.6 kg) [169]. These outcomes may be explained by low double bonds of ALA and its poor conversion rate to EPA and DHA, as shown in the FA profile of colostrum and milk in this study. The dietary ω6:ω3 ratio above 3:1 is considered safe to protect the animal from oxidative damage [170]. Our results suggest that not only the dietary ratio between ω6 and ω3 but also the type of fat source (total double bonds) have synergic effects on the oxidative stress level of the sows and piglets.

2.8 CONCLUSIONS

The current study showed that low dietary ω6:ω3 ratio in sow diet during gestation and lactation combined with the seaweed supplementation in piglets after weaning could not improve piglets' growth rate or antioxidant status. However, the sows' low ω6:ω3 ratio diet alone improved weaning survival rate, suckling piglets' weight gain, and total ω3 PUFAs (mainly ALA) in the colostrum and milk. Seaweed supplementation improved growth performance of piglets born

from sows which received the higher dietary ω6:ω3 ratio. These findings outline that maternal dietary interventions can significantly affect the progeny, and that seaweed supplementation is effective in improving performance in post-weaning piglets. However, interaction among these treatments remains unclear. Further studies are necessary to enhance the knowledge of maternal dietary interventions during gestation and lactation, and their effect on the progeny or to outline the efficacy of natural antimicrobials and antioxidants in the diets of piglets, also considering omics and epigenetic approaches.

Table 2-5 Growth performance of post-weaning piglets fed seaweed (SW) (full).

Sow diets (SD)	CR		LR		SEM [1]	*p*-value		
Piglet diets (PD) *	CT	SW	CT	SW		SD	PD	SD × PD
No. of piglets **	10	10	10	10				
BW [a] (kg)								
d 0	6.19	6.19	6.66	6.36	0.55	0.509	0.595	0.590
d 7	6.86	7.21	7.58	6.89	0.59	0.712	0.565	0.087
d 15	9.56	10.72	10.62	9.32	0.98	0.852	0.886	0.018
d 21	12.41 [b]	14.14 [a]	13.64	12.13	1.17	0.713	0.850	0.010
ADG [2] (g/d)								
d 0 to 7	51.86	101.30	157.50	100.20	62.74	0.106	0.901	0.099
d 7 to 15	346.85 [b]	447.64 [a]	375.05 [ab]	298.14 [bc]	60.95	0.310	0.698	0.007
d 15 to 21	471.65	567.97	527.00	491.98	73.17	0.780	0.409	0.083
d 0 to 15	202.76	279.59	275.82	211.51	55.73	0.955	0.824	0.017
d 0 to 21	276.15 [b]	358.55 [a]	345.63	289.71	52.20	0.993	0.616	0.013
FI[2] (kg/period)								
d 0 to 7	1.08	1.36	1.56	1.38	0.31	0.123	0.757	0.152
d 7 to 15	3.87	4.34	4.19	3.47	0.58	0.598	0.665	0.049
d 15 to 21	4.31 [b]	5.00[a]	4.45 [ab]	3.53[c]	0.48	0.127	0.644	0.002
d 0 to 15	5.18	5.92	5.60	4.70	0.84	0.596	0.851	0.060
d 0 to 21	9.63 [ab]	11.07[a]	9.96 [a]	8.13 [b]	1.17	0.234	0.743	0.009
ADFI[2] (g/d)								
d 0 to 7	154.46	194.17	222.59	196.79	44.58	0.123	0.757	0.152
d 7 to 15	483.86	542.20	523.48	433.50	72.35	0.598	0.665	0.049
d 15 to 21	717.62	833.07	741.10	588.15	80.39	0.127	0.644	0.002
d 0 to 15	345.07	394.71	373.65	313.38	56.11	0.596	0.851	0.060
d 0 to 21	458.59 [ab]	527.04 [a]	474.17 [a]	387.27 [b]	55.81	0.234	0.743	0.009
G : F [3]								
d 0 to 7	0.59	0.48	0.70	0.57	0.27	0.377	0.198	0.960
d 7 to 15	0.65	0.79	0.74	0.72	0.12	0.853	0.152	0.065
d 15 to 21	0.68	0.71	0.68	0.76	0.09	0.509	0.085	0.426
d 0 to 15	0.55 [b]	0.75 [a]	0.71	0.67	0.16	0.561	0.125	0.033
d 0 to 21	0.62	0.73	0.70	0.70	0.08	0.457	0.068	0.050

CR: sow diet with ω6:ω3 ratio=13:1 during gestation, starting from day 28 (G28) and 10:1 during lactation; LR: sow diet with ω6:ω3 ratio=4:1 from G28 until the end of lactation. CT: post-weaning piglets dietary supplemented without intact seaweed powder. SD: sow diets, PD: piglet diets. BW: body weight, ADG: average daily gain, ADFI: average daily feed intake, G:F: gain : feed ratio. * The trial was performed from weaning to d 21 of post-weaning with 4 g seaweed supplementation per kg of feed. Feed residual and daily feed intake of each piglet were recorded every morning, from day 0 (weaning) – 21 post-weaning to calculate average daily feed intake and feed conversion ratio. Individual body weight of piglets was measured on day 0, 7, 15 and 21 of post-weaning. ** Piglets were kept in individual pens (0.47 m2) with ad libitum feed and water. 1 SEM: Standard error of the means. Means are presented as least square means.a have normal distribution so Mixed procedure was performed. 3 do not have normal distribution so GENMOD procedure (GEE model) was performed.

Chapter 3 Plasma proteome changes in sows receiving a low dietary ω6:ω3 ratio

Journal of Proteomics: published 28 Mar 2022, Vol. 260, 30 May 2022, 104562
https://doi.org/10.1016/j.jprot.2022.104562

Thi Xuan Nguyen[1,2,5]
Alessandro Agazzi[1]
Suzanne McGill[2]
Stefan Weidt[2]
Quang Hanh Han[2,5]
Andrea Gelemanović[3]
Mark McLaughlin[2]
Matilde Piñeiro[4]
Giovanni Savoini[1]
Peter David Eckersall[2]
Richard Burchmore[2]

[1]Università degli Studi di Milano, Via dell'Università, 6, 26900 Lodi, Italy
[2]University of Glasgow, Bearsden Rd, G61 1QH, United Kingdom
[3]Mediterranean Institute for Life Sciences (MedILS), Meštrovićevo šetalište 45, 21000 Split, Croatia
[4]Acuvet Biotech, C/Bari, 25 dpdo, 50197 Zaragoza, Spain
[5]Vietnam National University of Agriculture, Hanoi, Vietnam

Thi Xuan Nguyen contribution: conceptualization and design of the study, funding acquisition and project administration, methodology, acquisition of data, formal analysis and interpretation of data, drafting the manuscript, critical revising the manuscript, approval of the final version to be submitted, corresponding author.

Other contributions: Conceptualization and design of the study: AA, GS, PDE, and RB; funding acquisition and project administration: RB, DE, GS; methodology: SM, SW, QHH, AG, MM, MP, RB, DE; acquisition of data: RB, DE; formal analysis and interpretation of data: AG; critical revising the manuscript: AA, QHH, AG, MM, MP, GS, DE, and RB; all authors approved the final version to be submitted.

3.1 HIGHLIGHTS

* Maternal low dietary ω6:ω3 fatty acid ratio during gestation and lactation affected acute phase proteins in sow plasma.

* Plasma protein profile significantly changed between later stages of gestation and lactation.

* Haptoglobin (HP) was identified in the comparisons between two dietary treatments and two stages of reproduction.

* The key Gene Ontology terms involved were acute phase response and high-density lipoprotein particle receptor binding.

3.2 SIGNIFICANCE

This study aimed to provide a proteomics insight into the beneficial effects of maternal diet supplementation with a low ω6:ω3 fatty acids ratio, based on previously reported performance and zootechnical data. The results suggest that a low dietary ω6:ω3 fatty acids ratio could enhance the cellular defence mechanisms against increased stresses and in particular to oxidative stress in sows during gestation and lactation, as reflected in proteomic changes of haptoglobin (HP), alpha-1-antitrypsin (SERPINA1) and serum amyloid P-component (APCS). Furthermore, significantly changed proteome profiles in sow plasma between late gestation and lactation phases have been revealed for the first time. This finding identified the adaptation mechanisms of sows to changing physiological events during reproduction.

3.3 GRAPHICAL ABSTRACT

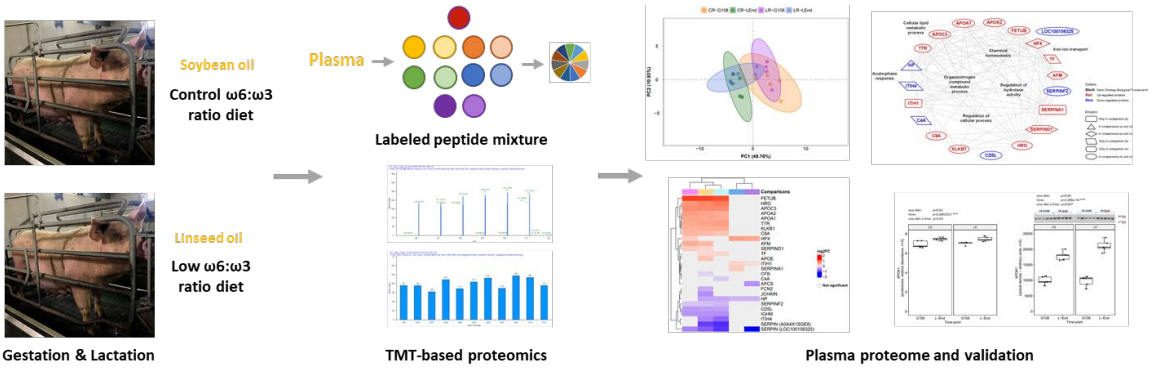

3.4 ABSTRACT

This study aimed to investigate the characteristic proteomic pattern of plasma from sows supplemented with low dietary ω6:ω3 fatty acids (FAs) ratio during gestation and lactation. Two dietary treatments (n = 8 each) comprised either a control ratio of ω6:ω3 FAs (CR, 13:1 during gestation and 10:1 during lactation) or a low ratio (LR, 4:1 during gestation and lactation) by adding soybean oil or linseed oil, respectively. High-resolution mass spectrometry-based quantitative proteomics was applied on plasma (n = 5 each) at day 108 of gestation (G108) and at the end of lactation (L-End), and a total of 379 proteins and 202 master proteins were identified. Out of these, four differentially abundant proteins between LR and CR samples at G108 may relate to serine-type endopeptidase inhibitor activity. Differentially abundant proteins in L-End versus G108 (12 up-regulated and 10 down-regulated) were positively correlated with the events that regulate plasma lipoproteins, stimulus- and defence-responses. These findings demonstrate the benefit of increased dietary ω3 FAs in modifying proteins involved in protective mechanisms against increased stresses in key life cycle phases in pigs. In addition, proteome changes from late gestation to late lactation disclosed the underlying mechanism of pigs in response to reproduction-related stimuli.

Keywords: plasma proteome, ω6:ω3 fatty acids, gestation, lactation, haptoglobin, high-density lipoprotein

3.5 INTRODUCTION

Nowadays, the pig diet has an imbalance in the ratio of omega-6 and omega-3 (ω6:ω3) polyunsaturated fatty acids (PUFAs) (ranging from 10:1 to 15:1) [171] because they consume an increased amount of ω6 FAs from corn and other grains [172] and a noticeably decreased amount of ω3 FAs such as from fish meal or linseed oil. Given the opposing physiological functions of ω6 and ω3 PUFAs [43], elevated intake of ω6 and poor intake of ω3 PUFAs can give rise to systemic inflammation and metabolic and inflammatory disorders [43]. Therefore, supplementation of low-ratio ω6:ω3 PUFAs, especially in the long-term, can reduce risk factors for inflammation-related diseases [173,174]. Nevertheless, there is no consensus on the optimal ratio of ω6:ω3 PUFAs for good health despite decades of research [174,175]. Several studies suggested that a ratio of ω6:ω3 PUFAs above 3:1 up to 6:1 is optimal for decreasing oxidative stress and lipoperoxidation [170]. However, other studies have proposed that a suitable ratio for reducing inflammation levels can range from 1:1 to 5:1 [173] or from 1:1 to 6:1 [176].

From a physiological and nutritional aspect, pregnancy is the most sensitive phase in the female life cycle [177,178] for both humans and animals. During pregnancy, sows undergo complex physiological changes such as weight gain, fetal and placental development [177]. Nutrient exchange between mother and fetus is only possible through the placenta - their temporary and unique metabolic link [178]. After birth, the neonates interact with their mother via breastfeeding, and maternal diet through gestation and lactation plays a significant role in early and long-term offspring's life growth, development, and health. In pigs, maternal nutrient requirements change according to the reproduction phases and massive metabolic alterations, such as increased oxidation levels, can occur in many tissues [179]. Antioxidant levels in sow diets should be re-assessed to avert elevated oxidative damage during late gestation and lactation and to improve sow productivity and health [180].

In the context of biological processes, the ω3 PUFAs are widely known for their antioxidant and anti-inflammatory properties by regulating the antioxidant signalling pathway and modulating inflammation [181]. Further, they are involved

in regulating platelet activity and hepatic lipid metabolism [174]. An updated meta-analysis of human studies revealed that low-ratio ω6:ω3 PUFAs supplementation remarkably decreased serum inflammatory factors, including tumour necrosis factor (TNF)-alpha and IL-6 levels [173]. This result was further confirmed in a mouse study [176]. Moreover, although the biological properties of ω3 PUFAs are well-recognized, the link between ω6 and ω3 PUFAs, their bioactive lipid metabolites and inflammation has not yet been entirely elucidated [174].

Proteomic studies in pigs have expanded in recent years [80,81]. Several studies have focused on proteins abundance in sows, such as changes in uterine endometrium [83,84], adipose tissue of fetuses [86], colostrum [88], and mammary tissue [87]. These reports disclosed the mechanisms underlying the molecular responses of sows to the internal and external stressors during gestation. However, inadequate attention has been given to the lactation stage in the sow. Therefore, an enhanced understanding of the protein profile from late gestation to late lactation would explain the molecular mechanisms contributing to a successful reproductive outcome. Furthermore, although numerous studies have investigated the beneficial effects of PUFAs supplementation during gestation and lactation stages [170][94,95,101,104,137,145,166,182], the underlying molecular mechanism of these effects remains to be elucidated. Furthermore, there is no available report in pigs focused on plasma proteome changes between late gestation and late lactation stages.

The present study tested the hypothesis that a low dietary ω6:ω3 fatty acid ratio could affect the plasma proteome during late pregnancy and lactation, two critical periods that reflect physiological adaptations of the sows to ensure maternal health, fetal and postnatal growth. Using a tandem mass tag (TMT)-based proteomics approach, this study provides evidence explaining the mechanism for enhanced survival rate and weight gain observed in piglets born from the mothers fed a low ω6:ω3 ratio in the diets [183]. Additionally, these data demonstrate the benefit of increased ω3 fatty acid in pig feed, which can be used as a complementary resource for human nutrition research.

3.6 MATERIALS AND METHODS

3.6.1 Animals and sample collection

The sow experiment was performed on a private swine farm (Arioli and Sangalli Agricultural Company S.S., Genzone, Italy). The experimental animal protocol was approved by the Ethical Committee of the University of Milan (OPBA 67/2018) and the Italian Ministry of Health (authorization n. 168/2019 PR). The study design with the results of performance, colostrum and milk fatty acid profiles, and oxidative status were previously described in detail in a report on the *in vivo* study results [183].

Sixteen sows were artificially inseminated at the 13th month of age (second parity) and delivered piglets at around 17th month of age. They had the similar bodyweight (202.57 ± 7.16 kg, mean ± SEM) and body condition score (2.36 ± 0.12, mean ± SEM) at the beginning of feeding trial period. Sows were randomly assigned to two isonitrogenous and isoenergetic diets (Table 2-1, Chapter 2), containing either a control ratio of ω6:ω3 PUFAs (CR, 13:1 during gestation, starting from day 28 (G28) and 10:1 during lactation) or a low ratio of ω6:ω3 PUFAs (LR, 4:1, from G28 until the end of lactation (L-End)) (Table 2-2, Chapter 2). They were housed in groups of 8 sows from 7 days after artificial insemination before moving to individual farrowing crates at day 108 of gestation, where they remained until the end of lactation.

Blood samples were collected at G108 and L-End before fresh feed was provided in the afternoon. Ethylenediaminetetraacetic acid (EDTA) tubes (K3E K3EDTA, 9 mL, REF 455036, Greiner Bio-One GmbH) were used for plasma collection. Blood samples were centrifuged (15 min; 3000× *g*; room temperature). The EDTA plasma was aspirated and transferred to microtubes (2.0 mL, Sarstedt AG & Co., Nümbrecht, Germany) before being stored at −80 °C until analysis.

3.6.2 Protein Identification and Quantification using the TMT approach

3.6.2.1 Protein quantification

The plasma samples were quantified for the total protein concentration by Bradford assay (Bio-Rad Protein Assay Dye Reagent Concentrate, Bio-Rad Laboratories GmbH, Müchen, Germany) using bovine serum albumin as standard. Samples were kept at -80 °C until analyses.

3.6.2.2 Protein digestion and Isobaric labeling – tandem mass tag

Samples were analysed for proteome profiling by applying a quantitative Tandem Mass Tagging (TMT) approach as previously described [184]. In general, 100 µg of total plasma protein per sample were converted to peptides using an in-solution digestion method (Filter-aided sample preparation, FASP) with 10 kDa cut-off filters. Briefly, samples (~1.20 µL) were mixed with SDT buffer (4% (w/v) sodium dodecyl sulfate (SDS), 0.1 M Tris/HCL pH 7.6, 0.1 M dithiothreitol (DTT) (Sigma Aldrich, St. Louis, MO, USA), alkylated by adding 0.05 M iodoacetamide (IAA) solution (20 min, room temperature in the dark) (Sigma Aldrich, St. Louis, MO, USA), and depleted of detrimental low-molecular-weight components by filtration with in 8M urea-containing solution (0.1 M Tris/HCL pH 8.5). Protein was digested overnight using 1 µg of trypsin (20 µg/mL, Promega, Madison, WI, USA) resuspended in 0.05 M ammonium bicarbonate (NH4HCO3) buffer, at 1:37 (w/w), at 37 °C. The released peptides were dissolved in 10% acetonitrile (ACN) in water and acidified by 1% trifluoroacetic acid (TFA, CF_3COOH) before vacuum centrifuged at 45 °C until completely dry.

A pooled internal standard (IS) was prepared with equal amounts of peptides from all samples to normalize the data. Subsequently, the peptides (lyophilized protein pellets) from samples and the IS were diluted using 0.1 M triethylammonium bicarbonate (TEAB, Thermo Scientific, Rockford, USA) before being tagged using a freshly prepared TMT11plex Label Reagent set (Thermo Scientific, Rockford, IL, USA). An amount of 25 µL of the appropriate TMT Label Reagent was added to each sample (50 µg protein pellets) for the labeling reaction (60 min, room temperature), and then 8 µL of 5% (w/v) hydroxylamine (Sigma Aldrich, St. Louis, MO, USA) was added to stop the reaction (45 min). Next, ten TMT-modified

peptide samples were combined with the IS (labeled with TMT 126 m/z) in equal amounts into a new microcentrifuge tube, aliquoted, dried, and stored at -80°C until analysis in the mass spectrometer. Two TMT11plex experiments were performed for a total of 20 samples (5 animals per group x 2 groups x 2-time points).

3.6.2.3 Liquid chromatography tandem mass spectrometer (LC-MS/MS)

Labeled dry peptides residues were solubilized in 20 µL of 5% (v/v) ACN with 0.5% (v/v) formic acid using the auto-sampler of a nanoflow uHPLC system (Thermo Scientific RSLCnano). Peptide ions were detected online by electrospray ionisation (ESI) mass spectrometry MS/MS with an Orbitrap Elite MS (Thermo Scientific). LC eluent was ionized by interfacing the LC coupling device to a NanoMate Triversa (Advion Bioscience) with an electrospray voltage of 1.7 kV. An injection volume of 5 µL of peptides was desalted and concentrated for 12 min on the trap column (0.3 × 5 mm) using a flow rate of 25 µL/min with 1% ACN and 0.1% formic acid.

Subsequently, the peptide was separated on a Pepmap C18 reversed-phase column (50 cm × 75 µm, particle size 3 µm, pore size 100 Å, Thermo Scientific) using a solvent gradient at a fixed solvent flow rate of 0.3 µL/min for the analytical column. The solvent compositions contain A) 0.1% formic acid in water and B) 0.08% formic acid in 80% ACN and 20% water. The solvent gradient was 4% (v/v) solvent B for 10 min, 4-60% (v/v) solvent B for 170 min, 60-99% (v/v) solvent B for 15 min, held at 99% (v/v) solvent B for 5 min. Then, the column was re-equilibrated at starting conditions (4% (v/v) solvent B for 10 min) before the next injection.

The mass spectrometer was operated in the Orbitrap Elite, using full-scan MS spectra (m/z 380–1800) at a high resolution of 60,000 RP. Ion fragmentation was performed with collision-induced dissociation (CID) and the top three precursor ions from the MS scan were detected in the linear ion trap. The three precursor ions were also subjected to high energy collision dissociation (HCD) in the HCD collision cell and were detected at a resolution of 30,000 (full-width half-maximum (FWHM) or mass resolving power defined at 400 m/z). Single-charged ions were omitted, and selected precursors ions were added to a dynamic exclusion list for 180 s.

3.6.3 MS/MS data processing

Raw MS/MS spectra were processed, and databases were searched to identify and quantify proteins using the Proteome Discoverer (version 2.4, Thermo Fisher Scientific) with Sequest HT algorithm against *Sus scrofa* FASTA files (downloaded from UniProtKB database on 18/02/2021; 104,940 sequences). The database search was performed with the parameters as follows: two trypsin missed cleavage sites, precursor mass tolerance threshold of 10 ppm and fragment tolerance of 0.02 Da, carbamidomethyl (C) fixed peptide modification; oxidation (M), deamidation (N, Q) and TMT six-plex (K, peptide N-terminus) variable modifications. The significant threshold of the peptide identification was calculated based on a false discovery rate (FDR) of ≤ 1% using the Percolator algorithm based on processing against a decoy database. Proteins were confidently identified with at least two peptides and 5% FDR. Only master proteins were considered for statistical analysis. Significantly altered proteins were defined at an adjusted *p*-value < 0.05, and possible altered proteins were defined at a *p*-value < 0.05. The mass spectrometry proteomics data have been deposited to the ProteomeXchange Consortium via PRIDE [185] partner repository with the dataset identifier PXD030880.

3.6.4 Statistical and Bioinformatics Analysis

3.6.4.1 Statistical analysis for proteomics data

The data at peptide spectrum match (PSM) level were exported from Proteome Discoverer and statistically analysed based on linear mixed-effects models with Empirical Bayes moderation using MSstatsTMT package version 2.0.0 [186] in R version 4.1.0 [187]. Proteins were quantified using only unique peptides and summarized using the median polish method. Each protein was normalized with reference channel (or pooled internal standard channel). The Benjamini-Hochberg procedure was employed to adjust for multiple pairwise comparisons for significant differential abundance of proteins ($p < 0.05$). The adjusted p-value was presented in the last column in Table 3-1.

The volcano plots, heatmaps, and PCA plots were created by applying packages *ggplot2* version 3.3.3 [188] and *ggrepel* version 0.9.1, *ggplot2* version 3.3.3 [188],

and *pheatmap* version 1.0.12, respectively. Venn diagrams were created using web tool Venny 2.1 (https://bioinfogp.cnb.csic.es/tools/venny/) [189].

3.6.4.2 Bioinformatics analysis

The accession numbers of master proteins were converted into the corresponding gene symbols using the online converter of UniProt database. Undefined proteins were replaced with the best match (i.e. largest overlap) on *Sus scrofa* orthologous genes of minimum 70% identity using SmartBLAST tool (https://blast.ncbi.nlm.nih.gov/smartblast/). The protein-protein interaction (PPI) network; Gene Ontology (GO) functional enrichment analysis covering three sub GOs: Biological Process (BP), Molecular Function (MF), and Cellular Component (CC), were retrieved by STRING database version 11.5 [190] using default settings as following: full network, the meaning of network edges = evidence, active interaction sources = all, the minimum required interaction score = medium confidence (0.4). Interactions between desired GO-BP pathways and proteins with significantly different abundances between comparisons were mapped with Cytoscape software v3.8.2 [191]. Significantly enriched (FDR < 0.05) GO terms were submitted into the REVIGO [192] web server (revigo.irb.hr) to omit dispensable terms, using the following settings: whole UniProt as the database, SimRel as semantic similarity measure considering a small similarity threshold of 0.5 at which the term was removed from the list and assigned to a cluster.

3.6.5 Validation of proteomics results

Proteomics results were validated by determining alteration in the non-depleted plasma contents of APOA1, HP, and ITIH4 (pig-MAP), which had shown significantly changed abundances by TMT proteomic analysis to explore the biological significance of the alterations in abundance. Antibody availability was also crucial in using these targets in the validation which uses the samples of the same animals as in proteomic analysis. As APOA1 was not the only apolipoprotein to be altered in abundance and in respect of lipoprotein metabolism of the sows during gestation and lactation, relevant lipid profile parameters in plasma, notably total cholesterol, HDL and LDL cholesterol, and triglyceride (TG), were also assessed.

The plasma level of APOA1 was determined using Western blot, as previously described [193]. Briefly, 10 µg of proteins of each plasma sample (5 samples/group/each time point) was denatured at 95 °C for 4 min in 4x Laemmli buffer and 1 M dithiothreitol (DTT) and separated by electrophoresis on 4-12% Bis-Tris precast Criterion XT gels (Bio-Rad, USA). Resolved proteins were transferred to nitrocellulose membranes which were then stained with 0.1% Ponceau S to confirm equal loading among samples. The membranes were blocked for 1 h with 5% (w/v) skim milk powder in 0.1% (v/v) Tween 20 in Tris-buffered saline (T-TBS) and then immersed overnight at 4 °C with rabbit polyclonal antibody to APOA1 at 1:20,000 dilution (PAA519Po01, Cloud-Clone Corp, USA). Then, the blot was incubated at room temperature with secondary antibody to rabbit IgG conjugated to horseradish peroxidase (HRP, 1:10,000; ab6721, Abcam Ltd. UK) for 1 h. Western blot signal was detected using the enhanced chemiluminescent (ECL) reaction (Thermo Fisher Scientific™, Meridian Rd., Rockford, USA) and visualized using radio-graphic film. The intensity of the protein bands was quantified using Image J NIH software (https://imagej.nih.gov/ij/).

The quantification of HP and ITIH4 (pig-MAP) was performed by ELISA using species-specific kits, as described by the manufacturer (ACUVET ELISA pig-HP and ACUVET ELISA pig-MAP, Acuvet Biotech, Zaragoza, Spain). HP assay used polyclonal antibodies specific for pig HP. The pig-MAP assay was based on two monoclonal antibodies [194]. Both assays use pig-specific standards and are calibrated according to the European Reference Serum for pig acute phase proteins (European Concerted Action QLK5-CT-1999-0153).

Total cholesterol and triglyceride concentrations were measured in the Veterinary Diagnostic Services, School of Veterinary Medicine, University of Glasgow using polychromatic and bichromatic endpoint techniques, respectively, using the biochemical autoanalyzer (Dimension® Xpand Plus™, Siemens Inc., USA). The HDL cholesterol level was determined using the HDL-cholesterol assay kit (ab65390; Abcam, Cambridge, UK) following the manufacturer's instructions, which included initial separation of HDL by precipitation from other lipoproteins followed by a colorimetric assay for cholesterol contained by the HDL. The level of LDL-cholesterol in plasma was determined using the Friedewald equation: LDL cholesterol = Total cholesterol − HDL cholesterol − Triglyceride/5 [195].

3.6.5.1 Statistical analysis for validation data

The proteomic validations for APOA1, HP, and ITIH4 (pig-MAP) were statistically analysed and compared with the proteomic results. Data were checked for normal distribution by the Shapiro-Wilk normality test and homogeneity of variance by Levene's test using R package *car* version 3.0-10. Differences between groups were determined using the linear mixed model by package *lme4* version 1.1-27, multiple pairwise comparisons were performed by the Tukey's post-hoc method and *p*-values were corrected for multiple testing by applying the Benjamini Hochberg method by *lsmeans* package version 2.30-0, separately for each biochemical assay. Fixed effects were sow diet, time, and their interactions. The random effect was an individual animal. Pearson correlation analysis was performed to assess the association between proteomics and validation results for HP and ITIH4 (pig-MAP) concentrations using R package *ggpubr* version 0.4.0. Spearman correlation analysis was applied for APOA1 because western blot results did not show a normal distribution.

The experimental design, pipeline for proteomics analysis (containing sample preparation, TMT labeling, and LC-MS/MS, data analysis, and quantitation), and validation of proteomics results are illustrated in Figure 3-1.

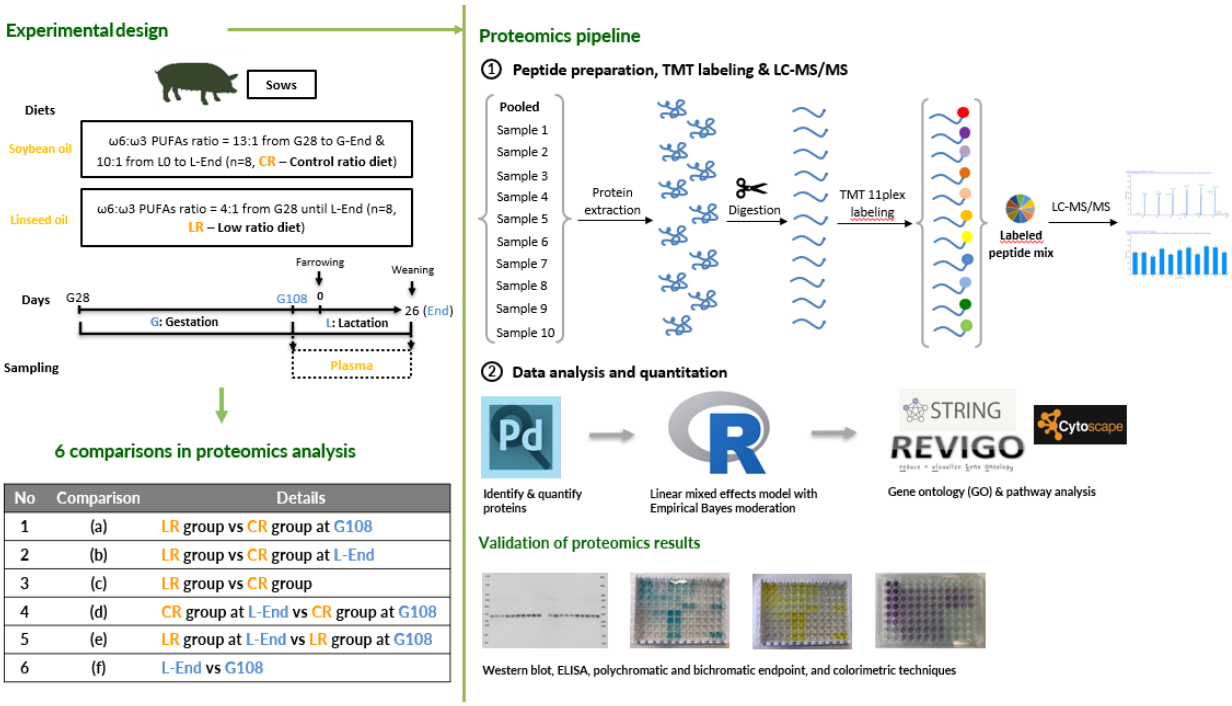

Figure 3-1 The experimental design, proteomics pipeline and validation of proteomics results. Proteomics pipeline contains: (1) Peptide preparation, TMT labeling and LC-MS/MS analysis, (2) Data analysis and quantitation: protein identification and quantitation using Proteome Discoverer, statistical analysis based on the linear mixed-effects model with empirical Bayes moderation (R package MSstatsTMT), bioinformatics analysis (Gene Ontology (GO) enrichment analysis).

3.7 RESULTS

3.7.1 Proteomic analysis

The TMT-based quantitative proteomics approach matched 1149 peptides, which represented 379 proteins and 202 "master" proteins. These terms will be explained as follows for a more comprehensive understanding of the results obtained. Each protein is denoted in UniProt by a distinguish accession number based on its isoform, and a protein can have many isoforms originating from the same gene, which are referred to a diverse set of protein sequences with different numbers of amino acids for the protein compared to the base primary gene (canonical) sequence [196]. The "master" protein is the primary translation product of the coding sequence and expresses at least one of the known protein isoforms, coded by the canonical sequence [197] - the most extended sequence that is most common and similar to orthologous sequences in different species [198]. Proteins are digested into peptides that could be unique for a specific protein or are shared between multiple proteins [199]. A unique peptide is defined as a different combination of amino acid sequence and modifications, regardless of the charge state of the precursor ions [200].

Identified proteins were excluded if they have no unique peptide, only one peptide, and singly charged ions. After filtering, 87 "master" proteins from all replicates and samples were quantified and remained for statistical analysis.

The principal component analysis (PCA) score plot showing the clustering of samples from four groups of sows are represented in Figure 3-2, containing CR group at G108 (CR-G108); CR group at L-End (CR- LEnd); LR group at G108 (LR-G108); and LR group at L-End (LR- LEnd). The analysis of the score plots showed that clusters of CR and LR groups at L-End were differentiated from the samples of both groups at G108, with the first two PCs explaining 60.69% of the total variance (Figure 3-2). Nevertheless, mixed distributions were shown for samples in LR and CR groups at each sampling time. In addition, the differentially abundant proteins (DAPs) were examined via six comparisons in Table 3-1 and Table 3-2. Details of these comparisons are described in Figure 3-1.

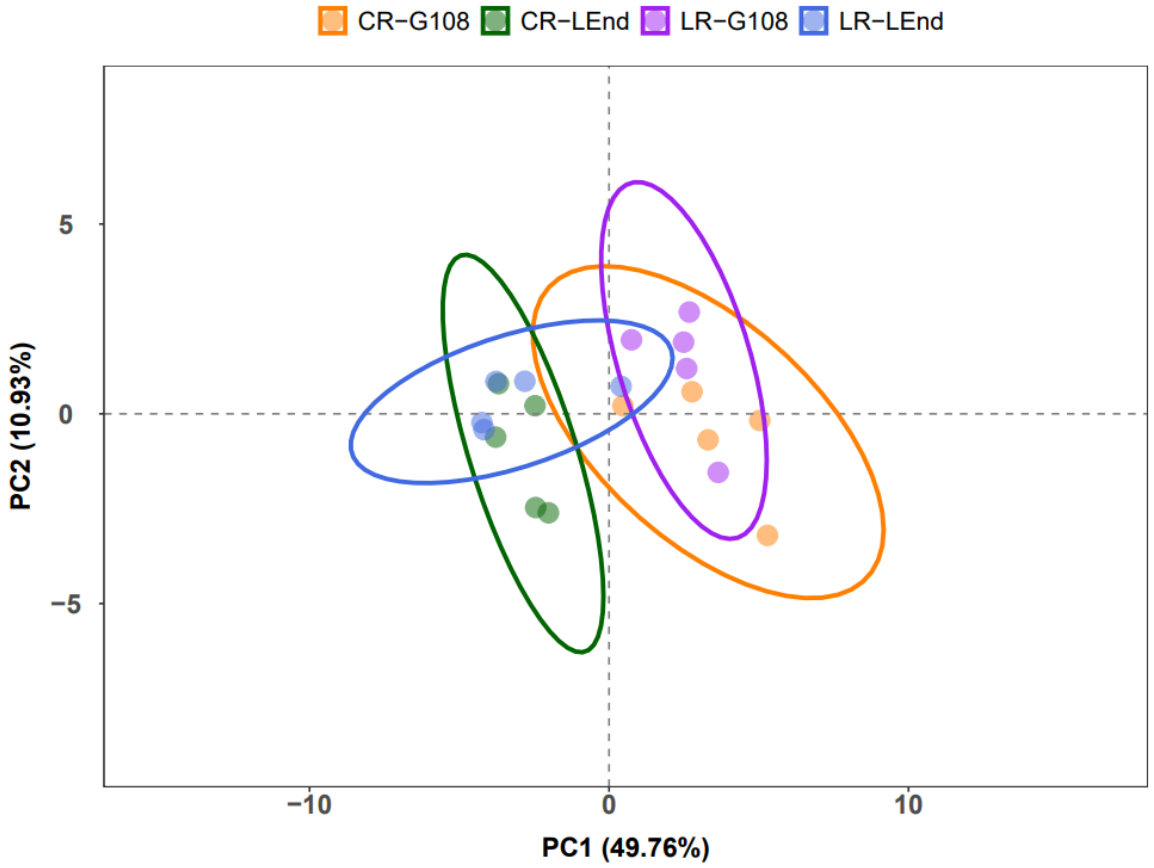

Figure 3-2 Principal component analysis (PCA) score plots showing the clustering of samples from four groups of sows. CR group at G108 (CR-G108, orange dots); CR group at L-End (CR-LEnd, green dots); LR group at G108 (LR-G108, purple dots); LR group at L-End (LR- LEnd, blue dots). The ellipses were drawn at 95% confidence interval of standard error. CR: sow diet with ω6:ω3 ratio=13:1 during gestation, starting from day 28 (G28) and 10:1 during lactation; LR: sow diet with ω6:ω3 ratio=4:1 from G28 until the end of lactation (L-End). G108 = day 108 of gestation.

Table 3-1 The differentially abundant proteins (DAPs) in sow plasma of six comparisons. (a) - LR group versus CR group at G108; (b) - LR group versus CR group at L-End; (c) - LR group versus CR group; (d) - CR group at L-End versus CR group at G108; (e) - LR group at L-End versus LR group at G108; (f) - L-End versus G108. Protein names marked with * were shown as "Uncharacterized protein" in the UniProt *Sus scrofa* database and thus were substituted with the best match on *Sus scrofa* database, using SMARTBLAST tool.

Protein name	Gene names	Accession number[1]	Number of peptides	log2FC[2]	*P*-value	Adjusted *p*-value
Comparison (a) - LR group versus CR group at G108						
Hemopexin	HPX	P50828	14	0.53	0.018	0.708
Alpha-1-antitrypsin/ Serpin Family A Member 1	SERPINA1	P50447	9	0.24	0.043	0.708
Inter-alpha-trypsin inhibitor heavy chain H1	ITIH1	A0A480SQD8	10	0.19	0.026	0.708
Haptoglobin	HP	Q8SPS7	21	-0.32	0.032	0.708
Comparison (b) - LR group versus CR group at L-End: no DAPs						
Comparison (c) - LR group versus CR group						
Hemopexin	HPX	P50828	14	0.49	0.002	0.214
Inter-alpha-trypsin inhibitor heavy chain H1	ITIH1	A0A480SQD8	10	0.12	0.019	0.480
Haptoglobin	HP	Q8SPS7	21	-0.33	0.042	0.734
Serum amyloid P-component	APCS	O19063	3	-0.53	0.022	0.480
SERPIN domain-containing protein	LOC100156325	A0A4X1SGC8	10	-1.23	0.021	0.480
Comparison (d) - CR group at L-End versus CR group at G108						
Fetuin-B isoform 1	FETUB	A0A480SUZ7	2	1.03	<0.001	0.013
Histidine-rich glycoprotein	HRG	A0A481B9A6	12	0.80	<0.001	0.023
Apolipoprotein C-III	APOC3	A0A5G2QLU1	3	0.68	0.006	0.070
Transthyretin	TTR	A0A5G2QIE9	2	0.56	0.041	0.211
Apolipoprotein A-I	APOA1	K7GM40	27	0.47	0.001	0.023
Plasma kallikrein *	KLKB1	A0A4X1VWY2	3	0.47	0.016	0.110
Apolipoprotein A-II	APOA2	A0A4X1VK69	3	0.46	0.008	0.083
Complement C8 alpha chain	C8A	F1S788	3	0.30	0.012	0.091
Transferrin	TF	P09571	54	0.17	0.037	0.204

[1]Accession number from UniProt protein database for Sus scrofa. 2log2FC is base 2 logarithm transformed of fold change value which represents the ratio of abundance levels in the first-mentioned group vs second-mentioned group. Adjusted p-value followed the Benjamini-Hochberg method. CR: sow diet with ω6:ω3 ratio=13:1 during gestation, starting from day 28 (G28) and 10:1 during lactation; LR: sow diet with ω6:ω3 ratio=4:1 from G28 until the end of lactation (L-End). G108 = day 108 of gestation.

(cont., 1).

Protein name	Gene names	Accession number[1]	Number of peptides	log2FC[2]	*P*-value	Adjusted *p*-value
Comparison (d) - CR group at L-End versus CR group at G108 (*cont.*)						
Complement C4 gamma chain	C4A	A0A4X1VBD2	18	-0.20	0.038	0.204
SERPIN domain-containing protein	SERPINF2	A0A4X1U6E7	2	-0.31	<0.001	0.013
Haptoglobin	HP	Q8SPS7	21	-0.40	0.009	0.083
CD5 antigen-like precursor *	CD5L	A0A4X1VVV3	4	-0.44	0.011	0.091
IgM heavy chain constant region *	IGHM	A0A287ALC1	22	-0.55	0.028	0.171
Inter-alpha-trypsin inhibitor heavy chain H4	ITIH4	A0A4X1VPB7	18	-0.80	0.005	0.070
SERPIN domain-containing protein	LOC100156325	A0A4X1SGU6	10	-1.06	0.006	0.070
SERPIN domain-containing protein		A0A4X1SGE8	11	-1.10	0.017	0.110
Comparison (e) - LR group at L-End versus LR group at G108						
Fetuin-B isoform 1	FETUB	A0A480SUZ7	2	1.10	<0.001	0.012
Apolipoprotein C-III	APOC3	A0A5G2QLU1	3	0.66	0.016	0.143
Histidine-rich glycoprotein	HRG	A0A481B9A6	12	0.60	0.010	0.135
Apolipoprotein A-II	APOA2	A0A4X1VK69	3	0.57	0.016	0.143
Apolipoprotein A-I	APOA1	K7GM40	27	0.50	<0.001	0.012
Transthyretin	TTR	A0A5G2QIE9	2	0.48	0.011	0.135
Afamin	AFM	F1RUM1	3	0.45	0.024	0.158
Plasma kallikrein *	KLKB1	A0A4X1VWY2	3	0.42	0.003	0.071
Complement C8 alpha chain	C8A	F1S788	3	0.40	<0.001	0.012
SERPIN domain-containing protein	SERPIND1	A0A4X1UYS0	3	0.24	0.036	0.224
Hemopexin	HPX	P50828	14	0.22	0.005	0.095
SERPIN domain-containing protein	SERPINF2	A0A4X1U6E7	2	-0.23	0.048	0.279
CD5 antigen-like precursor *	CD5L	A0A4X1VVV3	4	-0.49	0.022	0.158
IgM heavy chain constant region *	IGHM	A0A287ALC1	22	-0.51	0.019	0.151
SERPIN domain-containing protein	LOC100156325	A0A4X1SGU6	10	-0.61	0.016	0.143

[1]Accession number from UniProt protein database for Sus scrofa. 2log2FC is base 2 logarithm transformed of fold change value which represents the ratio of abundance levels in the first-mentioned group vs second-mentioned group. Adjusted p-value followed the Benjamini-Hochberg method. CR: sow diet with ω6:ω3 ratio=13:1 during gestation, starting from day 28 (G28) and 10:1 during lactation; LR: sow diet with ω6:ω3 ratio=4:1 from G28 until the end of lactation (L-End). G108 = day 108 of gestation.

(cont., 2).

Protein name	Gene names	Accession number[1]	Number of peptides	log2FC[2]	*P*-value	Adjusted *p*-value
Comparison (f) - L-End versus G108						
Fetuin-B isoform 1	FETUB	A0A480SUZ7	2	1.08	<0.001	<0.001
Histidine-rich glycoprotein	HRG	A0A481B9A6	12	0.70	<0.001	<0.001
Apolipoprotein C-III	APOC3	A0A5G2QLU1	3	0.69	<0.001	0.001
Transthyretin	TTR	A0A5G2QIE9	2	0.52	<0.001	0.006
Apolipoprotein A-II	APOA2	A0A4X1VK69	3	0.52	<0.001	0.002
Apolipoprotein A-I	APOA1	K7GM40	27	0.50	<0.001	<0.001
Plasma kallikrein *	KLKB1	A0A4X1VWY2	3	0.46	<0.001	0.001
Afamin	AFM	F1RUM1	3	0.37	0.006	0.033
Complement C8 alpha chain	C8A	F1S788	3	0.36	<0.001	<0.001
Apolipoprotein-E *	APOE	A0A4X1W1F9	8	0.30	0.023	0.099
SERPIN domain-containing protein	SERPIND1	A0A4X1UYS0	3	0.17	0.014	0.070
Transferrin	TF	P09571	54	0.16	0.007	0.038
C3/C5 convertase (Complement factor B)	CFB	K7GPT9	8	-0.15	0.020	0.093
SERPIN domain-containing protein	SERPINF2	A0A4X1U6E7	2	-0.26	<0.001	0.001
Ficolin-2	FCN2	A0A4X1SUF1	5	-0.36	0.033	0.130
Haptoglobin	HP	Q8SPS7	21	-0.41	0.009	0.045
CD5 antigen-like precursor *	CD5L	A0A4X1VVV3	4	-0.46	<0.001	0.002
IgM heavy chain constant region *	IGHM	A0A287ALC1	22	-0.53	0.001	0.007
Joining chain of multimeric IgA and IgM	JCHAIN	A0A287BQC8	2	-0.55	0.029	0.119
Inter-alpha-trypsin inhibitor heavy chain H4	ITIH4	A0A4X1VPB7	18	-0.60	0.001	0.007
SERPIN domain-containing protein	LOC100156325	A0A4X1SGU6	10	-0.84	<0.001	0.001
SERPIN domain-containing protein		A0A4X1SGE8	11	-1.00	0.004	0.027

[1]Accession number from UniProt protein database for Sus scrofa. 2log2FC is base 2 logarithm transformed of fold change value which represents the ratio of abundance levels in the first-mentioned group vs second-mentioned group. Adjusted p-value followed the Benjamini-Hochberg method. G108 = day 108 of gestation, L-End = the end of lactation.

Table 3-2 The differentially abundant proteins (DAPs) in sow plasma among five comparisons.

Gene	Description	log2FC				
		(a)	(c)	(d)	(e)	(f)
		LR-G108 vs CR-G108	LR vs CR	CR-LEnd vs CR-G108	LR-LEnd vs LR-G108	LEnd vs G108
AFM	Afamin	/	/	/	0.45	0.37
APCS	Serum amyloid P-component	/	-0.53	/	/	/
APOA1	Apolipoprotein A-I	/	/	0.47	0.5	0.5
APOA2	Apolipoprotein A-II	/	/	0.46	0.57	0.52
APOC3	Apolipoprotein C-III	/	/	0.68	0.66	0.69
APOE	Apolipoprotein-E *	/	/	/	/	0.3
C4A	Complement C4 gamma chain	/	/	-0.2	/	/
C8A	Complement C8 alpha chain	/	/	0.3	0.4	0.36
CD5L	CD5 antigen-like precursor *	/	/	-0.44	-0.49	-0.46
CFB	C3/C5 convertase (Complement factor B)	/	/	/	/	-0.15
FCN2	Ficolin-2	/	/	/	/	-0.36
FETUB	Fetuin-B isoform 1	/	/	1.03	1.1	1.08
HP	Haptoglobin	-0.32	-0.33	-0.4	/	-0.41
HPX	Hemopexin	0.53	0.49	/	0.22	/
HRG	Histidine-rich glycoprotein	/	/	0.8	0.6	0.7
IGHM	IgM heavy chain constant region *	/	/	-0.55	-0.51	-0.53
ITIH1	Inter-alpha-trypsin inhibitor heavy chain H1	0.19	0.12	/	/	/
ITIH4	Inter-alpha-trypsin inhibitor heavy chain H4	/	/	-0.8	/	-0.6
JCHAIN	Joining chain of multimeric IgA and IgM	/	/	/	/	-0.55
KLKB1	Plasma kallikrein *	/	/	0.47	0.42	0.46
SERPIN (A0A4X1SGE8)	SERPIN domain-containing protein	/	/	-1.1	/	-1
SERPIN (LOC100156325)	SERPIN domain-containing protein	/	-1.23	-1.06	-0.61	-0.84
SERPINA1	Alpha-1-antitrypsin/ Serpin Family A Member 1	0.24	/	/	/	/
SERPIND1	SERPIN domain-containing protein	/	/	/	0.24	0.17
SERPINF2	SERPIN domain-containing protein	/	/	-0.31	-0.23	-0.26
TF	Transferrin	/	/	0.17	/	0.16
TTR	Transthyretin	/	/	0.56	0.48	0.52

log2FC is base 2 logarithm transformed of fold change value which represents the ratio of abundance levels in the first-mentioned group vs second-mentioned group. Adjusted p-value followed the Benjamini-Hochberg method. CR: sow diet with ω6:ω3 ratio=13:1 during gestation, starting from day 28 (G28) and 10:1 during lactation; LR: sow diet with ω6:ω3 ratio=4:1 from G28 until the end of lactation (L-End). G108 = day 108 of gestation.

3.7.1.1 DAPs in the comparisons between LR and CR groups

Comparison (a): Plasma from low dietary ω6:ω3 ratio (LR) group at G108 showed 4 DAPs; 3 increased and one decreased) when compared to plasma from the control dietary ω6:ω3 ratio (CR) group at G108 (Table 3-1, $p < 0.05$). In comparison (b), plasma from LR sows at L-End versus CR sows at L-End gave no DAP. For comparison (c), plasma from LR sows versus CR sows regardless of sampling time yielded 5 DAPs (2 increased and 3 decreased) (Table 3-1, $p < 0.05$). Of these proteins, hemopexin (HPX) and inter-alpha-trypsin inhibitor heavy chain H1 (ITIH1) were increased, and haptoglobin (HP) was decreased in both (a) and (c) comparisons ($p < 0.05$, Table 3-1 and Table 3-2). Alpha-1-antitrypsin (SERPINA1) was up-regulated in comparison (a) and serum amyloid P-component (APCS) was down-regulated in comparison (c) ($p < 0.05$, Table 3-1). The separating and overlapping DAPs between comparisons (a) and (c) are shown in the Venn diagram (Figure 3-3A) and heatmap (Figure 3-4).

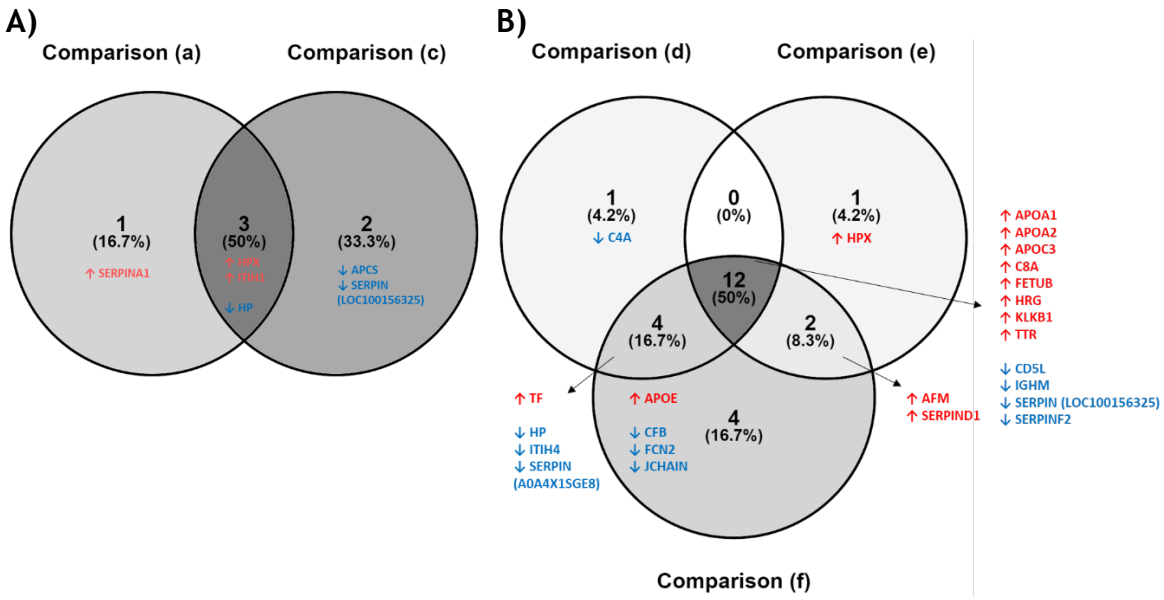

Figure 3-3 Venn diagram representing separated and overlapped differentially abundant proteins (DAPs) among: A) Comparison (a) - LR group versus CR group at G108 and comparison (c) - LR group versus CR group; and B) Comparison (d): CR group at L-End versus CR group at G108, comparison (e): LR group at L-End versus LR group at G108, and comparison (f): both CR and LR groups at L-End versus both groups at G108. CR: sow diet with ω6:ω3 ratio=13:1 during gestation, starting from day 28 (G28) and 10:1 during lactation; LR: sow diet with ω6:ω3 ratio=4:1 from G28 until the end of lactation (L-End). G108 = day 108 of gestation.

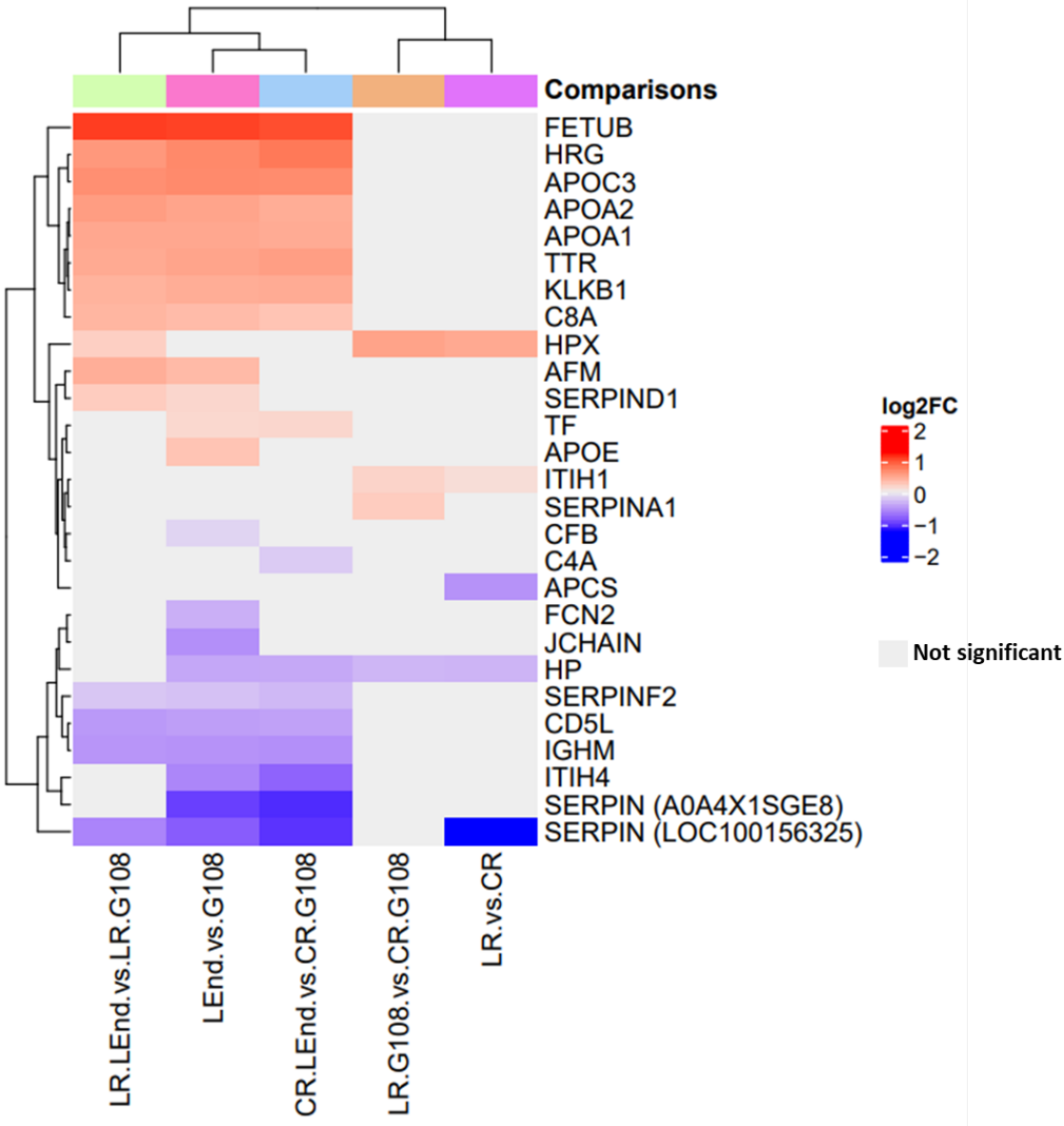

Figure 3-4 Heatmap of the 27 significant differentially abundant proteins (DAPs) among five comparisons : LR-G108 vs CR-G108 (yellow bar, (a)); LR vs CR (purple bar, (c)); CR-LEnd vs CR-G108 (baby blue bar, (d)); LR-LEnd vs LR-G108 (baby green bar, (e)); LEnd vs G108 (pink bar, (f)). CR: sow diet with ω6:ω3 ratio=13:1 during gestation, starting from day 28 (G28) and 10:1 during lactation; LR: sow diet with ω6:ω3 ratio=4:1 from G28 until the end of lactation (L-End). G108 = day 108 of gestation.

The DAPs between LR and CR groups at G108 - comparison (a) are shown in a volcano plot (Figure 3-5A). A mixed distribution with some overlaps of the samples based on the DAPs of this comparison is visualized in the PCA, with a high explained variance of 88.11% (Figure 3-5B), and the DAPs are shown in the hierarchically clustered heatmaps (Figure 3-5C).

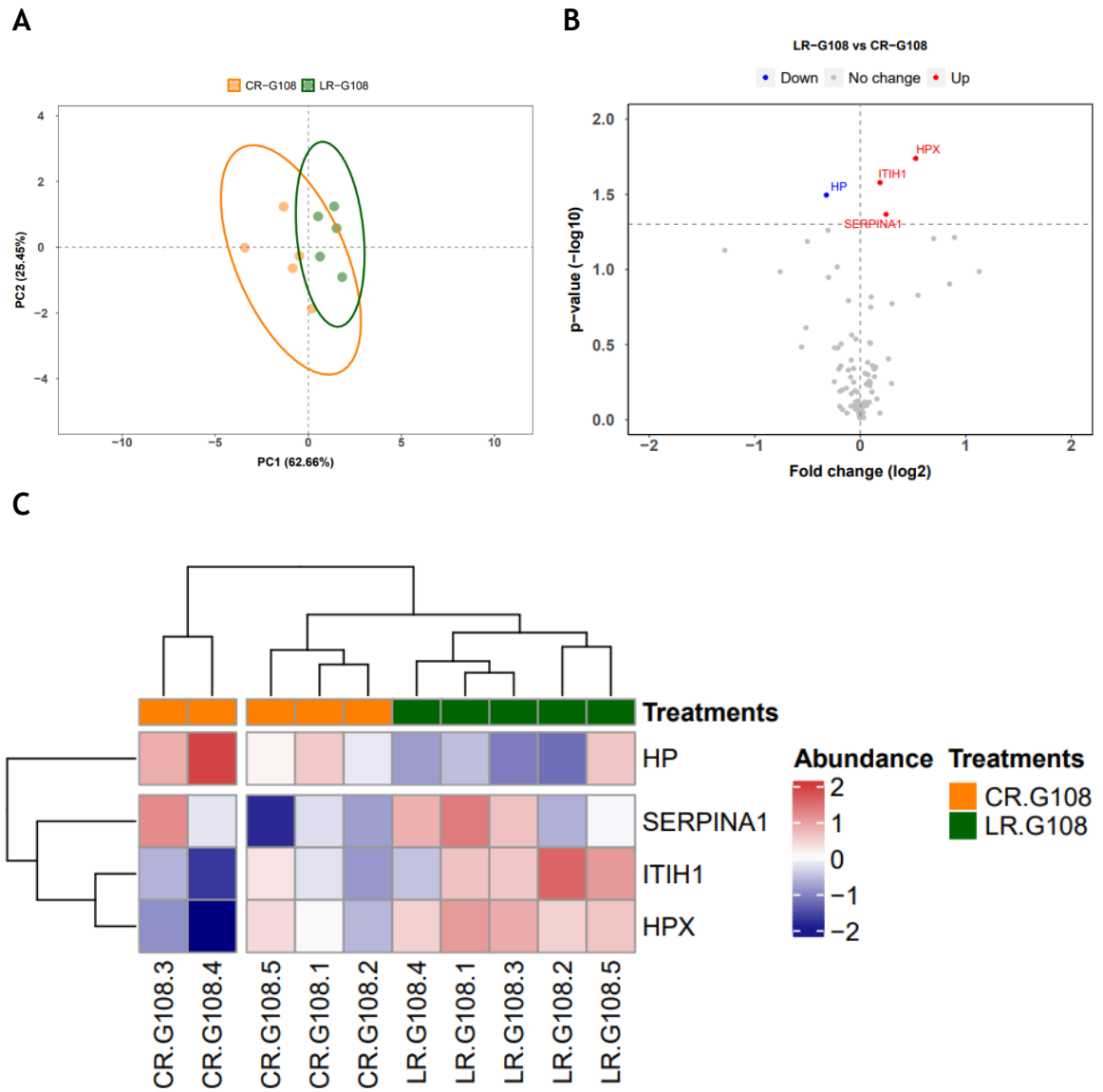

Figure 3-5 A- Principal Components Analysis (PCA) plot, B-Volcano plot, C-Heatmap in comparison (a) - LR versus CR at G108. A, B, and C show the clustering of samples, the differentially abundant proteins (DAPs), and highlighting the proteins changing, respectively. In the PCA, the ellipses represent 95% confidence region. Significant increased proteins in red, significant decreased proteins in blue, and non-significant proteins in grey. CR: sow diet with ω6:ω3 ratio=13:1 during gestation, starting from day 28 (G28) and 10:1 during lactation; LR: sow diet with ω6:ω3 ratio=4:1 from G28 until the end of lactation. G108 = day 108 of gestation.

3.7.1.2 DAPs in the comparisons between L-End and G108 sampling time

Looking at the sampling time, comparison (d) examined CR plasma at L-End compared to CR plasma at G108 and showed 17 DAPs (9 increased and 8 decreased) (Table 3-1, $p < 0.05$). Comparison (e) examined LR plasma at L-End versus LR plasma at G108 and yielded 15 DAPs (11 increased and 4 decreased) (Table 3-1, $p < 0.05$). Comparison (f) determined plasma from L-End versus G108 regardless of dietary treatment and found 22 DAPs (12 increased and 10 decreased) (Table 3-1, $p < 0.05$). Of these proteins, there are 8 proteins increased, and 4 proteins decreased in both (d) and (e); 10 proteins increased, and 4 proteins decreased in both (e) and (f); 9 proteins increased, and 7 proteins decreased in both (d) and (f) (Table 3-2). In all three comparisons, several proteins were all up-regulated such as apolipoprotein A1, A2, and C3 (APOA1, APOA2, APOC3); complement C8 alpha chain (C8A), fetuin-B isoform 1 (FETUB), and histidine-rich glycoprotein (HRG) and some proteins were all down-regulated including CD5 antigen-like precursor (CD5L) and SERPIN domain-containing proteins (SERPINF2 and SERPIN (LOC100156325)). The overlapped DAPs among these three comparisons are represented in the Venn diagram (Figure 3-3B) and heatmap (Figure 3-4).

The DAPs in comparisons (d), (e), and (f) are displayed in the volcano plots (Figures 3-6A, 3-7A, and 3-8A). The PCA plots show clear separations between samples in (d), (e), and (f), with the explained variances of 76.98% (Figure 3-6B), 75.95% (Figure 3-7B), and 62.63% (Figure 3-8B), respectively. The distinct proteome profiles of these comparisons are shown in the hierarchically clustered heatmaps (Figures 3-6C, 3-7C, and 3-8C, respectively).

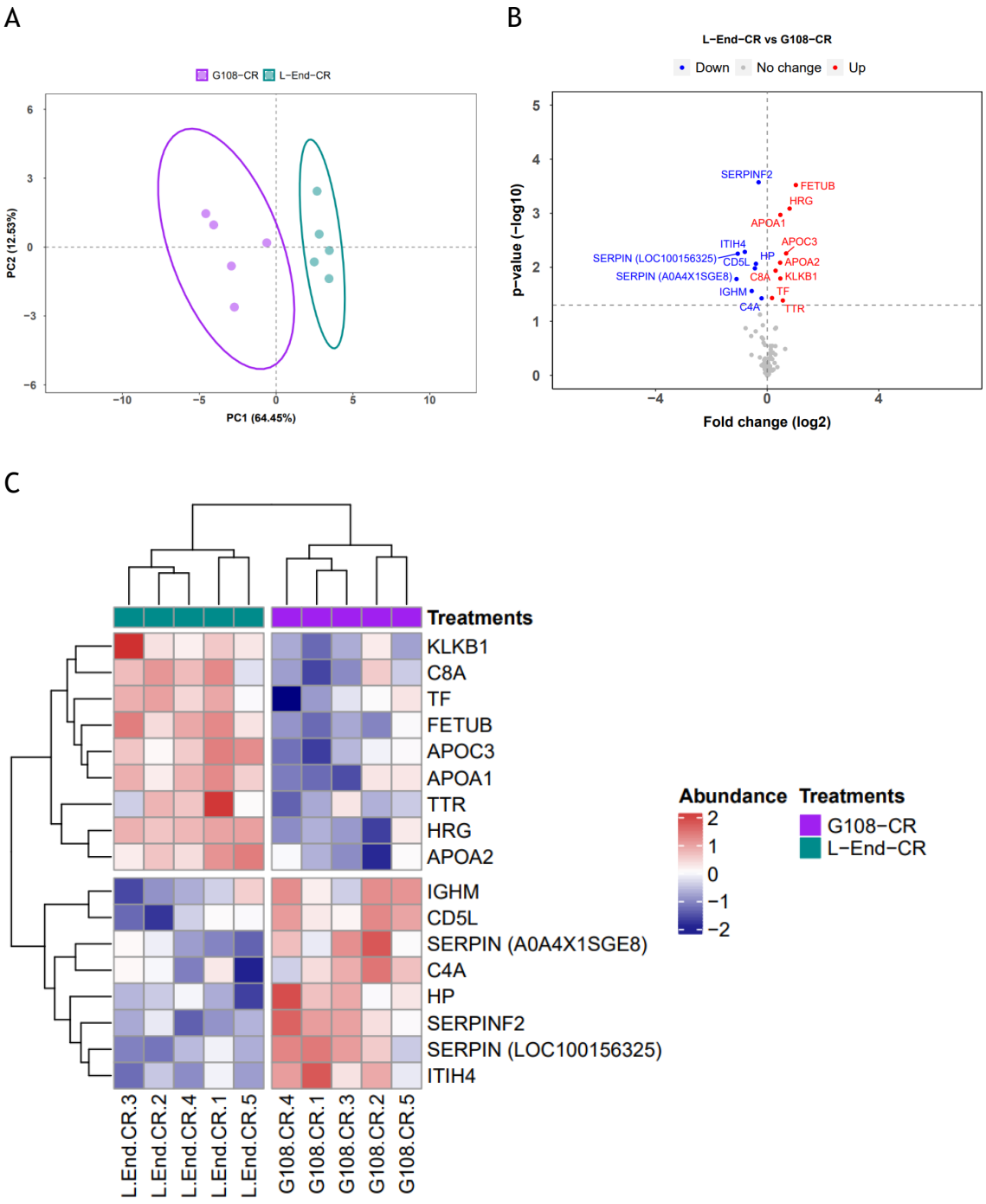

Figure 3-6 A- Principal Components Analysis (PCA) plot, B-Volcano plot, C-Heatmap in comparison (d) - CR at L-End versus CR at G108. A, B, and C show the clustering of samples, the differentially abundant proteins (DAPs), and highlighting the proteins changing, respectively. In the PCA, the ellipses represent 95% confidence region. Significant increased proteins in red, significant decreased proteins in blue, and non-significant proteins in grey. CR: sow diet with ω6:ω3 ratio=13:1 during gestation, starting from day 28 (G28) and 10:1 during lactation. G108 = day 108 of gestation. L-End = the end of lactation.

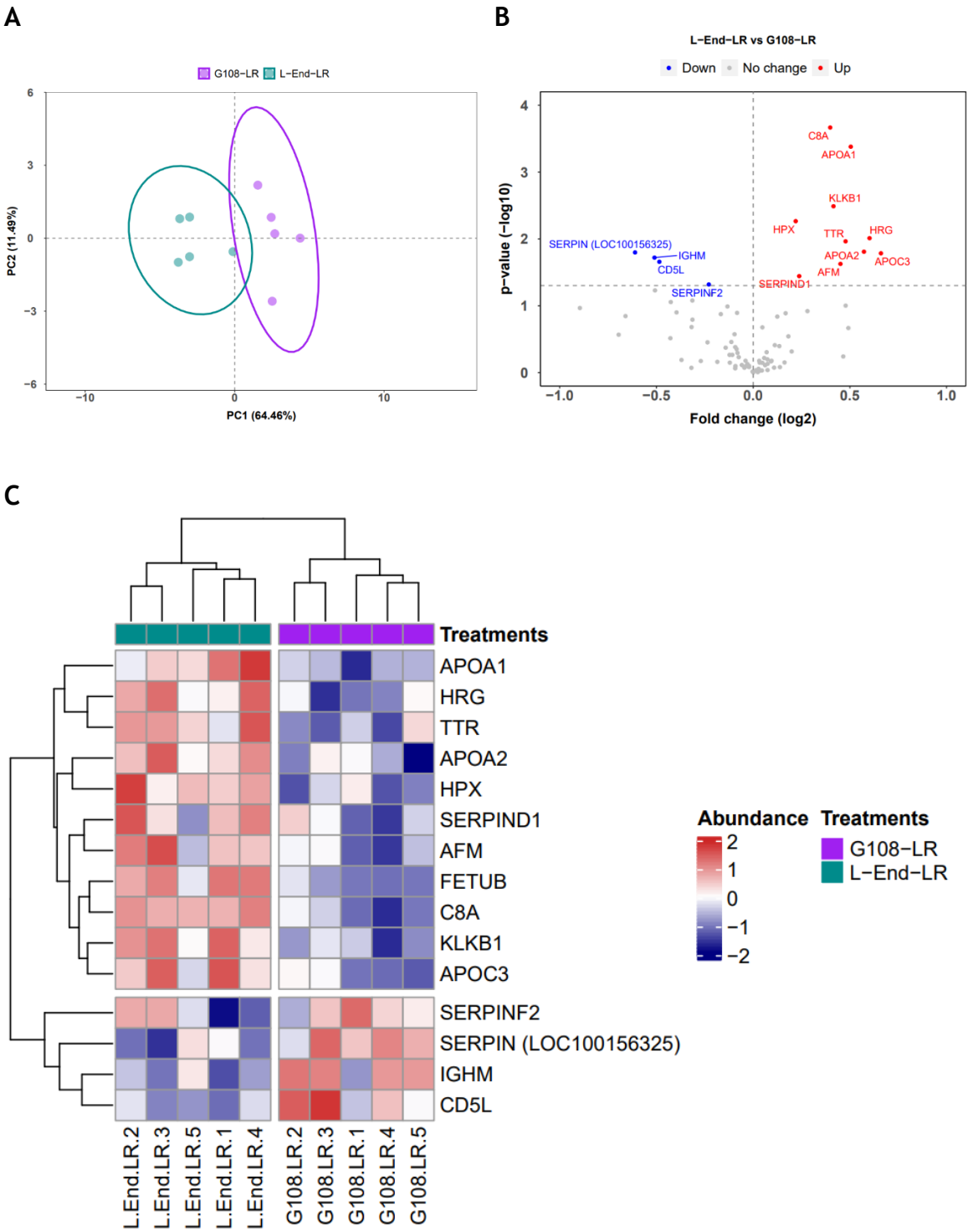

Figure 3-7 A- Principal Components Analysis (PCA) plot, B-Volcano plot, C-Heatmap in comparison (e) - LR at L-End versus LR at G108. A, B, and C show the clustering of samples, the differentially abundant proteins (DAPs), and highlighting the proteins changing, respectively. In the PCA, the ellipses represent 95% confidence region. Significant increased proteins in red, significant decreased proteins in blue, and non-significant proteins in grey. LR: sow diet with ω6:ω3 ratio=4:1 from G28 until the end of lactation (L-End). G108 = day 108 of gestation.

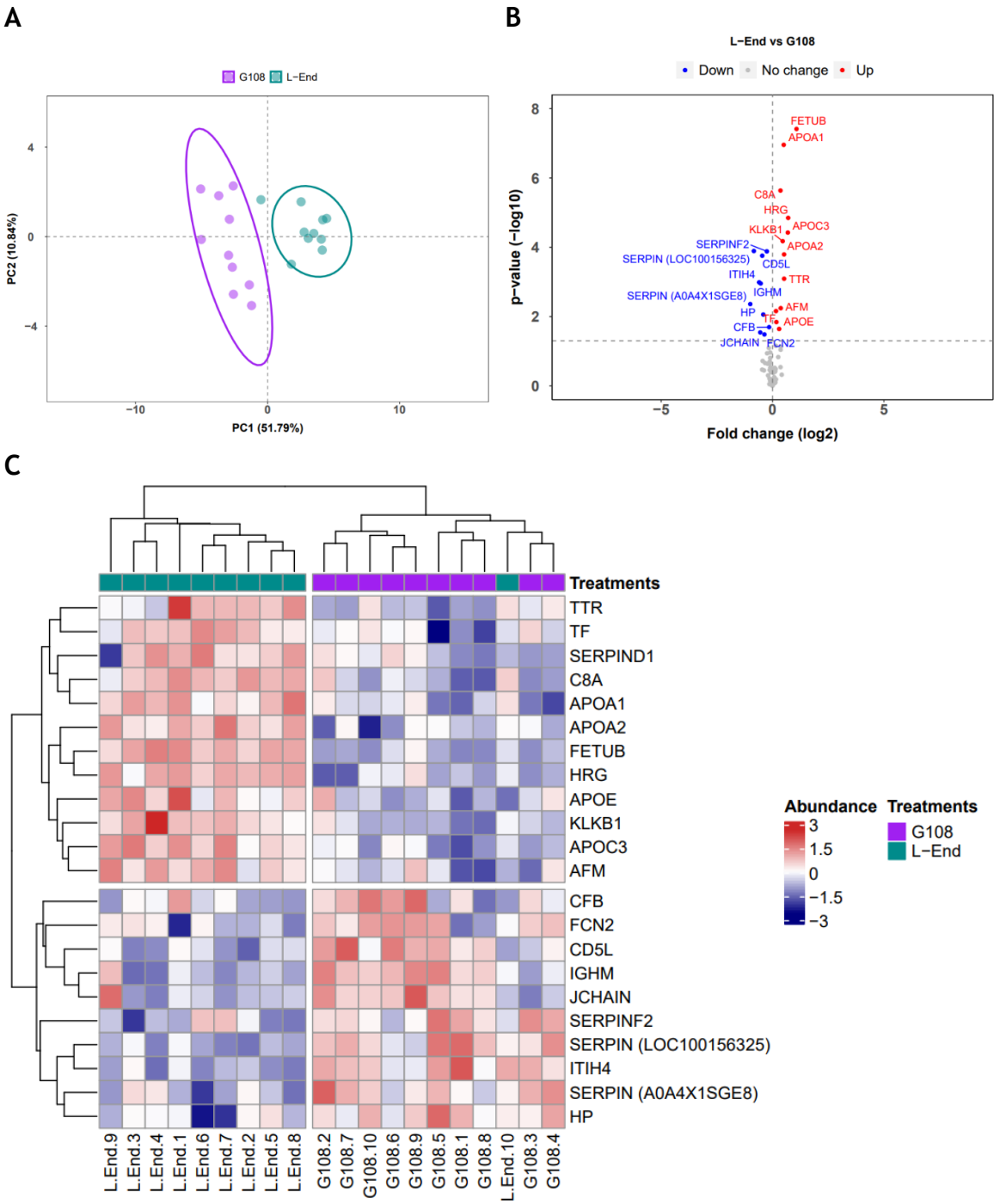

Figure 3-8 A-Principal Components Analysis (PCA) plot, B-Volcano plot, C-Heatmap in comparison (f) - L-End versus G108. A, B, and C show the clustering of samples, the differentially abundant proteins (DAPs), and highlighting the proteins changing, respectively. In the PCA, the ellipses represent 95% confidence region. Significant increased proteins in red, significant decreased proteins in blue, and non-significant proteins in grey. G108 = day 108 of gestation, L-End = the end of lactation.

3.7.1.3 Gene ontology (GO) enrichment of all identified proteins

The protein-protein interaction (PPI) network of all 87 master proteins kept in this work comprises 59 nodes and 628 edges (p < 1.0e-16). The functional enrichments showed 49, 19, and 8 GO terms on BP, MF, and CC, respectively (Table 3-3). The DAPs were primarily involved in response to stimulus [GO:0065007], response to stress [GO:0044238], and organonitrogen compound metabolic process [GO:1905907]. The main functions of these DAPs were serine-type endopeptidase activity [GO:0004252], enzyme regulator activity [GO:0030234], and lipoprotein particle receptor binding [GO:0070325]. They were primarily localized in the cellular anatomical entity [GO:0110165], extracellular space [GO:0005615], and protein-containing complex [GO:0032991]. The top 20, 10, and 5 GO terms in BP, MF, and CC categories, respectively, are illustrated in Figure 3-9.

3.7.1.4 Gene ontology enrichment in the comparisons between LR and CR groups

The DAP PPI network between LR and CR plasma at G108 - comparison (a) contains 4 nodes and 5 edges (p = 8.93e-10). Their list of enriched GO terms is presented in Table 3-4 and Figure 3-10. Regardless of sampling time, the PPI network in the DAPs between LR and CR plasma - comparison (c) contains 5 nodes and 3 edges (p = 1.68e-06), but no significant pathway enrichment was observed. GO analysis on the DAPs in comparison (a) disclosed the interaction between SERPINA1 and ITIH1 in the extracellular region and their contributions to the inhibitor activity of serine-type endopeptidase.

3.7.1.5 Gene ontology enrichment in the comparisons between L-End and G108 sampling times

The PPI network of comparison (d) (CR at L-End versus CR at G108), comparison (e) (LR at L-End versus LR at G108), and comparison (f) (L-End versus G108) contains 16 nodes and 43 edges, 15 nodes and 41 edges, and 21 nodes and 59 edges (p < 1.0e-16). The annotated GO terms corresponding to the DAPs of comparisons (d), (e), and (f) is presented in Tables 3-5, 3-6, and 3-7 (comparisons (d) and (e) do not have GO term in the BP category). The top 20, 5, and 3 leading GO terms in BP, MF, and CC categories, of the PPI network of DAPs in comparison (f), are illustrated in Figure 3-11.

Briefly, GO enrichment analysis on the DAPs in comparisons (d), (e), and (f) highlighted the role of APOA1 in the receptor-binding activity of high-density lipoprotein through its functionally linked to APOC3 in the extracellular space. GO analysis of comparison (f) underlined the interaction between APOA1, APOC3, APOE, complement factor B (CFB), HP, ITIH4 (pig-MAP), and transthyretin (TTR) and their participation in the metabolic process of the organonitrogen compound. APOA1 and APOC3 also contributed to chemical homeostasis through their interactions with transferrin (TF). Furthermore, CFB, HP, and ITIH4 (pig-MAP) play a role in defence response via their interactions with Ficolin-2 (FCN2); and the response to stimulus through their communication with FCN2, APOC3, and TTR. In addition, the contribution of HP and ITIH4 in the acute phase response was demonstrated.

To give an overview of the interaction between the DAPs and significantly enriched GO-BP terms, a network among three main comparisons (i.e. (a), (d), and (e)) was designed (Figure 3-12). In this network, up- and down-regulated proteins separately in each comparison and shared between two of them were mapped with their associated enriched GO terms.

Table 3-3 Gene Ontology (GO) terms on biological processes, molecular function and cellular components of all 87 master proteins kept in sow proteomics study.

GO term ID	Description	Adjusted p-value	Gene count	Matching proteins in PPI network
GO Biological Process (n = 49)				
GO:0043933	Biological regulation	1.29E-12	22	CFB, SERPINA1, HP, APOE, PLG, AMBP, C5, ALB, FGB, CLU, ITIH1, ITIH4, TF, AHSG, F2, C3, HPX, APOC3, APOA1, FCN2, TTR, F12
GO:0065007	Response to stimulus	1.46E-10	18	CFB, HP, PLG, C5, HBA, ALB, FGB, CLU, ITIH4, AHSG, F2, C3, HBB, APOC3, FCN2, TTR, F12, VTN
GO:0050896	Regulation of biological process	2.67E-10	19	CFB, SERPINA1, HP, APOE, PLG, AMBP, C5, ALB, CLU, ITIH1, ITIH4, AHSG, F2, C3, APOC3, APOA1, FCN2, TTR, F12
GO:0044238	Response to stress	1E-09	13	CFB, HP, PLG, C5, ALB, FGB, CLU, ITIH4, AHSG, F2, C3, FCN2, F12
GO:1905907	Organonitrogen compound metabolic process	8.1E-09	14	CFB, HP, APOE, PLG, AMBP, ITIH1, ITIH4, F2, HPX, APOC3, APOA1, ENSSSCG00000016483, TTR, F12
GO:1905952	Regulation of biological quality	1.63E-07	12	PLG, ALB, FGB, CLU, TF, F2, C3, HPX, APOC3, APOA1, TTR, F12
GO:0030212	Negative regulation of hydrolase activity	2.29E-07	7	SERPINA1, AMBP, ITIH1, ITIH4, AHSG, C3, APOC3
GO:0033700	Macromolecule metabolic process	3.61E-07	12	CFB, HP, APOE, PLG, AMBP, ITIH1, ITIH4, F2, APOC3, APOA1, ENSSSCG00000016483, F12
GO:0006950	Regulation of hydrolase activity	5.78E-07	8	SERPINA1, AMBP, ITIH1, ITIH4, AHSG, C3, APOC3, APOA1
GO:0002376	Regulation of proteolysis	9.22E-07	7	SERPINA1, AMBP, CLU, ITIH1, ITIH4, AHSG, C3
GO:0008152	Regulation of response to stimulus	1.04E-06	10	CFB, PLG, C5, CLU, AHSG, F2, C3, APOC3, FCN2, F12
GO:1900221	Inflammatory response	1.05E-06	7	HP, C5, CLU, ITIH4, AHSG, F2, C3
GO:0051179	Cellular process	1.29E-06	17	HP, APOE, AMBP, HBA, ALB, CLU, ITIH1, ITIH4, TF, F2, C3, HPX, HBB, APOC3, APOA1, TTR, VTN

GO term ID	Description	Adjusted p-value	Gene count	Matching proteins in PPI network
GO:0051239	Transport	1.96E-06	10	APOE, HBA, CLU, TF, HPX, HBB, APOC3, APOA1, TTR, VTN
GO:0032501	Regulation of molecular function	2.33E-06	11	SERPINA1, APOE, AMBP, CLU, ITIH1, ITIH4, AHSG, C3, APOC3, APOA1, TTR
GO:0019538	Protein metabolic process	2.41E-06	10	CFB, HP, APOE, PLG, AMBP, F2, APOC3, APOA1, ENSSSCG00000016483, F12
GO:0009605	Primary metabolic process	6.69E-06	12	CFB, HP, APOE, PLG, AMBP, F2, C3, APOC3, APOA1, ENSSSCG00000016483, TTR, F12
GO:0010941	Regulation of cellular process	1.43E-05	13	SERPINA1, HP, APOE, AMBP, ALB, CLU, ITIH1, ITIH4, AHSG, C3, APOC3, APOA1, TTR
GO:0090207	Acute phase response	2.08E-05	4	HP, ITIH4, AHSG, F2
GO:1901564	Complement activation	2.08E-05	4	CFB, C5, C3, FCN2
GO:0051004	Response to external stimulus	2.65E-05	8	CFB, HP, C5, ALB, FGB, CLU, C3, FCN2
GO:0044237	Positive regulation of biological process	3.32E-05	10	CFB, HP, APOE, C5, CLU, AHSG, F2, C3, APOA1, FCN2
GO:0048518	Cellular metabolic process	7.05E-05	11	APOE, AMBP, HBA, ITIH1, ITIH4, C3, HPX, HBB, APOC3, APOA1, TTR
GO:0006952	Blood coagulation	7.28E-05	4	PLG, FGB, F2, F12
GO:0002252	Immune effector process	9.56E-05	5	CFB, C5, CLU, C3, FCN2
GO:0032101	Regulation of cellular metabolic process	0.00016	9	SERPINA1, AMBP, CLU, ITIH1, ITIH4, AHSG, C3, APOC3, APOA1
GO:0006629	Defense response to other organism	0.00016	6	CFB, HP, C5, FGB, C3, FCN2
GO:0034382	Multicellular organismal process	0.00049	9	APOE, PLG, FGB, CLU, F2, APOC3, APOA1, ENSSSCG00000016483, F12
GO:0050794	Cholesterol efflux	0.00058	3	APOE, APOC3, APOA1
GO:0098869	Innate immune response	0.00061	5	CFB, C5, FGB, C3, FCN2

GO term ID	Description	Adjusted p-value	Gene count	Matching proteins in PPI network
GO:0071704	Regulation of vesicle-mediated transport	0.00098	4	CLU, AHSG, APOC3, APOA1
GO:0043170	Lipoprotein metabolic process	0.0014	3	APOE, APOC3, APOA1
GO:0048878	Organic substance transport	0.004	5	APOE, CLU, HPX, APOC3, APOA1
GO:0048519	Regulation of transport	0.0062	5	CLU, AHSG, C3, APOC3, APOA1
GO:0065009	Regulation of lipid localization	0.0076	3	C3, APOC3, APOA1
GO:0097006	Cellular oxidant detoxification	0.009	3	HP, HBA, HBB
GO:0044281	Cellular lipid metabolic process	0.0097	4	C3, APOC3, APOA1, TTR
GO:0009987	Phospholipid efflux	0.0118	2	APOC3, APOA1
GO:0044255	High-density lipoprotein particle assembly	0.0164	2	APOE, APOA1
GO:0071827	Plasma lipoprotein particle remodelling	0.0217	2	APOC3, APOA1
GO:0042157	Regulation of lipoprotein lipase activity	0.0217	2	APOC3, APOA1
GO:0065008	Complement activation, classical pathway	0.0258	2	C5, C3
GO:0030162	Regulation of cholesterol transport	0.0258	2	APOC3, APOA1
GO:0048583	Adaptive immune response	0.0303	3	C5, FGB, C3
GO:0006826	Iron ion transport	0.0309	2	TF, HPX

GO term ID	Description	Adjusted p-value	Gene count	Matching proteins in PPI network
GO:0031329	Regulation of cellular catabolic process	0.0309	3	CLU, APOC3, APOA1
GO:0006066	Alcohol metabolic process	0.0323	3	APOE, APOA1, TTR
GO:0033036	Macromolecule localization	0.0348	4	APOE, CLU, APOC3, APOA1
GO:0042744	Hydrogen peroxide catabolic process	0.0359	2	HBA, HBB
GO Molecular Function (n = 19)				
GO:0005488	Binding	7.83E-08	18	HP, APOE, AMBP, HBA, ALB, CLU, TF, F2, C3, HPX, HBB, APOC3, APOA1, ENSSSCG00000016483, FCN2, TTR, F12, VTN
GO:0004252	Serine-type endopeptidase activity	4.64E-07	6	CFB, HP, PLG, F2, ENSSSCG00000016483, F12
GO:0030234	Enzyme regulator activity	4.64E-07	8	SERPINA1, AMBP, ITIH1, ITIH4, AHSG, C3, APOC3, APOA1
GO:0043167	Ion binding	4.64E-07	13	APOE, HBA, ALB, TF, F2, HPX, HBB, APOC3, APOA1, ENSSSCG00000016483, FCN2, F12, VTN
GO:0070325	Lipoprotein particle receptor binding	1.5E-06	4	APOE, CLU, APOC3, APOA1
GO:0043169	Cation binding	4.32E-06	10	HBA, ALB, TF, F2, HPX, HBB, APOA1, ENSSSCG00000016483, FCN2, F12
GO:0098772	Molecular function regulator	3.33E-05	9	SERPINA1, AMBP, ITIH1, ITIH4, AHSG, C3, APOC3, APOA1, TTR
GO:0046872	Metal ion binding	3.93E-05	9	HBA, ALB, TF, F2, HPX, HBB, ENSSSCG00000016483, FCN2, F12
GO:0005515	Protein binding	0.00015	10	HP, APOE, AMBP, CLU, C3, HBB, APOC3, APOA1, FCN2, TTR
GO:0016787	Hydrolase activity	0.00026	7	CFB, HP, PLG, F2, HPX, ENSSSCG00000016483, F12
GO:0005102	Signalling receptor binding	0.00027	7	APOE, CLU, C3, APOC3, APOA1, FCN2, TTR
GO:0043177	Organic acid binding	0.0065	3	HBA, ALB, HBB

GO term ID	Description	Adjusted p-value	Gene count	Matching proteins in PPI network
GO:0008289	Lipid binding	0.0082	4	APOE, ALB, APOC3, APOA1
GO:0070653	High-density lipoprotein particle receptor binding	0.0091	2	APOC3, APOA1
GO:0030492	Hemoglobin binding	0.014	2	HP, HBB
GO:0020037	Heme binding	0.0202	3	AMBP, HBA, HBB
GO:0005344	Oxygen carrier activity	0.0273	2	HBA, HBB
GO:0019825	Oxygen binding	0.0273	2	HBA, HBB
GO:0001540	Amyloid-beta binding	0.0424	2	APOE, CLU
GO Cellular Component (n = 8)				
GO:0005576	Extracellular region	1.76E-23	24	CFB, SERPINA1, HP, APOE, PLG, AMBP, C5, ALB, FGB, CLU, ITIH1, ITIH4, TF, AHSG, F2, C3, HPX, APOC3, APOA1, ENSSSCG00000016483, FCN2, TTR, F12, VTN
GO:0005615	Extracellular space	2.69E-16	17	SERPINA1, HP, APOE, ALB, CLU, TF, AHSG, F2, C3, HPX, APOC3, APOA1, ENSSSCG00000016483, FCN2, TTR, F12, VTN
GO:0110165	Cellular anatomical entity	4.34E-14	26	CFB, SERPINA1, HP, APOE, PLG, AMBP, C5, HBA, ALB, FGB, CLU, ITIH1, ITIH4, TF, AHSG, F2, C3, HPX, HBB, APOC3, APOA1, ENSSSCG00000016483, FCN2, TTR, F12, VTN
GO:0031012	Extracellular matrix	0.001	4	APOE, AHSG, F2, FCN2
GO:0032991	Protein-containing complex	0.001	8	APOE, HBA, ALB, CLU, HBB, APOC3, APOA1, FCN2
GO:0034363	Intermediate-density lipoprotein particle	0.0097	2	APOE, APOC3
GO:0005833	Hemoglobin complex	0.0205	2	HBA, HBB
GO:0031838	Haptoglobin-hemoglobin complex	0.0205	2	HBA, HBB

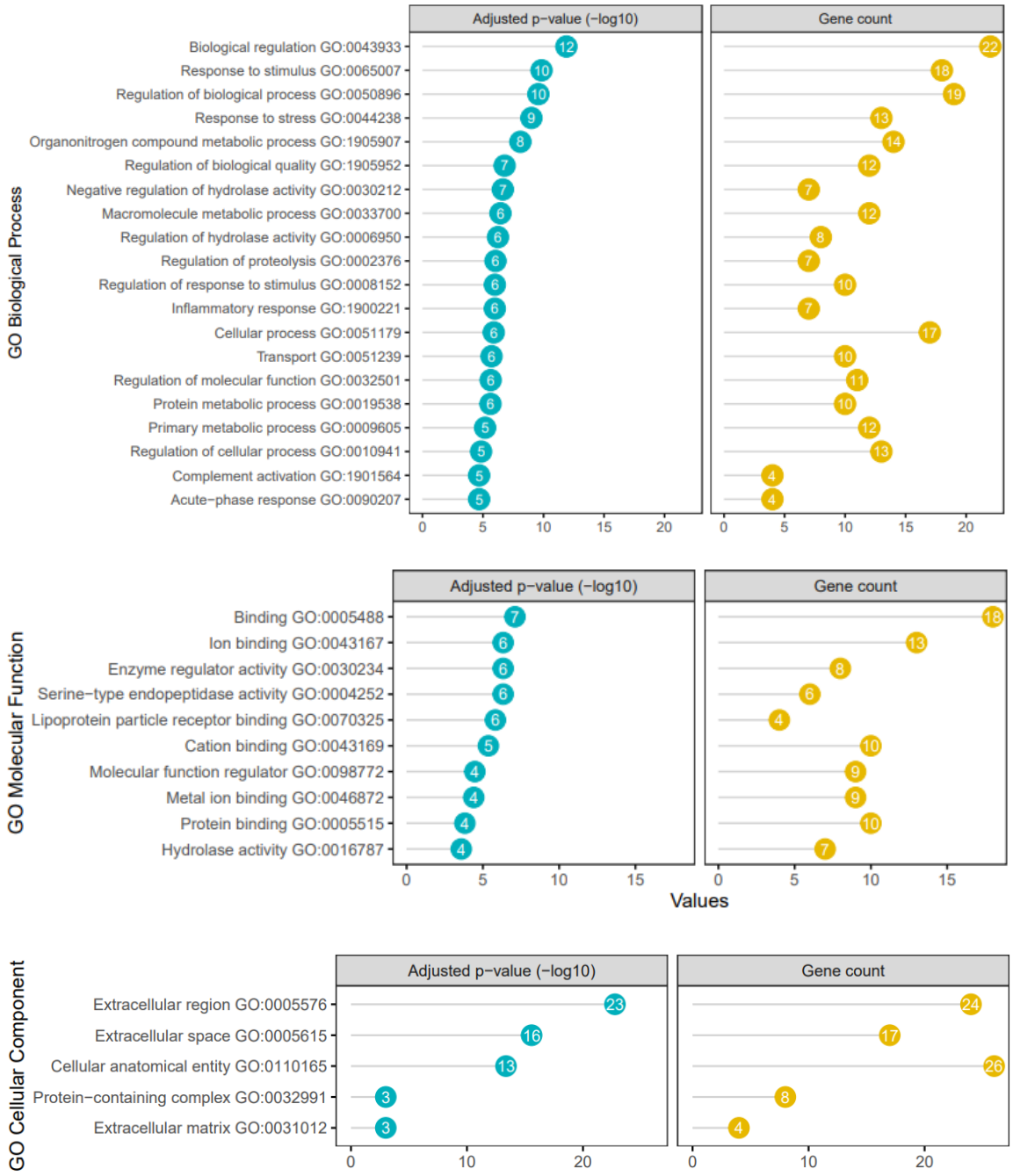

Figure 3-9 Top 20, 10, and 5 GO terms on biological processes, molecular function, and cellular component of all 87 sow plasma proteins with their corresponding gene count inside each term and their associated adjusted *p*-value (expressed as -log10), respectively.

Table 3-4 Gene Ontology (GO) terms on biological processes, molecular function and cellular components in comparison (a) - LR versus CR at G108.

GO term ID	Description	Adjusted p-value	Gene count	Matching proteins in PPI network
GO Biological Process (n = 1)				
GO:0065007	Biological regulation	0.0314	4	SERPINA1, HP, ITIH1, HPX
GO Molecular Function (n = 1)				
GO:0004867	Serine-type endopeptidase inhibitor activity	0.023	2	SERPINA1, ITIH1
GO Cellular Component (n = 2)				
GO:0005576	Extracellular region	0.0002	4	SERPINA1, HP, ITIH1, HPX
GO:0005615	Extracellular space	0.007	3	SERPINA1, HP, HPX

CR: sow diet with ω6:ω3 ratio=13:1 during gestation, starting from day 28 (G28) and 10:1 during lactation; LR: sow diet with ω6:ω3 ratio=4:1 from G28 until the end of lactation. G108 = day 108 of gestation.

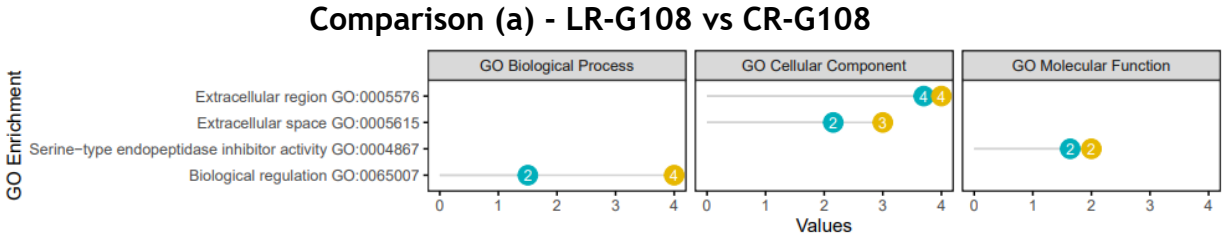

Figure 3-10 Gene ontology analysis of DAPs in comparison (a) - LR versus CR at G108 , with their corresponding gene count inside each term and their associated adjusted *p*-value (expressed as -log10). CR: sow diet with ω6:ω3 ratio=13:1 during gestation, starting from day 28 (G28) and 10:1 during lactation; LR: sow diet with ω6:ω3 ratio=4:1 from G28 until the end of lactation. G108 = day 108 of gestation.

Table 3-5 Gene Ontology (GO) terms on biological processes, molecular function and cellular components in comparison (d) - CR at L-End versus CR at G108.

GO term ID	Description	Adjusted p-value	Gene count	Matching proteins in PPI network
GO Molecular Function (n = 1)				
GO:0070653	High-density lipoprotein particle receptor binding	0.0161	2	APOC3, APOA1
GO Cellular Component (n = 3)				
GO:0005576	Extracellular region	0.00041	6	HP, ITIH4, TF, APOC3, APOA1, TTR
GO:0005615	Extracellular space	0.00091	5	HP, TF, APOC3, APOA1, TTR
GO:0042627	Chylomicron	0.0063	2	APOC3, APOA1

CR: sow diet with ω6:ω3 ratio=13:1 during gestation, starting from day 28 (G28) and 10:1 during lactation. G108 = day 108 of gestation. L-End = the end of lactation.

Table 3-6 Gene Ontology (GO) terms on biological processes, molecular function and cellular components in comparison (e) - LR at L-End versus LR at G108.

GO term ID	Description	Adjusted p-value	Gene count	Matching proteins in PPI network
GO Molecular Function (n = 1)				
GO:0070653	High-density lipoprotein particle receptor binding	0.0141	2	APOC3, APOA1
GO Cellular Component (n = 2)				
GO:0042627	Chylomicron	0.0165	2	APOC3, APOA1
GO:0005615	Extracellular space	0.0166	4	HPX, APOC3, APOA1, TTR

LR: sow diet with ω6:ω3 ratio=4:1 from G28 until the end of lactation (L-End). G108 = day 108 of gestation.

Table 3-7 Gene Ontology (GO) terms on biological processes, molecular function and cellular components in comparison (f) - L-End versus G108.

GO term ID	Description	Adjusted p-value	Gene count	Matching proteins in PPI network
GO Biological Process (n = 27)				
GO:0065007	Biological regulation	0.00042	9	CFB, HP, APOE, ITIH4, TF, APOC3, APOA1, FCN2, TTR
GO:1901564	Organonitrogen compound metabolic process	0.00052	7	CFB, HP, APOE, ITIH4, APOC3, APOA1, TTR
GO:0071827	Plasma lipoprotein particle organization	0.00055	3	APOE, APOC3, APOA1
GO:0097006	Regulation of plasma lipoprotein particle levels	0.00055	3	APOE, APOC3, APOA1
GO:0042157	Lipoprotein metabolic process	0.00056	3	APOE, APOC3, APOA1
GO:0043170	Macromolecule metabolic process	0.0013	6	CFB, HP, APOE, ITIH4, APOC3, APOA1
GO:0006629	Lipid metabolic process	0.0045	4	APOE, APOC3, APOA1, TTR
GO:0006810	Transport	0.0047	5	APOE, TF, APOC3, APOA1, TTR
GO:0019538	Protein metabolic process	0.0047	5	CFB, HP, APOE, APOC3, APOA1
GO:0034382	Chylomicron remnant clearance	0.0047	2	APOE, APOC3
GO:0044238	Primary metabolic process	0.0054	6	CFB, HP, APOE, APOC3, APOA1, TTR
GO:0033700	Phospholipid efflux	0.0063	2	APOC3, APOA1
GO:0006066	Alcohol metabolic process	0.0084	3	APOE, APOA1, TTR
GO:0006952	Defence response	0.0087	4	CFB, HP, ITIH4, FCN2
GO:0010896	Regulation of triglyceride catabolic process	0.0087	2	APOC3, APOA1
GO:0050896	Response to stimulus	0.0087	6	CFB, HP, ITIH4, APOC3, FCN2, TTR
GO:0051004	Regulation of lipoprotein lipase activity	0.01	2	APOC3, APOA1
GO:0065009	Regulation of molecular function	0.01	5	APOE, ITIH4, APOC3, APOA1, TTR
GO:0032374	Regulation of cholesterol transport	0.011	2	APOC3, APOA1

GO term ID	Description	Adjusted p-value	Gene count	Matching proteins in PPI network
GO:0048518	Positive regulation of biological process	0.0114	5	CFB, HP, APOE, APOA1, FCN2
GO:0050794	Regulation of cellular process	0.0128	6	HP, APOE, ITIH4, APOC3, APOA1, TTR
GO:0009987	Cellular process	0.0137	7	HP, APOE, ITIH4, TF, APOC3, APOA1, TTR
GO:0044281	Small molecule metabolic process	0.0153	4	APOE, ITIH4, APOA1, TTR
GO:0044255	Cellular lipid metabolic process	0.0163	3	APOC3, APOA1, TTR
GO:0006953	Acute phase response	0.0178	2	HP, ITIH4
GO:0044237	Cellular metabolic process	0.0359	5	APOE, ITIH4, APOC3, APOA1, TTR
GO:0048878	Chemical homeostasis	0.0383	3	TF, APOC3, APOA1
GO Molecular Function (n = 7)				
GO:0070325	Lipoprotein particle receptor binding	0.00014	3	APOE, APOC3, APOA1
GO:0005102	Signalling receptor binding	0.0028	5	APOE, APOC3, APOA1, FCN2, TTR
GO:0005515	Protein binding	0.0073	6	HP, APOE, APOC3, APOA1, FCN2, TTR
GO:0070653	High-density lipoprotein particle receptor binding	0.0073	2	APOC3, APOA1
GO:0005488	Binding	0.0142	7	HP, APOE, TF, APOC3, APOA1, FCN2, TTR
GO:0008289	Lipid binding	0.0331	3	APOE, APOC3, APOA1
GO:0043167	Ion binding	0.0464	5	APOE, TF, APOC3, APOA1, FCN2
GO Cellular Component (n = 3)				
GO:0005576	Extracellular region	7.41E-08	9	CFB, HP, APOE, ITIH4, TF, APOC3, APOA1, FCN2, TTR
GO:0005615	Extracellular space	3.08E-06	7	HP, APOE, TF, APOC3, APOA1, FCN2, TTR
GO:0034363	Intermediate-density lipoprotein particle	0.0015	2	APOE, APOC3

G108 = day 108 of gestation. L-End = the end of lactation.

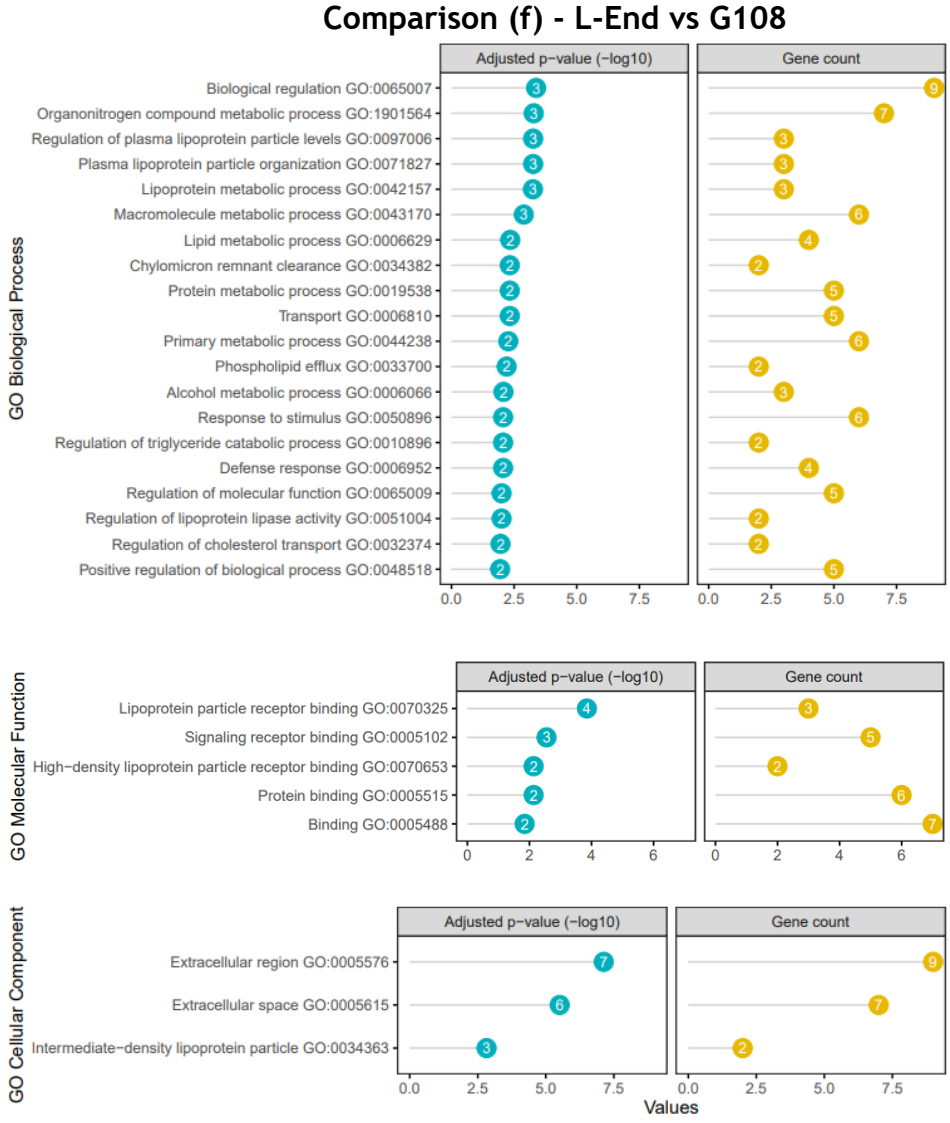

Figure 3-11 Gene ontology analysis of DAPs in comparison (f) - L-End versus G108 , with their corresponding gene count inside each term and their associated adjusted p-value (expressed as -log10). Top 20, 5, and all GO terms on biological processes, molecular function, and cellular component, respectively, are illustrated. CR: sow diet with ω6:ω3 ratio=13:1 during gestation, starting from day 28 (G28) and 10:1 during lactation; LR: sow diet with ω6:ω3 ratio=4:1 from G28 until the end of lactation (L-End). G108 = day 108 of gestation.

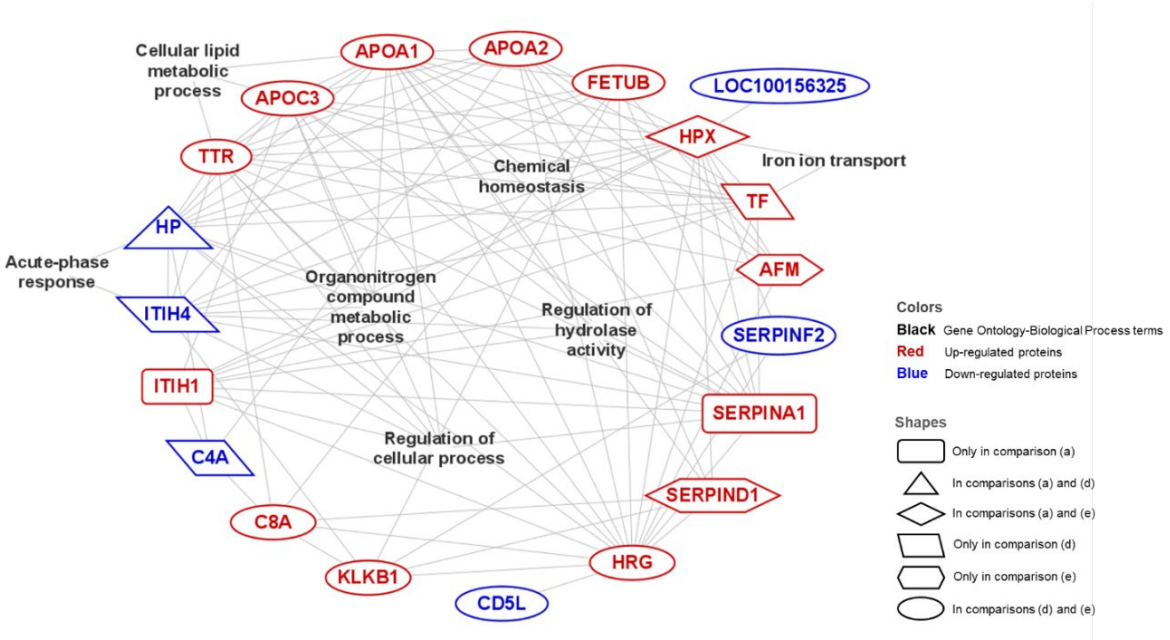

Figure 3-12 Network of DAPs among comparisons (a), (d), and (e) with significantly enriched Gene Ontology-Biological Process terms. Comparison (a) - LR versus CR at G108; (d) - CR at L-End versus CR at G108; and (e) - LR at L-End versus LR at G108. CR: sow diet with ω6:ω3 ratio=13:1 during gestation, starting from day 28 (G28) and 10:1 during lactation; LR: sow diet with ω6:ω3 ratio=4:1 from G28 until the end of lactation (L-End). G108 = day 108 of gestation.

3.7.2 Validation of proteomics results

Results of validation assays for apolipoprotein A1 (APOA1), haptoglobin (HP), and ITIH4 (pig-MAP), together with their respective protein abundance values determined by proteomics; is presented in Table 3-8 and visualized in Figure 3-13. In addition, plasma levels of total cholesterol, high-density lipoprotein (HDL) cholesterol, low-density lipoprotein (LDL) cholesterol, and triglyceride (TG) in four groups of sows are also shown in Figure 3-13.

3.7.2.1 Apolipoprotein A1

Western blot images of APOA1 in plasma samples from two groups of sows at two sampling times are presented in Figure 3-13A1. Clear bands corresponding to APOA1 (Mw 26 kDa) were detected in all samples. Statistical analysis of the band intensity for each group showed significant increases of APOA1 at L-End compared to G108 sampling time (Table 3-8, p = 0.001). However, there was no significant difference in APOA1 concentration between LR plasma compared to CR plasma. Moreover, no effect of interaction between sow diet and time was found. A significantly higher concentration of APOA1 was determined at L-End compared to

G108 within CR group (Table 3-8, p = 0.011), within LR group (Table 3-8, p = 0.037); in LR compared to CR groups and vice versa (Table 3-8, both p = 0.011). The relative abundance quantified by proteomics showed a similar increasing pattern of APOA1 at L-End compared to G108 (Figure 3-13A2, p < 0.001), as observed in validated APOA1 concentration. The overall evaluation found a strong correlation between validated APOA1 concentration and APOA1 proteomics relative abundance (Figure 3-14A, R = 0.68, p = 0.0013).

3.7.2.2 Haptoglobin (HP) and ITIH4 (pig-MAP)

HP and ITIH4 concentrations were significantly decreased at L-End compared to G108 (Figure 3-13B1 and 3-13C1, respectively, both p = 0.01). A significant decrease of HP concentration from G108 to L-End was found when compared CR group at G108 to LR group at L-End (Table 3-8, p = 0.015). The proteomics relative abundance showed a similar decreasing pattern of HP and ITIH4 at L-End compared to G108 (Figure 3-13B2 and 3-13C2, p = 0.0009 and p = 0.0003, respectively); as shown in their validated concentrations. The proteomics abundance pattern of HP was supported by a strong correlation between HP abundance and validated HP concentration (Figure 3-14B, R = 0.85, p = 2.3e-06). Similarly, validated ITIH4 concentration was strongly correlated to ITIH4 proteomics abundance (Figure 3-14C, R = 0.96, p = 4.2e-11). No effect of either sow diet or sow diet - time interaction was revealed.

3.7.2.3 Total cholesterol, HDL- and LDL-cholesterol, and triglyceride

Total cholesterol level significantly increased at L-End compared to G108 sampling time (Figure 3-13D1, p = 0.0001). A highly significant increase of total cholesterol at L-End compared to G108 was observed in the CR group (p = 0.002), in the LR group (p = 0.006), in LR compared to CR groups and vice versa (both p = 0.002). Effects of sow diet and sow diet-time interaction on total cholesterol level were not found. HDL-cholesterol significantly increased at L-End compared to G108 sampling time (Figure 3-13D2, p = 1.353e-06). A highly significant increase of HDL-cholesterol at L-End compared to G108 was observed in the CR group (Table 3-8, p = 0.001), in the LR group (Table 3-8, p = 0.001); in LR compared to CR groups, and vice versa (Table 3-8, both p < 0.001). Additionally, HDL-cholesterol level in plasma was not affected by either sow diet or sow diet-time interaction. Moreover, there were no significant differences between groups or sampling times for LDL-cholesterol and TG (Figure 3-13E1 and 3-13E2, respectively).

Table 3-8 Results of validation assays for the concentrations of apolipoprotein A1 (APOA1), haptoglobin (HP), and pig-MAP (ITIH4) are presented with their respective protein abundance values determined by proteomics. In addition, plasma levels of total cholesterol, high-density lipoprotein (HDL) cholesterol, low-density lipoprotein (LDL) cholesterol, and triglyceride (TG) in four groups of sows are shown. Difference between groups was analyzed separately for each tested protein and validation method.

Sow diet (S)		G108		L-End		SEM	*P*-value								
Time point (T)		CR (LSM)	LR (LSM)	CR (LSM)	LR (LSM)		S	T	S*T	LR-G108 vs CR-G108	CR-LEnd vs CR-G108	LR-LEnd vs CR-G108	CR-LEnd vs LR-G108	LR-LEnd vs LR-G108	LR-LEnd vs CR-LEnd
APOA1	Proteomics (relative abundance)	6.92^{a}	7.02^{a}	7.47^{b}	7.47^{b}	0.11	0.616	<0.001	0.626	0.583	0.018	0.012	0.018	0.026	0.992
	Western blot assay (optical density – arbitrary units)	9884^{a}	9695^{a}	17882^{b}	21076^{b}	713.00	0.890	0.001	0.412	0.626	0.011	0.011	0.011	0.037	0.591
HP	Proteomics (relative abundance)	7.53^{c}	7.21^{bc}	7.13^{ab}	6.78^{a}	0.12	0.064	<0.001	0.894	0.109	0.016	0.007	0.652	0.016	0.109
	ELISA assay (mg/mL)	1.70^{b}	1.28^{ab}	1.15^{ab}	0.96^{a}	0.15	0.080	0.010	0.400	0.110	0.061	0.015	0.550	0.211	0.448
pig-MAP (ITIH4)	Proteomics (relative abundance)	7.34^{b}	7.13^{b}	6.54^{a}	6.73^{a}	0.16	0.964	<0.001	0.071	0.394	0.002	0.031	0.031	0.031	0.394
	ELISA assay (mg/mL)	1.35^{a}	1.15^{a}	0.70^{a}	0.85^{a}	0.18	0.902	0.010	0.274	0.520	0.114	0.182	0.182	0.327	0.549
Total cholesterol	Total cholesterol measurement (mmol/L)	1.14^{a}	1.28^{a}	2.19^{b}	2.10^{b}	0.15	0.885	<0.001	0.423	0.615	0.002	0.002	0.002	0.006	0.661
HDL cholesterol	HDL cholesterol assay (mmol/L)	0.43^{a}	0.42^{a}	1.10^{b}	1.13^{b}	0.09	0.926	<0.001	0.842	0.940	0.001	<0.001	<0.001	0.001	0.940
LDL cholesterol	LDL cholesterol (mmol/L)	0.64^{a}	0.79^{a}	1.01^{a}	0.89^{a}	0.13	0.951	0.058	0.238	0.524	0.233	0.454	0.454	0.524	0.524
Triglyceride	Triglyceride measurement (mmol/L)	0.31^{a}	0.36^{a}	0.42^{a}	0.43^{a}	0.07	0.662	0.229	0.788	0.742	0.742	0.742	0.742	0.742	0.904

CR: sow diet with ω6:ω3 ratio=13:1 during gestation, starting from day 28 (G28) and 10:1 during lactation; LR: sow diet with ω6:ω3 ratio=4:1 from G28 until the end of lactation (L-End). G108 = day 108 of gestation. LSM = least square mean, SEM = standard error of the mean.

A1

sow diet: p=0.89
time: p=0.001 **
sow diet x time: p=0.41

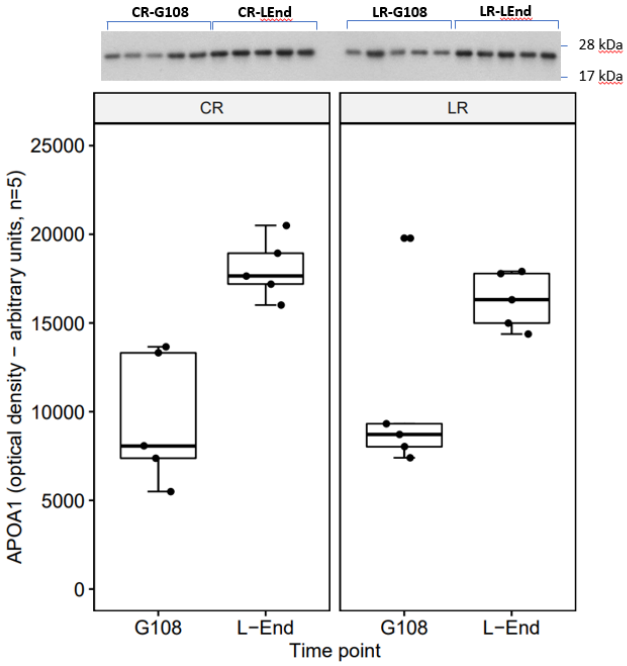

A2

sow diet: p=0.62
time: p=0.0002 ***
sow diet x time: p=0.63

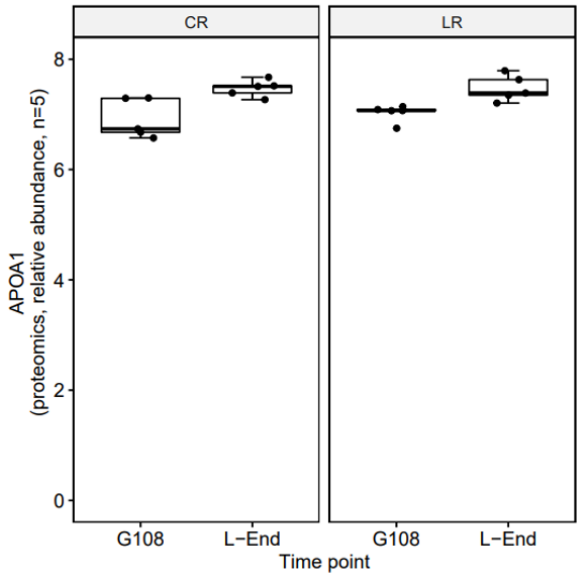

B1

sow diet: p=0.08
time: p=0.01 *
sow diet x time: p=0.40

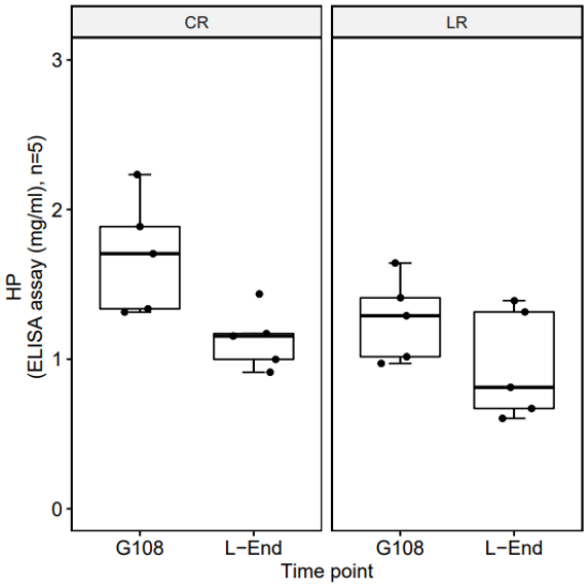

B2

sow diet: p=0.06
time: p=0.0009 ***
sow diet x time: p=0.89

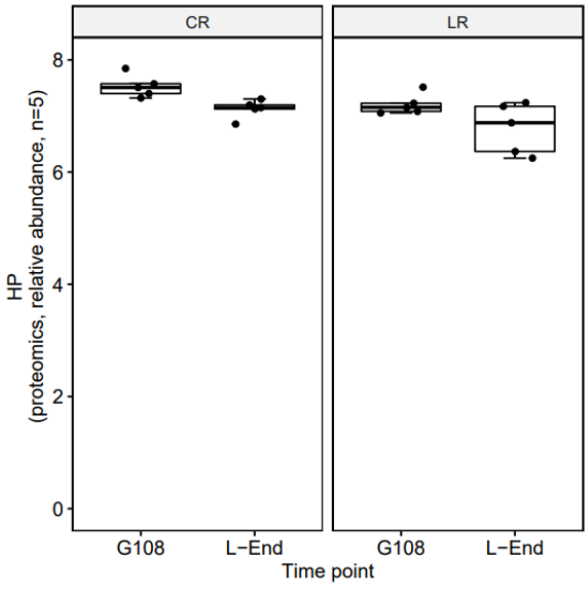

C1

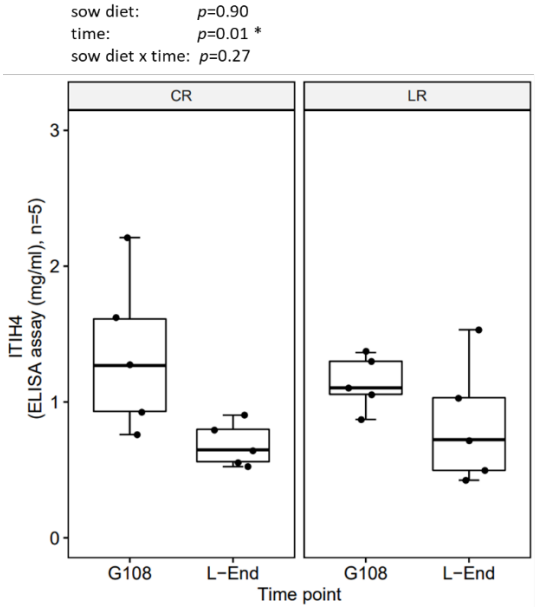
sow diet: p=0.90
time: p=0.01 *
sow diet x time: p=0.27
CR
LR
ITIH4 (ELISA assay (mg/ml), n=5)
G108
L−End
Time point

C2

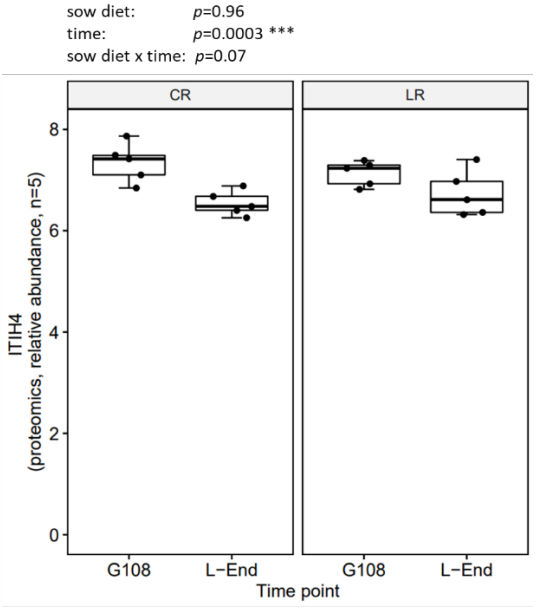
sow diet: p=0.96
time: p=0.0003 ***
sow diet x time: p=0.07
CR
LR
ITIH4 (proteomics, relative abundance, n=5)
G108
L−End
Time point

D1

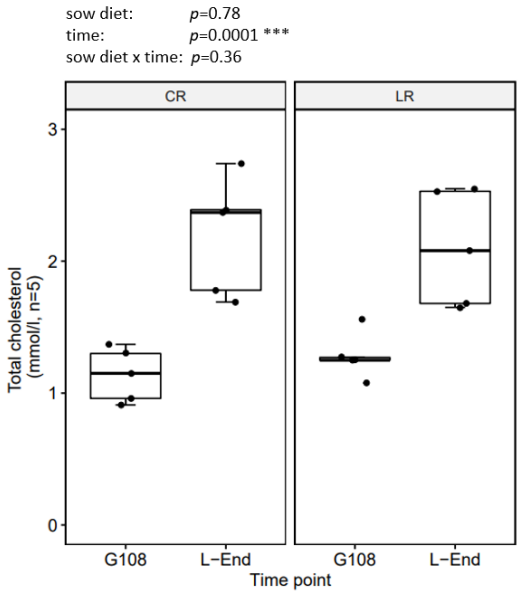
sow diet: p=0.78
time: p=0.0001 ***
sow diet x time: p=0.36
CR
LR
Total cholesterol (mmol/l, n=5)
G108
L−End
Time point

D2

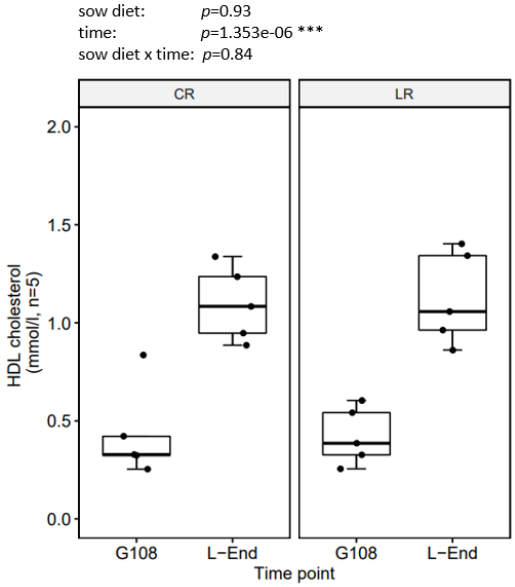
sow diet: p=0.93
time: p=1.353e-06 ***
sow diet x time: p=0.84
CR
LR
HDL cholesterol (mmol/l, n=5)
G108
L−End
Time point

E1

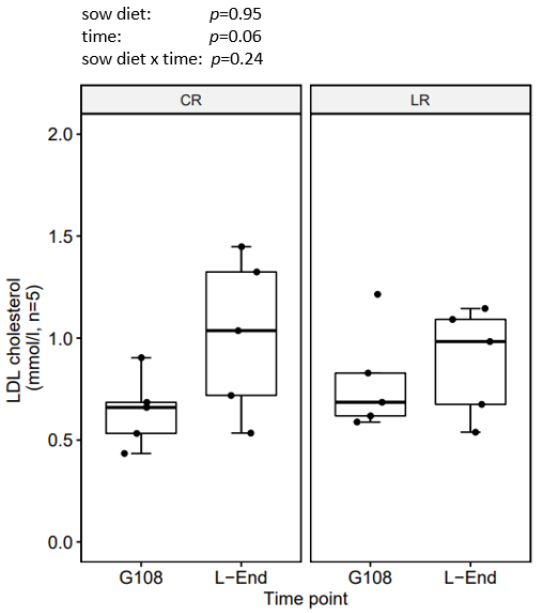

E2

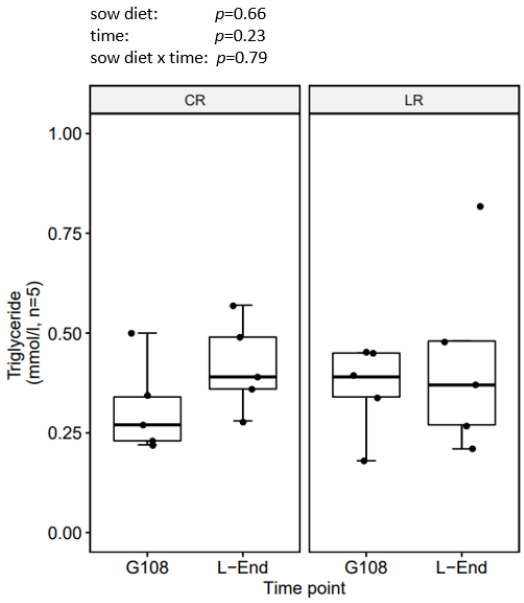

Figure 3-13 Boxplots of validation assays for the concentrations of apolipoprotein A1 (APOA1), haptoglobin (HP), and ITIH4 (pig-MAP) are presented with their respective abundance values determined by proteomics. Comparisons are A1 and A2 for APOA1; B1 and B2 for HP; C1 and C2 for ITIH4 (pig-MAP). In addition, plasma levels of total cholesterol, high-density lipoprotein (HDL) cholesterol, low-density lipoprotein (LDL) cholesterol, and triglyceride in four groups of sows are shown in D1, D2, E1, and E2, respectively. CR: sow diet with ω6:ω3 ratio=13:1 during gestation, starting from day 28 (G28) and 10:1 during lactation; LR: sow diet with ω6:ω3 ratio=4:1 from G28 until the end of lactation (L-End). G108 = day 108 of gestation.

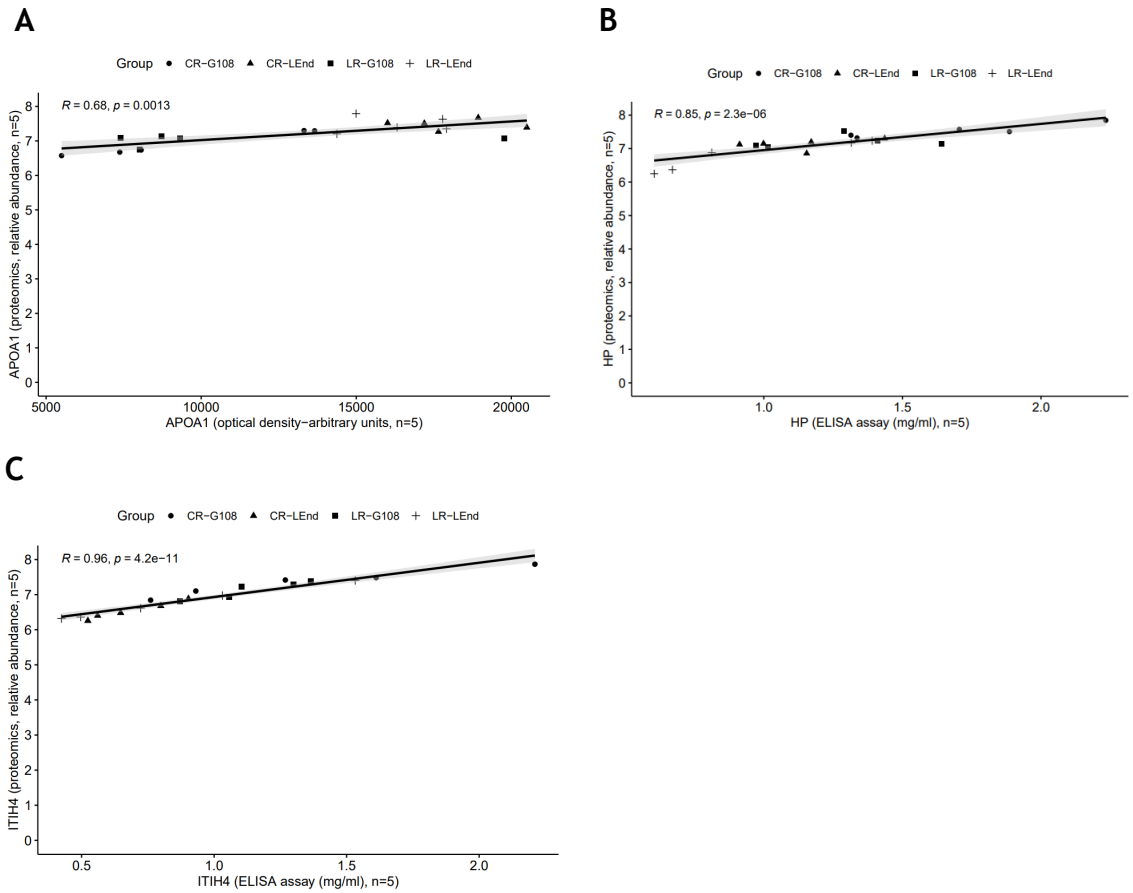

Figure 3-14 Correlations between relative protein abundance and validated protein concentration for A- apolipoprotein A1 (APOA1), B- haptoglobin (HP), and C- ITIH4 (pig-MAP). CR: sow diet with ω6:ω3 ratio=13:1 during gestation, starting from day 28 (G28) and 10:1 during lactation; LR: sow diet with ω6:ω3 ratio=4:1 from G28 until the end of lactation (L-End). G108 = day 108 of gestation.

3.8 DISCUSSION

While the dietary effects on sows have been well-studied [94,95,101,104,137,145,166,182,183,201] there have been a few previous studies on the plasma proteome beyond gestation, and this is the first report describing plasma proteome changes between late gestation and late lactation stages in sows supplemented with low dietary ω6:ω3 ratio. For several proteins, highly significant differences in abundance between G108 and L-End were observed; however other more modest differences (non-adjusted *p*-value < 0.05) may still be considered relevant, especially for guiding future research where larger group size or targeted quantitative proteomics would confirm significant differences.

3.8.1 Effect of sow dietary treatments: LR versus CR during G108 and L-End

Investigation of the effect of sows' diet, 4 and 5 proteins were changed in abundance following the change in the ratio between ω6 and ω3 PUFAs at G108 and regardless of time, respectively. Hemopexin (HPX) and alpha-1-antitrypsin (SERPINA1), implicated in inflammatory response regulation, and SERPINA1 and Inter-alpha-trypsin inhibitor heavy chain H1 (ITIH1), implicated in protease inhibition, were upregulated. Haptoglobin (HP) and Serum amyloid P-component (APCS), implicated in immune and inflammatory responses, were down-regulated. These observations support the hypothesis that low dietary ω6:ω3 fatty acids can modify the protein profile of plasma in sows during late gestation and lactation.

Haptoglobin (HP) is a specific positive acute phase protein (APP) with normal plasma levels ranging from 0.3 to 3 mg/mL [202]. HP primarily acts as an antioxidant and anti-inflammatory molecule by binding to free hemoglobin (HB) to detoxify HB and prevent its peroxidative side reactions to tissues [203]. In addition, HP functions as an immunomodulator in innate and adaptive cellular and humoral immune responses [204] by modulating helper T cell and lymphocyte function (that assists wound repair with minor cellular damage), inhibiting Th2 cytokine (anti-inflammatory) release, and weakly inhibiting Th1 cytokine (pro-inflammatory) release [205]. The ELISA assay validated the decreased abundance of HP in the plasma of LR-fed sows and showed a strong correlation with HP abundance quantified by proteomics.

In an earlier report in humans, the consumption of a low ω6:ω3 ratio was shown to lower plasma concentrations of HP and APCS, implying the activating effect of a low ω6:ω3 ratio intake on anti-inflammatory mechanisms [206]. Consistent with this observation, we also noticed the downregulation of HP and APCS in LR sows, suggesting that the anti-inflammatory mechanism was activated in these animals by the effect of a low ω6:ω3 ratio.

In contrast to the downregulation of HP and APCS, we found up-regulation of SERPINA1 in the plasma of LR sow. SERPINA1 is also an acute phase protein that inhibits proteases and stimulates the inflammatory response [207]. The increased abundance of SERPINA1 in plasma could be considered as a defence mechanism against excessive tissue damage at the final weeks of pregnancy.

3.8.2 Effect of time point: L-End versus G108 for LR and CR, separately and overall

The protein profile of sow plasma was measured in late gestation when the metabolic rate and energy expenditure in pregnant females is highest to meet the highest metabolic demand in the fetus [208], and proteome changes were found to move towards increased adipose tissue metabolism [86]. The lactating sows undergo accelerated catabolism because of the continued growth of mammary glands to produce a high milk yield, which can be a source of excessive oxidative stress [180]. Generally, sows in their late pregnancy and lactation suffer decreased antioxidative capacity and increased damage to immune cells due to excessive DNA oxidative attack [180]. An early study suggested that supplementing antioxidants can help fight against elevated oxidative stress and inflammation and restore the antioxidant defences of gestating and lactating sows [209].

Significant shifts were found over the late gestation-late lactation period affecting the plasma lipoproteins and the acute phase proteins. Related to the former, apolipoprotein A-1 (APOA1), A-2 (APOA2), and C-3 (APOC3) were all increased by L-End. They are soluble-multifunctional proteins that play a crucial role in lipid metabolism through regulating critical enzymes activity and acting as ligands to lipoprotein receptors [210]. Over the same period, positive acute phase proteins in pigs, haptoglobin (HP), and ITIH4 (or pig-MAP) were decreased in abundance. These findings imply that the end of pregnancy is associated with an acute phase

reaction demonstrated by the rise in the abundance of positive acute phase proteins and a decrease in negative acute phase proteins such as APOA1, while by the end of lactation, this acute phase reaction has dissipated. Western blot or immunoassay confirmed the changes of the plasma proteins in these groups. These findings support the hypothesis that plasma proteome profiles in pigs could be significantly altered during late gestation and lactation.

Apolipoproteins A1 (APOA1) and C3 (APOC3) are closely linked together because they are both in the same gene cluster, which was proposed to regulate the immune response to inflammation in pigs [211]. This effect is expressed by the decrease in HDL and the increase in TG and LDL [211]. Although no changes in TG and LDL were observed for sows at late gestation in our study, the mechanism of this action was partly shown because there was a decrease in plasma total cholesterol and HDL- cholesterol level in late gestating sows compared to late lactating sows. Indeed, this finding is further supported by the Gene Ontology enrichment analysis in which the interaction between APOA1 and APOC3 was shown in the HDL particle's receptor-binding activity.

APOA1 is a major negative APP in pigs due to its decreased level when the host is infected with bacteria [212], and this decrease is associated with decreased HDL levels in different acute phase responses (APR) [211]. Similar behavior of APOA1 during acute inflammation has been reported in humans [213], mice [214], and cows [215], suggesting APOA1 contribution in modulating some of the host acute phase reactions [213]. A chronic APR is caused by improper nutrient management and tissue stress or malfunction [216]. In the present work, a reduction of sow plasma HDL, APOA1, and APOA2 (the second most abundant HDL protein) was observed in late gestation versus late lactation, suggesting that sows had undergone elevated chronic systemic inflammation, oxidative damage, and lipid oxidation in late gestation versus late lactation. These observations support the hypothesis that the inflammatory responses changed in sows during different stages of reproduction. A Western blot assay confirmed the alteration in the proteomics result of APOA1, and the HDL-cholesterol assay showed a similar changing pattern on HDL cholesterol level.

APOC3 is primarily presented on the surface of chylomicrons, very low-density proteins (VLDL), and HDL [217], so it participates in regulating TG-rich lipoprotein [218] and plasma VLDL metabolism, also act as a pro-inflammatory factor *in vivo*

[219,220]. Comparing to plasma APOC3 levels in humans (~6 mg/dL) [221], mice (~4-5 mg/dL) [222] and cows (~6 mg/dL, in non-lactating stage); the pig has an unusual low level of ~50 ug/dL and consequently, a low circulating TG level [211]. Although the concentration of APOC3 was not measured in this study, HDL measurement showed a significantly lower level of ~7.7 mg/dL at G108 compared to ~20 mg/dL at L-End. HDL can promote cholesterol efflux and act as an antioxidant molecule in plasma, although this contribution is relatively small (1-2%) to the plasma's total antioxidant capacity [71]. HDL also has anti-inflammatory properties [71]. Therefore, this study's higher HDL level in late lactation contributes to decreased oxidative stress and inflammation in lactating sows compared to gestating sows.

Acute phase proteins, notably HP and ITIH4, were higher in abundance in plasma at G108 than L-End, and Gene Ontology enrichment analysis confirmed an interaction between these two main positive APPs. They both contributed to the organization of the extracellular region and participated in several biological processes, particularly acute phase and defence responses of the host to stimulus. Indeed, a significant correlation between plasma HP and ITIH4 concentrations was found (R = 0.62, p = 0.0037 for proteomics abundance; and R = 0.68, p = 0.001 for validated concentration, Figure 3-15A and B, respectively). The validation showing elevated HP and ITIH4 concentrations in the sows, particularly at late gestation, supports previous studies on the porcine APP [223]. The validated concentrations of HP and ITIH4 had strong correlations with the proteomics abundance, providing a reference for further research examining the role of the acute phase response in swine reproduction.

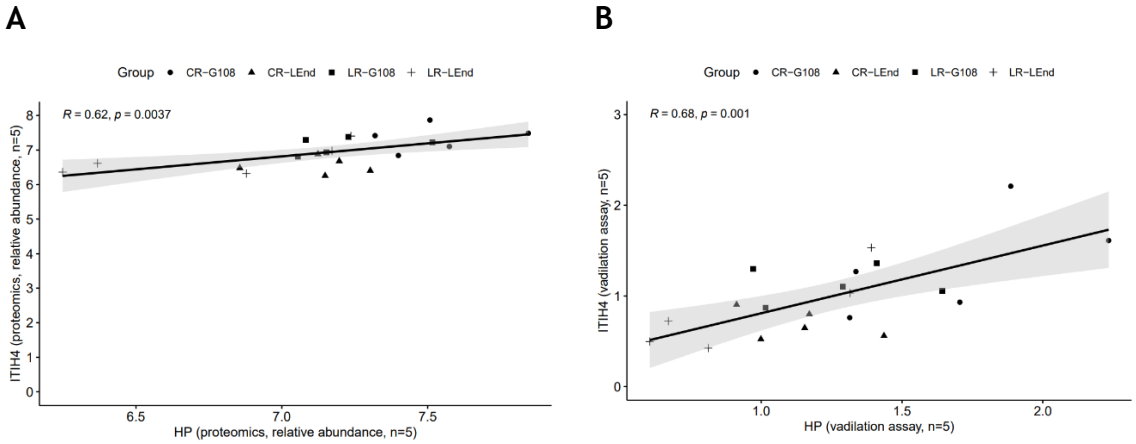

Figure 3-15 Correlations between ITIH4 (pig-MAP) and haptoglobin (HP) concentrations for A) proteomics abundance and B) validation assays. CR: sow diet with ω6:ω3 ratio=13:1 during gestation, starting from day 28 (G28) and 10:1 during lactation; LR: sow diet with ω6:ω3 ratio=4:1 from G28 until the end of lactation (L-End). G108 = day 108 of gestation.

Previous studies reported the crucial role of HP in modulating gamete interaction and early embryo development because it is up-regulated in the female reproductive fluid of pigs (*in vitro* study) [224], cows [225], and humans [226]. A recent study on sows confirmed the vital role of HP in early embryo development: it is excreted by the epithelium lining the oviduct and uterus throughout different stages of the oestrus cycle [227]. Linking HP function on lymphocyte modulation, it's increase in the oviduct and uterus throughout the luteal phase (and reaching a maximum on d 12 of pregnancy) implies HP's vital role in regulating maternal-embryonic communication [227]. These could be the underlying mechanism and explain the higher abundance of HP in late gestation compared to late lactation in this study. This finding is further validated by ELISA assay showing a similar altering pattern and a strong correlation with the proteomics result.

ITIH4 has an antiprotease activity and is also involved in the modulation of cell migration and proliferation [228], increasing rapidly in stressful conditions such as an injection, surgical trauma, or transportation [229,230]. In addition, ITIH4 may play a role in immune protection within the pig uterus and, thus, in pregnancy establishment [231]. These roles could explain a higher abundance of sow plasma ITIH4 in late gestation compared to late lactation in the present work. Moreover, ITIH4 concentrations of sows in this study agree with previous studies. ITIH4 concentration in healthy sows was 0.5 mg/mL (average at ~0.8 mg/mL [223]) and will be increased to 1.25 mg/mL at parturition; which are all below acute pathology level (6.11 mg/mL) [229].

3.9 CONCLUSIONS

The results revealed that low ω6:ω3 fatty acids ratio altered the plasma levels of several acute phase proteins in late gestating and late lactating sows. HP, SERPINA1, and APCS might be involved in protective mechanisms against accelerated oxidative impairment at later stages of gestation and lactation. Furthermore, the plasma proteome profile in sows was changed between late gestation and late lactation periods, in particular the relative abundance of apolipoproteins such as APOA1, APOA2, and APOC3 and positive acute phase proteins such as HP and ITIH4 (pig-MAP). These findings provide novel insights into animal adaptation's molecular mechanisms to changing stressors in different reproduction stages.

Chapter 4 Serum proteome changes associated with maternal dietary low ω6:ω3 ratio in piglets supplemented with seaweed

Journal of Proteomics: submitted 25/03/2022,
submission reference: JPROT-S-22-00165

Thi Xuan Nguyen[1,2,4]
Alessandro Agazzi[1]
Suzanne McGill[2]
Stefan Weidt[2]
Quang Hanh Han[2,4]
Andrea Gelemanović[3]
Mark McLaughlin[2]
Giovanni Savoini[1]
Peter David Eckersall[2]
Richard Burchmore[2]

[1]Università degli Studi di Milano, Via dell'Università, 6, 26900 Lodi, Italy
[2]University of Glasgow, Bearsden Rd, G61 1QH, United Kingdom
[3]Mediterranean Institute for Life Sciences (MedILS), Meštrovićevo šetalište 45, 21000 Split, Croatia
[4]Vietnam National University of Agriculture, Hanoi, Vietnam

Thi Xuan Nguyen contribution: conceptualization and design of the study, funding acquisition and project administration, methodology, acquisition of data, formal analysis and interpretation of data, drafting the manuscript, critical revising the manuscript, approval of the final version to be submitted, corresponding author.

Other contributions: Conceptualization and design of the study: AA, GS, PDE, and RB; funding acquisition and project administration: RB, DE, GS; methodology: SM, SW, QHH, AG, MM, RB, DE; acquisition of data: RB, DE; critical revising the manuscript: AA, QHH, AG, MM, GS, DE, and RB; all authors approved the final version to be submitted.

4.1 HIGHLIGHTS

* Maternal low dietary ω6:ω3 ratio (4:1) and offspring dietary seaweed supplementation affected the serum proteome in post-weaned piglets.

* Transferrin (TF) was significantly altered in abundance in comparison between two maternal dietary treatments and between weaning versus day 21 post-weaning.

* Acute phase proteins and apolipoproteins in serum were altered significantly in abundance between weaning versus day 21 post-weaning.

* The key pathways involved were coagulation cascade, platelet metabolism, and haemostasis in serum.

4.2 SIGNIFICANCE

This novel proteomic study in post-weaned piglets addresses the interplay between maternal and offspring nutritional interventions in a context of rapid and dynamic alterations in piglet metabolic status around weaning. This study also provides new insights into piglet serum proteome regulation during post-weaning, a critical development period in swine.

4.3 GRAPHICAL ABSTRACT

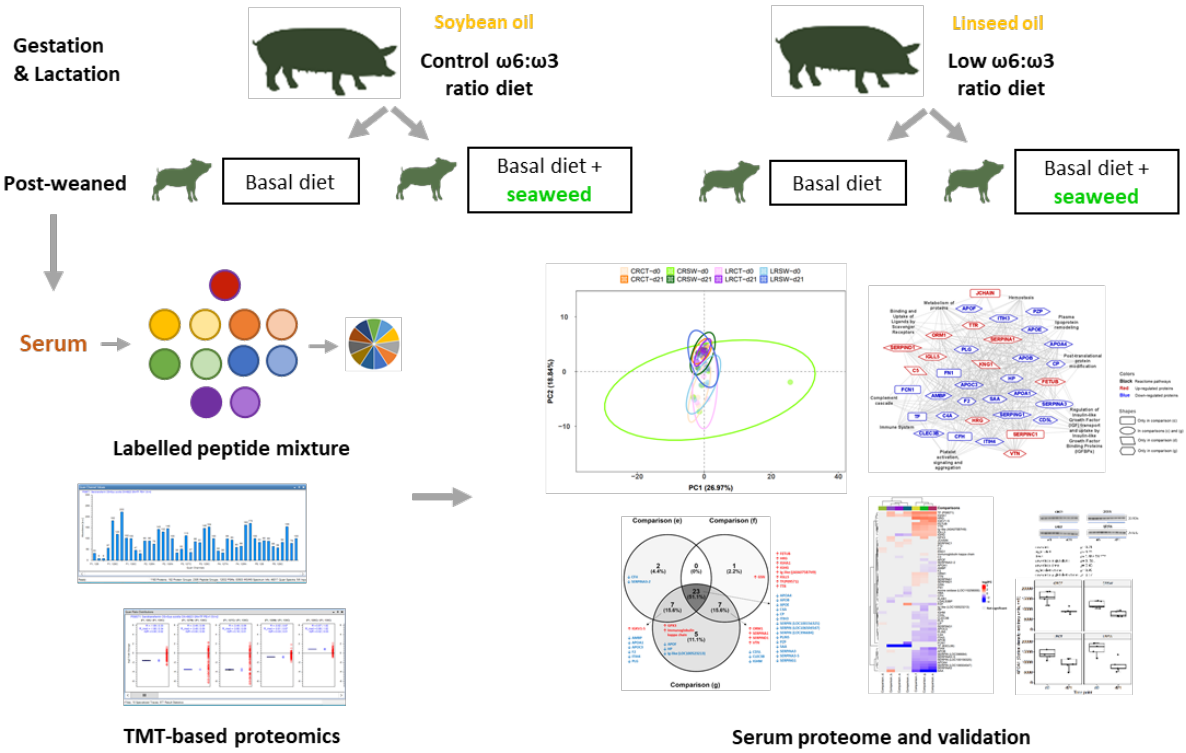

4.4 ABSTRACT

This study examines whether maternal low ω6:ω3 ratio diet and offspring seaweed (SW) supplementation can improve offspring immunity and performance by elucidating the effects on piglet serum proteome. A total of 16 sows were given either a standard (CR, 13:1) or low ω6:ω3 ratio diet (LR, 4:1) during pregnancy and lactation and their male weaned piglets were supplemented with SW powder (4 g/kg, SW) or not (CT) in a 21-day post-weaning (PW) diet. Four PW piglet groups were then identified based on dam and piglet treatment, namely CRCT, CRSW, LRCT, and LRSW (n = 10 each). Piglet serum collected at weaning and d21 PW were analysed (n = 5 each) using TMT-based quantitative proteomics and validated by appropriate assays. The differentially abundant proteins (n = 122) displayed positive effects of maternal LR diet on anti-inflammatory properties and innate immune stimulation. Progeny SW diet activated coagulation pathway, metabolism of platelets, and haemostasis, thus contributing to the cross-talk between coagulation cascade and inflammation. These data demonstrate the value of decreasing ω6:ω3 ratio in maternal diet and SW supplementation in PW piglet's diet to boost their immunity and anti-inflammation properties.

Keywords: pig proteome, weaning, ω6:ω3 fatty acids, seaweed, immunity, acute phase proteins, apolipoproteins, haemostasis

4.5 INTRODUCTION

Weaning is a critical familiarisation (adaptive) period in a pig's life to grow and develop fully in adulthood [232]. During weaning at an early age of ~3-4 weeks [233], piglets are trained to build a gradual adaptation to the introduction of solid feed [234], new social relationships, and a changing housing environment [235]. This permits adaptation of physiological and behavioural responses against different stressors and can thus ameliorate the effects of stress. During this sensitive growth stage, invading pathogens and inflammatory stimuli can negatively affect the biological system, so the host defence responses play a critical role in maintaining the balance of biological pathways [236]. The host defence consists of activated functions of non-specific innate and specific adaptive immune cells to preserve tissue homeostasis in response to inflammatory reactions caused by various stimuli [236]. Pathogens and tissue injuries from birth can stimulate innate immune cells [237–240] while long-lasting immune responses are maintained thanks to adaptive immune cells [241]. Nutritional intervention such as supplementation with antioxidant compounds might reduce weaning-related stress and intestinal barrier dysfunction in pigs [162], thus supporting the immune system.

Maternal dietary treatments drastically affect the growth and metabolic patterns of the offspring's prenatal, early postnatal, and juvenile growth and, in turn, mature phenotype [242,243]. Many studies in humans have shown the benefits of a low dietary ratio of omega 6:omega 3 (ω6:ω3) polyunsaturated fatty acids (PUFAs) on diminishing inflammation severity, particularly in the long-term [173,206], due to the anti-inflammatory and antioxidant properties of ω3 PUFAs [244,245]. Lowering the dietary ratio of ω6:ω3 in sows through increasing ω3 PUFAs from linseed oil has been reported to enhance their piglet's growth performance [246], levels of plasma immunoglobulins and hepatic gene expression [247].

In piglets, diet at weaning serves an essential role in controlling gut function, shaping the adaptive immune response, assisting the host defence against stimuli, and consequently contributing to the overall performance and health status [248]. In recent years, supplementing piglet diet with in-feed antibiotics alternatives

from sustainable sources has been rapidly developed [248]. *Ascophyllum nodosum* is a brown seaweed (SW) species, rich in bioactive ingredients such as phlorotannins and polyphenols [128,249–251]; and polysaccharides (laminarin, fucoidans and alginates [128], and ascophyllan [252]). Thus, it is a natural dietary source of antioxidants [168], antimicrobials and prebiotics [128,253], anti-inflammatory and immune regulators [127,254]. *A. nodosum* supplementation has been reported for its health benefits in pigs, mainly through its enhancement of gut health against pathogens and, consequently, has been proposed as an alternative to nutritional (in-feed) antibiotics [128,168,255]. However, the mechanism underlying the benefits of supplementing SW in pig diet has not been addressed so far.

An extensive review on the effects of alternatives to in-feed antibiotics in post-weaned piglets suggested that this type of study should pay equal attention to both physiological - functional approaches and gene expression [248]. Moreover, further investigations on the long-term effects of early- (prenatal to early postnatal or pre-weaning) and later- (post-weaning) nutritional programming are required to understand the underlying mechanisms of these dietary treatments in weaned piglet health and growth [248]. Studies considering the interplay between early- and later-life nutritional interventions will add to our understanding of the critical role of maternal diet in offspring growth and development [256].

This novel study describes the interplay between maternal low ω6:ω3 ingestion and offspring seaweed supplementation on offspring's serum (Chapter 4) and ileal protein profiles (Chapter 5) by quantitative proteomics, a method increasingly being used in studies of pig nutrition [110,257,258] here using the tandem mass tagged (TMT) approach. This study aims to provide a reference for future research on improving the life-long immune system of pigs. It is hypothesized that the mother's low ω6:ω3 diet and offspring seaweed supplementation diet will be suggestive of an additive effect on the offspring's immunity and growth. This chapter covers the protein profiles in serum of weaned piglets in exploring the underlying mechanisms, while Chapter 5 examines changes in the ileum proteome in the same piglets.

4.6 MATERIALS AND METHODS

4.6.1 Animals and sample collection

The feeding trial on piglets was conducted at the Animal Production Research and Teaching Centre of the Department of Veterinary Medicine and Animal Science, University of Milan (Lodi, Italy). The study protocol was approved by the Ethical Committee of the University of Milan (OPBA 67/2018) and the Italian Ministry of Health (authorization n. 168/2019 PR). The experimental design, growth performance, and blood oxidative status results were detailly described [183].

Briefly, a total of 40 male weaned piglets were designated from different mothers within a group, amongst two maternal dietary treatments containing either a control ratio of ω6:ω3 PUFAs (CR, 13:1 during gestation and 10:1 during lactation) or a low ratio of ω6:ω3 PUFAs (LR, 4:1, during gestation and lactation). Piglets were weaned at day 26 (± 1.76) of age with an average body weight of 6.46 kg (± 0.15) (mean ± SE). Piglets were fed a meal-based commercial diet (Table 2-3, Chapter 2) and supplemented with or without 4g seaweed powder *(A. nodosum;* Prodotti Arca S.r.l, Monza, Italy) per kg of feed, namely SW and CT groups, respectively. Four groups (*n* = 10 each) were formed: CRCT; CRSW; LRCT; and LRSW.

Blood samples were collected from the jugular vein from each piglet on weaning (d0) and day 21 post-weaning (d21 PW) using BD Vacutainer tubes (10 mL, REF 367896, BD-Plymouth, PL678P, UK). Blood samples were left to clot for a minimum of 60 min at room temperature, centrifuged (15 min; 3000× *g*; room temperature), and subsequently kept at −80 °C until analysis. Serum was selected because it is the standard source of biomaterials, and it contains slightly higher lipid levels compared to plasma [259].

4.6.2 Protein Identification and Quantification using the TMT approach

4.6.2.1 Protein quantification

Total protein concentration of the serum samples was measured by Bradford assay (Bio-Rad Protein Assay Dye Reagent Concentrate, Bio-Rad Laboratories GmbH, Müchen, Germany) using bovine serum albumin as standard.

4.6.2.2 Protein digestion and Isobaric labelling – tandem mass tag

The proteomic profiling of serum samples was performed using Tandem Mass Tag (TMT) labelling quantitative approach as described earlier [184]. For each sample, 37 µg protein was digested with trypsin using filter-aided sample preparation (FASP) [260] with 10 kDa molecular weight cut-off filters. Digesting proteins into peptides was executed overnight using 1 µg of trypsin (20 µg/mL, Promega, Madison, WI, USA) resuspended in 0.05 M ammonium bicarbonate (NH4HCO3) buffer, at 1:37 w/w, at 37 °C. The remaining peptides were collected using 10% ACN in water. Trypsin activity was inhibited by acidification with 1% trifluoroacetic acid (TFA, CF_3COOH) before entirely drying at 45 °C under a high vacuum.

Next, the peptides pellets obtained were diluted using 0.1 M triethylammonium bicarbonate (TEAB, Thermo Fisher Scientific, Rockford, USA) before being tagged using a freshly prepared TMT10plex Label Reagent set followed manufacturers instructions (Thermo Fisher Scientific, Rockford, IL, USA). All TMT-modified peptide samples were combined in equal amounts into a new microcentrifuge tube, aliquoted, SpeedVac lyophilized, and kept at -80 °C before tandem mass spectrometry analysis. In addition, an equal quantity of peptides from every sample was pooled and labelled by a TMT tag before adding to each TMT multiplexed sample as an internal standard (or linker) between multiple TMT sets. Five TMT10plex experiments were performed for a total of 40 samples (5 animals per group x 4 groups x 2 time points).

4.6.2.3 Liquid chromatography tandem mass spectrometer (LC-MS/MS)

Before analysis, peptides were dissolved in 20 µL of 5% (v/v) ACN with 0.5% (v/v) formic acid using the auto-sampler of a nanoflow uHPLC system (Thermo Fisher Scientific RSLCnano, Horsham, UK). Peptide ions were detected and characterized using electrospray ionisation (ESI) mass spectrometry MS/MS with an Orbitrap Elite MS (Thermo Fisher Scientific, Horsham, UK). LC eluent was ionized by interfacing the LC coupling device to a NanoMate Triversa (Advion Bioscience, Harlow, UK) with an electrospray voltage of 1.7 kV. Online desalting and trapping of peptides (5 µL) were performed for 12 min on the trap column (0.3 × 5 mm) using a flow rate of 25 µL/min with 1% ACN and 0.1% formic acid.

After desalting, the purified peptide was further separated on a Pepmap C18 reversed-phase column (50 cm × 75 µm, particle size 3 µm, pore size 100 Å, Thermo Fisher Scientific, Horsham, UK) using mobile phase A and B at a fixed flow rate of 0.3 µL/min for the analytical column. Mobile phase A was 0.1% formic acid in water and mobile phase B was 0.08% formic acid in 80% ACN and 20% water. The peptides were fractionated with a series of mobile phase B gradients: 4% v/v for 10 min, 4-60% v/v for 170 min, 60-99% v/v for 15 min, and held at 99% v/v for 5 min. The column was adjusted to the initial conditions and re-equilibrated under that condition for 10 min before the next sample injection.

Eluting peptides were analysed on an Orbitrap Elite mass spectrometer. Each MS scan (380 – 1800 m/z) was acquired at a resolution of 60000 FWHM, followed by CID fragmentation and detection of the top three precursor ions from the MS scan in the linear ion trap. The top three precursor ions are also subjected to HCD in the HCD collision cell, followed by detection in the Orbitrap at a resolution of 30000 FWHM, as defined at 400 m/z. Selected precursors were added to a dynamic exclusion list for 180s and single-charged ions were omitted from selection.

4.6.2.4 MS/MS data processing

Raw MS/MS spectra were processed in Proteome Discoverer (version 2.4, Thermo Fisher Scientific). The UniProtKB database was searched to identify and quantify proteins using the Sequest HT algorithm against *Sus scrofa* FASTA files (104,940 sequences; downloaded on 18/02/2021). Precursor ion mass tolerance of 10 ppm

and fragment tolerance of 0.02 Da were applied. Trypsin was selected as the enzyme with the option of two missed cleavage sites. Carbamidomethyl (C) was stated as the fixed modification. The dynamic modifications contain oxidation (M), deamidation (N, Q), and TMT six-plex (K, peptide N-terminus) were specified. The peptides were identified using the Percolator algorithm based on the search results against a decoy database. A false discovery rate (FDR) was set at 1% on the peptide level. At least two peptides and 5% FDR were required to report confidently identified proteins. The mass spectrometry proteomics data have been deposited to the ProteomeXchange Consortium via PRIDE [185] partner repository with the dataset identifier PXD032327.

4.6.3 Validation of proteomics results

For a comprehensive validation of proteomics results, alterations in the non-depleted sample contents of APOA1, HDL-cholesterol, SAA, and TF were determined. These proteins were selected based on their significant alterations in abundance analysis by TMT-based proteomic and accounting for their biological significance.

The concentration of **APOA1** in serum was measured using Western blot according to a previous method [193]. In brief, 10 µg of proteins of each sample (5 samples/group/time point) was denatured, followed by electrophoresis separation before transferring into nitrocellulose membranes. Membranes were then blocked in blocking solution and probed with rabbit polyclonal antibody to porcine APOA1 at 1:20,000 dilution (PAA519Po01, Cloud-Clone Corp, USA) by overnight incubation at 4°C. This primary antibody was later probed with secondary antibody HRP conjugated anti-rabbit IgG to horseradish peroxidase (1:10,000; ab6721, Abcam Ltd. UK) in T-TBS containing 5% milk powder for 1 h at room temperature. ECL substrate was added for protein detection (Thermo Fisher Scientific™, Meridian Rd., Rockford, USA) and ECL image was visualized using radiographic film (Hyperfilm ECL, Amersham Biosciences). The protein band intensity was measured using Image J NIH software (https://imagej.nih.gov/ij/).

HDL-cholesterol level was quantitatively analysed using the HDL-cholesterol assay kit (ab65390; Abcam, Cambridge, UK) following the manufacturer's instructions.

The HDL component was preliminarily separated using chemical precipitation from other lipoproteins. Then, the cholesterol contained by the HDL was determined using a colorimetric assay.

The quantification of **SAA** was implemented by ELISA using species-specific kits (Life Diagnostics pig SAA ELISA, Life Diagnostics Inc., West Chester, US). The assay uses peptide-specific pig SAA antibody for solid-phase immobilization. Pig SAA antibody conjugated with horseradish peroxidase (HRP) was used for detection.

The concentration of **TF** was estimated using Sodium-dodecyl Sulphate Polyacrylamide Gel Electrophoresis (SDS-PAGE), followed by Coomassie blue staining, and the band representing protein TF was subsequently confirmed by mass spectrometry. Generally, 20 μg of proteins of each sample (5 samples/group/time point) was denatured at 95 °C for 4 min in 4x Laemmli buffer and 1 M dithiothreitol (DTT). Serum proteins separated in polyacrylamide gel (4-12% Bis-Tris precast Criterion XT, Bio-Rad, USA) were stained using 0.1% Coomassie blue staining solution for 1 h at room temperature. Next, the gel was de-stained in acetic acid/methanol/distilled water (3:8:29, v/v). After visualizing the protein bands with Coomassie blue stain and scanning, gel images were measured using Image J NIH software to obtain protein band intensity. The TF band (~76.5 kDa) was above the albumin band (~69 kDa) in the gel. As described in detail below, a linear mixed model was used to evaluate TF band volume differences between treatments. To confirm the identity of the TF band protein-stained bands of ~76.5 kDa (n = 5/group/time point) were excised for in-gel digestion and subjected to MS identification, as described previously [261].

4.6.4 Statistical and Bioinformatics Analysis

4.6.4.1 Statistical analysis for proteomics data

The statistical analyses were performed using peptide spectrum match (PSM)-level data based on linear mixed-effects models with Empirical Bayes moderation using MSstatsTMT package version 2.0.0 [186] in R version 4.1.0 [187]. Proteins were quantified using unique peptides and summarized using the median polish method. Individual protein was normalized with the pooled internal standard channel. The Benjamini-Hochberg method was used to correct multiple pairwise comparisons (*p*

< 0.05). The statistical analysis used master proteins only. Significantly differentially abundant proteins were determined at an adjusted *p*-value < 0.05, and possibly changed proteins were determined at a *p*-value < 0.05.

The volcano plots were generated using packages *ggplot2* version 3.3.3 [188] and *ggrepel* version 0.9.1, PCA plots used *ggplot2* version 3.3.3 [188], and heatmaps used *pheatmap* version 1.0.12. Venn diagrams were generated using web tool Venny 2.1 (https://bioinfogp.cnb.csic.es/tools/venny/) [189].

4.6.4.2 Bioinformatics analysis

The accession numbers of identified master protein were converted into the corresponding gene ID using the UniProt retrieve/ID mapping tool. Undefined proteins were replaced with the best match on *Sus scrofa* orthologue annotated genes of minimum 70% identity using SmartBLAST tool (https://blast.ncbi.nlm.nih.gov/smartblast/). STRING database version 11.5 [190] was used to retrieve the protein-protein interaction (PPI) network, Reactome pathways, Gene Ontology (GO) analysis containing Biological Process (BP), Molecular Function (MF), and Cellular Component (CC). Enriched GO terms were further filtered using the REVIGO [192] webserver (revigo.irb.hr) to remove the redundant terms, applying the following settings: whole UniProt as the database, SimRel as semantic similarity measure considering a small similarity threshold of 0.5 at which the term was removed from the list and assigned to a cluster. Interactions between desired Reactome pathways and proteins with significantly different abundances between comparisons were mapped through Cytoscape software v3.8.2 [191].

4.6.4.3 Statistical analysis for validation data

The APOA1, SAA, and TF validation data were analysed and compared with results measured by proteomics. Before the data analysis, the normality of the data distribution for each variable was examined using the Shapiro-Wilk test and homogeneity of variance was checked using Levene's test. Difference between groups was investigated applying the linear mixed model, and multiple pairwise comparisons were corrected using the Benjamini-Hochberg false discovery control procedure. Fixed effects were sow diet, piglet diet, time, and their interactions.

The random effect was an individual animal. Pearson correlation analysis was applied to assess the association between proteomics and validation results for APOA1 concentrations. Spearman correlation was used for the validation data of SAA (data was normally distributed, but the variances were not equal) and abundance data of TF (not normally distributed).

The experimental design, pipeline for proteomics analysis (containing sample preparation, TMT labelling, and LC-MS/MS, data analysis, and quantitation), and validation of proteomics results are illustrated in Figure 4-1.

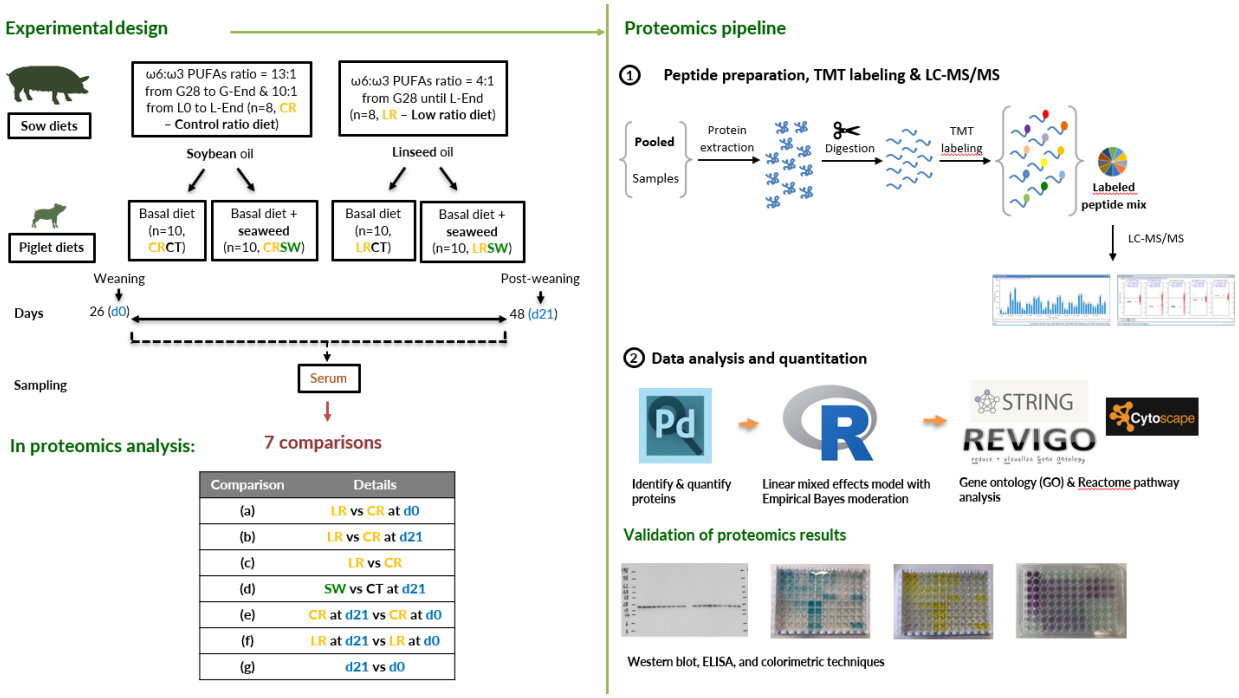

Figure 4-1 The experimental design, proteomics pipeline and validation of proteomics results. Proteomics pipeline contains: (1) Peptide preparation, TMT labelling, and LC-MS/MS analysis, (2) Data analysis and quantitation: protein identification and quantitation using Proteome Discoverer, statistical analysis based on the linear mixed-effects model with empirical Bayes moderation (R package MSstatsTMT), bioinformatics analysis (Gene Ontology (GO) and Reactome pathway enrichment analysis).

4.7 RESULTS

4.7.1 Proteomic analysis

The TMT mass spectrometry-based relative quantitation found 12832 features and mapped 2675 unique peptides, which represented 489 proteins and 260 master proteins. Proteins matched with no unique peptide or only one peptide were excluded. The master protein - primary translation product of the coding sequence

and expresses at least one of the known protein isoforms, coded by the canonical sequence [197], was used for statistical analysis. As a result, 122 master proteins have been quantified and remained for statistical analysis.

The principal component analysis (PCA) score plot displays the clustering of samples from 4 groups of piglets at 2 sampling times (Figure 4-2). The PCA disclosed that the samples of 4 groups clustered more closely at the same sampling time, whereas the samples of 4 groups at day 21 post-weaning (d21 PW) versus those at weaning (d0) were more homogeneous, with the first two principal components (PCs) explaining 45.81% of the total variance (Figure 4-2).

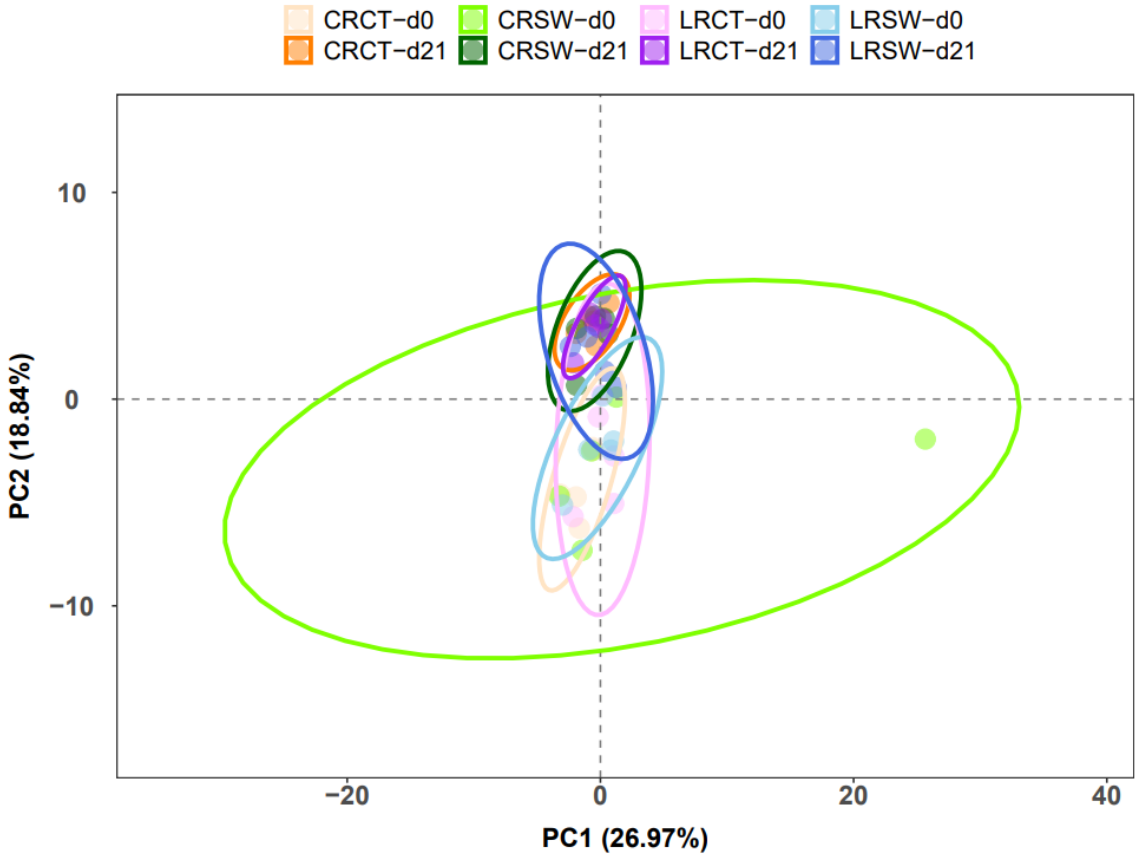

Figure 4-2 Principal component analysis (PCA) score plots showing the clustering of samples from four groups of piglet serum at two sampling time. Four groups contain CRCT: piglets fed no seaweed (SW, *Ascophyllum nodosum*), which nursed by sows fed dietary ω6:ω3 ratio = 13:1 during gestation, starting from day 28 (G28) and 10:1 during lactation at weaning day (bisque dots) and d21 post-weaning (dark orange dots); CRSW: piglets fed SW, which nursed by sows fed dietary ω6:ω3 ratio = 13:1 during gestation and 10:1 during lactation at weaning day (light green dots) and d21 post-weaning (dark green dots); LRCT: piglets fed no SW, which nursed by sows fed dietary ω6:ω3 ratio = 4:1 from G28 until the end of lactation at weaning day (plum dots) and d21 post-weaning (purple dots); LRSW: piglets fed SW, which nursed by sows fed dietary ω6:ω3 ratio = 4:1 from G28 until the end of lactation at weaning day (light blue dots) and d21 post-weaning (blue dots). The ellipses represent 95% confidence region.

The differentially abundant proteins (DAPs) in 7 comparisons are summarised in Table 4-1 (details are presented in Table 4-2) including (a) - LR vs CR at d0; (b) - LR vs CR at d21 PW; (c) - LR vs CR; (d) - SW vs CT at d21 PW; (e) - CR at d21 PW vs CR at d0; (f) - LR at d21 PW vs LR at d0; and (g) - d21 PW vs d0.

Table 4-1 The differentially abundant proteins (DAPs) in piglet serum among seven comparisons : (a) LR vs CR at weaning (d0); (b) LR vs CR at day 21 post-weaning (d21 PW); (c) - LR vs CR; (d) - SW vs CT at d21 PW; (e) - CR at d21 PW vs CR at d0; (f) - LR at d21 PW vs LR at d0; and (g) - d21 PW vs d0.

Protein name	Gene names	log2FC						
		Comparisons						
		(a)	(b)	(c)	(d)	(e)	(f)	(g)
		LR-d0 vs CR-d0	LR-d21 vs CR-d21	LR vs CR	SW-d21 vs CT-d21	CR-d21 vs CR-d0	LR-d21 vs LR-d0	d21 vs d0
Alpha-1-microglobulin	AMBP	/	/	/	/	-0.29	/	-0.21
Apolipoprotein A-I	APOA1	/	/	/	/	-0.18	/	-0.17
Apolipoprotein A-IV*	APOA4	/	/	/	/	-1.36	-1.21	-1.29
Apolipoprotein B	APOB	/	0.19	/	/	-1.02	-0.66	-0.84
Apolipoprotein C-III	APOC3	/	/	/	/	-0.76	/	-0.63
Apolipoprotein-E*	APOE	/	/	/	/	-0.75	-0.53	-0.64
Apolipoprotein F precursor*	APOF	/	/	/	/	/	/	-0.33
Complement C3	C3	-0.20	/	/	/	/	/	/
Complement C4A	C4A	/	/	/	/	-0.63	-0.57	-0.60
Complement C5a anaphylatoxin	C5	/	/	/	0.24	/	/	/
CD5 Molecule Like*	CD5L	/	/	/	/	/	-0.48	-0.36
Complement factor H isoform a	CFH	-0.37	/	-0.20	/	-0.24	/	/
C-type lectin domain family 3 member B	CLEC3B	/	/	/	/	/	-0.47	-0.42
Ceruloplasmin*	CP	/	/	/	0.16	-0.52	-0.24	-0.38
Coagulation factor XII	F12	0.23	/	/	/	/	/	/
Coagulation factor II	F2	/	/	/	/	-0.31	/	-0.23
Ficolin-1	FCN1	/	/	-1.67	/	/	/	/
Fetuin-B isoform 1	FETUB	/	/	/	/	0.97	1.15	1.07
Fibronectin	FN1	/	/	-0.21	/	/	/	/

log2FC is base 2 logarithm transformed of fold change value which represents the ratio of expression levels in the first-mentioned group vs second-mentioned group. Protein names marked with * were shown as "Uncharacterized protein" in the UniProt Sus scrofa database and thus were substituted with the best match on Sus scrofa database, using SMARTBLAST tool. CR: piglet born from sow fed diet with ω6:ω3 ratio=13:1 during gestation, starting from day 28 (G28) and 10:1 during lactation; LR: piglet born from sow fed diet with ω6:ω3 ratio=4:1 from G28 until the end of lactation (L-End). G108: day 108 of gestation.

(cont. 1)

Protein name	Gene names	log2FC						
		Comparisons						
		(a)	(b)	(c)	(d)	(e)	(f)	(g)
		LR-d0 vs CR-d0	LR-d21 vs CR-d21	LR vs CR	SW-d21 vs CT-d21	CR-d21 vs CR-d0	LR-d21 vs LR-d0	d21 vs d0
Glutathione peroxidase 3 precursor*	GPX3	/	0.46	/	/	/	/	0.81
Gelsolin	GSN	/	/	/	/	/	0.29	/
Haemoglobin subunit alpha	HBA	/	/	-0.56	/	/	/	/
Haptoglobin	HP	/	/	/	/	/	/	-0.79
Histidine-rich glycoprotein	HRG	/	/	/	/	1.51	1.67	1.60
IgA heavy chain constant region*	IGHA1	0.47	0.74	0.61	/	0.89	1.16	1.03
IgG heavy chain	IGHG	-0.79	/	-0.58	/	0.68	0.73	0.71
Ig-like domain-containing protein		/	/	/	/	0.65	0.90	0.78
IgM heavy chain constant region*	IGHM	/	/	/	-0.22	/	-0.34	-0.24
Immunoglobulin kappa chain**		/	/	/	/	/	/	0.18
Immunoglobulin kappa variable region*	IGKV1-5	/	/	/	/	1.41	/	1.11
Immunoglobulin lambda-like polypeptide 5 isoform 1*	IGLL5	/	/	/	/	0.61	0.64	0.62
Inter-Alpha-Trypsin Inhibitor Heavy Chain 3*	ITIH3	/	/	/	/	-0.73	-0.47	-0.60
Inter-alpha-trypsin inhibitor heavy chain H4 isoform 1	ITIH4	/	/	/	/	-1.45	/	-1.05
Joining chain of multimeric IgA and IgM	JCHAIN	/	0.35	0.32	/	/	/	/
Plasma kallikrein*	KLKB1	/	-0.27	/	/	/	/	/
Kininogen 1*	KNG1	/	/	/	0.18	/	/	/
Galectin-3-binding protein	LGALS3BP	/	-0.57	/	/	/	/	/

log2FC is base 2 logarithm transformed of fold change value which represents the ratio of expression levels in the first-mentioned group vs second-mentioned group. Protein names marked with * were shown as "Uncharacterized protein" in the UniProt Sus scrofa database and thus were substituted with the best match on Sus scrofa database, using SMARTBLAST tool. Proteins ** were shown as "Uncharacterized protein" in the UniProt Sus scrofa database and cannot find the best match on Sus scrofa database, thus were substituted with the best match on Homo sapiens database, using SMARTBLAST tool. CR: piglet born from sow fed diet with ω6:ω3 ratio=13:1 during gestation, starting from day 28 (G28) and 10:1 during lactation; LR: piglet born from sow fed diet with ω6:ω3 ratio=4:1 from G28 until the end of lactation (L-End). G108: day 108 of gestation.

(cont. 2)

Protein name	Gene names	log2FC						
		Comparisons						
		(a)	(b)	(c)	(d)	(e)	(f)	(g)
		LR-d0 vs CR-d0	LR-d21 vs CR-d21	LR vs CR	SW-d21 vs CT-d21	CR-d21 vs CR-d0	LR-d21 vs LR-d0	d21 vs d0
SERPIN domain-containing protein	LOC100156325	/	/	/	/	-0.84	-1.00	-0.92
Ig-like domain-containing protein	LOC100523213	/	/	/	/	/	/	-0.67
SERPIN domain-containing protein	LOC106504547	/	/	/	/	-1.72	-1.30	-1.51
Amine oxidase	LOC110256000	/	/	-0.26	/	/	/	/
SERPIN domain-containing protein	LOC396684	/	/	/	/	-1.05	-0.76	-0.90
Alpha-1 acid glycoprotein	ORM1	/	/	/	/	/	0.40	0.35
Plasminogen	PLG	/	/	/	/	-0.36	/	-0.40
Perilipin 5	PLIN5	/	/	/	/	-0.55	-0.54	-0.55
Alpha-2-Macroglobulin	PZP	/	/	1.23	/	-0.66	-0.40	-0.49
Serum amyloid A	SAA	/	1.18	/	/	-3.08	-1.95	-2.52
Alpha-1-antitrypsin/Serpin Family A Member 1	SERPINA1	/	/	/	/	/	0.29	0.21
Serpin A3-8*	SERPINA3	/	-0.24	-0.21	/	-2.14	-1.35	-1.74
Alpha-1-antichymotrypsin 2	SERPINA3-2	/	/	/	/	-0.32	/	/
Serpin A3-5*	SERPINA3-5	/	/	/	/	-0.84	-0.83	-0.84
Antithrombin-III	SERPINC1	0.26	/	0.20	/	/	/	/
SERPIN domain-containing protein	SERPIND1	/	/	/	/	/	0.29	0.20
Serpin family G member 1	SERPING1	/	/	/	/	-0.37	-0.36	-0.36
Transferrin (B3CL06)	TF	-3.14	-3.32	-3.33	/	/	/	/
Transferrin (P09571)	TF	/	0.78	0.79	/	1.43	1.41	1.42
Transthyretin	TTR	/	/	/	/	0.67	0.97	0.83
Vitronectin	VTN	/	/	/	/	/	0.32	0.28

log2FC is base 2 logarithm transformed of fold change value which represents the ratio of expression levels in the first-mentioned group vs second-mentioned group. Protein names marked with * were shown as "Uncharacterized protein" in the UniProt Sus scrofa database and thus were substituted with the best match on Sus scrofa database, using SMARTBLAST tool. CR: piglet born from sow fed diet with ω6:ω3 ratio=13:1 during gestation, starting from day 28 (G28) and 10:1 during lactation; LR: piglet born from sow fed diet with ω6:ω3 ratio=4:1 from G28 until the end of lactation (L-End). G108: day 108 of gestation.

Table 4-2 Detailed differentially abundant proteins (DAPs) in piglet serum of seven comparisons : (a) LR vs CR at weaning (d0); (b) LR vs CR at day 21 post-weaning (d21 PW); (c) - LR vs CR; (d) - SW vs CT at d21 PW; (e) - CR at d21 PW vs CR at d0; (f) - LR at d21 PW vs LR at d0; and (g) - d21 PW vs d0.

Protein name	Gene names	Accession number[1]	Number of peptides	log2FC[2]	*P*-value	Adjusted *p*-value
Comparison (a) – LR vs CR at d0						
IgA heavy chain constant region*	IGHA1	A0A480QMR6	4	0.47	0.045	0.771
Antithrombin-III	SERPINC1	A0A5G2QUE0	10	0.26	0.037	0.771
Coagulation factor XII	F12	A0A287BIP4	3	0.23	0.034	0.771
Complement C3	C3	I3LTB8	57	-0.20	0.030	0.771
Complement factor H isoform a	CFH	A0A480TLF3	10	-0.37	0.021	0.771
IgG heavy chain	IGHG	L8B0T2	9	-0.79	0.026	0.771
Transferrin	TF	B3CL06	51	-3.14	0.007	0.771
Comparison (b) – LR vs CR at d21 PW						
Serum amyloid A	SAA	A0A480PRQ0	2	1.18	0.007	0.283
Transferrin	TF	P09571	51	0.78	0.006	0.283
IgA heavy chain constant region*	IGHA1	A0A480QMR6	4	0.74	0.003	0.283
Glutathione peroxidase 3 precursor*	GPX3	A0A4X1TQP5	6	0.46	0.026	0.461
Joining chain of multimeric IgA and IgM	JCHAIN	A0A287BQC8	2	0.35	0.045	0.559
Apolipoprotein B	APOB	A0A4X1U273	25	0.19	0.037	0.522
Serpin A3-8*	SERPINA3	A0A4X1SG20	14	-0.24	0.029	0.461
Plasma kallikrein*	KLKB1	A0A4X1VWY2	2	-0.27	0.025	0.461
Galectin-3-binding protein	LGALS3BP	A0A5G2RLP2	5	-0.57	0.048	0.559
Transferrin	TF	B3CL06	51	-3.32	0.009	0.283
Comparison (c) – LR vs CR						
Alpha-2-Macroglobulin	PZP	A0A287A1B4	40	1.23	0.015	0.378
Transferrin	TF	P09571	51	0.79	0.029	0.475
IgA heavy chain constant region*	IGHA1	A0A480QMR6	4	0.61	0.012	0.378
Joining chain of multimeric IgA and IgM	JCHAIN	A0A287BQC8	2	0.32	0.042	0.475
Antithrombin-III	SERPINC1	A0A5G2QUE0	10	0.20	0.012	0.378
Complement factor H isoform a	CFH	A0A480TLF3	10	-0.20	0.043	0.475
Fibronectin	FN1	F1SS24	18	-0.21	0.047	0.475
Serpin A3-8*	SERPINA3	A0A4X1SG20	14	-0.21	0.007	0.378
Amine oxidase	LOC110256000	A0A5G2RD43	6	-0.26	0.049	0.475
Hemoglobin subunit alpha	HBA	P01965	7	-0.56	0.039	0.475
IgG heavy chain	IGHG	L8B0T2	9	-0.58	0.048	0.475
Ficolin-1	FCN1	A0A480N8F0	4	-1.67	0.027	0.475
Transferrin	TF	B3CL06	51	-3.33	<0.001	0.042

[1]Accession number from UniProt protein database for *Sus scrofa*. [2]log2FC is base 2 logarithm transformed of fold change value which represents the ratio of expression levels in the first-mentioned group vs second-mentioned group. Protein names marked with * were shown as "Uncharacterized protein" in the UniProt *Sus scrofa* database and thus were substituted with the best match on *Sus scrofa* database, using SMARTBLAST tool. CR: piglet born from sow fed diet with ω6:ω3 ratio=13:1 during gestation, starting from day 28 (G28) and 10:1 during lactation; LR: piglet born from sow fed diet with ω6:ω3 ratio=4:1 from G28 until the end of lactation.

(cont. 1)

Protein name	Gene names	Accession number[1]	Number of peptides	log2FC[2]	*P*-value	Adjusted *p*-value
Comparison (d) – SW vs CT at d21 PW						
Complement C5a anaphylatoxin	C5	F1SME1	3	0.24	0.012	0.856
Kininogen 1*	KNG1	A0A4X1UF91	6	0.18	0.027	0.856
Ceruloplasmin*	CP	K7GKN3	21	0.16	0.024	0.856
IgM heavy chain constant region*	IGHM	A0A287ALC1	18	-0.22	0.034	0.856
Comparison (e) – CR at d21 PW vs CR at d0						
Histidine-rich glycoprotein	HRG	A0A481B9A6	14	1.51	<0.001	<0.001
Transferrin	TF	P09571	51	1.43	<0.001	0.004
Immunoglobulin kappa variable region*	IGKV1-5	A0A286ZYQ7	4	1.41	0.010	0.045
Fetuin-B isoform 1	FETUB	A0A480SUZ7	2	0.97	<0.001	0.003
IgA heavy chain constant region*	IGHA1	A0A480QMR6	4	0.89	<0.001	0.008
IgG heavy chain	IGHG	L8B149	8	0.68	0.023	0.082
Transthyretin	TTR	A0A5G2QIE9	3	0.67	0.008	0.037
Ig-like domain-containing protein		A0A075B7H9	3	0.65	0.007	0.036
Immunoglobulin lambda-like polypeptide 5 isoform 1*	IGLL5	A0A287A1M4	4	0.61	0.025	0.085
Apolipoprotein A-I	APOA1	K7GM40	24	-0.18	0.015	0.060
Complement factor H isoform a	CFH	A0A480TLF3	10	-0.24	0.044	0.133
Alpha-1-microglobulin	AMBP	A0A480P2R0	2	-0.29	0.017	0.067
Coagulation factor II	F2	B3STX9	5	-0.31	0.033	0.109
Alpha-1-antichymotrypsin 2	SERPINA3-2	Q9GMA6	11	-0.32	0.023	0.083
Plasminogen	PLG	A0A4X1VQL9	19	-0.36	0.050	0.147
Serpin family G member 1	SERPING1	A0A5K1UE53	4	-0.37	0.020	0.077
Ceruloplasmin	CP	K7GKN3	21	-0.52	<0.001	<0.001
Perilipin 5	PLIN5	A0A5G2QKC5	2	-0.55	0.042	0.130
Complement C4A	C4A	A0A4X1VBD2	18	-0.63	0.005	0.028
Alpha-2-Macroglobulin *	PZP	A0A287BDU7	41	-0.66	0.002	0.010
Inter-Alpha-Trypsin Inhibitor Heavy Chain 3*	ITIH3	A0A4X1VPM1	2	-0.73	<0.001	0.001
Apolipoprotein-E*	APOE	A0A4X1W1F9	9	-0.75	0.002	0.010
Apolipoprotein C-III	APOC3	A0A5G2QLU1	2	-0.76	0.001	0.009
SERPIN domain-containing protein	LOC100156325	F1SCC6	12	-0.84	0.001	0.009
Serpin A3-5*	SERPINA3-5	A0A4X1SH92	17	-0.84	0.002	0.013
Apolipoprotein B	APOB	A0A4X1U273	25	-1.02	<0.001	<0.001

[1]Accession number from UniProt protein database for *Sus scrofa*. [2]log2FC is base 2 logarithm transformed of fold change value which represents the ratio of expression levels in the first-mentioned group vs second-mentioned group. Protein names marked with * were shown as "Uncharacterized protein" in the UniProt *Sus scrofa* database and thus were substituted with the best match on *Sus scrofa* database, using SMARTBLAST tool. CR: piglet born from sow fed diet with ω6:ω3 ratio=13:1 during gestation, starting from day 28 (G28) and 10:1 during lactation; LR: piglet born from sow fed diet with ω6:ω3 ratio=4:1 from G28 until the end of lactation. SW: piglet diet with seaweed supplementation, CT: piglet diet without seaweed supplementation.

(cont. 2)

Protein name	Gene names	Accession number[1]	Number of peptides	log2FC[2]	*P*-value	Adjusted *p*-value
Comparison (e) – CR at d21 PW vs CR at d0 (cont., 1)						
SERPIN domain-containing protein	LOC396684	F1SCC7	17	-1.05	0.001	0.009
Apolipoprotein A-IV*	APOA4	A0A4X1T1L0	13	-1.36	<0.001	<0.001
Inter-alpha-trypsin inhibitor heavy chain H4 isoform 1	ITIH4	A0A480IL91	28	-1.45	<0.001	0.005
SERPIN domain-containing protein	LOC106504547	A0A287AGW0	14	-1.72	<0.001	0.003
Alpha-1-antichymotrypsin	SERPINA3	A0A480Y8T9	13	-2.14	<0.001	<0.001
Serum amyloid A	SAA	A0A480PRQ0	2	-3.08	<0.001	<0.001
Immunoglobulin lambda-like polypeptide 5 isoform 1*	IGLL5	A0A287A1M4	4	0.61	0.025	0.085
Apolipoprotein A-I	APOA1	K7GM40	24	-0.18	0.015	0.060
Complement factor H isoform a	CFH	A0A480TLF3	10	-0.24	0.044	0.133
Alpha-1-microglobulin	AMBP	A0A480P2R0	2	-0.29	0.017	0.067
Coagulation factor II	F2	B3STX9	5	-0.31	0.033	0.109
Alpha-1-antichymotrypsin 2	SERPINA3-2	Q9GMA6	11	-0.32	0.023	0.083
Plasminogen	PLG	A0A4X1VQL9	19	-0.36	0.050	0.147
Serpin family G member 1	SERPING1	A0A5K1UE53	4	-0.37	0.020	0.077
Ceruloplasmin	CP	K7GKN3	21	-0.52	<0.001	<0.001
Perilipin 5	PLIN5	A0A5G2QKC5	2	-0.55	0.042	0.130
Complement C4A	C4A	A0A4X1VBD2	18	-0.63	0.005	0.028
Alpha-2-Macroglobulin *	PZP	A0A287BDU7	41	-0.66	0.002	0.010
Inter-Alpha-Trypsin Inhibitor Heavy Chain 3*	ITIH3	A0A4X1VPM1	2	-0.73	<0.001	0.001
Apolipoprotein-E*	APOE	A0A4X1W1F9	9	-0.75	0.002	0.010
Apolipoprotein C-III	APOC3	A0A5G2QLU1	2	-0.76	0.001	0.009
SERPIN domain-containing protein	LOC100156325	F1SCC6	12	-0.84	0.001	0.009
Serpin A3-5*	SERPINA3-5	A0A4X1SH92	17	-0.84	0.002	0.013
Apolipoprotein B	APOB	A0A4X1U273	25	-1.02	<0.001	<0.001
SERPIN domain-containing protein	LOC396684	F1SCC7	17	-1.05	0.001	0.009
Apolipoprotein A-IV*	APOA4	A0A4X1T1L0	13	-1.36	<0.001	<0.001
Inter-alpha-trypsin inhibitor heavy chain H4 isoform 1	ITIH4	A0A480IL91	28	-1.45	<0.001	0.005
SERPIN domain-containing protein	LOC106504547	A0A287AGW0	14	-1.72	<0.001	0.003
Alpha-1-antichymotrypsin	SERPINA3	A0A480Y8T9	13	-2.14	<0.001	<0.001
Serum amyloid A	SAA	A0A480PRQ0	2	-3.08	<0.001	<0.001

[1]Accession number from UniProt protein database for *Sus scrofa*. [2]log2FC is base 2 logarithm transformed of fold change value which represents the ratio of expression levels in the first-mentioned group vs second-mentioned group. Protein names marked with * were shown as "Uncharacterized protein" in the UniProt *Sus scrofa* database and thus were substituted with the best match on *Sus scrofa* database, using SMARTBLAST tool. CR: piglet born from sow fed diet with ω6:ω3 ratio=13:1 during gestation, starting from day 28 and 10:1 during lactation.

(cont. 3)

Protein name	Gene names	Accession number[1]	Number of peptides	log2FC[2]	*P*-value	Adjusted *p*-value
Comparison (f) – LR at d21 PW vs LR at d0						
Histidine-rich glycoprotein	HRG	A0A481B9A6	14	1.67	<0.001	<0.001
Transferrin	TF	P09571	51	1.41	0.005	0.040
IgA heavy chain constant region*	IGHA1	A0A480QMR6	4	1.16	<0.001	0.003
Fetuin-B isoform 1	FETUB	A0A480SUZ7	2	1.15	<0.001	0.002
Transthyretin	TTR	A0A5G2QIE9	3	0.97	0.003	0.039
Ig-like domain-containing protein		A0A075B7H9	3	0.90	0.001	0.023
IgG heavy chain	IGHG	L8B149	8	0.73	0.003	0.039
Immunoglobulin lambda-like polypeptide 5 isoform 1*	IGLL5	A0A287A1M4	4	0.64	0.013	0.066
Alpha-1 acid glycoprotein	ORM1	Q29014	11	0.40	0.019	0.087
Vitronectin	VTN	P48819	6	0.32	0.005	0.040
SERPIN domain-containing protein	SERPIND1	A0A4X1UYS0	3	0.29	0.039	0.143
Gelsolin	GSN	A0A287A6P1	2	0.29	0.039	0.143
Alpha-1-antitrypsin/Serpin Family A Member 1	SERPINA1	P50447	8	0.29	0.031	0.120
Ceruloplasmin	CP	K7GKN3	21	-0.24	0.030	0.120
IgM heavy chain constant region*	IGHM	A0A287ALC1	18	-0.34	0.031	0.120
Serpin family G member 1	SERPING1	A0A5K1UE53	4	-0.36	0.007	0.042
Alpha-2-Macroglobulin *	PZP	A0A287A1B4	40	-0.4	0.008	0.042
C-type lectin domain family 3 member B	CLEC3B	F1SRC8	3	-0.47	0.018	0.083
Inter-Alpha-Trypsin Inhibitor Heavy Chain 3*	ITIH3	A0A4X1VPM1	2	-0.47	0.001	0.010
CD5 Molecule Like*	CD5L	A0A4X1VVV3	4	-0.48	0.014	0.066
Apolipoprotein-E*	APOE	A0A4X1W1F9	9	-0.53	0.004	0.040
Perilipin 5	PLIN5	A0A5G2QKC5	2	-0.54	0.027	0.114

[1]Accession number from UniProt protein database for *Sus scrofa*. [2]log2FC is base 2 logarithm transformed of fold change value which represents the ratio of expression levels in the first-mentioned group vs second-mentioned group. Protein names marked with * were shown as "Uncharacterized protein" in the UniProt *Sus scrofa* database and thus were substituted with the best match on *Sus scrofa* database, using SMARTBLAST tool. CR: piglet born from sow fed diet with ω6:ω3 ratio=13:1 during gestation, starting from day 28 (G28) and 10:1 during lactation; LR: piglet born from sow fed diet with ω6:ω3 ratio=4:1 from G28 until the end of lactation.

(cont. 4)

Protein name	Gene names	Accession number[1]	Number of peptides	log2FC[2]	*P*-value	Adjusted *p*-value
Comparison (f) – LR at d21 PW vs LR at d0 (cont.)						
Complement C4A	C4A	A0A4X1VBD2	18	-0.57	<0.001	0.010
Apolipoprotein B	APOB	A0A4X1U273	25	-0.66	<0.001	<0.001
SERPIN domain-containing protein	LOC396684	F1SCC7	17	-0.76	0.007	0.042
Serpin A3-5*	SERPINA3-5	A0A4X1SH92	17	-0.83	0.005	0.040
SERPIN domain-containing protein	LOC100156325	F1SCC6	12	-1.00	0.008	0.042
Apolipoprotein A-IV*	APOA4	A0A4X1T1L0	13	-1.21	<0.001	<0.001
SERPIN domain-containing protein	LOC106504547	A0A287AGW0	14	-1.30	0.023	0.101
Alpha-1-antichymotrypsin (Fragment)	SERPINA3	A0A480Y8T9	13	-1.35	0.007	0.042
Serum amyloid A	SAA	A0A480PRQ0	2	-1.95	0.004	0.040
Comparison (g) – d21 PW vs d0						
Histidine-rich glycoprotein	HRG	A0A481B9A6	14	1.60	<0.001	<0.001
Transferrin	TF	P09571	51	1.42	<0.001	<0.001
Immunoglobulin kappa variable region*	IGKV1-5	A0A286ZYQ7	4	1.11	0.003	0.012
Fetuin-B isoform 1	FETUB	A0A480SUZ7	2	1.07	<0.001	<0.001
IgA heavy chain constant region*	IGHA1	A0A480QMR6	4	1.03	<0.001	<0.001
Transthyretin	TTR	A0A5G2QIE9	3	0.83	<0.001	<0.001
Glutathione peroxidase 3	GPX3	A0A4X1TQP5	6	0.81	0.015	0.043
Ig-like domain-containing protein		A0A075B7H9	3	0.78	<0.001	<0.001
IgG heavy chain	IGHG	L8B149	8	0.71	<0.001	<0.001
Immunoglobulin lambda-like polypeptide 5 isoform 1*	IGLL5	A0A287A1M4	4	0.62	<0.001	0.003
Alpha-1 acid glycoprotein	ORM1	Q29014	11	0.35	0.002	0.007
Vitronectin	VTN	P48819	6	0.28	0.003	0.011
Alpha-1-antitrypsin/Serpin Family A Member 1	SERPINA1	P50447	8	0.21	0.013	0.042
SERPIN domain-containing protein	SERPIND1	A0A4X1UYS0	3	0.20	0.026	0.070
Immunoglobulin kappa chain**		A0A4X1W4H6	9	0.18	0.043	0.106

[1]Accession number from UniProt protein database for *Sus scrofa*. [2]log2FC is base 2 logarithm transformed of fold change value which represents the ratio of expression levels in the first-mentioned group vs second-mentioned group. Protein names marked with * were shown as "Uncharacterized protein" in the UniProt *Sus scrofa* database and thus were substituted with the best match on *Sus scrofa* database, using SMARTBLAST tool. LR: piglet born from sow fed diet with ω6:ω3 ratio=4:1 from G28 until the end of lactation.

(cont. 5)

Protein name	Gene names	Accession number[1]	Number of peptides	log2FC[2]	*P*-value	Adjusted *p*-value
Comparison (g) - d21 PW vs d0 (cont.)						
Apolipoprotein A-I	APOA1	K7GM40	24	-0.17	0.002	0.007
Alpha-1-microglobulin	AMBP	A0A480P2R0	2	-0.21	0.011	0.035
Coagulation factor II	F2	B3STX9	5	-0.23	0.019	0.053
IgM heavy chain constant region*	IGHM	A0A287ALC1	18	-0.24	0.025	0.067
Apolipoprotein F precursor*	APOF	A0A4X1W7I8	2	-0.33	0.007	0.024
CD5 Molecule Like*	CD5L	A0A4X1VVV3	4	-0.36	0.028	0.073
Serpin family G member 1	SERPING1	A0A5K1UE53	4	-0.36	<0.001	0.001
Ceruloplasmin	CP	K7GKN3	21	-0.38	<0.001	<0.001
Plasminogen	PLG	A0A4X1VQL9	19	-0.40	0.014	0.043
C-type lectin domain family 3 member B	CLEC3B	F1SRC8	3	-0.42	0.008	0.026
Alpha-2-Macroglobulin *	PZP	A0A287BDU7	41	-0.49	<0.001	0.003
Perilipin 5	PLIN5	A0A5G2QKC5	2	-0.55	0.002	0.008
Inter-Alpha-Trypsin Inhibitor Heavy Chain 3*	ITIH3	A0A4X1VPM1	2	-0.60	<0.001	<0.001
Complement C4A	C4A	A0A4X1VBD2	18	-0.60	<0.001	<0.001
Apolipoprotein C-III	APOC3	A0A5G2QLU1	2	-0.63	<0.001	0.001
Apolipoprotein-E*	APOE	A0A4X1W1F9	9	-0.64	<0.001	<0.001
Ig-like domain-containing protein	LOC100523213	F1RL06	3	-0.67	0.020	0.057
Haptoglobin	HP	Q8SPS7	16	-0.79	0.015	0.043
Serpin A3-5*	SERPINA3-5	A0A4X1SH92	17	-0.84	<0.001	<0.001
Apolipoprotein B	APOB	A0A4X1U273	25	-0.84	<0.001	<0.001
SERPIN domain-containing protein	LOC396684	F1SCC7	17	-0.90	<0.001	<0.001
SERPIN domain-containing protein	LOC100156325	F1SCC6	12	-0.92	<0.001	<0.001
Inter-alpha-trypsin inhibitor heavy chain H4 isoform 1	ITIH4	A0A480IL91	28	-1.05	0.001	0.006
Apolipoprotein A-IV*	APOA4	A0A4X1T1L0	13	-1.29	<0.001	<0.001
SERPIN domain-containing protein	LOC106504547	A0A287AGW0	14	-1.51	<0.001	<0.001
Alpha-1-antichymotrypsin	SERPINA3	A0A480Y8T9	13	-1.74	<0.001	<0.001
Serum amyloid A	SAA	A0A480PRQ0	2	-2.52	<0.001	<0.001

[1]Accession number from UniProt protein database for *Sus scrofa*. [2]log2FC is base 2 logarithm transformed of fold change value which represents the ratio of expression levels in the first-mentioned group vs second-mentioned group. Protein names marked with * were shown as "Uncharacterized protein" in the UniProt *Sus scrofa* database and thus were substituted with the best match on *Sus scrofa* database, using SMARTBLAST tool. Proteins ** were shown as "Uncharacterized protein" in the UniProt *Sus scrofa* database and cannot find the best match on *Sus scrofa* database, thus were substituted with the best match on *Homo sapiens* database, using SMARTBLAST tool.

4.7.1.1 DAPs in LR vs CR groups (comparisons (a), (b), (c))

On d0, serum in LR piglets gave 7 DAPs (3 increased and 4 decreased) when compared to CR piglets (comparison (a), Table 4-1, $p < 0.05$), while on d21 PW, LR piglets exhibited 10 DAPs (6 increased and 4 decreased) when compared to CR piglets (comparison (b)). Irrespective of sampling time, LR piglets generated 13 DAPs (5 increased and 8 decreased) if compared to CR piglets (comparison (c), Table 4-1, $p < 0.05$). Among these proteins, transferrin (TF, B3CL06) was decreased in all three comparisons (a), (b), and (c), while TF (P09571) was increased in (b) and (c). Antithrombin-III (SERPINC1) was increased in both (a) and (c). Several DAPs were identified distinctly for each of the three comparisons, such as complement C3 (C3) was decreased, and coagulation factor XII (F12) was increased in (a). In (b), apolipoprotein B (APOB) and serum amyloid A protein (SAA) were increased while plasma kallikrein (KLKB1) was decreased. In (c), fibronectin (FN1) was decreased while alpha-2-Macroglobulin (PZP) was increased. The DAPs separated and overlapped among three comparisons (a), (b), and (c) are represented in the Venn diagram (Figure 4-3A) and heatmap (Figure 4-4).

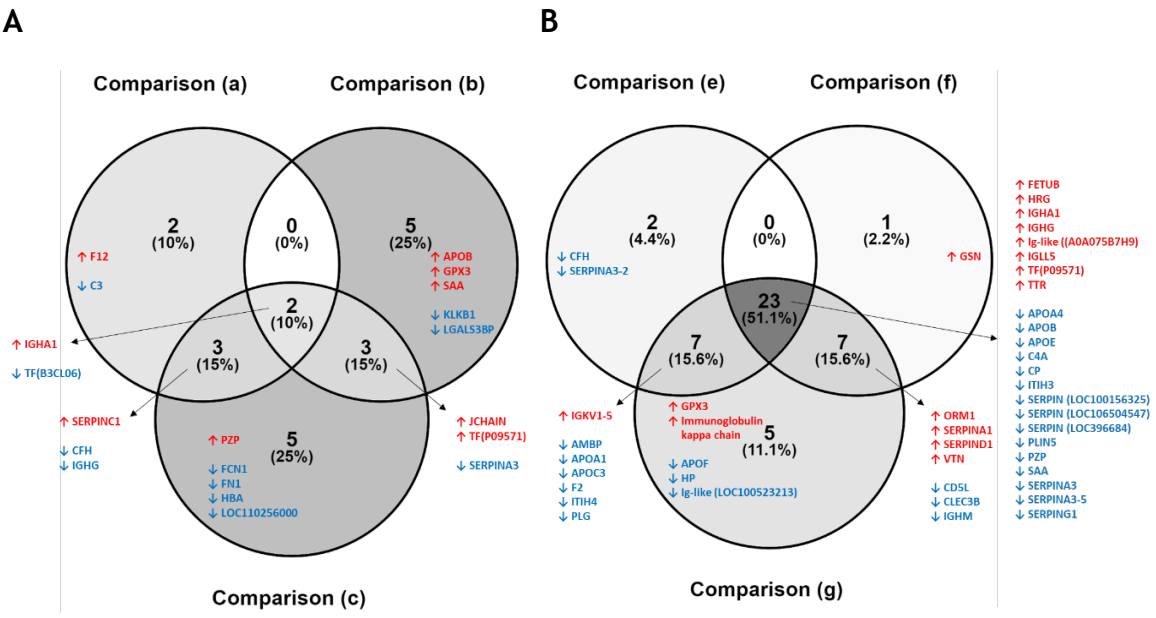

Figure 4-3 Venn diagram representing separated and overlapped differentially abundant proteins (DAPs) among six comparisons of piglet serum : A) Comparison (a) - LR vs CR at weaning (d0); Comparison (b) - LR vs CR at day 21 post-weaning (d21 PW); and Comparison (c) - LR vs CR; B) Comparison (e) - CR at d21 PW vs CR at d0; Comparison (f) - LR at d21 PW vs LR at d0; and Comparison (g) – d21 PW vs d0. CR: piglet born from sow fed diet with ω6:ω3 ratio=13:1 during gestation, starting from day 28 (G28) and 10:1 during lactation; LR: piglet born from sow fed diet with ω6:ω3 ratio=4:1 from G28 until the end of lactation. SW: piglet diet with seaweed supplementation, CT: piglet diet without seaweed supplementation.

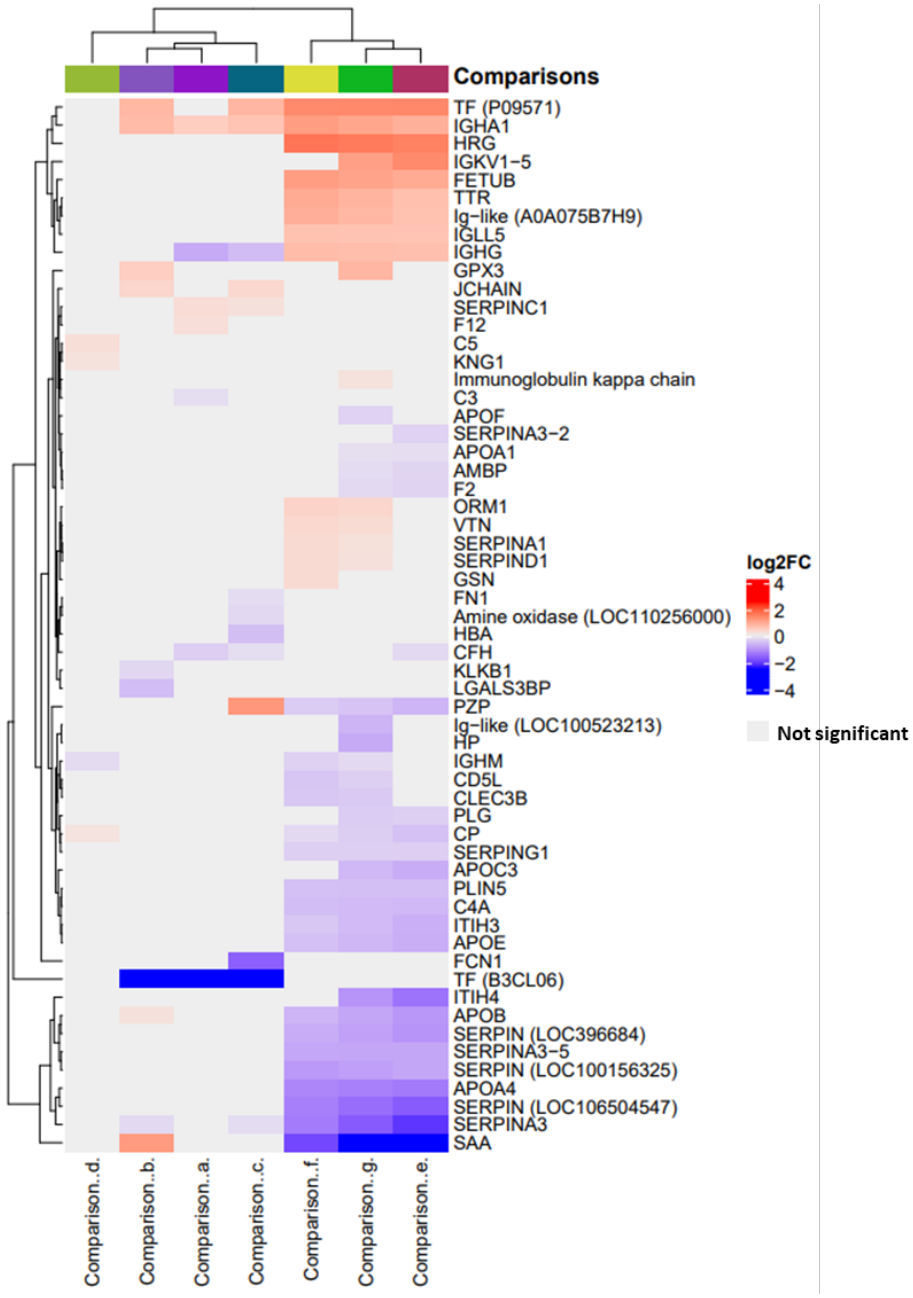

Figure 4-4 Heatmap of the significant differentially abundant proteins (DAPs) among seven comparisons of piglet serum : (a) - LR vs CR at d0; (b) - LR vs CR at d21 PW; (c) - LR vs CR; (d) - SW vs CT at d21 PW; (e) - CR at d21 PW vs CR at d0; (f) - LR at d21 PW vs LR at d0; and (g) - d21 PW vs d0. CR: piglet born from sow fed diet with ω6:ω3 ratio=13:1 during gestation, starting from day 28 (G28) and 10:1 during lactation; LR: piglet born from sow fed diet with ω6:ω3 ratio=4:1 from G28 until the end of lactation. SW: piglet diet with seaweed supplementation, CT: piglet diet without seaweed supplementation.

A mixed distribution with more overlaps of the samples between CR and LR groups towards the end of the post-weaning period is presented in the PCA of comparison (a), (b), and (c) (Figures 4-5A, 4-6A, and 4-7A, respectively). The total variance explained in the PCA procedure was gradually decreased from weaning (70.51%) to d21 PW (62.78%) and regardless of sampling time (50.30%). The volcano plots of DAPs in (a), (b), and (c) are shown in Figures 4-5B, 4-6B, and 4-7B, respectively. The hierarchical cluster heatmaps of the DAPs clearly showed a mixed distribution between LR and CR serum in (a), (b), and (c) (Figures 4-5C, 4-6C, and 4-7C, respectively).

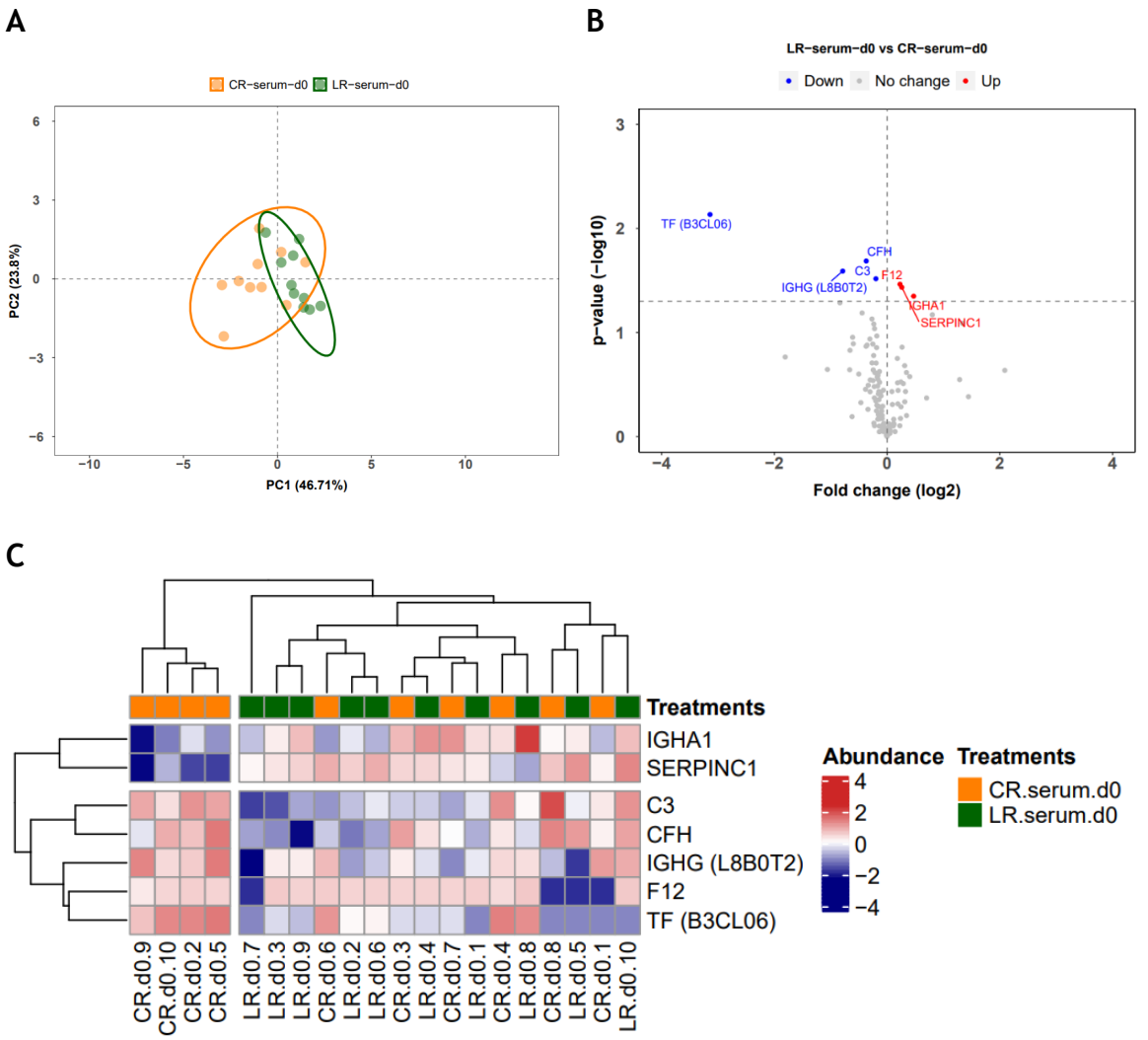

Figure 4-5 A-Principal Components Analysis (PCA) plot, B-Volcano plot, C-Heatmap in comparison (a) - LR versus CR at weaning day (d0). A, B, and C show the clustering of samples, the differentially abundant proteins (DAPs), and highlighting the proteins changing, respectively. In the PCA, the ellipses represent 95% confidence region. Significant increased proteins in red, significant decreased proteins in blue, and non-significant proteins in grey. CR: piglet born from sow fed diet with ω6:ω3 ratio=13:1 during gestation, starting from day 28 (G28) and 10:1 during lactation; LR: piglet born from sow fed diet with ω6:ω3 ratio=4:1 from G28 until the end of lactation.

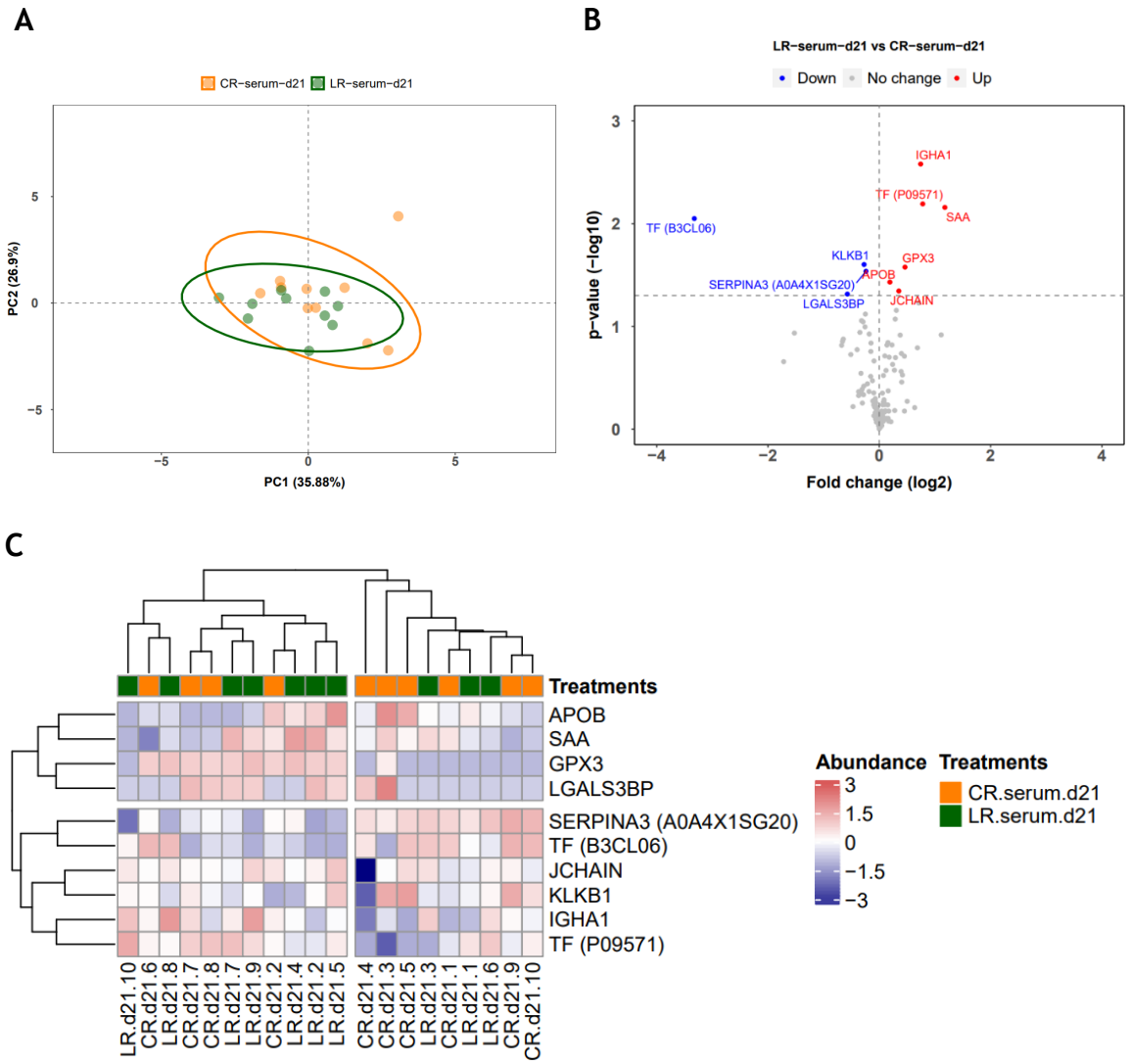

Figure 4-6 A-Principal Components Analysis (PCA) plot, B-Volcano plot, C-Heatmap in comparison (b) - LR versus CR at day 21 post-weaning (d21). A, B, and C show the clustering of samples, the differentially abundant proteins (DAPs), and highlighting the proteins changing, respectively. In the PCA, the ellipses represent 95% confidence region. Significant increased proteins in red, significant decreased proteins in blue, and non-significant proteins in grey. CR: piglet born from sow fed diet with ω6:ω3 ratio=13:1 during gestation, starting from day 28 (G28) and 10:1 during lactation; LR: piglet born from sow fed diet with ω6:ω3 ratio=4:1 from G28 until the end of lactation.

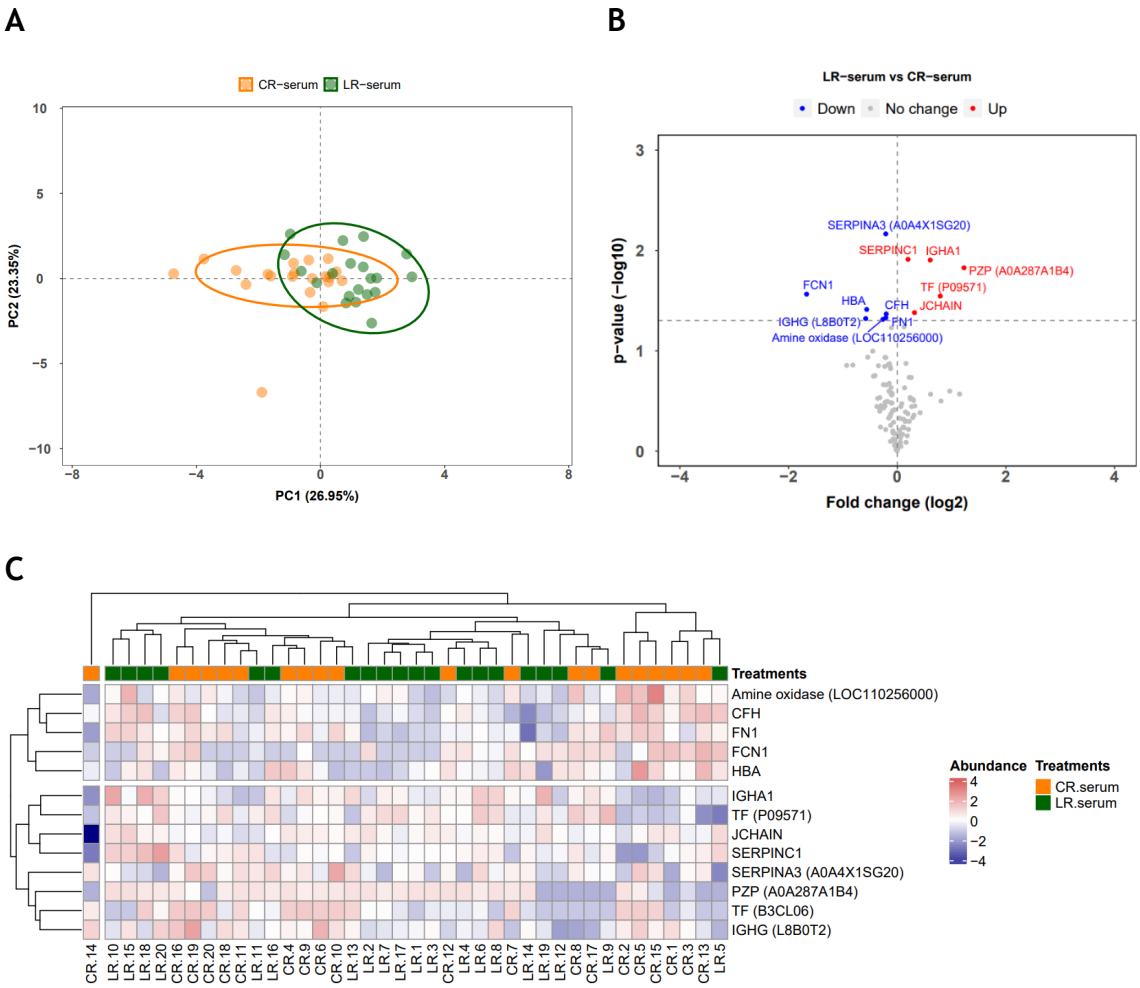

Figure 4-7 A-Principal Components Analysis (PCA) plot, B-Volcano plot, C-Heatmap in comparison (c) - LR versus CR. A, B, and C show the clustering of samples, the differentially abundant proteins (DAPs), and highlighting the proteins changing, respectively. In the PCA, the ellipses represent 95% confidence region. Significant increased proteins in red, significant decreased proteins in blue, and non-significant proteins in grey. CR: piglet born from sow fed diet with ω6:ω3 ratio=13:1 during gestation, starting from day 28 (G28) and 10:1 during lactation; LR: piglet born from sow fed diet with ω6:ω3 ratio=4:1 from G28 until the end of lactation.

4.7.1.2 DAPs in SW vs CT groups (comparison (d))

Taking into account the effect of the piglet diet, comparison (d) examined SW serum vs CT serum at d21 PW, and it yielded 4 DAPs ($p < 0.05$, Tables 4-1 and 4-2). As shown in Figure 4-8B, the volcano plot indicates three upregulated proteins comprising Complement C5a anaphylatoxin (C5), kininogen 1 (KNG1), and ceruloplasmin (CP), and one downregulated protein, IgM heavy chain constant region (IGHM). The PCA analysis showed a mixed cluster between SW and CT samples, with the first two components explaining a high rate (78.06%) of data variation (Figure 4-8A). This mixed cluster is also shown in the hierarchical cluster heatmaps of the DAPs between SW and CT serum (Figure 4-8C).

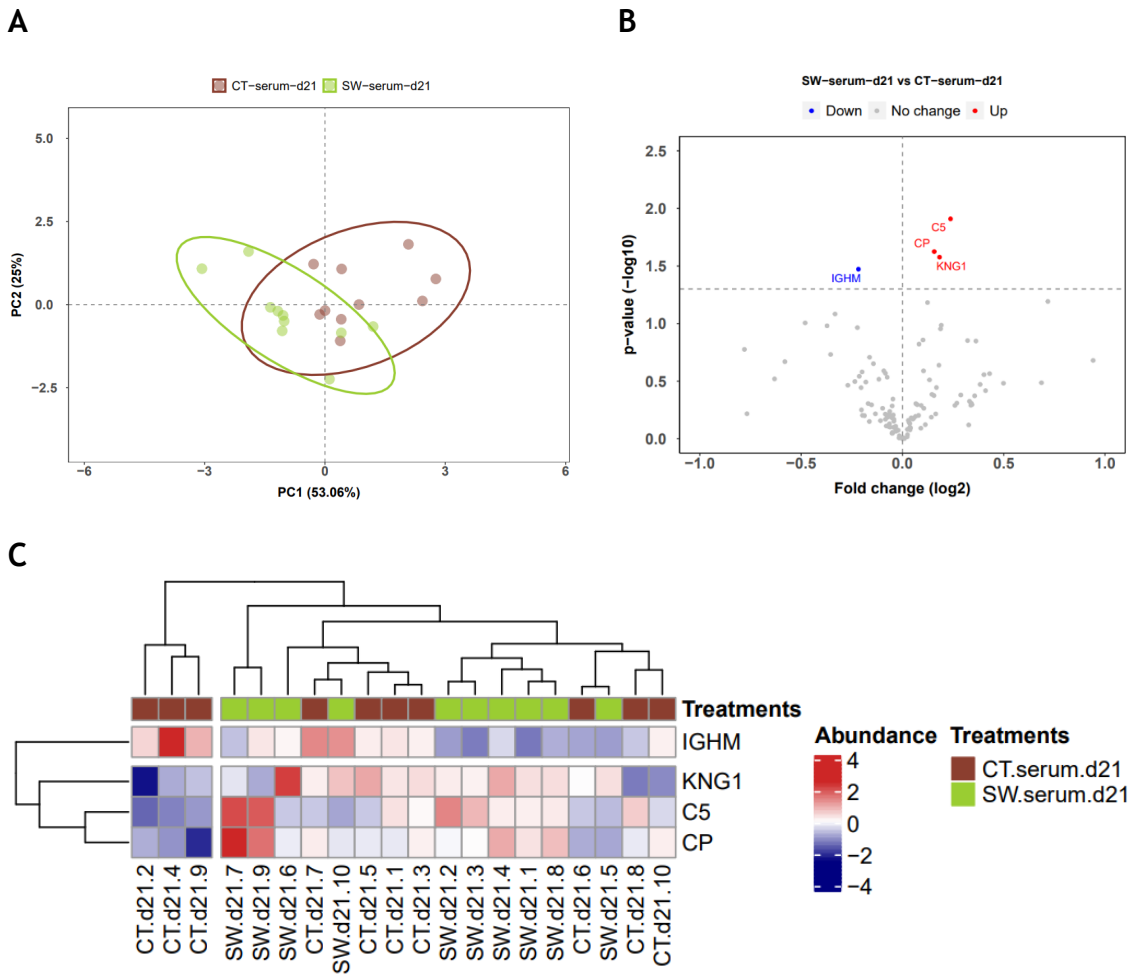

Figure 4-8 A-Principal Components Analysis (PCA) plot, B-Volcano plot, C-Heatmap in comparison (d) - SW versus CT at day 21 post-weaning (d21). A, B, and C show the clustering of samples, the differentially abundant proteins (DAPs), and highlighting the proteins changing, respectively. In the PCA, the ellipses represent 95% confidence region. Significant increased proteins in red, significant decreased proteins in blue, and non-significant proteins in grey. SW: piglet diet with seaweed supplementation, CT: piglet diet without seaweed supplementation.

4.7.1.3 DAPs in d21 PW vs d0 (comparisons (e), (f), (g))

Considering the sampling time, comparison (e) investigated CR serum at d21 PW versus CR serum at d0 and disclosed 32 DAPs (9 increased and 23 decreased) (Table 4-1, $p < 0.05$). Comparison (f) analysed LR serum at d21 PW versus LR serum at d0 and found 31 DAPs (13 increased and 18 decreased) (Table 4-1, $p < 0.05$). Irrespective of dietary treatment, comparison (g) determined serum from d21 PW versus d0 and revealed 42 DAPs (15 increased and 27 decreased) (Table 4-1, $p < 0.05$). A heatmap (Figure 4-4) showed that, among these proteins, there are 8 proteins increased, and 15 proteins decreased in both (e) and (f) comparisons; 11 proteins increased, and 18 proteins decreased in both (f) and (g); 8 proteins increased, and 21 proteins decreased in both (e) and (g). Moreover, these three comparisons (e, f, g) share similar increased-abundant proteins such as transferrin (TF, P09571), histidine-rich glycoprotein (HRG), fetuin-B isoform 1 (FETUB), transthyretin (TTR) and similar decreased-abundance proteins such as serum amyloid A (SAA), serpin-containing proteins; apolipoprotein A-IV, B and E (APOA4, APOB, APOE). The Venn diagram also illustrated the overlapped DAPs among these three comparisons (Figure 4-3B).

As shown in the PCA plots, the serum at d0 and d21 PW were distinctly clustered in comparisons (e), (f), and (g), with the explained variances of 68.56% (Figure 4-9A), 55.66% (Figure 4-10A), and 57.30% (Figure 4-11A), respectively. The hierarchically clustered heatmaps also displayed the distinct proteome profiles of these comparisons (Figures 4-9C, 4-10C, and 4-11C, respectively). The increased- and decreased- abundance proteins in (e), (f), and (g) are highlighted in the volcano plots (Figures 4-9B, 4-10B, and 4-11B, respectively).

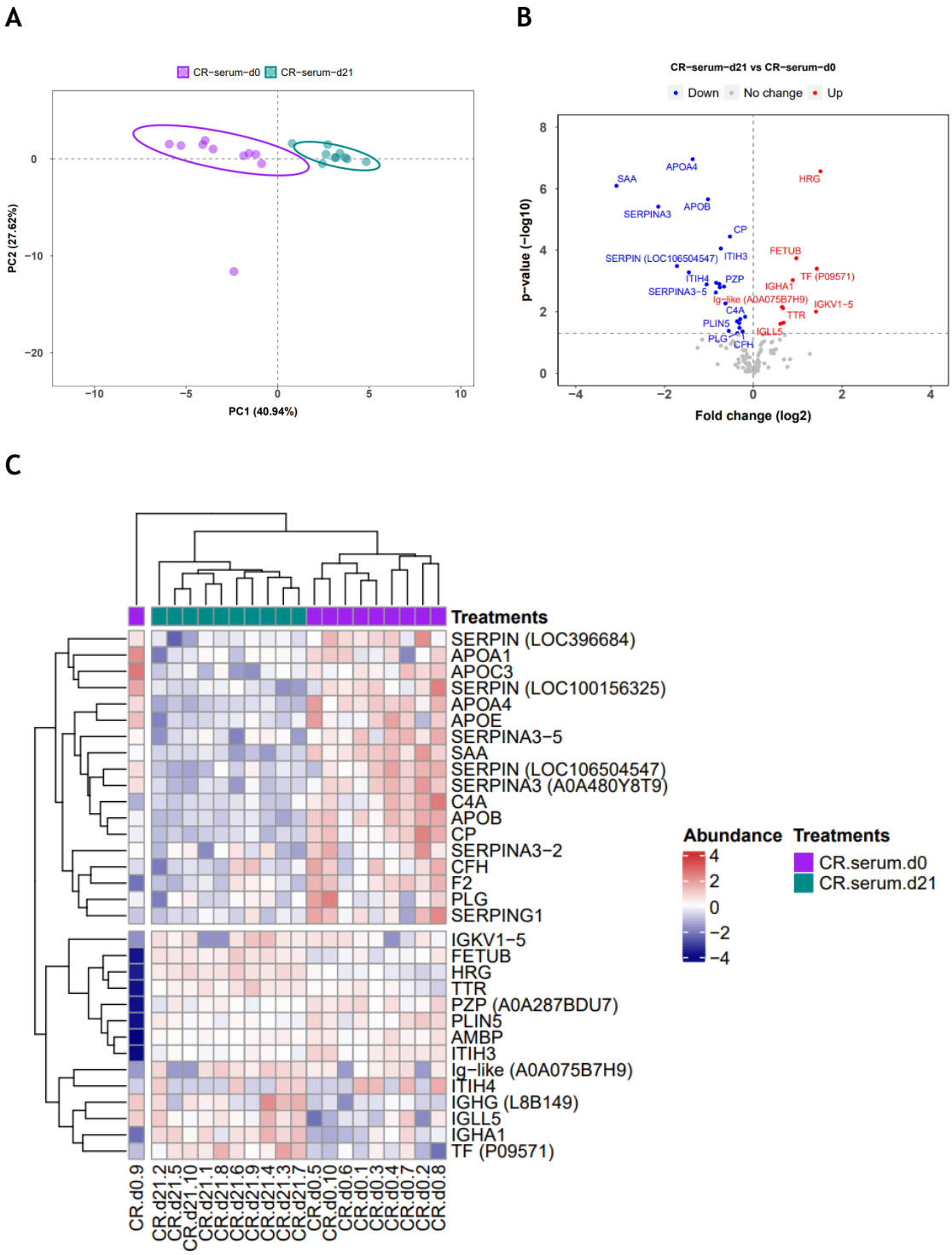

Figure 4-9 A-Principal Components Analysis (PCA) plot, B-Volcano plot, C-Heatmap in comparison (e) - CR at day 21 post-weaning (d21) versus CR at weaning day (d0). A, B, and C show the clustering of samples, the differentially abundant proteins (DAPs), and highlighting the proteins changing, respectively. In the PCA, the ellipses represent 95% confidence region. Significant increased proteins in red, significant decreased proteins in blue, and non-significant proteins in grey. CR: piglet born from sow fed diet with ω6:ω3 ratio=13:1 during gestation, starting from day 28 and 10:1 during lactation.

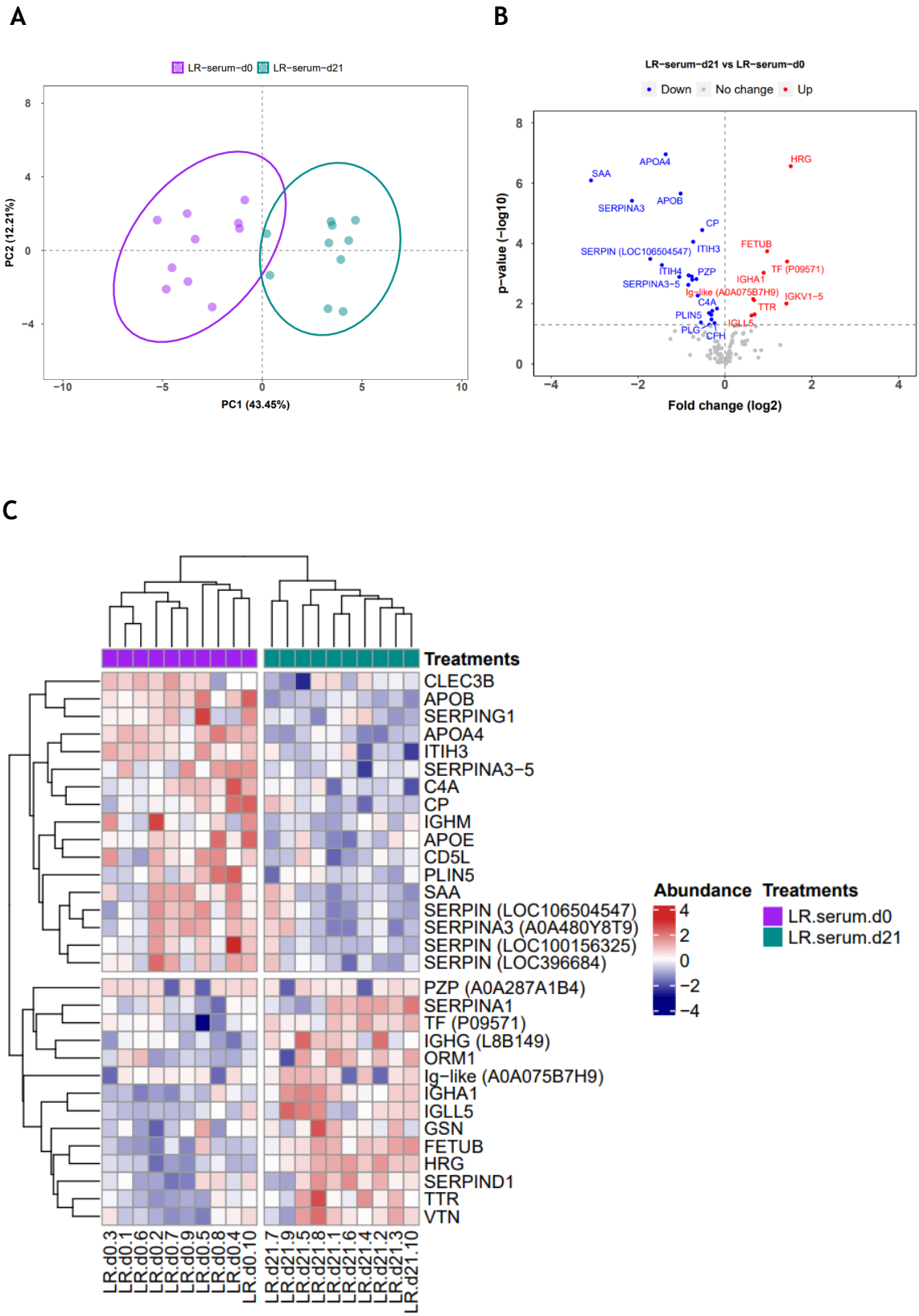

Figure 4-10 A-Principal Components Analysis (PCA) plot, B-Volcano plot, C-Heatmap in comparison (f) – LR at day 21 post-weaning (d21) versus LR at weaning day (d0). A, B, and C show the clustering of samples, the differentially abundant proteins (DAPs), and highlighting the proteins changing, respectively. In the PCA, the ellipses represent 95% confidence region. Significant increased proteins in red, significant decreased proteins in blue, and non-significant proteins in grey. CR: piglet born from sow fed diet with ω6:ω3 ratio=13:1 during gestation, starting from day 28 and 10:1 during lactation.

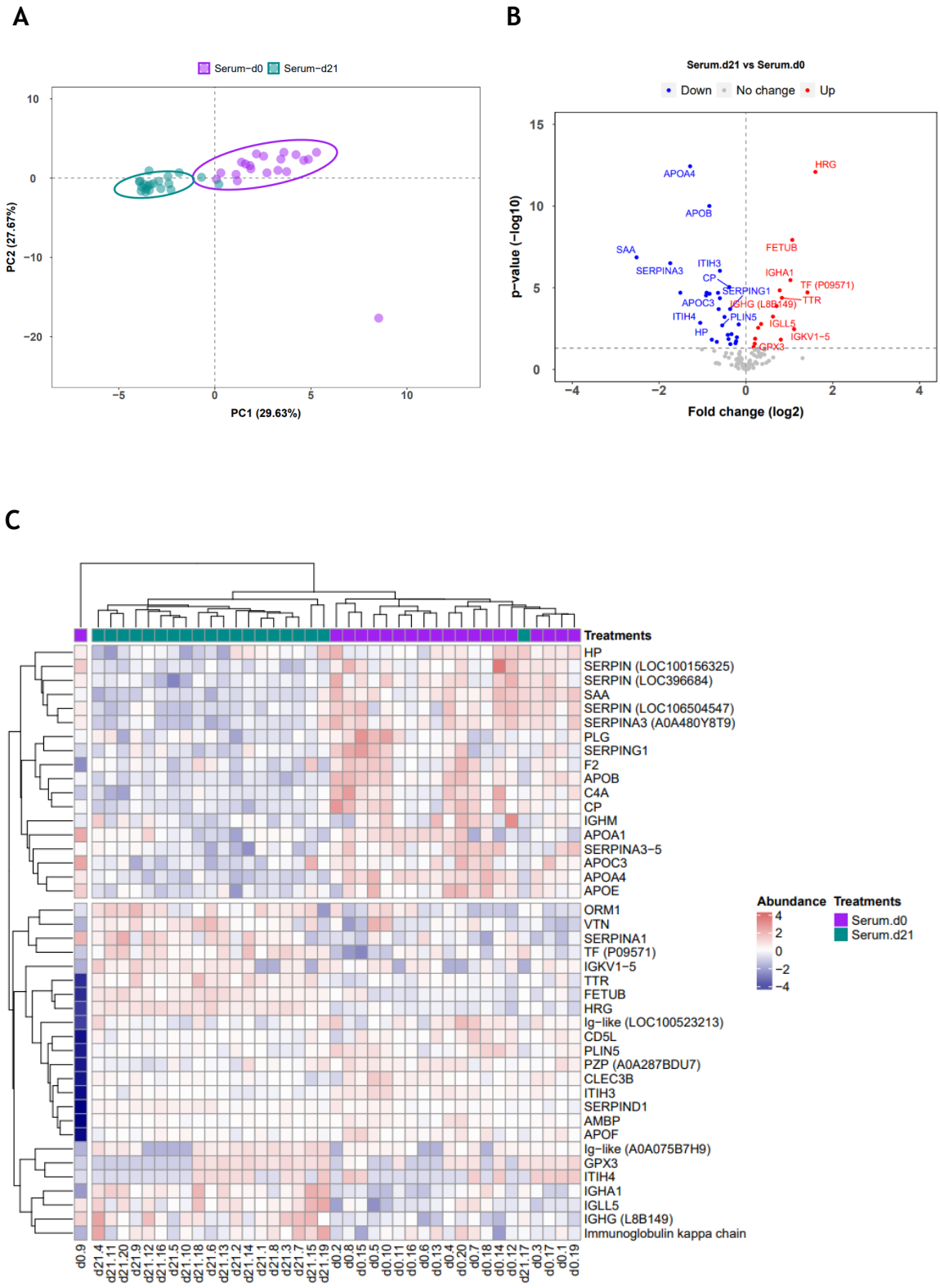

Figure 4-11 A-Principal Components Analysis (PCA) plot, B-Volcano plot, C-Heatmap in comparison (g) –day 21 post-weaning (d21) versus weaning day (d0). A, B, and C show the clustering of samples, the differentially abundant proteins (DAPs), and highlighting the proteins changing, respectively. In the PCA, the ellipses represent 95% confidence region. Significant increased proteins in red, significant decreased proteins in blue, and non-significant proteins in grey. CR: piglet born from sow fed diet with ω6:ω3 ratio=13:1 during gestation, starting from day 28 and 10:1 during lactation.

4.7.1.4 GO enrichment of all identified serum proteins

The analysis of protein-protein interaction (PPI) enrichment illustrates an association among 122 master proteins with 78 nodes and 1171 edges (p < 1.0e-16). The functional enrichments highlighted 99, 28, and 19 GO terms on biological processes (BP), molecular function (MF), and cellular components (CC), respectively. The top three enriched GO-BP terms were regulation of proteolysis [GO:0030162], vesicle-mediated transport [GO:0016192], and regulation of immune effector process [GO:0002697]. The top three enriched GO-MF terms were enzyme regulator activity [GO:0030234], heparin-binding [GO:0008201], and lipid binding [GO:0008289]. The top three enriched GO-CC terms were blood microparticle [GO:0072562], extracellular space [GO:0005615], and vesicle [GO:0031982]. The top 20, 10, and 5 GO terms on BP, MF, and CC, respectively, are shown in Figure 4-12.

All 122 serum master proteins

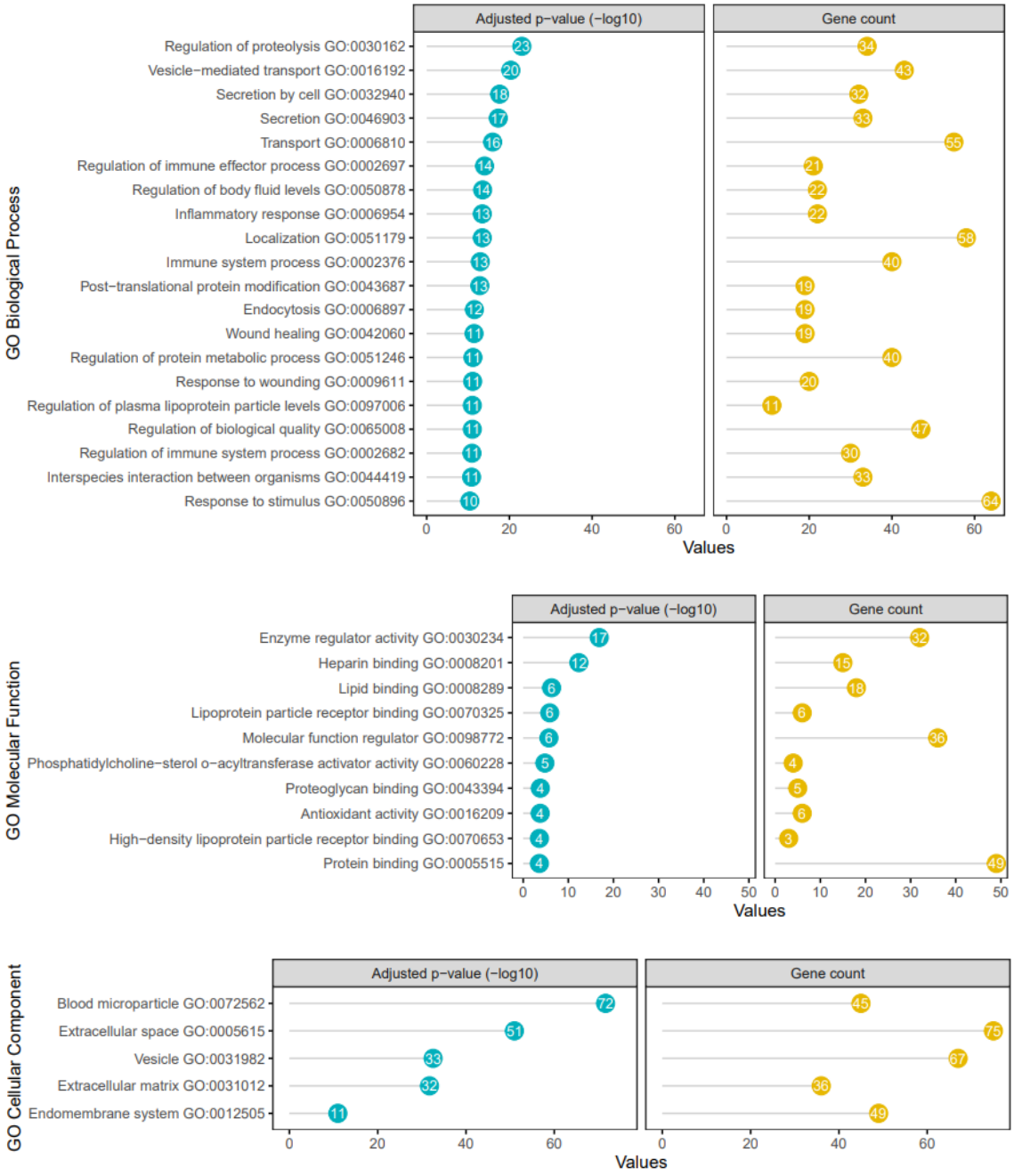

Figure 4-12 Gene ontology analysis of all 122 proteins kept in serum proteomics study with their corresponding gene count inside each term and their associated adjusted p-value (expressed as -log10).

4.7.1.5 GO and Reactome pathway enrichment in LR vs CR groups (comparisons (a), (b), (c))

The DAP PPI network between LR and CR serum at d0 - comparison (a) contains 5 nodes and 6 edges (p = 7.7e-09). No enriched GO terms on BP and MF were found. The list of enriched GO terms on CC and Reactome pathways is presented in Table 4-3. The PPI network in the LR serum compared to CR serum at d21 PW - comparison (b) comprises 8 nodes and 7 edges (p = 6.81e-08). The list of enriched GO terms on CC and Reactome pathways is presented in Table 4-4. Regardless of sampling time, the PPI network in the DAP between LR and CR serum - comparison (c) contains 9 nodes and 7 edges (p = 1.31e-05). No enriched GO terms on BP and Reactome pathways were observed. The list of enriched GO terms on MF and CC are presented in Table 4-5.

Reactome pathway analysis in comparison (a) highlighted the interaction among C3, SERPINC1, and TF in the regulation of Insulin-like Growth Factor (IGF) transport and uptake by Insulin-like Growth Factor Binding Proteins (IGFBPs) [HSA-381426], and post-translational protein phosphorylation [HSA-8957275]. In comparison (b), three Reactome pathways were enriched containing haemostasis [HSA-109582], binding and uptake of ligands by scavenger receptors [HSA-2173782], and scavenging by class B receptors [HSA-3000471].

4.7.1.6 GO and Reactome pathway enrichment in SW vs CT groups (comparisons (d))

The DAP PPI network between SW and CT serum at d21 PW - comparison (d) contains only 3 nodes and 1 edge (p = 0.038), and no significant pathways were detected. However, when the network is expanded with maximum 5 interactors shown in the first shell, 8 nodes and 17 edges were found (p = 3.75e-05). Moreover, their list of enriched GO terms on BP, CC, and Reactome pathways are presented in Table 4-6 underlined the role of C5 in regulating complement cascade [HSA-977606] and terminal pathway of complement [HSA-166665].

Table 4-3 Gene Ontology (GO) terms on biological processes, molecular function and cellular components in comparison (a) - LR versus CR at weaning. CR: piglet born from sow fed diet with ω6:ω3 ratio=13:1 during gestation, starting from day 28 (G28) and 10:1 during lactation; LR: piglet born from sow fed diet with ω6:ω3 ratio=4:1 from G28 until the end of lactation.

GO term ID	Description	Adjusted p-value	Gene count	Matching proteins in PPI network
GO Cellular Component (n = 2)				
GO:0072562	Blood microparticle	1.6E-05	4	C3, CFH, SERPINC1, TF
GO:0005783	Endoplasmic reticulum	4.9E-02	4	C3, F12, SERPINC1, TF
Pathway				
Reactome Pathways (n = 2)				
HSA-381426	Regulation of Insulin-like Growth Factor (IGF) transport and uptake by Insulin-like Growth Factor Binding Proteins (IGFBPs)	3.0E-02	3	C3, SERPINC1, TF
HSA-8957275	Post-translational protein phosphorylation	3.0E-02	3	C3, SERPINC1, TF

Table 4-4 Gene Ontology (GO) terms on cellular component and Reactome pathways in comparison (b) - LR versus CR at day 21 post-weaning. CR: piglet born from sow fed diet with ω6:ω3 ratio=13:1 during gestation, starting from day 28 (G28) and 10:1 during lactation; LR: piglet born from sow fed diet with ω6:ω3 ratio=4:1 from G28 until the end of lactation.

GO term ID	Description	Adjusted p-value	Gene count	Matching proteins in PPI network
GO Cellular Component (n = 5)				
GO:0072562	Blood microparticle	5.5E-05	4	JCHAIN, LGALS3BP, SERPINA3, TF
GO:0031983	Vesicle lumen	1.7E-03	4	APOB, LGALS3BP, SERPINA3, TF
GO:0071682	Endocytic vesicle lumen	9.2E-03	2	APOB, SAA
GO:0034364	High-density lipoprotein particle	1.7E-02	2	APOB, SAA
GO:0034774	Secretory granule lumen	4.0E-02	3	LGALS3BP, SERPINA3, TF
Pathway				
Reactome Pathways (n = 3)				
HSA-109582	Haemostasis	4.2E-04	6	APOB, JCHAIN, LGALS3BP, KLKB1, SERPINA3, TF
HSA-2173782	Binding and Uptake of Ligands by Scavenger Receptors	5.1E-03	3	APOB, JCHAIN, SAA
HSA-3000471	Scavenging by Class B Receptors	2.4E-02	2	APOB, SAA

Table 4-5 Gene Ontology (GO) terms on biological processes, molecular function and cellular components in comparison (c) - LR versus CR. CR: piglet born from sow fed diet with ω6:ω3 ratio=13:1 during gestation, starting from day 28 (G28) and 10:1 during lactation; LR: piglet born from sow fed diet with ω6:ω3 ratio=4:1 from G28 until the end of lactation.

GO term ID	Description	Adjusted p-value	Gene count	Matching proteins in PPI network
GO Molecular Function (n = 1)				
GO:0061134	Peptidase regulator activity	1.2E-02	4	PZP, FN1, SERPINC1, SERPINA3
GO Cellular Component (n = 6)				
GO:0072562	Blood microparticle	2.7E-11	7	JCHAIN, PZP, FN1, CFH, SERPINC1, SERPINA3, TF
GO:0005615	Extracellular space	4.8E-03	8	JCHAIN, PZP, FN1, CFH, SERPINC1, FCN1, SERPINA3, TF
GO:0031232	Extrinsic component of external side of plasma membrane	4.8E-03	2	FCN1, TF
GO:0031982	Vesicle	4.8E-03	8	JCHAIN, PZP, FN1, CFH, SERPINC1, FCN1, SERPINA3, TF
GO:0034774	Secretory granule lumen	4.8E-03	4	FN1, FCN1, SERPINA3, TF
GO:0062023	Collagen-containing extracellular matrix	4.8E-03	4	FN1, SERPINC1, FCN1, SERPINA3

Table 4-6 Gene Ontology (GO) terms on biological processes, molecular function and cellular components in comparison (d) - SW versus CT at day 21 post-weaning. The interaction network is expanded with maximum 5 interactors shown in the first shell. SW: piglet diet with seaweed supplementation, CT: piglet diet without seaweed supplementation.

GO term ID	Description	Adjusted p-value	Gene count	Matching proteins in PPI network
GO Biological Process (n = 6)				
GO:0019835	Cytolysis	2.4E-08	5	C5, C9, C6, C8A, C8B
GO:0006959	Humoral immune response	4.0E-07	6	C5, C9, C6, KNG1, C8A, C8B
GO:0006952	Defence response	5.8E-05	7	C5, C9, C6, KLKB1, KNG1, C8A, C8B
GO:0051707	Response to other organism	1.7E-03	6	C5, C9, C6, KNG1, C8A, C8B
GO:0007597	Blood coagulation, intrinsic pathway	1.5E-02	2	KLKB1, KNG1
GO:0048584	Positive regulation of response to stimulus	3.1E-02	6	C5, C9, C6, KLKB1, C8A, C8B
GO Cellular Component (n = 3)				
GO:0005579	Membrane attack complex	4.6E-12	5	C5, C9, C6, C8A, C8B
GO:0072562	Blood microparticle	3.7E-05	4	C9, CP, KNG1, C8A
GO:0005886	Plasma membrane	6.6E-03	8	C5, C9, C6, CP, KLKB1, KNG1, C8A, C8B
Reactome pathways (n = 2)				
HSA-166665	Terminal pathway of complement	5.2E-11	5	C5, C9, C6, C8A, C8B
HSA-977606	Regulation of Complement cascade	5.3E-08	5	C5, C9, C6, C8A, C8B

4.7.1.7 GO and Reactome pathway enrichment in d21 PW vs d0 (comparisons (e), (f), (g))

The PPI network in the DAPs of CR group at d21 PW versus d0 - comparison (e) contains 23 nodes and 148 edges (p < 1.0e-16). The PPI network in the DAPs of LR group at d21 PW versus d0 - comparison (f) comprises 23 nodes and 116 edges (p < 1.0e-16). Regardless of dietary treatments, the PPI network in d21 versus d0 serum - comparison (g) contains 31 nodes and 243 edges (p < 1.0e-16). The top 10 leading GO terms on BP, MF, and CC, and Reactome pathways of the PPI network of DAPs in (e), (f), and (g); are illustrated in Figures 4-13, 4-14, 4-15, respectively. For full GO terms and Reactome pathways list, see Appendix Tables S1, S2, S3.

Briefly, the pathways analysis in comparisons (e), (f), and (g) underscored the interactions of DAPs in multiple Reactome pathways such as platelet degranulation [HSA-114608], regulation of Insulin-like growth factor (IGF) transport and uptake by Insulin-like growth factor binding proteins (IGFBPs) [HSA-381426], haemostasis [HSA-109582], innate immune system [HSA-168249], and metabolism of proteins [HSA-392499].

Furthermore, a network among three main comparisons (i.e. (c), (d), and (g)) gives an overview of the interaction between the DAPs and significantly enriched Reactome pathways (Figure 4-16). In this network, the up- and down-regulated proteins with and between each comparison are shown with their related enriched Reactome pathways such as plasma lipoprotein remodelling [HSA-8963899], post-translational modification [HSA-597592], and complement cascade [HSA-166658].

Comparison (e) - CR serum at day 21 post-weaning versus CR serum at weaning day

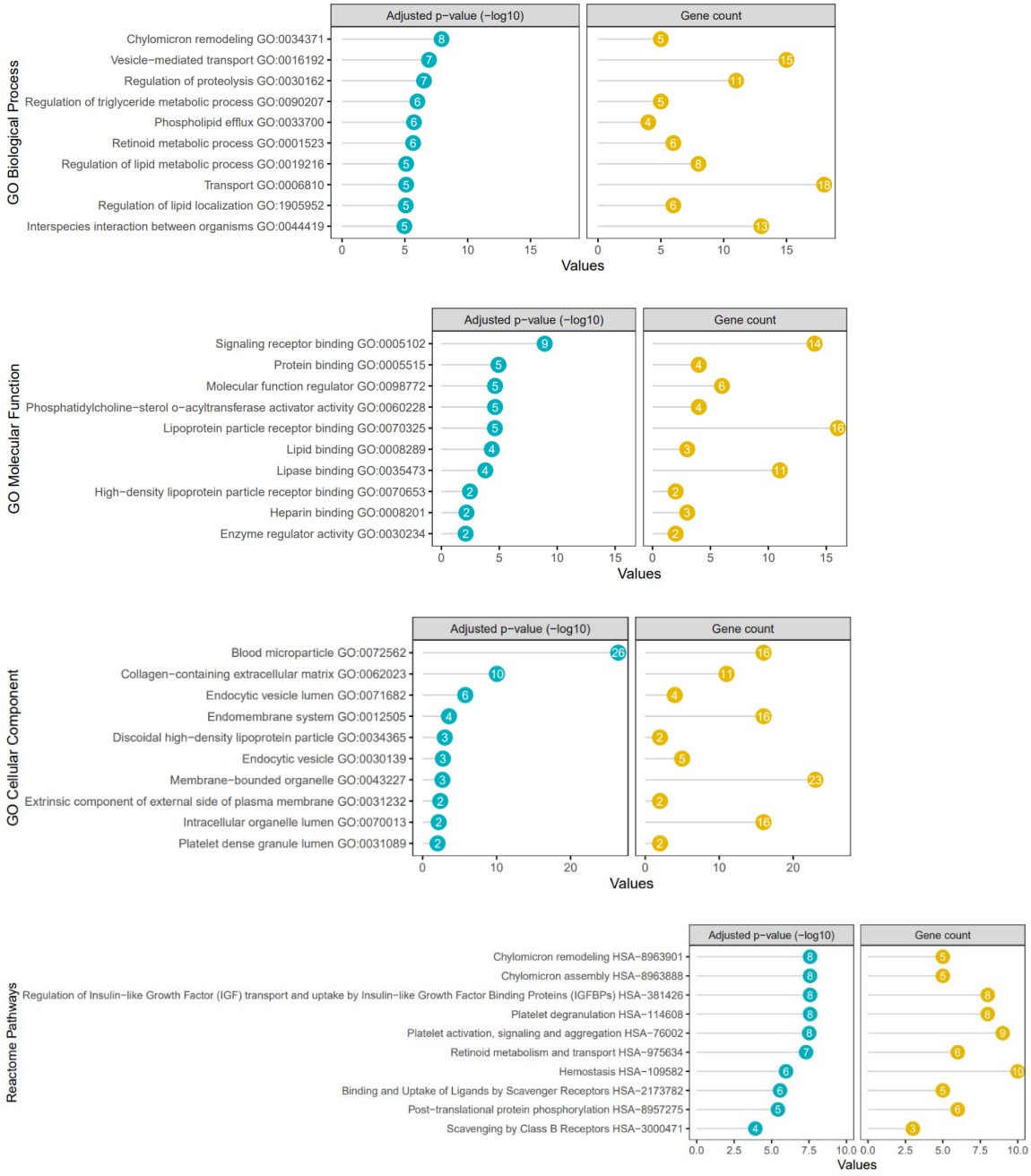

Figure 4-13 Gene ontology and Reactome pathways analysis of DAPs in comparison (e) - CR at day 21 post-weaning versus CR at weaning day , with their corresponding gene count inside each term and their associated adjusted *p*-value (expressed as -log10). Top 10 GO terms on biological processes, molecular function, and cellular component; and Reactome pathways are illustrated. CR: piglet born from sow fed diet with ω6:ω3 ratio=13:1 during gestation, starting from day 28 (G28) and 10:1 during lactation.

Comparison (f) - LR serum at day 21 post-weaning versus LR serum at weaning day

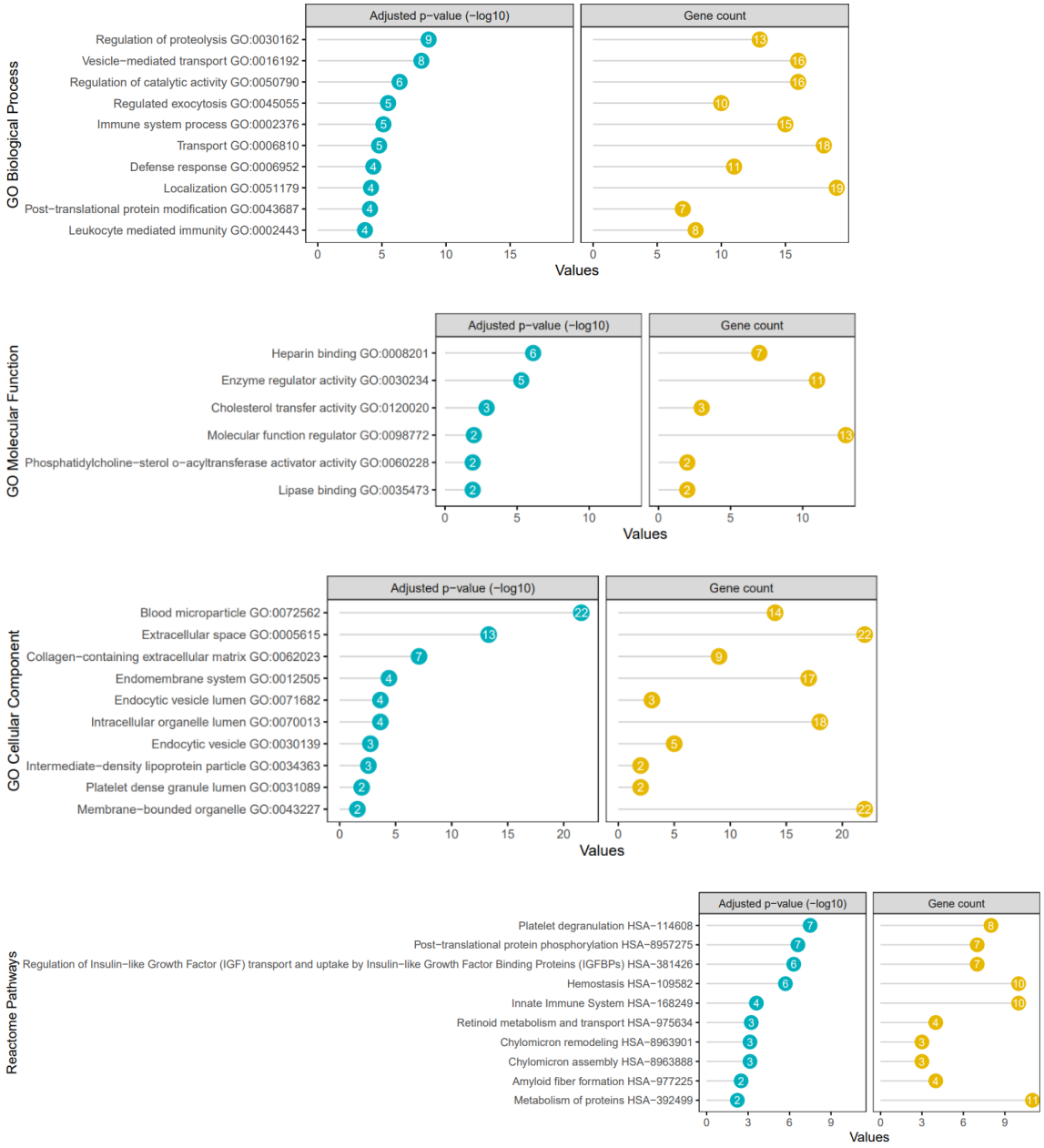

Figure 4-14 Gene ontology analysis of DAPs in comparison (f) - LR at day 21 post-weaning versus LR at weaning day , with their corresponding gene count inside each term and their associated adjusted *p*-value (expressed as -log10). Top 10 GO terms on biological processes and cellular component; Reactome pathways; and 6 GO terms on molecular function are illustrated. LR: piglet born from sow fed diet with ω6:ω3 ratio=4:1 from G28 until the end of lactation.

Comparison (g) - Serum at day 21 post-weaning versus serum at weaning day

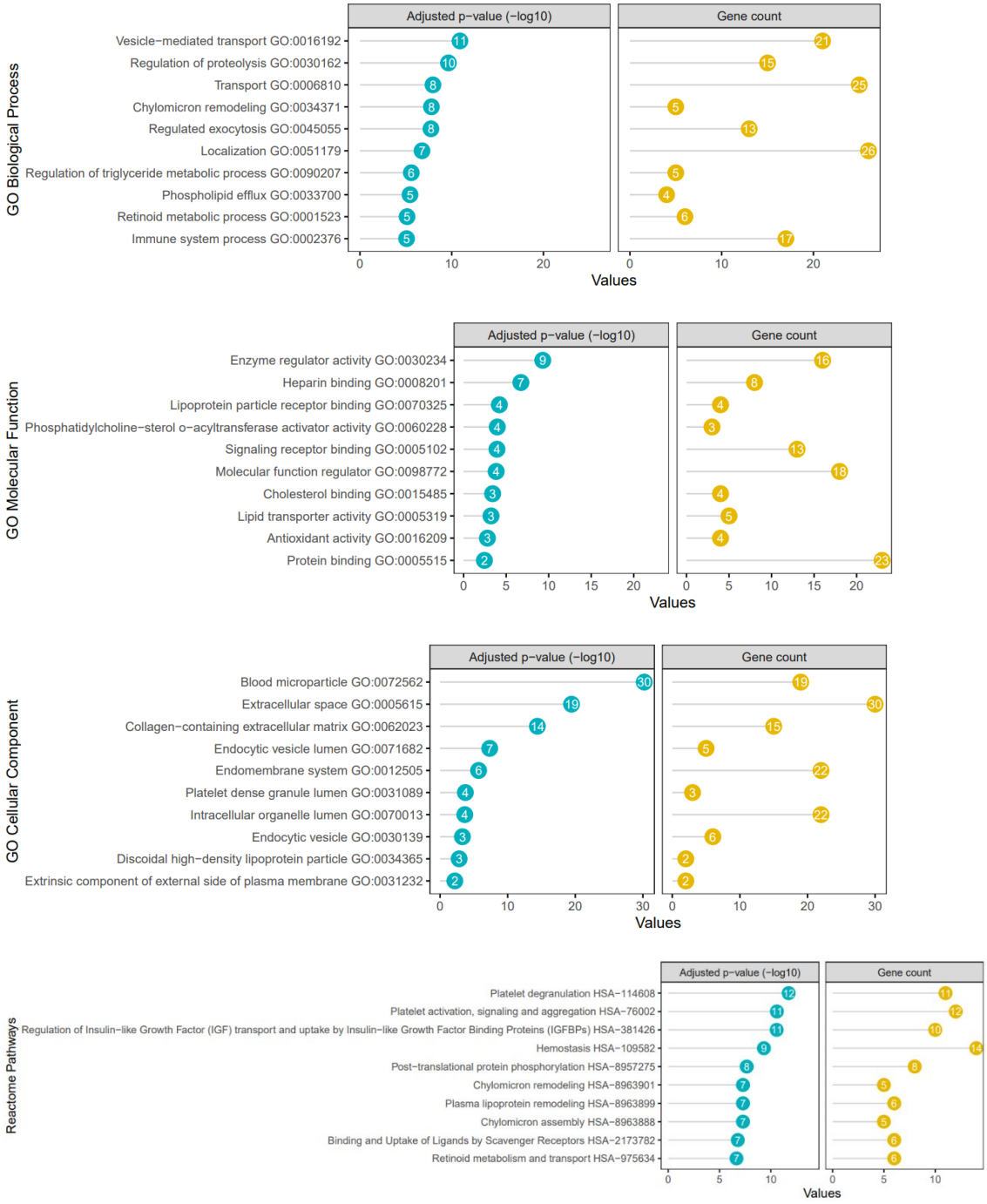

Figure 4-15 Gene ontology analysis of DAPs in comparison (g) - day 21 post-weaning versus weaning day , with their corresponding gene count inside each term and their associated adjusted p-value (expressed as -log10). Top 10 GO terms on biological processes, molecular function, and cellular component; and Reactome pathways are illustrated.

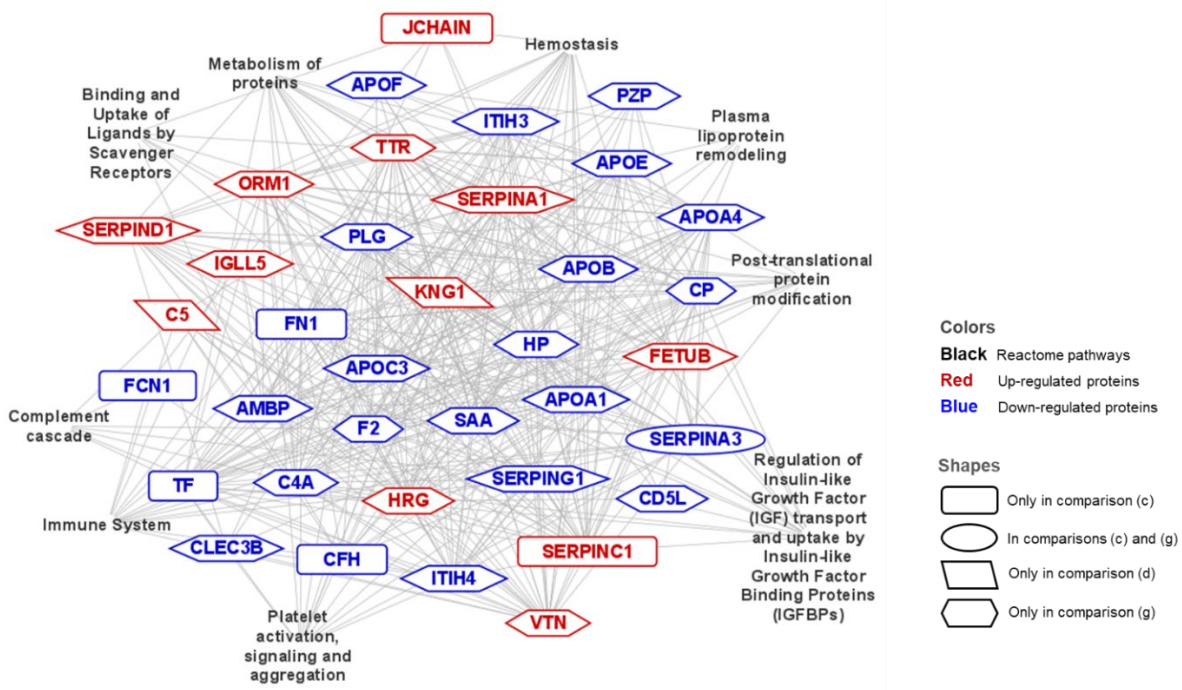

Figure 4-16 Network of the DAPs among comparisons (c), (d), and (g) of piglet serum with significantly enriched Reactome pathways. Comparison (c) - LR vs CR; (d) - SW vs CT at day 21 post-weaning; and (g) - day 21 post-weaning versus weaning day. CR: piglet born from sow fed diet with ω6:ω3 ratio=13:1 during gestation, starting from day 28 (G28) and 10:1 during lactation; LR: piglet born from sow fed diet with ω6:ω3 ratio=4:1 from G28 until the end of lactation. SW: piglet diet with seaweed supplementation, CT: piglet diet without seaweed supplementation.

4.7.2 Validation of proteomics results

Results of validation assays for apolipoprotein A1 (APOA1), serum amyloid A (SAA), and transferrin (TF) in serum samples, together with their respective protein abundance data determined by proteomics, are shown in Table 4-7 and visualized in Figure 4-17. Furthermore, serum levels of high-density lipoprotein (HDL) cholesterol in 4 groups of piglets at d0 and d21 PW are displayed in the same Table and Figure.

Table 4-7 Results of validation assays for the concentrations of apolipoprotein A1 (APOA1), serum amyloid A (SAA) and transferrin (TF) in serum samples are presented with their respective protein abundance values determined by proteomics. In addition, serum levels of high-density lipoprotein (HDL) cholesterol in eight groups of piglets are shown. Difference between groups was analysed separately for each tested protein and validation method.

Time point (T)	Sow diet (S)	Piglet diet (P)	APOA1		SAA		TF			HDL cholesterol
			Proteomics (relative abundance)	Western blot assay (optical density - arbitrary units)	Proteomics (relative abundance)	ELISA assay# (ng/mL)	Proteomics# (P09571, relative abundance)	Proteomics (B3CL06, relative abundance)	Coomassie blue and targeted MS (optical density - arbitrary units)	HDL cholesterol assay# (mmol/L)
Weaning (d0)	CR	CT	6.34	15870^{cd}	7.58^{e}	1.71^{bde}	5.62^{a}	6.82	20384^{a}	1.24
		SW	6.46	12018^{bc}	5.98^{cde}	1.51^{cde}	5.43^{a}	4.86	20501^{a}	1.00
	LR	CT	6.29	14905^{cd}	6.94^{de}	2.14^{e}	6.31^{abc}	2.91	23944^{ab}	1.28
		SW	6.37	16564^{d}	6.73^{e}	1.99^{de}	6.35^{ab}	4.07	22152^{ab}	1.32
d21 post-weaning (d21 PW)	CR	CT	6.20	9001^{ab}	3.80^{ab}	0.97^{ac}	6.84^{bcd}	7.01	24217^{b}	0.95
		SW	6.24	7466^{a}	3.60^{a}	0.92^{ab}	7.07^{bcd}	6.39	24035^{b}	0.88
	LR	CT	6.25	9074^{ab}	4.44^{abc}	1.22^{abcd}	7.9^{d}	3.01	24608^{b}	1.04
		SW	6.12	8213^{ab}	5.32^{bcd}	1.63^{abcde}	7.57^{cd}	3.98	24704^{b}	0.90
SEM			0.10	1219	0.50	0.21	0.40	1.13	982	0.11
P-value	S		ns	ns	ns	0.031 *	0.007	0.022*	0.077	ns
	P		ns	ns	ns	ns	ns	ns	ns	ns
	T		0.030	<0.001	<0.001	<0.001	<0.001	ns	<0.001	0.002
	S*P		ns	0.082	ns	ns	0.046	ns	ns	ns
	S*T		ns	ns	0.032	ns	<0.001	ns	0.066	ns
	P*T		ns	ns	0.020	0.044	0.002	ns	ns	ns
	S*P*T		ns	ns	ns	ns	0.001	ns	ns	ns
	CRCTd0-LRCTd0		ns	ns	ns	ns	ns	ns	0.050	ns
	CRCTd0-CRSWd0		ns	0.060	0.056	ns	ns	ns	ns	ns
	CRCTd0-LRSWd0		ns	ns	ns	ns	ns	ns	ns	ns

		APOA1		SAA		TF			HDL cholesterol
		Proteomics	Western blot assay	Proteomics	ELISA assay#	Proteomics# (P09571)	Proteomics (B3CL06)	Coomassie blue and targeted MS	HDL cholesterol assay#
P-value (cont.)	CRCTd0-CRCTd21	ns	0.001	<.0001	0.005	ns	ns	0.030	ns
	CRCTd0-LRCTd21	ns	0.001	<0.001	ns	0.006	ns	0.030	ns
	CRCTd0-CRSWd21	ns	<0.001	<0.001	0.059	0.099	ns	0.049	ns
	CRCTd0-LRSWd21	ns	<0.001	0.009	ns	0.018	ns	0.030	ns
	LRCTd0-CRSWd0	ns	ns	ns	ns	ns	ns	0.055	ns
	LRCTd0-LRSWd0	ns	ns	ns	ns	ns	ns	ns	ns
	LRCTd0-CRCTd21	ns	0.004	<0.001	0.007	ns	ns	ns	ns
	LRCTd0-LRCTd21	ns	0.005	<0.001	<0.001	ns	ns	ns	ns
	LRCTd0-CRSWd21	ns	<0.001	<0.001	0.006	ns	ns	ns	ns
	LRCTd0-LRSWd21	ns	0.001	0.056	ns	ns	ns	ns	ns
	CRSWd0-LRSWd0	ns	0.026	ns	ns	ns	ns	ns	ns
	CRSWd0-CRCTd21	ns	ns	0.011	ns	ns	ns	0.049	ns
	CRSWd0-LRCTd21	ns	ns	0.062	ns	0.006	ns	0.030	ns
	CRSWd0-CRSWd21	ns	0.026	<0.001	0.010	0.099	ns	0.030	ns
	CRSWd0-LRSWd21	ns	0.060	ns	ns	0.018	ns	0.030	ns
	LRSWd0-CRCTd21	ns	<0.001	0.001	0.012	ns	ns	ns	ns
	LRSWd0-LRCTd21	ns	<0.001	0.009	0.061	0.072	ns	ns	ns
	LRSWd0-CRSWd21	ns	<0.001	<0.001	0.010	ns	ns	ns	ns
	LRSWd0-LRSWd21	ns	<0.001	0.021	0.097	ns	ns	0.070	ns
	CRCTd21-LRCTd21	ns	ns	ns	ns	ns	ns	ns	ns
	CRCTd21-CRSWd21	ns	ns	ns	ns	ns	ns	ns	ns
	CRCTd21-LRSWd21	ns	ns	0.064	0.097	ns	ns	ns	ns
	LRCTd21-CRSWd21	ns	ns	ns	ns	ns	ns	ns	ns
	LRCTd21-LRSWd21	ns	ns	ns	ns	ns	ns	ns	ns
	CRSWd21-LRSWd21	ns	ns	0.044	0.080	ns	ns	ns	ns

A1

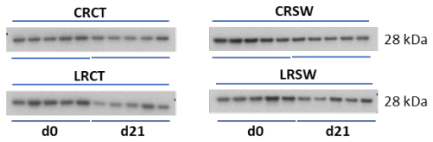

sow diet:	*p*= 0.21
piglet diet:	*p*= 0.19
time:	*p*= 1.88e-08 ***
sow diet x piglet diet :	*p*= 0. 08 .
sow diet x time:	*p*= 0.43
piglet diet x time:	*p*= 0.95
sow diet x piglet diet x time:	*p*= 0.17

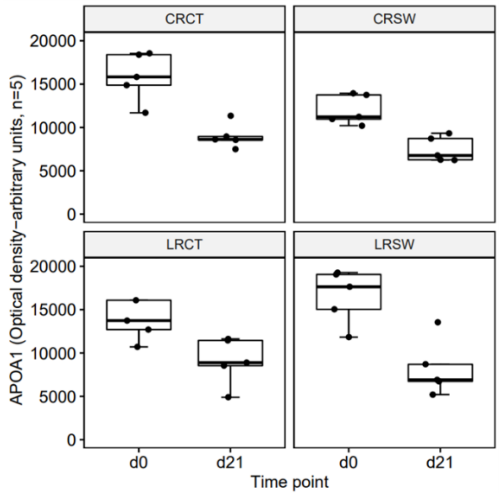

A2

sow diet:	*p*= 0.52
piglet diet:	*p*= 0.75
time:	*p*= 0.03 *
sow diet x piglet diet :	*p*= 0.49
sow diet x time:	*p*= 0.81
piglet diet x time:	*p*= 0.32
sow diet x piglet diet x time:	*p*= 0.61

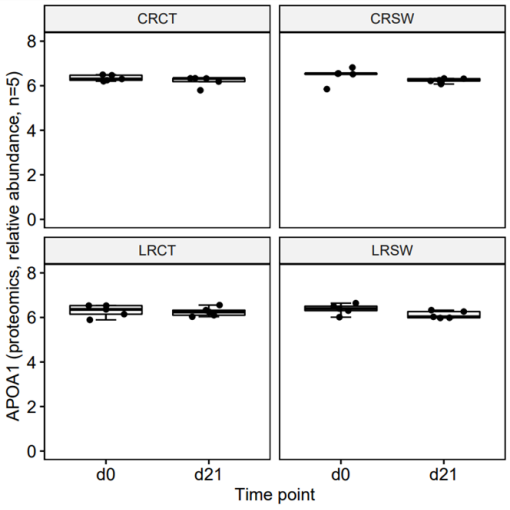

B1

sow diet:	*p*= 0.03 *
piglet diet:	*p*= 0.99
time:	*p*= 5e-07 ***
sow diet x piglet diet :	*p*= 0. 53
sow diet x time:	*p*= 0.88
piglet diet x time:	*p*= 0.04 *
sow diet x piglet diet x time:	*p*= 0.21

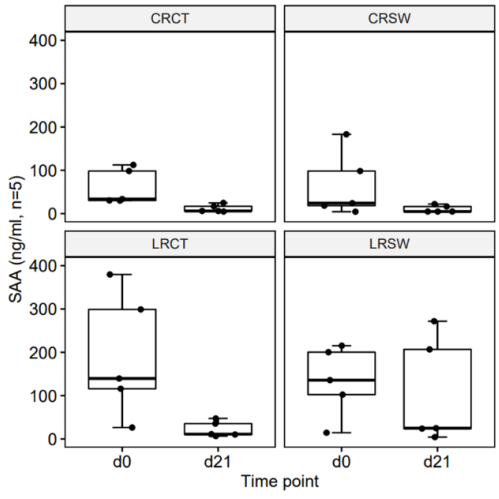

B2

sow diet:	*p*= 0.18
piglet diet:	*p*= 0.53
time:	*p*= 1.4e-08 ***
sow diet x piglet diet :	*p*= 0.17
sow diet x time:	*p*= 0.03 *
piglet diet x time:	*p*= 0.02 *
sow diet x piglet diet x time:	*p*= 0.75

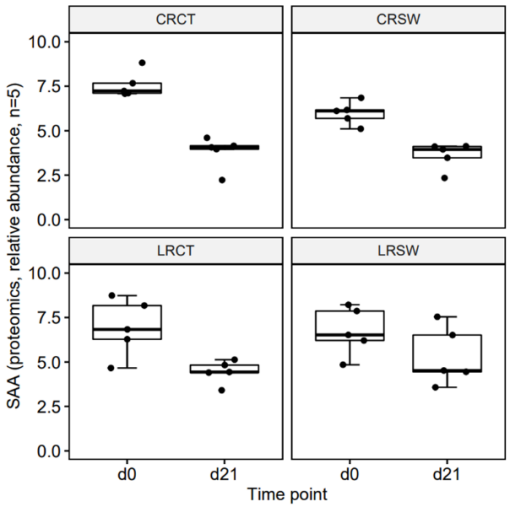

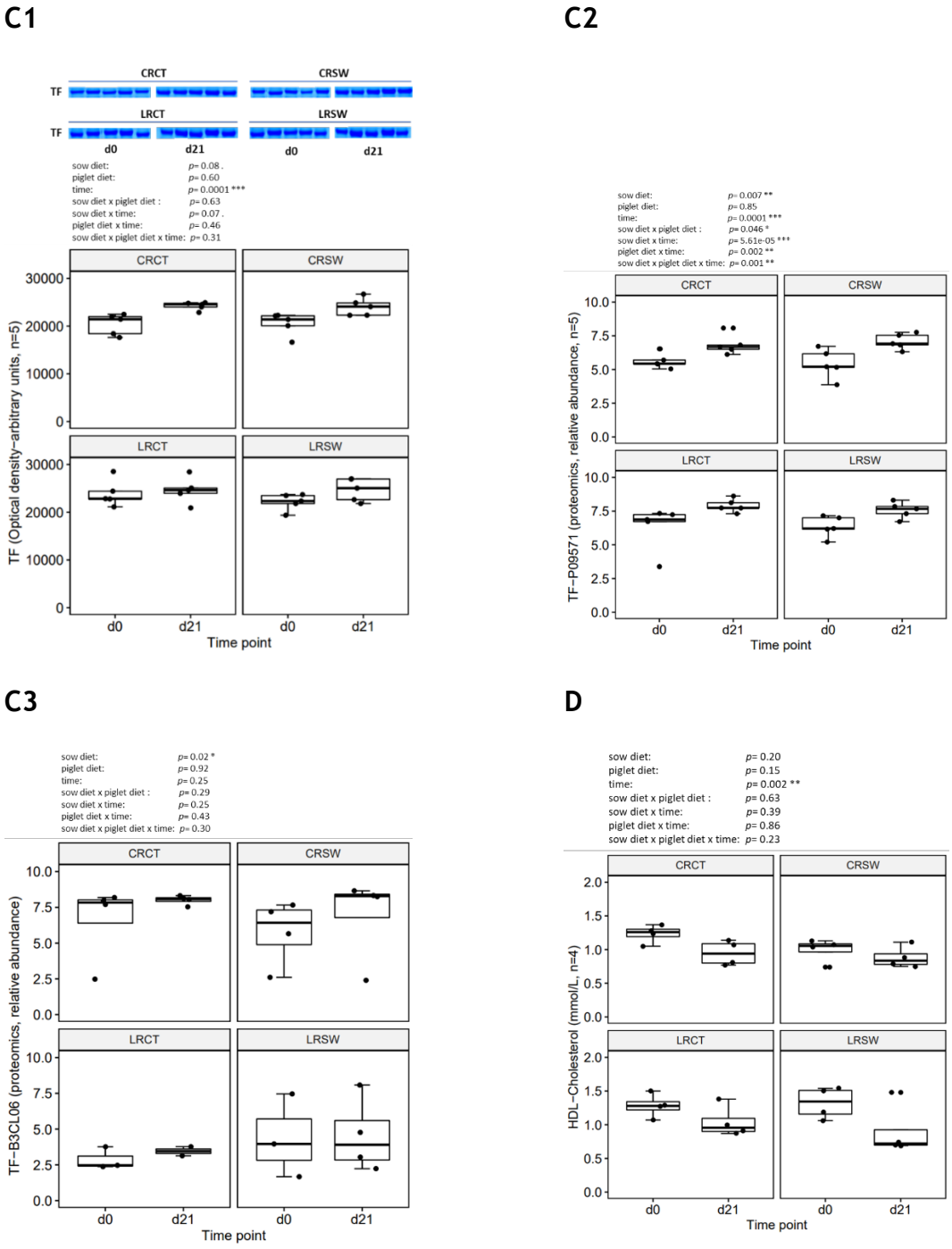

Figure 4-17 Boxplots of validation assays for the concentrations of apolipoprotein A1 (APOA1), serum amyloid A (SAA), and transferrin (TF) are presented with their respective abundance values determined by proteomics. Comparisons are A1 and A2 for APOA1; B1 and B2 for SAA; C1, C2 and C3 for TF. Moreover, plasma levels of high-density lipoprotein (HDL) cholesterol in eight groups of piglets are shown in D. CRCT: piglets fed no seaweed (SW, *Ascophyllum nodosum*), which nursed by sows fed dietary ω6:ω3 ratio = 13:1 during gestation, starting from day 28 (G28) and 10:1 during lactation. CRSW: piglets fed SW, which nursed by sows fed dietary ω6:ω3 ratio = 13:1 during gestation and 10:1 during lactation. LRCT: piglets fed no SW, which nursed by sows fed dietary ω6:ω3 ratio = 4:1 from G28 until the end of lactation. LRSW: piglets fed SW, which nursed by sows fed dietary ω6:ω3 ratio = 4:1 from G28 until the end of lactation. d0: weaning day, d21: d21 post-weaning.

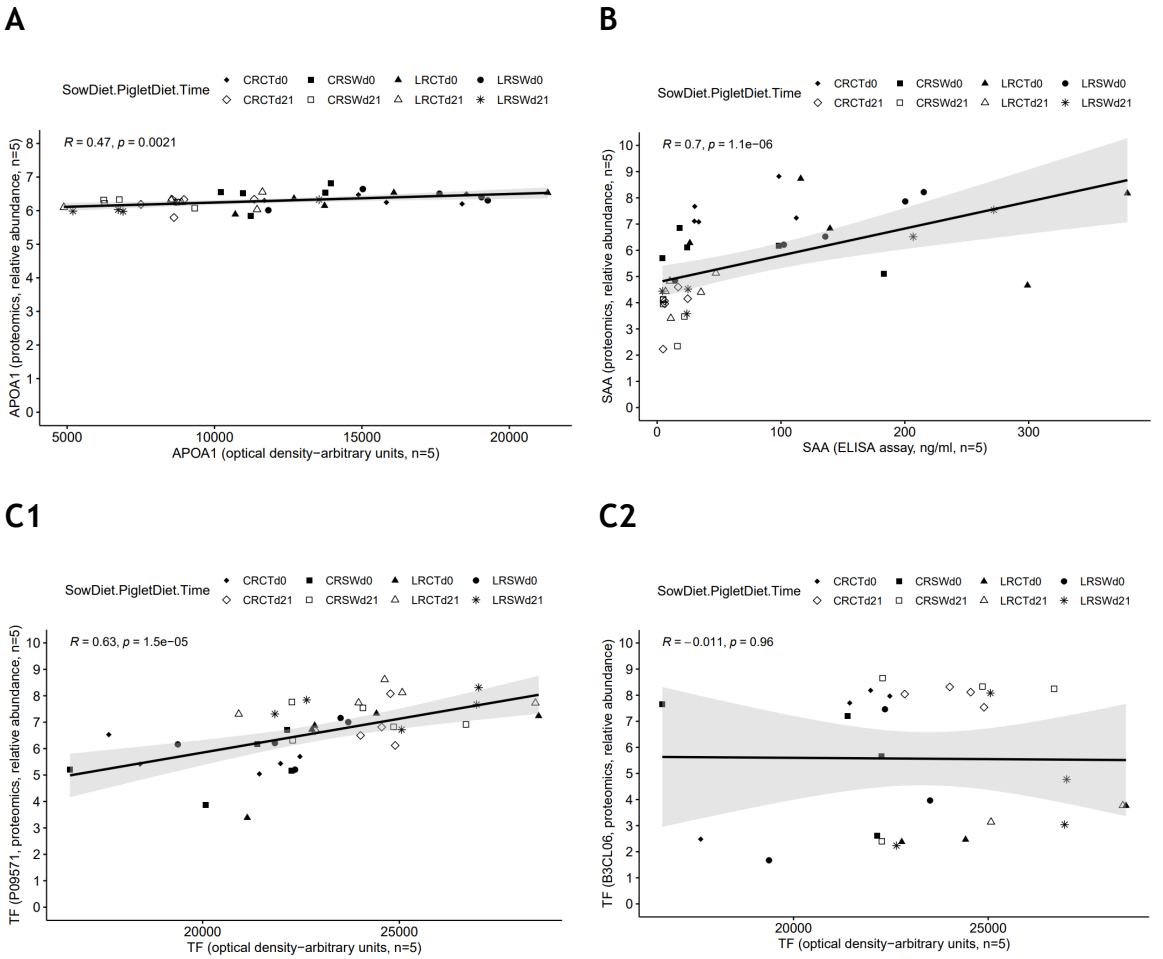

Figure 4-18 Correlations between relative protein abundance and validated protein concentration for A- apolipoprotein A1 (APOA1), B- serum amyloid A (SAA), and C- transferrin (TF). CRCT: piglets fed no seaweed (SW, *Ascophyllum nodosum*), which nursed by sows fed dietary ω6:ω3 ratio = 13:1 during gestation, starting from day 28 (G28) and 10:1 during lactation. CRSW: piglets fed SW, which nursed by sows fed dietary ω6:ω3 ratio = 13:1 during gestation and 10:1 during lactation. LRCT: piglets fed no SW, which nursed by sows fed dietary ω6:ω3 ratio = 4:1 from G28 until the end of lactation. LRSW: piglets fed SW, which nursed by sows fed dietary ω6:ω3 ratio = 4:1 from G28 until the end of lactation. d0: weaning day, d21: d21 post-weaning.

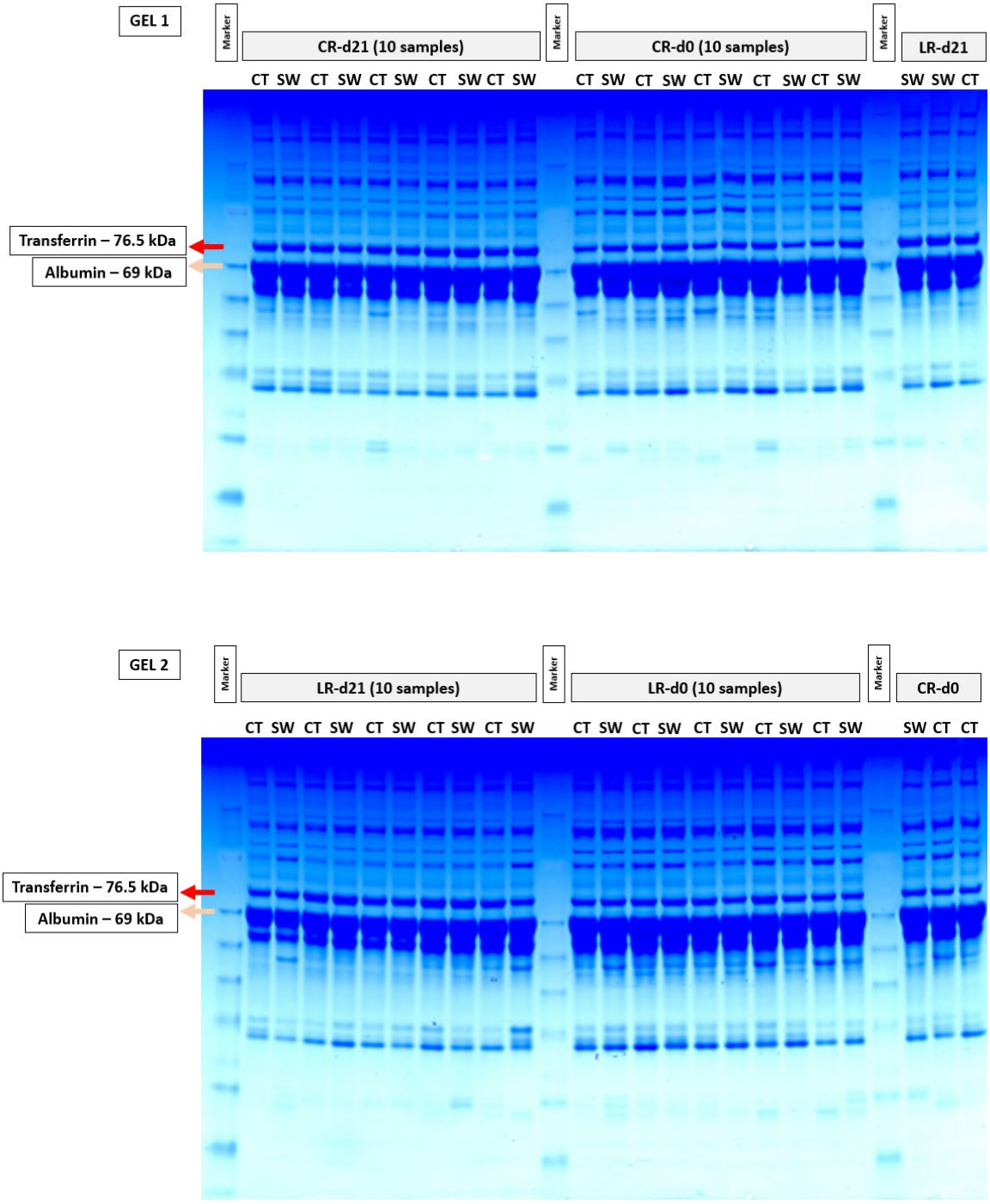

Figure 4-19 Images of two Coomassie blue-stained polyacrylamide gels were used to validate transferrin (TF). CR: piglet born from sow fed diet with ω6:ω3 ratio=13:1 during gestation, starting from day 28 (G28) and 10:1 during lactation, d0: weaning day, d21: d21 post-weaning.

4.7.2.1 Apolipoprotein A1 (APOA1)

Western blot analysis of APOA1 in serum is displayed in Figure 4-17. Clear bands at 26 kDa indicating the presence of APOA1 were detected in all samples. Protein band intensity was higher at d0 than at d21 PW (Table 4-7, $p < 0.001$). There were no significant effects of dietary treatments on the sows and piglets or their interactions with sampling times on APOA1 concentration. A significantly lower concentration of APOA1 was determined at d21 PW for all four groups (CRCT, CRSW, LRCT, and LRSW) compared to CRCT, LRCT, and LRSW at d0 (Table 4-7, $p < 0.001$). At d0, LRSW serum had a higher APOA1 concentration than CRSW serum (Table 4-7, $p = 0.026$). The proteomics relative abundance exhibited a similar increasing pattern of APOA1 at d21 PW compared to that at d0 (Figure 4-17A2, $p = 0.03$), as shown by the validated APOA1 concentration. The overall evaluation found a moderate positive linear correlation between validated APOA1 concentration and APOA1 proteomics relative abundance (Figure 4-18A, R = 0.47, $p = 0.0021$).

4.7.2.2 Serum amyloid A (SAA)

Concentrations of SAA was significant decreased at d21 PW compared to d0 (Figure 4-17B1, $p < 0.001$). Furthermore, the LR diet in sows increased the SAA concentration compared to the CR diet (Figure 4-17B1, $p = 0.031$). Regarding the interaction between piglet diets and sampling time, the concentration of SAA was decreased over time after weaning in both CT and SW groups (Figure 4-17B1, $p = 0.044$). A significant decrease of SAA concentration from d0 to d21 PW was shown when comparing CRCT and CRSW at d21 to LRCT and LRSW at d0 (Table 4-7, $p < 0.05$). The relative proteomics abundance presented a similar decreasing pattern of SAA at d21 compared to d0 (Figure 4-17B2, $p < 0.001$), especially when considering the effect of piglet diet over time (Figure 4-17B2, $p = 0.02$); as observed in the validated SAA concentration. The proteomics abundance pattern of SAA was supported by a significant correlation with validated SAA concentration (Figure 4-18B, R = 0.7, $p = 1.1e\text{-}06$).

4.7.2.3 Transferrin (TF)

The band intensity analysis showed a significant increase of TF at d21 compared to d0 (Figure 4-17C1, p = 0.0001). A highly significant increase of TF at d21 was shown in all four groups (CRCT, CRSW, LRCT, and LRSW) compared to CRCT and CRSW at d0 (Table 4-7, $p < 0.05$). Effects of dietary treatments on sow and piglet and their interactions with sampling time on TF band intensity were not found. The relative proteomics abundance presented a similar increasing pattern of TF (P09571) at d21 compared to d0 (Figure 4-17C2, p = 0.0001), as observed in the validated TF. However, this trend was not shown for the relative abundance of TF (B3CL06) (Figure 4-17C3, $p > 0.05$). The proteomics abundance pattern of TF (P09571) was moderately correlated with TF band intensity (Figure 4-18C1, R = 0.63, p = 1.5e-05). However, no correlation was found between the relative abundance of TF (B3CL06) and its band intensity (Figure 4-18C2, R = -0.011, p = 0.96). Images of two Coomassie blue-stained polyacrylamide gels used to validate TF were presented in Figure 4-19.

4.7.2.4 HDL-cholesterol

HDL-cholesterol level significantly decreased at d21 (~0.94 mmol/L) compared to d0 (~1.20 mmol/L) (Figure 4-17D, p = 0.002). However, the level of HDL-cholesterol in piglet serum was not affected by either sow diet, piglet diet, or their interaction with sampling time.

4.8 DISCUSSION

Maternal diet is critical to offspring growth, immune development, and intestinal functions [262–264]. During pregnancy and lactation, the nutritional program creates early-life adaptation and development and has long-term (permanent) effects on adult life [265]. Maternal micronutrients can function as enzyme substrates or cofactors responsible for the maintenance of genome stability, and macronutrients can affect the DNA-damage response through physiological regulation [264]. This is the first proteomics study of newly weaned (d0) and post-weaned (d21 PW) piglet serum, influenced by the interplay between maternal nutrition (a marker of early-life programming) and offspring nutrition (later-life programming). Although many DAPs with adjusted p-values < 0.05 were

highlighted, DAPs have more modest alterations with raw *p*-values < 0.05 may still be relevant for guiding further research if a larger sample size or targeted quantitative proteomics would prove significant alterations.

4.8.1 Effect of sow dietary treatments: LR vs CR groups (comparisons (a), (b), (c))

At weaning (d0), the relative abundance of C3, SERPINC1, and TF was influenced by maternal LR diet. These proteins were annotated by Reactome pathways associated with the regulation of Insulin-like Growth Factor (IGF) transport and uptake by Insulin-like Growth Factor Binding Proteins (IGFBPs) and post-translational protein phosphorylation. Complement component 3 (C3) is a critical component in the complement system. Complement C3 is well-established for its pro-inflammatory property, therefore, contributing to the innate and adaptive inflammation in response to stimuli [267]. The concentration of C3 was increased in most inflammatory conditions [268]; hence, the down-regulated of C3 in LR versus CR piglets at weaning in this study may relate to the anti-inflammatory property of low ω6:ω3 ratio in their mother's diet. The up-regulation of protein C3 in CR piglets may contribute to some key features of inflammation, such as hypo-fibrinolysis and hyper-coagulation [269]. Indeed, a short-term increased pig C3 serum level is an immune response during inflammation's sub-acute phase, such as after vaccinations/immunizations [270].

On d21 PW, 7 proteins were annotated by Reactome pathways related to haemostasis, binding and uptake of ligands by scavenger receptors, and scavenging by class B receptors. In the LR group, APOB, JCHAIN, SAA, and TF (P09571) were up-regulated while KLKB1, LGALS3BP, SERPINA3, and TF (B3CL06) were down-regulated when compared with CR group. Although two accession numbers of TF were identified, only P09571 was kept for discussion due to the strong correlation between its relative abundance measured by proteomics and band intensity validated by SDS-PAGE (Figure 4-18C1, R = 0.63, p = 1.5e-05). At the same time, there was no similar correlation in B3CL06 (Figure 4-18C2, R = -0.011, p = 0.96).

Addressing how maternal diet can affect piglet's immunity, acute phase proteins (APPs) are suitable parameters to consider because they regulate the acute phase response (APR) - the cornerstone of the innate immune system to restore homeostasis and promote the healing process [271]. Compared to two main positive APPs in pigs, i.e., pig-MAP and HP, SAA is fast but less prolonged released in the innate defence system against infection [271–273]. Pro-inflammatory cytokines (e.g., Interleukin-1ß (IL-1ß), Interleukin-6 (IL-6), and tumour necrosis factor-α (TNF-α)) regulate the hepatic release of SAA during the APR [273]. In a mice study [274], muscle release of SAA could synergize with Interleukin-6 (IL-6) to impair insulin/IGF-1 signalling and stimulate protein breakdown, thereby activating proteolytic pathways in muscle. Indeed, SAA can activate innate immune sensors such as Toll-like receptors 2 and 4 (TLR2 and TLR4), leading to activation of innate immunity and suppression of excessive inflammation and tissue damage [275–277]. In the current work, a significantly high level of SAA in LR piglets at d21 PW reflects that the innate defence system is strongly activated and participates in the inflammatory response.

In line with the results of the current study, Cai et al. (2005) and Sack Jr (2018) reported that SAA is a ligand for the scavenger receptor class B type 1 (SR-B1): SAA can bind to SR-B1 and participate in the selective uptake of high-density lipoprotein (HDL). During an APR in humans, hepatocytes' SAA synthesis is quickly released into the bloodstream, associated with HDL [279], and involved in lipid metabolism [275]. Acute phase SAA becomes the major apolipoprotein on HDL by displacing the APOA1 sub-unit, compromising HDL's role to protect against oxidation and prevent cholesterol accumulation (by promoting reverse cholesterol transport) [280]. Following maternal LR diet, serum level of SAA was increased in piglets at d21 PW compared to piglets on the CR diet and contributed to the host protective mechanism.

Another APP that participates in innate immune and inflammation regulation is transferrin (TF), an iron-carrier glycoprotein from the intestine to proliferative cells through the body [281]. In pigs, under physiological conditions, TF can prevent the formation of toxic non-TF bound iron ions (Fe^{2+} and Fe^{3+}) [282] by binding to 2 iron atoms [283] and resulting in ~30% of serum TF being saturated with iron [284]. Nevertheless, piglets are born with a low serum level of TF, ~1.8

mg/mL [283,285], and usually faced with an iron deficiency state [286]. Clinical studies in humans confirmed a low concentration of TF in newborns and their susceptibility to damage by non-TF bound iron ions [287,288]. Serum TF level will increase if inadequate iron is stored to meet higher iron requirements for absorption and transportation [285]. Piglet TF level can increase to ~6.1 mg/mL at day 42 post-birth [283,285] before staying constant. The gradual increase of TF was observed in the current study in piglets from weaning (d0 PW or d26 of life) to d21 PW (or d46 of life), and in LR versus CR piglets at d21 PW, reflecting increased TF synthesis in the liver and total body iron stores. By being actively involved in the active iron sites, TF is considered as an integral part of the protection system together with hemoglobin-haptoglobin complexes [289].

Besides the primary role as an iron-transport agent, TF is also regarded as a negative APP in pigs [271,290,291] and chickens [292]. The concentration of serum TF was decreased following inflammation to stimulate host defence and immune regulatory mechanisms [292]. Transferrin can act as an antioxidant and antimicrobial agent, protecting the host against tissue lipid peroxidation and pathogenic microorganisms, respectively [285,293]. Furthermore, TF is considered as a growth-promoting factor because it participates in DNA transcription and supports cell growth and proliferation [284]. Taken together, a higher level of TF in LR than CR piglets suggested the role of maternal diet in regulating the host response against inflammation, but its contribution to the growth rate in piglets has not been observed.

Regardless of sampling time, the relative abundance of PZP, FN1, SERPINC1, SERPINA3 was influenced by maternal LR diet. These proteins were annotated by enriched GO term referred to the regulation of peptidase activity.

Alpha-2-Macroglobulin (or Pregnancy-zone protein, PZP), an endopeptidase inhibitor, was up-regulated in LR versus CR group but down-regulated in d21 PW versus d0 in this study. The down-regulation of PZP in piglet serum from weaning to d21 PW in this study may follow the decrease in PZP concentration in their maternal blood during the lactation period [294]. Rubio-Aliaga et al. [295] reported that PZP might involve body weight regulation; however, the mechanism of this effect needs to be further studied. The concentration of fibronectin (FN1)

– a positive APP was down-regulated in LR versus CR serum, contributing to the enhanced host protective response [296] that is affected by low ω6:ω3 ratio in the maternal diet.

Two members of the serpins (serine proteinase inhibitors) family, Alpha-1-Antichymotrypsin (SERPINA3) was decreased while Antithrombin-III (SERPINC1) was increased in abundance in LR versus CR serum. Serpins are diverse in their functions but highly structurally conserved (similar) group of proteins [297] that are most abundant in humans [298] and higher organisms [299] such as swine, as shown in this study (Table 4-1). Apart from the central function in cellular homeostasis maintenance [298], serpins also have non-inhibitory roles related to various proteolytic pathways such as inflammation, coagulation, tissue remodelling, and angiogenesis [297,300,301]. SERPINA3 seems to be increased, and SERPINC1 decreased with the inflammation conditions [298]. So the down-regulation of SERPINA3 and up-regulation of SERPINC1 in the serum of LR piglets suggest the anti-inflammatory effect of low ω6:ω3 ratio in the maternal diet. Notably, SERPINA3 was strongly decreased in abundance on d21 PW versus d0, confirming that piglets at weaning time undergone higher inflammation state compared to the later stage of life, which is in agreement with previous observations [233].

4.8.2 Effect of piglet dietary treatments: SW vs CT groups (Comparison (d))

On d21 PW, the relative abundance of C5 and KNG1 was increased in the SW-fed piglets. These proteins were annotated by enriched GO terms referred to cytolysis, positive regulation of humoral immune and defence responses to stimuli, and blood coagulation (intrinsic pathway). The activated complement system produced anaphylatoxins – proinflammatory agents such as C5a that can activate innate immune cells, i.e., monocytes and neutrophils, and mediated endothelial permeability [302]. Additionally, C5a can trigger the endothelium to release inflammatory mediators such as Interleukin-6 (IL-6), thereby in-directly stimulating the innate immunity [303,304]. The enrichment of C5a in SW piglets at d21 PW in the current study suggests the essential role of C5a as a bridge to connect innate and adaptive immunity to enhance the host defence during

inflammation conditions [305]. Kininogen-1 (KNG1) is a coagulation factor [306], so it contributes to the activation of coagulation pathways [307], resulting in the formation of thrombin and fibrin to ensure the stability of blood clots at the site of injury [306]. Increased concentration of KNG1 in SW serum suggests an effect of SW on coagulation cascade regulation, as shown in this study. A similar observation was reported in a human study where the relationship between the altered level of KNG1 and blood coagulation was noted [307].

4.8.3 Effect of time point: d21 vs d0 (Comparisons (e), (f), (g))

The protein profiles at d21 PW and those at d0 were distinguished (as shown in the PCA score plot, Figure 4-11A), indicating the alterations in the proteomic patterns of the post-weaned piglets. The day 21 PW, serum lipoproteins (e.g., APOA1, APOB, APOE); pro-coagulation proteins (e.g., F2, HRG, ORM1); coagulation regulator, e.g., PLG; and acute phase proteins (e.g., HP, ITIH4, TF, SAA, SERPINA1) were changed in their relative abundance, compared to d0. These DAPs were annotated by 25 Reactome pathways; mostly referred to the metabolism of platelet, proteins, and Insulin-like Growth Factor (IGF), haemostasis, and innate immune system; regardless of maternal or offspring dietary treatments.

Apolipoproteins play a critical role in lipid transport throughout the lymphatic system, which regulates adaptive immunity and inflammation [308,309], particularly during the critical metabolic adaptation transition periods from gestation to lactation [308]. The decreased concentration of APOA1 and APOE in late pregnancy and increased concentration during lactation were reported in dairy cows [310] and sows - piglets' mothers of this study (unpublished data). Consequently, suckling piglets gained relatively high levels of apolipoproteins such as APOA1, APOB, and APOE from their mother; however, these concentrations fell considerably in post-weaning, as shown in the current work. Indeed, the changes in the apolipoprotein concentrations during weaning reflect piglet adaptation to dynamic and complex metabolic processes [311]. Apolipoproteins A1 containing lipoproteins (HDL) and APOB containing lipoproteins (chylomicrons, very-low density lipoprotein or VLDL, and low-density lipoprotein or LDL) are interrelated in lipoprotein metabolism [312]. Specifically, APOB containing lipoproteins transport lipids (primarily triglycerides (TG) and cholesterol) to provide energy

from the intestine and liver to other tissues, while APOA1 containing lipoproteins eliminate excess lipids (mainly cholesterol) from tissues and transport them to the liver [312]. Since HDL has multiple biological functions (anti-inflammatory, antioxidant, anti-thrombotic, and anti-apoptotic) [313]; a higher level of both APOA1 and HDL-cholesterol in piglets at weaning compared to d21 PW, as observed in this study, has shown that these changes are two of the host protective activities against weaning stress. In this study, while numerous apolipoproteins (APOA1, APOA4, APOB, APOC3, APOE, and APOF) were found to be altered in abundance between d0 and d21, validation was performed on APOA1 due to antibody availability, but the level of HDL was estimated via HDL-cholesterol assay. These methods confirmed that the concentrations of APOA1 and HDL were decreased towards d21 PW when a higher amount of adipose tissue was deposited [314].

The high levels of positive APPs (e.g., HP, ITIH4, SAA) and low levels of negative APPs (e.g., TF, TTR, and SERPINA1) in piglet serum at d0 were observed as a consequence of stress stimuli following separation from the mother, transportation, change to a new environment and social mixing (regrouping). These results match those observed in an earlier study [315]. Weaning stress induces appetite and feed intake suppression [315]. The stress may arise from accelerating catabolism [315], pushing animals into a state of immune challenge, negative energy balance, and reduced weight gain [316,317].

The DAPs in LR versus CR serum at d21 PW (i.e., APOB, JCHAIN, LGALS3BP, KLKB1, SERPINA3, TF); DAPs in CR at d21 PW versus d0 (HRG, APOB, APOA1, ITIH4, SERPING1, F2, PLG, SERPINA3, TF, ITIH3); DAPs in LR at d21 PW versus d0 (SERPIND1, HRG, APOB, ORM1, SERPING1, CLEC3B, SERPINA3, TF, ITIH3, SERPINA1); DAPs in d21 PW versus d0 (SERPIND1, HRG, APOB, APOA1, ORM1, ITIH4, SERPING1, CLEC3B, F2, PLG, SERPINA3, TF, ITIH3, SERPINA1) were assigned to the haemostasis-a pathway that is regulated by coagulation process and platelets to prevent bleeding caused by injured vessel [318]. Haemostasis is a complicated physiological process on the cell surfaces (i.e., endothelial cells and platelets), which represents the centre of the host defence and wound healing system [319,320]. These two types of cells regulate the coagulation system; hence, haemostasis in the normal state is an equilibrium between pro- and anti-

coagulation along with fibrinolysis and anti-fibrinolysis [319]. Impaired tissue homeostasis leads to fibrin clot formation inside damaged or injured vessels [321]. In humans, the haemostatic system of neonates is immature due to the immature coagulation system (most coagulation factors are only accounted for ~50% of adult levels) [322]. Consequently, the neonates are more sensitive and protective in response to various stimuli [323]. Similar to a previous report [324], multiple DAPs associated with haemostasis in this study showed the development of the haemostatic system in piglets from d0 to d21 PW.

Pathways related to platelets such as degranulation, activation, signalling, and aggregation were enriched in d21 PW versus d0 for both CR and LR groups with a series of proteins (HRG, APOA1, ITIH4, SERPING1, PLG, SERPINA3, TF, ITIH3). Platelets were shown, in previous studies, to be activated following the initiation of the complement and coagulation system [325]. Consequently, they took part in inflammatory and immune responses [326], in addition to their critical role in haemostasis as described above. Plasminogen (PLG), a down-regulated protein in d21 PW versus d0 in this study, is responsible for regulating blood complement and coagulation cascade system, thereby affecting homeostasis and the ability to recognize and abolish infectious bacteria [321]. These two cascade pathways stimulate the defence mechanism and innate immune cells in response to tissue damage/injury [327].

The data in this study demonstrated a significant difference in DAPs as early-onset physiological mechanisms to promote adaptation to inflammatory signalling [328]. Fetuin-B, a protease inhibitor that can regulate insulin-like and hepatocyte growth factors (which in turn are IGF and HGF) following systemic inflammation [329], was up-regulated in d21 PW versus d0 in both CR and LR groups. Another group of protease inhibitors such as Inter-alpha-trypsin inhibitor heavy chain (i.e., ITIH3, mainly) and Alpha-1-microglobulin (AMBP) is also associated with the inflammatory response with either inflammatory or anti-inflammatory properties, especially acute inflammation triggered by infection [330]. Indeed, the down-regulation of ITIH3 and AMBP in d21 PW versus d0 in this study was related to multiple biological processes such as vesicle-mediated transport and the regulation of proteolysis, localization, organonitrogen compound metabolic process. Coagulation factor XII (F12) was activated in LR versus CR serum at d0 to

quickly create enzymatic activity on the surface of pathological cells in response to inflammation [331]. Protein F12 also contributes to developing the protective system in weaning piglets by regulating the cross-talk that links coagulation pathways and inflammation, particularly in innate immunity [331].

4.9 CONCLUSIONS

The present study provides evidence that nutritional intervention strategies, such as reducing the ω6:ω3 ratio in maternal diet, can promote transmission of protective factors to the offspring, leading to better anti-inflammatory activities, activation of innate immunity, and contributing to the enhanced host protective response. Supplementing SW in post-weaned piglets stimulated coagulation cascade regulation and the connection between innate and adaptive immunity to enhance the host defence during inflammation conditions. The altered serum proteome profile between weaning and d21 post-weaning related to platelet metabolism, haemostasis, cross-talk between coagulation pathways and inflammation, particularly in the innate immune system. Particularly striking were the decreases in abundance of acute phase proteins such as serum amyloid and the increases in apolipoprotein and HDL between weaning and d21 post-weaning. These findings collectively demonstrate the efficiency of reducing ω6:ω3 ratio (to 4:1) in maternal diet and SW supplementation in the diet of post-weaned piglets to boost offspring's immunity and anti-inflammation properties.

Chapter 5 Ileal proteome changes associated with maternal dietary low ω6:ω3 ratio in piglets supplemented with seaweed

Journal of Proteomics: submitted 25/03/2022,
submission reference: JPROT-S-22-00166

Thi Xuan Nguyen[1,2,4]
Alessandro Agazzi[1]
Suzanne McGill[2]
Stefan Weidt[2]
Quang Hanh Han[2,4]
Andrea Gelemanović[3]
Mark McLaughlin[2]
Giovanni Savoini[1]
Peter David Eckersall[2]
Richard Burchmore[2]

[1]Università degli Studi di Milano, Via dell'Università, 6, 26900 Lodi, Italy
[2]University of Glasgow, Bearsden Rd, G61 1QH, United Kingdom
[3]Mediterranean Institute for Life Sciences (MedILS), Meštrovićevo šetalište 45, 21000 Split, Croatia
[4]Vietnam National University of Agriculture, Hanoi, Vietnam

Thi Xuan Nguyen contribution: conceptualization and design of the study, funding acquisition and project administration, methodology, acquisition of data, formal analysis and interpretation of data, drafting the manuscript, critical revising the manuscript, approval of the final version to be submitted, corresponding author.

Other contributions: Conceptualization and design of the study: AA, GS, PDE, and RB; funding acquisition and project administration: RB, DE, GS; methodology: SM, SW, QHH, AG, MM, RB, DE; acquisition of data: RB, DE; critical revising the manuscript: AA, QHH, AG, MM, GS, DE, and RB; all authors approved the final version to be submitted.

5.1 HIGHLIGHTS

* Long-term maternal dietary low ω6:ω3 ratio (4:1) and post-weaned pig diets supplemented with seaweed modified their ileal proteome.

* Maternal dietary low ω6:ω3 ratio exerted positive regulation of protein synthesis process; however, may induce uncontrolled proliferation and overexpression of cell cycle regulators in the offspring.

* Seaweed supplementation lowered the inflammation severity and promoted ileal epithelial growth in CRSW piglets but decreased the fat absorptive capacity in LRSW piglets.

5.2 SIGNIFICANCE

Weaning piglets undergo significant developmental changes in intestinal maturation. Present research assists in understanding the molecular mechanism that allows maternal combined with progeny dietary treatments to support piglet's ileal development from weaning to post-weaning. The results highlight the importance of nutritional management from the early stage (sows and newborn progeny) until later (post-weaning) to maintain piglet intestinal health and productivity.

5.3 GRAPHICAL ABSTRACT

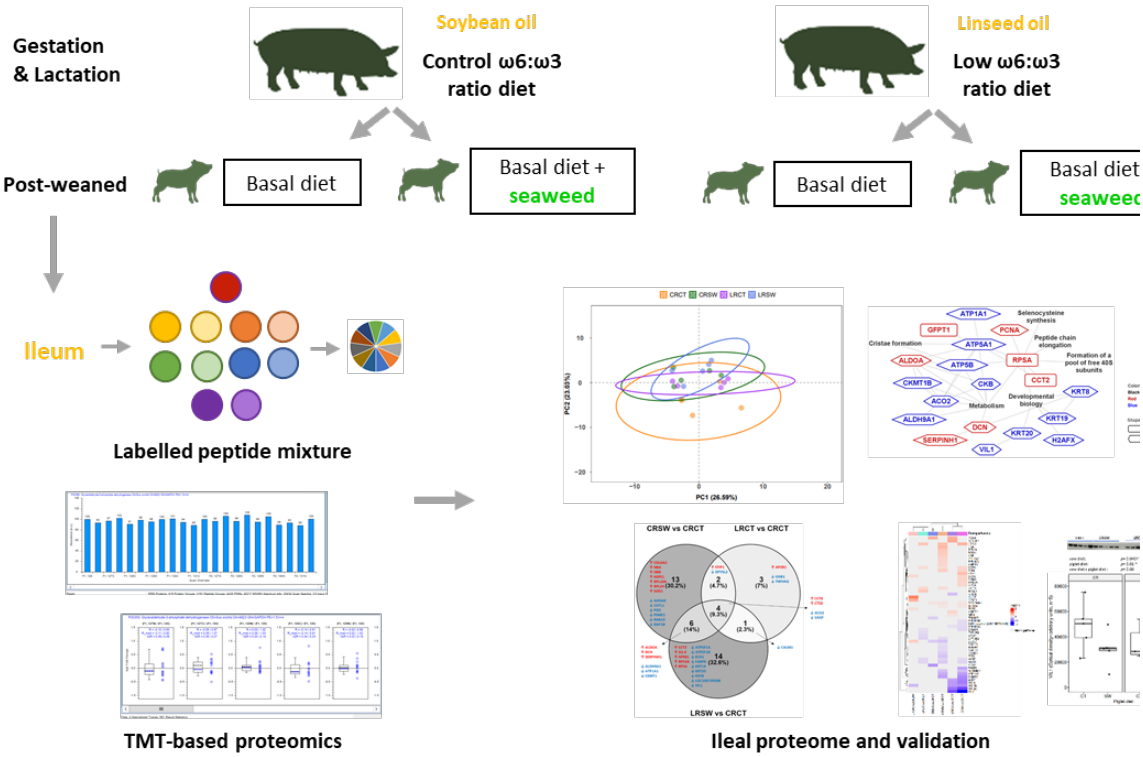

5.4 ABSTRACT

This study evaluates how long-term dietary low ω6:ω3 ratio in sows and offspring's seaweed (SW) intake affects piglet intestinal function and growth through modifying ileum proteome. Sows were assigned to either control diet (CR, ω6:ω3 ratio = 13:1) or treatment diet (LR, ω6:ω3 = 4:1) during gestation and lactation (n = 8 each). The male weaned offspring were received a basal diet with or without SW powder supplementation (4 g/kg) for 21 days, denoted as SW and CT groups, respectively. In total, four groups of weaned piglets were formed following maternal and offspring's diets combination, represented by CRCT, CRSW, LRCT, and LRSW (n = 10 each). Piglet ileum tissue was collected on day 22 post-weaning and analysed using TMT-based quantitative proteomics. The differentially abundant proteins (n = 300) showed the influence of maternal LR diet on protein synthesis, cell proliferation, and cell cycle regulation. In contrast, the SW diet lowered the inflammation severity and promoted ileal tissue development in CRSW piglets but reduced the fat absorption capacity in LRSW piglets. These results uncovered the mechanism behind the anti-inflammation and intestinal-boosting effects of maternal LR diet in piglets supplemented with SW.

Keywords: ileal proteome, ω6:ω3 fatty acids, seaweed, DNA and protein synthesis, weaned pigs, epithelial cells

5.5 INTRODUCTION

In pigs, weaning is a stressful event linked to significant intestinal changes [332]. Weaning stress triggers pro-inflammatory responses and stimulates epithelial proliferation (renewal) and differentiation, resulting in increased crypt depth, reduced intestinal villous height, and higher proportion of immature epithelial cells [332]. This process is essential to ensure an effective barrier function of the small intestine [333] and to progressively educate the mucosal immune system upon the antigenic challenge for health and normal growth maintenance [334]. Piglets in this critical phase must be well-equipped to protect the intestines and immune development, preventing an excessive reduction in feed consumption, intestinal inflammation, and dysbiosis [335].

Maternal effects include the environment experienced by the mother and nutrients belonging to the early life period that considerably influences offspring phenotype and growth [336,337]. Unbalanced maternal nutrition would lead to a mismatch in the maternal-offspring environment, suboptimal offspring growth [338], and health problems associated with metabolic dysfunction [339]. In pigs and mammals, the maternal effects continue during the lactation period and even for life. Therefore, the role of maternal nutrition is vital for offspring in response to early life stimuli [340], such as weaning stress. There have been no studies exploring the underlying mechanism of maternal-offspring nutritional interventions in initiating the development of piglets' ileal epithelial cells.

A high human modern dietary ω6:ω3 fatty acid ratio (~20:1) is associated with elevated pro-inflammatory mediators from ω6 and decreased the anti-inflammatory mediators from ω3, leading to excessive inflammation [43,45]. Consequently, lowering the dietary ω6:ω3 ratio might be a promising approach to decrease inflammation and allergies [42] and maintain good health [23]. Maternal dietary low ω6:ω3 ratio in swine with more ω3 fatty acids supplemented from linseed oil is effective in enhancing weaning survival rate [183], postnatal growth, and metabolic traits [183,341,342]. In addition, the post-weaning diet program is a crucial determinant of lifelong health and performance [343]. The brown seaweed *Ascophyllum nodosum* is a potential prebiotic and antibacterial dietary supplement for swine thanks to its high content of bioactive compounds such as

fucoidan (a type of polysaccharide) and laminarin [344]. The combined effects of maternal low ω6:ω3 ratio and offspring *Ascophyllum nodosum* diets on the molecular mechanism underlying offspring development are complicated and not addressed in swine.

Here, to better understand the mechanism behind effects of early- (maternal low ω6:ω3 intake) and later-life nutritional programming (offspring seaweed supplementation) on post-weaned piglet's ileal development, a Tandem Mass Tag (TMT)-based quantitative proteomics approach was applied. It was hypothesized that maternal-offspring dietary treatments would accelerate the ileal development in weaned piglets and relieve weaning distress through modifying the ileal protein profile. This study brings new insights into ileal developmental changes during post-weaning periods, which were affected by the associations between long-term maternal and offspring dietary treatments. The data in the current research provides additional evidence on piglets' dynamic molecular response to interactions between maternal low ω6:ω3 intake and post-weaned seaweed supplementation.

5.6 MATERIALS AND METHODS

5.6.1 Animals and sample collection

A feeding trial was performed with 40 male weaned piglets at the Animal Production Research and Teaching Centre of the Department of Veterinary Medicine and Animal Science, University of Milan (Lodi, Italy). The experiment protocol was approved by the Ethical Committee of the University of Milan (OPBA 67/2018) and the Italian Ministry of Health (authorization n. 168/2019 PR). The study design and zootechnical data were previously reported by Nguyen et al. [183].

After separating from the mothers, piglets weighing 6.46 kg (± 0.15) (mean ± SE) at day 26 (± 1.76) of age were selected from different mothers within a group, amongst two groups receiving either a control ratio of ω6:ω3 fatty acids (CR, 13:1 during gestation and 10:1 during lactation) or a low ratio (LR, 4:1, during gestation

and lactation). Piglets were provided a basal commercial diet [183] and supplemented with or without 4 g seaweed powder *(A. nodosum;* Prodotti Arca S.r.l, Monza, Italy) per kg of feed, namely SW and CT groups, respectively. In total, four groups (*n* = 10 each) were formed: CRCT, CRSW, LRCT, and LRSW. At the end of the post-weaning (PW) period (day 22), piglets were sacrificed to harvest ileum samples (~3 cm) using 2-mL cryogenic vials (Nalgene™, Thermo Scientific™). Samples were then frozen immediately and stored at −80 °C until analysed.

5.6.2 Protein Identification and Quantification using the TMT approach

5.6.2.1 Protein extraction and quantification

The protein in ileum samples (n = 5 per group x 4 groups) was extracted according to previously published methods [110,345]. In brief, cold cut frozen ileum tissue was homogenized using mortar and pestle in liquid nitrogen. Afterward, ~200 mg of fine ileum powder was sonicated in 500 µL lysis buffer (100 mM TEAB, 2% SDS), using a probe sonicator (OPTIMA, XL 100K, Germany) at 40% amplitude, following a sequence of 10-s on and 5-s off, three times on ice. The obtained homogenate was centrifuged at 14,000× *g* for 30 min at 4 °C. The supernatants (ileum extract) were separated from the pellets and total protein concentration was determined by the bicinchoninic acid method (BCA Assay, Pierce™ BCA Protein Assay Kit, Thermo Scientific, Meridian Rd., Rockford, IL, USA) with bovine serum albumin as standard. Samples were prepared and kept at -80 °C before analyses.

5.6.2.2 Protein digestion and TMT labelling

Tandem Mass Tag (TMT) labelling quantitative approach was applied to analyse the proteomic profiling of ileum samples as described previously [184]. 100 µg of protein (~4.63 µL) per sample was processed using the “in-solution” filter-aided sample preparation (FASP) with 10 kDa molecular weight cut-off filters (Merck Millipore, Carrigtohill, Ireland). Protein was denatured with 4% SDS and reduced using 0.1 M Tris/HCL pH 7.6 and 0.1 M DTT (Sigma Aldrich, St. Louis, MO, USA). Alkylation of cysteine residues was performed using 0.05 M IAA (Sigma Aldrich, St. Louis, MO, USA) in the dark for 20 min at room temperature. Tryptic digestion was

performed at 37 °C overnight using 1 µg of trypsin (Promega, Madison, WI, USA, 1:37) and then stopped using 1% TFA before vacuum-dried at 45 °C. The obtained peptides were labelled with freshly prepared TMT11plex (Thermo Fisher Scientific, Rockford, IL, USA), incubated for 60 min, quenched in 45 min and vacuum centrifuged until completely dry following the manufacturer's protocol. A pooled sample was prepared by taking an equal amount of peptide from each sample, labelled by a TMT tag and used as an internal standard between two TMT experiments.

5.6.2.3 Liquid chromatography tandem mass spectrometer (LC-MS/MS)

The labelled peptides were loaded onto a nanoflow uHPLC system (Thermo Fisher Scientific RSLCnano, Horsham, UK), detected using electrospray ionisation (ESI) mass spectrometry MS/MS with an Orbitrap Elite MS (Thermo Fisher Scientific, Horsham, UK). HPLC solvents contain 20 µL of 5% ACN and 0.5% formic acid. Ionization in LC-MS interfaces using a NanoMate Triversa (Advion Bioscience, Harlow, UK) with an electrospray voltage of 1.7 kV. The peptides (5 µL) were desalted using 1% ACN and 0.1% formic acid on the trap column (0.3 × 5 mm) at a flow rate of 25 µL/min for 12 min.

The purified peptides were then enriched on a Pepmap C18 reversed-phase column (50 cm × 75 µm, 3 µm, 100 Å, Thermo Fisher Scientific, Horsham, UK), and separated on an analytical column at a fixed flow rate of 0.3 µL/min. The solvent system used 0.1% aqueous formic acid as solvent A and 0.08% formic acid in 80% ACN as solvent B. Fractionation was run with 4% solvent B for 10 min, followed by 4-60% solvent B for 170 min, 60-99% solvent B for 15 min, and held at 99% solvent B for 5 min. The column was then adjusted to the initial set-up for re-equilibration (10 min) before injecting the following sample.

Eluting peptides were subjected to MS/MS analysis on an Orbitrap Elite MS. Each MS scan was within the m/z range of 380 – 1800. The top three precursor ions were fragmented using CID and HCD collision cells, detected in the Orbitrap at a resolution of 30000 FWHM, as defined at m/z 400. Precursor ions chosen were excluded after every 180s, and single-charged ions were omitted from selection.

5.6.3 MS/MS data processing

The MS/MS data were searched against the UniProt *Sus scrofa* database (104,940 sequences; downloaded on 18/02/2021) for protein identification and relative quantification using Sequest HT search engine in Proteome Discoverer (v2.4, Thermo Fisher Scientific). The search parameters were as follows: tryptic peptides with two missed-cleavage allowed, carbamidomethylation at cysteine residue was stated as fixed modification, oxidation at methionine, deamidation at asparagine and glutamine residues, and TMT labelling at lysine residue and peptide N-terminus were stated as variable. The mass tolerance for the precursor ions was 10 ppm and that for fragment ions was 0.02 Da. A false discovery rate (FDR) of 1% was applied at the peptide level. Proteins were identified containing at least two peptides with 5% FDR. The mass spectrometry proteomics data have been deposited to the ProteomeXchange Consortium via PRIDE [185] partner repository with the dataset identifier PXD032326.

5.6.4 Validation of proteomics results

To validate ileum proteomics results, evaluating changes in the non-depleted sample contents of villin-1 (VIL1) and Proliferating cell nuclear antigen (PCNA) were implemented, which were chosen based on their significant abundance changes, biological meaning and antibody availability. The concentration of VIL1 and PCNA in ileum extraction samples was quantified using Western blot, detailed as described elsewhere [193]. Briefly, an amount of 2 μg and 10 μg ileum proteins per sample was used for VIL1 and PCNA immunoassays, respectively. The presence of VIL1 in ileum samples was captured and detected using rabbit polyclonal antibody to villin diluted in 1:1,000 (ab233155, Abcam Ltd. UK), followed by secondary antibody conjugated donkey anti-rabbit IgG to horseradish peroxidase (HRP) diluted in 1:10,000 (ab7125, Abcam Ltd. UK). Ileum PCNA was detected using goat polyclonal antibody raised against synthetic peptide of PCNA at 1:1,000 dilution (pab27564, Abnova, Taipei, Taiwan) as the primary antibody and HRP-conjugated donkey anti-goat IgG 1:5,000 as the secondary antibody.

The experimental design, pipeline for proteomics analysis (containing sample preparation, TMT labelling, and LC-MS/MS, data analysis, and quantitation), and validation of proteomics are illustrated in Figure 5-1.

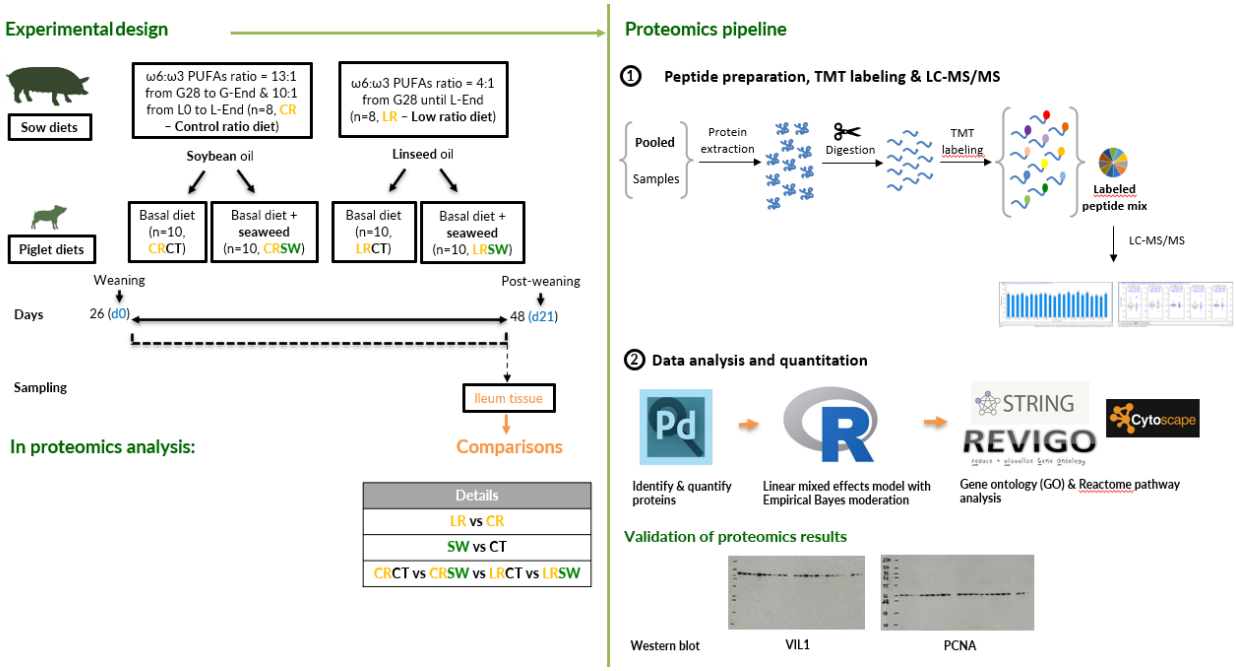

Figure 5-1 The experimental design, proteomics pipeline and validation of proteomics results. Proteomics pipeline contains: (1) Peptide preparation, TMT labelling, and LC-MS/MS analysis, (2) Data analysis and quantitation: protein identification and quantitation using Proteome Discoverer, statistical analysis based on the linear mixed-effects model with empirical Bayes moderation (R package MSstatsTMT), bioinformatics analysis (Gene Ontology (GO) and Reactome pathway enrichment analysis).

5.6.5 Statistical and Bioinformatics Analysis

5.6.5.1 Statistical analysis for proteomics data

The peptide spectrum match (PSM)-level data were analysed using linear mixed-effects models with Empirical Bayes moderation on MSstatsTMT package v2.0.0 [186] in R v4.1.0 [187]. Protein was quantified based on unique peptides only and summarization using the median polish method. Protein normalization was performed using the internal standard channel. Only master proteins were subjected to the statistical analysis. Proteins were significantly changed at an adjusted *p*-value < 0.05 and possibly altered at a *p*-value < 0.05. The Benjamini-Hochberg correction was applied to adjust the *p*-values ($p < 0.05$).

The volcano plots were illustrated using packages *ggplot2* v3.3.3 [188] and *ggrepel* v0.9.1, PCA plots used *ggplot2* v3.3.3 [188], and heatmaps used *pheatmap* v1.0.12. Venn diagrams were performed using web tool Venny 2.1 (https://bioinfogp.cnb.csic.es/tools/venny/) [189].

5.6.5.2 Bioinformatics analysis

For identified master protein, the UniProt retrieve/ID mapping tool was used to convert their accession numbers into the corresponding gene ID. For undefined proteins, their best match on *Sus scrofa* orthologue annotated genes (minimum 70% identity) were used instead using the SmartBLAST tool (https://blast.ncbi.nlm.nih.gov/smartblast/). Differential abundant proteins (DAPs) were imported into the STRING database v11.5 [190] and retrieved the protein-protein interaction (PPI) network, Reactome pathways, Gene Ontology (GO) analysis containing Biological Process (BP), Molecular Function (MF), and Cellular Component (CC) using the default parameters. Extremely similar GO terms were filtered using the REVIGO [192] (revigo.irb.hr), with the following settings: whole UniProt as the database, SimRel as semantic similarity measure at a threshold of 0.5. The network showing interactions between desired Reactome pathways and DAPs between comparisons were illustrated using Cytoscape software v3.8.2 [191].

5.6.5.3 Statistical analysis for validation data

The validation data on VIL1 and PCNA were analysed and checked for their correlation with proteomics data. Data normalization and variance homogeneity were checked by the Shapiro-Wilk and Levene's test. Difference between groups was discovered using the linear mixed model, and p-values were adjusted using the Benjamini-Hochberg post hoc pairwise testing. Fixed effects were sow diet, piglet diet, time, and their interactions. The random effect was an individual piglet. Spearman correlation analysis assessed the relationship between proteomics and validation results for both VIL1 and PCNA.

5.7 RESULTS

5.7.1 Proteomic analysis

The proteomics analysis generated 4428 features and mapped 2216 unique peptides, which represented 1237 proteins and 671 master proteins. After filtering proteins with no unique peptide, only one peptide, and singly charged ions, 300 master proteins were quantified and reserved for statistical analysis.

5.7.1.1 DAPs in LR vs CR and SW vs CT groups

The DAPs were determined via two comparisons: LR vs CR and SW vs CT (Table 5-1). Comparison between LR and CR discovered 5 DAPs (4 increased and one decreased) and comparison SW vs CT revealed 19 DAPs (5 increased and 14 decreased) (Table 5-1, $p < 0.05$). No DAPs were shared between these two comparisons (Venn diagram, Figure 5-2A). The DAPs were determined distinctly for comparison LR vs CR comprising increased-abundant proteins such as Glutamine--fructose-6-phosphate transaminase (GFPT1), T-complex protein 1 subunit beta (CCT2), and 40S ribosomal protein SA (RPSA), and one decreased-abundant protein (calmodulin 1, CALM1). In comparison SW vs CT, the leading increased-abundant protein was proliferating cell nuclear antigen (PCNA) and the leading decreased-abundant proteins were villin-1 (VIL1) and keratin proteins (KRT8, KRT19, KRT20) ($p < 0.05$, Table 5-1).

Table 5-1 The differentially abundant proteins (DAPs) in piglet ileum at day 22 of post-weaning of two comparisons: LR vs CR and SW vs CT.

Protein name	Gene names	Accession number[1]	Number of peptides	log2FC[2]	*P*-value	Adjusted *p*-value
LR vs CR						
Glutamine-fructose-6-phosphate transaminase (isomerizing)	GFPT1	E1U318	2	0.32	0.042	0.963
T-complex protein 1 subunit beta	CCT2	A0A5G2QMG1	2	0.17	0.009	0.963
PDZ and LIM domain protein 7	PDLIM7	A0A4X1SEG0	3	0.16	0.026	0.963
40S ribosomal protein SA	RPSA	A0A480SME4	4	0.14	0.044	0.963
Calmodulin 1	CALM1	A0A4X1ST02	3	-0.10	0.030	0.963
SW vs CT						
Proliferating cell nuclear antigen	PCNA	X5FB24	2	0.51	0.005	0.368
Cathepsin D	CTSD	A0A480M5F4	2	0.29	0.034	0.678
Decorin	DCN	F1SQ10	4	0.19	0.009	0.407
Collagen-binding protein	SERPINH1	A0A480U2E1	10	0.09	0.002	0.368
Fructose-bisphosphate aldolase	ALDOA	A0A4X1U0N5	11	0.06	0.046	0.678
ATP synthase subunit alpha	ATP5A1	A0A287AGU2	13	-0.09	0.023	0.582
ATP synthase subunit beta	ATP5B	A0A481D142	17	-0.10	0.019	0.573
Aconitate hydratase, mitochondrial (Aconitase)	ACO2	F1SRC5	2	-0.13	0.036	0.678
Creatine kinase	CKB	A0A4X1TV43	8	-0.13	0.025	0.582
Proteasome activator complex subunit 1	PSME1	Q64L94	4	-0.18	0.018	0.573
4-trimethylaminobutyraldehyde dehydrogenase	ALDH9A1	F1S232	2	-0.23	0.025	0.582
Sodium/potassium-transporting ATPase subunit alpha	ATP1A1	A0A4X1SW39	2	-0.33	0.049	0.678
Creatine kinase U-type, mitochondrial	CKMT1B	Q29577	2	-0.40	0.048	0.678
Histone H2A	H2AFX	A0A5G2QMX0	3	-0.41	0.037	0.678
Keratin, type I cytoskeletal 19	KRT19	A0A480IFL7	11	-0.47	0.003	0.368
Keratin, type II cytoskeletal 8	KRT8	A0A4X1WBI1	18	-0.51	0.006	0.368
Enoyl coenzyme A hydratase 1	ECH1	A0A4X1T0M5	2	-0.53	0.009	0.407
Keratin, type I cytoskeletal 20	KRT20	A0A5G2QPZ4	6	-0.75	0.006	0.368
Villin-1	VIL1	Q29261	2	-0.98	0.018	0.573

[1]Accession number from UniProt protein database for *Sus scrofa*. [2]log2FC is base 2 logarithm transformed of fold change value which represents the ratio of expression levels in the first-mentioned group vs second-mentioned group. CR: mother diet with ω6:ω3 ratio = 13:1 during gestation, starting from day 28 (G28) and 10:1 during lactation; LR: mother diet with ω6:ω3 ratio = 4:1 from G28 until the end of lactation. SW: piglet diet with seaweed supplementation, CT: piglet diet without seaweed supplementation.

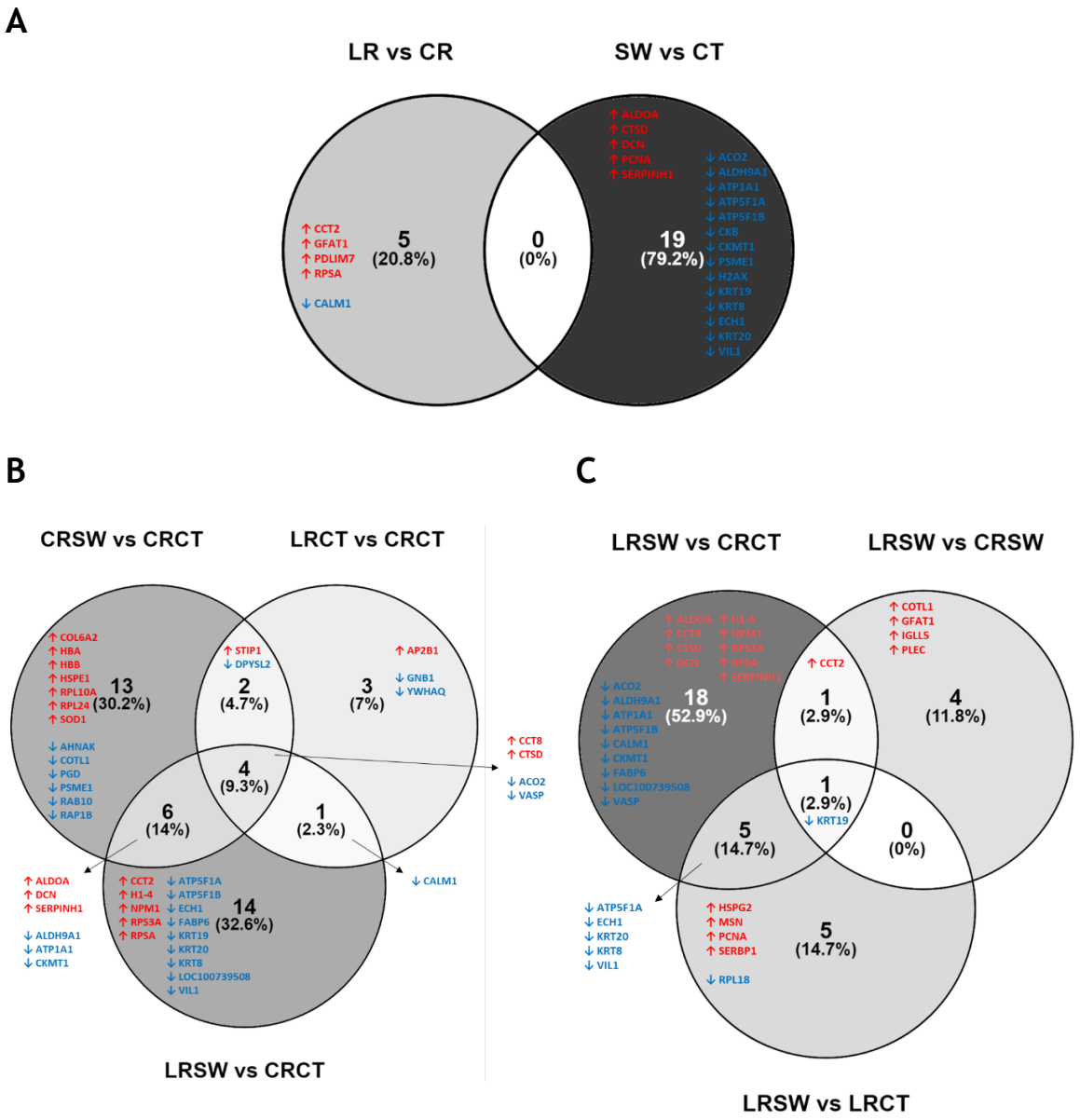

Figure 5-2 Venn diagram representing separated and overlapped differentially abundant proteins (DAPs) between two comparisons of piglet ileum: LR vs CR and SW vs CT. CR: piglet born from sow fed diet with ω6:ω3 ratio = 13:1 during gestation, starting from day 28 (G28) and 10:1 during lactation; LR: piglet born from sow fed diet with ω6:ω3 ratio = 4:1 from G28 until the end of lactation. SW: piglet diet with seaweed supplementation, CT: piglet diet without seaweed supplementation. CRCT: piglets fed no seaweed (SW, *Ascophyllum nodosum*), which nursed by sows fed dietary ω6:ω3 ratio = 13:1 during gestation, starting from day 28 (G28) and 10:1 during lactation. CRSW: piglets fed SW, which nursed by sows fed dietary ω6:ω3 ratio = 13:1 during gestation and 10:1 during lactation. LRCT: piglets fed no SW, which nursed by sows fed dietary ω6:ω3 ratio = 4:1 from G28 until the end of lactation. LRSW: piglets fed SW, which nursed by sows fed dietary ω6:ω3 ratio = 4:1 from G28 until the end of lactation.

5.7.1.2 DAPs in the comparisons among all 4 groups (CRCT, LRCT, CRSW, and LRSW)

The PCA score plot shows a mixed grouping of ileum samples from 4 groups of piglets at day 22 post-weaning (Figure 5-3), containing CRCT, LRCT, CRSW, and LRSW groups. The first two PCs contributed a cumulative variance rate of 47.66% of the overall variance. The DAPs in piglet ileum among these 4 groups are examined in six comparisons and presented in Table 5-2.

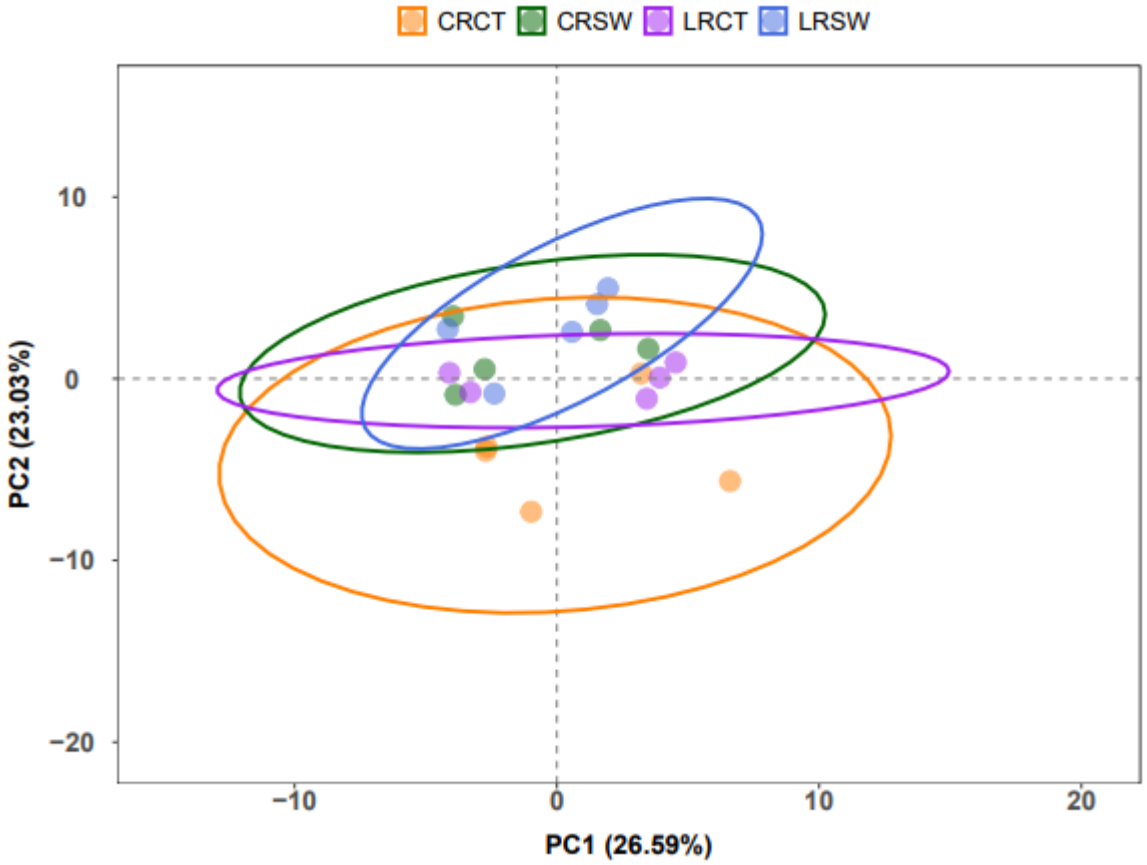

Figure 5-3 Principal component analysis (PCA) score plots showing the clustering of samples from four groups of piglet ileum containing CRCT: piglets fed no seaweed (SW, *Ascophyllum nodosum*), which nursed by sows fed dietary ω6:ω3 ratio = 13:1 during gestation, starting from day 28 (G28) and 10:1 during lactation. CRSW: piglets fed SW, which nursed by sows fed dietary ω6:ω3 ratio = 13:1 during gestation and 10:1 during lactation. LRCT: piglets fed no SW, which nursed by sows fed dietary ω6:ω3 ratio = 4:1 from G28 until the end of lactation. LRSW: piglets fed SW, which nursed by sows fed dietary ω6:ω3 ratio = 4:1 from G28 until the end of lactation. The ellipses represent 95% confidence region.

Table 5-2 The differentially abundant proteins (DAPs) in piglet ileum at day 22 post-weaning among 4 groups containing CRCT, CRSW, LRCT and LRSW.

Protein name	Gene names	Accession number[1]	Number of peptides	log2FC[2]						*P*-value					
				CRSW vs CRCT	CRSW vs LRCT	LRCT vs CRCT	LRSW vs CRCT	LRSW vs CRSW	LRSW vs LRCT	CRSW vs CRCT	CRSW vs LRCT	LRCT vs CRCT	LRSW vs CRCT	LRSW vs CRSW	LRSW vs LRCT
Aconitate hydratase, mitochondrial (Aconitase)	ACO2	F1SRC5	2	-0.26	/	-0.17	-0.18	/	/	0.003	/	0.033	0.030	/	/
Neuroblast differentiation-associated protein AHNAK isoform X1**	AHNAK	A0A4X1VKL9	6	-0.16	/	/	/	/	/	0.021	/	/	/	/	/
4-rimethylaminobutyraldehyde dehydrogenase	ALDH9A1	F1S232	2	-0.33	/	/	-0.35	/	/	0.044	/	/	0.025	/	/
Fructose-bisphosphate aldolase	ALDOA	A0A4X1U0N5	11	0.08	/	/	0.10	/	/	0.039	/	/	0.016	/	/
AP-2 complex, beta subunit	AP2B1	A0A4X1T8Q4	2	/	/	0.34	/	/	/	/	/	0.017	/	/	/
Sodium/potassium-transporting ATPase subunit alpha	ATP1A1	A0A4X1SW39	2	-0.47	/	/	-0.59	/	/	0.038	/	/	0.012	/	/
ATP synthase subunit alpha	ATP5A1	A0A287AGU2	13	/	/	/	-0.15	/	-0.11	/	/	/	0.010	/	0.049
ATP synthase subunit beta	ATP5B	A0A481D142	17	/	/	/	-0.14	/	/	/	/	/	0.031	/	/
Calmodulin 1	CALM1	A0A4X1ST02	3	/	/	-0.12	-0.18	/	/	/	/	0.047	0.007	/	/
T-complex protein 1 subunit beta	CCT2	A0A5G2QMG1	2	/	/	/	0.24	0.20	/	/	/	/	0.011	0.025	/
T-complex protein 1 subunit theta	CCT8	A0A480X895	2	0.16	/	0.16	0.21	/	/	0.038	/	0.038	0.008	/	/

Protein names marked with ** were shown as "Uncharacterized protein" in the UniProt *Sus scrofa* database and cannot find the best match on *Sus scrofa* database, thus were substituted with the best match on *Homo sapiens* database, using SMARTBLAST tool. [1]Accession number from UniProt protein database for *Sus scrofa*. [2]log2FC is base 2 logarithm transformed of fold change value which represents the ratio of expression levels in the first-mentioned group vs second-mentioned group. CRCT: piglets fed no seaweed (SW, *Ascophyllum nodosum*), which nursed by sows fed dietary ω6:ω3 ratio = 13:1 during gestation, starting from day 28 (G28) and 10:1 during lactation. CRSW: piglets fed SW, which nursed by sows fed dietary ω6:ω3 ratio = 13:1 during gestation and 10:1 during lactation. LRCT: piglets fed no SW, which nursed by sows fed dietary ω6:ω3 ratio = 4:1 from G28 until the end of lactation. LRSW: piglets fed SW, which nursed by sows fed dietary ω6:ω3 ratio = 4:1 from G28 until the end of lactation.

(cont., 1).

Protein name	Gene names	Accession number[1]	Number of peptides	log2FC[2]						*P*-value					
				CRSW vs CRCT	CRSW vs LRCT	LRCT vs CRCT	LRSW vs CRCT	LRSW vs CRSW	LRSW vs LRCT	CRSW vs CRCT	CRSW vs LRCT	LRCT vs RCT	LRSW vs CRCT	LRSW vs CRSW	LRSW vs LRCT
Creatine kinase U-type, mitochondrial	CKMT1B	Q29577	2	-0.57	/	/	-0.74	/	/	0.036	/	/	0.010	/	/
Collagen alpha-2(VI) chain isoform 2C2	COL6A2	A0A480W6C8	9	0.23	/	/	/	/	/	0.048	/	/	/	/	/
Coactosin-like protein 1	COTL1	A0A4X1T354	3	-0.31	-0.25	/	/	0.29	/	0.002	0.011	/	/	0.004	/
Cathepsin D	CTSD	A0A480M5F4	2	0.41	/	0.36	0.52	/	/	0.021	/	0.042	0.006	/	/
Decorin	DCN	F1SQ10	4	0.30	/	/	0.23	/	/	0.004	/	/	0.020	/	/
Dihydropyrimidinase-related protein 2	DPYSL2	G9F6X9	3	-0.16	/	-0.20	/	/	/	0.049	/	0.020	/	/	/
Enoyl coenzyme A hydratase 1	ECH1	A0A4X1T0M5	2	/	/	/	-0.81	/	-0.56	/	/	/	0.005	/	0.039
Fatty acid binding protein 6	FABP6	F1RR40	6	/	/	/	-0.55	/	/	/	/	/	0.017	/	/
Glutamine-fructose-6-phosphate transaminase	GFPT1	E1U318	2	/	/	/	/	0.54	/	/	/	/	/	0.015	/
G protein subunit beta 1	GNB1	A0A287A7Q3	2	/	/	-0.17	/	/	/	/	/	0.008	/	/	/
Histone H1.4	HIST1H1E	A0A480QWI4	8	/	/	/	0.44	/	/	/	/	/	0.023	/	/
Histone H2A	H2AX	A0A5G2QMX0	3	/	-0.67	/	/	/	/	/	0.017	/	/	/	/

[1]Accession number from UniProt protein database for *Sus scrofa*. [2]log2FC is base 2 logarithm transformed of fold change value which represents the ratio of expression levels in the first-mentioned group vs second-mentioned group. CRCT: piglets fed no seaweed (SW, *Ascophyllum nodosum*), which nursed by sows fed dietary ω6:ω3 ratio = 13:1 during gestation, starting from day 28 (G28) and 10:1 during lactation. CRSW: piglets fed SW, which nursed by sows fed dietary ω6:ω3 ratio = 13:1 during gestation and 10:1 during lactation. LRCT: piglets fed no SW, which nursed by sows fed dietary ω6:ω3 ratio = 4:1 from G28 until the end of lactation. LRSW: piglets fed SW, which nursed by sows fed dietary ω6:ω3 ratio = 4:1 from G28 until the end of lactation.

(cont., 2).

Protein name	Gene names	Accession number[1]	Number of peptides	log2FC[2]						*P*-value					
				CRSW vs CRCT	CRSW vs LRCT	LRCT vs CRCT	LRSW vs CRCT	LRSW vs CRSW	LRSW vs LRCT	CRSW vs CRCT	CRSW vs LRCT	LRCT vs CRCT	LRSW vs CRCT	LRSW vs CRSW	LRSW vs LRCT
Hemoglobin subunit alpha	HBA	P01965	6	0.48	/	/	/	/	/	0.005	/	/	/	/	/
Hemoglobin subunit beta	HBB	P02067	8	0.27	/	/	/	/	/	0.017	/	/	/	/	/
10 kDa heat shock protein, mitochondrial (Chaperonin 10)	HSPE1	F1SMZ6	4	0.21	/	/	/	/	/	0.044	/	/	/	/	/
Heparan sulfate proteoglycan 2	HSPG2	A0A287ATP0	4	/	/	/	/	/	0.24	/	/	/	/	/	0.035
Immunoglobulin lambda-like polypeptide 5 precursor*	IGLL5	A0A4X1T0Z9	2	/	/	/	/	0.93	/	/	/	/	/	0.048	/
Keratin, type I cytoskeletal 19	KRT19	A0A480IFL7	11	/	/	/	-0.72	-0.39	-0.62	/	/	/	0.001	0.040	0.003
Keratin, type I cytoskeletal 20	KRT20	A0A5G2QPZ4	6	/	/	/	-1.24	/	-0.90	/	/	/	0.001	/	0.012
Keratin, type II cytoskeletal 8	KRT8	A0A4X1WBI1	18	/	/	/	-0.82	/	-0.62	/	/	/	0.002	/	0.011
GST class-pi	LOC100739508	A0A287BQ81	4	/	/	/	-0.15	/	/	/	/	/	0.033	/	/
Moesin	MSN	A0A4X1VQZ3	5	/	/	/	/	/	0.10	/	/	/	/	/	0.032
Nucleoplasmin domain-containing protein	NPM1	A0A4X1U9Z4	6	/	/	/	0.24	/	/	/	/	/	0.018	/	/
Proliferating cell nuclear antigen	PCNA	X5FB24	2	/	0.54	/	/	/	0.56	/	0.047	/	/	/	0.029
PDZ and LIM domain protein 7	PDLIM7	A0A4X1SEG0	3	/	-0.24	/	/	/	/	/	0.017	/	/	/	/
6-phosphogluconate dehydrogenase, decarboxylating	PGD	A0A480YSA5	2	-0.32	/	/	/	/	/	0.046	/	/	/	/	/

Protein names marked with * were shown as "Uncharacterized protein" in the UniProt *Sus scrofa* database, thus were substituted with the best match on *Sus scrofa* database, using SMARTBLAST tool. [1]Accession number from UniProt protein database for *Sus scrofa*. [2]log2FC is base 2 logarithm transformed of fold change value which represents the ratio of expression levels in the first-mentioned group vs second-mentioned group. CRCT: piglets fed no seaweed (SW, *Ascophyllum nodosum*), which nursed by sows fed dietary ω6:ω3 ratio = 13:1 during gestation, starting from day 28 (G28) and 10:1 during lactation. CRSW: piglets fed SW, which nursed by sows fed dietary ω6:ω3 ratio = 13:1 during gestation and 10:1 during lactation. LRCT: piglets fed no SW, which nursed by sows fed dietary ω6:ω3 ratio = 4:1 from G28 until the end of lactation. LRSW: piglets fed SW, which nursed by sows fed dietary ω6:ω3 ratio = 4:1 from G28 until the end of lactation.

(cont., 3).

Protein name	Gene names	Accession number[1]	Number of peptides	log2FC[2]						*P*-value					
				CRSW vs CRCT	CRSW vs LRCT	LRCT vs CRCT	LRSW vs CRCT	LRSW vs CRSW	LRSW vs LRCT	CRSW vs CRCT	CRSW vs LRCT	LRCT vs CRCT	LRSW vs CRCT	LRSW vs CRSW	LRSW vs LRCT
Plectin (Fragment)	PLEC	K9IVQ6	3	/	/	/	/	0.15	/	/	/	/	/	0.047	/
Proteasome activator complex subunit 1	PSME1	Q64L94	4	-0.23	/	/	/	/	/	0.032	/	/	/	/	/
Ras-related protein Rab-10	RAB10	A0A4X1TSZ3	2	-0.16	/	/	/	/	/	0.033	/	/	/	/	/
Ras-related protein Rap-1b	RAP1B	A0A5G2QA99	2	-0.12	/	/	/	/	/	0.045	/	/	/	/	/
60S ribosomal protein L10A	RPL10A	A0A4X1T0H0	2	0.22	/	/	/	/	/	0.039	/	/	/	/	/
Ribosomal protein L18 (Fragment)	RPL18	Q0QEV2	2	/	/	/	/	/	-0.34	/	/	/	/	/	0.033
Ribosomal protein L24	RPL24	A0A287A286	2	0.35	/	/	/	/	/	0.042	/	/	/	/	/
40S ribosomal protein S3a	RPS3A	B6V8C8	3	/	/	/	0.22	/	/	/	/	/	0.036	/	/
40S ribosomal protein SA	RPSA	A0A480SME4	4	/	/	/	0.22	/	/	/	/	/	0.027	/	/
SERPINE1 mRNA binding protein 1	SERBP1	A0A5G2QNW1	2	/	/	/	/	/	0.60	/	/	/	/	/	0.045
Collagen-binding protein	SERPINH1	A0A480U2E1	10	0.12	0.09	/	0.08	/	/	0.004	0.016	/	0.033	/	/
Superoxide dismutase 1 (Fragment)	SOD1	Q95ME5	2	0.32	/	/	/	/	/	0.026	/	/	/	/	/
Stress-induced phosphoprotein 1	STIP1	A0A0B8RZ32	3	0.16	/	0.20	/	/	/	0.043	/	0.013	/	/	/
Vasodilator-stimulated phosphoprotein	VASP	A0A481C371	2	-0.20	/	-0.18	-0.15	/	/	0.012	/	0.021	0.047	/	/
Villin-1	VIL1	Q29261	2	/	/	/	-1.56	/	-1.18	/	/	/	0.007	/	0.014
14-3-3 protein theta	YWHAQ	A0A5G2QM17	7	/	/	-0.14	/	/	/	/	/	0.042	/	/	/

[1]Accession number from UniProt protein database for *Sus scrofa*. [2]log2FC is base 2 logarithm transformed of fold change value which represents the ratio of expression levels in the first-mentioned group vs second-mentioned group. CRCT: piglets fed no seaweed (SW, *Ascophyllum nodosum*), which nursed by sows fed dietary ω6:ω3 ratio = 13:1 during gestation, starting from day 28 (G28) and 10:1 during lactation. CRSW: piglets fed SW, which nursed by sows fed dietary ω6:ω3 ratio = 13:1 during gestation and 10:1 during lactation. LRCT: piglets fed no SW, which nursed by sows fed dietary ω6:ω3 ratio = 4:1 from G28 until the end of lactation. LRSW: piglets fed SW, which nursed by sows fed dietary ω6:ω3 ratio = 4:1 from G28 until the end of lactation.

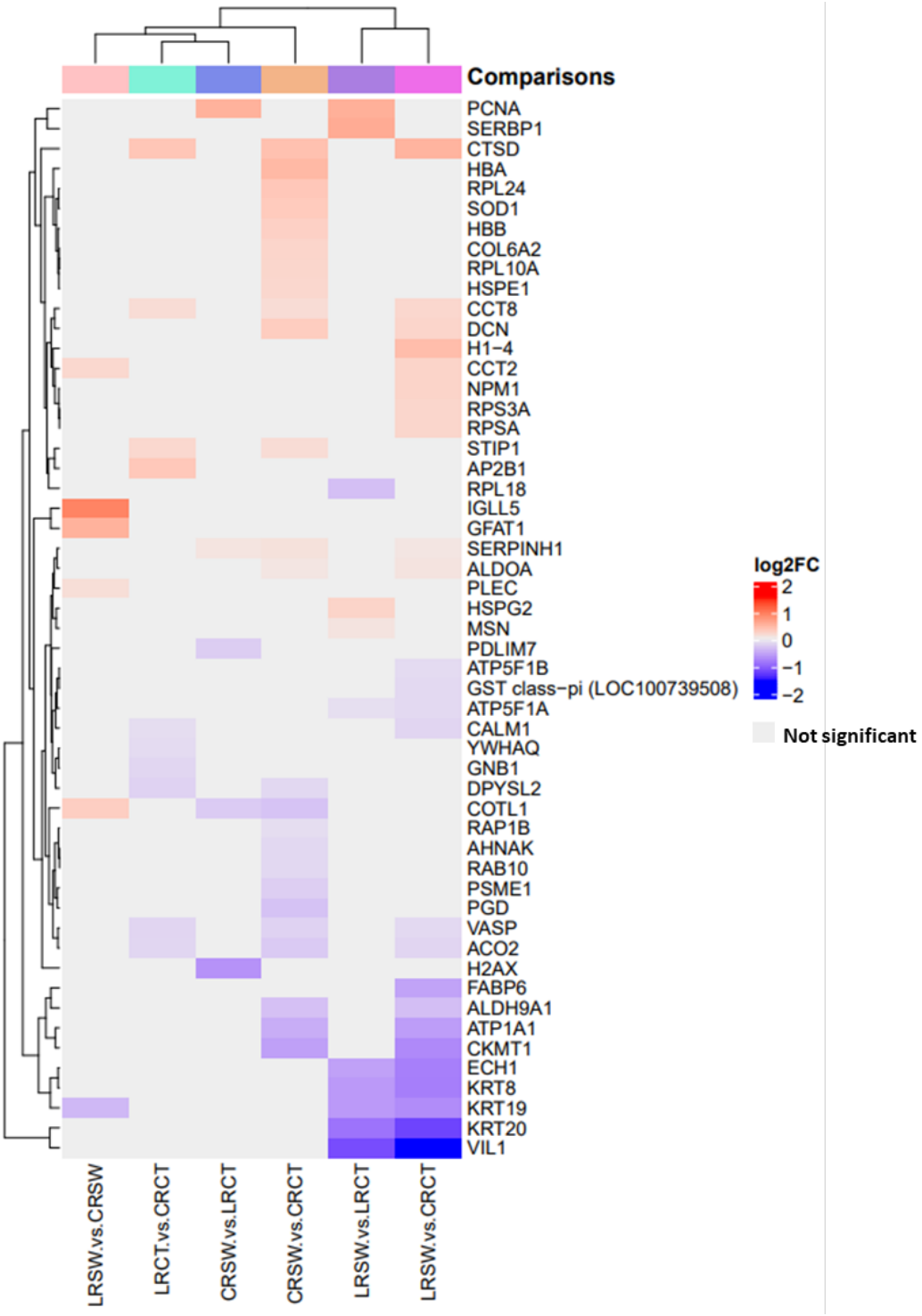

Figure 5-4 Heatmap of the significant differentially abundant proteins (DAPs) among four groups of piglet ileum containing CRCT: piglets fed no seaweed (SW, *Ascophyllum nodosum*), which nursed by sows fed dietary ω6:ω3 ratio = 13:1 during gestation, starting from day 28 (G28) and 10:1 during lactation. CRSW: piglets fed SW, which nursed by sows fed dietary ω6:ω3 ratio = 13:1 during gestation and 10:1 during lactation. LRCT: piglets fed no SW, which nursed by sows fed dietary ω6:ω3 ratio = 4:1 from G28 until the end of lactation. LRSW: piglets fed SW, which nursed by sows fed dietary ω6:ω3 ratio = 4:1 from G28 until the end of lactation.

The unique and shared DAPs in comparing LRCT, CRSW, and LRSW with CRCT groups are indicated in the Venn diagram (Figure 5-2B) and heatmap (Figure 5-4). As shown in these two figures, these three comparisons shared 4 similar DAPs (3 increased and one decreased). Groups SW (CRSW and LRSW) versus CRCT group revealed 6 DAPs (3 increased and 3 decreased). Groups LR (LRCT and LRSW) versus the CRCT group yielded only one decreased-abundant protein, calmodulin 1 - CALM1.

Furthermore, the LRSW group was compared to three remaining groups (CRCT, CRSW, and LRCT) using a Venn diagram (Figure 5-2C) and heatmap (Figure 5-4). These two figures display only one overlap DAP (keratin19 - KRT19), which was decreased among the three comparisons. The comparisons between the LRSW group versus CT groups (CRCT and LRCT) discovered 5 DAPs that were all decreased in abundances, such as ATP synthase subunit alpha (ATP5A1), keratin proteins (KRT8, KRT20), and villin-1 (VIL1). Comparing the LRSW group versus CR groups (CRCT and CRSW) revealed only one DAP (T-complex protein 1 subunit beta - CCT2), which was increased in abundance.

5.7.1.3 GO enrichment of all identified ileum proteins

The protein-protein interaction (PPI) enrichment analysis shows an association among 300 master proteins, with 288 nodes and 5696 edges (p < 1.0e-16). The functional enrichments emphasised 172, 54, and 60 GO terms on biological processes (BP), molecular function (MF), and cellular components (CC), respectively. The top three enriched GO-BP terms were symbiotic process [GO:0044403], cellular localization [GO:0051641], and translational initiation [GO:0006413]. The DAPs primarily participated in RNA binding [GO:0003723], structural molecule activity [GO:0005198], and protein binding [GO:0005515]. The DAPs mostly located in extracellular space [GO:0005615], vesicle [GO:0031982], and cytosol [GO:0005829]. The top 20, 10, and 5 GO terms on BP, MF, and CC, respectively, are presented in Figure 5-5.

All 300 ileum master proteins

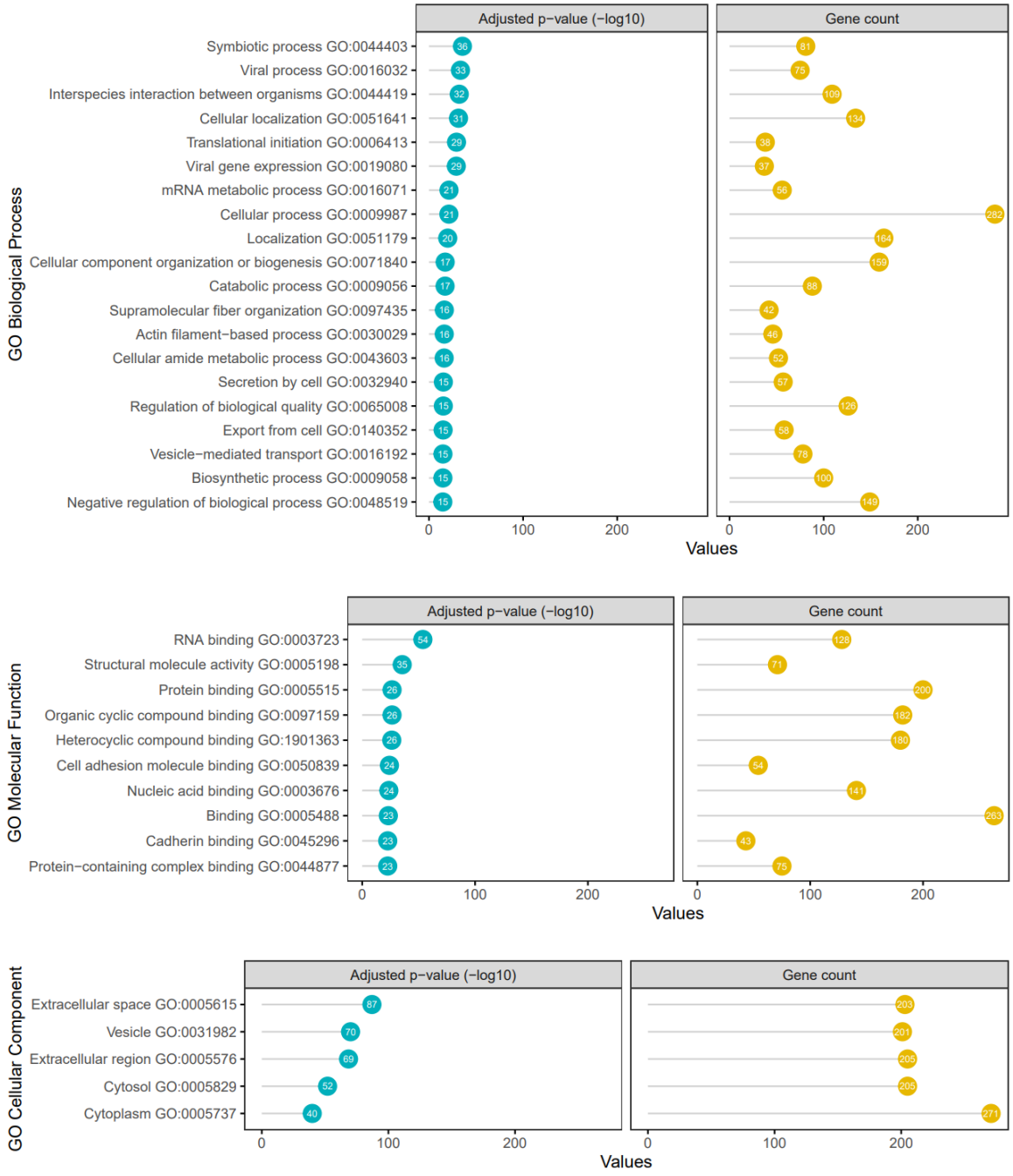

Figure 5-5 Gene ontology analysis of all 300 proteins kept in ileum proteomics study with their corresponding gene count inside each term and their associated adjusted p-value (expressed as -log10). Top 20, 10, and 5 GO terms on biological processes, molecular function, and cellular component, respectively, are illustrated.

5.7.1.4 GO and Reactome pathway enrichment in LR vs CR groups

The DAP PPI network enrichment between LR and CR ileum was not significant (p = 0.407). So, the network was expanded with a maximum of 5 interactors in the first shell, and the result showed 10 nodes and 21 edges (p = 0.0003). GO analysis highlighted top three enriched BP terms were translational initiation [GO:0006413], cytoplasmic translation [GO:0002181], and transport [GO:0006810]. The top three enriched Reactome pathways were peptide chain elongation [HSA-156902], SRP-dependent co-translational protein targeting to membrane [HSA-1799339], and selenocysteine synthesis [HSA-2408557]. Lists of enriched GO terms and Reactome pathways are presented in Figure 5-6 and Appendix Table S4.

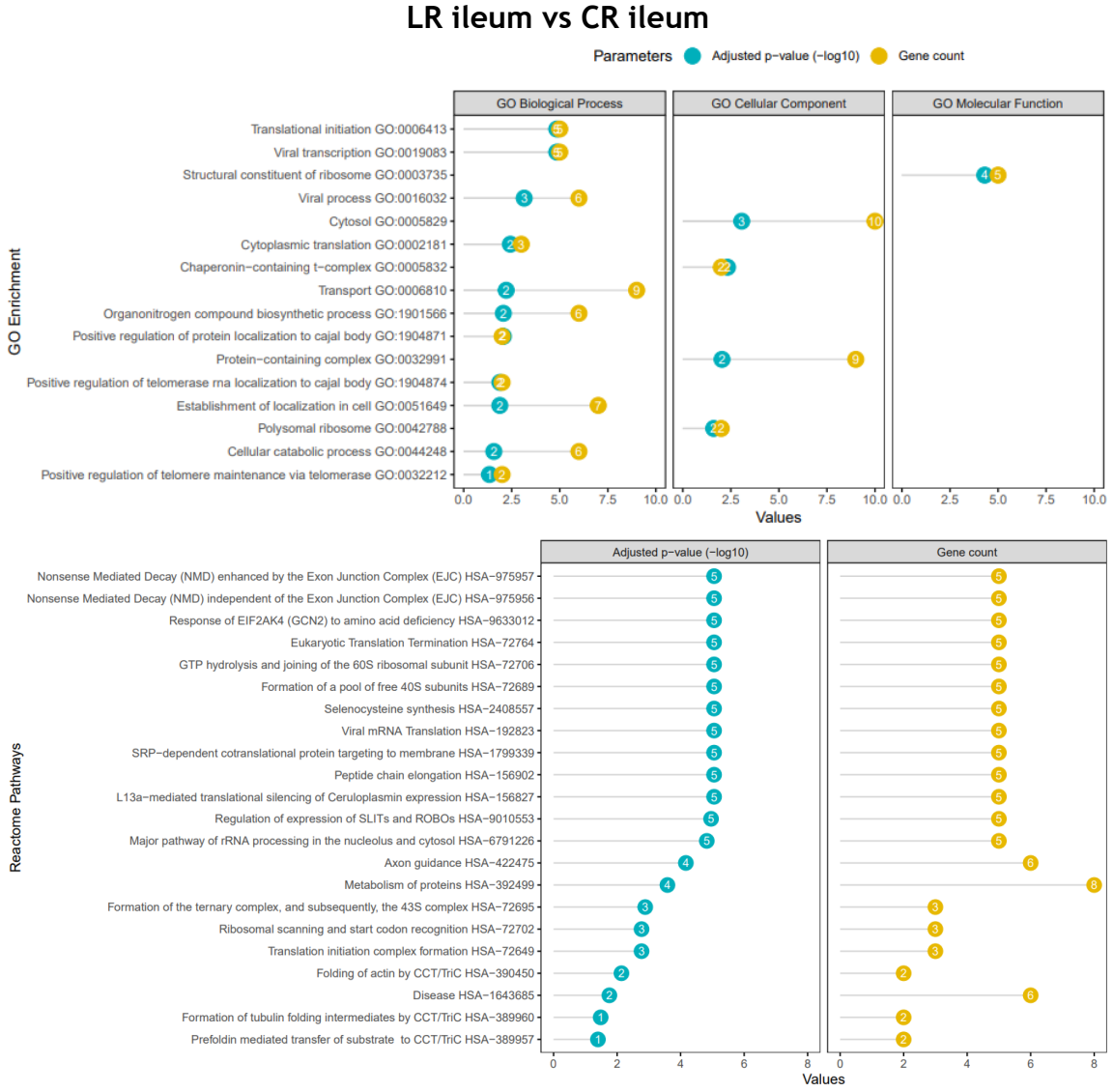

Figure 5-6 Gene ontology analysis of DAPs in comparison LR ileum versus CR ileum, with their corresponding gene count inside each term and their associated adjusted *p*-value (expressed as -log10). Interaction networks were created with maximum 5 interactors shown in the first shell. CR: piglet born from sow fed diet with ω6:ω3 ratio=13:1 during gestation, starting from day 28 (G28) and 10:1 during lactation; LR: piglet born from sow fed diet with ω6:ω3 ratio=4:1 from G28 until the end of lactation.

5.7.1.5 GO and Reactome pathway enrichment in SW vs CT groups

The PPI network between SW and CT ileum contains 19 nodes and 16 edges (p = 5.91e-05). Only three GO-CC terms were enriched containing extracellular space [GO:0005615], extracellular exosome [GO:0070062], and proton-transporting ATP synthase complex, catalytic core f(1) [GO:0045261]. The expanded network with maximum 5 interactors in the first shell shows 24 nodes and 31 edges (p = 0.0001). The DAPs were particularly involved in cristae formation [GO:0042407], biosynthetic process [GO:0009058], and proton transmembrane transport [GO:1902600]. The top three enriched Reactome pathways were the formation of ATP by chemiosmotic coupling [HSA-163210], cristae formation [HSA-8949613], and the citric acid (TCA) cycle and respiratory electron transport [HSA-1428517]. Lists of enriched GO terms and Reactome pathways are presented in Figure 5-7 and Appendix Table S5.

Additionally, a network among comparisons LR vs CR and SW vs CT provides an overview of the interaction between the DAPs and significantly enriched Reactome pathways (Figure 5-8). This network presents the up- and down-regulated proteins distinctively for each comparison and their association with related Reactome pathways such as metabolism [HSA-1430728], developmental biology [HSA-1266738], and peptide chain elongation [HSA-156902].

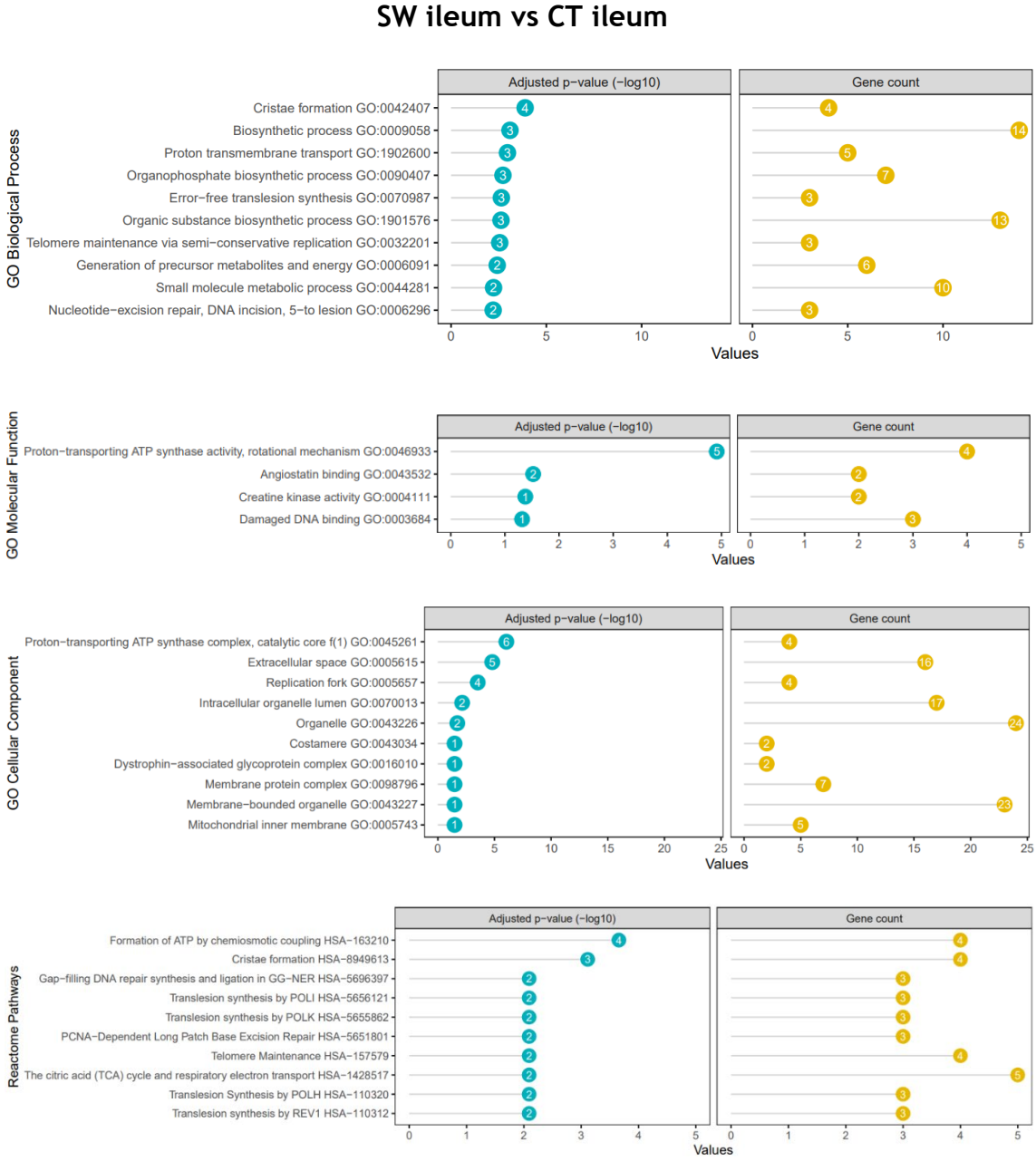

Figure 5-7 Gene ontology analysis of DAPs in comparison SW ileum versus CT ileum, with their corresponding gene count inside each term and their associated adjusted *p*-value (expressed as -log10). Top 10 GO terms on biological processes and cellular component; Reactome pathways; and 4 GO terms on molecular function are illustrated. SW: piglet diet with seaweed supplementation, CT: piglet diet without seaweed supplementation.

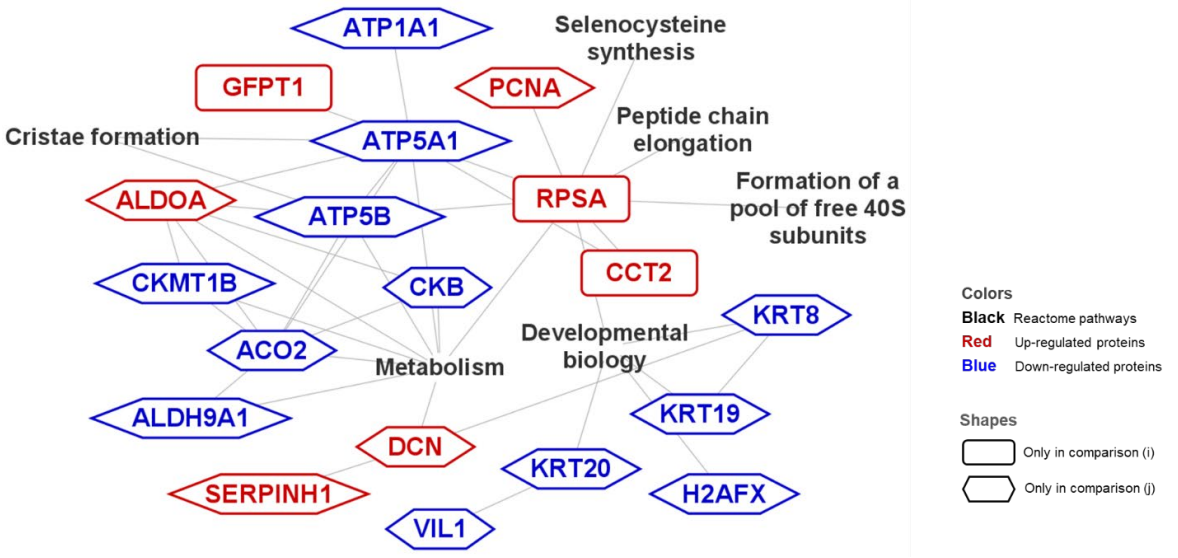

Figure 5-8 Network of the significant differentially abundant proteins (DAPs) between comparisons LR vs CR and SW vs CT with significantly enriched Reactome pathways. Interaction networks were created with maximum 5 interactors shown in the first shell. CR: piglet born from sow fed diet with ω6:ω3 ratio=13:1 during gestation, starting from day 28 (G28) and 10:1 during lactation; LR: piglet born from sow fed diet with ω6:ω3 ratio=4:1 from G28 until the end of lactation. SW: piglet diet with seaweed supplementation, CT: piglet diet without seaweed supplementation.

5.7.1.6 GO and Reactome pathway enrichment in LRCT, CRSW, and LRSW vs CRCT groups

The PPI network enrichment in LRCT - CRCT comparison was not significant (p = 0.221). Thus, maximum 5 interactors were added in the first shell of the network to have 17 nodes and 22 edges (p = 0.016). The DAPs were involved in 13 BP, particularly response to stimulus [GO:0050896], regulation of cellular component organization [GO:0051128], and protein folding [GO:0006457]. The functional enrichment analysis highlighted 51 Reactome pathways, particularly the metabolism of proteins [HSA-392499], integration of energy metabolism [HSA-163685], and transport of small molecules [HSA-382551]. A list of enriched GO terms and Reactome pathways are shown in Figure 5-9 and Appendix Table S6.

Comparing CRSW and CRCT ileum, the PPI network contains 26 nodes and 29 edges (p = 7.95e-08). GO analysis highlighted three enriched BP such as neutrophil degranulation [GO:0043312], regulated exocytosis [GO:0045055], and export from cell [GO:0140352]. Seven Reactome pathways were enriched, including immune system [HSA-168256], neutrophil degranulation [HSA-6798695], and metabolism of amino acids and derivatives [HSA-71291]. The expanded network with maximum 5 interactors in the first shell shows 31 nodes and 60 edges (p = 2.84e-11). In the

expanded network, 15 GO-BP terms were highlighted, particularly transport [GO:0006810], biosynthetic process [GO:0009058], and export from cell [GO:0140352]. Twenty-three Reactome pathways were enriched, particularly the metabolism of proteins [HSA-392499], metabolism of amino acids and derivatives [HAS-71291], and cellular responses to stress [HAS-2262752]. A list of enriched GO terms and Reactome pathways are shown in Figure 5-10 and Appendix Table S7.

The PPI network in LRSW versus CRCT contains 24 nodes and 27 edges (p = 1.29e-05). Three significant enriched GO-BP terms were supramolecular fiber organization [GO:0097435], the establishment of localization in cell [GO:0051649], and ATP biosynthetic process [GO:0006754]. The expanded network with maximum 5 interactors in the first shell shows 29 nodes and 51 edges (p = 1.07e-07). The top three enriched GO-BP terms were organonitrogen compound biosynthetic process [GO:1901566], transport [GO:0006810], and nuclear-transcribed mRNA catabolic process, nonsense-mediated decay [GO:0000184]. The top three enriched Reactome pathways were metabolism [HSA-1430728], formation of ATP by chemiosmotic coupling [HSA-163210], and peptide chain elongation [HSA-156902]. A list of enriched GO terms and Reactome pathways are shown in Figure 5-11 and Appendix Table S8.

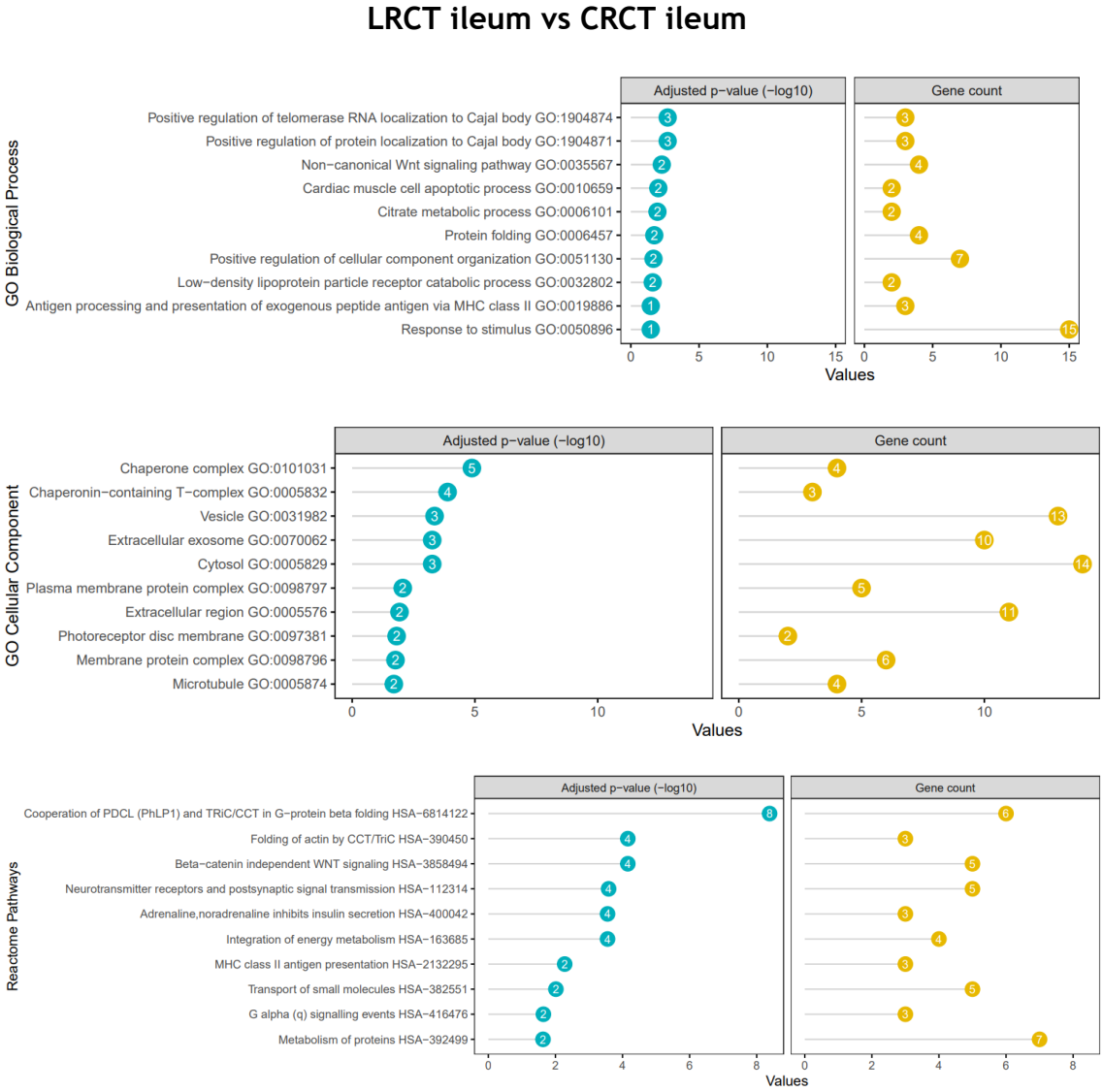

Figure 5-9 Gene ontology analysis of DAPs in comparison between LRCT and CRCT ileum, with their corresponding gene count inside each term and their associated adjusted p-value (expressed as -log10). Top 10 GO terms on biological processes, cellular component, and Reactome pathways are illustrated. CRCT: piglets fed no seaweed (SW, *Ascophyllum nodosum*), which nursed by sows fed dietary ω6:ω3 ratio = 13:1 during gestation, starting from day 28 (G28) and 10:1 during lactation. LRCT: piglets fed no seaweed, which nursed by sows fed dietary ω6:ω3 ratio = 4:1 from G28 until the end of lactation.

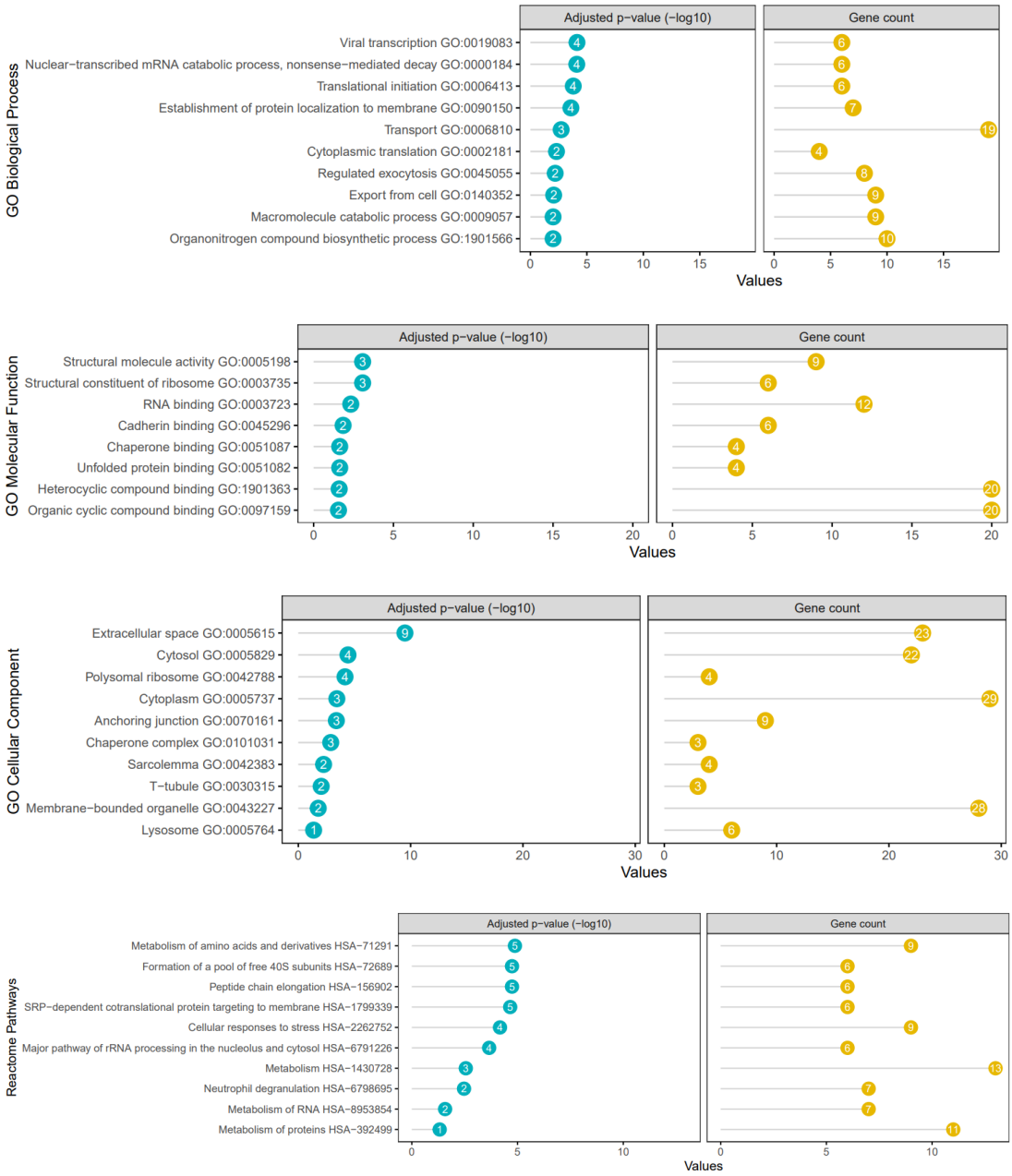

Figure 5-10 Gene ontology analysis of DAPs in comparison between CRSW and CRCT ileum, with their corresponding gene count inside each term and their associated adjusted *p*-value (expressed as -log10). Top 10 GO terms on biological processes and cellular component; Reactome pathways; and 8 GO terms on molecular function are illustrated. CRCT: piglets fed no seaweed (SW, *Ascophyllum nodosum*), which nursed by sows fed dietary ω6:ω3 ratio = 13:1 during gestation, starting from day 28 (G28) and 10:1 during lactation. CRSW: piglets fed SW, which nursed by sows fed dietary ω6:ω3 ratio = 13:1 from G28 until the end of lactation.

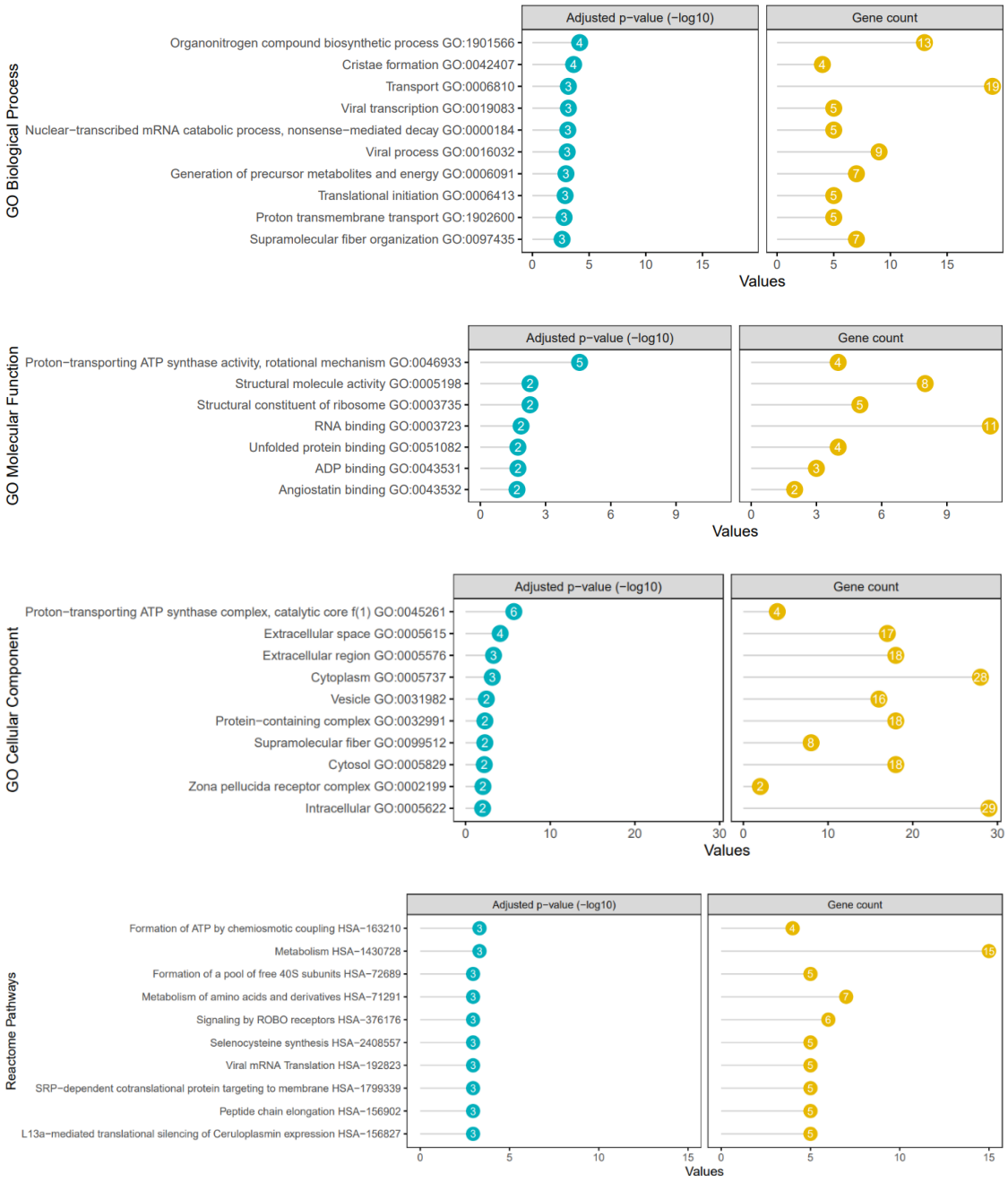

Figure 5-11 Gene ontology analysis of DAPs in comparison between LRSW and CRCT ileum, with their corresponding gene count inside each term and their associated adjusted *p*-value (expressed as -log10). Top 10 GO terms on biological processes and cellular component; Reactome pathways; and 7 GO terms on molecular function are illustrated. CRCT: piglets fed no seaweed (SW, *Ascophyllum nodosum*), which nursed by sows fed dietary ω6:ω3 ratio = 13:1 during gestation, starting from day 28 (G28) and 10:1 during lactation. LRSW: piglets fed SW, which nursed by sows fed dietary ω6:ω3 ratio = 4:1 from G28 until the end of lactation.

5.7.2 Validation of proteomics results

Results of validation assays for villin (VIL1) and proliferating cell nuclear antigen (PCNA) are visualized in Figure 5-12 and shown in Table 5-3.

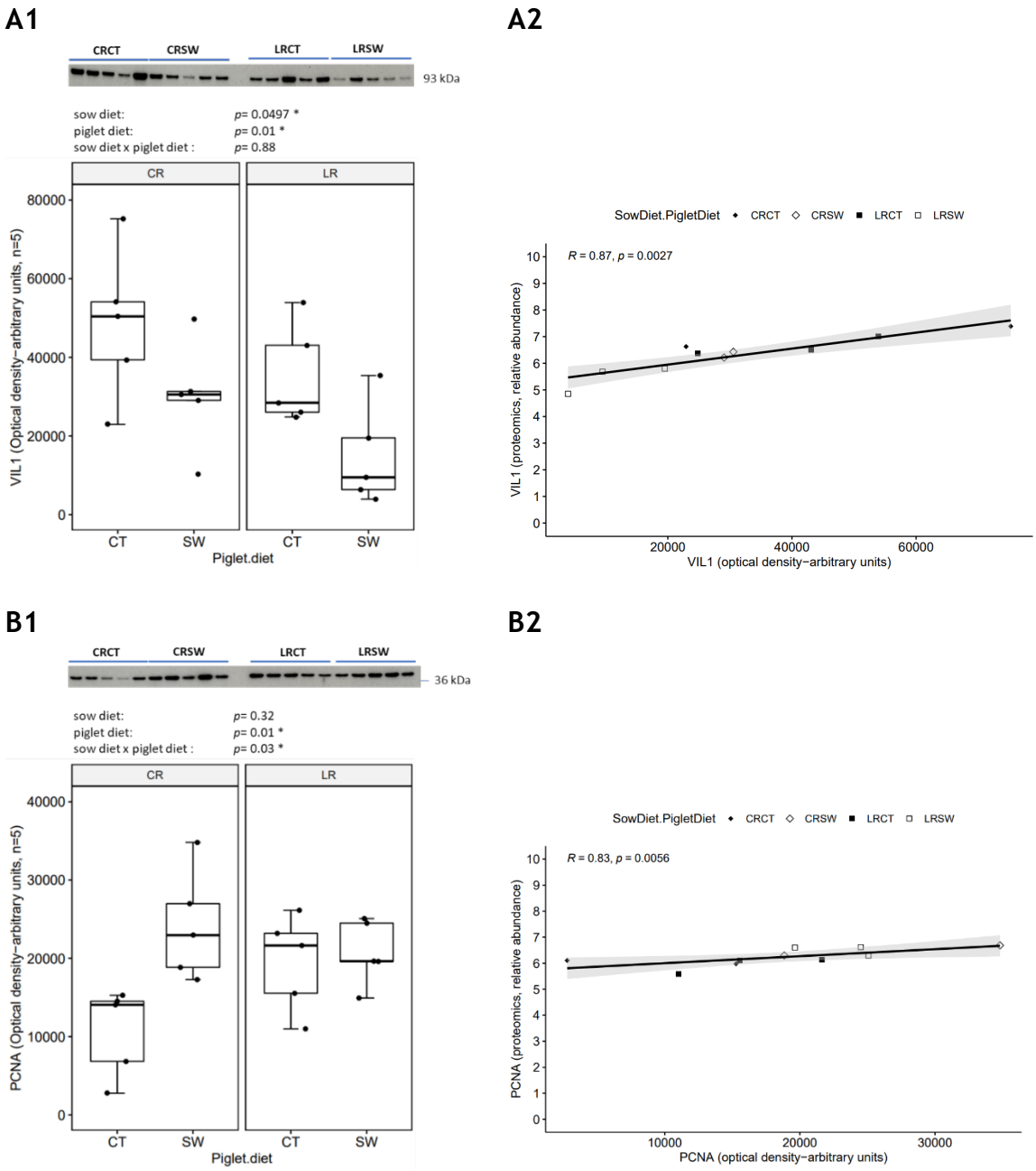

Figure 5-12 Boxplots of validation assays for the concentrations of villin (VIL1) and proliferating cell nuclear antigen (PCNA) in ileum samples are presented with their correlation with respective protein abundance quantified by proteomics. CRCT: piglets fed no seaweed (SW, *Ascophyllum nodosum*), which nursed by sows fed dietary ω6:ω3 ratio = 13:1 during gestation, starting from day 28 (G28) and 10:1 during lactation. CRSW: piglets fed SW, which nursed by sows fed dietary ω6:ω3 ratio = 13:1 during gestation and 10:1 during lactation. LRCT: piglets fed no SW, which nursed by sows fed dietary ω6:ω3 ratio = 4:1 from G28 until the end of lactation. LRSW: piglets fed SW, which nursed by sows fed dietary ω6:ω3 ratio = 4:1 from G28 until the end of lactation.

Table 5-3 Results of validation assays for the concentrations of villin (VIL1) and proliferating cell nuclear antigen (PCNA) in ileum samples are presented. Their respective protein abundance values are not shown because of low abundance values were determined by proteomics. Difference between groups was analysed separately for each tested protein and validation method.

Sow diet (S)	Piglet diet (P)	VIL1	PCNA
		Western blot assay (optical density – arbitrary units)	
CR	**CT**	48415^{b}	10693^{a}
	SW	30176^{ab}	24178^{b}
LR	**CT**	35266^{ab}	19504^{ab}
	SW	14932^{a}	20750^{b}
SEM		6687	2604
P-value			
S		0.0497 *	ns
P		0.011 *	0.012 *
S*P		ns	0.032 *
CR CT - LR CT		ns	0.059
CR CT - CR SW		ns	0.012 *
CR CT - LR SW		0.016 *	0.044 *
LR CT - CR SW		ns	ns
LR CT - LR SW		ns	ns
CR SW - LR SW		ns	ns

CRCT: piglets fed no seaweed (SW, *Ascophyllum nodosum*), which nursed by sows fed dietary ω6:ω3 ratio = 13:1 during gestation, starting from day 28 (G28) and 10:1 during lactation. CRSW: piglets fed SW, which nursed by sows fed dietary ω6:ω3 ratio = 13:1 during gestation and 10:1 during lactation. LRCT: piglets fed no SW, which nursed by sows fed dietary ω6:ω3 ratio = 4:1 from G28 until the end of lactation. LRSW: piglets fed SW, which nursed by sows fed dietary ω6:ω3 ratio = 4:1 from G28 until the end of lactation.

5.7.2.1 Villin (VIL1)

Western blot images for VIL1 in ileum samples from four groups of piglets are presented in Figure 5-12 and Table 5-3. Clear bands at 93 kDa showing the presence of VIL1 were detected in all samples. VIL1 band intensity in LR ileum was lower than in CR ileum (Figure 5-12A1, p = 0.0497), and VIL1 band intensity in SW ileum was lower than CT ileum (Figure 5-12A1, p = 0.01). A significantly lower concentration of VIL1 was determined in LRSW compared to CRCT ileum (Table 5-3, p = 0.016). However, there was no interaction between the sow diet and the piglet diet. A strong positive linear correlation between validated VIL1 concentration and VIL1 relative abundance (Figure 5-12A2, R = 0.87, p = 0.0027) suggests an accurate reflection of VIL1 proteomics data level present in four piglet groups.

5.7.2.2 Proliferating cell nuclear antigen (PCNA)

Western blot analysis for PCNA is shown in Figure 5-12 and Table 5-3. Clear bands at 36 kDa representing the presence of PCNA were detected in all samples. PCNA band intensity in SW ileum was higher than CT ileum (Figure 5-12B1, $p = 0.01$), and this trend was shown in CRSW and CRCT groups (Table 5-3, $p = 0.012$). There was a significant interaction between the sow diet and the piglet diet (Figure 5-12B1, $p = 0.03$): a significantly higher concentration of PCNA was determined in LRSW than the CRCT ileum (Table 5-3, $p = 0.044$). The effect of the sow diet on the concentration of PCNA was not significant. The overall evaluation highlighted a strong positive linear correlation between the validated PCNA concentration and PCNA proteomics relative abundance (Figure 5-12B2, $R = 0.83$, $p = 0.0056$).

5.8 DISCUSSION

Intestinal protective barrier and nutrient uptake are greatly affected by the continuous renewal of epithelial cells and crypt-villus structure [346]. Weaning induced significant alterations in intestinal structure and function [347] and hampered the immature mucosal immune system [334]. Factors such as maternal and offspring dietary management could drive mucosal immune development and progeny performance [262–264]. By investigating the combined effects of dietary treatments in sows and their offspring on offspring's development, this study aimed to stimulate a rapid maturation of the piglet intestine and immune system to resist weaning challenges. DAPs with modest differences (non-adjusted p-value < 0.05) were regarded as relevant because they are likely to give valid biological changes via validation assays on several proteins, as presented later.

5.8.1 Effect of sow dietary treatments: LR vs CR groups

The maternal LR diet affected the relative abundance of GFPT1, CCT2, PDLIM7, RPSA, and CALM1. Proteins RPSA, CCT2, and GFPT1 were annotated by Reactome pathways referred to peptide chain elongation, selenocysteine synthesis, and metabolism of proteins.

Ribosomes are the cellular machines where the message in mRNA is translated to proteins (also known as protein synthesis) [348]; thus, ribosomes contribute

considerably to the host response to infection [349]. The protein production starts with the translation initiation step to regulate mRNA translation, followed by the elongation step to add a newly translated amino acid to the protein chain, concluding with a stop codon [349]. Each ribosome in humans contains a small (40S) and large (60S) subunit [350]. The 40S ribosomal protein SA (RPSA) can contribute to the initiation step of mRNA translation and trans-translation events [351]. It also participates in the maturation of the 18S rRNA element of the 40S ribosomal subunit [352]. The increased abundance of protein RPSA in LR versus CR ileum in this study may relate to the positive regulation of protein synthesis process [348], thereby contributing to immune response activation [349].

Chaperonin-containing T-complex protein 1 (CCT) is a macromolecular protein folding complex that consists of eight subunit proteins (CCT1-8) [353] relating to cell cycling dysregulation and leading to uncontrolled proliferation [354]. The subunit beta (CCT2) may drive cell division and attract proliferative factors in humans, affecting crucial survival and growth components [354]. CCT2 can regulate cell proliferation; thus, the upregulation of CCT2 in LR versus CR ileum in this study can induce uncontrolled proliferation and is associated with the overexpression of cell cycle regulators [354].

Glutamine-fructose-6-phosphate transaminase (GFPT1) is an important enzyme that participates in protein glycosylation (glycans biosynthesis) which could enhance the solubility and stability of newly formed peptides [355]. The glycosylation is a crucial cellular post-translational modification where glycosyl residue is transferred from a donor comprising a nucleoside phosphate to an acceptor molecule by glycosyltransferases [356]. The glycosylation process contributes to inflammation states, so GFPT1 protein plays a role in the host response to inflammation [356]. In this study, the changes in GFPT1 protein and, in turn, glycosylation process in LR versus CR ileum may relate to inflammatory conditions [356].

Taken together, the increased expression of RPSA, CCT2, and GFPT1 in LR ileum relate to the host response to inflammatory stimuli and thus, affect piglet' growth performance, as observed in the in vivo study [183].

5.8.2 Effect of piglet dietary treatments: SW vs CT groups

In the SW piglets, 11 proteins (i.e., ACO2, ATP5B, ATP5A1, DCN, CKB, CKMT1B, ALDH9A1, PSME1, ALDOA, PCNA) were annotated by Reactome pathways mostly referred to metabolism, the citric acid (TCA) cycle, and respiratory electron transport, synthesis of DNA, protein localization, mitochondrial protein import, and creatine metabolism.

ATP synthase subunit alpha and beta (ATP5A1 and ATP5B, respectively) were down-regulated in SW ileum. They are two subunits of mitochondrial ATP synthase involved in regulating mitochondrial complexes and ATP synthesis [357]. The mitochondrial ATP synthase can function as a regulator of inflammatory responses expressed through changes in ATP concentrations [358]. Diminishing ATP synthesis by disrupting or inhibiting ATP synthase activity targets cancer treatment [358]. The reduced ATP subunits reflect the cellular response toward anti-inflammation [358] and are related to this study's SW supplementation in piglet diet.

The SW supplementation decreased creatine kinase activity, an indicator of tissue injury [359], in piglets ileum at d21 PW. A lower serum creatine kinase activity was also reported in male mice who received curcumin – a yellow pigment of turmeric in the diet [359]. A similar effect of seaweed and curcumin was possibly due to their natural antioxidant property against cellular oxidative damage [360]. This observation suggests the modulatory impact of SW supplementation in the post-weaning diet on creatine kinase activity in piglet ileum. Recent studies on juvenile rainbow trout [361] and juvenile carp [362] described that the decrease in muscle creatine and ATP concentrations might be responsible for the decreased myogenesis and growth performance. Although the concentration of muscle creatine in fish is higher than that in mammals due to different locomotor activity [363], these findings are still helpful references to explain the similar pattern in mammals. Collectively, the decreased expression of ATP synthase subunits and creatine kinase in SW-fed piglets born from LR-fed mothers may be associated with the decline in myogenesis and, consequently, growth rate as reported in the in vivo study [183].

Proliferating cell nuclear antigen (PCNA), a marker of cell proliferation [364], was upregulated in SW versus CT ileum (specifically, in CRSW and LRSW versus LRCT) in this study. The PCNA is an auxiliary protein of DNA polymerise-δ that participates in DNA synthesis, replication, and repair; cell proliferation, and cell cycle initiation [365,366]. The concentration of PCNA is decreased in the inactive cells; however, it increases before DNA replication [366]. PCNA is increased through phosphorylation during the cell cycle, so DNA replication and cellular proliferation are stimulated [364]. The increased expression of PCNA in the SW group could result from the increased proliferation behavior of cells [364], DNA synthesis, and repair associated with the SW diet.

Ileal epithelial keratin (KRT8, 19, and 20) and villin-1 (VIL1) were not involved in any Reactome pathways, but are the most significant down-regulated proteins, thus, relevant to mention the abundance pattern and possible biological meanings of these proteins as follows.

Keratin type II cytoskeletal 8 (KRT8, acidic keratin) and type I cytoskeletal 19 and 20 (KRT19 and 20, basic keratin) [367] were decreased expressions in SW piglets. Keratins are intermediate filament proteins expressed in epithelia of the gastrointestinal tract in mammals [368] that support the structure of cell and tissue homeostasis [369]. Keratins also contribute to the host protection against stress/inflammation [370,371] through maintaining epithelial barrier functions [372]. A review from Polari et al. [369] found that keratins alteration in expression level might contribute to the differentiation-proliferation balance of the epithelial cell. Protein K8 and K19 are the primary keratins in small and large intestines [369]. Furthermore, keratins are involved in many post-translational modifications (PTMs), so increased keratin expression was associated with cancer development where PTMs are dysregulated [371]. The decreased level of K8, K19, and K20 in SW ileum may relate to their role in epithelial cell metabolism [370] and the possible effect of SW on lowering the inflammation severity in post-weaning piglets.

Villin-1 (VIL1), an indicator of absorptive cells in the brush border [373], was decreased expressions in SW piglets (specifically, in LRSW versus CRCT and LRCT). The tendency of a down-regulation in villin mRNA expression was observed in the

jejunal tissue of neonatal piglets on d7 versus d0, reflecting declined jejunal villus height of 7-d-old piglets [374]. This is one of the indicators of the fast intestinal development in suckling pigs, together with the increased villus width and number of crypts [374]. As located in the epithelial brush border, villin functions as a crucial regulator of epithelial structure and microvilli physiological functions [375]. Alteration of villin concentration may induce the remodelling of intestinal epithelial cells structure, and consequently, alter brush border integrity [375]. Microvilli development could enlarge the intestinal epithelial cells' contact area, absorption, and secretory surface [375].

The agreement between Western blot validation results and relative protein abundance measured by proteomics (Figure 5-12, $R \geq 0.83$, $p < 0.01$) for both VIL1 and PCNA shows that despite the adjusted *p*-value giving no significant results, the non-adjusted p-values are likely giving valid biological changes. Validation on VIL1 and PCNA identified by two peptides and relatively low in abundance confirm crucial biologically relevant aspects disclosed by the TMT quantitative proteomics data [79]. This approach increases the confidence level in protein identification [79].

Collectively, the upregulation of PCNA and downregulation of VIL1 in SW piglets observed in this study suggests that SW supplementation stimulates the rapid renewal of the ileal epithelium by promoting cell proliferation but diminishes the absorption capacity of ileal epithelial cells at the same time.

5.8.3 Combined effects of sow and piglet dietary treatments: LRCT, CRSW, and LRSW vs CRCT groups

In the comparisons among 4 groups containing CRCT, CRSW, LRCT, and LRSW, a series of 6 pairwise comparisons revealed 53 DAPs, of which the majority of DAPs was in CRSW vs CRCT and LRSW vs CRCT (25 DAPs), followed by LRSW vs LRCT and LRCT vs CRCT (11 and 10 DAPs, respectively), and the lowest DAPs was in LRSW vs CRSW and CRSW vs LRCT (6 and 5 DAPs, respectively). This discussion focuses on the distinct DAPs and associated Reactome pathways in three main comparisons: LRCT, CRSW, and LRSW vs CRCT groups with their expanded networks (maximum 5 interactors in the first shell).

Among three comparisons, LRCT vs CRCT affected the interaction between AP2B1 and GNB1 in multiple pathways, especially neurotransmitter receptors and postsynaptic signal transmission and transport of small molecules. The beta subunit of Adaptin protein (AP)-2 complex (AP2B1) was up-regulated in LRCT vs CRCT ileum in this study and also in the muscle of gilts in another study where found AP2B1 joined in lipid metabolism [376]. AP2B1 was involved in the immune response to stimuli in cattle [377]. In line with this study, Shin et al. [378] reported the role of AP2B1 in the synaptic vesical cycle and neural functions. The upregulation of AP2B1 is a defence mechanism against stimuli such as heavy metals [379]. In contrast with AP2B1, G protein subunit beta 1 (GNB1) was downregulated in LRCT vs CRCT, which engaged in regulating transmembrane signal transduction [380–382], cellular response to hypoxia [381], and boosting virus budding at the cell membrane to stimulate progeny virus release [383]. The LRCT diet was associated with enriched regulation of signal transmission between neurons in the brain and contributed to the immune response against stimuli.

Comparison CRSW-CRCT affected the relative abundance of 13 proteins such as COTL1, HBB, RAB10, RAP1B, RPL10A, RPL24, SOD1, PGD, and PSME1. These proteins were annotated by Reactome pathways referred to the metabolism of proteins, RNA, and amino acids and derivatives, neutrophil degranulation, and cellular responses to stress. Oxygen binding and transport proteins, hemoglobin (subunit A – HBA and subunit B – HBB) was increased-abundant in CRSW than CRCT. It is supposed that this may contribute to the enhancement in the CRSW's oxygen storage and transfer capacity [384,385], thus, improving oxygen supply to ileal tissue against stressors such as weaning- or transport-related hypoxia [386] and consequently, enhancing CRSW's intestinal health. Ribosomal proteins such as RPL10A and RPL24 were overabundant in CRSW piglets, promoting protein synthesis and driving the regeneration of ileal tissue [387]. In addition, a negative regulator of the cell cycle/adhesion and mediator of protein degradation, proteasome activator complex subunit 1 (PSME1) [388,389], was downregulated in CRSW ileum. A protein that regulates actin cytoskeleton activity, coactosin-like protein 1 (COLT1) [390] can promote lamellipodia protrusion in motile cells such as endothelial, immune, and epithelial cells [391]. Both PSME1 and COTL1 were upregulated in inflammatory-, tumour- or cancer-associated events [389,392–396]. Referring to the benefits of CRSW diet on improving piglet growth

performance as reported in the previous study [183], the downregulation of PSME1 and COTL1 in CRSW ileum had no harmful effects or their effects were masked from the positive effects of hemoglobin and ribosomal proteins.

In the LRSW vs CRCT piglets, 14 proteins (including ATP5A1, ATP5B, CCT2, ECH1, FABP6, KRT8, KRT19, KRT20, RPSA, and RPS3A) were annotated by Reactome pathways mostly referred to metabolism, organelle biogenesis and maintenance, developmental Biology, and protein localization. An enzyme that participates in mitochondrial fatty acid ß-oxidation, Enoyl coenzyme A hydratase 1 (ECH1) [397] was downregulated in LRSW. This finding is supported by a previous study that reported the underlying beneficial effects of dietary ω3 PUFA supplementation in the insulin signalling improvement process via down-regulating ECH1 and inhibiting peroxisomal ß-oxidation [398]. LRSW piglets had downregulation of Fatty acid-binding protein 6 (FABP6) - an ileum-specific bile acid transporter, implicating a reduction in efficiency of dietary fat absorption [399,400] due to impaired bile acid production/absorption in ileum as a consequence of early inflammatory reaction [401,402]. A cell cycle-associated protein that organizes chromatin structure and regulates gene transcription via chromatin remodelling, Histone protein - HIST1H1E [403,404], although was not involved in any pathways, is still worth mentioning because its upregulation in LRSW piglets may reflect an increased formation of chromatin fiber [405], facilitating DNA replication, DNA repair, and genome stability [404]. Together these observations suggest that the decreased fat absorption capacity may be associated with unexpected growth development of LRSW piglets as observed in the previous study [183], although they may have insulin signalling improvement and genome stability.

5.9 CONCLUSIONS

This study showed that maternal dietary low ω6:ω3 ratio (LR) exerted its positive regulation of protein synthesis process and contributed to enhanced intestinal function via modulating ileal proteome in piglets. However, maternal LR diet may induce uncontrolled proliferation and overexpression of cell cycle regulators in the offspring, which may be responsible for the lower growth performance of piglets, as shown in the *in vivo* experiment of this study. Seaweed (SW) supplementation can reduce inflammation severity and stimulate the rapid

renewal of the ileal epithelium and ileal tissue development in CRSW piglets but diminish the fat absorption capacity of epithelial cells in LRSW piglets. Overall, lowering dietary ω6:ω3 ratio (to 4:1) in sows and SW supplementation in weaned piglet's diet benefitted piglet's intestinal development and anti-inflammation activity against weaning challenges.

Chapter 6 General Discussion & Conclusions

6.1 MAIN MESSAGES

1. Zootechnical performance: Maternal LR diet during gestation and lactation combined with the SW supplementation in post-weaned piglets did not enhance piglet's growth or antioxidant status. Nevertheless, the maternal LR diet alone increased total ω3 PUFAs (mainly α-linolenic acid - ALA) in the colostrum and milk, improving the weaning survival rate and suckling piglets' weight gain. Additionally, SW supplementation enhanced piglets' growth from sows fed CR diet.

2. Sow plasma proteomics: LR diet altered the plasma levels of several acute phase proteins (APPs) such as HP, SERPINA1, and APCS that might be involved in protective mechanisms against accelerated stresses and, in particular, oxidative stress at later stages of gestation and lactation. Furthermore, significant shifts were found over the late gestation-late lactation period affecting the plasma lipoproteins and the APPs. The end of pregnancy is associated with an acute phase reaction (APR) demonstrated by the increased abundance of positive APPs (i.e., HP and ITIH4 (pig-MAP)) and a decrease in negative APPs, i.e., APOA1, while by the end of lactation, this APR has dissipated and APOA1, APOA2, and APOC3 were all increased.

3. Piglet serum proteomics: maternal LR diet enhanced piglet host protective response via positive effects on anti-inflammatory activities and innate immunity. Post-weaned piglets' SW diet stimulated coagulation cascade regulation and the connection between innate and adaptive immunity to enhance the host defence during inflammation conditions. The altered serum proteome profile between d21 PW and weaning related to platelet metabolism, haemostasis, cross-talk between coagulation pathways and inflammation, particularly in the innate immune system.

4. Piglet ileum proteomics: maternal LR diet positively regulated protein synthesis process but may induce uncontrolled proliferation and overexpression of cell cycle regulators in the offspring. SW supplementation reduced the inflammation severity in post-weaning piglets and promoted ileal epithelial growth in CRSW piglets but decreased the fat absorptive capacity in LRSW piglets. Overall, maternal LR diet and offspring SW diet

benefitted piglet's intestinal development and anti-inflammation activity against weaning challenges.

The ω3 PUFAs are characterized as micronutrients and are usually deficient in animal diets. Frequently excessive animal consumption of ω6 PUFAs from corn and other grains compared to ω3 PUFAs (or high dietary ω6:ω3 ratio) leads to various performance and health problems in animals and also affect human health – the primary consumers of animal products. In recent years, lowering the ratio between ω6 and ω3 PUFAs in animal diets has gained increasing attention as a nutritional intervention to enhance performance and health.

This thesis aimed to improve growth performance and immune system in weaned pigs through early nutritional programs (maternal LR diet during gestation and lactation) combined with later-life nutritional interventions (post-weaned SW diet). Effects LR in sow diet and SW supplementation in piglet diet on performance, colostrum and milk FA profiles, and oxidative status, were studied *in vivo* (Chapter 2). The performance and zootechnical data showed the effects of maternal LR diet during gestation and lactation alone or in combination with the SW supplementation in post-weaned piglets on piglet growth and antioxidant status. Also, the influence of SW supplementation alone on piglet growth was revealed. To discover the fundamental molecular processes that activate biological systems such as reproduction and oxidative status, influenced by gestational and lactational LR diet, sow plasma proteomic pattern changes and related biological pathways associated with LR diet were characterized (Chapter 3). Moreover, the alterations in the serum and ileal proteomes and related pathways induced by the interplay between maternal LR diet and offspring SW diet were studied (Chapters 4 and 5).

This final Chapter discusses the findings of the studies described in this thesis. Additionally, implications of the results for future feeding regimes practices are addressed.

6.2 OMEGA 6 : OMEGA3 RATIOS IN SWINE NUTRITION AND ZOOTECHNICAL PERFORMANCE

6.2.1 ALA and the conversion to EPA and DHA in sow milk

This study used soybean oil and linseed oil as the source of ω6 and ω3. These contain large amounts of linoleic acid (LA, 18:2ω-6) and α-linolenic acid (ALA, 18:3ω-3), respectively. ALA is stored in adipose tissue and primarily serves as a substrate for synthesizing long-chain omega-3 PUFAs eicosapentaenoic acid (EPA, 20:5ω-3), especially in females during pregnancy and lactation and in newborns [406]. A more balanced ω6:ω3 ratio (decreased LA and increased ALA intake) will ensure the ALA – EPA conversion [148,151]. Nevertheless, the conversion efficiency from ALA to EPA is poor (i.e., 0.2 - 5%) and even poorer from ALA to docosahexaenoic acid (DHA, 22:6ω-3) (i.e., 0.05 - 0.5%) [148,149], primarily due to the low bioavailability of ALA after a high proportion of ALA (59%) is ß-oxidised in the mitochondria [150]. Furthermore, the lack of elongase-2 (ELOVL2) expression to elongate C22:5 ω3 to C24:5 ω3 [37], supports the EPA's synthesis. Also, the competition between LA and ALA for enzyme Δ-6 desaturase, which has a higher affinity for ALA; thus, high LA intake prevents the conversion from ALA to EPA [148,151]. Chapter 1 showed that the increased intake of ALA resulted in high concentrations of ALA and, consequently, EPA but not DHA in the sow milk. This observation accords with a review in human studies by Baker et al. [406]. Overall, our results demonstrate that the enriched ω3 diet by adding linseed oil effectively improves the EPA but has little effect on DHA concentrations in sow milk.

6.2.2 Sow's reproductive performance

Maternal LR diet enhanced weaning survival rate and sucking piglet's weight gain compared with CR diet (Chapter 2). The enrichment of total ω3 PUFAs in the colostrum and milk in LR-fed sow could positively modulate the intestinal microflora, thus promoting the intestinal health in suckling piglets by inhibiting Toll-like receptor 4 (TLR4) and signalling to decrease inflammation [137]. These findings match those observed in previous studies indicating the association between low ω6:ω3 ratio in the maternal diet with piglet growth improvement [94,95,104]. Although LR sows had fewer piglets born alive than CR sows, their

performance was in line with earlier data in sows that received low ω6:ω3 ratios (from 1:1 to 5:1) [138]. The unexpected result of decreased piglets born alive in the LR-fed sow could be explained by some unaccounted factors such as a low heritability of this trait (0.04 - 0.29) [140,141], although the two sow groups were kept in identical housing environments monitoring for the same light and temperature during the feeding trial.

6.2.3 Piglet's growth performance

The study described in Chapter 1 was the first one that accounted for a possible combined positive effect of maternal LR diet and post-weaned SW (*A. nodosum*) diet on piglet growth and oxidative status. Results disclosed that BW, ADG, ADFI, and G:F improved in SW-fed piglets born from CR-fed sows compared with CT-fed piglets. The supplementation of SW can add more ω3 PUFAs and lower ω6:ω3 ratios in SW-fed piglets that born from CR-fed sows due to its high contents of EPA (C20:5 ω3) and low ω6:ω3 ratio of 2.75 [142]. Nevertheless, LR and SW diets' combined effect is still unclear. These observations seem to be consistent with other research, which found no or minimal effect of a meagre ratio of ω6:ω3 (0.38) [143] or *A. nodosum* extract [125,255] on growth performance of growing-finishing pigs. The main effects of a low ratio between ω6 and ω3 were improved total ω3 PUFAs (including ALA, EPA, and DHA) and reduced ω6:ω3 ratio in pork [143].

6.2.4 Oxidative status in sows and piglets

Pregnancy, parturition, and lactation in sows and weaning in piglets are all linked to elevated levels of oxidative stress due to intensive metabolism [157,160] and resulted in the increased oxidative products (i.e., ROM, NO, and H2O2) in plasma [161,162].

In sows, the LR diet tended to increase AOPP concentrations at the end of gestation, so the decreased number of piglets born and piglets born alive might be caused by the involvement of AOPP levels in embryonic mortality [158]. Nevertheless, the increased tendency of AOPPs in LR sows did not seem to produce intracellular ROS (H202) because d-ROMs levels of LR and CR sows at the end of gestation were similar. Moreover, the LR diet did not influence lipid peroxidation

of sow plasma, possibly due to the rapid hepatic absorption of malondialdehyde measured in the TBARS assay before being eliminated in urine without influencing TBARS levels in blood circulation [159]. Additionally, FRAP values of LR sows were similar at the end of gestation and tended to increase at the beginning of lactation, compared with CR sows, as a result of activated sow's antioxidant system with increased protein oxidation.

Although no effects of maternal LR diet and piglet SW diet on piglet oxidative status, the higher ADG and G:F ratio of the LRCT and CRSW piglets showed the benefits of LR and SW diets on stimulating antioxidants and reducing excessive ROS production. Several reasons can explain the positive effects on piglet growth rates. First, growth performance reflects overall influences over a period, whereas plasma measurements are single tests at a time point [163]. Second, the bioactivity of ω3 PUFAs in the maternal diet and SW-derived elements (i.e., ascophyllan, laminarin, fucoidans, and phlorotannins) in the piglet diet [164] can promote piglet intestinal health through its immunomodulatory, anti-inflammatory, antioxidant, and antimicrobial properties [127,167,168]. Third, maternal LR diet with optimal ω6:ω3 ratio might regulate progeny immune response and improve anti-inflammatory activity against pathogens [165] or post-weaning stress [166].

6.3 OMEGA 6 : OMEGA3 RATIOS AND PROTEOMICS

The observations in Chapter 2 support the idea that maternal dietary interventions can remarkably affect the offspring, and dietary supplementation with SW can effectively enhance post-weaned piglet performance. Nevertheless, the molecular mechanism of the interaction between dietary treatments in sows and piglets remains to be addressed. Thus, the effects of nutritional interventions on molecular outcomes in sows and their progeny were studied in Chapters 3, 4 and 5, respectively.

6.3.1 Sow plasma proteomics

ALA may participate in some lipoprotein-related pathways in plasma [175], such as inflammation and platelet aggregation, with a high content provided in a long-

term study because more EPA is synthesized from ALA [406]. Plant-derived ω3 PUFA ALA primarily functions as a regulator for converting LA to AA and as a substrate for EPA synthesis [174]. These effects of ALA were observed on sow plasma (Chapter 2). Results in Chapter 3 showed that LR diet during a sixteen-week intervention trial altered several acute phase proteins' plasma levels in late gestating and late lactating sows. In the LR group, the down-regulation of HP and Serum amyloid P-component (APCS) and up-regulation of alpha-1-antitrypsin (SERPINA1) may relate to the mechanism of anti-inflammation and protease inhibition [206,207]. Consequently, these acute phase proteins might participate in the host defence mechanisms against accelerated oxidative damage in key life cycle chapters in sows.

In comparing the plasma proteome of late gestation to that of late lactation, substantial alterations were observed over this stage, affecting the plasma lipoproteins and the acute phase proteins in particular. Related to the former, apolipoprotein A-1 (APOA1), A-2 (APOA2), and C-3 (APOC3) were all up-regulated by the end of lactation. They are multifunctional proteins that play significant roles in lipid metabolism through regulating critical enzymes activity and functioning as ligands to lipoprotein receptors [212]. Over the same stage, positive acute phase proteins in pigs, haptoglobin (HP), and ITIH4 (or pig-MAP) were down-regulated. These observations suggest that the end of gestation is linked to an acute phase reaction demonstrated by the increase in positive acute phase proteins and a decline in negative acute phase proteins such as APOA1, while by the end of lactation, this acute phase reaction has dissipated.

This study also aimed to explain the mechanism of improved survival rate and weight gain of piglets born from the LR sows, as reported in the *in vivo* study (Chapter 2). A diet supplemented with FA primarily regulates the concentration of milk fat [87], whose main component is TG (>95%) and is closely linked to neonatal growth [407]. Better postnatal survival of newborns is associated with higher body fat content mass [408]. Piglets born from LR sows could have a higher fat deposition, increased TG turnover rate, and circulating lipids during later stages of fetal life and, thus, increased energy metabolism in postnatal life [408], compared to piglets born from CR sows. Consequently, LR piglets are more physiological mature at birth [408], and they survive better than CR piglets.

However, this needs further validation because we did not measure TG in milk, and plasma TG level was similar between the two dietary treatments.

Overall, results in Chapter 3 provide additional insights into the benefit of LR diet in altering proteins that involve in the protective system against gestational and lactational stresses and sow adaptation's molecular mechanisms to stimuli in different reproduction stages.

6.3.2 Piglet serum proteomics

Weaning is a critical adaptive period in a pig's life to grow and develop fully in adulthood [232]. Piglets in this critical period must be well-equipped to protect the intestines and immune development, preventing an excessive reduction in feed consumption, intestinal inflammation, and dysbiosis [335]. Maternal and offspring nutritional interventions might alleviate weaning-related stress and intestinal barrier dysfunction in pigs [162], thus, supporting the immune system and development of piglets.

Serum proteome profiles of newly weaned (d0) and post-weaned (d21 PW) piglets influenced by maternal and post-weaned diets were revealed in Chapter 4. The neonates are more sensitive and protective in response to various stimuli [323]. The data in Chapter 4 demonstrated a significant difference in DAPs as early-onset physiological mechanisms to promote adaptation to inflammatory signalling [328].

Maternal diet is critical to offspring growth, immune development, and intestinal functions [262–264]. On d0, the downregulation of complement C3 in LR piglets may be associated with the anti-inflammatory property of low ω6:ω3 ratio in their mother's diet. On d21 PW, a significantly high level of positive APP - serum amyloid A (SAA) and negative APP - transferrin (TF), in LR piglets reflects that the innate defence system is strongly activated and participates in the inflammatory response. Regardless of sampling time, maternal LR diet decreased the levels of fibronectin (FN1) – a positive APP, and alpha-1-Antichymotrypsin (SERPINA3) - a serine proteinase inhibitor, however antithrombin-III (SERPINC1) was increased in abundance. SERPINA3 seems to be increased, and SERPINC1 decreased with the inflammation conditions [298]. These alterations in LR piglets suggested the anti-inflammatory effect of low ω6:ω3 ratio in the maternal diet and contributed to

the enhanced host protective response. Coagulation factor XII (F12) was activated in LR versus CR serum at d0 to quickly create enzymatic activity on the surface of pathological cells in response to inflammation [331]. Protein F12 also contributes to developing the protective system in weaning piglets by regulating the cross-talk that links coagulation pathways and inflammation, particularly in innate immunity [331].

In piglets, the weaning diet serves a crucial role in controlling gut function, shaping adaptive immunity, supporting the host defence against stimuli, thereby affecting the overall performance and health [248]. This study supplemented *Ascophyllum nodosum* to weaned piglets (d0 – d21 PW), a brown seaweed (SW) species with in-feed antibiotics properties due to rich in bioactive ingredients such as phlorotannins and polyphenols [128,249–251]; and polysaccharides (laminarin, fucoidans, and alginates [128], and ascophyllan [252]). The effect of piglet dietary treatments: SW versus CT groups was assessed on d21 PW. The enrichment of complement C5a in SW piglets at d21 PW suggests the essential role of C5a as a bridge to connect innate and adaptive immunity to enhance the host defence during inflammation conditions [305]. Additionally, the increased concentration of kininogen-1 (KNG1), a coagulation factor, in SW serum suggests an effect of SW on coagulation cascade regulation.

Regarding the effect of time points, the proteomic patterns of the post-weaned piglets were significantly altered from d0 to d21 PW. Specifically, serum lipoproteins (e.g., APOA1, APOB, APOE); pro-coagulation proteins (e.g., F2, HRG, ORM1); coagulation regulator, e.g., PLG; and acute phase proteins (e.g., HP, ITIH4, TF, SAA, SERPINA1) were changed in their relative abundance on d21 PW, compared to d0.

As observed in Chapter 3, APOA1 and APOE concentrations were decreased in late pregnancy and increased during lactation. Accordingly, suckling piglets gained relatively high levels of APOA1, APOB, and APOE from their mother; however, these concentrations fell significantly during post-weaning. The serum level of high-density lipoprotein (HDL) was estimated in Chapter 4. Due to multiple biological functions of HDL such as anti-inflammatory, antioxidant, anti-thrombotic, and anti-apoptotic [313]; a higher level of both APOA1 and HDL-cholesterol in piglets at d0 versus d21 PW suggests that these changes related to

the host protective activities against weaning stress. Moreover, high levels of positive APPs (e.g., HP, ITIH4, SAA) and low levels of negative APPs (e.g., TF, TTR, and SERPINA1) on d0 were observed as a consequence of stress stimuli following separation from the mother, transportation, change to a new environment and social mixing (regrouping). These results match those reported in an earlier study [315].

Similar to a previous report [324], multiple DAPs (such as APOB, SERPINA3, and TF) associated with haemostasis showed the development of the haemostatic system in piglets from d0 to d21 PW. Haemostasis development promotes effective host defence and wound healing system [319,320].

Altogether, findings in Chapter 4 reveal the benefits of reducing ω6:ω3 ratio in maternal LR diet and SW supplementation in PW piglet's diet to boost piglet immunity and anti-inflammation properties.

6.3.3 Piglet ileum proteomics

Weaning is a stressful event linked to significant intestinal changes in pigs [332]. Long-term maternal and post-weaned dietary treatments can modify piglet ileal proteome (on d22 PW), and these results are presented in Chapter 5.

Maternal LR diet increased the abundance of the 40S ribosomal protein SA (RPSA), chaperonin-containing T-complex protein 1 subunit beta (CCT2), and glutamine-fructose-6-phosphate transaminase (GFPT1) in LR ileum, and these alterations may relate to the host response to inflammatory stimuli, affecting piglet' growth performance, as observed in the in vivo study (Chapter 2). The upregulation of RPSA in LR ileum may relate to the positive regulation of the protein synthesis process [348]. However, the upregulation of CCT2 in LR ileum can induce uncontrolled proliferation and is associated with the overexpression of cell cycle regulators [354]. Moreover, the changes in GFPT1 protein and, in turn, glycosylation process in LR ileum may relate to inflammatory conditions [356].

SW dietary supplementation in post-weaned piglets increased the abundance of proliferating cell nuclear antigen (PCNA) but decreased the abundance of villin-1 (VIL1) in the ileum. These changes suggest that SW stimulates the rapid renewal

of the ileal epithelium by promoting cell proliferation while diminishing the absorption capacity of ileal epithelial cells. Indeed, PNCA is a marker of cell proliferation [364] and participates in DNA synthesis, replication, and repair; cell proliferation, and cell cycle initiation [365,366]. VIL1 indicates absorptive cells in the brush border [373] because it regulates epithelial structure and microvilli physiological functions [375], the main absorption site. Additionally, the decreased expression of ATP synthase subunits and keratin proteins (KRT8, 19, and 20) may relate to cellular response toward anti-inflammation [358] or lowering the inflammation severity [370,371]. Nevertheless, the downregulation of creatine kinase in LRSW piglets may be associated with the decline in myogenesis [361,362], and consequently, LRSW piglets had a lower growth rate as reported in the in vivo study (Chapter 2).

The interplay between maternal and post-weaned diets was assessed through the comparisons among 4 groups containing CRCT, CRSW, LRCT, and LRSW, and the focus was on three main comparisons: LRCT, CRSW, and LRSW versus CRCT groups. The LRCT diet was associated with enriched regulation of signal transmission between neurons in the brain and contributed to the immune response against stimuli. In CRSW piglet, oxygen storage and supply to ileal tissue against stressors were improved via the upregulation of hemoglobin (subunit A – HBA and subunit B – HBB) [384–386], protein synthesis and the regeneration of ileal tissue were promoted through the overabundance of ribosomal proteins (RPL10A and RPL24) [387], thus, enhancing intestinal health. The LRSW piglets decreased fat absorption capacity, which may be associated with their unexpected growth development, as observed in Chapter 2, although they may improve insulin signalling and genome stability. These observations were evident in the downregulation of enoyl coenzyme A hydratase 1 (ECH1), an enzyme that participates in the insulin signalling improvement process [398] and fatty acid-binding protein 6 (FABP6) - an ileum-specific bile acid transporter [399,400], and the upregulation of histone protein (HIST1H1E) - a component of chromatin fiber [405] that facilitates DNA replication, DNA repair, and genome stability [404].

Results in Chapter 5 uncovered the mechanism behind the anti-inflammation and intestinal-boosting effects of maternal LR diet in piglets supplemented with SW.

6.4 SCOPE FOR FURTHER INVESTIGATIONS

Although substantial effort has been made during experimental design and performance, there are still several areas for further improvements in the investigations described in this thesis.

1. Besides recording body condition scores and live body weight, the sow's feed intake and backfat thickness should be measured during gestation and lactation, while leptin concentrations were assessed on the sow's plasma. Leptin regulates feed intake and energy metabolism, influencing the sow's body weight gain/loss and reproductive performance [409]. The feed intake was not measured because the sow trial was executed in a commercial farm where dry feed was mixed with water in the feeder. The information about feed intake and back fat measurements may expand our understanding of leptin levels under dietary treatments.

2. The health status of sows and piglets was observed in this study (data not shown); diarrhea measurement (such as diarrhea score or index) should be performed to provide evidence and our comprehension of dietary treatment effects on the postweaning piglet's response.

3. TBARS was used to measure lipid peroxidation. Though the TBARS assay is the most common method to measure lipid peroxidation, this assessment frequently overestimates the lipid damage because it investigates non-specific aldehydes [410]. Consequently, more specific methods such as determining MDA directly without derivatization, measuring MDA-TBA derivative by high-performance liquid chromatography (HPLC), or F2-isoprostanes (ISP) assays [411] or mass spectrometry techniques [412], instead of TBARS assay, would be performed to obtain a better result of the oxidized lipid. Moreover, lipid peroxidation products should also be measured in the liver where lipid is metabolized and, in the urine, where lipid is abolished.

4. Although the required sample size was calculated (n = 10), accounting for the minimum number of animals for animal welfare and a statistically significant effect of dietary treatments (EU Directive 2010/63), a larger sample size (n = 12-15) might be valuable to estimate better the changes on sows and their respective

offspring under treatment effects. Especially our proteomics study design is relatively complicated with many variables; the sample size for proteomics analysis was relatively small (n = 5), accounting for genetic heterogeneity from different sows. So, the dietary treatment effect on protein profile is small. Thus, we have also considered examining DAPs with unadjusted *p*-value < 0.05, arguing that even with a small effect of change, it could be biologically relevant, and our results could encourage further research on the same topic. We suppose that further studies with a larger sample size for proteomics analysis (n = 9 – 12) would potentially give significant results with adjusted *p*-values <0.05. In our study, we decided to use raw *p*-values < 0.05 as a threshold to filter out potentially biologically interesting proteins, which should be examined in more detail in further studies to fully understand the molecular mechanism behind these observed associations due to the low number of DAPs identified based on adjusted *p*-values.

5. We used multiplexed proteomics – one of the best current methods for relative protein identification and quantitation. This approach can misrepresent fold changes in protein expression due to ratio distortion or compression problems [63,413]. Specifically, the ratio for the peptides of interest between control and treatment may be compressed, resulting in underestimating the fold change in peptides upon the co-isolation and co-fragmentation of peptides with similar m/z and retention time (including the interfering peptides were labelled with identical isobaric tags) [63]. Consequently, the obtained *p*-values and adjusted *p*-values are higher, equivalent to fewer proteins passing the adjusted thresholds, so multiple testing adjustment procedures may fail to detect any true positives even if many exist [413]. Applying multiple testing adjustment methods in proteomics studies with low power is a helpful tool but should not be considered as a necessary stamp [413]. Indeed, a recent meta-analysis of 100 proteomics papers published in 2019 further supports this view found that multiple testing adjustments were employed in just < 1/5 of papers (24/100) [414].

6. No depletion of high-abundance proteins or peptides was executed in this thesis to avoid the potential bias of depletion in shotgun proteomics that relates to the unintended removal of several potential important non-targeted proteins such as plasma albumin, antitrypsin, transferrin, haptoglobin, etc. [266]. However,

ProteoMiner technology could be applied appropriately in future studies to enrich low abundant proteins (by decreasing the dynamic range of peptides after proteolysis) and increase the number of identified proteins in biological samples [415].

7. Finally, a simple experimental design with fewer experimental factors would be more efficient in the statistical analysis of proteomics data.

6.5 GENERAL CONCLUSIONS

This thesis provides evidence in supporting the benefits of long-term dietary supplementation with low ω6:ω3 PUFAs ratio (LR) on sow colostrum - milk fatty acid profiles and reproductive performance. Proteomic analyses identified the relation between LR diet and acute phase proteins (APPs; i.e., HP, SERPINA1, and APCS) in protective mechanisms against accelerated reproduction-related stresses. In addition, potential regulators of females' gestation and lactation such as positive APPs (HP and ITIH4 or pig-MAP), negative APP (APOA1), and apolipoproteins (APOA2 and APOC3) were revealed. During post-weaning, growth of piglets from sows fed control diet was not affected by the maternal LR diet but was improved by offspring's seaweed (SW) supplemented diet. Serum proteomics analyses highlighted the contribution of C3, SAA, SERPINA3, SERPINC1, and TF in piglet host protective mechanisms in response to maternal LR diet. Post-weaned piglets' SW diet enriched C5a and KNG1, two stimulators of coagulation cascade regulation and the connection between innate and adaptive immunity. The potential regulator proteins associated with the early development of piglet post-weaning were also underlined, including serum lipoproteins (APOA1, APOB, APOE); pro-coagulation proteins (F2, HRG, ORM1); coagulation regulator (PLG); and APPs (HP, ITIH4, TF, SAA, SERPINA1).

Ileal proteomic analyses suggested that maternal LR diet affected RPSA regarding protein synthesis process, GFPT1 regarding the host response to inflammatory stimuli, and CCT2 regarding uncontrolled proliferation and overexpression of cell cycle regulators. SW supplementation affected potential regulators of the anti-inflammation (ATP5A1 and ATP5B), ileal epithelial growth in CRSW piglets (HBA, HBB, RPL10A, and RPL24); fat absorptive capacity (FABP6), insulin signalling (ECH1), and genome stability (HIST1H1E) in LRSW piglets. A summary of the main

results obtained in this thesis is presented in Figure 6-1. Understanding the potential roles of these protein regulators will provide insights into how nutrition programs can be enhanced to improve pig performance and health over sensitive periods in development. Effective nutrition management will meet the needs of increasing demand for high-quality and safe animal products.

In summary, the results presented here provide the basis of future studies toward the effects of maternal and offspring's nutritional interventions, such as anti-inflammatories and alternatives to in-feed antibiotics diets, on piglet development. The interplay between early- and later-life nutrition, as environmental factors will shape the genetic and epigenetic signature of offspring, and thus, have long-term effects on the onset and development of the immune system, intestinal health, and growth rate, particularly in crucial developmental points in the life cycles of animals [416]. These factors make this field an interesting but complex area of research. Any research highlighting the importance of early- and later-life nutritional programming during critical periods of a pig's life would drive the pig production industry towards sustainable development and benefit human health.

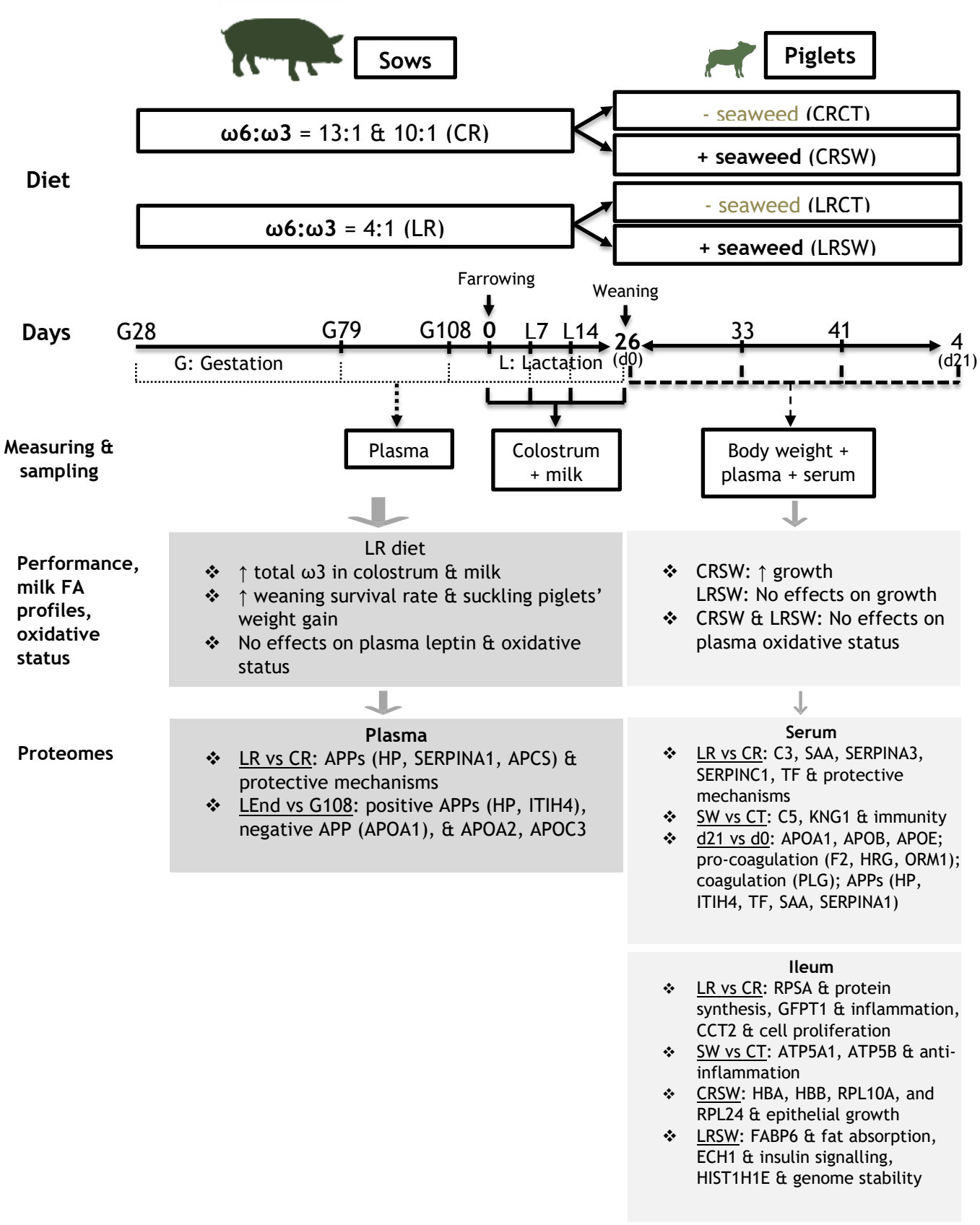

Figure 6-1 A summary of main results obtained in this thesis.

Appendices

Appendix Table S1. Gene Ontology (GO) terms on biological processes, molecular function and cellular components in comparison (e) - CR serum at day 21 post-weaning versus CR serum at weaning day. CR: piglet born from sow fed diet with ω6:ω3 ratio = 13:1 during gestation, starting from day 28 (G28) and 10:1 during lactation.

GO term ID	Description	Adjusted p-value	Gene count	Matching proteins in PPI network
		GO Biological Process (n = 54)		
GO:0034371	Chylomicron remodelling	1.2E-08	5	APOC3, APOB, APOA1, APOE, APOA4
GO:0016192	Vesicle-mediated transport	1.2E-07	15	HRG, APOB, APOA1, TTR, APOE, AMBP, ITIH4, SERPING1, F2, PLG, SERPINA3, SAA, TF, ITIH3, IGLL5
GO:0030162	Regulation of proteolysis	3.0E-07	11	HRG, APOE, PZP, FETUB, AMBP, ITIH4, SERPING1, F2, SERPINA3, C4A, ITIH3
GO:0090207	Regulation of triglyceride metabolic process	1.0E-06	5	APOC3, APOA1, APOE, APOA4, PLIN5
GO:0033700	Phospholipid efflux	1.9E-06	4	APOC3, APOA1, APOE, APOA4
GO:0001523	Retinoid metabolic process	2.2E-06	6	APOC3, APOB, APOA1, TTR, APOE, APOA4
GO:0006810	Transport	7.9E-06	18	APOC3, HRG, APOB, APOA1, TTR, APOE, CP, AMBP, ITIH4, SERPING1, F2, PLG, APOA4, SERPINA3, SAA, TF, ITIH3, IGLL5
GO:0019216	Regulation of lipid metabolic process	7.9E-06	8	APOC3, APOB, APOA1, APOE, F2, APOA4, PLIN5, SERPINA3
GO:1905952	Regulation of lipid localization	8.5E-06	6	APOC3, APOB, APOA1, APOE, APOA4, PLIN5
GO:0044419	Interspecies interaction between organisms	1.1E-05	13	HRG, APOB, APOE, AMBP, SERPING1, F2, PLG, APOA4, CFH, SAA, TF, C4A, IGLL5
GO:0006898	Receptor-mediated endocytosis	2.0E-05	6	APOB, APOA1, APOE, AMBP, SAA, IGLL5
GO:0070328	Triglyceride homeostasis	3.4E-05	4	APOC3, APOA1, APOE, APOA4
GO:0051179	Localization	3.4E-05	19	APOC3, HRG, APOB, APOA1, TTR, APOE, CP, AMBP, ITIH4, SERPING1, F2, PLG, APOA4, PLIN5, SERPINA3, SAA, TF, ITIH3, IGLL5
GO:0065009	Regulation of molecular function	3.9E-05	18	APOC3, HRG, APOA1, TTR, APOE, PZP, FETUB, AMBP, ITIH4, SERPING1, F2, APOA4, PLIN5, SERPINA3, SAA, TF, C4A, ITIH3
GO:0032489	Regulation of cdc42 protein signal transduction	4.5E-05	3	APOC3, APOA1, APOE
GO:0042157	Lipoprotein metabolic process	7.4E-05	5	APOC3, APOB, APOA1, APOE, APOA4

GO term ID	Description	Adjusted p-value	Gene count	Matching proteins in PPI network
GO Biological Process (n = 54, cont.)				
GO:0002376	Immune system process	1.5E-04	13	HRG, APOB, TTR, SERPING1, F2, PLG, APOA4, CFH, SERPINA3, SAA, TF, C4A, IGLL5
GO:0010876	Lipid localization	3.0E-04	6	APOC3, APOB, APOA1, APOE, APOA4, PLIN5
GO:0009605	Response to external stimulus	4.6E-04	12	HRG, APOB, APOA1, APOE, SERPING1, F2, APOA4, CFH, SAA, TF, C4A, IGLL5
GO:0043687	Post-translational protein modification	5.1E-04	6	APOB, APOA1, APOE, CP, TF, C4A
GO:0065008	Regulation of biological quality	7.1E-04	15	APOC3, HRG, APOB, APOA1, TTR, APOE, CP, SERPING1, F2, PLG, APOA4, PLIN5, SERPINA3, SAA, TF
GO:0048519	Negative regulation of biological process	7.5E-04	17	APOC3, HRG, APOA1, APOE, PZP, FETUB, AMBP, ITIH4, SERPING1, F2, PLG, APOA4, PLIN5, SERPINA3, SAA, C4A, ITIH3
GO:0006950	Response to stress	7.7E-04	14	HRG, APOA1, APOE, ITIH4, SERPING1, F2, PLG, APOA4, CFH, SERPINA3, SAA, TF, C4A, IGLL5
GO:0002697	Regulation of immune effector process	9.9E-04	6	APOA1, SERPING1, F2, CFH, C4A, IGLL5
GO:0062012	Regulation of small molecule metabolic process	1.4E-03	6	APOC3, APOB, APOA1, APOE, APOA4, PLIN5
GO:0010543	Regulation of platelet activation	1.4E-03	3	HRG, APOE, F2
GO:0010903	Negative regulation of very-low-density lipoprotein particle remodelling	1.7E-03	2	APOC3, APOA1
GO:0032879	Regulation of localization	2.1E-03	12	APOC3, HRG, APOB, APOA1, APOE, F2, PLG, APOA4, PLIN5, SAA, TF, C4A
GO:0065007	Biological regulation	2.2E-03	23	APOC3, HRG, APOB, APOA1, TTR, APOE, PZP, CP, FETUB, AMBP, ITIH4, SERPING1, F2, PLG, APOA4, CFH, PLIN5, SERPINA3, SAA, TF, C4A, ITIH3, IGLL5
GO:0050878	Regulation of body fluid levels	2.5E-03	6	HRG, APOE, SERPING1, F2, PLG, SAA
GO:1901564	Organonitrogen compound metabolic process	2.6E-03	16	APOC3, APOB, APOA1, TTR, APOE, CP, AMBP, ITIH4, SERPING1, F2, PLG, APOA4, SAA, TF, C4A, ITIH3
GO:0007596	Blood coagulation	2.8E-03	5	HRG, SERPING1, F2, PLG, SAA
GO:0009611	Response to wounding	3.1E-03	6	HRG, APOA1, SERPING1, F2, PLG, SAA

GO term ID	Description	Adjusted p-value	Gene count	Matching proteins in PPI network
GO Biological Process (n = 54, cont.)				
GO:0050794	Regulation of cellular process	3.1E-03	22	APOC3, HRG, APOB, APOA1, TTR, APOE, PZP, FETUB, AMBP, ITIH4, SERPING1, F2, PLG, APOA4, CFH, PLIN5, SERPINA3, SAA, TF, C4A, ITIH3, IGLL5
GO:0051649	Establishment of localization in cell	3.1E-03	11	HRG, APOA1, TTR, APOE, ITIH4, SERPING1, F2, PLG, SERPINA3, TF, ITIH3
GO:0006066	Alcohol metabolic process	3.5E-03	5	APOB, APOA1, TTR, APOE, APOA4
GO:0048583	Regulation of response to stimulus	3.9E-03	14	APOC3, HRG, APOA1, APOE, AMBP, SERPING1, F2, PLG, CFH, PLIN5, SAA, TF, C4A, IGLL5
GO:0051641	Cellular localization	3.9E-03	12	HRG, APOA1, TTR, APOE, ITIH4, SERPING1, F2, PLG, PLIN5, SERPINA3, TF, ITIH3
GO:0019538	Protein metabolic process	5.6E-03	14	APOC3, APOB, APOA1, TTR, APOE, CP, AMBP, SERPING1, F2, PLG, APOA4, SAA, TF, C4A
GO:0006641	Triglyceride metabolic process	7.6E-03	3	APOC3, APOB, APOE
GO:0051006	Positive regulation of lipoprotein lipase activity	8.0E-03	2	APOA1, APOA4
GO:0006826	Iron ion transport	8.0E-03	3	HRG, CP, TF
GO:0002252	Immune effector process	8.3E-03	7	TTR, SERPING1, F2, CFH, SERPINA3, C4A, IGLL5
GO:0042158	Lipoprotein biosynthetic process	1.5E-02	3	APOB, APOA1, APOE
GO:0043170	Macromolecule metabolic process	1.6E-02	16	APOC3, APOB, APOA1, TTR, APOE, CP, AMBP, ITIH4, SERPING1, F2, PLG, APOA4, SAA, TF, C4A, ITIH3
GO:0062014	Negative regulation of small molecule metabolic process	2.0E-02	3	APOC3, APOE, PLIN5
GO:0061024	Membrane organization	2.0E-02	6	APOB, APOA1, APOE, APOA4, TF, IGLL5
GO:0006954	Inflammatory response	2.3E-02	5	ITIH4, F2, SERPINA3, SAA, C4A
GO:0044267	Cellular protein metabolic process	2.7E-02	12	APOB, APOA1, TTR, APOE, CP, AMBP, F2, PLG, APOA4, SAA, TF, C4A
GO:0016042	Lipid catabolic process	2.8E-02	4	APOC3, APOB, APOE, APOA4
GO:0044403	Symbiotic process	3.0E-02	6	HRG, APOE, AMBP, F2, PLG, CFH

GO term ID	Description	Adjusted p-value	Gene count	Matching proteins in PPI network
GO Biological Process (n = 54, cont.)				
GO:0040011	Locomotion	3.3E-02	7	HRG, APOB, APOA1, F2, PLG, SAA, IGLL5
GO:0016477	Cell migration	3.6E-02	6	APOB, APOA1, F2, PLG, SAA, IGLL5
GO:0030212	Hyaluronan metabolic process	4.7E-02	2	ITIH4, ITIH3
GO Molecular Function (n = 12)				
GO:0005102	Signalling receptor binding	1.2E-09	14	APOC3, HRG, APOA1, APOE, PZP, FETUB, AMBP, ITIH4, SERPING1, F2, APOA4, SERPINA3, C4A, ITIH3
GO:0005515	Protein binding	1.2E-05	4	APOB, APOA1, APOE, APOA4
GO:0060228	Phosphatidylcholine-sterol o-acyltransferase activator activity	2.3E-05	4	APOC3, APOB, APOA1, APOE
GO:0098772	Molecular function regulator	2.3E-05	6	HRG, APOB, APOE, F2, CFH, SAA
GO:0070325	Lipoprotein particle receptor binding	2.4E-05	16	APOC3, HRG, APOA1, TTR, APOE, PZP, FETUB, AMBP, ITIH4, SERPING1, F2, APOA4, SERPINA3, SAA, C4A, ITIH3
GO:0008289	Lipid binding	4.4E-05	3	APOA1, APOE, APOA4
GO:0035473	Lipase binding	1.6E-04	11	APOC3, HRG, APOB, APOA1, TTR, APOE, F2, PLG, SAA, TF, IGLL5
GO:0070653	High-density lipoprotein particle receptor binding	3.4E-03	2	APOC3, APOA1
GO:0008201	Heparin binding	6.8E-03	3	APOC3, APOA1, APOA4
GO:0030234	Enzyme regulator activity	8.0E-03	2	APOB, PLIN5
GO:0120020	Cholesterol transfer activity	8.8E-03	18	APOC3, HRG, APOB, APOA1, TTR, APOE, PZP, CP, AMBP, F2, PLG, APOA4, CFH, PLIN5, SAA, TF, C4A, IGLL5
GO:0015485	Cholesterol binding	3.7E-02	6	APOC3, APOB, APOA1, APOE, F2, APOA4

GO term ID	Description	Adjusted p-value	Gene count	Matching proteins in PPI network
		GO Cellular Component (n = 11)		
GO:0072562	Blood microparticle	3.6E-27	16	HRG, APOA1, APOE, PZP, CP, AMBP, ITIH4, SERPING1, F2, PLG, APOA4, CFH, SERPINA3, TF, C4A, IGLL5
GO:0062023	Collagen-containing extracellular matrix	9.0E-11	11	APOC3, HRG, APOA1, APOE, AMBP, ITIH4, SERPING1, F2, PLG, APOA4, SERPINA3
GO:0071682	Endocytic vesicle lumen	1.7E-06	4	APOB, APOA1, APOE, SAA
GO:0012505	Endomembrane system	2.7E-04	16	APOC3, HRG, APOB, APOA1, TTR, APOE, CP, ITIH4, SERPING1, F2, PLG, APOA4, SERPINA3, TF, C4A, ITIH3
GO:0034365	Discoidal high-density lipoprotein particle	1.0E-03	2	APOA1, APOE
GO:0030139	Endocytic vesicle	1.8E-03	5	APOB, APOA1, APOE, SAA, TF
GO:0043227	Membrane-bounded organelle	2.1E-03	23	APOC3, HRG, APOB, APOA1, TTR, APOE, PZP, CP, FETUB, AMBP, ITIH4, SERPING1, F2, PLG, APOA4, CFH, PLIN5, SERPINA3, SAA, TF, C4A, ITIH3, IGLL5
GO:0031232	Extrinsic component of external side of plasma membrane	4.1E-03	2	PLG, TF
GO:0070013	Intracellular organelle lumen	6.7E-03	16	HRG, APOB, APOA1, TTR, APOE, CP, ITIH4, SERPING1, F2, PLG, APOA4, SERPINA3, SAA, TF, C4A, ITIH3
GO:0031089	Platelet dense granule lumen	9.3E-03	2	ITIH4, ITIH3
GO:0009986	Cell surface	1.7E-02	6	HRG, APOA1, AMBP, PLG, TF, IGLL5

Pathway	Description	Adjusted p-value	Gene count	Matching proteins in PPI network
	Reactome Pathways (n = 21)			
HSA-114608	Platelet degranulation	2.7E-08	8	HRG, APOA1, ITIH4, SERPING1, PLG, SERPINA3, TF, ITIH3
HSA-381426	Regulation of Insulin-like Growth Factor (IGF) transport and uptake by Insulin-like Growth Factor Binding Proteins (IGFBPs)	2.7E-08	8	APOB, APOA1, APOE, CP, F2, PLG, TF, C4A
HSA-8963888	Chylomicron assembly	2.7E-08	5	APOC3, APOB, APOA1, APOE, APOA4
HSA-8963901	Chylomicron remodelling	2.7E-08	5	APOC3, APOB, APOA1, APOE, APOA4
HSA-76002	Platelet activation, signalling and aggregation	3.0E-08	9	HRG, APOA1, ITIH4, SERPING1, F2, PLG, SERPINA3, TF, ITIH3
HSA-975634	Retinoid metabolism and transport	4.9E-08	6	APOC3, APOB, APOA1, TTR, APOE, APOA4
HSA-109582	Haemostasis	1.1E-06	10	HRG, APOB, APOA1, ITIH4, SERPING1, F2, PLG, SERPINA3, TF, ITIH3
HSA-2173782	Binding and Uptake of Ligands by Scavenger Receptors	2.7E-06	5	APOB, APOA1, APOE, AMBP, SAA
HSA-8957275	Post-translational protein phosphorylation	3.7E-06	6	APOB, APOA1, APOE, CP, TF, C4A
HSA-3000471	Scavenging by Class B Receptors	1.2E-04	3	APOB, APOA1, SAA
HSA-418594	G alpha (i) signalling events	2.6E-04	7	APOC3, APOB, APOA1, TTR, APOE, APOA4, SAA
HSA-977606	Regulation of Complement cascade	3.2E-04	4	SERPING1, F2, CFH, C4A
HSA-8964058	HDL remodelling	3.5E-04	3	APOC3, APOA1, APOE
HSA-3000480	Scavenging by Class A Receptors	1.5E-03	3	APOB, APOA1, APOE
HSA-977225	Amyloid fiber formation	1.8E-03	4	APOA1, TTR, APOA4, SAA
HSA-392499	Metabolism of proteins	3.5E-03	11	APOB, APOA1, TTR, APOE, CP, F2, PLG, APOA4, SAA, TF, C4A
HSA-8964043	Plasma lipoprotein clearance	6.8E-03	3	APOB, APOA1, APOE
HSA-168249	Innate Immune System	9.3E-03	8	APOB, TTR, SERPING1, F2, CFH, SERPINA3, SAA, C4A
HSA-382551	Transport of small molecules	9.3E-03	7	APOC3, APOB, APOA1, APOE, CP, APOA4, TF
HSA-388396	GPCR downstream signalling	1.4E-02	8	APOC3, APOB, APOA1, TTR, APOE, F2, APOA4, SAA
HSA-8964026	Chylomicron clearance	1.7E-02	2	APOB, APOE

Appendix Table S2. Gene Ontology (GO) terms on biological processes, molecular function and cellular components in comparison (f) - LR serum at day 21 post-weaning versus LR serum at weaning day. LR: piglet born from sow fed diet with ω6:ω3 ratio = 4:1 from G28 until the end of lactation.

GO term ID	Description	Adjusted p-value	Gene count	Matching proteins in PPI network
GO Biological Process (n = 39)				
GO:0030162	Regulation of proteolysis	2.3E-09	13	SERPIND1, VTN, HRG, APOE, PZP, FETUB, SERPING1, CLEC3B, GSN, SERPINA3, C4A, ITIH3, SERPINA1
GO:0016192	Vesicle-mediated transport	8.3E-09	16	VTN, HRG, APOB, TTR, APOE, ORM1, SERPING1, CLEC3B, CD5L, GSN, SERPINA3, SAA, TF, ITIH3, SERPINA1, IGLL5
GO:0050790	Regulation of catalytic activity	4.2E-07	16	SERPIND1, VTN, HRG, APOE, PZP, FETUB, SERPING1, APOA4, GSN, PLIN5, SERPINA3, SAA, TF, C4A, ITIH3, SERPINA1
GO:0045055	Regulated exocytosis	3.3E-06	10	HRG, TTR, ORM1, SERPING1, CLEC3B, GSN, SERPINA3, TF, ITIH3, SERPINA1
GO:0002376	Immune system process	7.6E-06	15	VTN, HRG, APOB, TTR, ORM1, SERPING1, APOA4, CD5L, GSN, SERPINA3, SAA, TF, C4A, SERPINA1, IGLL5
GO:0006810	Transport	1.7E-05	18	VTN, HRG, APOB, TTR, APOE, ORM1, CP, SERPING1, CLEC3B, APOA4, CD5L, GSN, SERPINA3, SAA, TF, ITIH3, SERPINA1, IGLL5
GO:0006952	Defence response	4.7E-05	11	HRG, ORM1, SERPING1, APOA4, CD5L, GSN, SERPINA3, SAA, C4A, SERPINA1, IGLL5
GO:0051179	Localization	7.1E-05	19	VTN, HRG, APOB, TTR, APOE, ORM1, CP, SERPING1, CLEC3B, APOA4, CD5L, GSN, PLIN5, SERPINA3, SAA, TF, ITIH3, SERPINA1, IGLL5
GO:0043687	Post-translational protein modification	8.5E-05	7	SERPIND1, APOB, APOE, CP, TF, C4A, SERPINA1
GO:0002443	Leukocyte mediated immunity	2.1E-04	8	TTR, ORM1, SERPING1, GSN, SERPINA3, C4A, SERPINA1, IGLL5
GO:0065009	Regulation of molecular function	5.5E-04	17	SERPIND1, VTN, HRG, TTR, APOE, PZP, FETUB, SERPING1, APOA4, GSN, PLIN5, SERPINA3, SAA, TF, C4A, ITIH3, SERPINA1
GO:0050878	Regulation of body fluid levels	6.0E-04	7	SERPIND1, VTN, HRG, APOE, SERPING1, SAA, SERPINA1
GO:0080090	Regulation of primary metabolic process	1.4E-03	18	SERPIND1, VTN, HRG, APOB, APOE, PZP, FETUB, SERPING1, CLEC3B, APOA4, GSN, PLIN5, SERPINA3, SAA, TF, C4A, ITIH3, SERPINA1
GO:0065008	Regulation of biological quality	1.6E-03	15	SERPIND1, VTN, HRG, APOB, TTR, APOE, CP, SERPING1, APOA4, GSN, PLIN5, SERPINA3, SAA, TF, SERPINA1

GO term ID	Description	Adjusted p-value	Gene count	Matching proteins in PPI network
GO Biological Process (n = 39, cont.)				
GO:0006950	Response to stress	1.7E-03	14	SERPIND1, HRG, APOE, ORM1, SERPING1, APOA4, CD5L, GSN, SERPINA3, SAA, TF, C4A, SERPINA1, IGLL5
GO:0001523	Retinoid metabolic process	2.4E-03	4	APOB, TTR, APOE, APOA4
GO:0065007	Biological regulation	4.6E-03	23	SERPIND1, VTN, HRG, APOB, TTR, APOE, ORM1, PZP, CP, FETUB, SERPING1, CLEC3B, APOA4, CD5L, GSN, PLIN5, SERPINA3, SAA, TF, C4A, ITIH3, SERPINA1, IGLL5
GO:0009605	Response to external stimulus	5.3E-03	11	SERPIND1, HRG, APOB, APOE, SERPING1, APOA4, GSN, SAA, TF, C4A, IGLL5
GO:0061024	Membrane organization	5.8E-03	7	APOB, APOE, APOA4, GSN, TF, SERPINA1, IGLL5
GO:0044419	Interspecies interaction between organisms	5.8E-03	10	HRG, APOB, APOE, SERPING1, APOA4, GSN, SAA, TF, C4A, IGLL5
GO:0051649	Establishment of localization in cell	6.0E-03	11	HRG, TTR, APOE, ORM1, SERPING1, CLEC3B, GSN, SERPINA3, TF, ITIH3, SERPINA1
GO:1905952	Regulation of lipid localization	6.1E-03	4	APOB, APOE, APOA4, PLIN5
GO:0002682	Regulation of immune system process	6.2E-03	9	VTN, HRG, APOE, ORM1, SERPING1, CD5L, GSN, C4A, IGLL5
GO:0048519	Negative regulation of biological process	6.8E-03	16	SERPIND1, VTN, HRG, APOE, ORM1, PZP, FETUB, SERPING1, APOA4, GSN, PLIN5, SERPINA3, SAA, C4A, ITIH3, SERPINA1
GO:0051641	Cellular localization	7.5E-03	12	HRG, TTR, APOE, ORM1, SERPING1, CLEC3B, GSN, PLIN5, SERPINA3, TF, ITIH3, SERPINA1
GO:0050776	Regulation of immune response	1.0E-02	7	VTN, HRG, APOE, SERPING1, CD5L, C4A, IGLL5
GO:0034382	Chylomicron remnant clearance	1.1E-02	2	APOB, APOE
GO:0010873	Positive regulation of cholesterol esterification	1.2E-02	2	APOE, APOA4
GO:0006826	Iron ion transport	1.4E-02	3	HRG, CP, TF
GO:0019216	Regulation of lipid metabolic process	1.9E-02	5	APOB, APOE, APOA4, PLIN5, SERPINA3
GO:0033700	Phospholipid efflux	1.9E-02	2	APOE, APOA4
GO:0042632	Cholesterol homeostasis	2.1E-02	3	APOB, APOE, APOA4
GO:0001775	Cell activation	2.4E-02	7	HRG, TTR, ORM1, GSN, SERPINA3, SAA, SERPINA1
GO:0042159	Lipoprotein catabolic process	2.5E-02	2	APOB, APOE
GO:0019538	Protein metabolic process	3.7E-02	13	SERPIND1, APOB, TTR, APOE, CP, SERPING1, APOA4, CD5L, GSN, SAA, TF, C4A, SERPINA1

GO term ID	Description	Adjusted p-value	Gene count	Matching proteins in PPI network
GO Biological Process (n = 39, cont.)				
GO:0050896	Response to stimulus	4.0E-02	18	SERPIND1, VTN, HRG, APOB, TTR, APOE, ORM1, SERPING1, CLEC3B, APOA4, CD5L, GSN, SERPINA3, SAA, TF, C4A, SERPINA1, IGLL5
GO:0008203	Cholesterol metabolic process	4.7E-02	3	APOB, APOE, APOA4
GO:0042157	Lipoprotein metabolic process	4.7E-02	3	APOB, APOE, APOA4
GO:0010954	Positive regulation of protein processing	4.9E-02	2	CLEC3B, GSN
GO:0008201	Heparin binding	7.7E-07	7	SERPIND1, VTN, HRG, APOB, APOE, CLEC3B, SAA
GO:0030234	Enzyme regulator activity	5.1E-06	11	SERPIND1, HRG, APOE, PZP, FETUB, SERPING1, APOA4, SERPINA3, C4A, ITIH3, SERPINA1
GO:0120020	Cholesterol transfer activity	1.3E-03	3	APOB, APOE, APOA4
GO:0098772	Molecular function regulator	9.9E-03	13	SERPIND1, HRG, TTR, APOE, PZP, FETUB, SERPING1, APOA4, SERPINA3, SAA, C4A, ITIH3, SERPINA1
GO:0035473	Lipase binding	1.2E-02	2	APOB, PLIN5
GO:0060228	Phosphatidylcholine-sterol o-acyltransferase activator activity	1.2E-02	2	APOE, APOA4
GO Cellular Component (n = 10)				
GO:0072562	Blood microparticle	2.7E-22	14	VTN, HRG, APOE, ORM1, PZP, CP, SERPING1, APOA4, CD5L, GSN, SERPINA3, TF, C4A, IGLL5
GO:0005615	Extracellular space	4.9E-14	22	SERPIND1, VTN, HRG, APOB, TTR, APOE, ORM1, PZP, CP, FETUB, SERPING1, CLEC3B, APOA4, CD5L, GSN, SERPINA3, SAA, TF, C4A, ITIH3, SERPINA1, IGLL5
GO:0062023	Collagen-containing extracellular matrix	8.2E-08	9	VTN, HRG, APOE, ORM1, SERPING1, CLEC3B, APOA4, SERPINA3, SERPINA1
GO:0012505	Endomembrane system	4.0E-05	17	SERPIND1, VTN, HRG, APOB, TTR, APOE, ORM1, CP, SERPING1, CLEC3B, APOA4, GSN, SERPINA3, TF, C4A, ITIH3, SERPINA1
GO:0070013	Intracellular organelle lumen	2.3E-04	18	SERPIND1, VTN, HRG, APOB, TTR, APOE, ORM1, CP, SERPING1, CLEC3B, APOA4, GSN, SERPINA3, SAA, TF, C4A, ITIH3, SERPINA1

GO term ID	Description	Adjusted p-value	Gene count	Matching proteins in PPI network
GO Cellular Component (n = 10, cont.)				
GO:0071682	Endocytic vesicle lumen	2.3E-04	3	APOB, APOE, SAA
GO:0030139	Endocytic vesicle	1.8E-03	5	APOB, APOE, GSN, SAA, TF
GO:0034363	Intermediate-density lipoprotein particle	2.7E-03	2	APOB, APOE
GO:0031089	Platelet dense granule lumen	1.1E-02	2	CLEC3B, ITIH3
GO:0043227	Membrane-bounded organelle	2.6E-02	22	SERPIND1, VTN, HRG, APOB, TTR, APOE, ORM1, PZP, CP, FETUB, SERPING1, CLEC3B, APOA4, GSN, PLIN5, SERPINA3, SAA, TF, C4A, ITIH3, SERPINA1, IGLL5
Reactome Pathways (n = 14)				
HSA-114608	Platelet degranulation	3.2E-08	8	HRG, ORM1, SERPING1, CLEC3B, SERPINA3, TF, ITIH3, SERPINA1
HSA-8957275	Post-translational protein phosphorylation	2.5E-07	7	SERPIND1, APOB, APOE, CP, TF, C4A, SERPINA1
HSA-381426	Regulation of Insulin-like Growth Factor (IGF) transport and uptake by Insulin-like Growth Factor Binding Proteins (IGFBPs)	5.0E-07	7	SERPIND1, APOB, APOE, CP, TF, C4A, SERPINA1
HSA-109582	Haemostasis	2.0E-06	10	SERPIND1, HRG, APOB, ORM1, SERPING1, CLEC3B, SERPINA3, TF, ITIH3, SERPINA1
HSA-168249	Innate Immune System	2.5E-04	10	VTN, APOB, TTR, ORM1, SERPING1, GSN, SERPINA3, SAA, C4A, SERPINA1
HSA-975634	Retinoid metabolism and transport	5.9E-04	4	APOB, TTR, APOE, APOA4
HSA-8963888	Chylomicron assembly	7.3E-04	3	APOB, APOE, APOA4
HSA-8963901	Chylomicron remodelling	7.3E-04	3	APOB, APOE, APOA4
HSA-977225	Amyloid fiber formation	3.2E-03	4	TTR, APOA4, GSN, SAA
HSA-392499	Metabolism of proteins	6.0E-03	11	SERPIND1, APOB, TTR, APOE, CP, APOA4, GSN, SAA, TF, C4A, SERPINA1
HSA-2173782	Binding and Uptake of Ligands by Scavenger Receptors	1.9E-02	3	APOB, APOE, SAA

HSA-8964026	Chylomicron clearance	2.6E-02	2	APOB, APOE
HSA-977606	Regulation of Complement cascade	2.6E-02	3	VTN, SERPING1, C4A
HSA-3000471	Scavenging by Class B Receptors	3.0E-02	2	APOB, SAA

Appendix Table S3. Gene Ontology (GO) terms on biological processes, molecular function and cellular components in comparison (g) - Serum at day 21 post-weaning versus serum at weaning day.

GO term ID	Description	Adjusted p-value	Gene count	Matching proteins in PPI network
		GO Biological Process (n = 56)		
GO:0016192	Vesicle-mediated transport	1.3E-11	21	VTN, HRG, APOB, APOA1, TTR, APOE, ORM1, AMBP, ITIH4, SERPING1, CLEC3B, F2, PLG, HP, CD5L, SERPINA3, SAA, TF, ITIH3, SERPINA1, IGLL5
GO:0030162	Regulation of proteolysis	2.3E-10	15	SERPIND1, VTN, HRG, APOE, PZP, FETUB, AMBP, ITIH4, SERPING1, CLEC3B, F2, SERPINA3, C4A, ITIH3, SERPINA1
GO:0006810	Transport	1.1E-08	25	VTN, APOC3, HRG, APOB, APOA1, TTR, APOE, ORM1, CP, AMBP, ITIH4, SERPING1, CLEC3B, F2, PLG, HP, APOA4, CD5L, SERPINA3, APOF, SAA, TF, ITIH3, SERPINA1, IGLL5
GO:0034371	Chylomicron remodelling	1.6E-08	5	APOC3, APOB, APOA1, APOE, APOA4
GO:0045055	Regulated exocytosis	1.8E-08	13	HRG, APOA1, TTR, ORM1, ITIH4, SERPING1, CLEC3B, PLG, HP, SERPINA3, TF, ITIH3, SERPINA1
GO:0051179	Localization	1.7E-07	26	VTN, APOC3, HRG, APOB, APOA1, TTR, APOE, ORM1, CP, AMBP, ITIH4, SERPING1, CLEC3B, F2, PLG, HP, APOA4, CD5L, PLIN5, SERPINA3, APOF, SAA, TF, ITIH3, SERPINA1, IGLL5
GO:0090207	Regulation of triglyceride metabolic process	2.5E-06	5	APOC3, APOA1, APOE, APOA4, PLIN5
GO:0033700	Phospholipid efflux	3.5E-06	4	APOC3, APOA1, APOE, APOA4
GO:0001523	Retinoid metabolic process	7.3E-06	6	APOC3, APOB, APOA1, TTR, APOE, APOA4
GO:0002376	Immune system process	8.3E-06	17	VTN, HRG, APOB, TTR, ORM1, SERPING1, F2, PLG, HP, APOA4, CD5L, SERPINA3, SAA, TF, C4A, SERPINA1, IGLL5
GO:0050878	Regulation of body fluid levels	1.9E-05	9	SERPIND1, VTN, HRG, APOE, SERPING1, F2, PLG, SAA, SERPINA1
GO:0043687	Post-translational protein modification	2.1E-05	8	SERPIND1, APOB, APOA1, APOE, CP, TF, C4A, SERPINA1
GO:0006954	Inflammatory response	2.1E-05	9	ORM1, ITIH4, F2, HP, CD5L, SERPINA3, SAA, C4A, SERPINA1
GO:0006950	Response to stress	2.3E-05	19	SERPIND1, HRG, APOA1, APOE, ORM1, ITIH4, SERPING1, F2, PLG, HP, APOA4, CD5L, GPX3, SERPINA3, SAA, TF, C4A, SERPINA1, IGLL5

GO term ID	Description	Adjusted p-value	Gene count	Matching proteins in PPI network
GO Biological Process (n = 56, cont.)				
GO:0065009	Regulation of molecular function	2.7E-05	22	SERPIND1, VTN, APOC3, HRG, APOA1, TTR, APOE, PZP, FETUB, AMBP, ITIH4, SERPING1, F2, HP, APOA4, PLIN5, SERPINA3, SAA, TF, C4A, ITIH3, SERPINA1
GO:1905952	Regulation of lipid localization	3.6E-05	6	APOC3, APOB, APOA1, APOE, APOA4, PLIN5
GO:0019216	Regulation of lipid metabolic process	6.1E-05	8	APOC3, APOB, APOA1, APOE, F2, APOA4, PLIN5, SERPINA3
GO:0070328	Triglyceride homeostasis	8.8E-05	4	APOC3, APOA1, APOE, APOA4
GO:0032489	Regulation of cdc42 protein signal transduction	9.0E-05	3	APOC3, APOA1, APOE
GO:0007596	Blood coagulation	9.2E-05	7	SERPIND1, HRG, SERPING1, F2, PLG, SAA, SERPINA1
GO:0002443	Leukocyte mediated immunity	9.8E-05	9	TTR, ORM1, SERPING1, F2, HP, SERPINA3, C4A, SERPINA1, IGLL5
GO:0048519	Negative regulation of biological process	1.2E-04	22	SERPIND1, VTN, APOC3, HRG, APOA1, APOE, ORM1, PZP, FETUB, AMBP, ITIH4, SERPING1, F2, PLG, HP, APOA4, PLIN5, SERPINA3, SAA, C4A, ITIH3, SERPINA1
GO:0010876	Lipid localization	1.3E-04	7	APOC3, APOB, APOA1, APOE, APOA4, PLIN5, APOF
GO:0051649	Establishment of localization in cell	1.5E-04	15	HRG, APOA1, TTR, APOE, ORM1, ITIH4, SERPING1, CLEC3B, F2, PLG, HP, SERPINA3, TF, ITIH3, SERPINA1
GO:0009611	Response to wounding	2.5E-04	8	SERPIND1, HRG, APOA1, SERPING1, F2, PLG, SAA, SERPINA1
GO:0042157	Lipoprotein metabolic process	2.6E-04	5	APOC3, APOB, APOA1, APOE, APOA4
GO:0051641	Cellular localization	3.8E-04	16	HRG, APOA1, TTR, APOE, ORM1, ITIH4, SERPING1, CLEC3B, F2, PLG, HP, PLIN5, SERPINA3, TF, ITIH3, SERPINA1
GO:0044419	Interspecies interaction between organisms	4.1E-04	13	HRG, APOB, APOE, AMBP, SERPING1, F2, PLG, HP, APOA4, SAA, TF, C4A, IGLL5
GO:0002697	Regulation of immune effector process	5.3E-04	7	VTN, APOA1, SERPING1, F2, CD5L, C4A, IGLL5
GO:0080090	Regulation of primary metabolic process	7.2E-04	22	SERPIND1, VTN, APOC3, HRG, APOB, APOA1, APOE, PZP, FETUB, AMBP, ITIH4, SERPING1, CLEC3B, F2, APOA4, PLIN5, SERPINA3, SAA, TF, C4A, ITIH3, SERPINA1
GO:0065008	Regulation of biological quality	8.2E-04	18	SERPIND1, VTN, APOC3, HRG, APOB, APOA1, TTR, APOE, CP, SERPING1, F2, PLG, APOA4, PLIN5, SERPINA3, SAA, TF, SERPINA1
GO:0006066	Alcohol metabolic process	1.5E-03	6	APOB, APOA1, TTR, APOE, APOA4, APOF

GO term ID	Description	Adjusted p-value	Gene count	Matching proteins in PPI network
GO Biological Process (n = 56, cont.)				
GO:0002682	Regulation of immune system process	1.6E-03	11	VTN, HRG, APOA1, APOE, ORM1, AMBP, SERPING1, F2, CD5L, C4A, IGLL5
GO:0019538	Protein metabolic process	1.6E-03	18	SERPIND1, APOC3, APOB, APOA1, TTR, APOE, CP, AMBP, SERPING1, F2, PLG, HP, APOA4, CD5L, SAA, TF, C4A, SERPINA1
GO:1901564	Organonitrogen compound metabolic process	1.6E-03	20	SERPIND1, APOC3, APOB, APOA1, TTR, APOE, CP, AMBP, ITIH4, SERPING1, F2, PLG, HP, APOA4, CD5L, SAA, TF, C4A, ITIH3, SERPINA1
GO:0051702	Interaction with symbiont	1.9E-03	4	HRG, APOE, F2, PLG
GO:0060191	Regulation of lipase activity	2.4E-03	4	APOC3, APOA1, APOA4, PLIN5
GO:0009605	Response to external stimulus	2.6E-03	13	SERPIND1, HRG, APOB, APOA1, APOE, SERPING1, F2, HP, APOA4, SAA, TF, C4A, IGLL5
GO:0006982	Response to lipid hydroperoxide	2.7E-03	2	APOA4, GPX3
GO:0010543	Regulation of platelet activation	2.9E-03	3	HRG, APOE, F2
GO:0050896	Response to stimulus	4.6E-03	24	SERPIND1, VTN, APOC3, HRG, APOB, APOA1, TTR, APOE, ORM1, ITIH4, SERPING1, CLEC3B, F2, PLG, HP, APOA4, CD5L, GPX3, SERPINA3, SAA, TF, C4A, SERPINA1, IGLL5
GO:0062012	Regulation of small molecule metabolic process	6.6E-03	6	APOC3, APOB, APOA1, APOE, APOA4, PLIN5
GO:0065007	Biological regulation	7.5E-03	29	SERPIND1, VTN, APOC3, HRG, APOB, APOA1, TTR, APOE, ORM1, PZP, CP, FETUB, AMBP, ITIH4, SERPING1, CLEC3B, F2, PLG, HP, APOA4, CD5L, PLIN5, SERPINA3, SAA, TF, C4A, ITIH3, SERPINA1, IGLL5
GO:0040011	Locomotion	9.5E-03	9	SERPIND1, VTN, HRG, APOB, APOA1, F2, PLG, SAA, IGLL5
GO:0032879	Regulation of localization	1.3E-02	13	VTN, APOC3, HRG, APOB, APOA1, APOE, F2, PLG, APOA4, PLIN5, SAA, TF, C4A
GO:0043170	Macromolecule metabolic process	1.3E-02	20	SERPIND1, APOC3, APOB, APOA1, TTR, APOE, CP, AMBP, ITIH4, SERPING1, F2, PLG, HP, APOA4, CD5L, SAA, TF, C4A, ITIH3, SERPINA1

GO term ID	Description	Adjusted p-value	Gene count	Matching proteins in PPI network
GO Biological Process (n = 56, cont.)				
GO:0061024	Membrane organization	1.8E-02	7	APOB, APOA1, APOE, APOA4, TF, SERPINA1, IGLL5
GO:0006826	Iron ion transport	1.8E-02	3	HRG, CP, TF
GO:0001775	Cell activation	1.8E-02	8	HRG, TTR, ORM1, F2, HP, SERPINA3, SAA, SERPINA1
GO:0046486	Glycerolipid metabolic process	2.4E-02	5	APOC3, APOB, APOA1, APOE, APOA4
GO:0042159	Lipoprotein catabolic process	2.6E-02	2	APOB, APOE
GO:0010810	Regulation of cell-substrate adhesion	2.8E-02	4	VTN, HRG, APOA1, PLG
GO:0016477	Cell migration	3.3E-02	7	VTN, APOB, APOA1, F2, PLG, SAA, IGLL5
GO:0032652	Regulation of interleukin-1 production	4.0E-02	3	APOA1, ORM1, SAA
GO:0062014	Negative regulation of small molecule metabolic process	4.6E-02	3	APOC3, APOE, PLIN5
GO:0048583	Regulation of response to stimulus	4.7E-02	15	VTN, APOC3, HRG, APOA1, APOE, AMBP, SERPING1, F2, PLG, CD5L, PLIN5, SAA, TF, C4A, IGLL5
GO Molecular Function (n = 14)				
GO:0030234	Enzyme regulator activity	5.0E-10	16	SERPIND1, APOC3, HRG, APOA1, APOE, PZP, FETUB, AMBP, ITIH4, SERPING1, F2, APOA4, SERPINA3, C4A, ITIH3, SERPINA1
GO:0008201	Heparin binding	1.9E-07	8	SERPIND1, VTN, HRG, APOB, APOE, CLEC3B, F2, SAA
GO:0070325	Lipoprotein particle receptor binding	6.3E-05	4	APOC3, APOB, APOA1, APOE
GO:0060228	Phosphatidylcholine-sterol o-acyltransferase activator activity	1.1E-04	3	APOA1, APOE, APOA4
GO:0005102	Signalling receptor binding	1.2E-04	13	VTN, APOC3, HRG, APOB, APOA1, TTR, APOE, F2, PLG, APOF, SAA, TF, IGLL5
GO:0098772	Molecular function regulator	1.5E-04	18	SERPIND1, APOC3, HRG, APOA1, TTR, APOE, PZP, FETUB, AMBP, ITIH4, SERPING1, F2, APOA4, SERPINA3, SAA, C4A, ITIH3, SERPINA1
GO:0015485	Cholesterol binding	3.9E-04	4	APOC3, APOA1, APOA4, APOF
GO:0005319	Lipid transporter activity	6.0E-04	5	APOB, APOA1, APOE, APOA4, APOF

GO term ID	Description	Adjusted p-value	Gene count	Matching proteins in PPI network
GO Molecular Function (n = 14, cont.)				
GO:0016209	Antioxidant activity	1.6E-03	4	APOE, HP, APOA4, GPX3
GO:0005515	Protein binding	3.6E-03	23	VTN, APOC3, HRG, APOB, APOA1, TTR, APOE, PZP, CP, AMBP, CLEC3B, F2, PLG, HP, APOA4, PLIN5, GPX3, APOF, SAA, TF, C4A, SERPINA1, IGLL5
GO:0070653	High-density lipoprotein particle receptor binding	5.0E-03	2	APOC3, APOA1
GO:0035473	Lipase binding	1.3E-02	2	APOB, PLIN5
GO:0004252	Serine-type endopeptidase activity	2.0E-02	4	F2, PLG, HP, CD5L
GO:0008289	Lipid binding	2.9E-02	7	APOC3, APOB, APOA1, APOE, F2, APOA4, APOF
GO term ID	**Description**	**Adjusted p-value**	**Gene count**	**Matching proteins in PPI network**
GO Cellular Component (n = 12)				
GO:0072562	Blood microparticle	6.3E-31	19	VTN, HRG, APOA1, APOE, ORM1, PZP, CP, AMBP, ITIH4, SERPING1, F2, PLG, HP, APOA4, CD5L, SERPINA3, TF, C4A, IGLL5
GO:0005615	Extracellular space	3.5E-20	30	SERPIND1, VTN, APOC3, HRG, APOB, APOA1, TTR, APOE, ORM1, PZP, CP, FETUB, AMBP, ITIH4, SERPING1, CLEC3B, F2, PLG, HP, APOA4, CD5L, GPX3, SERPINA3, APOF, SAA, TF, C4A, ITIH3, SERPINA1, IGLL5
GO:0062023	Collagen-containing extracellular matrix	4.0E-15	15	VTN, APOC3, HRG, APOA1, APOE, ORM1, AMBP, ITIH4, SERPING1, CLEC3B, F2, PLG, APOA4, SERPINA3, SERPINA1
GO:0071682	Endocytic vesicle lumen	4.5E-08	5	APOB, APOA1, APOE, HP, SAA
GO:0012505	Endomembrane system	2.0E-06	22	SERPIND1, VTN, APOC3, HRG, APOB, APOA1, TTR, APOE, ORM1, CP, ITIH4, SERPING1, CLEC3B, F2, PLG, HP, APOA4, SERPINA3, TF, C4A, ITIH3, SERPINA1
GO:0031089	Platelet dense granule lumen	1.8E-04	3	ITIH4, CLEC3B, ITIH3

GO term ID	Description	Adjusted p-value	Gene count	Matching proteins in PPI network
GO Cellular Component (n = 12, cont.)				
GO:0070013	Intracellular organelle lumen	2.2E-04	22	SERPIND1, VTN, HRG, APOB, APOA1, TTR, APOE, ORM1, CP, ITIH4, SERPING1, CLEC3B, F2, PLG, HP, APOA4, SERPINA3, SAA, TF, C4A, ITIH3, SERPINA1
GO:0030139	Endocytic vesicle	4.9E-04	6	APOB, APOA1, APOE, HP, SAA, TF
GO:0034365	Discoidal high-density lipoprotein particle	1.5E-03	2	APOA1, APOE
GO:0031232	Extrinsic component of external side of plasma membrane	6.5E-03	2	PLG, TF
GO:0043227	Membrane-bounded organelle	7.9E-03	29	SERPIND1, VTN, APOC3, HRG, APOB, APOA1, TTR, APOE, ORM1, PZP, CP, FETUB, AMBP, ITIH4, SERPING1, CLEC3B, F2, PLG, HP, APOA4, PLIN5, GPX3, SERPINA3, SAA, TF, C4A, ITIH3, SERPINA1, IGLL5
GO:0009986	Cell surface	1.5E-02	7	HRG, APOA1, AMBP, PLG, CD5L, TF, IGLL5
Pathway				
Reactome Pathways (n = 25)				
HSA-114608	Platelet degranulation	1.8E-12	11	HRG, APOA1, ORM1, ITIH4, SERPING1, CLEC3B, PLG, SERPINA3, TF, ITIH3, SERPINA1
HSA-76002	Platelet activation, signalling and aggregation	2.6E-11	12	HRG, APOA1, ORM1, ITIH4, SERPING1, CLEC3B, F2, PLG, SERPINA3, TF, ITIH3, SERPINA1
HSA-381426	Regulation of Insulin-like Growth Factor (IGF) transport and uptake by Insulin-like Growth Factor Binding Proteins (IGFBPs)	2.7E-11	10	SERPIND1, APOB, APOA1, APOE, CP, F2, PLG, TF, C4A, SERPINA1
HSA-109582	Haemostasis	4.8E-10	14	SERPIND1, HRG, APOB, APOA1, ORM1, ITIH4, SERPING1, CLEC3B, F2, PLG, SERPINA3, TF, ITIH3, SERPINA1
HSA-8957275	Post-translational protein phosphorylation	2.2E-08	8	SERPIND1, APOB, APOA1, APOE, CP, TF, C4A, SERPINA1
HSA-8963888	Chylomicron assembly	5.2E-08	5	APOC3, APOB, APOA1, APOE, APOA4
HSA-8963899	Plasma lipoprotein remodelling	5.2E-08	6	APOC3, APOB, APOA1, APOE, APOA4, APOF

Pathway	Description	Adjusted p-value	Gene count	Matching proteins in PPI network
Reactome Pathways (n = 25, cont.)				
HSA-8963901	Chylomicron remodelling	5.2E-08	5	APOC3, APOB, APOA1, APOE, APOA4
HSA-2173782	Binding and Uptake of Ligands by Scavenger Receptors	1.7E-07	6	APOB, APOA1, APOE, AMBP, HP, SAA
HSA-975634	Retinoid metabolism and transport	2.2E-07	6	APOC3, APOB, APOA1, TTR, APOE, APOA4
HSA-168249	Innate Immune System	3.0E-04	11	VTN, APOB, TTR, ORM1, SERPING1, F2, HP, SERPINA3, SAA, C4A, SERPINA1
HSA-3000471	Scavenging by Class B Receptors	3.1E-04	3	APOB, APOA1, SAA
HSA-8964058	HDL remodelling	9.3E-04	3	APOC3, APOA1, APOE
HSA-977606	Regulation of Complement cascade	1.1E-03	4	VTN, SERPING1, F2, C4A
HSA-2168880	Scavenging of heme from plasma	1.6E-03	3	APOA1, AMBP, HP
HSA-418594	G alpha (i) signalling events	2.0E-03	7	APOC3, APOB, APOA1, TTR, APOE, APOA4, SAA
HSA-392499	Metabolism of proteins	3.0E-03	13	SERPIND1, APOB, APOA1, TTR, APOE, CP, F2, PLG, APOA4, SAA, TF, C4A, SERPINA1
HSA-3000480	Scavenging by Class A Receptors	3.2E-03	3	APOB, APOA1, APOE
HSA-5653656	Vesicle-mediated transport	4.6E-03	8	APOB, APOA1, APOE, AMBP, HP, SAA, TF, SERPINA1
HSA-977225	Amyloid fiber formation	5.3E-03	4	APOA1, TTR, APOA4, SAA
HSA-140837	Intrinsic Pathway of Fibrin Clot Formation	5.6E-03	3	SERPIND1, SERPING1, F2
HSA-382551	Transport of small molecules	7.8E-03	8	APOC3, APOB, APOA1, APOE, CP, APOA4, APOF, TF
HSA-8964043	Plasma lipoprotein clearance	1.4E-02	3	APOB, APOA1, APOE
HSA-8964041	LDL remodelling	2.0E-02	2	APOB, APOF
HSA-8964026	Chylomicron clearance	2.7E-02	2	APOB, APOE

Appendix Table S4. Gene Ontology (GO) terms on biological processes, molecular function and cellular components in comparison LR versus CR ileum. The network is expanded with maximum 5 interactors shown in the first shell. CR: piglet born from sow fed diet with ω6:ω3 ratio = 13:1 during gestation, starting from day 28 (G28) and 10:1 during lactation; LR: piglet born from sow fed diet with ω6:ω3 ratio = 4:1 from G28 until the end of lactation.

GO term ID	Description	Adjusted p-value	Gene count	Matching proteins in PPI network
GO Biological Process (n = 11)				
GO:0019083	Viral transcription	1.4E-05	5	RPL18A, RPL19, RPS12, RPS16, RPSA
GO:0006413	Translational initiation	1.4E-05	5	RPL18A, RPL19, RPS12, RPS16, RPSA
GO:0016032	Viral process	7.1E-04	6	RPL18A, RPL19, RPS12, RPS16, RPSA, CALM1
GO:0002181	Cytoplasmic translation	3.7E-03	3	RPL18A, RPL19, RPSA
GO:0006810	Transport	6.1E-03	9	RPL18A, RPL19, RPS12, RPS16, CCT7, CCT2, RPSA, PDLIM7, CALM1
GO:1904871	Positive regulation of protein localization to Cajal body	8.6E-03	2	CCT7, CCT2
GO:1901566	Organonitrogen compound biosynthetic process	8.6E-03	6	RPL18A, RPL19, RPS12, RPS16, RPSA, GFPT1
GO:1904874	Positive regulation of telomerase RNA localization to Cajal body	1.3E-02	2	CCT7, CCT2
GO:0051649	Establishment of localization in cell	1.3E-02	7	RPL18A, RPL19, RPS12, RPS16, CCT2, RPSA, CALM1
GO:0044248	Cellular catabolic process	2.7E-02	6	RPL18A, RPL19, RPS12, RPS16, RPSA, CALM1
GO:0032212	Positive regulation of telomere maintenance via telomerase	4.6E-02	2	CCT7, CCT2
GO Molecular Function (n = 1)				
GO:0003735	Structural constituent of ribosome	4.9E-05	5	RPL18A, RPL19, RPS12, RPS16, RPSA
GO Cellular Component (n = 4)				
GO:0005829	Cytosol	8.6E-04	10	RPL18A, RPL19, RPS12, RPS16, CCT7, CCT2, RPSA, PDLIM7, CALM1, GFPT1
GO:0005832	Chaperonin-containing t-complex	4.7E-03	2	CCT7, CCT2
GO:0032991	Protein-containing complex	9.1E-03	9	RPL18A, RPL19, RPS12, RPS16, CCT7, CCT2, RPSA, PDLIM7, CALM1
GO:0042788	Polysomal ribosome	2.5E-02	2	RPL18A, RPL19

Pathway	Description	Adjusted p-value	Gene count	Matching proteins in PPI network
	Reactome Pathways (n = 22)			
HSA-156827	L13a-mediated translational silencing of Ceruloplasmin expression	8.8E-06	5	RPL18A, RPL19, RPS12, RPS16, RPSA
HSA-156902	Peptide chain elongation	8.8E-06	5	RPL18A, RPL19, RPS12, RPS16, RPSA
HSA-1799339	SRP-dependent co-translational protein targeting to membrane	8.8E-06	5	RPL18A, RPL19, RPS12, RPS16, RPSA
HSA-192823	Viral mRNA Translation	8.8E-06	5	RPL18A, RPL19, RPS12, RPS16, RPSA
HSA-2408557	Selenocysteine synthesis	8.8E-06	5	RPL18A, RPL19, RPS12, RPS16, RPSA
HSA-72689	Formation of a pool of free 40S subunits	8.8E-06	5	RPL18A, RPL19, RPS12, RPS16, RPSA
HSA-72706	GTP hydrolysis and joining of the 60S ribosomal subunit	8.8E-06	5	RPL18A, RPL19, RPS12, RPS16, RPSA
HSA-72764	Eukaryotic Translation Termination	8.8E-06	5	RPL18A, RPL19, RPS12, RPS16, RPSA
HSA-9633012	Response of EIF2AK4 (GCN2) to amino acid deficiency	8.8E-06	5	RPL18A, RPL19, RPS12, RPS16, RPSA
HSA-975956	Nonsense Mediated Decay (NMD) independent of the Exon Junction Complex (EJC)	8.8E-06	5	RPL18A, RPL19, RPS12, RPS16, RPSA
HSA-975957	Nonsense Mediated Decay (NMD) enhanced by the Exon Junction Complex (EJC)	8.8E-06	5	RPL18A, RPL19, RPS12, RPS16, RPSA
HSA-9010553	Regulation of expression of SLITs and ROBOs	1.1E-05	5	RPL18A, RPL19, RPS12, RPS16, RPSA
HSA-6791226	Major pathway of rRNA processing in the nucleolus and cytosol	1.5E-05	5	RPL18A, RPL19, RPS12, RPS16, RPSA
HSA-422475	Axon guidance	6.8E-05	6	RPL18A, RPL19, RPS12, RPS16, RPSA, PDLIM7
HSA-392499	Metabolism of proteins	2.6E-04	8	RPL18A, RPL19, RPS12, RPS16, CCT7, CCT2, RPSA, GFPT1
HSA-72695	Formation of the ternary complex, and subsequently, the 43S complex	1.3E-03	3	RPS12, RPS16, RPSA
HSA-72649	Translation initiation complex formation	1.7E-03	3	RPS12, RPS16, RPSA
HSA-72702	Ribosomal scanning and start codon recognition	1.7E-03	3	RPS12, RPS16, RPSA
HSA-390450	Folding of actin by CCT/TriC	7.3E-03	2	CCT7, CCT2
HSA-1643685	Disease	1.8E-02	6	RPL18A, RPL19, RPS12, RPS16, RPSA, GFPT1
HSA-389960	Formation of tubulin folding intermediates by CCT/TriC	3.3E-02	2	CCT7, CCT2
HSA-389957	Prefoldin mediated transfer of substrate to CCT/TriC	4.0E-02	2	CCT7, CCT2

Appendix Table S5. Gene Ontology (GO) terms on biological processes, molecular function and cellular components in comparison SW versus CT ileum. The network is expanded with maximum 5 interactors shown in the first shell. SW: piglet diet with seaweed supplementation, CT: piglet diet without seaweed supplementation.

GO term ID	Description	Adjusted p-value	Gene count	Matching proteins in PPI network
	GO Biological Process (n = 18)			
GO:0042407	Cristae formation	1.3E-04	4	ATP5D, ATP5E, ATP5B, ATP5A1
GO:0009058	Biosynthetic process	8.1E-04	14	DCN, RFC2, ATP5D, ATP5E, RPA1, CDK4, ATP5B, CKB, CKMT1B, ALDH9A1, PCNA, ALDOA, ATP5A1, SERPINH1
GO:1902600	Proton transmembrane transport	1.1E-03	5	ATP5D, ATP5E, ATP5B, ATP5A1, ATP1A1
GO:0090407	Organophosphate biosynthetic process	1.9E-03	7	ATP5D, ATP5E, ATP5B, CKB, CKMT1B, ALDOA, ATP5A1
GO:0070987	Error-free translesion synthesis	2.3E-03	3	RFC2, RPA1, PCNA
GO:1901576	Organic substance biosynthetic process	2.4E-03	13	DCN, RFC2, ATP5D, ATP5E, RPA1, CDK4, ATP5B, CKB, CKMT1B, ALDH9A1, PCNA, ALDOA, ATP5A1
GO:0032201	Telomere maintenance via semi-conservative replication	2.8E-03	3	RFC2, RPA1, PCNA
GO:0006091	Generation of precursor metabolites and energy	3.8E-03	6	ATP5D, ACO2, ATP5E, ATP5B, ALDOA, ATP5A1
GO:0044281	Small molecule metabolic process	5.9E-03	10	DCN, ATP5D, ACO2, ECH1, ATP5E, ATP5B, CKB, CKMT1B, ALDOA, ATP5A1
GO:0006296	Nucleotide-excision repair, DNA incision, 5-to lesion	6.2E-03	3	RFC2, RPA1, PCNA
GO:0097435	Supramolecular fiber organization	7.6E-03	6	KRT20, VIL1, KRT19, ALDOA, SERPINH1, KRT8
GO:0008152	Metabolic process	1.3E-02	20	DCN, RFC2, ATP5D, ACO2, ECH1, CTSD, ATP5E, RPA1, CDK4, ATP5B, CKB, CKMT1B, ALDH9A1, PCNA, PSME1, ALDOA, ATP5A1, H2AFX, SERPINH1, ATP1A1
GO:0006600	Creatine metabolic process	1.7E-02	2	CKB, CKMT1B
GO:1901137	Carbohydrate derivative biosynthetic process	1.9E-02	6	DCN, ATP5D, ATP5E, ATP5B, ALDOA, ATP5A1
GO:0019725	Cellular homeostasis	1.9E-02	7	RFC2, RPA1, ATP5B, CKB, PCNA, ALDOA, ATP1A1

GO term ID	Description	Adjusted p-value	Gene count	Matching proteins in PPI network
GO Biological Process (n = 18, cont.)				
GO:1900264	Positive regulation of DNA -directed DNA polymerase activity	2.0E-02	2	RFC2, PCNA
GO:0071704	Organic substance metabolic process	2.3E-02	19	DCN, RFC2, ATP5D, ACO2, ECH1, CTSD, ATP5E, RPA1, CDK4, ATP5B, CKB, CKMT1B, ALDH9A1, PCNA, PSME1, ALDOA, ATP5A1, H2AFX, SERPINH1
GO:0010632	Regulation of epithelial cell migration	3.6E-02	4	DCN, VIL1, ATP5B, ATP5A1
GO Molecular Function (n = 4)				
GO:0046933	Proton-transporting ATP synthase activity, rotational mechanism	1.2E-05	4	ATP5D, ATP5E, ATP5B, ATP5A1
GO:0043532	Angiostatin binding	3.0E-02	2	ATP5B, ATP5A1
GO:0004111	Creatine kinase activity	4.2E-02	2	CKB, CKMT1B
GO:0003684	Damaged DNA binding	4.8E-02	3	RPA1, PCNA, H2AFX
GO Cellular Component (n = 13)				
GO:0045261	Proton-transporting ATP synthase complex, catalytic core f(1)	8.9E-07	4	ATP5D, ATP5E, ATP5B, ATP5A1
GO:0005615	Extracellular space	1.6E-05	16	DCN, ECH1, CTSD, VIL1, ATP5B, CKB, ALDH9A1, KRT19, PCNA, PSME1, ALDOA, ATP5A1, H2AFX, SERPINH1, ATP1A1, KRT8
GO:0005657	Replication fork	3.0E-04	4	RFC2, RPA1, PCNA, H2AFX
GO:0070013	Intracellular organelle lumen	7.1E-03	17	DCN, RFC2, ATP5D, ACO2, ECH1, CTSD, ATP5E, RPA1, CDK4, ATP5B, PCNA, PSME1, ALDOA, ATP5A1, H2AFX, SERPINH1, KRT8
GO:0043226	Organelle	1.9E-02	24	DCN, RFC2, KRT20, ATP5D, ACO2, ECH1, CTSD, ATP5E, VIL1, RPA1, CDK4, ATP5B, CKB, CKMT1B, ALDH9A1, KRT19, PCNA, PSME1, ALDOA, ATP5A1, H2AFX, SERPINH1, ATP1A1, KRT8
GO:0005743	Mitochondrial inner membrane	3.4E-02	5	ATP5D, ATP5E, ATP5B, CKMT1B, ATP5A1
GO:0043227	Membrane-bounded organelle	3.4E-02	23	DCN, RFC2, ATP5D, ACO2, ECH1, CTSD, ATP5E, VIL1, RPA1, CDK4, ATP5B, CKB, CKMT1B, ALDH9A1, KRT19, PCNA, PSME1, ALDOA, ATP5A1, H2AFX, SERPINH1, ATP1A1, KRT8
GO:0098796	Membrane protein complex	3.4E-02	7	ATP5D, ATP5E, ATP5B, KRT19, ATP5A1, ATP1A1, KRT8

GO term ID	Description	Adjusted p-value	Gene count	Matching proteins in PPI network
GO Cellular Component (n = 13, cont.)				
GO:0016010	Dystrophin-associated glycoprotein complex	3.4E-02	2	KRT19, KRT8
GO:0043034	Costamere	3.4E-02	2	KRT19, KRT8
GO:0016327	Apicolateral plasma membrane	3.4E-02	2	KRT19, KRT8
GO:0005622	Intracellular	4.1E-02	24	DCN, RFC2, KRT20, ATP5D, ACO2, ECH1, CTSD, ATP5E, VIL1, RPA1, CDK4, ATP5B, CKB, CKMT1B, ALDH9A1, KRT19, PCNA, PSME1, ALDOA, ATP5A1, H2AFX, SERPINH1, ATP1A1, KRT8
GO:0042383	Sarcolemma	4.5E-02	3	KRT19, ATP1A1, KRT8
Pathway				
Reactome Pathways (n = 31)				
HSA-163210	Formation of ATP by chemiosmotic coupling	2.2E-04	4	ATP5D, ATP5E, ATP5B, ATP5A1
HSA-8949613	Cristae formation	7.7E-04	4	ATP5D, ATP5E, ATP5B, ATP5A1
HSA-110312	Translesion synthesis by REV1	8.1E-03	3	RFC2, RPA1, PCNA
HSA-110320	Translesion synthesis by POLH	8.1E-03	3	RFC2, RPA1, PCNA
HSA-1428517	The citric acid (TCA) cycle and respiratory electron transport	8.1E-03	5	ATP5D, ACO2, ATP5E, ATP5B, ATP5A1
HSA-157579	Telomere Maintenance	8.1E-03	4	RFC2, RPA1, PCNA, H2AFX
HSA-5651801	PCNA-Dependent Long Patch Base Excision Repair	8.1E-03	3	RFC2, RPA1, PCNA
HSA-5655862	Translesion synthesis by POLK	8.1E-03	3	RFC2, RPA1, PCNA
HSA-5656121	Translesion synthesis by POLI	8.1E-03	3	RFC2, RPA1, PCNA
HSA-5696397	Gap-filling DNA repair synthesis and ligation in GG-NER	8.1E-03	3	RFC2, RPA1, PCNA
HSA-69186	Lagging Strand Synthesis	8.1E-03	3	RFC2, RPA1, PCNA
HSA-69242	S Phase	8.1E-03	5	RFC2, RPA1, CDK4, PCNA, PSME1
HSA-73884	Base Excision Repair	8.1E-03	4	RFC2, RPA1, PCNA, H2AFX

Pathway	Description	Adjusted p-value	Gene count	Matching proteins in PPI network
		Reactome Pathways (n = 31, cont.)		
HSA-110314	Recognition of DNA damage by PCNA-containing replication complex	9.3E-03	3	RFC2, RPA1, PCNA
HSA-5656169	Termination of translesion DNA synthesis	9.9E-03	3	RFC2, RPA1, PCNA
HSA-1430728	Metabolism	1.1E-02	11	DCN, ATP5D, ACO2, ATP5E, ATP5B, CKB, CKMT1B, ALDH9A1, PSME1, ALDOA, ATP5A1
HSA-174417	Telomere C-strand (Lagging Strand) Synthesis	1.1E-02	3	RFC2, RPA1, PCNA
HSA-5693567	HDR through Homologous Recombination (HRR) or Single Strand Annealing (SSA)	1.1E-02	4	RFC2, RPA1, PCNA, H2AFX
HSA-69239	Synthesis of DNA	1.1E-02	4	RFC2, RPA1, PCNA, PSME1
HSA-69206	G1/S Transition	1.2E-02	4	RPA1, CDK4, PCNA, PSME1
HSA-5696400	Dual Incision in GG-NER	1.2E-02	3	RFC2, RPA1, PCNA
HSA-69278	Cell Cycle, Mitotic	1.8E-02	6	RFC2, RPA1, CDK4, PCNA, PSME1, H2AFX
HSA-69481	G2/M Checkpoints	1.8E-02	4	RFC2, RPA1, PSME1, H2AFX
HSA-9609507	Protein localization	2.1E-02	4	ACO2, ECH1, ATP5B, ATP5A1
HSA-912446	Meiotic recombination	2.2E-02	3	RPA1, CDK4, H2AFX
HSA-1268020	Mitochondrial protein import	3.3E-02	3	ACO2, ATP5B, ATP5A1
HSA-5685942	HDR through Homologous Recombination (HRR)	3.3E-02	3	RFC2, RPA1, PCNA
HSA-6782135	Dual incision in TC-NER	3.3E-02	3	RFC2, RPA1, PCNA
HSA-6782210	Gap-filling DNA repair synthesis and ligation in TC-NER	3.3E-02	3	RFC2, RPA1, PCNA
HSA-71288	Creatine metabolism	3.8E-02	2	CKB, CKMT1B
HSA-69473	G2/M DNA damage checkpoint	5.0E-02	3	RFC2, RPA1, H2AFX

Appendix Table S6. Gene Ontology (GO) terms on biological processes, molecular function and cellular components, respectively, after reducing the redundancy between GO terms by REVIGO and Reactome pathways corresponding to comparison between LRCT and CRCT ileum. The network is expanded with maximum 5 interactors shown in the first shell. CRCT: piglets fed no seaweed (SW, *Ascophyllum nodosum*), which nursed by sows fed dietary ω6:ω3 ratio = 13:1 during gestation, starting from day 28 (G28) and 10:1 during lactation. LRCT: piglets fed no SW, which nursed by sows fed dietary ω6:ω3 ratio = 4:1 from G28 until the end of lactation.

GO term ID	Description	Adjusted p-value	Gene count	Matching proteins in PPI network
		GO Biological Process (n = 13)		
GO:1904871	Positive regulation of protein localization to Cajal body	2.0E-03	3	CCT7, CCT6A, CCT8
GO:1904874	Positive regulation of telomerase RNA localization to Cajal body	2.0E-03	3	CCT7, CCT6A, CCT8
GO:0035567	Non-canonical WNT signalling pathway	5.4E-03	4	AP2S1, CALM1, GNB1, AP2B1
GO:0010659	Cardiac muscle cell apoptotic process	9.7E-03	2	GNGT1, GNB1
GO:0006101	Citrate metabolic process	1.1E-02	2	ACO2, ACLY
GO:0006457	Protein folding	1.9E-02	4	CCT7, CCT6A, CCT8, GNB1
GO:0051130	Positive regulation of cellular component organization	2.2E-02	7	VASP, CCT7, CCT6A, CCT8, CAPN2, YWHAQ, AP2B1
GO:0032802	Low-density lipoprotein particle receptor catabolic process	2.5E-02	2	AP2S1, AP2B1
GO:0051128	Regulation of cellular component organization	2.8E-02	9	VASP, CCT7, AP2S1, CCT6A, CCT8, CAPN2, DPYSL2, YWHAQ, AP2B1
GO:0016056	Rhodopsin mediated signalling pathway	2.8E-02	2	GNGT1, GNB1
GO:0019886	Antigen processing and presentation of exogenous peptide antigen via MHC class II	3.5E-02	3	CTSD, AP2S1, AP2B1
GO:0050896	Response to stimulus	3.5E-02	15	ACO2, CTSD, VASP, GNG13, GNGT1, ACLY, AP2S1, CCT8, CAPN2, DPYSL2, CALM1, STIP1, YWHAQ, GNB1, AP2B1

GO term ID	Description	Adjusted p-value	Gene count	Matching proteins in PPI network
GO Cellular Component (n = 15)				
GO:0048268	Clathrin coat assembly	4.6E-02	2	AP2S1, AP2B1
GO:0101031	Chaperone complex	1.3E-05	4	CCT7, CCT6A, CCT8, STIP1
GO:0005832	Chaperonin-containing T-complex	1.3E-04	3	CCT7, CCT6A, CCT8
GO:0031982	Vesicle	4.4E-04	13	CTSD, VASP, ACLY, CCT7, AP2S1, CCT6A, CCT8, CAPN2, DPYSL2, CALM1, YWHAQ, GNB1, AP2B1
GO:0005829	Cytosol	5.5E-04	14	ACO2, VASP, ACLY, CCT7, AP2S1, CCT6A, CCT8, CAPN2, DPYSL2, CALM1, STIP1, YWHAQ, GNB1, AP2B1
GO:0070062	Extracellular exosome	5.5E-04	10	CTSD, VASP, ACLY, CCT7, CCT6A, CCT8, CAPN2, DPYSL2, YWHAQ, GNB1
GO:0098797	Plasma membrane protein complex	8.7E-03	5	GNG13, GNGT1, AP2S1, GNB1, AP2B1
GO:0005576	Extracellular region	1.2E-02	11	CTSD, VASP, ACLY, CCT7, CCT6A, CCT8, CAPN2, DPYSL2, CALM1, YWHAQ, GNB1
GO:1904813	ficolin-1-rich granule lumen	1.4E-02	3	CTSD, ACLY, CCT8
GO:0097381	Photoreceptor disc membrane	1.6E-02	2	GNGT1, GNB1
GO:0098796	Membrane protein complex	1.7E-02	6	GNG13, GNGT1, AP2S1, CALM1, GNB1, AP2B1
GO:0005874	Microtubule	2.0E-02	4	CCT7, CCT6A, CCT8, CALM1
GO:0005775	Vacuolar lumen	2.3E-02	3	CTSD, ACLY, CCT8
GO:0032991	Protein-containing complex	3.8E-02	11	GNG13, GNGT1, CCT7, AP2S1, CCT6A, CCT8, CALM1, STIP1, YWHAQ, GNB1, AP2B1
GO:0098552	Side of membrane	4.2E-02	4	GNG13, GNGT1, CAPN2, GNB1
GO:0001917	Photoreceptor inner segment	4.7E-02	2	GNGT1, GNB1
Reactome Pathways (n = 51)				
HSA-6814122	Cooperation of PDCL (PhLP1) and TRiC/CCT in G-protein beta folding	4.1E-09	6	GNG13, GNGT1, CCT7, CCT6A, CCT8, GNB1
HSA-3858494	Beta-catenin independent WNT signalling	7.0E-05	5	GNG13, GNGT1, AP2S1, GNB1, AP2B1
HSA-390450	Folding of actin by CCT/TriC	7.0E-05	3	CCT7, CCT6A, CCT8

Pathway	Description	Adjusted p-value	Gene count	Matching proteins in PPI network
		Reactome Pathways (n = 51, cont.)		
HSA-389960	Formation of tubulin folding intermediates by CCT/TriC	2.6E-04	3	CCT7, CCT6A, CCT8
HSA-392170	ADP signalling through P2Y purinoceptor 12	2.6E-04	3	GNG13, GNGT1, GNB1
HSA-392451	G beta:gamma signalling through PI3Kgamma	2.6E-04	3	GNG13, GNGT1, GNB1
HSA-392851	Prostacyclin signalling through prostacyclin receptor	2.6E-04	3	GNG13, GNGT1, GNB1
HSA-418217	G beta:gamma signalling through PLC beta	2.6E-04	3	GNG13, GNGT1, GNB1
HSA-418592	ADP signalling through P2Y purinoceptor 1	2.6E-04	3	GNG13, GNGT1, GNB1
HSA-428930	Thromboxane signalling through TP receptor	2.6E-04	3	GNG13, GNGT1, GNB1
HSA-500657	Presynaptic function of Kainate receptors	2.6E-04	3	GNG13, GNGT1, GNB1
HSA-8964315	G beta:gamma signalling through BTK	2.6E-04	3	GNG13, GNGT1, GNB1
HSA-8964616	G beta:gamma signalling through CDC42	2.6E-04	3	GNG13, GNGT1, GNB1
HSA-1296041	Activation of G protein gated Potassium channels	2.8E-04	3	GNG13, GNGT1, GNB1
HSA-163685	Integration of energy metabolism	2.8E-04	4	GNG13, GNGT1, ACLY, GNB1
HSA-202040	G-protein activation	2.8E-04	3	GNG13, GNGT1, GNB1
HSA-389957	Prefoldin mediated transfer of substrate to CCT/TriC	2.8E-04	3	CCT7, CCT6A, CCT8
HSA-400042	Adrenaline,noradrenaline inhibits insulin secretion	2.8E-04	3	GNG13, GNGT1, GNB1

Pathway	Description	Adjusted p-value	Gene count	Matching proteins in PPI network
	Reactome Pathways (n = 51, cont.)			
HSA-456926	Thrombin signalling through proteinase activated receptors (PARs)	2.8E-04	3	GNG13, GNGT1, GNB1
HSA-997272	Inhibition of voltage gated Ca2+ channels via Gbeta/gamma subunits	2.8E-04	3	GNG13, GNGT1, GNB1
HSA-420092	Glucagon-type ligand receptors	2.9E-04	3	GNG13, GNGT1, GNB1
HSA-390471	Association of TriC/CCT with target proteins during biosynthesis	4.0E-04	3	CCT7, CCT6A, CCT8
HSA-381676	Glucagon-like Peptide-1 (GLP1) regulates insulin secretion	4.8E-04	3	GNG13, GNGT1, GNB1
HSA-432040	Vasopressin regulates renal water homeostasis via Aquaporins	5.0E-04	3	GNG13, GNGT1, GNB1
HSA-437239	Recycling pathway of L1	5.9E-04	3	AP2S1, DPYSL2, AP2B1
HSA-418597	G alpha (z) signalling events	6.1E-04	3	GNG13, GNGT1, GNB1
HSA-8939211	ESR-mediated signalling	1.0E-03	4	CTSD, GNG13, GNGT1, GNB1
HSA-4086398	Ca2+ pathway	1.1E-03	3	GNG13, GNGT1, GNB1
HSA-182218	Nef Mediated CD8 Down-regulation	1.2E-03	2	AP2S1, AP2B1
HSA-167590	Nef Mediated CD4 Down-regulation	1.8E-03	2	AP2S1, AP2B1
HSA-9009391	Extra-nuclear estrogen signalling	1.8E-03	3	GNG13, GNGT1, GNB1
HSA-416482	G alpha (12/13) signalling events	2.0E-03	3	GNG13, GNGT1, GNB1
HSA-2485179	Activation of the phototransduction cascade	2.4E-03	2	GNGT1, GNB1
HSA-8866427	VLDLR internalisation and degradation	2.7E-03	2	AP2S1, AP2B1
HSA-5140745	WNT5A-dependent internalization of FZD2, FZD5 and ROR2	2.9E-03	2	AP2S1, AP2B1

Pathway	Description	Adjusted p-value	Gene count	Matching proteins in PPI network
	Reactome Pathways (n = 51, cont.)			
HSA-177504	Retrograde neurotrophin signalling	3.2E-03	2	AP2S1, AP2B1
HSA-5099900	WNT5A-dependent internalization of FZD4	3.6E-03	2	AP2S1, AP2B1
HSA-416993	Trafficking of GluR2-containing AMPA receptors	4.4E-03	2	AP2S1, AP2B1
HSA-2132295	MHC class II antigen presentation	5.3E-03	3	CTSD, AP2S1, AP2B1
HSA-8964038	LDL clearance	5.3E-03	2	AP2S1, AP2B1
HSA-9660821	ADORA2B mediated anti-inflammatory cytokines production	6.8E-03	3	GNG13, GNGT1, GNB1
HSA-382551	Transport of small molecules	9.7E-03	5	GNG13, GNGT1, AP2S1, GNB1, AP2B1
HSA-163359	Glucagon signalling in metabolic regulation	1.3E-02	2	GNG13, GNB1
HSA-2514859	Inactivation, recovery and regulation of the phototransduction cascade	1.3E-02	2	GNGT1, GNB1
HSA-5663205	Infectious disease	1.6E-02	5	GNG13, GNGT1, AP2S1, GNB1, AP2B1
HSA-416476	G alpha (q) signalling events	2.3E-02	3	GNG13, GNGT1, GNB1
HSA-392499	Metabolism of proteins	2.4E-02	7	CTSD, GNG13, GNGT1, CCT7, CCT6A, CCT8, GNB1
HSA-3928665	EPH-ephrin mediated repulsion of cells	2.6E-02	2	AP2S1, AP2B1
HSA-422475	Axon guidance	3.0E-02	4	VASP, AP2S1, DPYSL2, AP2B1
HSA-1643685	Disease	3.7E-02	6	GNG13, GNGT1, AP2S1, CAPN2, GNB1, AP2B1

Appendix Table S7. Gene Ontology (GO) terms on biological processes, molecular function and cellular components, respectively, after reducing the redundancy between GO terms by REVIGO and Reactome pathways corresponding to comparison between CRSW and CRCT ileum. The network is expanded with maximum 5 interactors shown in the first shell. CRCT: piglets fed no seaweed (SW, *Ascophyllum nodosum*), which nursed by sows fed dietary ω6:ω3 ratio = 13:1 during gestation, starting from day 28 (G28) and 10:1 during lactation. CRSW: piglets fed SW, which nursed by sows fed dietary ω6:ω3 ratio = 13:1 from G28 until the end of lactation.

GO term ID	Description	Adjusted p-value	Gene count	Matching proteins in PPI network
		GO Biological Process (n = 15)		
GO:0019083	Viral transcription	7.5E-05	6	RPL18A, RPL19, RPS12, RPS16, RPL10A, RPL24
GO:0000184	Nuclear-transcribed mRNA catabolic process, nonsense-mediated decay	7.8E-05	6	RPL18A, RPL19, RPS12, RPS16, RPL10A, RPL24
GO:0006413	Translational initiation	1.6E-04	6	RPL18A, RPL19, RPS12, RPS16, RPL10A, RPL24
GO:0090150	Establishment of protein localization to membrane	2.6E-04	7	RPL18A, RPL19, RPS12, RPS16, RAB10, RPL10A, RPL24
GO:0006810	Transport	1.9E-03	19	RPL18A, RPL19, RPS12, CTSD, RAP1B, RPS16, CCT7, COTL1, RAB10, SOD1, CCT8, DPYSL2, HBB, RPL10A, SCN2A, PSME1, RPL24, ALDOA, ATP1A1
GO:0002181	Cytoplasmic translation	4.9E-03	4	RPL18A, RPL19, RPL10A, RPL24
GO:0045055	Regulated exocytosis	6.4E-03	8	CTSD, RAP1B, COTL1, RAB10, SOD1, CCT8, HBB, ALDOA
GO:0140352	Export from cell	8.7E-03	9	CTSD, RAP1B, COTL1, RAB10, SOD1, CCT8, HBB, ALDOA, ATP1A1
GO:1901566	Organonitrogen compound biosynthetic process	9.8E-03	10	DCN, RPL18A, RPL19, RPS12, RPS16, CKMT1B, ALDH9A1, RPL10A, RPL24, ALDOA
GO:0009057	Macromolecule catabolic process	9.8E-03	9	DCN, RPL18A, RPL19, RPS12, CTSD, RPS16, RPL10A, PSME1, RPL24
GO:0009056	Catabolic process	1.1E-02	12	DCN, RPL18A, RPL19, RPS12, CTSD, RPS16, PGD, HBB, RPL10A, PSME1, RPL24, ALDOA

GO term ID	Description	Adjusted p-value	Gene count	Matching proteins in PPI network
GO Biological Process (n = 15, cont.)				
GO:0007339	Binding of sperm to zona pellucida	1.3E-02	3	CCT7, CCT8, ALDOA
GO:0009058	Biosynthetic process	3.6E-02	13	DCN, RPL18A, RPL19, RPS12, RPS16, SOD1, PGD, CKMT1B, ALDH9A1, RPL10A, RPL24, ALDOA, SERPINH1
GO:0051289	Protein homotetramerization	3.7E-02	3	VASP, ALDH9A1, ALDOA
GO:1904851	Positive regulation of establishment of protein localization to telomere	4.4E-02	2	CCT7, CCT8
GO Molecular Function (n = 8)				
GO:0003735	Structural constituent of ribosome	8.5E-04	6	RPL18A, RPL19, RPS12, RPS16, RPL10A, RPL24
GO:0005198	Structural molecule activity	8.5E-04	9	DCN, RPL18A, RPL19, RPS12, RPS16, COL6A2, RPL10A, AHNAK, RPL24
GO:0003723	RNA binding	4.7E-03	12	DCN, RPL18A, RPL19, RPS12, HSPE1, RPS16, STIP1, RPL10A, AHNAK, RPL24, ALDOA, SERPINH1
GO:0045296	Cadherin binding	1.4E-02	6	VASP, RAB10, CCT8, AHNAK, RPL24, ALDOA
GO:0051082	Unfolded protein binding	2.3E-02	4	HSPE1, CCT7, CCT8, SERPINH1
GO:0051087	Chaperone binding	2.3E-02	4	HSPE1, SOD1, STIP1, ATP1A1
GO:1901363	Heterocyclic compound binding	2.5E-02	20	DCN, RPL18A, RPL19, RPS12, HSPE1, RAP1B, RPS16, CCT7, RAB10, PGD, CCT8, CKMT1B, HBB, STIP1, RPL10A, AHNAK, RPL24, ALDOA, SERPINH1, ATP1A1
GO:0097159	Organic cyclic compound binding	2.8E-02	20	DCN, RPL18A, RPL19, RPS12, HSPE1, RAP1B, RPS16, CCT7, RAB10, PGD, CCT8, CKMT1B, HBB, STIP1, RPL10A, AHNAK, RPL24, ALDOA, SERPINH1, ATP1A1
GO Cellular Component (n = 12)				
GO:0005615	Extracellular space	3.2E-10	23	DCN, HSPE1, CTSD, VASP, RAP1B, RPS16, CCT7, COTL1, RAB10, SOD1, PGD, CCT8, COL6A2, DPYSL2, HBB, ALDH9A1, RPL10A, AHNAK, PSME1, RPL24, ALDOA, SERPINH1, ATP1A1

GO term ID	Description	Adjusted p-value	Gene count	Matching proteins in PPI network

GO Cellular Component (n = 12, cont.)				
GO:0005829	Cytosol	3.8E-05	22	ACO2, RPL18A, RPL19, RPS12, VASP, RAP1B, RPS16, CCT7, COTL1, RAB10, SOD1, PGD, CCT8, DPYSL2, HBB, ALDH9A1, STIP1, RPL10A, AHNAK, PSME1, RPL24, ALDOA
GO:0042788	Polysomal ribosome	6.9E-05	4	RPL18A, RPL19, RPL10A, RPL24
GO:0005737	Cytoplasm	3.7E-04	29	DCN, ACO2, RPL18A, RPL19, RPS12, HSPE1, CTSD, VASP, RAP1B, RPS16, CCT7, COTL1, RAB10, SOD1, PGD, CCT8, CKMT1B, COL6A2, DPYSL2, HBB, ALDH9A1, STIP1, RPL10A, AHNAK, PSME1, RPL24, ALDOA, SERPINH1, ATP1A1
GO:0070161	Anchoring junction	4.1E-04	9	RPL19, VASP, RAP1B, RPS16, RAB10, RPL10A, SCN2A, AHNAK, ATP1A1
GO:0101031	Chaperone complex	1.3E-03	3	CCT7, CCT8, STIP1
GO:0042383	Sarcolemma	5.6E-03	4	COL6A2, SCN2A, AHNAK, ATP1A1
GO:0030315	T-tubule	9.2E-03	3	SCN2A, AHNAK, ATP1A1
GO:0005832	Chaperonin-containing t-complex	1.3E-02	2	CCT7, CCT8
GO:0043227	Membrane-bounded organelle	1.7E-02	28	DCN, ACO2, RPL19, RPS12, HSPE1, CTSD, VASP, RAP1B, RPS16, CCT7, COTL1, RAB10, SOD1, PGD, CCT8, CKMT1B, COL6A2, DPYSL2, HBB, ALDH9A1, STIP1, RPL10A, AHNAK, PSME1, RPL24, ALDOA, SERPINH1, ATP1A1
GO:0043226	Organelle	1.7E-02	29	DCN, ACO2, RPL18A, RPL19, RPS12, HSPE1, CTSD, VASP, RAP1B, RPS16, CCT7, COTL1, RAB10, SOD1, PGD, CCT8, CKMT1B, COL6A2, DPYSL2, HBB, ALDH9A1, STIP1, RPL10A, AHNAK, PSME1, RPL24, ALDOA, SERPINH1, ATP1A1
GO:0005764	Lysosome	4.3E-02	6	DCN, CTSD, RAP1B, SOD1, CCT8, AHNAK

GO term ID	Description	Adjusted p-value	Gene count	Matching proteins in PPI network
Reactome Pathways (n = 23)				
HSA-422475	Axon guidance	5.3E-06	11	RPL18A, RPL19, RPS12, VASP, RPS16, COL6A2, DPYSL2, RPL10A, SCN2A, PSME1, RPL24
HSA-376176	Signalling by ROBO receptors	6.3E-06	8	RPL18A, RPL19, RPS12, VASP, RPS16, RPL10A, PSME1, RPL24
HSA-71291	Metabolism of amino acids and derivatives	1.3E-05	9	RPL18A, RPL19, RPS12, RPS16, CKMT1B, ALDH9A1, RPL10A, PSME1, RPL24
HSA-156902	Peptide chain elongation	1.8E-05	6	RPL18A, RPL19, RPS12, RPS16, RPL10A, RPL24
HSA-192823	Viral mRNA Translation	1.8E-05	6	RPL18A, RPL19, RPS12, RPS16, RPL10A, RPL24
HSA-2408557	Selenocysteine synthesis	1.8E-05	6	RPL18A, RPL19, RPS12, RPS16, RPL10A, RPL24
HSA-72689	Formation of a pool of free 40S subunits	1.8E-05	6	RPL18A, RPL19, RPS12, RPS16, RPL10A, RPL24
HSA-72764	Eukaryotic Translation Termination	1.8E-05	6	RPL18A, RPL19, RPS12, RPS16, RPL10A, RPL24
HSA-9010553	Regulation of expression of SLITs and ROBOs	1.8E-05	7	RPL18A, RPL19, RPS12, RPS16, RPL10A, PSME1, RPL24
HSA-9633012	Response of EIF2AK4 (GCN2) to amino acid deficiency	1.8E-05	6	RPL18A, RPL19, RPS12, RPS16, RPL10A, RPL24
HSA-975956	Nonsense Mediated Decay (NMD) independent of the Exon Junction Complex (EJC)	1.8E-05	6	RPL18A, RPL19, RPS12, RPS16, RPL10A, RPL24
HSA-156827	L13a-mediated translational silencing of Ceruloplasmin expression	2.2E-05	6	RPL18A, RPL19, RPS12, RPS16, RPL10A, RPL24
HSA-1799339	SRP-dependent cotranslational protein targeting to membrane	2.2E-05	6	RPL18A, RPL19, RPS12, RPS16, RPL10A, RPL24
HSA-72706	GTP hydrolysis and joining of the 60S ribosomal subunit	2.2E-05	6	RPL18A, RPL19, RPS12, RPS16, RPL10A, RPL24
HSA-975957	Nonsense Mediated Decay (NMD) enhanced by the Exon Junction Complex (EJC)	2.4E-05	6	RPL18A, RPL19, RPS12, RPS16, RPL10A, RPL24
HSA-2262752	Cellular responses to stress	6.8E-05	9	RPL18A, RPL19, RPS12, RPS16, SOD1, STIP1, RPL10A, PSME1, RPL24

GO term ID	Description	Adjusted p-value	Gene count	Matching proteins in PPI network
Reactome Pathways (n = 23, cont.)				
HSA-6791226	Major pathway of rRNA processing in the nucleolus and cytosol	2.2E-04	6	RPL18A, RPL19, RPS12, RPS16, RPL10A, RPL24
HSA-1430728	Metabolism	2.8E-03	13	DCN, ACO2, RPL18A, RPL19, RPS12, RPS16, PGD, CKMT1B, ALDH9A1, RPL10A, PSME1, RPL24, ALDOA
HSA-6798695	Neutrophil degranulation	3.4E-03	7	CTSD, RAP1B, COTL1, RAB10, CCT8, HBB, ALDOA
HSA-5663205	Infectious disease	1.4E-02	8	RPL18A, RPL19, RPS12, RPS16, RPL10A, PSME1, RPL24, ATP1A1
HSA-8953854	Metabolism of RNA	2.7E-02	7	RPL18A, RPL19, RPS12, RPS16, RPL10A, PSME1, RPL24
HSA-1643685	Disease	3.3E-02	10	DCN, RPL18A, RPL19, RPS12, RAP1B, RPS16, RPL10A, PSME1, RPL24, ATP1A1
HSA-392499	Metabolism of proteins	4.8E-02	11	RPL18A, RPL19, RPS12, CTSD, RPS16, CCT7, RAB10, CCT8, RPL10A, PSME1, RPL24

Appendix Table S8. Gene Ontology (GO) terms on biological processes, molecular function and cellular components, respectively, after reducing the redundancy between GO terms by REVIGO and Reactome pathways corresponding to comparison between LRSW and CRCT ileum. The network is expanded with maximum 5 interactors shown in the first shell. CRCT: piglets fed no seaweed (SW, *Ascophyllum nodosum*), which nursed by sows fed dietary ω6:ω3 ratio = 13:1 during gestation, starting from day 28 (G28) and 10:1 during lactation. LRSW: piglets fed SW, which nursed by sows fed dietary ω6:ω3 ratio = 4:1 from G28 until the end of lactation.

GO term ID	Description	Adjusted p-value	Gene count	Matching proteins in PPI network
		GO Biological Process (n = 23)		
GO:1901566	Organonitrogen compound biosynthetic process	6.8E-05	13	DCN, ATP5D, RPL18A, RPL19, RPS12, ATP5E, ATP5B, CKMT1B, RPS3A, RPSA, ALDH9A1, ALDOA, ATP5A1
GO:0042407	Cristae formation	2.3E-04	4	ATP5D, ATP5E, ATP5B, ATP5A1
GO:0019083	Viral transcription	6.7E-04	5	RPL18A, RPL19, RPS12, RPS3A, RPSA
GO:0006810	Transport	6.7E-04	19	ATP5D, ECH1, RPL18A, RPL19, RPS12, CTSD, ATP5E, VIL1, ATP5B, CCT8, NPM1, CCT2, RPS3A, RPSA, CALM1, FABP6, ALDOA, ATP5A1, ATP1A1
GO:0000184	Nuclear-transcribed mRNA catabolic process, nonsense-mediated decay	7.5E-04	5	RPL18A, RPL19, RPS12, RPS3A, RPSA
GO:0016032	Viral process	8.5E-04	9	RPL18A, RPL19, RPS12, NPM1, RPS3A, RPSA, CALM1, KRT19, KRT8
GO:0006091	Generation of precursor metabolites and energy	1.1E-03	7	ATP5D, ACO2, ATP5E, ATP5B, CALM1, ALDOA, ATP5A1
GO:0006413	Translational initiation	1.3E-03	5	RPL18A, RPL19, RPS12, RPS3A, RPSA
GO:1902600	Proton transmembrane transport	1.6E-03	5	ATP5D, ATP5E, ATP5B, ATP5A1, ATP1A1
GO:0097435	Supramolecular fiber organization	2.4E-03	7	KRT20, VASP, VIL1, KRT19, ALDOA, SERPINH1, KRT8
GO:0009058	Biosynthetic process	4.8E-03	14	DCN, ATP5D, RPL18A, RPL19, RPS12, ATP5E, ATP5B, CKMT1B, RPS3A, RPSA, ALDH9A1, ALDOA, ATP5A1, SERPINH1
GO:0007339	Binding of sperm to zona pellucida	9.0E-03	3	CCT8, CCT2, ALDOA
GO:0072594	Establishment of protein localization to organelle	1.1E-02	6	ECH1, RPL18A, RPL19, RPS12, RPS3A, RPSA
GO:0044419	Interspecies interaction between organisms	1.4E-02	11	DCN, RPL18A, RPL19, RPS12, VIL1, NPM1, RPS3A, RPSA, CALM1, KRT19, KRT8

GO term ID	Description	Adjusted p-value	Gene count	Matching proteins in PPI network
		GO Biological Process (n = 23, cont.)		
GO:0044281	Small molecule metabolic process	2.5E-02	10	DCN, ATP5D, ACO2, ECH1, ATP5E, ATP5B, CKMT1B, CALM1, ALDOA, ATP5A1
GO:0051289	Protein homo-tetramerization	2.7E-02	3	VASP, ALDH9A1, ALDOA
GO:0009057	Macromolecule catabolic process	2.8E-02	8	DCN, RPL18A, RPL19, RPS12, CTSD, RPS3A, RPSA, CALM1
GO:0090407	Organophosphate biosynthetic process	2.9E-02	6	ATP5D, ATP5E, ATP5B, CKMT1B, ALDOA, ATP5A1
GO:1904871	Positive regulation of protein localization to Cajal body	3.7E-02	2	CCT8, CCT2
GO:0007010	Cytoskeleton organization	3.8E-02	8	KRT20, VASP, VIL1, NPM1, CALM1, KRT19, ALDOA, KRT8
GO:0002181	Cytoplasmic translation	3.8E-02	3	RPL18A, RPL19, RPSA
GO:0030029	Actin filament-based process	4.1E-02	6	VASP, VIL1, KRT19, ALDOA, ATP1A1, KRT8
GO:1901137	Carbohydrate derivative biosynthetic process	4.3E-02	6	DCN, ATP5D, ATP5E, ATP5B, ALDOA, ATP5A1
		GO Molecular Function (n = 7)		
GO:0046933	Proton-transporting ATP synthase activity, rotational mechanism	2.7E-05	4	ATP5D, ATP5E, ATP5B, ATP5A1
GO:0003735	Structural constituent of ribosome	5.2E-03	5	RPL18A, RPL19, RPS12, RPS3A, RPSA
GO:0005198	Structural molecule activity	5.2E-03	8	DCN, KRT20, RPL18A, RPL19, RPS12, RPS3A, RPSA, KRT19
GO:0003723	RNA binding	1.3E-02	11	DCN, RPL18A, RPL19, RPS12, NPM1, HIST1H1E, RPS3A, RPSA, ALDOA, ATP5A1, SERPINH1
GO:0043531	ADP binding	1.9E-02	3	HIST1H1E, ATP5A1, ATP1A1
GO:0051082	Unfolded protein binding	1.9E-02	4	CCT8, NPM1, CCT2, SERPINH1
GO:0043532	Angiostatin binding	2.1E-02	2	ATP5B, ATP5A1
		GO Cellular Component (n = 22)		
GO:0045261	Proton-transporting ATP synthase complex, catalytic core f(1)	2.0E-06	4	ATP5D, ATP5E, ATP5B, ATP5A1
GO:0005615	Extracellular space	8.2E-05	17	DCN, ECH1, CTSD, VASP, VIL1, ATP5B, CCT8, CCT2, RPS3A, RPSA, ALDH9A1, KRT19, ALDOA, ATP5A1, SERPINH1, ATP1A1, KRT8

GO term ID	Description	Adjusted p-value	Gene count	Matching proteins in PPI network
		GO Cellular Component (n = 22, cont.)		
GO:0005576	Extracellular region	5.0E-04	18	DCN, ECH1, CTSD, VASP, VIL1, ATP5B, CCT8, CCT2, RPS3A, RPSA, ALDH9A1, CALM1, KRT19, ALDOA, ATP5A1, SERPINH1, ATP1A1, KRT8
GO:0005737	Cytoplasm	7.0E-04	28	DCN, KRT20, ATP5D, ACO2, ECH1, RPL18A, RPL19, RPS12, CTSD, ATP5E, VASP, VIL1, ATP5B, CCT8, NPM1, CCT2, CKMT1B, RPS3A, RPSA, ALDH9A1, CALM1, KRT19, FABP6, ALDOA, ATP5A1, SERPINH1, ATP1A1, KRT8
GO:0031982	Vesicle	3.5E-03	16	ECH1, CTSD, VASP, VIL1, ATP5B, CCT8, CCT2, RPS3A, RPSA, ALDH9A1, CALM1, KRT19, ALDOA, ATP5A1, ATP1A1, KRT8
GO:0032991	Protein-containing complex	5.2E-03	18	DCN, ATP5D, RPL18A, RPL19, RPS12, ATP5E, ATP5B, CCT8, NPM1, CCT2, HIST1H1E, RPS3A, RPSA, CALM1, KRT19, ATP5A1, ATP1A1, KRT8
GO:0099512	Supramolecular fiber	5.3E-03	8	DCN, KRT20, CCT8, CCT2, CALM1, KRT19, ALDOA, KRT8
GO:0005829	Cytosol	6.2E-03	18	KRT20, ACO2, ECH1, RPL18A, RPL19, RPS12, VASP, CCT8, NPM1, CCT2, RPS3A, RPSA, ALDH9A1, CALM1, KRT19, FABP6, ALDOA, KRT8
GO:0002199	Zona pellucida receptor complex	8.9E-03	2	CCT8, CCT2
GO:0005622	Intracellular	9.8E-03	29	DCN, KRT20, ATP5D, ACO2, ECH1, RPL18A, RPL19, RPS12, CTSD, ATP5E, VASP, VIL1, ATP5B, CCT8, NPM1, CCT2, CKMT1B, HIST1H1E, RPS3A, RPSA, ALDH9A1, CALM1, KRT19, FABP6, ALDOA, ATP5A1, SERPINH1, ATP1A1, KRT8
GO:0005775	Vacuolar lumen	1.1E-02	4	DCN, CTSD, CCT8, CCT2
GO:0005832	Chaperonin-containing t-complex	1.1E-02	2	CCT8, CCT2
GO:0043226	Organelle	2.2E-02	28	DCN, KRT20, ATP5D, ACO2, ECH1, RPL18A, RPL19, RPS12, CTSD, ATP5E, VASP, VIL1, ATP5B, CCT8, NPM1, CCT2, CKMT1B, HIST1H1E, RPS3A, RPSA, ALDH9A1, CALM1, KRT19, ALDOA, ATP5A1, SERPINH1, ATP1A1, KRT8

GO term ID	Description	Adjusted p-value	Gene count	Matching proteins in PPI network
GO Cellular Component (n = 22, cont.)				
GO:0043229	Intracellular organelle	2.4E-02	27	DCN, KRT20, ATP5D, ACO2, ECH1, RPL18A, RPL19, RPS12, CTSD, ATP5E, VASP, VIL1, ATP5B, CCT8, NPM1, CCT2, CKMT1B, HIST1H1E, RPS3A, RPSA, CALM1, KRT19, ALDOA, ATP5A1, SERPINH1, ATP1A1, KRT8
GO:1990904	Ribonucleoprotein complex	2.6E-02	6	RPL18A, RPL19, RPS12, NPM1, RPS3A, RPSA
GO:0045111	Intermediate filament cytoskeleton	2.6E-02	4	KRT20, CCT8, KRT19, KRT8
GO:0016010	Dystrophin-associated glycoprotein complex	2.6E-02	2	KRT19, KRT8
GO:0016327	Apicolateral plasma membrane	2.6E-02	2	KRT19, KRT8
GO:0005743	Mitochondrial inner membrane	3.4E-02	5	ATP5D, ATP5E, ATP5B, CKMT1B, ATP5A1
GO:1904813	ficolin-1-rich granule lumen	4.2E-02	3	CTSD, CCT8, ALDOA
GO:0005856	Cytoskeleton	4.3E-02	10	KRT20, VASP, VIL1, CCT8, NPM1, CCT2, CALM1, KRT19, ALDOA, KRT8
GO:0042383	Sarcolemma	4.7E-02	3	KRT19, ATP1A1, KRT8
Pathway				
Reactome Pathways (n = 25)				
HSA-1430728	Metabolism	4.8E-04	15	DCN, ATP5D, ACO2, RPL18A, RPL19, RPS12, ATP5E, ATP5B, CKMT1B, RPS3A, RPSA, ALDH9A1, FABP6, ALDOA, ATP5A1
HSA-163210	Formation of ATP by chemiosmotic coupling	4.8E-04	4	ATP5D, ATP5E, ATP5B, ATP5A1
HSA-156827	L13a-mediated translational silencing of Ceruloplasmin expression	1.1E-03	5	RPL18A, RPL19, RPS12, RPS3A, RPSA
HSA-156902	Peptide chain elongation	1.1E-03	5	RPL18A, RPL19, RPS12, RPS3A, RPSA
HSA-1799339	SRP-dependent cotranslational protein targeting to membrane	1.1E-03	5	RPL18A, RPL19, RPS12, RPS3A, RPSA
HSA-192823	Viral mRNA Translation	1.1E-03	5	RPL18A, RPL19, RPS12, RPS3A, RPSA
HSA-2408557	Selenocysteine synthesis	1.1E-03	5	RPL18A, RPL19, RPS12, RPS3A, RPSA
HSA-376176	Signalling by ROBO receptors	1.1E-03	6	RPL18A, RPL19, RPS12, VASP, RPS3A, RPSA

Pathway	Description	Adjusted p-value	Gene count	Matching proteins in PPI network
Reactome Pathways (n = 25, cont.)				
HSA-71291	Metabolism of amino acids and derivatives	1.1E-03	7	RPL18A, RPL19, RPS12, CKMT1B, RPS3A, RPSA, ALDH9A1
HSA-72689	Formation of a pool of free 40S subunits	1.1E-03	5	RPL18A, RPL19, RPS12, RPS3A, RPSA
HSA-72706	GTP hydrolysis and joining of the 60S ribosomal subunit	1.1E-03	5	RPL18A, RPL19, RPS12, RPS3A, RPSA
HSA-72764	Eukaryotic Translation Termination	1.1E-03	5	RPL18A, RPL19, RPS12, RPS3A, RPSA
HSA-8949613	Cristae formation	1.1E-03	4	ATP5D, ATP5E, ATP5B, ATP5A1
HSA-9633012	Response of EIF2AK4 (GCN2) to amino acid deficiency	1.1E-03	5	RPL18A, RPL19, RPS12, RPS3A, RPSA
HSA-975956	Nonsense Mediated Decay (NMD) independent of the Exon Junction Complex (EJC)	1.1E-03	5	RPL18A, RPL19, RPS12, RPS3A, RPSA
HSA-975957	Nonsense Mediated Decay (NMD) enhanced by the Exon Junction Complex (EJC)	1.1E-03	5	RPL18A, RPL19, RPS12, RPS3A, RPSA
HSA-1852241	Organelle biogenesis and maintenance	2.9E-03	6	ATP5D, ATP5E, ATP5B, CCT8, CCT2, ATP5A1
HSA-9010553	Regulation of expression of SLITs and ROBOs	3.4E-03	5	RPL18A, RPL19, RPS12, RPS3A, RPSA
HSA-1428517	The citric acid (TCA) cycle and respiratory electron transport	4.2E-03	5	ATP5D, ACO2, ATP5E, ATP5B, ATP5A1
HSA-6791226	Major pathway of rRNA processing in the nucleolus and cytosol	4.5E-03	5	RPL18A, RPL19, RPS12, RPS3A, RPSA
HSA-1266738	Developmental Biology	1.1E-02	9	KRT20, RPL18A, RPL19, RPS12, VASP, RPS3A, RPSA, KRT19, KRT8
HSA-72695	Formation of the ternary complex, and subsequently, the 43S complex	3.2E-02	3	RPS12, RPS3A, RPSA
HSA-72649	Translation initiation complex formation	4.2E-02	3	RPS12, RPS3A, RPSA
HSA-72702	Ribosomal scanning and start codon recognition	4.2E-02	3	RPS12, RPS3A, RPSA
HSA-9609507	Protein localization	4.4E-02	4	ACO2, ECH1, ATP5B, ATP5A1

List of References

[1] D.S. Rosero, R. Dean Boyd, J. Odle, E. van Heugten, Optimizing dietary lipid use to improve essential fatty acid status and reproductive performance of the modern lactating sow: A review, J. Anim. Sci. Biotechnol. 7 (2016) 2–18. https://doi.org/10.1186/S40104-016-0092-X.

[2] B.J. Kerr, T.A. Kellner, G.C. Shurson, Characteristics of lipids and their feeding value in swine diets, J. Anim. Sci. Biotechnol. 6 (2015) 1–23. https://doi.org/10.1186/s40104-015-0028-x.

[3] B.K. Yoon, J.A. Jackman, E.R. Valle-Gonzalez, N.-J. Cho, Antibacterial Free Fatty Acids and Monoglycerides: Biological Activities, Experimental Testing, and Therapeutic Applications, Int. J. Mol. Sci. 19 (2018) 1–40. https://doi.org/10.3390/ijms19041114.

[4] T.J. Cole, K.L. Short, S.B. Hooper, The science of steroids, Semin. Fetal Neonatal Med. 24 (2019) 170–175. https://doi.org/10.1016/j.siny.2019.05.005.

[5] A.K. Azad, J. Gao, J. Ma, T. Li, B. Tan, X. Huang, J. Yin, Opportunities of prebiotics for the intestinal health of monogastric animals, Anim. Nutr. 6 (2020) 379–388. https://doi.org/10.1016/j.aninu.2020.08.001.

[6] C. Lauridsen, Effects of dietary fatty acids on gut health and function of pigs pre- and post-weaning, J. Anim. Sci. 98 (2020) 1–12. https://doi.org/10.1093/jas/skaa086.

[7] P. Jones, T. Rideout, Lipids, sterols, and their metabolites, in: A. Ross, B. Caballero, R. Cousins, K. Tucker, T. Ziegler (Eds.), Mod. Nutr. Heal. Dis., 11th ed., Lippincott Williams and Wilkins, Philadelphia, 2012: pp. 65–87.

[8] M. Hamosh, Lingual and gastric lipases, Nutrition. 6 (1990) 421–428. http://europepmc.org/abstract/MED/2134569.

[9] A. Langlois, T. Corring, F. Levenez, J.-C. Cuber, J.-A. Chayvialle, Effects of pancreatic polypeptide on biliary flow and bile acid secretion stimulated by secretin and cholecystokinin in the conscious pig, Regul. Pept. 27 (1990) 139–147.

[10] A. Vandermeers, M.C. Vandermeers-Piret, J. Rathé, J. Christophe, On human pancreatic triacylglycerol lipase: isolation and some properties, Biochim Biophys Acta. 370 (1974) 257.

[11] U. Bracco, Effect of triglyceride structure on fat absorption, Am. J. Clin. Nutr. 60 (1994) 1002S.

[12] H. Westergaard, J.M. Dietschy, The Mechanism Whereby Bile Acid Micelles Increase the Rate of Fatty Acid and Cholesterol Uptake into the Intestinal Mucosal Cell, J. Clin. Invest. 58 (1976) 97–108.

[13] J.R. Hirschey, N. Kumar, T. Turnaoglu, K.R. Gluesenkamp, S. Graham, Review of Low-Cost Organic and Inorganic Phase Change Materials with Phase Change Temperature between 0°C and 65°C, in: 6th Int. High Perform. Build. Conf., Purdue, 2021: pp. 0–10.

[14] P.C. Calder, Fatty acids and inflammation: The cutting edge between food and pharma, Eur. J. Pharmacol. 668 (2011) S50–S58. https://doi.org/10.1016/j.ejphar.2011.05.085.

[15] W.M.N. Ratnayake, C. Galli, Fat and Fatty Acid Terminology, Methods of Analysis and Fat Digestion and Metabolism: A Background Review Paper, Ann. Nutr. Metab. 55 (2009) 8–43. https://doi.org/10.1159/000228994.

[16] U.N. Das, Essential fatty acids: biochemistry, physiology and pathology, Biotechnol. J. 1 (2006) 420–439. https://doi.org/10.1002/biot.200600012.

[17] A.R. Eynard, G. Repossi, Role of ω3 polyunsaturated fatty acids in diabetic retinopathy: a morphological and metabolically cross talk among blood retina barriers damage, autoimmunity and chronic inflammation, Lipids Health Dis. 18 (2019) 1–15.

[18] S.M. Innis, Perinatal biochemistry and physiology of long-chain polyunsaturated fatty acids, J. Pediatr. 3476 (2003) 1–8.

[19] H.K. Maehre, I.-J. Jensen, E.O. Elvevoll, K.-E. Eilertsen, ω-3 Fatty Acids and Cardiovascular Diseases: Effects, Mechanisms and Dietary Relevance, Int. J. Mol. Sci. 16 (2015) 22636–22661. https://doi.org/10.3390/ijms160922636.

[20] C.N. Serhan, J. Dalli, R.A. Colas, J.W. Winkler, N. Chiang, Protectins and maresins : New pro-resolving families of mediators in acute in fl ammation and resolution bioactive metabolome

☆, Biochim. Biophys. Acta - Mol. Cell Biol. Lipids. 1851 (2015) 397–413. https://doi.org/10.1016/j.bbalip.2014.08.006.

[21] A.T. Høstmark, Intended Ranges and Correlations between Percentages of Variables Like Oleic Acid, Eicosapentaenoic Acid, and Arachidonic Acid, Foods. 10 (2021) 1–13.

[22] A. Hellström, A. Pivodic, L. Gränse, P. Lundgren, U. Sjöbom, A.K. Nilsson, H. Söderling, Association of Docosahexaenoic Acid and Arachidonic Acid Serum Levels With Retinopathy of Prematurity in Preterm Infants, JAMA Netw. Open. 4 (2021) 1–12. https://doi.org/10.1001/jamanetworkopen.2021.28771.

[23] R.K. Saini, Y.S. Keum, Omega-3 and omega-6 polyunsaturated fatty acids: Dietary sources, metabolism, and significance — A review, Life Sci. 203 (2018) 255–267. https://doi.org/10.1016/j.lfs.2018.04.049.

[24] J.T. Brenna, N. Salem, A.J. Sinclair, S.C. Cunnane, a-Linolenic acid supplementation and conversion to n-3 long-chain polyunsaturated fatty acids in humans, Prostaglandins, Leukot. Essent. Fat. Acids. 80 (2009) 85–91. https://doi.org/10.1016/j.plefa.2009.01.004.

[25] M. Ivan, P.S. Mir, K.M. Koenig, L.M. Rode, L. Neill, T. Entz, Z. Mir, Effects of dietary sunflower seed oil on rumen protozoa population and tissue concentration of conjugated linoleic acid in sheep, Small Rumin. Res. 41 (2001) 215–227.

[26] K. Albracht-Schulte, N.S. Kalupahana, L. Ramalingam, S. Wang, S.M. Rahman, J. Robert-McComb, N. Moustaid-Moussa, Omega-3 fatty acids in obesity and metabolic syndrome: a mechanistic update, J. Nutr. Biochem. 58 (2018) 1–16. https://doi.org/10.1016/j.jnutbio.2018.02.012.

[27] O. Kose, M. Tuter, H.A. Aksoy, Immobilized Candida antarctica lipase-catalyzed alcoholysis of cotton seed oil in a solvent-free medium, Bioresour. Technol. 83 (2002) 125–129.

[28] R. Howell, F. Collins, Factors Affecting Linolenic and Linoleic Acid Content of Soybean Oil, Agron. J. 49 (1957) 593–597.

[29] H.M. Karvonen, A. Aro, N.S. Tapola, I. Salminen, M.I.J. Uusitupa, E.S. Sarkkinen, Effect of a-Linolenic Acid-Rich Camelina sativa Oil on Serum Fatty Acid Composition and Serum Lipids in Hypercholesterolemic Subjects, Metabolism. 51 (2002) 1253–1260. https://doi.org/10.1053/meta.2002.35183.

[30] A. Fröhlich, B. Rice, Evaluation of Camelina sativa oil as a feedstock for biodiesel production, Ind. Crops Prod. 21 (2005) 25–31. https://doi.org/10.1016/j.indcrop.2003.12.004.

[31] E.P. on G.M.O. (GMO), Scientific Opinion on application (EFSA-GMO-UK-2009-76) for the placing on the market of soybean MON 87769 genetically modified to contain stearidonic acid, for food and feed uses, import and processing under Regulation (EC) No 1829/2003 from Monsanto, EFSA J. 12 (2014) 3–41.

[32] S.L. Holdt, S. Kraan, Bioactive compounds in seaweed : functional food applications and legislation, J. Appl. Phycol. 23 (2011) 543–597. https://doi.org/10.1007/s10811-010-9632-5.

[33] D. Li, O. Bode, H. Drummond, A. Sinclair, Ome-ga-3 (n–3) fatty acids, in: F. Gunstone (Ed.), Lipids Funct. Foods Nutraceuti-Cals, The Oily Press, UK, 2002: pp. 225– 262.

[34] J. Roy, C. Vigor, J. Vercauteren, G. Reversat, B. Zhou, A. Surget, L. Larroquet, A. Lanuque, F. Sandres, F. Terrier, C. Oger, J.-M. Galano, G. Corraze, T. Durand, Characterization and modulation of brain lipids content of rainbow trout fed with 100% plant based diet rich in omega-3 long chain polyunsaturated fatty acids DHA and EPA, Biochimie. 178 (2020) 137–147. https://doi.org/10.1016/j.biochi.2020.06.010.

[35] N. Kaur, V. Chugh, A.K. Gupta, Essential fatty acids as functional components of foods- a review, J Food Sci Technol. 51 (2014) 2289–2303. https://doi.org/10.1007/s13197-012-0677-0.

[36] S.C. Cunnane, M.J. Anderson, Pure linoleate deficiency in the rat: Influence on growth, accumulation of n-6 polyunsaturates, and [1-14C]linoleate oxidation, J. Lipid Res. 38 (1997) 805–812.

[37] G. Barceló-Coblijn, E.J. Murphy, Alpha-linolenic acid and its conversion to longer chain n-3 fatty acids: Benefits for human health and a role in maintaining tissue n-3 fatty acid levels, Prog. Lipid Res. 48 (2009) 355–374. https://doi.org/10.1016/j.plipres.2009.07.002.

[38] H. Sprecher, Metabolism of highly unsaturated n-3 and n-6 fatty acids, Biochim. Biophys. Acta. 1486 (2000) 219–231.

[39] A.K. Duttaroy, Docosahexaenoic acid supports feto-placental growth and protects cardiovascular and cognitive function: A mini review, J Lipid Sci Technol. 118 (2016) 1439–1449. https://doi.org/10.1002/ejlt.201500496.

[40] D. Ibrahim, R. El-sayed, S.I. Khater, E.N. Said, S.A.M. El-mandrawy, Changing dietary n-6:n-3 ratio using different oil sources affects performance, behavior, cytokines mRNA expression and meat fatty acid profile of broiler chickens, Anim. Nutr. 4 (2018) 44–51. https://doi.org/10.1016/j.aninu.2017.08.003.

[41] A.P. Simopoulos, The importance of the ratio of omega-6/omega-3 essential fatty acids, Biomed. Pharmacother. 56 (2002) 365–379. https://doi.org/10.1016/S0753-3322(02)00253-6.

[42] J.J. Dinicolantonio, J. O'keefe, J.H. O'keefe, The Importance of Maintaining a Low Omega-6/Omega-3 Ratio for Reducing the Risk of Autoimmune Diseases, Asthma, and Allergies, Mo. Med. 118 (2021) 453. /pmc/articles/PMC8504498/%0A/pmc/articles/PMC8504498/?report=abstract%0Ahttps://www.ncbi.nlm.nih.gov/pmc/articles/PMC8504498/.

[43] A.P. Simopoulos, An increase in the Omega-6/Omega-3 fatty acid ratio increases the risk for obesity, Nutrients. 8 (2016) 1–17. https://doi.org/10.3390/nu8030128.

[44] P. Haggarty, Fatty Acid Supply to the Human Fetus, Annu. Rev. Nutr. 30 (2010) 237–255. https://doi.org/10.1146/annurev.nutr.012809.104742.

[45] J.J. DiNicolantonio, J. O'Keefe, The Importance of Maintaining a Low Omega-6/Omega-3 Ratio for Reducing the Risk of Inflammatory Cytokine Storms., Mo. Med. 117 (2020) 539–542.

[46] P. Shrestha, X.-R. Zhou, S.V. Pillai, J. Petrie, R. de Feyter, S. Singh, Comparison of the Substrate Preferences of ω3 Fatty Acid Desaturases for Long Chain Polyunsaturated Fatty Acids, Int. J. Mol. Sci. 20 (2019) 1–13.

[47] R. Boyd, R. Kensinger, Metabolic precursors for milk synthesis. The Lactating Sow., Wageningen Press, Wageningen, The Netherlands, 1998.

[48] J. Chambaz, D. Ravel, M.C. Manier, D. Pepin, N. Mulliez, G. Bereziat, Essential fatty acids interconversion in the human fetal liver, Biol. Neonate. 47 (1985) 136–140.

[49] J.R. Silva, B. Burger, C.M.C. Kühl, T. Candreva, M.B.P. Anjos, H.G. Rodrigues, Wound Healing and Omega-6 Fatty Acids: From Inflammation to Repair, Mediators Inflamm. 2018 (2018) 1–17.

[50] L. Paulesu, J. Bhattacharjee, N. Bechi, R. Romagnoli, S. Jantra, F. Ietta, Pro-inflammatory Cytokines in Animal and Human Gestation, Curr. Pharm. Des. 16 (2010) 3601–3615.

[51] O.A. Akerele, S.K. Cheema, A balance of omega-3 and omega-6 polyunsaturated fatty acids is important in pregnancy, J. Nutr. Intermed. Metab. 5 (2016) 23–33. https://doi.org/10.1016/j.jnim.2016.04.008.

[52] C.L. Elliott, J.A.Z. Loudon, N. Brown, D.M. Slater, P.R. Bennett, M.H.F. Sullivan, IL-1β and IL-8 in human fetal membranes: Changes with gestational age, labor, and culture conditions, Am. J. Reprod. Immunol. 46 (2001) 260–267. https://doi.org/10.1034/j.1600-0897.2001.d01-11.x.

[53] P.C. Calder, Omega-3 polyunsaturated fatty acids and inflammatory processes: Nutrition or pharmacology?, Br. J. Clin. Pharmacol. 75 (2013) 645–662. https://doi.org/10.1111/j.1365-2125.2012.04374.x.

[54] A. Yamashita, K. Kawana, K. Tomio, A. Taguchi, Y. Isobe, R. Iwamoto, K. Masuda, H. Furuya, T. Nagamatsu, K. Nagasaka, T. Arimoto, K. Oda, O. Wada-Hiraike, T. Yamashita, Y. Taketani, J.X. Kang, S. Kozuma, H. Arai, M. Arita, Y. Osuga, T. Fujii, Increased tissue levels of omega-3 polyunsaturated fatty acids prevents pathological preterm birth, Sci. Rep. 3 (2013) 1–7. https://doi.org/10.1038/srep03113.

[55] C.J. Lo, K.C. Chiu, M. Fu, R. Lo, S. Helton, Fish oil decreases macrophage tumor necrosis factor gene transcription by altering the NFκB activity, J. Surg. Res. 82 (1999) 216–221. https://doi.org/10.1006/jsre.1998.5524.

[56] C. Lecchi, G. Invernizzi, A. Agazzi, M. Ferroni, L.F. Pisani, G. Savoini, F. Ceciliani, In vitro modulation of caprine monocyte immune functions by ω-3 polyunsaturated fatty acids, Vet. J. 189 (2011) 353–355. https://doi.org/10.1016/j.tvjl.2010.09.001.

[57] E.D. Merkley, D.S. Wunschel, K.L. Wahl, K.H. Jarman, Applications and challenges of forensic proteomics, Forensic Sci. Int. 297 (2019) 350–363. https://doi.org/10.1016/j.forsciint.2019.01.022.

[58] K. Suhre, M.I. McCarthy, J.M. Schwenk, Genetics meets proteomics: perspectives for large population-based studies, Nat. Rev. Genet. 22 (2021) 19–37. https://doi.org/10.1038/s41576-020-0268-2.

[59] J.R. Yates, Recent technical advances in proteomics [version 1; peer review: 2 approved], F1000Research. 8 (2019) 1–8.

[60] Z.R. Gregorich, Y. Ge, Top-down proteomics in health and disease: Challenges and opportunities, Proteomics. 14 (2014) 1195–1210. https://doi.org/10.1002/pmic.201300432.

[61] Y. Zhang, B.R. Fonslow, B. Shan, M. Baek, J.R. Yates, Protein Analysis by Shotgun/Bottom-up Proteomics, Chem. Rev. 113 (2013) 2343–2394.

[62] P.B. Pandeswari, V. Sabareesh, Middle-down approach: a choice to sequence and characterize proteins/proteomes by mass spectrometry, RSC Adv. 9 (2019) 313–344. https://doi.org/10.1039/c8ra07200k.

[63] N. Pappireddi, L. Martin, M. Wühr, A Review on Quantitative Multiplexed Proteomics, HHS Public Access. 20 (2019) 1210–1224. https://doi.org/10.1002/cbic.201800650.A.

[64] O.T. Schubert, H.L. Röst, B.C. Collins, G. Rosenberger, R. Aebersold, Quantitative proteomics: challenges and opportunities in basic and applied research, Nat. Publ. Gr. 12 (2017) 1289–1294. https://doi.org/10.1038/nprot.2017.040.

[65] S.A. Gerber, J. Rush, O. Stemman, M.W. Kirschner, S.P. Gygi, Absolute quantification of proteins and phosphoproteins from cell lysates by tandem MS, PNAS. 100 (2003) 6940–6945. https://doi.org/10.1073/pnas.0832254100.

[66] J. Park, P.D. Piehowski, C. Wilkins, M. Zhou, J. Mendoza, G.M. Fujimoto, B.C. Gibbons, J.B. Shaw, Y. Shen, A.K. Shukla, R.J. Moore, T. Liu, V.A. Petyuk, N. Tolić, L. Paša-tolić, R.D. Smith, S.H. Payne, S. Kim, Informed-Proteomics: open-source software package for top-down proteomics, Nat. Methods. 14 (2018) 909–914. https://doi.org/10.1038/nmeth.4388.

[67] J.R. Yates, C.I. Ruse, A. Nakorchevsky, Proteomics by Mass Spectrometry: Approaches, Advances, and Applications, Annu. Rev. Biomed. Eng. 11 (2009) 49–79. https://doi.org/10.1146/annurev-bioeng-061008-124934.

[68] A. Gorg, W. Weiss, M.J. Dunn, Current two dimensional electrophoresis technology for proteomics, 4 (2004) 3665–3685.

[69] S.R. Langley, J. Dwyer, I. Drozdov, X. Yin, M. Mayr, Proteomics: from single molecules to biological pathways, Cardiovasc. Res. 97 (2013) 612–622. https://doi.org/10.1093/cvr/cvs346.

[70] K. Chandramouli, P.-Y. Qian, Proteomics: Challenges, Techniques and Possibilities to Overcome Biological Sample Complexity, Hum. Genomics Proteomics. 1 (2009). https://doi.org/10.4061/2009/239204.

[71] M. Sonnett, E. Yeung, M. Wühr, Accurate, Sensitive, and Precise Multiplexed Proteomics Using the Complement Reporter Ion Cluster, Anal. Chem. 90 (2018) 5032–5039. https://doi.org/10.1021/acs.analchem.7b04713.

[72] C.S. Hughes, S. Moggridge, T. Müller, P.H. Sorensen, G.B. Morin, J. Krijgsveld, Single-pot, solid-phase-enhanced sample preparation for proteomics experiments, Nat. Protoc. 14 (2019).

[73] M. Mann, R.C. Hendrickson, A. Pandey, ANALYSIS OF PROTEINS AND PROTEOMES BY MASS SPECTROMETRY, Annu. Rev. Biochem. 70 (2001) 437–473.

[74] L.C. Gillet, A. Leitner, R. Aebersold, Mass Spectrometry Applied to Bottom-Up Proteomics: Entering the High-Throughput Era for Hypothesis Testing, Annu. Rev. Anal. Chem. 9 (2016) 449–472. https://doi.org/10.1146/annurev-anchem-071015-041535.

[75] F. Calderon-Celis, J.R. Encinar, A. Sanz-Medel, Standardization approaches in absolute quantitative proteomics with mass spectrometry, Mass Spectrom. Rev. 37 (2018) 715–737.

[76] J.K. Eng, B. Fischer, J. Grossmann, M.J. MacCoss, A Fast SEQUEST Cross Correlation Algorithm, J. Proteome Res. 7 (2008) 4598–4602.

[77] C. Chen, J. Hou, J.J. Tanner, J. Cheng, Bioinformatics Methods for Mass Spectrometry-Based Proteomics Data Analysis, Int. J. Mol. Sci. 21 (2020).

[78] J.S. Cottrell, Protein identification using MS/MS data, J. Proteomics. 74 (2011) 1842–1851. https://doi.org/10.1016/j.jprot.2011.05.014.

[79] D.C. Handler, D. Pascovici, M. Mirzaei, V. Gupta, G.H. Salekdeh, P.A. Haynes, The Art of Validating Quantitative Proteomics Data, Proteomics. 18 (2018). https://doi.org/10.1002/pmic.201800222.

[80] J. Kolakowska, A. Franczak, R.K.R. Saini, S. Souchelnytskyi, Progress and challenges in the proteomics of domestic pig in research on the female reproductive system, J. Elem. 21 (2016) 1055–1069. https://doi.org/10.5601/jelem.2016.21.1.1104.

[81] A.M. de Almeida, E. Bendixen, Pig proteomics: a review of a species in the crossroad between biomedical and food sciences, J. Proteomics. 75 (2012) 4296–4314. https://doi.org/10.1016/j.jprot.2012.04.010.

[82] C. Kasper, D. Ribeiro, A.M. De Almeida, C. Larzul, L. Liaubet, E. Murani, Omics Application in Animal Science—A Special Emphasis on Stress Response and Damaging Behaviour in Pigs, Genes (Basel). 11 (2020) 1–24.

[83] B. Moza Jalali, P. Likszo, D.J. Skarzynski, Proteomic and network analysis of pregnancy-induced changes in the porcine endometrium on Day 12 of gestation, Mol. Reprod. Dev. 83 (2016) 827–841. https://doi.org/10.1002/mrd.22733.

[84] J. Chae, J. Kim, S.G. Lee, Y. Jeon, D. Kim, Y. Soh, K.S. Seo, H.K. Lee, N. Choi, J. Ryu, S. Kang, S. Cho, D. Lee, H.M. Chung, D.-B. Koo, Proteomic analysis of pregnancy-related proteins from pig uterus endometrium during pregnancy, Proteome Sci. 9 (2011) 1–16.

[85] J. Kolakowska, E.M. Drzewiecka, W. Kozlowska, A. Zmijewska, S. Souchelnytskyi, A. Franczak, Proteomic profile alterations inporcine conceptuses during early stages of development, Reprod. Biol. 21 (2021) 100481. https://doi.org/10.1016/j.repbio.2021.100481.

[86] F. Gondret, B. Guével, M.C. Père, H. Quesnel, Y. Billon, E. Com, L. Canario, I. Louveau, L. Liaubet, Proteomic analysis of adipose tissue during the last weeks of gestation in pure and crossbred Large White or Meishan fetuses gestated by sows of either breed, J. Anim. Sci. Biotechnol. 9 (2018) 1–16. https://doi.org/10.1186/s40104-018-0244-2.

[87] L. Che, M. Xu, K. Gao, L. Wang, X. Yang, X. Wen, H. Xiao, M. Li, Z. Jiang, Mammary tissue proteomics in a pig model indicates that dietary valine supplementation increases milk fat content via increased de novo synthesis of fatty acid, Food Sci. Nutr. (2021) 6213–6223. https://doi.org/10.1002/fsn3.2574.

[88] G. Yin, L. Wang, X. Zhao, L. Yu, D. Huang, Proteomics analysis of colostrum samples from sows housed under different conditions, Animals. 10 (2020) 1–10. https://doi.org/10.3390/ani10020355.

[89] J.W. Li, J. Hu, M. Wei, Y.Y. Guo, P.S. Yan, The effects of maternal obesity on porcine placental efficiency and proteome, Animals. 9 (2019). https://doi.org/10.3390/ani9080546.

[90] O. Sarr, I. Louveau, C. Kalbe, C.C. Metges, C. Rehfeldt, F. Gondret, Prenatal exposure to maternal low or high protein diets induces modest changes in the adipose tissue proteome of newborn piglets, J. Anim. Sci. 88 (2010) 1626–1641. https://doi.org/10.2527/jas.2009-2542.

[91] O. Sarr, I. Louveau, I. Le Huërou-Luron, F. Gondret, Adipose tissue proteomes of intrauterine growth-restricted piglets artificially reared on a high-protein neonatal formula, J. Nutr. Biochem. 23 (2012) 1417–1424. https://doi.org/10.1016/j.jnutbio.2011.09.002.

[92] B. Donovan, A. Suarez-Trujillo, T. Casey, U.K. Aryal, D. Conklin, L.L. Williams, R.C. Minor, Inclusion of oat and yeast culture in sow gestational and lactational diets alters immune and antimicrobial associated proteins in milk, Animals. 11 (2021) 1–18. https://doi.org/10.3390/ani11020497.

[93] Y. Lin, L. Li, Y. Li, K. Wang, D. Wei, S. Xu, B. Feng, L. Che, Z. Fang, J. Li, Y. Zhuo, D. Wu, Interpretation of fiber supplementation on offspring testicular development in a pregnant sow model from a proteomics perspective, Int. J. Mol. Sci. 20 (2019). https://doi.org/10.3390/ijms20184549.

[94] W. Yao, J. Li, J. jun Wang, W. Zhou, Q. Wang, R. Zhu, F. Wang, P. Thacker, Effects of dietary ratio of n-6 to n-3 polyunsaturated fatty acids on immunoglobulins, cytokines, fatty acid composition, and performance of lactating sows and suckling piglets, J. Anim. Sci. Biotechnol. 3 (2012) 1–8. https://doi.org/10.1186/2049-1891-3-43.

[95] J. Yin, K.Y. Lee, J.K. Kim, I.H. Kim, Effects of different n-6 to n-3 polyunsaturated fatty acids ratio on reproductive performance, fecal microbiota and nutrient digestibility of gestation-lactating sows and suckling piglets, Anim. Sci. J. 88 (2017) 1744–1752. https://doi.org/10.1111/asj.12819.

[96] A. Agazzi, G. Invernizzi, A. Campagnoli, M. Ferroni, A. Fanelli, D. Cattaneo, A. Galmozzi, M. Crestani, V. Dell'Orto, G. Savoini, Effect of different dietary fats on hepatic gene expression in transition dairy goats, Small Rumin. Res. 93 (2010) 31–40. https://doi.org/10.1016/j.smallrumres.2010.04.027.

[97] G. Savoini, A. Agazzi, G. Invernizzi, D. Cattaneo, L. Pinotti, A. Baldi, Polyunsaturated fatty acids and choline in dairy goats nutrition: Production and health benefits, Small Rumin. Res. 88 (2010) 135–144. https://doi.org/10.1016/j.smallrumres.2009.12.021.

[98] C. Lecchi, G. Invernizzi, A. Agazzi, S. Modina, P. Sartorelli, G. Savoini, F. Ceciliani, Research in Veterinary Science Effects of EPA and DHA on lipid droplet accumulation and mRNA abundance of PAT proteins in caprine monocytes, Res. Vet. Sci. 94 (2013) 246–251. https://doi.org/10.1016/j.rvsc.2012.09.019.

[99] Y. Duan, F. Li, L. Li, J. Fan, X. Sun, Y. Yin, n-6 : n-3 PUFA ratio is involved in regulating lipid metabolism and inflammation in pigs, (2014) 445–451. https://doi.org/10.1017/S0007114513002584.

[100] G. Invernizzi, S. Modina, D. Corbani, V. Bronzo, L.F. Pisani, J.M. Caputo, A. Agazzi, V. Dell'Orto, G. Savoini, Hepatic and subcutaneous adipose tissue variations in transition dairy goats fed saturated or unsaturated fat supplemented diets, Small Rumin. Res. (2016). https://doi.org/10.1016/j.smallrumres.2016.09.009.

[101] S. Tanghe, J. Missotten, K. Raes, S. De Smet, The effect of different concentrations of linseed oil or fish oil in the maternal diet on the fatty acid composition and oxidative status of sows and piglets, J. Anim. Physiol. Anim. Nutr. (Berl). 99 (2015) 938–949. https://doi.org/10.1111/jpn.12243.

[102] A. Szostak, M. Og, M.F.W. Pas, E. Po, E. Juszczuk-kubiak, T. Blicharski, C.S. Pareek, J.R. Dunkelberger, O. Horba, M. Pierzcha, Effect of a diet enriched with omega-6 and omega-3 fatty acids on the pig liver transcriptome, Genes Nutr. 11 (2016) 1–17. https://doi.org/10.1186/s12263-016-0517-4.

[103] S.I. Lee, K.S. Kang, Omega-3 fatty acids modulate cyclophosphamide induced markers of immunosuppression and oxidative stress in pigs, Sci. Rep. 9 (2019) 1–8. https://doi.org/10.1038/s41598-019-39458-x.

[104] A. De Greeff, P. Bikker, E. Bruininx, H. Zwolschen, H. Fijten, P. Zetteler, Increased fat and polyunsaturated fatty acid content in sow gestation diet has no effect on gene expression in progeny during the first 7 days of life, J. Anim. Physiol. Anim. Nutr. (Berl). 100 (2016) 127–135. https://doi.org/10.1111/jpn.12345.

[105] S.C. Kyriakis, V.K. Tsiloyiannis, K. Sarris, A.C. Tsinas, C. Alexopoulos, L. Jansegers, The effect of probiotic LSP 122 on the control of post-weaning diarrhoea syndrome of piglets, Res. Vet. Sci. 67 (1999) 223–228.

[106] C. Alexopoulos, I.E. Georgoulakis, A. Tzivara, C.S. Kyriakis, A. Govaris, S.C. Kyriakis, Field evaluation of the effect of a probiotic-containing Bacillus licheniformis and Bacillus subtilis spores on the health status, performance, and carcass quality of grower and finisher pigs, J. Vet. Med. Ser. A Physiol. Pathol. Clin. Med. 51 (2004) 306–312. https://doi.org/10.1111/j.1439-0442.2004.00637.x.

[107] A. Estrada, M.D. Drew, A. Van Kessel, Effect of the dietary supplementation of fructooligosaccharides and Bifidobacterium longum to early-weaned pigs on performance and fecal bacterial populations, Can. J. Anim. Sci. 81 (2001) 141–148.

[108] C. Corino, S.C. Modina, A. Di Giancamillo, S. Chiapparini, R. Rossi, Seaweeds in pig nutrition, Animals. 9 (2019) 1–26. https://doi.org/10.3390/ani9121126.

[109] A.A.M. Chaves, C.F. Martins, D.F.P. Carvalho, D.M. Ribeiro, M. Lordelo, J.P.B. Freire, A.M. de Almeida, A viewpoint on the use of microalgae as an alternative feedstuff in the context of pig and poultry feeding—a special emphasis on tropical regions, Trop. Anim. Health Prod. 53 (2021). https://doi.org/10.1007/s11250-021-02800-5.

[110] D.M. Ribeiro, C.F. Martins, J. Kuleš, A. Horvatić, N. Guillemin, J.P.B. Freire, P.D. Eckersall, A.M. Almeida, J.A.M. Prates, Influence of dietary Spirulina inclusion and lysozyme

supplementation on the longissimus lumborum muscle proteome of newly weaned piglets, J. Proteomics. 244 (2021) 104274. https://doi.org/10.1016/j.jprot.2021.104274.

[111] D.A. Gahan, M.B. Lynch, J.J. Callan, J.T.O. Sullivan, J.V.O. Doherty, Performance of weanling piglets offered low- , medium- or high-lactose diets supplemented with a seaweed extract from Laminaria spp ., Animal. 3 (2009) 24–31. https://doi.org/10.1017/S1751731108003017.

[112] S. Gupta, N. Abu-Ghannam, Bioactive potential and possible health effects of edible brown seaweeds, Trends Food Sci. Technol. 22 (2011) 315–326. https://doi.org/10.1016/j.tifs.2011.03.011.

[113] V. Dhargalkar, N. Pereira, Seaweed: Promising plant of the millennium, Sci. Cult. 71 (2005) 60–66.

[114] T.N. Zvyagintseva, N.M. Shevchenko, A.O. Chizhov, T.N. Krupnova, E. V Sundukova, V. V Isakov, Water-soluble polysaccharides of some far-eastern brown seaweeds. Distribution, structure, and their dependence on the developmental conditions, J. Exp. Mar. Bio. Ecol. 294 (2003) 1–13. https://doi.org/10.1016/S0022-0981(03)00244-2.

[115] J.M. O'Connell, T. Sweeney, J.J. Callan, J. V. O'Doherty, The effect of cereal type and exogenous enzyme supplementation in pig diets on nutrient digestibility, intestinal microflora, volatile fatty acid concentration and manure ammonia emissions from finisher pigs, Anim. Sci. 81 (2005) 357–364. https://doi.org/10.1079/ASC42040357.

[116] W. Schoenherr, D. Pollmann, J. Coalson, Titration of Macro- GuardTM-S on growth performance of nursery pigs, J. Anim. Sci. 72 (1994) 57.

[117] J. Majtán, G. Kogan, E. Kováčová, K. Bíliková, J. Šimúth, Stimulation of TNF- α Release by Fungal Cell Wall Polysaccharides, Zeitschrift Für Naturforsch. C. 60 (2005) 921–926.

[118] W.A.J.P. Wijesinghe, Y. Jeon, Biological activities and potential industrial applications of fucose rich sulfated polysaccharides and fucoidans isolated from brown seaweeds : A review, Carbohydr. Polym. 88 (2012) 13–20. https://doi.org/10.1016/j.carbpol.2011.12.029.

[119] C. Zhuang, H. Itoh, T. Mizuno, H. Ito, Antitumor Active Fucoidan from the Brown Seaweed , Umitoranoo (Sargassum thunbergii), Biosci. Biotechnol. Biochem. 59 (1995) 563–567. https://doi.org/10.1271/bbb.59.563.

[120] J. Lee, K. Hayashi, M. Hashimoto, T. Nakano, T. Hayashi, Novel Antiviral Fucoidan from Sporophyll of Undaria pinnatifida (Mekabu), Chem. Pharm. Bull. 52 (2004) 1091–1094.

[121] M.O. McClure, J.P. Moore, D.F. Blanc, P. Scotting, G.M.W. Cook, R.J. Keynes, J.N. Weber, D. Davies, R.A. Weiss, Investigations into the Mechanism by Which Sulfated Polysaccharides Inhibit HIV Infection In Vitro, AIDS Res. Hum. Retroviruses. 8 (1992) 19–26.

[122] S. Eom, Y. Kim, S. Kim, Antimicrobial effect of phlorotannins from marine brown algae, Food Chem. Toxicol. 50 (2012) 3251–3255. https://doi.org/10.1016/j.fct.2012.06.028.

[123] J. Michiels, E. Skrivanova, J. Missotten, A. Ovyn, J. Mrazek, S. De Smet, N. Dierick, Intact brown seaweed (Ascophyllum nodosum) in diets of weaned piglets: Effects on performance, gut bacteria and morphology and plasma oxidative status, J. Anim. Physiol. Anim. Nutr. (Berl). 96 (2012) 1101–1111. https://doi.org/10.1111/j.1439-0396.2011.01227.x.

[124] S. Kandasamy, W. Khan, F. Evans, A.T. Critchley, B. Prithiviraj, Tasco®: A Product of Ascophyllum nodosum Enhances Immune Response of Caenorhabditis elegans Against Pseudomonas aeruginosa Infection, Mar. Drugs. 10 (2012) 84–105. https://doi.org/10.3390/md10010084.

[125] J.L. Turner, S.S. Dritz, J.J. Higgins, J.E. Minton, Effects of Ascophyllum nodosum extract on growth performance and immune function of young pigs challenged with Salmonella typhimurium, J. Anim. Sci. 80 (2002) 1947–1953. https://doi.org/10.2527/2002.8071947x.

[126] T. Sweeney, J. V. O'Doherty, Marine macroalgal extracts to maintain gut homeostasis in the weaning piglet, Domest. Anim. Endocrinol. 56 (2016) S84–S89. https://doi.org/10.1016/j.domaniend.2016.02.002.

[127] B. Bahar, J. V. O'Doherty, T.J. Smyth, T. Sweeney, A comparison of the effects of an Ascophyllum nodosum ethanol extract and its molecular weight fractions on the inflammatory immune gene expression in-vitro and ex-vivo, Innov. Food Sci. Emerg. Technol. 37 (2016) 276–285. https://doi.org/10.1016/j.ifset.2016.07.027.

[128] N. Dierick, A. Ovyn, S. De Smet, Effect of feeding intact brown seaweed Ascophyllum nodosum on some digestive parameters and on iodine content in edible tissues in pigs, J. Sci. Food Agric. 89 (2009) 584–594. https://doi.org/10.1002/jsfa.3480.

[129] P.C. Calder, Polyunsaturated Fatty Acids, Inflammation, and Immunity, Lipids. 36 (2001) 1007–1024.

[130] H. Sauerwein, U. Heintges, M. Hennies, T. Selhorst, A. Daxenberger, Growth hormone induced alterations of leptin serum concentrations in dairy cows as measured by a novel enzyme immunoassay, Livest. Prod. Sci. 87 (2004) 189–195. https://doi.org/10.1016/j.livprodsci.2003.08.001.

[131] M. Alberti, A., Bolognini, L., Macciantelli, D., Caratelli, The radical cation of N,N-diethl-para-phenylendiamine: A possible indicator of oxidative stress in biological samples, Res. Chem. Intermed. 26 (2000) 253–267. https://doi.org/10.1108/09596119910272739.

[132] P. Regenhard, D. Nakov, H. Sauerwein, Applicability of a spectrophotometric method for assessment of oxidative stress in poultry, Maced. Vet. Rev. (2014). https://doi.org/10.14432/j.macvetrev.2013.10.002.

[133] V. Witko-Sarsat, M. Friedlander, C. Capeillère-Blandin, T. Nguyen-Khoa, A.T. Nguyen, J. Zingraff, P. Jungers, B. Descamps-Latscha, Advanced oxidation protein products as a novel marker of oxidative stress in uremia, Kidney Int. 49 (1996) 1304–1313. https://doi.org/10.1038/ki.1996.186.

[134] M.M. Bradford, A rapid and sensitive method for the quantitation of microgram quantities of protein utilizing the principle of protein-dye binding, Anal. Biochem. (1976). https://doi.org/10.1016/0003-2697(76)90527-3.

[135] J.M.C. Gutteridge, G.J. Quinlan, Malondialdehyde formation from lipid peroxides in the thiobarbituric acid test: The role of lipid radicals, iron salts, and metal chelators, J. Appl. Biochem. (1983).

[136] I.F.F. Benzie, J.J. Strain, The ferric reducing ability of plasma (FRAP) as a measure of “antioxidant power”: The FRAP assay, Anal. Biochem. 239 (1996) 70–76. https://doi.org/10.1006/abio.1996.0292.

[137] J. Chen, Q. Xu, Y. Li, Z. Tang, W. Sun, X. Zhang, J. Sun, Z. Sun, Comparative effects of dietary supplementations with sodium butyrate, medium-chain fatty acids, and n-3 polyunsaturated fatty acids in late pregnancy and lactation on the reproductive performance of sows and growth performance of suckling piglets, J. Anim. Sci. 97 (2019) 4256–4267. https://doi.org/10.1093/jas/skz284.

[138] A. Cools, D. Maes, G. Papadopoulos, J.A. Vandermeiren, E. Meyer, K. Demeyere, S. De Smet, G.P.J. Janssens, Dose-response effect of fish oil substitution in parturition feed on erythrocyte membrane characteristics and sow performance, J. Anim. Physiol. Anim. Nutr. (Berl). 95 (2011) 125–136. https://doi.org/10.1111/j.1439-0396.2010.01119.x.

[139] M.S. Lund, M. Puonti, L. Rydhmer, J. Jensen, Relationship between litter size and perinatal and pre-weaning survival in pigs, Anim. Sci. 74 (2002) 217–222. https://doi.org/10.1017/S1357729800052383.

[140] J. Dobrzański, E. Sell-kubiak, E.F. Knol, Estimation of litter size variability phenotypes in Large White sows, J. Anim. Breed. Genet. 00 (2020) 1–12. https://doi.org/10.1111/jbg.12465.

[141] E.G. Camargo, D. Botelho, D. Marques, A.P. De Figueiredo, Genetic study of litter size and litter uniformity in Landrace pigs, Rev. Bras. Zootec. 49 (2020) 1–12.

[142] V.J.T. Van Ginneken, J.P.F.G. Helsper, W. De Visser, H. Van Keulen, W.A. Brandenburg, Polyunsaturated fatty acids in various macroalgal species from north Atlantic and tropical seas, Lipids Health Dis. 10 (2011) 4–11. https://doi.org/10.1186/1476-511X-10-104.

[143] R. Leikus, V. Juskiene, R. Juska, R. Juodka, D. Stankeviciene, R. Nainiene, A. Siukscius, Effect of linseed oil sediment in the diet of pigs on the growth performance and fatty acid profile of meat, Rev. Bras. Zootec. 47 (2018) 1–8. https://doi.org/10.1590/rbz4720170104.

[144] S. Tanghe, E. Cox, V. Melkebeek, S. De Smet, S. Millet, Effect of fatty acid composition of the sow diet on the innate and adaptive immunity of the piglets after weaning, Vet. J. 200 (2014) 287–293. https://doi.org/10.1016/j.tvjl.2014.02.025.

[145] F. De Quelen, G. Boudry, J. Mourot, Linseed oil in the maternal diet increases long chain-PUFA status of the foetus and the newborn during the suckling period in pigs, Br. J. Nutr. 104 (2010) 533–543. https://doi.org/10.1017/S0007114510000772.

[146] H. Zhu, H. Wang, S. Wang, Z. Tu, L. Zhang, X. Wang, Y. Hou, C. Wang, J. Chen, Y. Liu, Flaxseed Oil Attenuates Intestinal Damage and Inflammation by Regulating Necroptosis and TLR4/NOD Signaling Pathways Following Lipopolysaccharide Challenge in a Piglet Model, Mol. Nutr. Food Res. 62 (2018) 1–11. https://doi.org/10.1002/mnfr.201700814.

[147] T. Greupner, L. Kutzner, F. Nolte, A. Strangmann, H. Kohrs, A. Hahn, N.H. Schebb, J.P. Schuchardt, Effects of a 12-week high-α-linolenic acid intervention on EPA and DHA concentrations in red blood cells and plasma oxylipin pattern in subjects with a low EPA and DHA status, Food Funct. 9 (2018) 1587–1600. https://doi.org/10.1039/c7fo01809f.

[148] G.C. Burdge, P.C. Calder, Conversion of α-linolenic acid to longer-chain polyunsaturated fatty acids in human adults, Reprod. Nutr. Dev. 45 (2005) 581–597. https://doi.org/10.1051/rnd.

[149] M. Plourde, S.C. Cunnane, Extremely limited synthesis of long chain polyunsaturates in adults: Implications for their dietary essentiality and use as supplements, Appl. Physiol. Nutr. Metab. 32 (2007) 619–634. https://doi.org/10.1139/H07-034.

[150] C. Poumès-Ballihaut, B. Langelier, F. Houlier, J.M. Alessandri, G. Durand, C. Latge, P. Guesnet, Comparative bioavailability of dietary α-linolenic and docosahexaenoic acids in the growing rat, Lipids. 36 (2001) 793–800. https://doi.org/10.1007/s11745-001-0786-5.

[151] T. Greupner, L. Kutzner, S. Pagenkopf, H. Kohrs, A. Hahn, N.H. Schebb, J.P. Schuchardt, Effects of a low and a high dietary LA/ALA ratio on long-chain PUFA concentrations in red blood cells, Food Funct. 9 (2018) 4742–4754. https://doi.org/10.1039/c8fo00735g.

[152] O. Gruzdeva, D. Borodkina, E. Uchasova, Y. Dyleva, O. Barbarash, Leptin resistance: Underlying mechanisms and diagnosis, Diabetes, Metab. Syndr. Obes. Targets Ther. 12 (2019) 191–198. https://doi.org/10.2147/DMSO.S182406.

[153] S. Fukumitsu, K. Aida, N. Ueno, S. Ozawa, Y. Takahashi, M. Kobori, Flaxseed lignan attenuates high-fat diet-induced fat accumulation and induces adiponectin expression in mice, Br. J. Nutr. 100 (2008) 669–676. https://doi.org/10.1017/S0007114508911570.

[154] M. Baranowski, J. Enns, H. Blewett, U. Yakandawala, P. Zahradka, C.G. Taylor, Dietary flaxseed oil reduces adipocyte size, adipose monocyte chemoattractant protein-1 levels and T-cell infiltration in obese, insulin-resistant rats, Cytokine. 59 (2012) 382–391. https://doi.org/10.1016/j.cyto.2012.04.004.

[155] A.W. Tekeleselassie, Y.M. Goh, M.A. Rajion, M. Motshakeri, M. Ebrahimi, A high-fat diet enriched with low omega-6 to omega-3 fatty acid ratio reduced fat cellularity and plasma leptin concentration in sprague-dawley rats, Sci. World J. 2013 (2013) 1–7. https://doi.org/10.1155/2013/757593.

[156] J. Ukropec, J.E. Reseland, D. Gasperikova, E. Demcakova, L. Madsen, R.K. Berge, A.C. Rustan, I. Klimes, C.A. Drevon, E. Sebökova, The Hypotriglyceridemic Effect of Dietary n-3 FA Is Associated with Increased β-Oxidation and Reduced Leptin Expression, Lipids. 38 (2003) 1023–1029. https://doi.org/10.1007/s11745-006-1156-z.

[157] M.A. Camkurt, E. Findikli, F.I. Tolun, M. Bakacak, N.G. Bal, H. Sakalli, M. Güneş, Probable preventive effects of placenta from oxidative stress; Evaluation of total antioxidant status, total oxidant status and oxidative stress index in fetal cord blood during the delivery, Psychiatry Res. 240 (2016) 222–225. https://doi.org/10.1016/j.psychres.2016.03.054.

[158] P. Celi, M. Merlo, L. Da Dalt, A. Stefani, O. Barbato, G. Gabai, Relationship between late embryonic mortality and the increase in plasma advanced oxidised protein products (AOPP) in dairy cows, Reprod. Fertil. Dev. 23 (2011) 527–533. https://doi.org/10.1071/RD10268.

[159] S.C. Lindblom, Impacts of feeding peroxidized oils on growth and oxidative status in swine and poultry. Master of science, Iwoa State University, Ames, Iowa, 2017. https://lib.dr.iastate.edu/etd.

[160] E. Barba-Vidal, S.M. Martín-Orué, L. Castillejos, Review: Are we using probiotics correctly in post-weaning piglets?, Animal. 12 (2018) 2489–2498. https://doi.org/10.1017/S1751731118000873.

[161] H. Sauerwein, S. Schmitz, S. Hiss, Effects of a dietary application of a yeast cell wall extract on innate and acquired immunity, on oxidative status and growth performance in weanling piglets

and on the ileal epithelium in fattened pigs, J. Anim. Physiol. Anim. Nutr. (Berl). 91 (2007) 369–380. https://doi.org/10.1111/j.1439-0396.2006.00663.x.

[162] L.H. Zhu, K.L. Zhao, X.L. Chen, J.X. Xu, Impact of weaning and an antioxidant blend on intestinal barrier function and antioxidant status in pigs, J. Anim. Sci. 90 (2012) 2581–2589. https://doi.org/10.2527/jas.2011-4444.

[163] Y. V. Silva-Guillen, C. Arellano, R.D. Boyd, G. Martinez, E. Van Heugten, Growth performance, oxidative stress and immune status of newly weaned pigs fed peroxidized lipids with or without supplemental vitamin e or polyphenols, J. Anim. Sci. Biotechnol. 11 (2020) 1–11. https://doi.org/10.1186/s40104-020-0431-9.

[164] H.P.S. Makkar, G. Tran, V. Heuzé, S. Giger-Reverdin, M. Lessire, F. Lebas, P. Ankers, Seaweeds for livestock diets: A review, Anim. Feed Sci. Technol. 212 (2016) 1–17. https://doi.org/10.1016/j.anifeedsci.2015.09.018.

[165] A. V. Lee, L. You, S.Y. Oh, Z. Li, R.E. Fisher-Heffernan, T.R.H. Regnault, C.F.M. de Lange, L. Huber, N.A. Karrow, Microalgae supplementation to late gestation sows and its effects on the health status of weaned piglets fed diets containing high- or low-quality protein sources, Vet. Immunol. Immunopathol. 218 (2019). https://doi.org/10.1016/j.vetimm.2019.109937.

[166] J.M. McAfee, H.G. Kattesh, M.D. Lindemann, B.H. Voy, C.J. Kojima, N.C. Burdick Sanchez, J.A. Carroll, B.E. Gillespie, A.M. Saxton, Effect of omega-3 polyunsaturated fatty acid (n-3 PUFA) supplementation to lactating sows on growth and indicators of stress in the postweaned pig, J. Anim. Sci. 97 (2019) 4453–4463. https://doi.org/10.1093/jas/skz300.

[167] G. Corona, Y. Ji, P. Anegboonlap, S. Hotchkiss, C. Gill, P. Yaqoob, J.P.E. Spencer, I. Rowland, Gastrointestinal modifications and bioavailability of brown seaweed phlorotannins and effects on inflammatory markers, Br. J. Nutr. 115 (2016) 1240–1253. https://doi.org/10.1017/S0007114516000210.

[168] M. Dell'Anno, S. Sotira, R. Rebucci, S. Reggi, B. Castiglioni, L. Rossi, In vitro evaluation of antimicrobial and antioxidant activities of algal extracts, Ital. J. Anim. Sci. 19 (2020) 103–113. https://doi.org/10.1080/1828051X.2019.1703563.

[169] J. Leskovec, V. Rezar, A.N. Svete, Antioxidative effects of olive polyphenols compared to vitamin e in piglets fed a diet rich in n-3 pufa, Animals. 9 (2019) 1–11. https://doi.org/10.3390/ani9040161.

[170] Y. Yang, C.J. Hu, X. Zhao, K. Xiao, M. Deng, L. Zhang, X. Qiu, J. Deng, Y. Yin, C. Tan, Dietary energy sources during late gestation and lactation of sows: effects on performance, glucolipid metabolism, oxidative status of sows, and their offspring, J. Anim. Sci. 97 (2019) 4608–4618. https://doi.org/10.1093/jas/skz297.

[171] M. Kouba, J. Mourot, A review of nutritional effects on fat composition of animal products with special emphasis on n-3 polyunsaturated fatty acids, Biochimie. 93 (2011) 13–17. https://doi.org/10.1016/j.biochi.2010.02.027.

[172] A.P. Simopoulos, Omega-3 fatty acids in health and disease and in growth and development, Am. J. Clin. Nutr. 54 (1991) 438–463. https://doi.org/10.1093/ajcn/54.3.438.

[173] Y. Wei, Y. Meng, N. Li, Q. Wang, L. Chen, The effects of low-ratio n-6/n-3 PUFA on biomarkers of inflammation: a systematic review and meta-analysis, Food Funct. 12 (2021) 30–40. https://doi.org/10.1039/d0fo01976c.

[174] I. Djuricic, P.C. Calder, Beneficial outcomes of omega-6 and omega-3 polyunsaturated fatty acids on human health: an update for 2021, Nutrients. 13 (2021). https://doi.org/10.3390/nu13072421.

[175] N. Blondeau, R.H. Lipsky, M. Bourourou, M.W. Duncan, P.B. Gorelick, A.M. Marini, Alpha-linolenic acid: an omega-3 fatty acid with neuroprotective properties - ready for use in the stroke clinic?, Biomed Res. Int. 2015 (2015) 1–8. https://doi.org/10.1155/2015/519830.

[176] Y. Dai, L. Zhang, Z. Yan, Z. Li, M. Fu, C. Xue, J. Wang, A low proportion n-6/n-3 PUFA diet supplemented with Antarctic krill (: Euphausia superba) oil protects against osteoarthritis by attenuating inflammation in ovariectomized mice, Food Funct. 12 (2021) 6766–6779. https://doi.org/10.1039/d1fo00056j.

[177] P. Corrales, A. Vidal-Puig, G. Medina-Gómez, Obesity and pregnancy, the perfect metabolic storm, Eur. J. Clin. Nutr. (2021). https://doi.org/10.1038/s41430-021-00914-5.

[178] C.E. Bowman, Z. Arany, M.J. Wolfgang, Regulation of maternal–fetal metabolic communication, Springer International Publishing, 2021. https://doi.org/10.1007/s00018-020-03674-w.

[179] D.E. Bauman, Regulation of nutrient partitioning during lactation: homeostasis and homeorhesis revisited, in: Rumin. Physiol. Dig. Metab. Growth, Reprod., CABI Publishing, 2000: pp. 311–328. https://books.google.co.uk/books?id=_cxUuEaITRsC&source=gbs_navlinks_s.

[180] S.W. Kim, A.C. Weaver, Y.B. Shen, Y. Zhao, Improving efficiency of sow productivity: nutrition and health, J. Anim. Sci. Biotechnol. 4 (2013) 2–9. https://doi.org/10.1186/2049-1891-4-26.

[181] F. Oppedisano, R. Macrì, M. Gliozzi, V. Musolino, C. Carresi, J. Maiuolo, F. Bosco, S. Nucera, M.C. Zito, L. Guarnieri, F. Scarano, C. Nicita, A.R. Coppoletta, S. Ruga, M. Scicchitano, R. Mollace, E. Palma, V. Mollace, The anti-inflammatory and antioxidant properties of n-3 PUFAs: their role in cardiovascular protection, Biomedicines. 8 (2020) 1–18. https://doi.org/10.3390/biomedicines8090306.

[182] H. Wang, H.M. Yun, I.H. Kim, Evaluation of dietary-coated omega-3 fatty acid supplementation on reproduction performance, growth performance, nutrient digestibility, and blood profiles in lactating sows and suckling piglets, Can. J. Anim. Sci. 101 (2021) 473–480. https://doi.org/10.1139/cjas-2019-0074.

[183] T.X. Nguyen, A. Agazzi, M. Comi, V. Bontempo, I. Guido, S. Panseri, H. Sauerwein, P.D. Eckersall, R. Burchmore, G. Savoini, Effects of Low ω 6 : ω 3 Ratio in Sow Diet and Seaweed Supplement in Piglet Diet on Performance , Colostrum and Milk Fatty Acid Profiles , and Oxidative Status, Animals. 10 (2020). https://doi.org/10.3390/ani10112049.

[184] S. Martinez-Subiela, A. Horvatic, D. Escribano, L. Pardo-Marin, M. Kocaturk, V. Mrljak, R. Burchmore, J.J. Ceron, Z. Yilmaz, Identification of novel biomarkers for treatment monitoring in canine leishmaniosis by high-resolution quantitative proteomic analysis, Vet. Immunol. Immunopathol. 191 (2017) 60–67. https://doi.org/10.1016/j.vetimm.2017.08.004.

[185] Y. Perez-Riverol, A. Csordas, J. Bai, M. Bernal-Llinares, S. Hewapathirana, D.J. Kundu, A. Inuganti, J. Griss, G. Mayer, M. Eisenacher, E. Pérez, J. Uszkoreit, J. Pfeuffer, T. Sachsenberg, Ş. Yilmaz, S. Tiwary, J. Cox, E. Audain, M. Walzer, A.F. Jarnuczak, T. Ternent, A. Brazma, J.A. Vizcaíno, The PRIDE database and related tools and resources in 2019: Improving support for quantification data, Nucleic Acids Res. 47 (2019) D442–D450. https://doi.org/10.1093/nar/gky1106.

[186] T. Huang, M. Choi, M. Tzouros, S. Golling, N.J. Pandya, B. Banfai, T. Dunkley, O. Vitek, T. Huang, M. Choi, M. Tzouros, S. Golling, MSstatsTMT: statistical detection of differentially abundant proteins in experiments with isobaric labeling and multiple mixtures, Mol. Cell. Proteomics. 19 (2020) 1706–1723. https://doi.org/10.1074/mcp.RA120.002105.

[187] T. R Core Team, R: A Language and Environment for Statistical Computing - Reference Index - Version 4.1.0 (2021-05-18), (2021) 1–3728.

[188] H. Wickham, ggplot2: Elegant Graphics for Data Analysis. Second edition. Springer., 2016. http://link.springer.com/10.1007/978-0-387-98141-3.

[189] J.C. Oliveros, Venny. An interactive tool for comparing lists with Venn's diagrams., (2021). https://bioinfogp.cnb.csic.es/tools/venny/index.html (accessed November 9, 2021).

[190] D. Szklarczyk, A.L. Gable, K.C. Nastou, D. Lyon, R. Kirsch, S. Pyysalo, N.T. Doncheva, M. Legeay, T. Fang, P. Bork, L.J. Jensen, C. Von Mering, The STRING database in 2021 : customizable protein – protein networks , and functional characterization of user-uploaded gene / measurement sets, Nucleic Acids Res. 49 (2021) 605–612. https://doi.org/https://doi.org/10.1093/nar/gkaa1074.

[191] P. Shannon, A. Markiel, O. Ozier, N.S. Baliga, J.T. Wang, D. Ramage, N. Amin, B. Schwikowski, T. Ideker, Cytoscape: a software environment for integrated models of biomolecular interaction networks, Genome Res. 13 (2003) 2498–2504. https://doi.org/10.1101/gr.1239303.metabolite.

[192] F. Supek, M. Bosˇnjak, N. Sˇkunca, T. Sˇmuc, REVIGO summarizes and visualizes long lists of Gene Ontology terms, PLoS One. 6 (2011) e21800. https://doi.org/10.1371/journal.pone.0021800.

[193] R. Baka, D. Eckersall, A. Horvatic, A. Gelemanovic, V. Mrljak, M. McLaughlin, L. V. Athanasiou, N. Papaioannou, I. Stylianaki, H.Q. Hanh, C.C. Chadwick, Z. Polizopoulou,

Quantitative proteomics of cerebrospinal fluid using tandem mass tags in dogs with recurrent epileptic seizures, J. Proteomics. 231 (2021) 103997. https://doi.org/10.1016/j.jprot.2020.103997.

[194] M. Piñeiro, F. Lampreave, M.A. Alava, Development and validation of an ELISA for the quantification of pig Major Acute phase Protein (pig-MAP), Vet. Immunol. Immunopathol. 127 (2009) 228–234. https://doi.org/10.1016/j.vetimm.2008.10.318.

[195] W.T. Friedewald, R.I. Levy, D.S. Fredrickson, Estimation of the concentration of low-density lipoprotein cholesterol in plasma, without use of the preparative ultracentrifuge, Clin. Chem. 18 (1972) 499–502. https://academic.oup.com/clinchem/article-abstract/18/6/499/5676160?redirectedFrom=fulltext.

[196] L.M. Smith, N.L. Kelleher, Proteoform: a single term describing protein complexity, Nat. Methods. 10 (2013) 186–187. https://doi.org/10.1038/nmeth.2369.

[197] A. Archakov, A. Aseev, V. Bykov, A. Grigoriev, V. Govorun, V. Ivanov, A. Khlunov, A. Lisitsa, S. Mazurenko, A.A. Makarov, E. Ponomarenko, R. Sagdeev, K. Skryabin, Gene-centric view on the human proteome project: The example of the Russian roadmap for chromosome 18, Proteomics. 11 (2011) 1853–1856. https://doi.org/10.1002/pmic.201000540.

[198] S.N. Naryzhny, M.A. Maynskova, V.G. Zgoda, N.L. Ronzhina, O.A. Kleyst, I. V. Vakhrushev, A.I. Archakov, Virtual-experimental 2DE approach in chromosome-centric human proteome project, J. Proteome Res. 15 (2016) 525–530. https://doi.org/10.1021/acs.jproteome.5b00871.

[199] Y. Zhang, Z. Wen, M.P. Washburn, L. Florens, Refinements to label free proteome quantitation: how to deal with peptides shared by multiple proteins, Anal. Chem. 82 (2010) 2272–2281. https://doi.org/10.1021/ac9023999.

[200] C.D. Wenger, D.H. Phanstiel, M.V. Lee, D.J. Bailey, J.J. Coon, COMPASS: a suite of pre- and post-search proteomics software tools for OMSSA, Proteomics. 11 (2011) 1064–1074. https://doi.org/10.1002/pmic.201000616.

[201] Y. Yang, C.J. Hu, X. Zhao, K. Xiao, M. Deng, L. Zhang, X. Qiu, J. Deng, Y. Yin, C. Tan, Dietary energy sources during late gestation and lactation of sows: Effects on performance, glucolipid metabolism, oxidative status of sows, and their offspring, J. Anim. Sci. 97 (2019) 4608–4618. https://doi.org/10.1093/jas/skz297.

[202] A.P. Levy, R. Asleh, S. Blum, N.S. Levy, R. Miller-Iotan, S. Kalet-litman, Y. Anbinder, O. Lache, F.M. Nakhoul, R. Asaf, D. Farbstein, M. Pollak, Y.Z. Soloveichik, M. Strauss, J. Alshiek, A. Livshits, A. Schwartz, H. Awad, K. Jad, H. Goldenstein, Haptoglobin: basic and clinical aspects, Antioxid. Redox Signal. 12 (2009) 293–304.

[203] A.I. Alayash, Haptoglobin: old protein with new functions, Clin. Chim. Acta. 412 (2011) 493–498. https://doi.org/10.1016/j.cca.2010.12.011.

[204] I.K. Quaye, Haptoglobin , inflammation and disease, Trans. R. Soc. Trop. Med. Hyg. 102 (2008) 735—742. https://doi.org/10.1016/j.trstmh.2008.04.010.

[205] M. Arredouani, P. Matthijs, E. Hoeyveld, A. Kasran, H. Baumann, J.L. Ceuppens, Haptoglobin directly affects T cells and suppresses T helper cell type 2 cytokine release, Immunology. 108 (2003) 144–151.

[206] J.J. Dinicolantonio, J.H. O'Keefe, Importance of maintaining a low omega-6/omega-3 ratio for reducing inflammation, Open Hear. 5 (2018) 3–6. https://doi.org/10.1136/openhrt-2018-000946.

[207] R. Cannarella, A. Crafa, F. Barbagallo, L.M. Mongioì, R.A. Condorelli, A. Aversa, A.E. Calogero, S. La Vignera, Seminal plasma proteomic biomarkers of oxidative stress, Int. J. Mol. Sci. 21 (2020) 1–13. https://doi.org/10.3390/ijms21239113.

[208] S.B. Seidelmann, B. Claggett, S. Cheng, M. Henglin, A. Shah, L.M. Steffen, A.R. Folsom, E.B. Rimm, W.C. Willett, S.D. Solomon, Dietary carbohydrate intake and mortality: a prospective cohort study and meta-analysis, Lancet Public Heal. 3 (2018) e419–e428. https://doi.org/10.1016/S2468-2667(18)30135-X.

[209] B.J. et al. Agarwal, A., Aponte-Mellado, A., Premkumar, The effects of oxidative stress on female reproduction: a review, Reprod. Biol. Endocrinol. 49 (2012). https://doi.org/https://doi.org/10.1186/1477-7827-10-49.

[210] A. Mehta, M.D. Shapiro, Apolipoproteins in vascular biology and atherosclerotic disease, Nat. Rev. Cardiol. (2021). https://doi.org/10.1038/s41569-021-00613-5.

[211] M.A. Navarro, R. Carpintero, S. Acı, J.M. Arbone, L. Calleja, R. Carnicer, J.C. Surra, M.A. Guzma, Immune-regulation of the apolipoprotein A-I / C-III / A-IV gene cluster in experimental inflammation, Cytokine. 31 (2005) 52–63. https://doi.org/10.1016/j.cyto.2005.03.002.

[212] R. Carpintero, M. Pin˜eiro, M. Andre, M. Iturralde, M.A. Alava, P.M.H. Heegaard, J.L. Jobert, F. Madec, F. Lampreave, The concentration of apolipoprotein A-I decreases during experimentally induced acute-phase processes in pigs, Infect. Immun. 73 (2005) 3184–3187. https://doi.org/10.1128/IAI.73.5.3184.

[213] D. Burger, J.-M. Dayer, High-density lipoprotein-associated apolipoprotein A-I : the missing link between infection and chronic inflammation ?, Autoimmun. Rev. 1 (2002) 111–117.

[214] E. Lindhorst, D. Young, W. Bagshaw, M. Hyland, Acute inflammation , acute phase serum amyloid A and cholesterol metabolism in the mouse, Biochim. Biophys. Acta. 1339 (1997) 143–154. https://doi.org/10.1016/s0167-4838(96)00227-0.

[215] S. Oikawa, N. Katoh, H. Itoh, T. Miyamoto, M. Konno, T. Kajita, Decreased serum apolipoprotein A-I concentrations in cows infected with Salmonella Typhimurium, Can J Vet Res. 61 (1997) 182–186.

[216] N. Venteclef, T. Jakobsson, K.R. Steffensen, E. Treuter, Metabolic nuclear receptor signaling and the inflammatory acute phase response, Trends Endocrinol. Metab. 22 (2011) 333–343. https://doi.org/10.1016/j.tem.2011.04.004.

[217] C.S. Gangabadage, J. Zdunek, M. Tessari, S. Nilsson, G. Olivecrona, S.S. Wijmenga, Structure and dynamics of human apolipoprotein CIII, J. Biol. Chem. 283 (2008) 17416–17427. https://doi.org/10.1074/jbc.M800756200.

[218] A. Sahebkar, L.E. Simental-Mendía, D.P. Mikhailidis, M. Pirro, M. Banach, C.R. Sirtori, Ž. Reiner, Effect of omega-3 supplements on plasma apolipoprotein C-III concentrations: a systematic review and meta-analysis of randomized controlled trials, Ann. Med. 50 (2018) 565–575. https://doi.org/10.1080/07853890.2018.1511919.

[219] T. Gong, R. Zhou, ApoC3: an ‘alarmin’ triggering sterile inflammation, Nat. Immunol. 21 (2020) 9–16.

[220] I. Valladolid-acebes, P. Berggren, L. Juntti-berggren, Apolipoprotein CIII is an important piece in the type-1 diabetes jigsaw puzzle, Int. J. Mol. Sci. 22 (2021).

[221] A. Onat, G. Hergenc, E. Ayhan, M. Ugur, H. Kaya, M. Tuncer, G. Can, Original article: metabolism serum apolipoprotein C-III in high-density lipoprotein: a key diabetogenic risk factor in Turks, Diabet. Med. 26 (2009) 981–988. https://doi.org/10.1111/j.1464-5491.2009.02814.x.

[222] J. Fruchart-Najib, E. Bauge, L.-S. Niculescu, T. Pham, B. Thomas, C. Rommens, Z. Majd, B. Brewer, L.A. Pennacchio, J. Fruchart, Mechanism of triglyceride lowering in mice expressing human apolipoprotein A5, Biochem. Biophys. Res. Commun. 319 (2004) 397–404. https://doi.org/10.1016/j.bbrc.2004.05.003.

[223] C. Pineiro, M. Pineiro, J. Morales, M. Andres, E. Lorenzo, M. del Pozo, M.A. Alava, F. Lampreave, Pig-MAP and haptoglobin concentration reference values in swine from commercial farms, Vet. J. 179 (2009) 78–84. https://doi.org/10.1016/j.tvjl.2007.08.010.

[224] A.S. Georgiou, E. Sostaric, C.H. Wong, A.P.L. Snijders, P.C. Wright, H.D. Moore, A. Fazeli, Gametes alter the oviductal secretory proteome, Mol. Cell. Proteomics. 4 (2005) 1785–1796. https://doi.org/10.1074/mcp.M500119-MCP200.

[225] K. Lavery, A. Way, G. Killian, Identification and immunohistochemical localization of a haptoglobin-like protein in the tissues and fluids of the bovine (Bos taurus) ovary and oviduct, Reproduction. 125 (2003) 837–846.

[226] T. Parmar, G. Sachdeva, L. Savardekar, R.R. Katkam, V. Salvi, D.D. Manjramkar, P. Meherji, C.P. Puri, Protein repertoire of human uterine fluid during the mid-secretory phase of the menstrual cycle, Hum. Reprod. 23 (2008) 379–386.

[227] F.A. García-Vázquez, C. Moros-Nicolás, R. López-Úbeda, E. Rodríguez-Tobón, A. Guillén-Martínez, J.W. Ross, C. Luongo, C. Matás, I. Hernández-Caravaca, M. Avilés, M.J. Izquierdo-Rico, Evidence of haptoglobin in the porcine female genital tract during oestrous cycle and its effect on in vitro embryo production, Sci. Rep. 11 (2021) 1–14. https://doi.org/10.1038/s41598-021-90810-6.

[228] C.D. Bhanumathy, Y. Tang, S.P.S. Monga, V. Katuri, J.A. Cox, B. Mishra, L. Mishra, Itih-4, a serine protease inhibitor regulated in interleukin-6-dependent liver formation: role in liver development and regeneration, Dev. Dyn. 223 (2002) 59–69. https://doi.org/10.1002/dvdy.1235.

[229] M.A. Alava, N. Gonzalez-Ramon, P. Heegaard, S. Guzylack, M.J.M. Toussaint, C. Lipperheide, F. Madec, E. Gruys, P.D. Eckersall, F. Lampreave, A. Pineiro, Pig-MAP, porcine acute phase proteins and standardisation of assays in Europe, Comp. Haematol. Int. 7 (1997) 208–213.

[230] M. Piñeiro, C. Piñeiro, R. Carpintero, J. Morales, F.M. Campbell, P.D. Eckersall, M.J.M. Toussaint, F. Lampreave, Characterisation of the pig acute phase protein response to road transport, Vet. J. 173 (2007) 669–674. https://doi.org/10.1016/j.tvjl.2006.02.006.

[231] R.D. Geisert, M.D. Ashworth, J.R. Malayer, Expression of inter-α-trypsin inhibitor heavy chains in endometrium of cyclic and pregnant gilts, Reproduction. 126 (2003) 621–627. https://doi.org/10.1530/rep.0.1260621.

[232] D.C.M. Terrin G., Di Chiara M., Sabatini G., Senterre T., Enteral Nutrition in Preterm Neonates., in: D.A. Guandalini S. (Ed.), Textb. Pediatr. Gastroenterol. Hepatol. Nutr., Springer, Cham., 2022: pp. 65–85. https://doi.org/https://doi.org/10.1007/978-3-030-80068-0_6.

[233] R. Choudhury, A. Middelkoop, J. Boekhorst, W.J.J. Gerrits, B. Kemp, J.E. Bolhuis, M. Kleerebezem, Early life feeding accelerates gut microbiome maturation and suppresses acute post-weaning stress in piglets, Environ. Microbiol. 23 (2021) 7201–7213. https://doi.org/10.1111/1462-2920.15791.

[234] Z.W. Mu C., Pi Y., Zhang C., Microbiomes in the Intestine of Developing Pigs: Implications for Nutrition and Health, in: W. G. (Ed.), Recent Adv. Anim. Nutr. Metab. Adv. Exp. Med. Biol. Vol 1354, Springer, Cham, 2022: pp. 161–176. https://doi.org/https://doi.org/10.1007/978-3-030-85686-1_9.

[235] S. Sugiharto, M.S. Hedemann, C. Lauridsen, Plasma metabolomic profiles and immune responses of piglets after weaning and challenge with E. coli, J. Anim. Sci. Biotechnol. 5 (2014) 1–8. https://doi.org/10.1186/2049-1891-5-17.

[236] S. Udit, K. Blake, I.M. Chiu, Somatosensory and autonomic neuronal regulation of the immune response, Nat. Rev. Neurosci. 0123456789 (2022). https://doi.org/10.1038/s41583-021-00555-4.

[237] C. V. Jakubzick, G.J. Randolph, P.M. Henson, Monocyte differentiation and antigen-presenting functions, Nat. Rev. Immunol. 17 (2017) 349–362. https://doi.org/10.1038/nri.2017.28.

[238] V. Papayannopoulos, Neutrophil extracellular traps in immunity and disease, Nat. Rev. Immunol. 18 (2018) 134–147. https://doi.org/10.1038/nri.2017.105.

[239] K.D. Stone, C. Prussin, D.D. Metcalfe, IgE, mast cells, basophils, and eosinophils, J. Allergy Clin. Immunol. 125 (2010) S73–S80. https://doi.org/10.1016/j.jaci.2009.11.017.

[240] H. Spits, D. Artis, M. Colonna, A. Diefenbach, J.P. Di Santo, G. Eberl, S. Koyasu, R.M. Locksley, A.N.J. McKenzie, R.E. Mebius, F. Powrie, E. Vivier, Innate lymphoid cells-a proposal for uniform nomenclature, Nat. Rev. Immunol. 13 (2013) 145–149. https://doi.org/10.1038/nri3365.

[241] N.M. Chapman, H. Chi, Metabolic adaptation of lymphocytes in immunity and disease, Immunity. 55 (2022) 14–30. https://doi.org/10.1016/j.immuni.2021.12.012.

[242] A. Barbero, S. Astiz, C.J. Lopez-bote, M.L. Perez-solana, M. Ayuso, Maternal Malnutrition and Offspring Sex Determine Juvenile Obesity and Metabolic Disorders in a Swine Model of Leptin Resistance, PLoS One. 8 (2013) 1–14. https://doi.org/10.1371/journal.pone.0078424.

[243] K.E. Govoni, S.A. Reed, S.A. Zinn, Cell biology symposium: metabolic responses to stress: from animal to cell: Poor maternal nutrition during gestation: effects on offspring whole-body and tissue-specific metabolism in livestock species, J. Anim. Sci. 97 (2019) 3142–3152. https://doi.org/10.1093/jas/skz157.

[244] Q. Du, L. Zhou, M. Li, F. Lyu, J. Liu, Y. Ding, Omega-3 polyunsaturated fatty acid encapsulation system: Physical and oxidative stability , and medical applications, Food Front. (2022) 1–17. https://doi.org/10.1002/fft2.134.

[245] M.E. Berger, S. Smesny, S.W. Kim, C.G. Davey, S. Rice, Z. Sarnyai, M. Schlögelhofer, M.R. Schäfer, M. Berk, P.D. McGorry, G.P. Amminger, Omega-6 to omega-3 polyunsaturated fatty acid

ratio and subsequent mood disorders in young people with at-risk mental states: A 7-year longitudinal study, Transl. Psychiatry. 7 (2017) 1–6. https://doi.org/10.1038/tp.2017.190.

[246] J.M. Ahn, M.R. Hoque, Y.J. Choi, I.H. Kim, Effects of flaxseed oil supplementation on lactating sows and their offspring, Korean J. Agric. Sci. 48 (2021) 11–19. https://doi.org/10.7744/kjoas.20200059.

[247] X.L. Chen, N. Wang, M.L. Tian, L. Wang, T. Liu, X.W. Zhang, B.M. Shi, A.S. Shan, Dietary linseed oil in the maternal diet affects immunoglobulins , tissue fatty acid composition and expression of lipid metabolism-related genes in piglets, J. Anim. Physiol. Anim. Nutr. (Berl). 101 (2017) 257–265. https://doi.org/10.1111/jpn.12599.

[248] J.-P. Lalles, C.A. Montoya, Dietary alternatives to in-feed antibiotics , gut barrier function and inflammation in piglets post-weaning: Where are we now ?, Anim. Feed Sci. Technol. 274 (2021). https://doi.org/10.1016/j.anifeedsci.2021.114836.

[249] Z. Tamanai-Shacoori, F. Chandad, A. Rebillard, J. Cillard, M. Bonnaure-mallet, Silver-Zeolite Combined to Polyphenol-Rich Extracts of Ascophyllum nodosum: Potential Active Role in Prevention of Periodontal Diseases, PLoS One. 9 (2014) 1–8. https://doi.org/10.1371/journal.pone.0105475.

[250] G. Corona, M.M. Coman, Y. Guo, S. Hotchkiss, C. Gill, P. Yaqoob, J.P. Spencer, I. Rowland, Effect of simulated gastrointestinal digestion and fermentation on polyphenolic content and bioactivity of brown seaweed phlorotannin-rich extracts, Mol. Nutr. Food Res. 61 (2017) 1–10. https://doi.org/10.1002/mnfr.201700223.

[251] L. Ford, C. Curry, M. Campbell, K. Theodoridou, G. Sheldrake, J. Dick, L. Stella, P.J. Walsh, Effect of phlorotannins from brown seaweeds on the in vitro digestibility of pig feed, Animals. 10 (2020) 1–16. https://doi.org/10.3390/ani10112193.

[252] Z. Jiang, T. Okimura, T. Yokose, Y. Yamasaki, K. Yamaguchi, T. Oda, Effects of sulfated fucan , ascophyllan , from the brown Alga Ascophyllum nodosum on various cell lines : A comparative study on ascophyllan and fucoidan, JBIOSC. 110 (2010) 113–117. https://doi.org/10.1016/j.jbiosc.2010.01.007.

[253] M. Costa, C. Cardoso, C. Afonso, N.M. Bandarra, J.A.M. Prates, Current knowledge and future perspectives of the use of seaweeds for livestock production and meat quality : a systematic review, J. Anim. Physiol. Anim. Nutr. (Berl). (2021) 1–28. https://doi.org/10.1111/jpn.13509.

[254] W. Zhang, J.Y. Du, Z. Jiang, T. Okimura, T. Oda, Q. Yu, J.O. Jin, Ascophyllan purified from Ascophyllum nodosum induces Th1 and Tc1 immune responses by promoting dendritic cell maturation, Mar. Drugs. 12 (2014) 4148–4164. https://doi.org/10.3390/md12074148.

[255] G.E. Gardiner, A.J. Campbell, J. V. O'Doherty, E. Pierce, P.B. Lynch, F.C. Leonard, C. Stanton, R.P. Ross, P.G. Lawlor, Effect of Ascophyllum nodosum extract on growth performance, digestibility, carcass characteristics and selected intestinal microflora populations of grower-finisher pigs, Anim. Feed Sci. Technol. 141 (2008) 259–273. https://doi.org/10.1016/j.anifeedsci.2007.06.011.

[256] H. Toh, J.A. Thomson, P. Jiang, Maternal high-fiber diet protects offspring against type 2 diabetes, Nutrients. 13 (2021) 1–10. https://doi.org/10.3390/nu13010094.

[257] J.A.M. Prates, J.P.B. Freire, A.M. de Almeida, C. Martins, D.M. Ribeiro, H. Osório, M.A.S. Pinho, P.A. Lopes, J.M.J. Correia, R.M.A. Pinto, T. Costa, E. Corrent, T. Chalvon-Demersay, Influence of dietary supplementation with an amino acid mixture on inflammatory markers, immune status and serum proteome in lps-challenged weaned piglets, Animals. 11 (2021). https://doi.org/10.3390/ani11041143.

[258] D.M. Ribeiro, D. Coelho, H. Osório, C. Martins, J.P. Bengala Freire, J. Almeida, O. Moreira, A.M. Almeida, J.A.M. Prates, Effect of dietary incorporation of Chlorella vulgaris and CAZyme supplementation on the hepatic proteome of finishing pigs, J. Proteomics. 256 (2022) 104504. https://doi.org/10.1016/j.jprot.2022.104504.

[259] D. Wolrab, R. Jirásko, E. Cífková, M. Höring, D. Mei, M. Chocholoušková, O. Peterka, J. Idkowiak, T. Hrnčiarová, L. Kuchař, R. Ahrends, R. Brumarová, D. Friedecký, G. Vivo-Truyols, P. Škrha, J. Škrha, R. Kučera, B. Melichar, G. Liebisch, R. Burkhardt, M.R. Wenk, A. Cazenave-Gassiot, P. Karásek, I. Novotný, K. Greplová, R. Hrstka, M. Holčapek, Lipidomic profiling of human serum enables detection of pancreatic cancer, Nat. Commun. 13 (2022) 1–16. https://doi.org/10.1038/s41467-021-27765-9.

[260] J.R. Wiśniewski, A. Zougman, N. Nagaraj, M. Mann, Universal sample preparation method for proteome analysis, Nat. Methods. 6 (2009) 359–362. https://doi.org/10.1038/nmeth.1322.

[261] M.J. Ormsby, E. Grahame, R. Burchmore, R.L. Davies, Comparative bioinformatic and proteomic approaches to evaluate the outer membrane proteome of the fish pathogen Yersinia ruckeri, J. Proteomics. 199 (2019) 135–147. https://doi.org/10.1016/j.jprot.2019.02.014.

[262] C.N. Hsu, Y.L. Tain, Early-life programming and reprogramming of adult kidney disease and hypertension: The interplay between maternal nutrition and oxidative stress, Int. J. Mol. Sci. 21 (2020). https://doi.org/10.3390/ijms21103572.

[263] Q. Shang, S. Liu, H. Liu, S. Mahfuz, X. Piao, Maternal supplementation with a combination of wheat bran and sugar beet pulp during late gestation and lactation improves growth and intestinal functions in piglets, Food Funct. 12 (2021) 7329–7342. https://doi.org/10.1039/d1fo00014d.

[264] S. Wang, C.A. Maxwell, N.M. Akella, Diet as a potential moderator for genome stability and immune response in pediatric leukemia, Cancers (Basel). 13 (2021) 1–17. https://doi.org/10.3390/cancers13030413.

[265] S.N. Mousavi, F. Koohdani, F. Shidfar, M.B. Eslaminejad, Comparison of maternal isocaloric high carbohydrate and high fat diets on osteogenic and adipogenic genes expression in adolescent mice offspring, Nutr. Metab. 13 (2016) 1–10. https://doi.org/10.1186/s12986-016-0130-x.

[266] C. Tu, P.A. Rudnick, M.Y. Martinez, K.L. Cheek, S.E. Stein, R.J.C. Slebos, D.C. Liebler, Depletion of Abundant Plasma Proteins and Limitations of Plasma Proteomics, J. Proteome Res. 9 (2010) 4982–4991.

[267] A. Klos, A.J. Tenner, K.-O. Johswich, R.R. Ager, E.S. Reis, J. Köhl, The role of the anaphylatoxins in health and disease, Mol. Immunol. 46 (2009) 2753–2766. https://doi.org/10.1016/j.molimm.2009.04.027.

[268] M.J. Page, J. Bester, E. Pretorius, The inflammatory effects of TNF-α and complement component 3 on coagulation, Sci. Rep. 8 (2018) 1–9. https://doi.org/10.1038/s41598-018-20220-8.

[269] J.S. Sundsmo, D.S. Fair, Relationships Among the Complement , Kinin , Coagulation , and Fibrinolytic Systems, Springer Semin. Immunopathol. 6 (1983) 231–258.

[270] K. Wimmers, S. Mekchay, K. Schellander, S. Ponsuksili, Molecular characterization of the pig C3 gene and its association with complement activity, Immunogenetics. 54 (2003) 714–724. https://doi.org/10.1007/s00251-002-0524-y.

[271] C. Cray, Acute phase proteins in animals, 1st ed., Elsevier Inc., 2012. https://doi.org/10.1016/B978-0-12-394596-9.00005-6.

[272] M. Clapperton, S.C. Bishop, M. Piñeiro, F.M. Campbell, E.J. Glass, The association between plasma levels of acute phase proteins, haptoglobin, alpha-1 acid glycoprotein (AGP), Pig-MAP, transthyretin and serum amyloid A (SAA) in Large White and Meishan pigs, Vet. Immunol. Immunopathol. 119 (2007) 303–309. https://doi.org/10.1016/j.vetimm.2007.05.008.

[273] G.H. Sack Jr, Serum amyloid A – a review, Mol. Med. 24 (2018) 1–27.

[274] L. Zhang, J. Du, Z. Hu, G. Han, P. Delafontaine, G. Garcia, W.E. Mitch, IL-6 and serum amyloid A synergy mediates angiotensin Il-Lnduced muscle wasting, J. Am. Soc. Nephrol. 20 (2009) 604–612. https://doi.org/10.1681/ASN.2008060628.

[275] R.D. Ye, L. Sun, Emerging functions of serum amyloid A in inflammation, J. Leukoc. Biol. 98 (2015) 923–929. https://doi.org/10.1189/jlb.3vmr0315-080r.

[276] S. Khanmohammadi, N. Rezaei, Role of Toll-like receptors in the pathogenesis of COVID-19, J. Med. Virol. 93 (2021) 2735–2739.

[277] Z. Olumee-Shabon, C. Chattopadhaya, M.J. Myers, Proteomics profiling of swine serum following lipopolysaccharide stimulation, Rapid Commun Mass Spectrom. 34 (2020) 1–12. https://doi.org/10.1002/rcm.8639.

[278] L. Cai, M.C. De Beer, F.C. De Beer, D.R. Van Der Westhuyzen, Serum amyloid a is a ligand for scavenger receptor class B type I and inhibits high density lipoprotein binding and selective lipid uptake, J. Biol. Chem. 280 (2005) 2954–2961. https://doi.org/10.1074/jbc.M411555200.

[279] E.P. Benditt, N. Eriksen, Amyloid protein SAA is associated with high density lipoprotein from human serum, Proc. Natl. Acad. Sci. U. S. A. 74 (1977) 4025–4028. https://doi.org/10.1073/pnas.74.9.4025.

[280] V.L. King, J. Thompson, L.R. Tannock, Serum amyloid A in atherosclerosis, Curr. Opin. Lipidol. 22 (2011) 302–307. https://doi.org/10.1097/MOL.0b013e3283488c39.

[281] A.S. Ogun, A. Adeyinka, Biochemistry, Transferrin. [Updated 2021 Jul 31], StatPearls [Internet]. Treasure Isl. StatPearls Publ. (2022). https://www.ncbi.nlm.nih.gov/books/NBK532928/.

[282] M.D. Knutson, Non-transferrin-bound iron transporters, Free Radic. Biol. Med. 133 (2019) 101–111. https://doi.org/10.1016/j.freeradbiomed.2018.10.413.

[283] K. Thorén-Tolling, K. Martinsson, On the Transferrin Concentration in Serum of Sows and Growing Pigs and in sow Colostrum, Acta Vet. Scand. 15 (1974) 120–134. https://doi.org/10.1186/BF03547499.

[284] G. de Jong, J.P. van Dijk, H.G. van Eijk, The biology of transferrin, Clin. Chim. Acta. 190 (1990) 1–46. https://doi.org/10.1016/0009-8981(90)90278-Z.

[285] K. Thoren-Tolling, Studies of serum-transferrin and some hematologic parameters in vitamin E and selenium deficient pigs, Ann. Rech. Vet. 15 (1984) 387–394.

[286] C. Tóthová, R. Link, P. Kyzeková, O. Nagy, Serum protein electrophoretic pattern in piglets during the early postnatal period, Sci. Rep. 11 (2021) 1–10. https://doi.org/10.1038/s41598-021-96957-6.

[287] P.. Scott, H.. Berger, C. Kenward, P. Scott, B.. Wharton, Effect of gestational age and intrauterine nutrition on plasma transferrin and iron in the newborn, Arch. Dis. Child. 50 (1975) 796–798.

[288] K.J. Collard, Iron Homeostasis in the Neonate, Pediatrics. 123 (2009) 1208–1216. https://doi.org/10.1542/peds.2008-1047.

[289] F. Carrascoza, R. Silaghi-Dumitrescu, The dynamics of hemoglobin-haptoglobin complexes. Relevance for oxidative stress, J. Mol. Struct. 1250 (2022) 131703. https://doi.org/10.1016/j.molstruc.2021.131703.

[290] A. Camacho, J. Guitian, E. Pallas, J. Gestal, S. Olmeda, H. Goethert, S. Telford, A. Spielman, Serum protein response and renal failure in canine Babesia annae infection, Vet. Res. 36 (2005) 713–722. https://doi.org/10.1051/vetres.

[291] K. Skovgaard, S. Mortensen, M. Boye, K.T. Poulsen, F.M. Campbell, P. David Eckersall, P.M.H. Heegaard, Rapid and widely disseminated acute phase protein response after experimental bacterial infection of pigs, Vet. Res. 40 (2009). https://doi.org/10.1051/vetres/2009006.

[292] Ł.S. Jarosz, A. Ciszewski, S. Grabowski, A. Marek, Z. Grądzki, B. Żylińska, A. Rysiak, The effect of feed supplementation with a copper-glycine chelate and copper sulphate on cellular and humoral immune parameters in chickens, Food Agric. Immunol. 32 (2021) 373–402. https://doi.org/10.1080/09540105.2021.1954143.

[293] L. De Puysseleyr, K. De Puysseleyr, J. Rybarczyk, P. Vander Donck, W.H. De Vos, D. Vanrompay, Transferrins reduce replication of Chlamydia suis in McCoy cells, Pathogens. 10 (2021) 1–10. https://doi.org/10.3390/pathogens10070858.

[294] J. Folkersen, B. Teisner, N. Grunnet, J.G. Grudzinskas, J.G. Westergaard, P. Hindersson, Circulating levels of pregnancy zone protein: normal range and the influence of age and gender, Clin. Chim. Acta. (1981) 139–145.

[295] I. Rubio-Aliaga, L.F. Marvin-Guy, P. Wang, S. Wagniere, R. Mansourian, A. Fuerholz, W.H.M. Saris, A. Astrup, E.C.M. Mariman, M. Kussmann, Mechanisms of weight maintenance under high- and low-protein, low-glycaemic index diets, Mol. Nutr. Food Res. 55 (2011) 1603–1612. https://doi.org/10.1002/mnfr.201100081.

[296] J.F. Dhainaut, N. Marin, A. Mignon, C. Vinsonneau, C. Sprung, Hepatic response to sepsis: Interaction between coagulation and inflammatory processes, Crit. Care Med. 29 (2001). https://doi.org/10.1097/00003246-200107001-00016.

[297] R.H.P. Law, Q. Zhang, S. Mcgowan, A.M. Buckle, G.A. Silverman, W. Wong, C.J. Rosado, C.G. Langendorf, R.N. Pike, P.I. Bird, J.C. Whisstock, An overview of the serpin superfamily, Genome Biol. 7 (2006) 216.1-216.11. https://doi.org/10.1186/gb-2006-7-5-216.

[298] J. Peltier, J. Roperch, S. Audebert, J. Borg, L. Camoin, Quantitative proteomic analysis exploring progression of colorectal cancer : Modulation of the serpin family, J. Proteomics. 148 (2016) 139–148. https://doi.org/10.1016/j.jprot.2016.07.031.

[299] N.D. Rawlings, D.P. Tolle, A.J. Barrett, Evolutionary families of peptidase inhibitors, Biochem. J. 378 (2004) 705–716.

[300] G.A. Silverman, P.I. Bird, R.W. Carrell, F.C. Church, P.B. Coughlin, P.G.W. Gettins, J.A. Irving, D.A. Lomas, C.J. Luke, R.W. Moyer, P.A. Pemberton, E.R. Donnell, G.S. Salvesen, J. Travis, J.C. Whisstock, The Serpins Are an Expanding Superfamily of Structurally, J. Biol. Chem. 276 (2001) 33293–33296. https://doi.org/10.1074/jbc.R100016200.

[301] J.A. Huntington, Shape-shifting serpins – advantages of a mobile mechanism, TRENDS Biochem. Sci. 31 (2006) 427–435. https://doi.org/10.1016/j.tibs.2006.06.005.

[302] I.U. Schraufstatter, K. Trieu, L. Sikora, R. Discipio, Complement C3a and C5a Induce Different Signal Transduction Cascades in Endothelial Cells, J. Immunol. 169 (2002) 2102–2110. https://doi.org/10.4049/jimmunol.169.4.2102.

[303] S. Sayah, A.M. Ischenko, A. Zhakhov, A.-S. Bonnard, M. Fontaine, Expression of Cytokines by Human Astrocytomas Following Stimulation by C3a and C5a Anaphylatoxins : Specific Increase in Interleukin-6 mRNA Expression, J. Neurochem. 72 (1999) 2426–2436.

[304] D. Desai, P.U. Dugel, Complement cascade inhibition in geographic atrophy: a review, Eye. (2022). https://doi.org/10.1038/s41433-021-01765-x.

[305] R. Guo, P.A. Ward, Role of C5a in inflammatory responses, Annu. Rev. Immunol. 23 (2005) 821–852. https://doi.org/10.1146/annurev.immunol.23.021704.115835.

[306] H.D.N. Tran, S.S. Moonshi, Z.P. Xu, H.T. Ta, Biomaterials Science balance : between thrombosis and haemorrhage, Biomater. Sci. 10 (2022) 10–50. https://doi.org/10.1039/d1bm01351c.

[307] J. Calvet, A. Berenguer-Llergo, M. Gay, M. Massanella, P. Domingo, M. Llop, E. Sánchez-Jiménez, M. Arévalo, J. Carrillo, N. Albiñana, G. Arauz-Garofalo, C. Orellana, J.F. Delgado, A. Serrano, A. Llobell, E. Graell, M.G. Manrique, M. Moreno, C. Galisteo, E. Casado, N. Navarro, A. Gómez, S.G. Cirera, M. Rusiñol, E. Costa, B. Clotet, M. Vilaseca, J. Blanco, J. Gratacós, Biomarker candidates for progression and clinical management of COVID - 19 associated pneumonia at time of admission, Sci. Rep. 12 (2022) 1–10. https://doi.org/10.1038/s41598-021-04683-w.

[308] E. Boschetti, L.E. Hernández-Castellano, P.G. Righetti, Progress in farm animal proteomics: The contribution of combinatorial peptide ligand libraries, J. Proteomics. 197 (2019) 1–13. https://doi.org/10.1016/j.jprot.2019.02.005.

[309] R. Kumar, U. Anand, R.N. Priyadarshi, Lymphatic dysfunction in advanced cirrhosis: Contextual perspective and clinical implications, World J. Hepatol. 13 (2021) 300–314. https://doi.org/10.4254/wjh.v13.i3.300.

[310] A.K. Kurpińska, A. Jarosz, M. Ozgo, W.F. Skrzypczak, Changes in lipid metabolism during last month of pregnancy and first two months of lactation in primiparous cows - Analysis of apolipoprotein expression pattern and changes in concentration of total cholesterol, HDL, LDL, triglycerides, Pol. J. Vet. Sci. 18 (2015) 291–298. https://doi.org/10.1515/pjvs-2015-0038.

[311] M. Saladrigas-García, M. D'Angelo, H.L. Ko, P. Nolis, Y. Ramayo-Caldas, J.M. Folch, P. Llonch, D. Solà-Oriol, J.F. Pérez, S.M. Martín-Orúe, Understanding host-microbiota interactions in the commercial piglet around weaning, Sci. Rep. 11 (2021) 1–18. https://doi.org/10.1038/s41598-021-02754-6.

[312] D. Sviridov, A.T. Remaley, High-Density Lipoprotein mimetics: promises and challenges, Biochem J. 472 (2015) 249–259. https://doi.org/10.1042/BJ20150832.High-Density.

[313] K.A. Rye, P.J. Barter, Thematic review series: High density lipoprotein structure, function, and metabolism cardioprotective functions of HDLs 1, J. Lipid Res. 55 (2014) 168–179. https://doi.org/10.1194/jlr.R039297.

[314] P. Khanal, D. Pandey, S. Binti Ahmad, S. Safayi, H.N. Kadarmideen, M. Olaf Nielsen, Differential impacts of late gestational over–and undernutrition on adipose tissue traits and

associated visceral obesity risk upon exposure to a postnatal high-fat diet in adolescent sheep, Physiol. Rep. 8 (2020) 1–21. https://doi.org/10.14814/phy2.14359.

[315] C. Piñeiro, M. Piñeiro, J. Morales, R. Carpintero, F.M. Campbell, P.D. Eckersall, M.J.M. Toussaint, M.A. Alava, F. Lampreave, Pig acute-phase protein levels after stress induced by changes in the pattern of food administration, Animal. 1 (2007) 133–139. https://doi.org/10.1017/S1751731107283909.

[316] M.E. Spurlock, Regulation of Metabolism and Growth during Immune Challenge: An Overview of Cytokine Function, J. Anim. Sci. 75 (1997) 1773–1783. https://doi.org/10.2527/1997.7571773x.

[317] R.W. Johnson, Inhibition of Growth by Pro-Inflammatory Cytokines: An Integrated View, J. Anim. Sci. 75 (1997) 1244–1255. https://doi.org/10.2527/1997.7551244x.

[318] C.B. Keragala, D.F. Draxler, Z.K. McQuilten, R.L. Medcalf, Haemostasis and innate immunity – a complementary relationship: A review of the intricate relationship between coagulation and complement pathways, Br. J. Haematol. 180 (2018) 782–798. https://doi.org/10.1111/bjh.15062.

[319] M. Hoffman, D.M. Monroe, A cell-based model of hemostasis, Thromb. Haemost. 85 (2001) 958–965. https://doi.org/10.1055/s-0037-1615947.

[320] S. Petros, Trauma-Induced Coagulopathy, Hamostaseologie. 39 (2019) 020–027. https://doi.org/10.1055/s-0039-1677853.

[321] D. Barthel, S. Schindler, P.F. Zipfel, Plasminogen is a complement inhibitor, J. Biol. Chem. 287 (2012) 18831–18842. https://doi.org/10.1074/jbc.M111.323287.

[322] S. Pal, A. Curley, S.J. Stanworth, Interpretation of clotting tests in the neonate, Arch. Dis. Child. Fetal Neonatal Ed. 100 (2015) 270–274. https://doi.org/10.1136/archdischild-2014-306196.

[323] P. Monagle, V. Ignjatovic, H. Savoia, Blood Reviews Hemostasis in neonates and children : Pitfalls and dilemmas, Blood Rev. 24 (2010) 63–68. https://doi.org/10.1016/j.blre.2009.12.001.

[324] V.R. y Formoso, R.B. Mota, H. Soares, Developmental hemostasis in the neonatal period, World J. Pediatr. 18 (2022) 7–15. https://doi.org/10.1007/s12519-021-00492-3.

[325] J.W.M. Heemskerk, E.M. Bevers, T. Lindhout, Platelet activation and blood coagulation, Thromb. Haemost. 88 (2002) 186–193. https://doi.org/10.1055/s-0037-1613209.

[326] M.R. Thomas, R.F. Storey, The role of platelets in inflammation, Thromb. Haemost. 1114 (2015) 449–458.

[327] S. Subramaniam, K. Jurk, L. Hobohm, S. Jackel, M. Saffarzadeh, K. Schwierczek, P. Wenzel, F. Langer, C. Reinhardt, W. Ruf, Distinct contributions of complement factors to platelet activation and fibrin formation in venous thrombus development, Blood. 129 (2017) 2291–2302. https://doi.org/10.1182/blood-2016-11-749879.

[328] L. Youssef, J. Miranda, M. Blasco, C. Paules, F. Crovetto, M. Palomo, S.T. Moix, H.G. Calderó, O.T. Ceide, Complement and coagulation cascades activation is the main pathophysiological pathway in early - onset severe preeclampsia revealed by maternal proteomics, Sci. Rep. (2021) 1–13. https://doi.org/10.1038/s41598-021-82733-z.

[329] FETUB fetuin B [Homo sapiens (human)], Gene ID 26998. (2022). https://www.ncbi.nlm.nih.gov/gene?Db=gene&Cmd=DetailsSearch&Term=26998 (accessed January 15, 2022).

[330] L. Zhuo, K. Kimata, Structure and function of inter-α-trypsin inhibitor heavy chains, Connect. Tissue Res. 49 (2008) 311–320. https://doi.org/10.1080/03008200802325458.

[331] J.H. Foley, E.M. Conway, Cross Talk Pathways between Coagulation and Inflammation, Circ. Res. 118 (2016) 1392–1408. https://doi.org/10.1161/CIRCRESAHA.116.306853.

[332] C. Xi, Y. Zehong, H. Huiling, D. Wentao, W. Aiping, D. Yanbin, G. Weihang, D. Song, C. Bo, L. Jiali, S. Nannan, C. Zhibin, G. Wenfeng, L. Yanwu, G. Yong, Differentiation and Proliferation of Intestinal Stem Cells and its Underlying Regulated Mechanisms during Weaning, Curr. Protein Pept. Sci. 20 (2019). https://doi.org/https://dx.doi.org/10.2174/1389203720666190125101834.

[333] N. Verdile, R. Mirmahmoudi, T.A.L. Brevini, F. Gandolfi, Evolution of pig intestinal stem cells from birth to weaning, Animal. 13 (2019) 2830–2839. https://doi.org/10.1017/S1751731119001319.

[334] C.R. Stokes, The development and role of microbial-host interactions in gut mucosal immune development, J. Anim. Sci. Biotechnol. 8 (2017) 8–17. https://doi.org/10.1186/s40104-016-0138-0.

[335] F. Correa, D. Luise, P. Bosi, P. Trevisi, Weaning differentially affects the maturation of piglet peripheral blood and jejunal Peyer's patches, Sci. Rep. 12 (2022) 1–12. https://doi.org/10.1038/s41598-022-05707-9.

[336] T.A. Mousseau, C.W. Fox, The adaptive significance of maternal effects, Trends Ecol. Evol. 13 (1998) 403–407. https://doi.org/10.1016/S0169-5347(98)01472-4.

[337] L.M. Dixon, N.H.C. Sparks, K.M.D. Rutherford, Early experiences matter: A review of the effects of prenatal environment on offspring characteristics in poultry, Poult. Sci. 95 (2016) 489–499. https://doi.org/10.3382/ps/pev343.

[338] E.H. Van Der Waaij, H. Van Den Brand, J.A.M. Van Arendonk, B. Kemp, Effect of match or mismatch of maternal-offspring nutritional environment on the development of offspring in broiler chickens, Animal. 5 (2011) 741–748. https://doi.org/10.1017/S1751731110002387.

[339] J. Fisch, V. Feistauer, A.C. de Moura, A.O. Silva, V. Bollis, M. Porawski, S. Almeida, R.P. Guedes, A.G. Barschak, M. Giovenardi, Maternal feeding associated to post-weaning diet affects metabolic and behavioral parameters in female offspring, Physiol. Behav. 204 (2019) 162–167. https://doi.org/10.1016/j.physbeh.2019.02.026.

[340] C.W. Kuzawa, A.W. Kim, Early environments, developmental plasticity, and chronic degenerative disease, Elsevier Inc., 2022. https://doi.org/10.1016/b978-0-12-822652-0.00020-1.

[341] A. Heras-molina, J.L. Pesántez-pacheco, C. Garcia-contreras, M. Vázquez-gómez, A. López, R. Benítez, Y. Núñez, S. Astiz, C. Óvilo, B. Isabel, A. González-bulnes, Maternal supplementation with polyphenols and omega-3 fatty acids during pregnancy: Prenatal effects on growth and metabolism, Animals. 11 (2021). https://doi.org/10.3390/ani11061699.

[342] H.Y. Sun, I.H. Kim, Coated omega-3 fatty acid from linseed oil positively affect sow immunoglobulin G concentration and pre-weaning performance of piglet, Anim. Feed Sci. Technol. 269 (2020) 114676. https://doi.org/10.1016/j.anifeedsci.2020.114676.

[343] L.M.S. Bouwman, J.M.S. Fernandez-Calleja, H.J.M. Swarts, I. van der Stelt, A. Oosting, J. Keijer, E.M. van Schothorst, No Adverse Programming by Post-Weaning Dietary Fructose ofBody Weight, Adiposity, Glucose Tolerance, or Metabolic Flexibility, Mol. Nutr. Food Res. 62 (2018) 1–10.

[344] B. Venardou, J. V. O'doherty, M. Garcia-Vaquero, C. Kiely, G. Rajauria, M.J. McDonnell, M.T. Ryan, T. Sweeney, Evaluation of the Antibacterial and Prebiotic Potential of Ascophyllum nodosum and Its Extracts Using Selected Bacterial Members of the Pig Gastrointestinal Microbiota, Mar. Drugs. 20 (2022). https://doi.org/10.3390/md20010041.

[345] K. Yu, M. Matzapetakis, A. Horvatić, M. Terré, A. Bach, J. Kuleš, N. Yeste, N. Gómez, L. Arroyo, E. Rodríguez-tomàs, R. Peña, N. Guillemin, A.M. De Almeida, P. David, A. Bassols, Metabolome and proteome changes in skeletal muscle and blood of pre- weaning calves fed leucine and threonine supplemented diets, J. Proteomics. 216 (2020) 103677. https://doi.org/10.1016/j.jprot.2020.103677.

[346] H. Gehart, H. Clevers, Tales from the crypt: new insights into intestinal stem cells, Nat. Rev. Gastroenterol. Hepatol. 16 (2018) 19–34. https://doi.org/10.1038/s41575-018-0081-y.

[347] M. Wang, L. Wang, X. Tan, L. Wang, X. Xiong, Y. Wang, Q. Wang, H. Yang, Y. Yin, The developmental changes in intestinal epithelial cell proliferation, differentiation, and shedding in weaning piglets, Anim. Nutr. (2022). https://doi.org/10.1016/j.aninu.2021.11.006.

[348] R.A. Hall, E.W.J. Wallace, Post-transcriptional control of fungal cell wall synthesis, Cell Surf. 8 (2022) 100074. https://doi.org/10.1016/j.tcsw.2022.100074.

[349] J. Wei, A. Hui, Review of Ribosome Interactions with SARS-CoV-2 and COVID-19 mRNA Vaccine, Life. 12 (2022). https://doi.org/https:// doi.org/10.3390/life12010057.

[350] B. Nieto, S.G. Gaspar, G. Moriggi, D.G. Pestov, X.R. Bustelo, M. Dosil, Identification of distinct maturation steps involved in human 40S ribosomal subunit biosynthesis, Nat. Commun. 11 (2020). https://doi.org/10.1038/s41467-019-13990-w.

[351] A. Wadood, A. Shareef, A.U. Rehman, S. Muhammad, B. Khurshid, R.S. Khan, S. Shams, S.G. Afridi, In Silico Drug Designing for ala438 Deleted Ribosomal Protein S1 (RpsA) on the Basis

of the Active Compound Zrl 15, ACS Omega. 7 (2022) 397–408. https://doi.org/10.1021/acsomega.1c04764.

[352] A. Mahdaviani, M. Fallahpour, F. Seif, H. Alyasine, Soheila, Abolhassanif, A. Bousfihah, M.-R. Barbouchei, P. Olbrichj, Defects in intrinsic and innate immunity, in: R.Y. Asghar Aghamohammadi, Hassan Abolhassani, Nima Rezaei (Ed.), Inborn Errors Immun., Academic Press, 2021: pp. 219–243. https://doi.org/10.1016/B978-0-12-821028-4.00002-6.

[353] Q. Liu, Y. Qi, X. Kong, X. Wang, W. Zhang, J. Zhai, Y. Yang, Y. Fang, J. Wang, Molecular and Clinical Characterization of CCT2 Expression and Prognosis via Large-Scale Transcriptome Pro fi le of Breast Cancer, Front. Oncol. 11 (2021). https://doi.org/10.3389/fonc.2021.614497.

[354] H. Ghozlan, A. Showalter, E. Lee, X. Zhu, A.R. Khaled, Chaperonin-Containing TCP1 Complex (CCT) Promotes Breast Cancer Growth Through Correlations With Key Cell Cycle Regulators, Front. Oncol. 11 (2021) 1–24. https://doi.org/10.3389/fonc.2021.663877.

[355] A.G. Engel, Congenital Myasthenic Syndromes in 2018, Curr. Neurol. Neurosci. Rep. 18 (2018). https://doi.org/10.1007/s11910-018-0852-4.

[356] I. Tvaroška, Glycosyltransferases as targets for therapeutic intervention in cancer and inflammation: molecular modeling insights, Versita, 2022. https://doi.org/10.1007/s11696-021-02026-7.

[357] Q. Wang, H. Unwalla, I. Rahman, Dysregulation of Mitochondrial Complexes and Dynamics by Chronic Cigarette Smoke Exposure in MitoQC Reporter Mice, Mitochondrion. 63 (2022) 43–50. https://doi.org/10.1016/j.mito.2022.01.003.

[358] T. Wang, F. Ma, H. Qian, Defueling the cancer: ATP synthase as an emerging target in cancer therapy, Mol. Ther. - Oncolytics. 23 (2021) 82–95. https://doi.org/10.1016/j.omto.2021.08.015.

[359] J.O. Olanlokun, W.O. Abiodun, O. Ebenezer, N.A. Koorbanally, O.O. Olorunsogo, Curcumin modulates multiple cell death, matrix metalloproteinase activation and cardiac protein release in susceptible and resistant Plasmodium berghei-infected mice, Biomed. Pharmacother. 146 (2022).

[360] K.I. Priyadarsini, The chemistry of curcumin: From extraction to therapeutic agent, Molecules. 19 (2014) 20091–20112. https://doi.org/10.3390/molecules191220091.

[361] H. Alami-Durante, D. Bazin, M. Cluzeaud, S. Fontagné-Dicharry, S. Kaushik, I. Geurden, Effect of dietary methionine level on muscle growth mechanisms in juvenile rainbow trout (Oncorhynchus mykiss), Aquaculture. 483 (2018) 273–285. https://doi.org/10.1016/j.aquaculture.2017.10.030.

[362] Y. Yun, D. Song, Z. He, J. Mi, L. Wang, G. Nie, Effects of methionine supplementation in plant protein based diet on growth performance and fillet quality of juveniles Yellow River carp (Cyprinus carpio haematopterus), Aquaculture. 549 (2022).

[363] A. Borchel, M. Verleih, A. Rebl, C. Kühn, T. Goldammer, Creatine metabolism differs between mammals and rainbow trout (Oncorhynchus mykiss), Springerplus. 3 (2014) 1–9. https://doi.org/10.1186/2193-1801-3-510.

[364] E. Chen, N.J. Liu, Y. Zhao, M. Tang, L.P. Ou, X.H. Wu, C.L. Luo, Panobinostat reverses HepaCAM gene expression and suppresses proliferation by increasing histone acetylation in prostate cancer, Gene. 808 (2022) 145977. https://doi.org/10.1016/j.gene.2021.145977.

[365] H.D. Nguyen, A.-K. Bielinsky, HDM2 ERKs PCNA, J. Cell Biol. 190 (2010) 487–489. https://doi.org/10.1002/jcc.20084.

[366] H. Tamura, Expression of p63 and Proliferating Cell Nuclear Antigen in Oral Submucous Fibrosis, J. Int. Soc. Prev. Community Dent. 11 (2021) 448–456. https://doi.org/10.4103/jispcd.JISPCD.

[367] S. Werner, L. Keller, K. Pantel, Molecular Aspects of Medicine Epithelial keratins : Biology and implications as diagnostic markers for liquid biopsies, Mol. Aspects Med. 72 (2020) 100817. https://doi.org/10.1016/j.mam.2019.09.001.

[368] C.-G. Stenvall, A. Tayyab, Mina, T. Grönroos, M.A. Ilomäki, K. Viiri, K.M. Ridge, L. Polari, D.M. Toivola, Targeted deletion of keratin 8 in intestinal epithelial cells disrupts tissue integrity and predisposes to tumorigenesis in the colon, Cell. Mol. Life Sci. 79 (2022) 1–17. https://doi.org/10.1007/s00018-021-04081-5.

[369] L. Polari, C.M. Alam, J.H. Nyström, T. Heikkilä, M. Tayyab, S. Baghestani, D.M. Toivola, Keratin intermediate filaments in the colon: guardians of epithelial homeostasis, Int. J. Biochem. Cell Biol. 129 (2020). https://doi.org/10.1016/j.biocel.2020.105878.

[370] T.O. Helenius, J.O. Misiorek, J.H. Nyström, L.E. Fortelius, A. Habtezion, J. Liao, M.N. Asghar, H. Zhang, S. Azhar, M.B. Omary, D.M. Toivola, Keratin 8 absence down-regulates colonocyte HMGCS2 and modulates colonic ketogenesis and energy metabolism, Mol. Biol. Cell. 26 (2015) 2298–2310. https://doi.org/10.1091/mbc.E14-02-0736.

[371] C.A. Evans, B.M. Corfe, Seminars in Cell and Developmental Biology Colorectal keratins : Integrating nutrition , metabolism and colorectal health, Semin. Cell Dev. Biol. (2021). https://doi.org/10.1016/j.semcdb.2021.08.010.

[372] L. Wang, S. Srinivasan, A.L. Theiss, D. Merlin, S. V. Sitaraman, Interleukin-6 induces keratin expression in intestinal epithelial cells: Potential role of keratin-8 in interleukin-6-induced barrier function alterations, J. Biol. Chem. 282 (2007) 8219–8227. https://doi.org/10.1074/jbc.M604068200.

[373] C. Zhong, D. Tong, Y. Zhang, X. Wang, H. Yan, H. Tan, C. Gao, DL -methionine and DL -methionyl- DL -methionine increase intestinal development and activate Wnt / b -catenin signaling activity in domestic pigeons (Columba livia), Poult. Sci. 101 (2019) 101644. https://doi.org/10.1016/j.psj.2021.101644.

[374] L. Yin, J. Li, Y. Zhang, Q. Yang, C. Yang, Z. Yi, Y. Yin, Q. Wang, J. Li, N. Ding, Z. Zhang, H. Yang, Y. Yin, Changes in progenitors and differentiated epithelial cells of neonatal piglets, Anim. Nutr. 8 (2022) 265–276. https://doi.org/10.1016/j.aninu.2021.10.008.

[375] D. Delacour, J. Salomon, S. Robine, D. Louvard, Plasticity of the brush border — the yin and yang of intestinal homeostasis, Nat. Rev. Gastroenterol. Hepatol. (2016). https://doi.org/10.1038/nrgastro.2016.5.

[376] K. Piórkowska, A comprehensive transcriptome analysis of skeletal muscles in two Polish pig breeds differing in fat and meat quality traits, Genet. Mol. Biol. 41 (2018) 125–136. https://doi.org/http://dx.doi.org/10.1590/1678-4685-GMB-2016-0101.

[377] S. Ben-Jemaa, G. Senczuk, E. Ciani, R. Ciampolini, G. Catillo, M. Boussaha, F. Pilla, B. Portolano, S. Mastrangelo, Genome-Wide Analysis Reveals Selection Signatures Involved in Meat Traits and Local Adaptation in Semi-Feral Maremmana Cattle, Front. Genet. 12 (2021) 1–12. https://doi.org/10.3389/fgene.2021.675569.

[378] J. Shin, A. Nile, J. Oh, Role of adaptin protein complexes in intracellular trafficking and their impact on diseases, Bioengineered. 12 (2021) 8259–8278. https://doi.org/10.1080/21655979.2021.1982846.

[379] J. Lee, M. Tokumoto, Y. Fujiwara, M. Satoh, Gene expression analysis using DNA microarray in HK-2 human proximal tubular cells treated with cadmium, J. Toxicol. Sci. 38 (2013) 959–962.

[380] M. Freissmuth, P.J. Casey, A.G. Gilman, G proteins control diverse pathways of transmembrane signaling, FASEB J. 3 (1989) 2125–2131. https://doi.org/doi:10.1096/fasebj.3.10.2546847.

[381] H. Najafi, M. Totonchi, M. Sadeghizadeh, Predicted Cellular and Molecular Actions of Lithium in the Treatment of Bipolar Disorder: An In Silico Study, CNS Drugs. 34 (2020) 521–533. https://doi.org/10.1007/s40263-020-00723-7.

[382] M. Nobles, D. Montaigne, S. Sebastian, L. Birnbaumer, A. Tinker, Differential effects of inhibitory G protein isoforms on G protein-gated inwardly rectifying K+ currents in adult murine atria, Am J Physiol Cell Physiol. 314 (2018) 616–626. https://doi.org/10.1152/ajpcell.00271.2016.

[383] F. Li, J. Liu, J. Yang, H. Sun, Z. Jiang, C. Wang, X. Zhang, Y. Yu, C. Zhao, J. Pu, Y. Sun, K.-C. Chang, J. Liu, H. Sun, H9N2 virus-derived M1 protein promotes H5N6 virus release in mammalian cells: Mechanism of avian influenza virus inter- species infection in humans, PLos Pathog. 17 (2021) 1–24. https://doi.org/10.1371/journal.ppat.1010098.

[384] M. Li, X. Tian, X. Li, M. Huang, S. Huang, Y. Wu, M. Jiang, Diverse energy metabolism patterns in females in Neodon fuscus, Lasiopodomys brandtii , and Mus musculus revealed by comparative transcriptomics under hypoxic conditions, Sci. Total Environ. 783 (2021) 147130. https://doi.org/10.1016/j.scitotenv.2021.147130.

[385] B. Kim, D. Ahn, S. Kang, J. Jeong, E. Jo, J. Kim, H. Park, De novo Assembly and Annotation of the Blood Transcriptome of the Southern Elephant Seal Mirounga leonina from the South Shetland Islands , Antarctica, Ocean Sci. J. 54 (2019) 307–315.

[386] J.S. Johnson, M.A. Aardsma, A.W. Duttlinger, K.R. Kpodo, Early life thermal stress: Impact on future thermotolerance , stress response , behavior , and intestinal morphology in piglets exposed to a heat stress challenge during simulated transport, J. Anim. Sci. 96 (2018) 1640–1653. https://doi.org/10.1093/jas/sky107.

[387] Y. Jia, L. Li, Y. Lin, D.J. Siegwart, J.M. Ready, Y. Jia, L. Li, Y. Lin, P. Gopal, S. Shen, K. Zhou, X. Yu, T. Sharma, In vivo CRISPR screening identifies BAZ2 chromatin remodelers as druggable regulators of mammalian liver regeneration Article In vivo CRISPR screening identifies BAZ2 chromatin remodelers as druggable regulators of mammalian liver regeneration, Cell Stem Cell. 29 (2022) 1–14. https://doi.org/10.1016/j.stem.2022.01.001.

[388] Z. Mbita, R. Hull, F. Mokoena, C. Lai, Z. Dlamini, RBBP6 interactome: RBBP6 isoform 3/DWNN and Nek6 interaction is critical for cell cycle regulation and may play a role in carcinogenesis, Informatics Med. Unlocked. 23 (2021) 100522. https://doi.org/10.1016/j.imu.2021.100522.

[389] Q. Wang, F. Pan, S. Li, R. Huang, X. Wang, S. Wang, X. Liao, The prognostic value of the proteasome activator subunit gene family in skin cutaneous melanoma, J. Cancer. 10 (2019) 2205–2219. https://doi.org/10.7150/jca.30612.

[390] F.A. Simmen, Y. Su, R. Xiao, Z. Zeng, The Krüppel-like factor 9 (KLF9) network in HEC-1-A endometrial carcinoma cells suggests the carcinogenic potential of dys-regulated KLF9 expression, Reprod. Biol. Endocrinol. 6 (2008) 1–11. https://doi.org/10.1186/1477-7827-6-41.

[391] J. Kim, M.J. Shapiro, A.O. Bamidele, P. Gurel, P. Thapa, H.N. Higgs, K.E. Hedin, V.S. Shapiro, D.D. Billadeau, Coactosin-Like 1 Antagonizes Cofilin to Promote Lamellipodial Protrusion at the Immune Synapse, PLoS One. 9 (2014) 1–11. https://doi.org/10.1371/journal.pone.0085090.

[392] S. Guo, P. Yang, X. Jiang, X. Li, Y. Wang, Genetic and epigenetic silencing of mircoRNA-506-3p enhances COTL1 oncogene expression to foster non-small lung cancer progression, Oncotarget. 8 (2017) 644–657.

[393] E. Jin, S. Shim, H. Kim, S. Chae, Polymorphisms of COTL1 gene identified by proteomic approach and their association with autoimmune disorders, Exp. Mol. Med. 41 (2009) 354–361. https://doi.org/10.3858/emm.2009.41.5.040.

[394] S. Rai, S. Bhatnagar, Hyperlipidemia, Disease Associations, and Top 10 Potential Drug Targets: A Network View, Omi. A J. Integr. Biol. 20 (2016) 152–169. https://doi.org/10.1089/omi.2015.0172.

[395] Y. Guo, X. Dong, J. Jin, Y. He, The Expression Patterns and Prognostic Value of the Proteasome Activator Subunit Gene Family in Gastric Cancer Based on Integrated Analysis, Front. Cell Dev. Biol. 9 (2021). https://doi.org/10.3389/fcell.2021.663001.

[396] S. Ge, H. Huang, W. Huang, R. Ji, J. Chen, S. Wu, L. Wang, PSME4 Activates mTOR Signaling and Promotes the Malignant Progression of Hepatocellular Carcinoma, Int. J. Gen. Med. 15 (2022) 885–895.

[397] A. Braeuning, A. Oberemm, J. Görte, L. Böhmert, S. Juling, Comparative proteomic analysis of silver nanoparticle effects in human liver and intestinal cells, J. Appl. Toxicol. 38 (2018) 638–648. https://doi.org/10.1002/jat.3568.

[398] A. Camargo, O.A. Rangel-zúñiga, P. Peña-orihuela, C. Marín, P. Pérez-martínez, J. Delgado-lista, F.M. Gutierrez-mariscal, M.M. Malagón, H.M. Roche, F. José, F. Perez-jimenez, J. Lopez-miranda, Postprandial changes in the proteome are modulated by dietary fat in patients with, J. Nutr. Biochem. 24 (2013) 318–324. https://doi.org/10.1016/j.jnutbio.2012.06.014.

[399] S.M. Habib, B.L. Zwicker, L. Wykes, L.B. Agellon, Sexually dimorphic response of mice to the Western-style diet caused by deficiency of fatty acid binding protein 6 (Fabp6), Physiol. Rep. 9 (2021) 1–10. https://doi.org/10.14814/phy2.14733.

[400] S. Peng, Y. Li, Q. Chen, Q. Hu, Y. He, L. Che, P. Jiang, Intestinal and Mucosal Microbiome Response to Oral Challenge of Enterotoxigenic Escherichia coli in Weaned Pigs, Pathogens. 11 (2022) 1–12.

[401] J.H. Uribe, M.C. Romero, S.Z. López, C. Arce, R. Bautista, A. Carvajal, S. Cirera, M.G. Claros, J.J. Garrido, Transcriptional analysis of porcine intestinal mucosa infected with Salmonella Typhimurium revealed a massive inflammatory response and disruption of bile acid absorption in ileum, Vet. Res. 47 (2016) 1–10. https://doi.org/10.1186/s13567-015-0286-9.

[402] S. Gilani, G.S.H.G. Nattrass, S.M.K.R. Barekatain, R.E.A.F.C.D. Tran, R.J. Hughes, Gene expression and morphological changes in the intestinal mucosa associated with increased permeability induced by short-term fasting in chickens, J. Anim. Physiol. Anim. Nutr. (Berl). 102 (2018) 653–661. https://doi.org/10.1111/jpn.12808.

[403] S.H. Yoon, J. Choi, W.J. Lee, J.T. Do, Genetic and Epigenetic Etiology Underlying Autism Spectrum Disorder, J. Clin. Med. 9 (2020) 1–27.

[404] C. Cytrynbaum, S. Choufani, R. Weksberg, Epigenetic signatures in overgrowth syndromes: Translational opportunities, Anim. J. Med. Genet. 181C (2019) 491–501. https://doi.org/10.1002/ajmg.c.31745.

[405] M.T. Andrews, Molecular interactions underpinning the phenotype of hibernation in mammals, J. Exp. Biol. 222 (2019). https://doi.org/10.1242/jeb.160606.

[406] E.J. Baker, E.A. Miles, G.C. Burdge, P. Yaqoob, P.C. Calder, Metabolism and functional effects of plant-derived omega-3 fatty acids in humans, Prog. Lipid Res. 64 (2016) 30–56. https://doi.org/10.1016/j.plipres.2016.07.002.

[407] S.M. Innis, Dietary triacylglycerol structure and its role in infant nutrition, Adv. Nutr. 2 (2011) 275–283. https://doi.org/10.3945/an.111.000448.

[408] P. Herpin, J. Le Dividich, N. Amaral, Effect of selection for lean tissue growth on body composition and physiological state of the pig at birth., J. Anim. Sci. 71 (1993) 2645–2653. https://doi.org/10.2527/1993.71102645x.

[409] C.R. Barb, G.J. Hausman, C.A. Lents, Energy Metabolism and Leptin: Effects on Neuroendocrine Regulation of Reproduction in the Gilt and Sow, Reprod. Domest. Anim. 43 (2008) 324–330. https://doi.org/10.1111/j.1439-0531.2008.01173.x.

[410] P. Monaghan, N.B. Metcalfe, R. Torres, Oxidative stress as a mediator of life history trade-offs: Mechanisms, measurements and interpretation, Ecol. Lett. 12 (2009) 75–92. https://doi.org/10.1111/j.1461-0248.2008.01258.x.

[411] J. Lykkesfeldt, O. Svendsen, Oxidants and antioxidants in disease: Oxidative stress in farm animals, Vet. J. 173 (2007) 502–511. https://doi.org/10.1016/j.tvjl.2006.06.005.

[412] H. Yin, L. Xu, N.A. Porter, Free radical lipid peroxidation: Mechanisms and analysis, Chem. Rev. 111 (2011) 5944–5972. https://doi.org/10.1021/cr200084z.

[413] D. Pascovici, D.C.L. Handler, J.X. Wu, P.A. Haynes, Multiple testing corrections in quantitative proteomics: A useful but blunt tool, Proteomics. 16 (2016) 2448–2453. https://doi.org/10.1002/pmic.201600044.

[414] D.C.L. Handler, P.A. Haynes, Statistics in Proteomics: A Meta-analysis of 100 Proteomics Papers Published in 2019, J. Am. Soc. Mass Spectrom. 31 (2020) 1337−1343. https://doi.org/10.1021/jasms.9b00142.

[415] A. Fröhlich, F. Gaupels, H. Sarioglu, C. Holzmeister, M. Spannagl, J. Durner, C. Lindermayr, Looking deep Inside: Detection of low-abundance proteins in leaf extracts of Arabidopsis and phloem exudates of pumpkin, Plant Physiol. 159 (2012) 902–914. https://doi.org/10.1104/pp.112.198077.

[416] R. Gabbianelli, E. Damiani, Epigenetics and neurodegeneration: role of early-life nutrition, J. Nutr. Biochem. 57 (2018) 1–13. https://doi.org/10.1016/j.jnutbio.2018.01.014.

About the author

Curriculum Vitae

List of Publications

Training Activities

CURRICULUM VITAE

Thi Xuan Nguyen was born on October 06, 1987, in Hanoi, Vietnam. In 2009 she graduated from Hanoi University of Agriculture with a Bachelor's degree in "Veterinary and Animal Sciences". Next, she worked full-time for three years as a lecturer and researcher at the same University. In 2013, she started her Research Master program on "Animal Sciences" at Wageningen University thanks to the Netherlands Fellowship Program (NFP - Nuffic Fellowship) from Dutch Minister for Education, Culture and Science. Her major specialization was "Animal Nutrition", and minor specialization was "Feed Technology". For the specialization Animal Nutrition, she studied the effect of sainfoin silage (*Onobrychis viciifolia*) on nutrient flow and biohydrogenation in dairy cows at the laboratory of Animal Nutrition Group (Wageningen University). For the minor specialization Feed Technology, she performed shear processing on soy proteins and evaluated the effects of this procedure on structural, chemical changes, and the *in vitro* digestibility at the laboratory of Food Process Engineering Group, Food Chemistry, and Animal Nutrition Group (Wageningen University). In 2015, after graduating MSc study, Xuan came back to work as a lecturer at the Department of Animal Production, Vietnam National University of Agriculture, Hanoi, Vietnam.

In 2018, Xuan started her PhD research within the framework of MANNA (European Joint Doctorate in Molecular Animal Nutrition) - European Union's Horizon 2020 research & innovation program H2020-MSCA- ITN-2017- EJD: Marie Skłodowska-Curie Innovative Training Networks – Grant agreement n°: 765423. Her project focused on the effects of divergent dietary ratios between omega 6 and omega 3 on sow's and their offspring's performance and oxidative status. These results have been described in Chapter 2 (sow trial at Arioli and Sangalli Agricultural Company S.S., Genzone, Italy; and piglet trial at Centro Clinico- Veterinario e Zootecnico-Sperimentale d'Ateneo di Lodi, Università degli Studi di Milano, Italy) under supervision of Prof. Dr. Giovanni Savoini and Prof. Dr. Alessandro Agazzi. This thesis's proteomics studies (Chapter 3, 4, and 5) were performed at the Glasgow Polyomics, College of Veterinary, Medical and Life sciences, University of Glasgow (Glasgow, UK) under the supervision of Dr. Richard Burchmore and Prof. Dr. David Eckersall.

LIST OF PUBLICATIONS

Peer Reviewed Scientific Publications

A. Agazzi, V. Perricone, F.O. Zorini, S. Sandrini, E. Mariani, Xian-Ren Jiang, A. Ferrari, M. Crestani, **T.X. Nguyen**, V. Bontempo, C. Domeneghini and G. Savoini. Dietary Mannan Oligosaccharides Modulate Gut Inflammatory Response and Improve Duodenal Villi Height in Post-Weaning Piglets Improving Feed Efficiency. Animals **2020**, 10(8), 1283; https://doi.org/10.3390/ani10081283.

T.X. Nguyen, A. Agazzi, M. Comi, V. Bontempo, I. Guido, S. Panseri, H. Sauerwein, P.D. Eckersall, R. Burchmore, G. Savoini. Effects of Low ω6:ω3 Ratio in Sow Diet and Seaweed Supplement in Piglet Diet on Performance, Colostrum and Milk Fatty Acid Profiles, and Oxidative Status. Animals **2020**, 10, 2049. https://doi.org/10.3390/ani10112049.

T.X. Nguyen, A. Agazzi, S. McGill, S. Weidt, Q.H. Han, A. Gelemanović, M. McLaughlin, M. Piñeiro, G. Savoini, P.D. Eckersall, R. Burchmore. Abundance of plasma proteins in response to divergent ratios of dietary ω6:ω3 fatty acids in gestating and lactating sows using a quantitative proteomics approach. Journal of Proteomics (published online 28 Mar **2022**, Vol. 260, 30 May 2022, 104562); https://doi.org/10.1016/j.jprot.2022.104562.

T.X. Nguyen, A. Agazzi, S. McGill, S. Weidt, Q.H. Han, A. Gelemanović, M. McLaughlin, G. Savoini, P.D. Eckersall, R. Burchmore. Proteomic changes associated with maternal dietary low ω6:ω3 ratio in piglets supplemented with seaweed Part I: Serum proteomes. Journal of Proteomics (submitted 25/03/**2022**, submission reference: JPROT-S-22-00165).

T.X. Nguyen, A. Agazzi, S. McGill, S. Weidt, Q.H. Han, A. Gelemanović, M. McLaughlin, G. Savoini, P.D. Eckersall, R. Burchmore. Proteomic changes associated with maternal dietary low ω6:ω3 ratio in piglets supplemented with seaweed Part II: Ileum proteomes. Journal of Proteomics (submitted 25/03/**2022**, submission reference: JPROT-S-22-00166).

Conference Proceedings

F.O. Zorini, E. Mariani, **T.X. Nguyen**, G. Invernizzi. Evaluation of feed efficiency in Italian Holstein Friesian heifers and lactating cows. APSA 23rd congress, Sorrento, June 11-14, **2019**. Italian Journal of Animal Science. Volume 1, supplement 1, p. 59.

T.X. Nguyen[§], A. Agazzi, M. Comi, V. Bontempo, G. Invernizzi, H. Sauerwein, M. Pinerio, D. Eckersall, R. Burchmore and G. Savoini. Performance, colostrum and milk fatty acid profile in sows fed divergent ω-6:ω-3 fatty acids ratios. Book of abstracts of the 71st Annual Meeting of the European Federation of Animal Science, Virtual Meeting, December 01 - 04, **2020**. Wageningen Academic Publishers, The Netherlands. ISBN: 978-90-8686-349-5, p. 129.

T.X. Nguyen[§], A. Agazzi, M. Comi, V. Bontempo, G. Invernizzi, H. Sauerwein, M. Pinerio, D. Eckersall, R. Burchmore and G. Savoini. Performance, oxidative status and serum proteome in piglets from sows fed at divergent ω6:ω3 ratios. Book of abstracts of the 71st Annual Meeting of the European Federation of Animal Science, Virtual Meeting, December 01 - 04, **2020**. Wageningen Academic Publishers, The Netherlands. ISBN: 978-90-8686-349-5, p. 264.

T.X. Nguyen[§], A. Gelemanović, S. McGill, S. Weidt, M. Piñeiro, A. Agazzi, G. Savoini, P.D. Eckersall, R. Burchmore. TMT proteomics analysis of plasma in pigs fed low dietary ω6:ω3 ratio during gestation and lactation. BSPR Interact **2021**, July 06 – 07, virtual version.

M. Cau, A. Agazzi, **T. X. Nguyen**, M. McLaughlin, A. S. Bonastre. Assessment of the fecal microbiota from sow to piglet and the impact of different ratios of dietary polyunsaturated fatty acids. Book of abstracts of the ISAG **2021**, Virtual conference, International Society for Animal Genetics, July 26 - 30, p. 106.

[§] Presenting author

T.X. Nguyen[§], A. Gelemanović, S. McGill, S. Weidt, M. Piñeiro, A. Agazzi, P.D. Eckersall, R. Burchmore, G. Savoini. Altered serum proteomes in newly weaned piglets born from the sows receiving a low ratio of ω6:ω3. Book of abstracts of the 72nd Annual Meeting of the European Federation of Animal Science, Davos, Switzerland, August 30 – September 03, **2021**. Wageningen Academic Publishers, The Netherlands. ISBN: 978-90-8686-366-2, p. 631.

T.X. Nguyen[§], A. Agazzi, S. McGill, S. Weidt, Q.H. Han, A. Gelemanović, M. McLaughlin, M. Piñeiro, G. Savoini, P.D. Eckersall, R. Burchmore. Effect of a diet rich in omega-3 fatty acid on acute-phase proteins and high-density lipoproteins in the plasma proteome of gestating and lactating sows: a sixteen-week intervention trial. PROTEOMIC FORUM | EuPA **2022** | XIV Annual Congress European Proteomic Association Proteomics Association, April 03 - 07, Leipzig, Germany.

[§] Presenting author

TRAINING ACTIVITIES

MANNA

MANNA Core Course (including a presentation, 10.5 ECTS credits) 2018
SCENE, Glasgow, UK; October 01-10

1st Summer School in OMICS (including a progress presentation, 3 ECTS credits) 2019
Lodi, Italy; July 22-24

MANNA Milan mid-term meeting 2019
Milan, Italy; May 13

MANNA Bonn mid-term meeting 2019
Bonn, Germany; May 27

Proteomic tutorial 2020
Online course via Zoom; April 20 – 24

2nd Summer School in management skills and media communication (including a progress 2020
presentation, 3 ECTS credits)
University of Zagreb and University of Glasgow,
Online course via Zoom; September 21 – 25

Bioinformatics workshop (focusing on metabolomics and transcriptomics) 2021
MANNA consortium, online via Zoom; March 02 – 04

3rd Summer School (including a progress presentation, 3 ECTS credits) 2021
From Research to Commercial Products and Applications: Perspectives and insights for the transition from PhD to job opportunities
University of Bonn, online via Zoom; July 26 – 29

University of Milan (Unimi)

Unimi - Optional courses

Statistics for molecular and cellular biology (3 ECTS credits) 2019
Milan; January

Bionformatics tools to study omic data (2 ECTS credits) 2019
Milan; January

Genomics & Proteomics (5 ECTS credits) 2019
Milan; February

Scientific writing (2 ECTS credits) 2019
Milan; February

Bioinformatics and functional genomics (2 ECTS credits) 2019
Milan; February

Integrated structural biology (3 ECTS credits) 2019
Milan; March

Digital imaging and image integrity in scientific publication (2 ECTS credits) 2019
Milan; April

How to communicate your research (2 ECTS credits) 2019
Milan; May

Statistics for veterinary and animal science -1 (4 ECTS credits) 2019
Milan; March – May

Pathology of laboratory animals (2 ECTS credits) 2019
Milan; April – May

Statistics for veterinary and animal science -2 (3 ECTS credits) 2019
Milan; June

TRAINING ACTIVITIES *(cont.)*

Laboratory diagnostics and clinical research (2 ECTS credits) Milan; June	2019
The intestinal microbiota: interactions with host and diet (2 ECTS credits) Milan; June	2019
Italian course Milan; March – June	2019
Animal microbiome (3 ECTS credits) Online via Zoom; April 29 – May	2020
Unimi - Transferable skill courses	
Protecting and enhancing the Value of research results on the market Milan; November 29	2019
Research Integrity – Natural and physical sciences Milan; December 09	2019
Fake news, dissemination and scientific research Milan; April 16	2020
GRANTMANSHIP II Online via Teams; September	2020
Behind the Scene of a Peer Reviewed Journal Online via Teams; October 13	2020
Unimi - Presentations	
1st Unimi winter presentations Doctorate program in Veterinary Science, Lodi, Italy; January 16	2020
2nd Unimi winter presentations Doctorate program in Veterinary Science, online via Teams; February 12	2021
Unimi - Seminars	
Microbiota in pigs Milan, Italy; November 09	2018
9th Proteonet Meeting – OMICs Integration Milan, Italy; April 05	2019
Animal by-products for feed: a new roadmap for sustainable development Milan; November 21	2019
Erasmus seminar: Aflatoxin in milk Lodi; December 05	2019
University of Glasgow (Uofg)	
Uofg - Mandatory and optional courses	
Research Integrity webinar (Mandatory, 1 credit) Online; November 07	2018
Research Data Management Webinar (Mandatory, 1 credit) Online; February 13	2019
Working Towards Research Impact (1 credit) Online via Zoom; June 18	2019
Establishing a Writing Practice SCI (1 credit) Glasgow; October 07	2019
Effective writing 1 SCI (1 credit) Glasgow; October 10	2019

TRAINING ACTIVITIES *(cont.)*	
Effective writing 2 SCI (1 credit) Glasgow; October 15	2019
Writing for Publication SCI (1 credit) Glasgow; October 16	2019
Structuring a Dissertation SCI (1 credit) Glasgow; October 21	2019
Project Management (1 credit) Glasgow; January 20	2020
Omic Technologies for the Biomedical Sciences: from Genomics to Metabolomics (BIOL5197 – Masters Course) Glasgow; February – March	2020
Introduction bioinformatics live course Online via Zoom; May 18 - 22	2020
Metagenomics live course Online via Zoom; June 09 - 11	2020
Bioinformatics and R for Wet Lab Biologists – Part I (3 credits) Glasgow, online via Zoom; March 22 – April 02	2021
Bioinformatics and R for Wet Lab Biologists – Part II (Signatures, Clinical data & Biomarkers, 2 credits) Glasgow, online via Zoom; April 26 - 30	2021
Uofg - MVLS Credit	
Postgraduate Research Student Induction Course (Mandatory, 1 credit) Glasgow, October 03	2019
Programming for Biologists (Recommended, 1 credit) Online via Zoom; April 01, 08, 15	2020
Preparing for the Viva (Mandatory, 2 credits) Glasgow; February 17	2020
Successful writing (Recommended, 2 credits) Glasgow; January 23	2020
Introduction to Writing your Thesis (Mandatory, 2 credits) Online via Zoom, May 05	2021
External courses	
The 13th Mass Spectrometry in Biotechnology and Medicine (MSBM) Dubrovnik, Croatia; July 07 - 13	2019
Proteome Discoverer workshop Live sessions via Teams, ThermoFisher scientific; December 15 - 17	2020
Hands-on Introduction to R Core Facility Bioinformatics, University of Bonn, online via Zoom; April – May	2021
Uofg - Presentations	
PGR seminar Glasgow; January 24	2020
Physiology and Welfare SIG seminar Online via Zoom; June 23	2021
Uofg - Seminars	
PGR seminar Glasgow; every Friday afternoon	2019 - 2022

TRAINING ACTIVITIES *(cont.)*	
Physiology and Welfare SIG seminar Online via Zoom; every Wednesday afternoon	2020
iPS Proteomes in Health and Disease Glasgow; January 22	2020
Scientific conferences	
23rd Congress of the Animal Science and Production Association (ASPA): New challenges in Animal Science Sorrento, Italy; June 11 - 14	2019
70th Annual Meeting of the European Federation of Animal Science (EAAP 2019) Ghent, Belgium; August 26 - 30	2019
71st Annual Meeting of the European Federation of Animal Science (EAAP 2020) Online; December 01 - 04	2020
BSPR Interact 2021 Virtual meeting; July 06 - 07	2021
72nd Annual Meeting of the European Federation of Animal Science (EAAP 2021) Davos, Switzerland; August 30 - September 03	2021
PROTEOMIC FORUM | EuPA 2022 | XIV Annual Congress European Proteomic Association Leipzig, Germany; April 03 - 07	2022
Other activities	
Poster Session – Induction Day (1 credit) Glasgow; October 03	2019
MEETmeTONIGHT 2019: "Questions for Science" activity Milan; September 27 - 28	2019
Three Minute Thesis (3MT®) – an academic competition for research students (2 credits) Glasgow; March 05	2020
Careers Event: Working at the Lighthouse Lab (1 credit) Online via Zoom, December 15	2020


6
3